AD 674775

PROCEEDINGS OF CONFERENCE
ON
POLYMER STRUCTURE & MECHANICAL PROPERTIES

APRIL 19-21, 1967

HUNTER AUDITORIUM
U. S. ARMY NATICK LABORATORIES
NATICK, MASSACHUSETTS

SPONSORED BY
U. S. ARMY NATICK LABORATORIES
U. S. NAVY, OFFICE OF NAVAL RESEARCH
U. S. AIR FORCE
NATIONAL AERONAUTICS AND SPACE ADMINISTRATION
ADVISORY BOARD ON MILITARY PERSONNEL SUPPLIES
NATIONAL ACADEMY OF SCIENCES

Reproduced by the
CLEARINGHOUSE
for Federal Scientific & Technical
Information Springfield Va. 22151

458

PROCEEDINGS OF CONFERENCE

on

POLYMER STRUCTURE AND MECHANICAL PROPERTIES

April 19-21, 1967

Hunter Auditorium
U. S. Army Natick Laboratories
Natick, Massachusetts

Sponsored by

U. S. Army Natick Laboratories
U. S. Navy, Office of Naval Research
U. S. Air Force
National Aeronautics and Space Administration
Advisory Board on Military Personnel Supplies
National Academy of Sciences

BLANK PAGE

TABLE OF CONTENTS

Page

Introductory Remarks - No manuscript

Field H. Winslow
General Chairman of Conference
Bell Telephone Laboratories, Inc.

William M. Mantz
Commanding General
U. S. Army Natick Laboratories

Dale H. Sieling
Scientific Director
U. S. Army Natick Laboratories

Introduction to the Proceedings 1
J. H. Faull, Jr. and N. S. Schneider

SESSION 1: MECHANICAL PROPERTIES OF RUBBERY POLYMERS
Chairman: J. H. Faull, Jr.
Office of Naval Research

Paper No. 1 - Deformation and Fracture of Elastomers 4
A. N. Gent, University of Akron

Paper No. 2 - Relationship Between Crosslink Type and Mechanical Properties 29
L. Mullins, Natural Rubber Producers' Research Association, Herts, England

Comments after Paper No. 2 46
Arthur V. Tobolsky, Princeton University

Paper No. 3 - Equations of State for Elastomers 48
Turner Alfrey, Jr., The Dow Chemical Company

SESSION 2: MECHANICAL PROPERTIES OF GLASSY POLYMERS
Chairman: Nathaniel S. Schneider
U. S. Army Natick Laboratories

Paper No. 4 - Plastic Yield Behavior of Glassy Polymers 61
Rodney D. Andrews, Jr., Stevens Institute of Technology

Discussion on Paper No. 4 73
Allan S. Hoffman, Massachusetts Institute of Technology

TABLE OF CONTENTS (continued)

Page

Paper No. 5 - A Working Hypothesis of Polymer Fracture 77
P. I. Vincent, Imperial Chemical Industries, Ltd., Hertfordshire, England

Discussion on Paper No. 5 90
I. V. Yannas, Massachusetts Institute of Technology

Paper No. 6 - Cyclic Stress-Strain Behavior of the Dry Polycarbonate Craze 91
R. P. Kambour and R. W. Kopp, General Electric Company

SESSION 3: MORPHOLOGY OF CRYSTALLINE POLYMERS
Chairman: Eric Baer
Case Institute of Technology

Paper No. 7 - Polymer Crystals - Good and Bad 132
H. D. Keith, Bell Telephone Laboratories, Inc.

Discussion on Paper No. 7 147
B. Wunderlich, Rensselaer Polytechnic Institute

Paper No. 8 - On the Structure of Disordered Regions in Polyethylene Single Crystals and in Drawn Polyethylene 148
E. W. Fischer, H. Goddar and G. F. Schmidt, Universitat Mainz, Mainz, W. Germany

Paper No. 9 - Regular Crystallographic Chain-Folding in Polyethylene Crystals 183
P. H. Lindenmeyer, Chemstrand Research Center, Inc.

Contributed papers on Session 3:

Density and Heat of Fusion of Folded Chain Polyethylene Crystals 215
Fumiyuki Hamada and Bernhard Wunderlich
Rensselaer Polytechnic Institute

Some New Avenues in Polymer Single Crystal Studies 246
A. Keller, University of Bristol, England

TABLE OF CONTENTS (continued)

Page

The Regularity of Polymer Fold Surfaces 260
D. C. Bassett, University of Reading, U.K.

Characterization of Chain Folds in Crystalline Polymers. A Statistical Problem 275
T. G. Fox and Hershel Markovitz, Carnegie-Mellon University

SESSION 4: MECHANICAL PROPERTIES OF CRYSTALLINE POLYMERS
Chairman: Shiro Matsuoka
Bell Telephone Laboratories, Inc.

Paper No. 10 - Mechanical Properties of Crystalline Polymers
John D. Hoffman
National Bureau of Standards
No Manuscript

Paper No. 11 - Mechanical Properties of Polymer Single Crystals and Extended Chain Crystals--Discussion of Defect Region and Loose Chains Attached to Them..... 284
Motowo Takayanagi, Kyushu University, Japan

Paper No. 12 - Deformation of Crystalline Polymers
Phillip H. Geil
Case Institute of Technology
No Manuscript

Contributed paper on Session 4:

High Shear Flow of Partially Crystalline Polymers 294
(partially presented at Conference)
Roger Porter, University of Massachusetts

SESSION 5: POLYMER TRANSITIONS AND RELAXATION PROCESSES
Chairman: Raymond F. Boyer
Dow Chemical Company

Paper No. 13 - Effect of Secondary Transitions and Relaxations on Polymer Properties 299
Raymond F. Boyer, Dow Chemical Company

Discussion on Paper No. 13 437
Donald J. Plazek, Mellon Institute

TABLE OF CONTENTS (continued)

Page

Paper No. 14 - Multiple Transitions in Polyalkyl Methacrylates . . 380
Robert A. Haldon and Robert Simha,
University of Southern California

Paper No. 15 - Properties of Ethylene-Methacrylic Acid Copolymers and Their Sodium Salts; Mechanical Relaxations . .410
W. J. MacKnight, L. W. McKenna and B. E. Read,
University of Massachusetts

General Contribution:

Studies in the Field of Polymer Structure and Mechanical Properties 430
E. H. Andrews, Queen Mary College, England

Attendance List 447

Introduction to the Proceedings

This conference had its origins in the recognized need to obtain a critical review and discussion of recent progress and current problems in the area of polymer solid state structure and mechanical properties that would provide useful leads and general guidance to military programs. To achieve this purpose an effort was made to obtain as the main conference speakers the outstanding research scientists working on the various subjects treated in the conference.

Credit for the success of the conference belongs largely to Dr. Field Winslow, whose time as General Chairman was generously donated by the Bell Telephone Laboratories. It was he who proposed the agenda outline with its five sessions, each to handle a separate topic area by three talks: a critical review by a recognized leader in the field, followed by two current research reports of more than passing significance; thus it was hoped to set the stage for definitive discussions by other leaders in the field who had in turn been invited to the conference for that purpose. Success, Dr. Winslow insisted, would depend on certain conditions, among them acceptance by a large enough representation of the top scientists from all over the world, creation of the atmosphere of a working group not unlike a Gordon Research Conference, and a restriction of attendance to assure meaningful interactions. While the conditions were met and success recognized by all attending, it was inevitable that some important people and some important points of view were missing; many more people, regretfully, could not be accommodated as attendees.

It is appropriate to express our appreciation, as well, to the several chairmen who had the responsibility for organizing the individual sessions. Finally, well deserved recognition must be accorded Dr. Frank Fisher, Executive Director, Advisory Board on Military Supplies of N R Council. His assistance and support in all phases of the business of the Conference were invaluable to the organizers, and his attention to the innumerable details of organization were responsible for the smooth operation of the Conference.

Originally a Proceedings was not contemplated. However, as the conference progressed it became apparent that much material had, in fact, been prepared in a form suitable for a more permanent record. It was also recognized that the sponsoring agencies and, indeed, the research scientists themselves could use a Proceedings for future research program planning and reference. It was then determined that many, all contributing to this document, would offer manuscripts for a Proceedings composed of papers, discussion and even afterthoughts, provided that distribution would be limited to invitees, sponsoring agencies and their active research contractors in the field. Unfortunately much of the definitive and lively discussion presented from the floor is lost, owing to acoustical difficulties with the recording. This has been partially made up by several more lengthy discussions not fully presented at the conference itself, herein included as "contributions," and printed following the invited papers for the appropriate session.

In many cases authors clearly stated what they felt to be important future directions of research. The reader might well profit by searching these out. By way of example, a few will be mentioned. In Session No. 1, Professor Gent listed six areas for further research, ranging from fracture phenomenology to mechanism of tear deviations; a more detailed comparison of the failure of swollen against unswollen rubbers could pinpoint viscoelastic factors whereby earlier theories might be revised. Dr. Mullins believes much is yet to be learned of the importance to strength of the nature of cross links and their interaction with the viscoelastic environment, especially concerning the role of bond breaking and redistribution under stress. Alfrey detailed a new approach to large deformation viscoelastic theory which is more likely to be more structure related than the useful Mooney-Rivlin invariant approach and even applicable to much higher extension ratios. Craze theory was linked to Tg change by Andrews and a new approach opened up by Kambour with obvious lines of investigation opening up for many materials not studied. The role of free volume was raised by Hoffman, and Tobolsky proposed a new definition of free volume for polymers in relation to strain, as an approach to failure mechanisms.

In Session 3, Morphology of Crystalline Polymers, the conference reached a high level of activity and interaction. Keith anticipated this in his review statement calling for a reevaluation of ten years of progress in this field. Folded chain theory dominated the presentations and discussion, involving all three agenda presentations and eliciting in addition four major contributions which are reproduced in full for these Proceedings. In fact, folded chain theory carried over into other sessions, most notably perhaps in the novel and clarifying work of Takayanagi. Unfortunately the steering committee did not reserve enough time for these deliberations, although the generous documents here reproduced together may make some amends. Much work remains to be done but the conference provided a rich collection of leads and approaches which should bear fruit.

Finally, attention might be drawn to the contribution by E. H. Andrews, printed at the end, in which an excellent photomicrograph is included as part of his provocative theory of nucleation and polymer crystal growth in stress environments.

The organizers and sponsors of this conference are grateful to the participants who in many cases came from afar and who gave so generously of their time and thought. Those who supplied written manuscript for this Proceedings under rather unfavorable circumstances are particularly to be thanked; admittedly a more complete and polished Proceedings would be welcome, but it is felt that a best effort document circulated to a limited working group may well be justified at this time.

Basic polymer research has not been reviewed before by a conference of this sort sponsored jointly by the several military agencies. Polymer technology has long been a major materials concern to all these agencies, and various aspects have been repeatedly made the subject of joint conferences. It is becoming increasingly recognized that technology programs without related basic research programs advance slowly and less certainly. A successful conference such as this serves not only to provide a medium for technical coordination and advance, but also to provide a credible reference in the all-important defense for the funding of basic research programs. Thus, it should be contemplated that this conference is not to stand alone but to be followed by others covering, as well, other topics in polymer science.

J. H. FAULL, Jr.,
Office of Naval Research

N. S. Schneider,
U. S. Army Natick Laboratories

DEFORMATION AND FRACTURE OF ELASTOMERS

A. N. Gent

Institute of Polymer Science
The University of Akron

ABSTRACT

Part of the energy expended in deforming elastomers is dissipated in overcoming the viscous resistance to motion of the molecular chains and in breaking structures associated with fillers or crystalline regions. These energy losses have recently been shown to govern a wide variety of mechanical properties: tensile strength, tear resistance, resistance to surface cracking by ozone, sliding friction and abrasion. A review is given of these findings. In addition, attention is drawn to modes of failure which might be properly termed "elastic instabilities," as they can be predicted quantitatively from the elastic properties alone.

1. Introduction

Elastomers are not perfectly elastic; some part of the energy spent in deforming them is dissipated due to a variety of causes. The principal energy-dissipating mechanisms are:

(i) Internal friction or viscosity, as the molecular chains rearrange their positions and segments of them slide past each other.

(ii) Strain-induced crystallization. Under the orienting influence of a deformation, sufficiently regular molecules may form microcrystalline assemblies. Any further deformation can only be accomplished by disrupting the crystallites with a corresponding dissipation of energy.

(iii) Structural breakdown of a filled elastomer (two-phase) system. Hard filler particles, generally of carbon black, stiffen elastomers in two ways: by forming long associated chains of particles and by adhering strongly to the molecules in contact with each particle. Both of these associations are destroyed at least partially by a deformation, the particle chains at quite small deformations and the elastomer-particle bonds at large ones.

The dissipation of energy internally has usually been regarded as a serious disadvantage of elastomers. Recently, however, it has been shown to be responsible for the resistance to a wide variety of fracture processes: tensile rupture, tearing, surface cracking by ozone, and abrasion. These findings are reviewed here. Also, the existence of unstable states is pointed out, at which an elastic deformation becomes inhomogeneous. Small regions then become highly deformed, often to the point of rupture. In these cases the criterion for fracture is an <u>elastic</u> one, involving the relations between applied loads and deformations.

2. <u>Tensile Rupture</u>

Strength measurements at different rates of elongation $\dot{\epsilon}$ and temperatures T are found to depend upon a single variable $\dot{\epsilon}\eta_T$, where η is the segmental viscosity (Figure 1; Smith, 1958). Variations with temperature are thus due to corresponding viscosity changes. Moreover, the master curve under iso-viscous conditions has the form expected of a viscosity-controlled quantity; it rises sharply with increased rate of elongation to a maximum value at high rates when the segments do not move and the material breaks as a brittle glass (Bueche, 1955). The breaking elongation at first rises with increasing rate of elongation,

reflecting the enhanced strength, and then falls at higher rates as the segments become unable to respond sufficiently rapidly (Figure 2).

An alternative measure of tensile rupture is the work W_b required to break the rubber per unit volume. It varies with the rate of elongation in a similar manner to the elongation at break, passing through a maximum value with increasing rate, or with decreasing temperature at a constant rate. The variation closely resembles that obtained for energy dissipation under small deformation, indicating the close parallel between energy dissipation and energy required to rupture. A more striking demonstration is afforded by the recent observation of Grosch, Harwood and Payne (1966) that a direct relationship exists between W_b and the energy dissipated W_d in stretching to the breaking elongation, irrespective of the mechanism of energy loss, i.e., for filled and unfilled, strain-crystallizing and amorphous elastomers, Figure 3. Their empirical relation is

$$W_b = 4 \cdot 1 \; W_d^{2/3},$$

W_b and W_d being measured in joules/cm^3. Those materials which require the most energy to bring about rupture, i.e., the strongest elastomers, are precisely those in which the major part of the energy is dissipated before rupture.

3. Tear Strength

It is important to recognize that the tear strength $\underline{\theta}$ is also not a constant value for a particular material; it depends strongly upon the temperature and rate of tear, i.e., the rate at which material is deformed to rupture at the tear tip. Several critical values of $\underline{\theta}$ may be distinguished. The smallest possible value is given by the surface energy, about 50 ergs/cm^2 for non-polar hydrocarbons. This value is indeed found to govern the growth of surface cracks due to chemical scission of the elastomer molecules (by atmospheric ozone), when the function of the applied forces is merely to separate molecules already broken (see section 6). Another critical value of $\underline{\theta}$ is that necessary to break all the molecules crossing a random plane. This has been estimated to be of the order of 10^4 ergs/cm^2 for typical hydrocarbon elastomers (Thomas, 1966). Measurements of the minimum value of $\underline{\theta}$ necessary to cause <u>any</u> cut growth by mechanical rupture are in reasonable agreement with this value (Lake and Lindley, 1965).

In simple tearing measurements the observed values of $\underline{\theta}$ are considerably large, ranging from 10^5 to 10^8 ergs/cm^2. The reason for the enhanced strength is made clear by considering the process by which the energy $\underline{\theta}$ is dissipated at the tear tip. Thomas (1955) has shown that $\underline{\theta}$ can be expressed in terms of the effective diameter $\underline{d}$ of the tip of the tear and the

"intrinsic" breaking energy $\underline{\overline{W_b}}$ of the material by the approximate relation

$$\theta = \overline{W_b} .$$

The "intrinsic" breaking energy may be defined as the energy required to break unit volume of the material in the absence of a significant nick or flaw. It will be generally similar to, but larger than, the value of $\underline{W_b}$ determined for carefully prepared tensile test-pieces in which chance edge flaws are minimized. Both $\underline{\overline{W_b}}$ and $\underline{d}$ depend upon the conditions of tear. However, for unfilled non-crystallizing elastomers, $\underline{d}$ remains small (of the order of 0.01 cm) and relatively constant. In these cases Greensmith (1960) has shown that $\underline{\theta}$ is proportional to $\underline{W_b}$ and changes in a parallel fashion with temperature and rate of tearing (rate of extension). Mullins (1959) has also shown that $\underline{\theta}$ is proportional to a measure of the viscous stress component. Thus the internal viscosity determines the intrinsic breaking energy and the tear resistance for such materials. The effective diameter $\underline{d}$ of the tip of a growing tear also depends upon the elastic and viscous properties to some degree (Gent and Henry, 1967) so that the tear energy $\underline{\theta}$ shows a complex temperature dependence. It is still governed by the internal energy dissipation, however, and is found to be the same for elastomers of widely-different chemical composition under conditions of equal segmental mobility (Figure 4; Mullins, 1959).

In strain-crystallizing elastomers (for example, natural rubber) the tear resistance and tensile strength are greatly enhanced. Such materials show mechanical energy dissipation as discussed in the Introduction, and their strength has been accounted for in this way (Andrews, 1963). Adding reinforcing particulate fillers to non-crystallizing elastomers brings about a similar strengthening. This effect is principally due to a pronounced change in the character of the tear process, from relatively smooth tearing in unfilled materials to a discontinuous stick-slip process, in which the tear develops laterally or even circles around under increasing force until a new tear breaks ahead and the tear force drops abruptly. The process then repeats itself (Figure 5). This form of tearing has been termed "knotty" tearing (Greensmith, 1956).

The mechanism of tear deviation is still obscure. It may occur because the maximum stresses lie off the tear axis, due to anisotropic elastic behavior of the strained material around the tear tip or to a "frozen" stress mechanism proposed by Andrews (1963), or because the filled materials have anisotropic strength. Pronounced knotty tearing occurs only within a limited range of tear rates and temperatures, depending upon the particular filler and elastomer employed (Greensmith, 1956). There are some indications that this effect is associated with the viscoelastic response of the polymer, but the conditions required involve much higher temperatures and lower rates of extension than the main rubber-to-glass transition region.

4. Sliding Friction

Friction is naturally associated with energy dissipation. The principal mechanism of dissipation again turns out to be energy losses within the elastomer, but the connection between the coefficient of friction μ and the internal viscosity, for example, is complex; two distinct modes of deformation having been distinguished (Grosch, 1963). The first is due to indentation by surface asperities on the track and the second arises from molecular adhesions which are formed and broken during sliding.

On a lubricated rough track the value of μ increases with increasing sliding velocity and then passes through a maximum (Figure 6). The relation closely resembles the dependence of the energy absorption per deformation cycle upon the frequency of deformation. Indeed, the speed of sliding at which μ has a maximum value, divided by the spacing between asperities, corresponds accurately to the frequency of deformation at which the energy dissipation is a maximum at the same temperature. The dominant role of energy dissipation in lubricated sliding friction is thus established. For sliding over a clean smooth surface the relation for μ is found to be similar, but displaced toward lower velocities. It corresponds, therefore, to "asperities" of much closer spacing than those in the rough surface.

The spacings are calculated to be only about 60Å, by comparing the comparing the velocity for maximum friction with the frequency for maximum energy absorption. Thus, friction between dry smooth surfaces is associated with deformations on a molecular scale. It has therefore been attributed to transitory molecular adhesions between elastomer and track The high frictional coefficient is, however, again due to dissipation of energy in the rubber as it undergoes local shearing deformations around the temporary bonds, and not due to the strength of the bonds themselves This is shown by the characteristic dependence on speed and temperature.

On dry rough surfaces the effects of both surface asperities and molecular adhesions are evident in the master relation for μ as a function of the speed of sliding (Figure 6). On lubricated smooth surfaces both deformation processes are minimized and the coefficient of friction is correspondingly small.

5. Wear Due to Sliding

As both the tear resistance and the tearing (frictional) force depend upon temperature in accord with viscosity-controlled processes, it is not surprising that the abrasive wear as a function of spped of sliding should do so. A suitable measure of the rate of wear is provided by the ratio A/μ of the volume A abraded away per unit normal load and unit

sliding distance to the coefficient of friction μ. This ratio, termed the abradibility, represents the abraded volume per unit energy dissipated in sliding.

It is found to decrease with increasing speed, pass through a minimum and then rise again at high speeds. This behavior resenbles the variation of the reciprocal of the breaking energy W_b with rate of deformation (a reciprocal relationship because high abradibility corresponds to low strength). Indeed, Grosch and Schallamach (1965) found a general parallel between A/μ and $1/W_b$ (Figure 7). Moreover, the coefficient of proportionality was found to be similar, about 10^{-3}, for all the unfilled elastomers examined. This coefficient represents the volume of rubber abraded away by unit energy applied frictionally to a material for which unit energy per unit volume is necessary to cause tensile rupture. It may be regarded as a measure of the inefficiency of rupture by tangential surface tractions; large volumes are deformed but only small volumes are removed.

6. Resistance to Ozone Cracking

In an atmosphere containing ozone, stretched strips of unsaturated elastomers develop surface cracks. These cracks grow in width and depth and either sever the strip or cause a serious loss of strength. From experiments with initial cuts of different length and with elastomers of dif-

ferent degrees of crosslinking, and hence different values of Young s modulus, Braden and Gen (1960, 1961) found that the minimum stresses for cracking to occur corresponded to a critical energy requirement of about 50 ergs/cm^2 of new surface This suggests that the critical condition is a very simple one: the stored elastic energy must be sufficient to meet surface energy requirements. The critical stresses to cause cracking in uncut test-pieces corresponded to cuts about 10^{-3}cm deep, using the same energy criterion. It was therefore deduced that normal ozone cracks start from surface nicks or flaws equivalent to cuts of this size.

Provided the critical stress was exceeded, the rate of crack growth did not depend significantly upon the applied stress over a wide range of stresses. However, it depended markedly upon temperature. Rates of growth were determined over a wide temperature range for a series of butadienestyrene rubbers containg from 0 to 80 per cent styrene (Gent and McGrath, 1965). When plotted against the temperature diffierence T-Tg between the test temperature and the glass temperature for each material, they were found to form a single, relation (Figure 8) suggesting that segmental mobility is the primary factor determining the rate of growth of an ozone crack. The Williams, Landel and Ferry relation for segmental mobility (Ferry, 1961) was found to describe the ex-

perimental results well at low temperatures. At higher temperatures the observed rates did not continue to increase with increasing segmental mobility but approached a constant value. This was due to the limited concentration of ozone; the incidence of ozone molecules had become rate-determining, rather than the segmental mobility. However, over a temperature range up to about $T_g + 60^{\circ}C$ at this particular ozone concentration, the rates of ozone crack growth were clearly determined by the internal viscosity of the rubber, rather than by strictly chemical factors. This is apparently due to the need for movement of the rubber molecules in and near the crack tip to yield new surfaces for reaction (Gent and Mc Grath, 1965).

7. Elastic Instabilities

Novel instabilities can occur for materials capable of undergoing large elastic deformations. For example, the uniform inflation of a long rubber tube becomes unstable at a critical degree of inflaction and the tube develops a pronounced "blister". In such cases, where the deformation becomes markedly non-uniform, the specimen will obviously rupture prematurely. For materials of limited extensibility fracture can therefore be calculated quantitatively from purely elastic considerations, and will be largely independent of the detailed fracture properties of the material. The cavitation of elastomers under a negative hydrostatic

pressure (triaxial tension) is an example of this type of fracture. Gent and Lindley (1958) have shown experimentally that the critical stress at which cavitation occurs is not greatly dependent on the tensile strength or extensibility of the elastomer. Instead it is directly proportional to the elastomer modulus (Figure 9). Indeed, quantitative agreement was obtained with the calculated stress at which the elastic expansion of a hypothetical small hole in the elastomer would become indefinitely large. It seems likely that other cases of fracture by elastic instability also exist, as yet unrecognized.

8. Conclusions and Recommended Research

A review of several diverse fracture processes in elastomers has been presented in terms of a general unifying concept: the inefficiency with which the energy of deformation is expended in molecular rupture. The experimental evidence has been briefly discussed, using amorphous unfilled elastomers as the primary examples because their energy dissipation in viscous processes follows a characteristic dependence upon speed of deformation (or frequency) and temperature. The effects of strain-induced crystallization and the presence of reinforcing particulate fillers have also been shown to be encompassed by the same general principles, so that it has proved possible to account for the main features of the tensile strength, tear resistance, abrasive wear and ozone cracking

of elastomers in this way.

It is clear that an elastomer having the greatest degree of energy dissipation consistent with satisfacoty: service performance should be chosen for maximum strength. Two aspects of this general correlation between strength and dissipative properties should be emphasized, however:

(i) It is not always a simple relationship. In sliding friction, for example, two mechanisms of dissipation have been identified, whose relative importance depends upon the geometry of the track, the speed of sliding and the detailed nature of the viscoelastic response of the rubber.

(ii) Ideally an elastomer should develop energy-dissipating features only at high extensions so that it is resilient under normal service conditions and yet strong at sites of stress concentration. Strain-crystallizing elastomers show precisely this behavior, and filled materials do so also but to a lesser degree.

The detailed structure of elastomer networks has not been dealt with here The average length of the molecular chains which comprise the network is found to govern the extensibility under conditions of low internal viscosity (Greensmith, Mullins and Thomas, 1963). Significant effects would also be expected from the distribution of chain lengths, of which little is known, and from the presence of physical entanglements

in addition to permanent chemical crosslinks between chains. No study of such effects has yet been made. Indeed, the study of general fracture processes under conditions of low internal viscosity, and the effects of network structure upon them, seem appropriate areas for future research.

Acknowledgments

This review was prepared in connection with a program of research supported by the National Science Foundation. A brief earlier version was presented at the Conference on Elastom-Plastics Technology, Detroit, in May, 1965, and a more comprehensive one forms part of a "Treatise on Fracture", to be edited by H. Liebowitz and published by Academic Press in 1968. The author is indebted to an earlier review by Grosch and Mullins (1962), in which the general relationship between hysteresis and various strength properties was outlined. Other recent reviews by Greensmith, Mullins and Thomas (1963), Landel and Fedors (1964) and Halpin (1965) should be consulted for further details.

REFERENCES

Andrews, E. H. (1963) Rubb Chem. Technol., 36, 325

Braden, M., and Gent, A.N. (1960) J Appl. Polym Sci , 3, 100

Braden, M., and Gent, A.N. (1961) Kautschuk U. Gummi, 14, WT157.

Bueche, F. (1955) J. Appl. Phys., 26, 1133.

Ferry, J.D. (1961) "Viscoelastic Properties of Polymers", Wiley, N.Y.

Gent, A.N., and Henry, A.W. (967) in press.

Gent, A.N., and Lindley, P.B. (.958) Proc. Roy. Soc. (London), A249, 195.

Gent, A.N., and McGrath, J.E. (1965) J. Polym. Sci., A2, 1473.

Greensmith, H.W. (1956) J. Polym. Sci., 21, 175

Greensmith, H.W. (1960) J. Appl. Polym. Sci., 3, 183.

Greensmith, H.W, Mullins, L and Thomas, A.G. (1963) Chap. 10 in "The Chemistry and Physics of Rubberlike Substances" ed. by L Bateman, Wiley, New York.

Grosch, K.A. (1963) Proc. Roy. Soc. (London), A274, 21.

Grosch, K.A., Harwood, J.A.C., and Payne, A.R. (1966) Nature, 212, 497.

Grosch, K.A., and Mullins, L. (1962) Rev. Gen. Caoutch., 39, 1781.

Grosch, K.A., and Schallamach, A. (1965) Trans. Instn Rubb. Inc., 41, T80

Halpin, J.C. (1965) Rubb. Chem. Technol., 38, 1007.

Lake, G.J., and Lindley, P.B. (1965) J. Appl. Polym. Sci., 9, 1233.

Landel, R.F., and Fedors, R.F. (1964) Chap. IIIB in "Rupture Processes in Polymeric Solids" ed. by B. Rosen, Interscience, New York.

Mullins, L. (1959) Trans. Instn Rubb. Ind., 35, 213.

Smith, T.L. (1958) J. Polym. Sci., 32, 99

Thomas, A.G. (1955) J. Polym. Sci., 18, 177.

Thomas, A.G. (1966) Unpublished work.

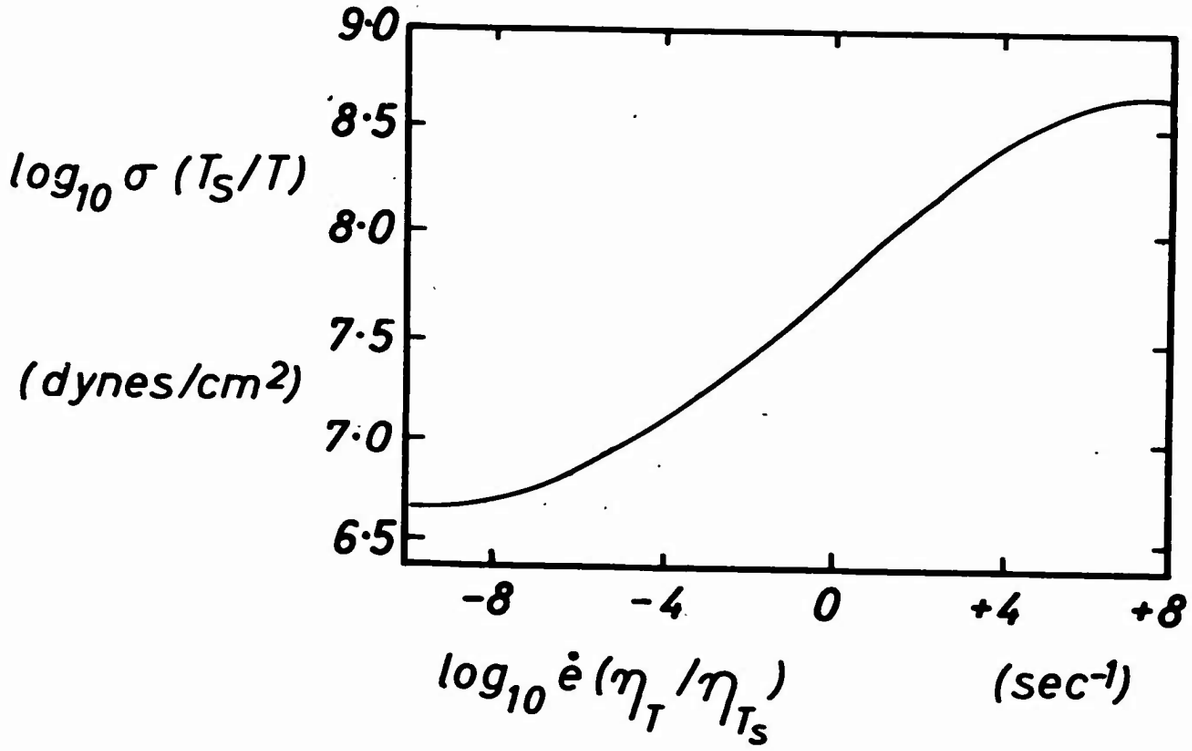

Master relation for tensile strength σ as a function of rate of elongation $\dot{e}$ reduced to $T_S = -10^{\circ}C$ ($T_g + 50^{\circ}C$). [After T. L. Smith (1958)].

FIGURE 1

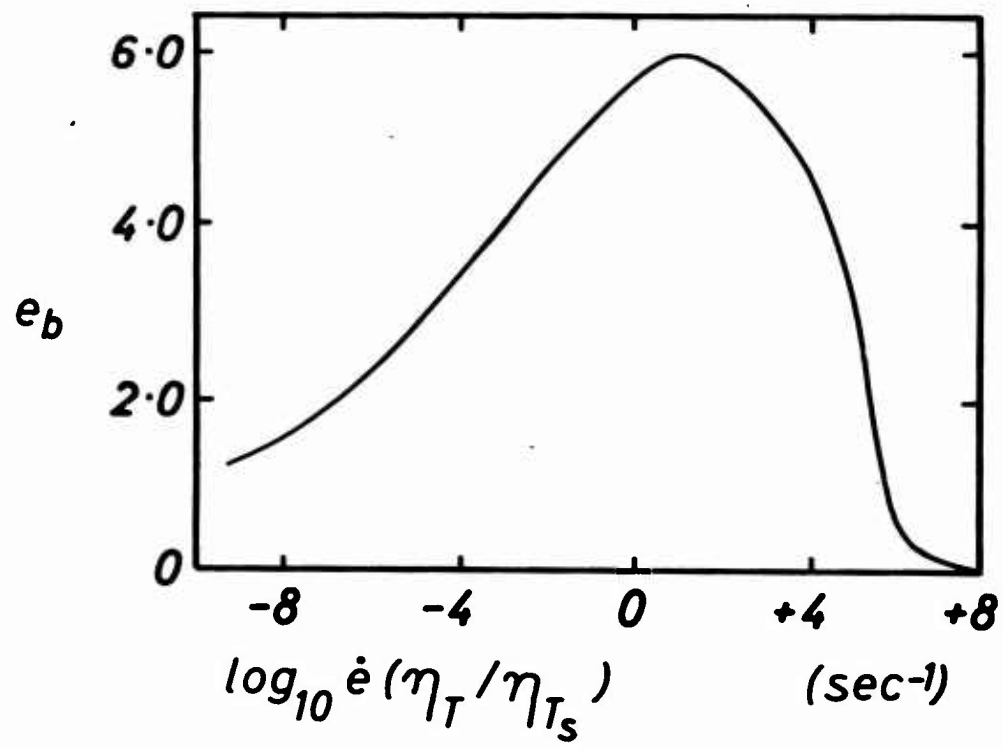

Master relation for breaking elongation e_b as a function of rate of elongation $\dot{e}$ reduced to -10°C (Tg + 50°C). After T. L. Smith (1958)

FIGURE 2

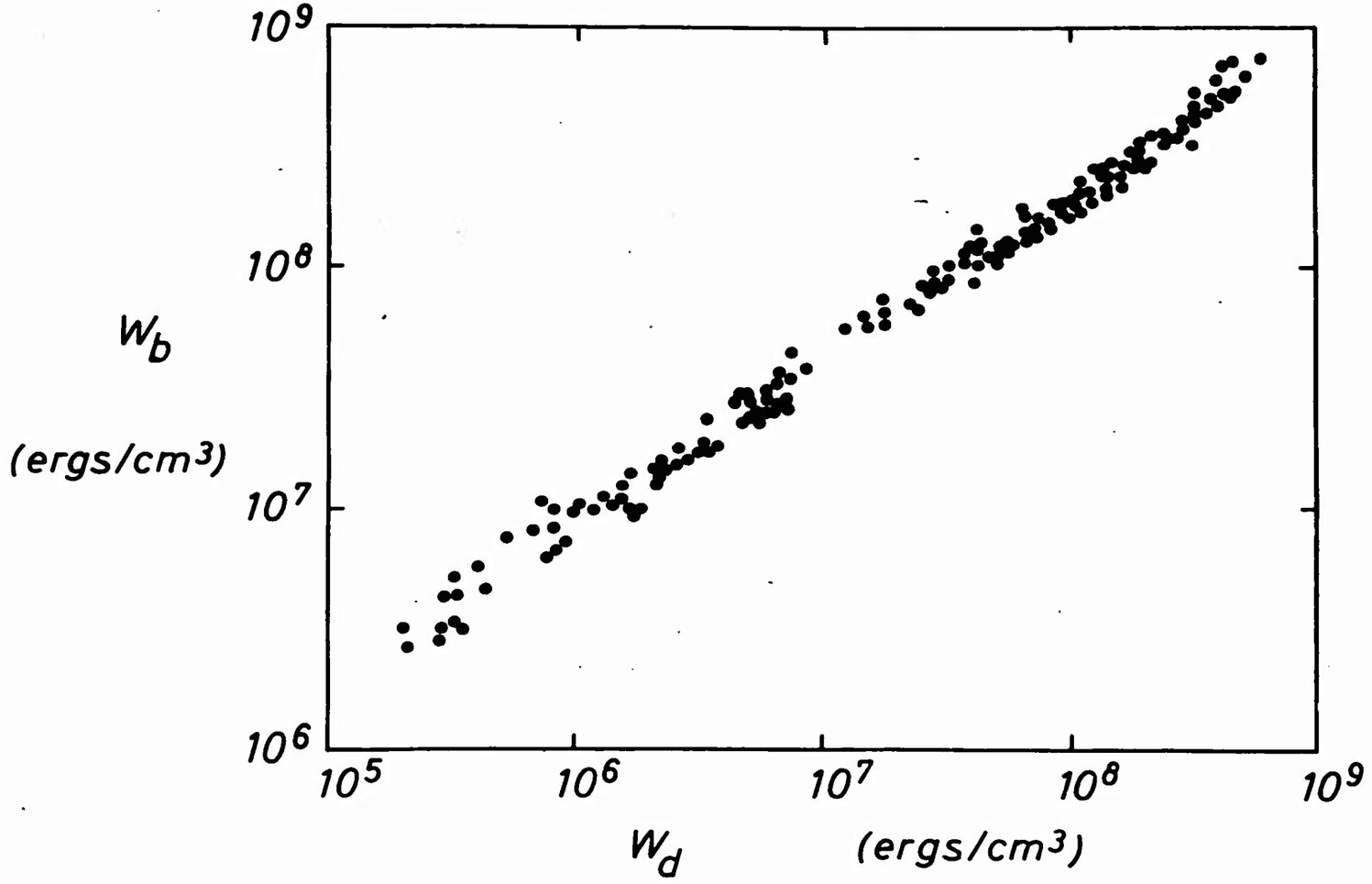

Relation between work-to-break W_b and energy dissipated W_d for a wide variety of elastomer systems (Grosch, Harwood and Payne, 1966).

FIGURE 3

Master relation for tear energy θ as a function of the rate of tearing r reduced to Tg + 20°C for vulcanizates of butadiene-styrene (△, □) and butadiene-acrylonitrile (●, ▲) copolymers. After L Mullins (1959)

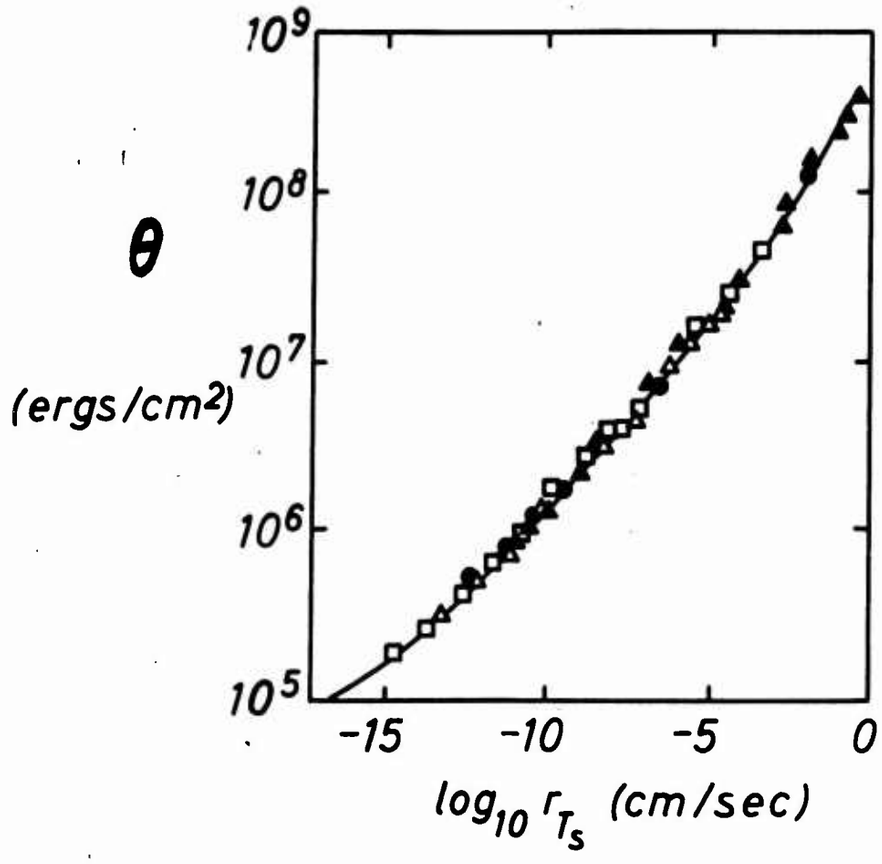

FIGURE 4

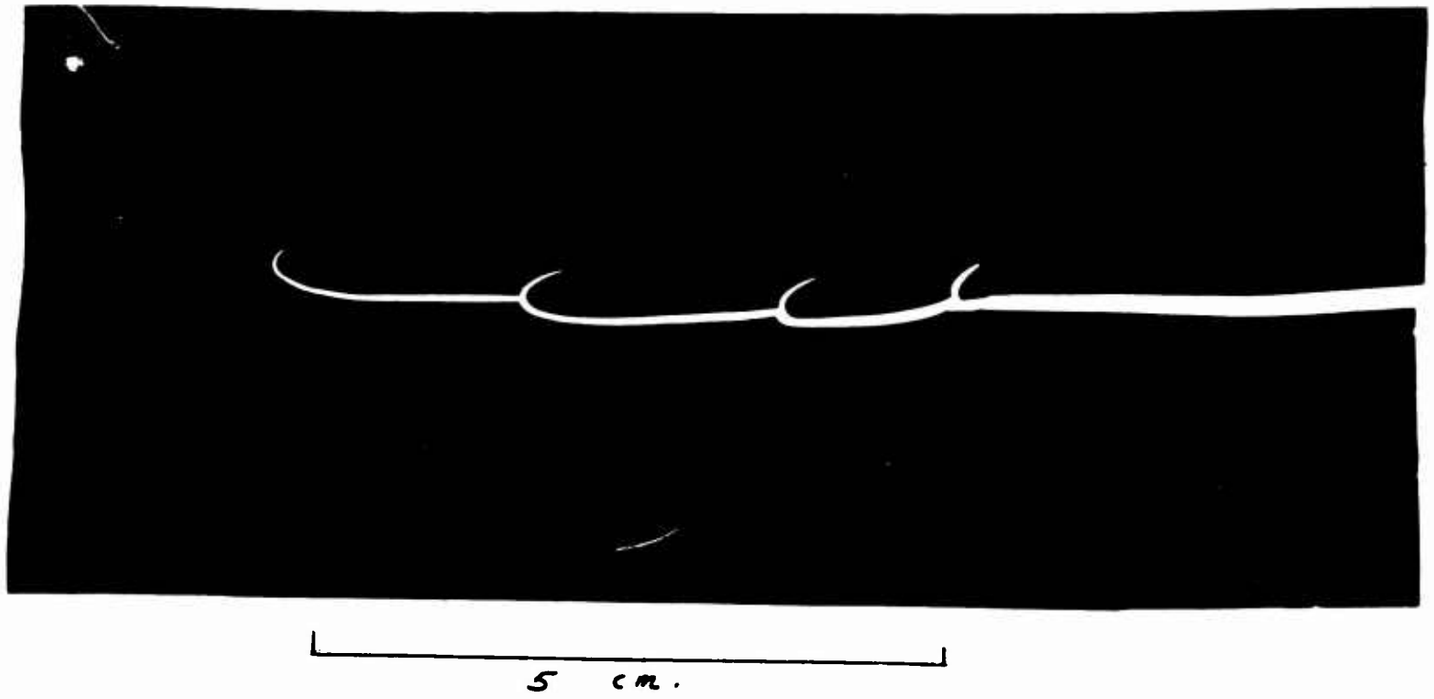

Example of "knotty" tearing (Gent and Henry, 1967).

FIGURE 5

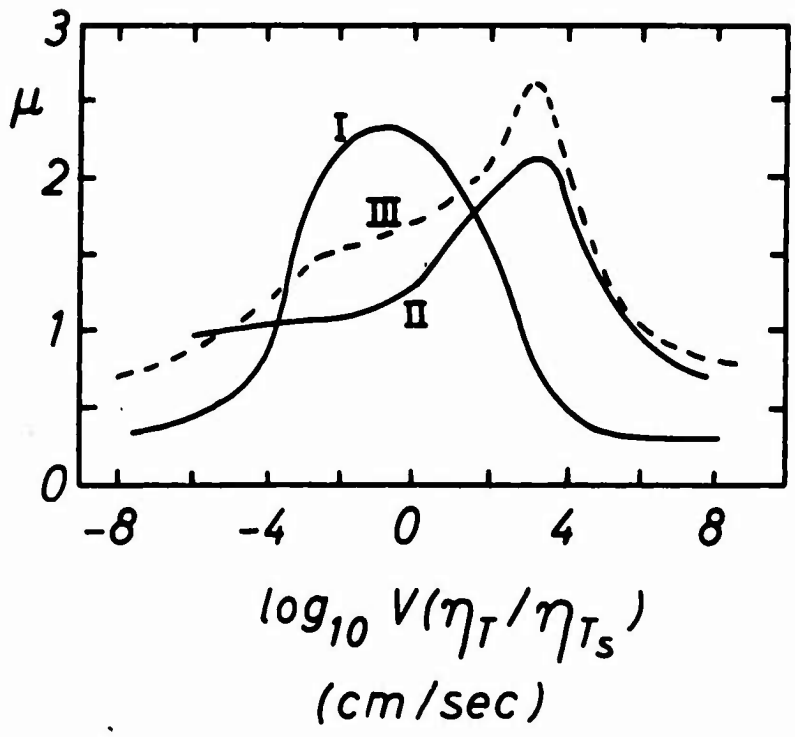

Coefficient of sliding friction μ for a butadiene-acrylonitrile vulcanizate vs speed of sliding V reduced to 20°C. Curve I, dry smooth track; curve II, lubricated rough track; curve III, dry rough track. From K.A. Grosch (1963).

FIGURE 6

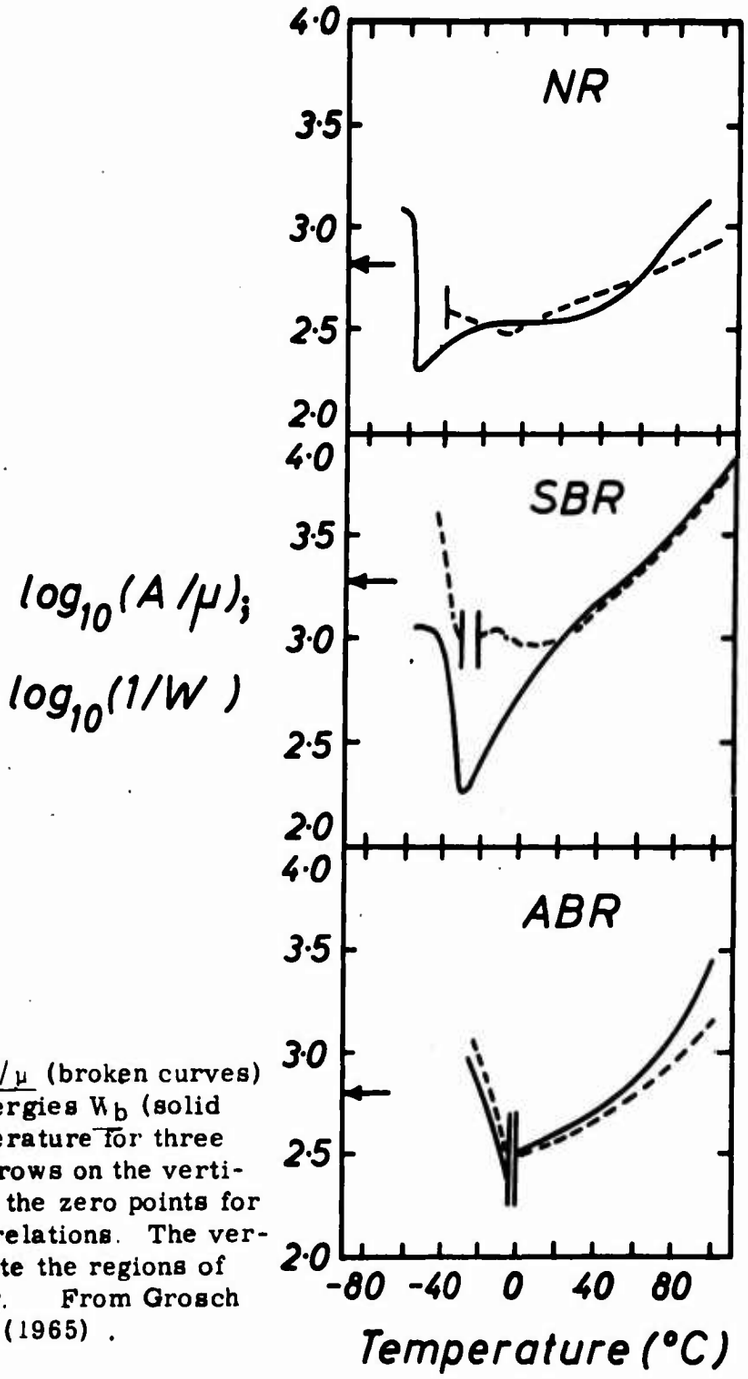

Abradibilities A/μ (broken curves) and breaking energies W_b (solid curves) vs temperature for three elastomers. Arrows on the vertical axis indicate the zero points for the abradibility relations. The vertical bars indicate the regions of stick-slip sliding. From Grosch and Schallamach (1965).

FIGURE 7

Rate of ozone crack growth vs temperature difference T-Tg for butadiene-styrene copolymers. Styrene content, per cent by weight: ◇, o; ▽, 25; △, 56; ○, 67; □, 80. From A. N. Gent and J. E. McGrath (1965).

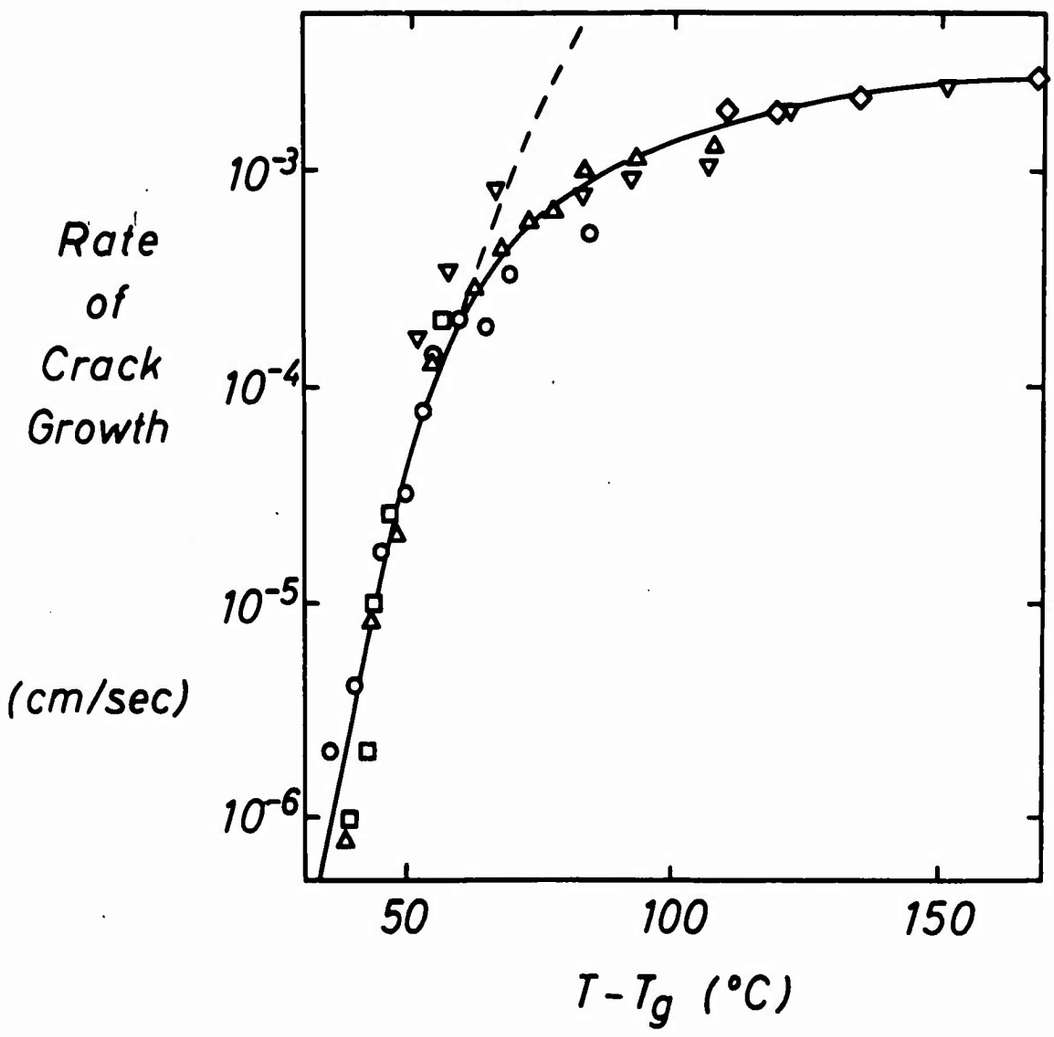

FIGURE 8

Relation between cracking stress S and Young's modulus E of the vulcanizate (Gent and Lindley, 1958).

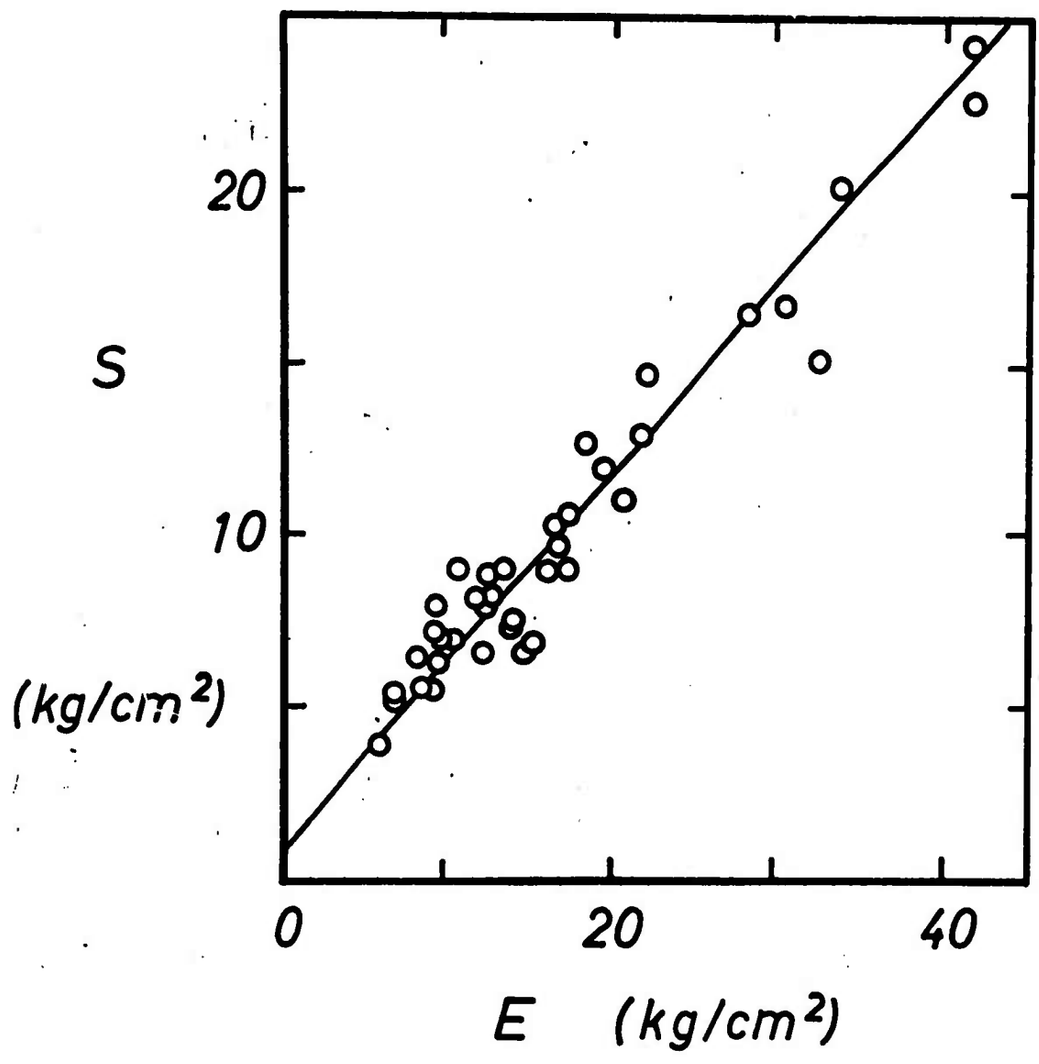

FIGURE 9

Lecture to Conference on Polymer Structure and Mechanical Properties held at U.S. Army Natick Laboratories, April 1967
Relationship between Crosslink Type and Mechanical Properties.

---

by L. Mullins
Natural Rubber Producers' Research Association

Traditionally the process of vulcanization involves the formation of a stable crosslinked network from the long polymer chains by the judicious admixture of sulphur, fatty acid, metal oxide, accelerators and the generous application of heat. This is a surprisingly complex chemical process to achieve the apparently simple purpose of the introduction of a few crosslinks. Simpler processes are known but these lead to vulcanizates with inferior properties to those obtained by conventional sulphur vulcanization. Chemical properties as evidenced--for example--by resistance to ageing are also altered markedly in passing from the base polymer to certain vulcanizates.

Now we know that if we take a rubber and vulcanize it to the same extent by different vulcanizing systems the resultant vulcanizates may have widely differing strength properties - tensile strength - fatigue strength - cut growth resistance - tear resistance - or resistance to just wearing out. (Figure 1). With natural rubber tensile strengths of in excess of 300 kg cm^{-2} are obtained for certain types of accelerated sulphur vulcanizates, falling to values of between 200 to 300 kg. cm^{-2} for other sulphur vulcanizates in which less sulphur is used, falling to less than 200 kg. cm^{-2} for peroxide vulcanizates and finally to less than 100 kg. cm^{-2} for vulcanizates produced by high energy radiation. To

complete the picture a value in excess of 700 kg. cm^{-2} is produced by vulcanizates containing pendent carboxyl groups and vulcanized with zinc soaps. With SBR - rubbers in which strain induced crystallisation is absent - values of 21.0 and 12.5 kg. cm^{-2} are obtained for accelerated sulphur and peroxide cures respectively in contrast to values of in excess of 700 kg. cm^{-2} for carboxyl type crosslinks under certain conditions of testing.

These differences in strength must stem from:-

i) differences in the actual crosslink,

ii) chemical modification of the main chain during vulcanization,

iii) changes in the effective initial molecular weight of the base polymer.

Knowledge on the contribution of these aspects has been exceedingly hard to come by and work at NRPRA is currently proceeding on a number of complimentary and interrelated fronts in an attempt to give information of how the vulcanizing system affects mechanical properties.

i) The first of these is to develop techniques to provide information about the detailed vulcanizate structure - so called chemical probes. The essential features of much of this work have been published, although the probes are continuously being refined. It is the application of these probes to determine the nature of crosslinks in vulcanized articles made from different vulcanizing systems and to trace the changing fate of these crosslinks during the life of the articles to which attention is currently directed.

ii) The second front is an attempt to make vulcanizates as comparable as possible with respect to crosslink density, base polymer, non-rubbers, etc. and to have as the only variable the known nature of the crosslink itself.

iii) The third front is an attempt to confirm the existence of mechanisms which have been invoked to account for differences in properties of vulcanizates prepared from different vulcanizing systems.

As already indicated in tracing the effect of vulcanizing systems it is necessary for us to consider a variety of crosslink types (Figure 2).

i) First direct C-C crosslinks without the intervention of sulphur or other groupings between polymer chains. These are produced by organic peroxides or high energy radiation.

ii) Secondly crosslinks produced by conventional sulphur vulcanization may be of a variety of types depending upon the exact conditions of vulcanization - the detailed amount and nature of ingredients and the temperature and period of vulcanization. Crosslink types may vary from mono-sulphides to disulphides to polysulphides.

iii) A further type of crosslink involves not co-valent bonds but ionic linkages as exemplified by the crosslinks formed by metal carboxylates.

iv) Perhaps I ought to add a fourth type - in view of development of thermolastic rubber - the domain types or crystalline type of crosslink.

On the provision of techniques to unravel the detailed nature of sulphur vulcanizates, briefly methods have been developed which enable us to quantitatively determine the actual nature of crosslink tupes in sulphur vulcanizates, it is now possible with so-called chemical probes

to count the number of monosulphide, disulphide and polysulphide crosslinks and to determine how much sulphur is used wastefully in cyclic sulphides and pendent chains.

The technique involves

i) Determination total number crosslinks

ii) Treatment with a solution propane-2-thiol (0.4M) plus piperidine (0.4M) in n.heptane. This destroys all polysulphides but leaves di and mono sulphides intact.

iii) Determination of residual number crosslinks

iv) Treatment in vacuo for 24 hrs. with a solution of n-hexane thiol (1M) in neat piperidine. This destroys all polysulphides and disulphides but leaves monosulphides intact.

v) Determination residual number crosslinks

vi) Calculation of monosulphides by difference

vii) Treatment with triphenylphosphine which converts polysulphidic crosslinks to mono or di. From knowledge of the network concentration and crosslink type and combined sulphur before and after treatment the combined sulphur present other than in crosslinks can be found.

We have now the possibility of tracing the effect of sulphur crosslink type on physical properties, and of selecting vulcanizing systems to give required crosslink types.

Vulcanizates have been prepared as similar as possible in all respects other than crosslink type.

Peroxide	(Carbon-Carbon)
CBS, 6; S, 0.4;	(Monosulphide 90%)
CBS, 1.0; S, 2.5;	(Polysulphide 70%)

Figures 3 and 4 show the progressive change in crosslink type which occurs with prolonged vulcanization. This also occurs during thermal ageing or during the service life of articles. Table 1 gives data on some mechanical properties of these vulcanizates.

We have been closely following the changes in crosslink type during a variety of service applications, in tyres, in engine mountings, in couplings, etc.

Let me illustrate the possibilities with an investigation which was carried out on truck tyres, where we were interested in tread looseness developing in service. Here using 900 x 20 (12 ply) tyre we took number consecutively from a production run as follows. Control tyres, tyres for rig testing on ribbed drum to promote tread lift tyres were removed as soon as tread lift observed, tyres for service on the driving wheels of a petrol tanker (24 ton 8 wheeler 400 m.p. day, 45 m.p.hr., 27,000 miles, surface temperature 65°C.).

The results showed that in the controls the overall concentration of crosslinks was uniform but that after the rig test the concentration was greater everywhere and greatest under the outside ribs while in the service test the concentration was similar to the control.

The results also showed that there was a progressive change in crosslink type towards monosulphidic crosslinks. Indeed in carcass of heavy treads - subject to retreading a number of times - the crosslink type

must be monosulphidic for most of the life of the tyre (Figure 5).

Now I would like to move from the more practical more empirical aspects of our work to the more theoretical more hypothetical.

It is found that the strength of rubbers increases progressively with type of crosslink in the order C-C < C-S-C < C-S-S-C < C-S-S_x-S-C < ionic. The strengths are in inverse order to their bond energies and it is tempting to ascribe differences in strength to differences in strength of the crosslinks themselves.

Crosslinks with lower bond energies contribute to higher tensile strength due to the ability of these crosslinks to relieve local stress concentrations. The mechanism involved is that due to the random nature of the cr[illegible] linked network - it is in constant thermal motion - at any instance some of the chains are subject to abnormally high stress. If the chains are securely anchored by strong crosslinks the chances are that the chains will break and neighbouring chains subject to enhanced stresses. If the points of anchorage are weak the crosslinks yield and the stress concentration released by redistribution of the load. A characteristic of multiple sulphur and ionic bonds is their readiness to participate in exchange reactions of breaking and reforming and so to provide a bond rearrangement which can continuously adjust itself and thus permit the deformed network as a whole to support a higher stress.

This hypothesis is supported by the results of an investigation into the breaking and reforming of crosslinks during stressing. Here by measuring the permanent set remaining after stressing to large extensions we get information of number of bonds reformed in deformed state

and changes in equilibrium volume swelling give fraction of crosslinks which break.

Two network theory enables a quantitative estimate to be given to fraction which break and fraction which recombine.

Found tendency to break greater in crosslinks with lower bond energy, tendency to reform also greater in crosslinks with lower bond energy. Thus the redistribution of crosslinks which occurs in conventional sulphur CBS is greater than in TMTD which in turn is greater than in peroxide vulcanizates. (Table 2).

Further support obtained by swelling in a radical acceptor di-n-butyl tetrasulphide. Breaking is found to be similar for both control and treated samples but recombination is less. This shown by reduced set and increased swelling.

In another context studying the effect of crosslink type on softening resulting from previous stretching we have examined same three types of vulcanizing system and have shown that permanent changes of the network on stressing depend on the vulcanizing system.

There is thus evidence for the breaking and redistribution of crosslinks on stressing which supports the proposed mechanism for the effect of crosslink type on strength.

This process in which redistribution of crosslinks leads to strength inevitably leads to a loss in elastic properties viz:- creep, set, stress relaxation, and hysteresis.

Another aspect of the effect of crosslink type on strength of natural rubber is shown by recent work on the change in tensile strength

with temperature.

If follow the change in tensile strength with temperature then observe a critical temperature above which the strength falls abruptly. This is due to the rubber crystallizing in bulk at lower temperatures. The critical temperature depends among other things on the type of vulcanizing system (Figure 6). It is interesting to note that rubbers with lower strength have lower critical temperatures. It has however been known for a long while that the ease with which rubbers crystallize at low temperatures depends on vulcanizing system but significantly the weaker rubbers are those which crystallize most readily.

Here again the role of crosslinks which break and reform appears important. Slippage of crosslinks in addition to permitting stress redistribution permits more perfect alignment of the chains which in turn results in more effective crystallisation which shows more permanence at high temperature.

It is interesting to compare the curves of tensile strength against temperature with the effect of the size of a small cut on tear strength. Here the abrupt full in tear strength is attributed to a change from tearing in rubber where the bulk is crystalline to tearing in rubber where rupture occurs at a strain less than that required to make the bulk crystalline.

The chemical properties of rubbers as reflected by their resistance to thermal and oxidative ageing are also markedly altered by the nature of the crosslink. Vulcanizates with C-C or monosulphide crosslinks show the expected good thermal stability while those with polysulphide cross-

links show post curing reflecting the readiness of the crosslinks to undergo sulphur bond interchange. Oxidative degradation of the former types of vulcanizates occurs primarily as a result of scission of the main chains and can be suppressed by conventional antioxidants but with the latter type conventional antioxidants act as relatively poor inhibitors.

TABLE 2

Vulcanizing System	Set %	Fraction Breaking %	Fraction Recombining %
Peroxide	1.7	6	0.6
TMTD	2.5	10	0.9
Sulphur/CBS	9.0	12	3.4
Sulphur/CBS (with radical acceptor)	-	14	1.4

Breaking and Recombination of Crosslinks on

Stressing (150 $kg.cm^{-2}$)

Crosslink Type	Poly-sulphide (a)	Mono-sulphide (b)	Carbon-Carbon (c)
Tensile Strength	300kg.cm^{-2}	250kg.cm^{-2}	220kg.cm^{-2}
Permanent Set (130kg.cm^{-2})	9.0%	2.5%	1.7%
Compression Set (24 hr. at 70°C, 25% strain)	43%	11%	12%
De Mattia Flex Life (Grade C)	113Kc.	41Kc.	25Kc.
De Mattia Cut Growth (4-8mm)	75Kc.	36Kc.	18Kc.

TABLE I

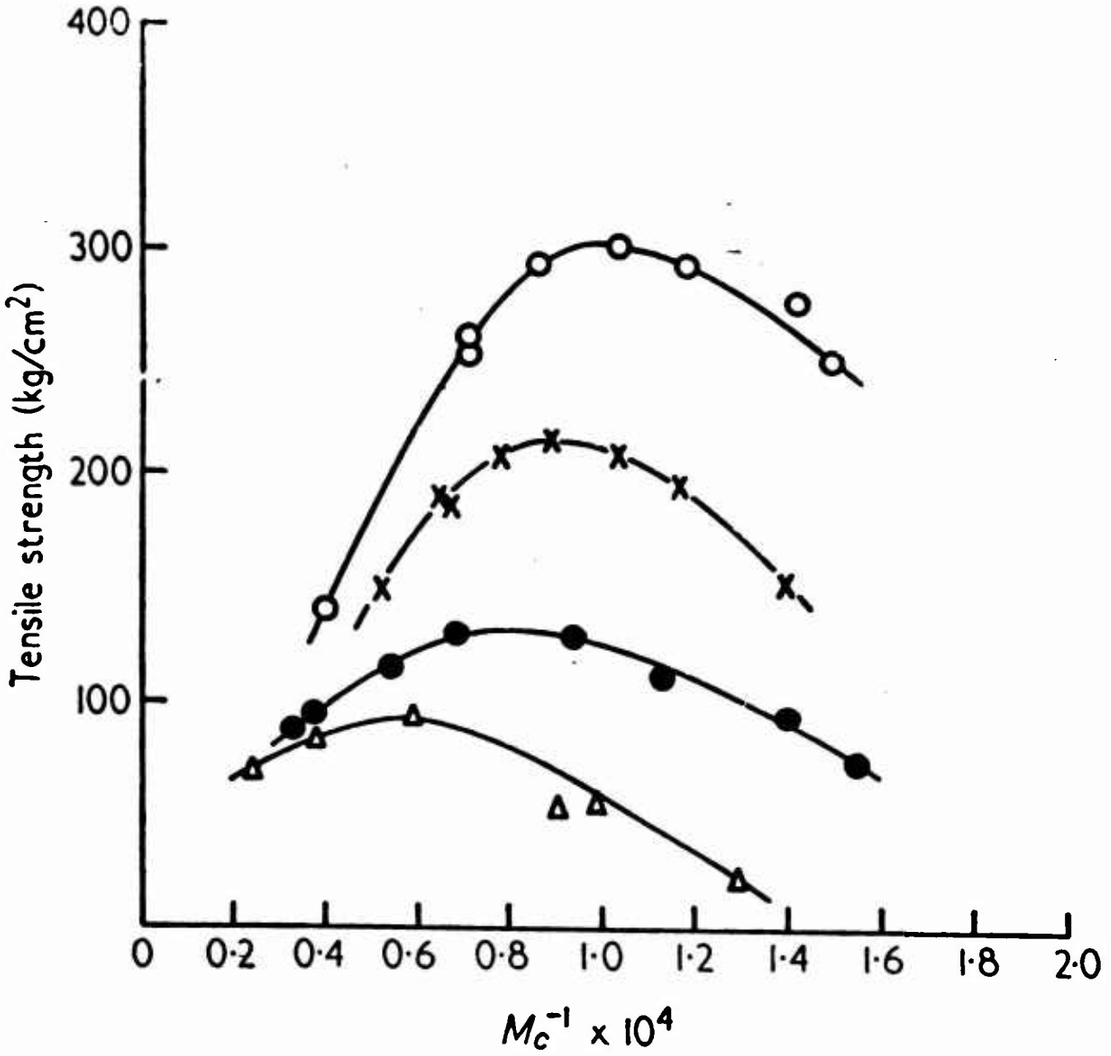

Tensile strength of pure gum natural rubber vulcanizates plotted against $1/M_c$ for various vulcanizing systems. ○ accelerated sulphur; × TMT sulphurless; ● peroxide; △ high energy radiation

Fig. 1

STRUCTURAL FEATURES OF AN ACCELERATED SULPHUR VULCANIZATE NETWORK OF NR

(X = accelerator fragment
x ⩾ 3, y ⩾ 1)

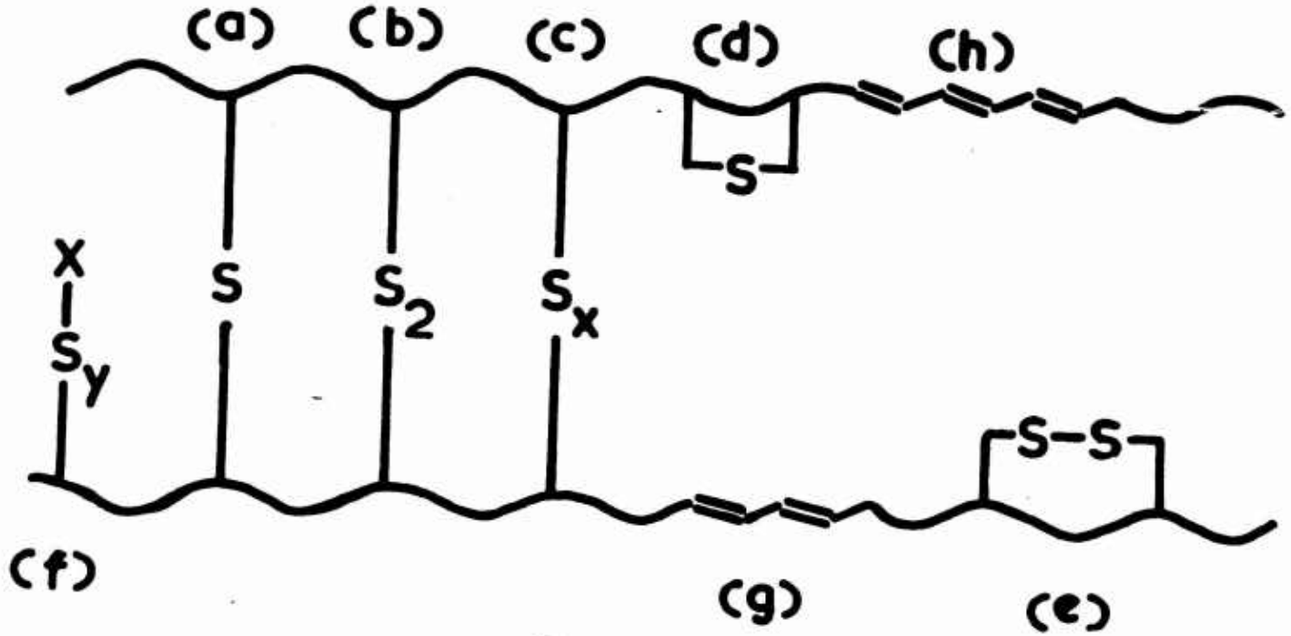

Fig. 2

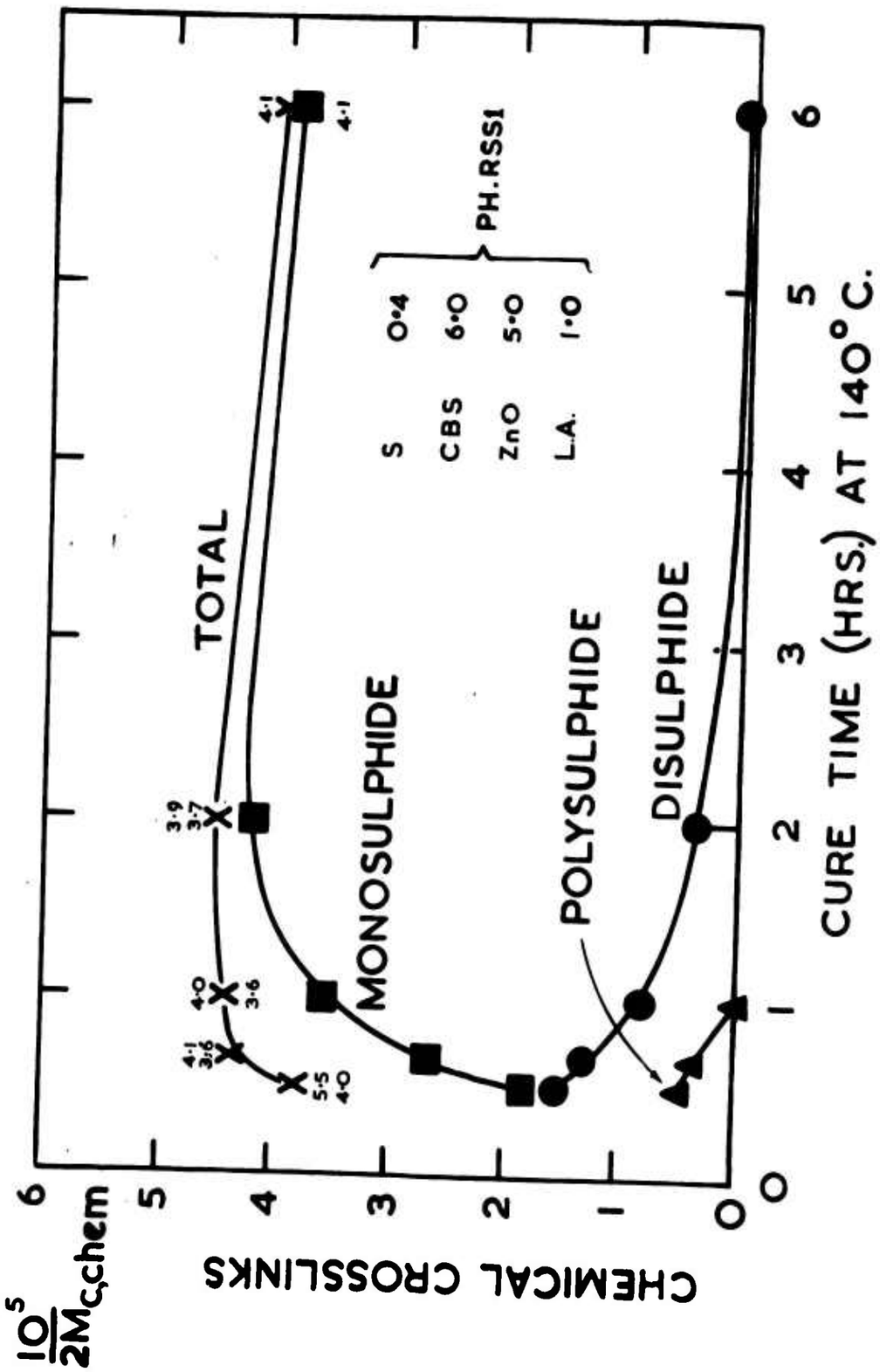
$\frac{10^5}{2M_{c,chem}}$
CHEMICAL CROSSLINKS
CURE TIME (HRS.) AT 140°C.
TOTAL
MONOSULPHIDE
POLYSULPHIDE
DISULPHIDE
PH.RSS1
S 0·4
CBS 6·0
ZnO 5·0
L.A. 1·0
3·9
3·7
4·0
3·6
4·1
3·6
5·5
4·0
4·1
4·1

Fig. 3

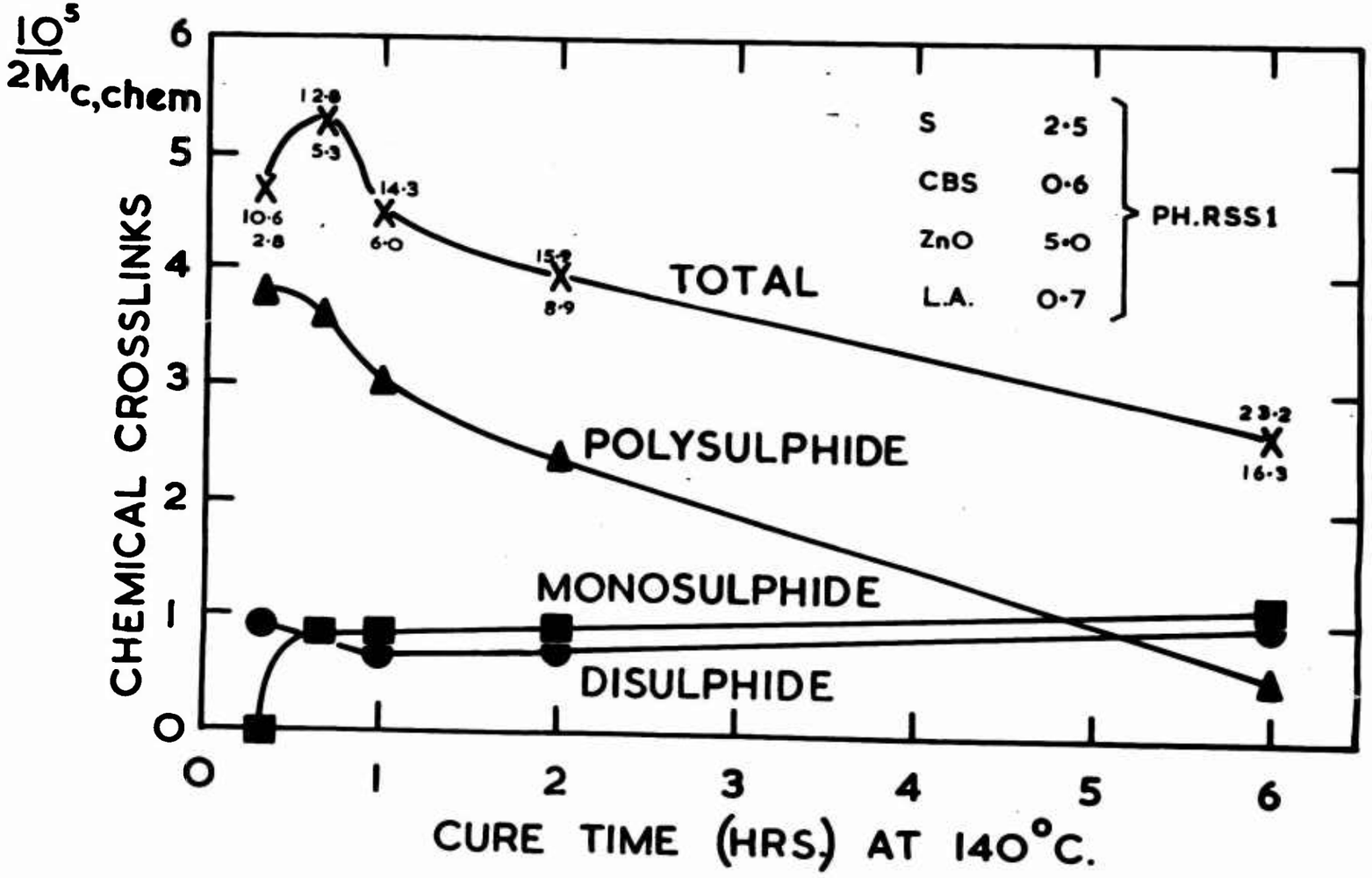
$\frac{1}{2}\frac{10^5}{M_{c,chem}}$
CHEMICAL CROSSLINKS
CURE TIME (HRS.) AT 140°C.
TOTAL
POLYSULPHIDE
MONOSULPHIDE
DISULPHIDE
S 2·5
CBS 0·6
ZnO 5·0
L.A. 0·7
PH.RSS1
10·6
2·8
12·8
5·3
14·3
6·0
15·2
8·9
23·2
16·3

Fig. 4

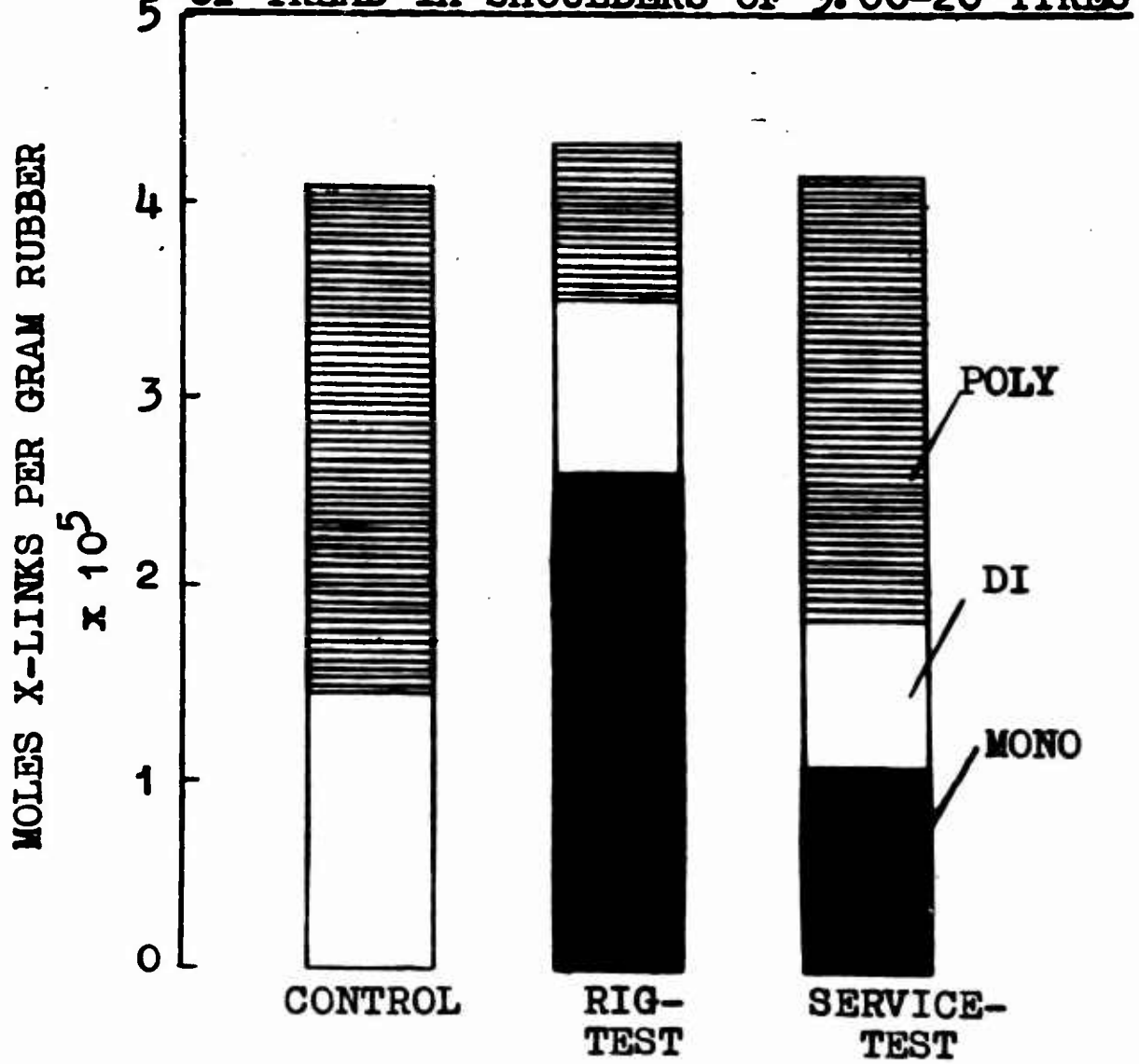
CONCENTRATIONS OF X-LINK TYPES at BASE of TREAD in SHOULDERS OF 9.00-20 TYRES
MOLES X-LINKS PER GRAM RUBBER x 10^5
5
4
3
2
1
0
POLY
DI
MONO
CONTROL
RIG-TEST
SERVICE-TEST

Fig. 5

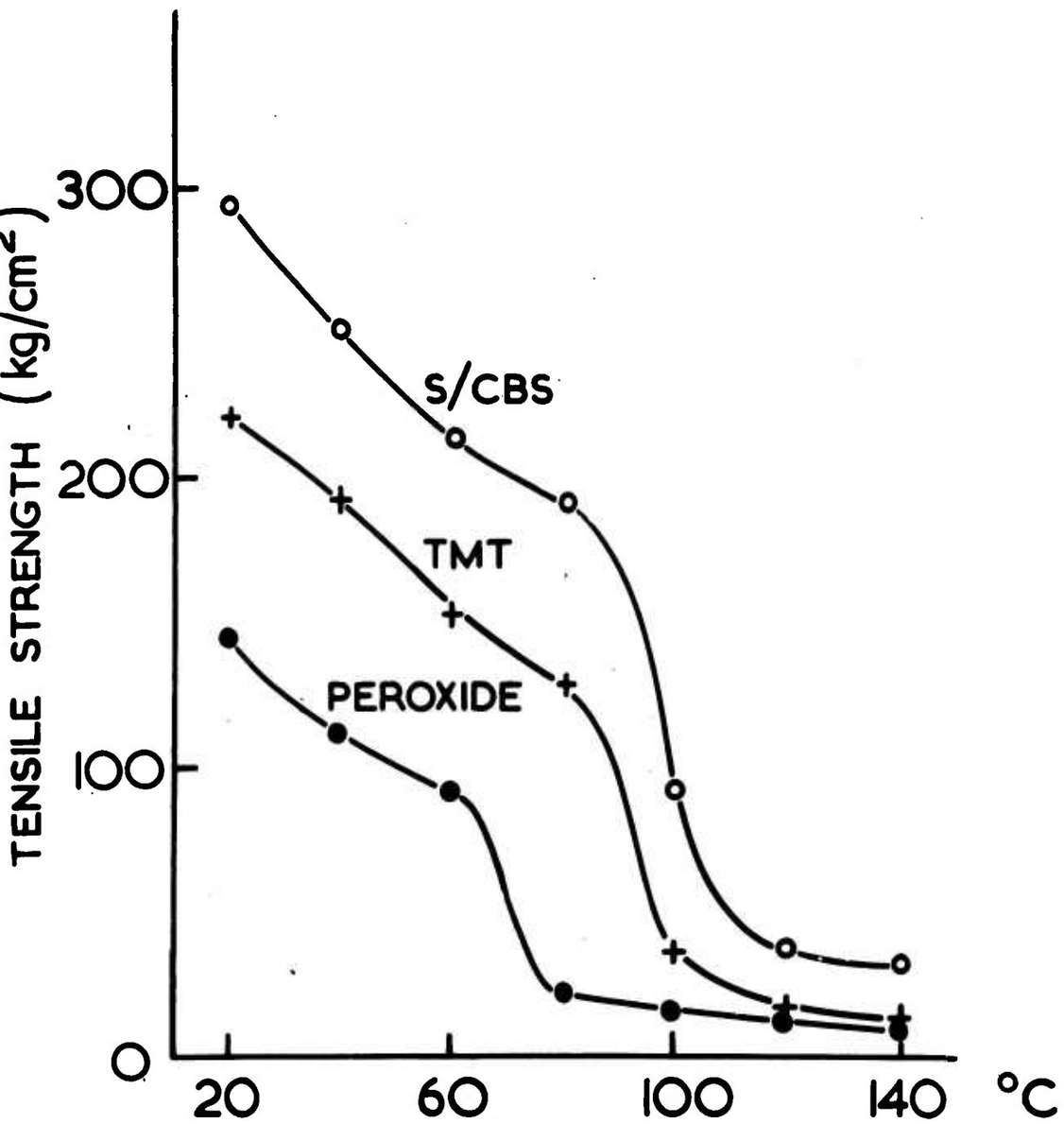
TENSILE STRENGTH (kg/cm²)
300
200
100
0
S/CBS
TMT
PEROXIDE
20
60
100
140
°C

FIG. 6

Comments after talk by Dr. Mullins

Arthur V. Tobolsky

The tensile strength of rubbers crosslinked to equivalent extents by carbon-carbon linkages, monosulfide linkages, disulfide linkages, polysulfide linkages and salt linkages are known to increase in this order. This is also the order of decreasing bond strength of these crosslinkages[1].

Several authors have concluded that the high strength values result from a breaking and remaking of the weak crosslinks during the tensile test, as reviewed in reference (1).

Tensile strength tests are carried out at room temperature in a matter of seconds. The relaxation time of polysulfide linkages at room temperature is of the order of many hours. In my opinion it remains to be fully demonstrated that an appreciable fraction of weak linkages break and remake during the time of a tensile test.

Furthermore, Lal and Scott[2] have shown that networks containing polysulfide crosslinkages can be treated with reagents which convert these linkages to stable linkages, without much loss in tensile strength.

It appears that a supplementary or alternative theory to explain the high tensile strengths of weak crosslinkage networks is desirable.

One possibility that should be considered is the following: during vulcanization by peroxides the crosslinkages are formed in an irreversible fashion, which might produce built in stresses or strains. During vulcanizations which produce polysulfide bonds the crosslinkages break and remake, thus producing a network which may be relatively free from internal stresses and strains. The difference in tensile strength might arise from a difference in the network structure, internally strained versus relaxed, according to this hypothesis.

This hypothesis is quite consistent with the results of Lal and Scott. Once the network is formed in an internally relaxed condition, the tensile strength remains high even when weak crosslinkages are replaced by strong ones.

Comments after talk by Dr. Mullins (continued) - A. V. Tobolsky

A problem remains which is not explained by the hypotheses of reference (1) or by the one suggested here. Thiokol rubbers containing polysulfide linkages along the main chain do not have high tensile strengths.

References

1. L. Bateman, L. Mullins et al "Chemistry and Physics of Rubberlike Substances", Chapter 19, MacLarend and Sons, Ltd., London 1963.

2. J. Lal and K. W. Scott, J. of Polymer Sci., C9, 113, 1965.

EQUATIONS OF STATE FOR ELASTOMERS

Turner Alfrey, Jr.

The Dow Chemical Company

INTRODUCTION:

No completely satisfactory analysis of the large-strain elastic behavior of rubbery materials has been developed.

In one sense, the problem is solved. If a unique strain-energy function exists, it must be expressible in terms of the three strain invariants:

$$W = W(I_1, I_2, I_3) \tag{1}$$

(it being assumed that the material is initially isotropic). In the case of an incompressible elastomer, the third invariant is a constant, and hence:

$$W = W(I_1, I_2) \tag{2}$$

The Mooney-Rivlin equation is an example of this type of expression, which utilizes the linear terms of a power series in I_1 and I_2:

$$W = C_1 (I_1-3) + C_2 (I_2-3) \tag{3}$$

Although the strain energy function must be expressible as a function of I_1 and I_2, there is no assurance that this will be a simple function. The utility of the Mooney-Rivlin Equation is definitely limited, and attempts to develop more elaborate versions of Equation (2) have met with only partial success.

It therefore seems worth-while to examine other, completely different, approaches to a strain-energy function for large strains.

Landel has suggested the formulation of W in terms of the principle strains, rather than the strain invariants. In particular, he has used a separable strain-energy function of the form:

$$W = f(\lambda_1) + f(\lambda_2) + f(\lambda_3) \qquad (4)$$

In this report, we shall introduce a method of representing arbitrarily large multiaxial strains in incompressible elastomers, by points on a triangular coordinate system. We then assume that the strain-energy is a smooth function of the strain, and are led to a strain-energy function of the form employed by Landel, for moderate strains.

MATHEMATICAL DEVELOPMENT:

Consider a hysteresis-free incompressible elastomer, deformed in three mutually perpendicular directions to arbitrary extension-ratios: λ_1, λ_2, and λ_3. The corresponding principle stresses are σ_1, σ_2, and σ_3. The strain energy density is W.

Because of the incompressibility condition, the state of strain is defined by any two principle extension-ratios, and hence can be represented by a point on a two-dimensional map. One method of representing multi-axial strains on a plane, which has the desirable feature of giving equal status to λ_1, λ_2, and λ_3, is described below.

A triangular grid of lines inclined at 0°, 120°, and 240° is set up. The origin is located at the center. The logarithms of the extension-ratios are plotted on the triangular coordinate system, as indicated in Figure 1. Either natural or Briggsian logarithms may be employed. We shall use the latter:

$$L_1 = \log_{10} \lambda_1$$

$$L_2 = \log_{10} \lambda_2 \qquad (5)$$

$$L_3 = \log_{10} \lambda_3$$

Figure 2 indicates the general character of the strain energy function W, when represented on such a triangular diagram. Clearly, the contour lines of constant W must exhibit trigonal symmetry, and must approach circular shape for small strains.

We wish to examine the restrictions on $W(\lambda_1, \lambda_2, \lambda_3)$ which can be deduced from the minimal assumptions of smoothness and symmetry. As a background for this, we shall briefly consider the expansion of a smooth function in terms of polar coordinates, r and θ.

POLAR COORDINATE EXPANSION OF A SMOOTH FUNCTION:

Consider a scalar function of two independent variables:

$$W = f(x,y) \qquad (6)$$

In the neighborhood of the point (x=o, y=o), the function is continuous, finite, single-valued, and "smooth" (all derivatives finite and continuous throughout the region considered). Such a function can be represented by a two-dimensional Taylor series:

$$W = A + Bx + Cy + Dx^2 + Exy + Fy^2 + Gx^3 + Hx^2y + \cdots \qquad (7)$$

where A, B, C, etc. are numerical coefficients.

Let us now represent the same scalar function W in terms of polar coordinates:

$$W = g(r, \theta) \qquad (8)$$

In the vicinity of the origin, this function can be expanded into a series of terms of the type $r^n \sin(m\theta)$. If W is a smooth function, the following restriction on the integers n and m hold:

(1) n and m are both odd or both even.
(2) $n \geq m$.

Thus, W can be written as:

$$
\begin{aligned}
W = &\left[A_0 + A_2 r^2 + A_4 r^4 + A_6 r^6 + \right] \text{---} \\
&+ \left[B_1 r + B_3 r^3 + B_5 r^5 + \text{---}\right] \sin\theta \\
&+ \left[C_1 r + C_3 r^3 + C_5 r^5 + \text{---}\right] \cos\theta \\
&+ \left[D_2 r^2 + D_4 r^4 + D_6 r^6 + \text{---}\right] \sin 2\theta \\
&+ \left[E_2 r^2 + E_4 r^4 + E_6 r^6 + \text{---}\right] \cos 2\theta \\
&+ \left[F_3 r^3 + F_5 r^5 + F_7 r^7 + \text{---}\right] \sin 3\theta \\
&+ \left[G_3 r^3 + G_5 r^5 + G_7 r^7 + \text{---}\right] \cos 3\theta \\
&+ \text{----}
\end{aligned}
$$

If the function W has some sort of <u>symmetry</u>, further restrictions can be made on the allowable terms of such an expansion. In particular,

$$
\begin{aligned}
\text{if } W(r,\theta) &= W\left(r,\theta + \tfrac{2\pi}{3}\right) = W\left(r,\theta + \tfrac{4\pi}{3}\right) \\
&= W(r,-\theta) = W\left(r,-\theta + \tfrac{2\pi}{3}\right) = W\left(r,-\theta + \tfrac{4\pi}{3}\right)
\end{aligned} \tag{10}
$$

$$
\begin{aligned}
\text{then } W = &\left[A_0 + A_2 r^2 + A_4 r^4 + A_6 r^6 + \text{---}\right] \\
&+ \left[B_3 r^3 + B_5 r^5 + B_7 r^7 + \text{--}\right] \cos 3\theta \\
&+ \left[C_6 r^6 + C_8 r^8 + C_{10} r^{10} + \text{---}\right] \cos 6\theta \\
&+ \left[D_9 r^9 + D_{11} r^{11} + \text{---}\right] \cos 9\theta \\
&+ \text{---}
\end{aligned} \tag{11}
$$

Rearranging this series in order of increasing powers of r, we obtain:

$$W = A_0 + A_2 r^2 + B_3 r^3 \cos 3\theta + A_4 r^4 + B_5 r^5 \cos 3\theta + \\ + (A_6 + C_6 \cos 6\theta) r^6 + B_7 r^7 \cos 3\theta + \text{---} \qquad (12)$$

Restrictions on W (L_1, L_2, L_3).

Returning to the triangular diagram of multiaxial strain (L_1, L_2, L_3), and the strain-energy function W, let us establish a polar coordinate system (r, θ) as indicated in Figure 3. Any state of multiaxial strain (λ_1, λ_2, λ_3) can be expressed in terms of r and θ:

$$\begin{aligned} L_3 &= r \cos \theta \\ L_2 &= r \cos \left(\theta - \tfrac{2\pi}{3}\right) \\ L_1 &= r \cos \left(\theta + \tfrac{2\pi}{3}\right) \end{aligned} \qquad (13)$$

Or, if we express r and θ in terms of L_1, L_2, L_3:

$$r = \sqrt{L_3^2 + \tfrac{1}{3} L_2^2 - \tfrac{2}{3} L_1 L_2 + \tfrac{1}{3} L_1^2} = \left(\tfrac{\sqrt{6}}{3}\right) \cdot \sqrt{L_1^2 + L_2^2 + L_3^2} \qquad (14)$$

$$\theta = \cos^{-1} \left\{ \frac{L_3}{\sqrt{L_3^2 + \tfrac{1}{3} L_2^2 - \tfrac{2}{3} L_1 L_2 + \tfrac{1}{3} L_1^2}} \right\} \qquad (15)$$

Now, let us examine the consequences of making the minimal assumption that W (L_1, L_2, L_3) must exhibit the qualities of smoothness and symmetry discussed in the preceding section. Setting W=0 for the unstrained state, we obtain:

$$W = A_2 r^2 + B_3 r^3 \cos 3\theta + A_4 r^4 + B_5 r^5 \cos 3\theta + (A_6 + C_6 \cos 6\theta) r^6 + B_7 r^7 \cos 3\theta + A_8 r^8 + C_8 r^8 \cos 6\theta + (B_9 \cos 3\theta + D_9 \cos 9\theta) r^9 + A_{10} r^{10} + C_{10} r^{10} \cos 6\theta + \cdots \quad (16)$$

Let us examine these terms individually, starting with the first:

$$A_2 r^2 = A_2 \cdot \left(\frac{3}{2}\right) \cdot (L_1^2 + L_2^2 + L_3^2) \quad (17)$$

$$B_3 r^3 \cos 3\theta = B_3 r^3 \left[4 \cos 3\theta - 3 \cos \theta\right] = B_3 (L_1^3 + L_2^3 + L_3^3) \quad (18)$$

$$A_4 r^4 = A_4 \cdot \left(\frac{4}{9}\right) \cdot (L_1^2 + L_2^2 + L_3^2)^2 = A_4 \cdot \left(\frac{8}{9}\right) \cdot (L_1^4 + L_2^4 + L_3^4) \quad (19)$$

$$B_5 r^5 \cos (3\theta) = B_5 r^5 \left[4 \cos 3\theta - 3 \cos \theta\right] = B_5 \cdot K (L_1^5 + L_2^5 + L_3^5) \quad (20)$$

Each of the above terms, and hence the entire $W (L_1, L_2, L_3)$ -- through the 5th power term -- is separable, with no cross terms.

$$W = f (L_1) + f (L_2) + f (L_3) \quad (21)$$

This of course implies:

$$W = g(\lambda_1) + g(\lambda_2) + g(\lambda_3) \quad (22)$$

which is precisely Landel's assumption.

On the other hand, this simple separability does not continue indefinitely. The reader can easily verify that the term $A_8 r^8$, for example, does <u>not</u> reduce to $K (L_1^8 + L_2^8 + L_3^8)$.

We are thus led to the conclusion that Landel's equation of state for rubber is not exactly correct for strains of all magnitudes, but that up through the 5th power terms of a power series expansion the Landel separation is rigorously correct. Landel's equation should fit well over a considerably wider range than the Mooney-Rivlin Equation, but should fail at extremely large strains (approaching the ultimate extension).

Figure 1.

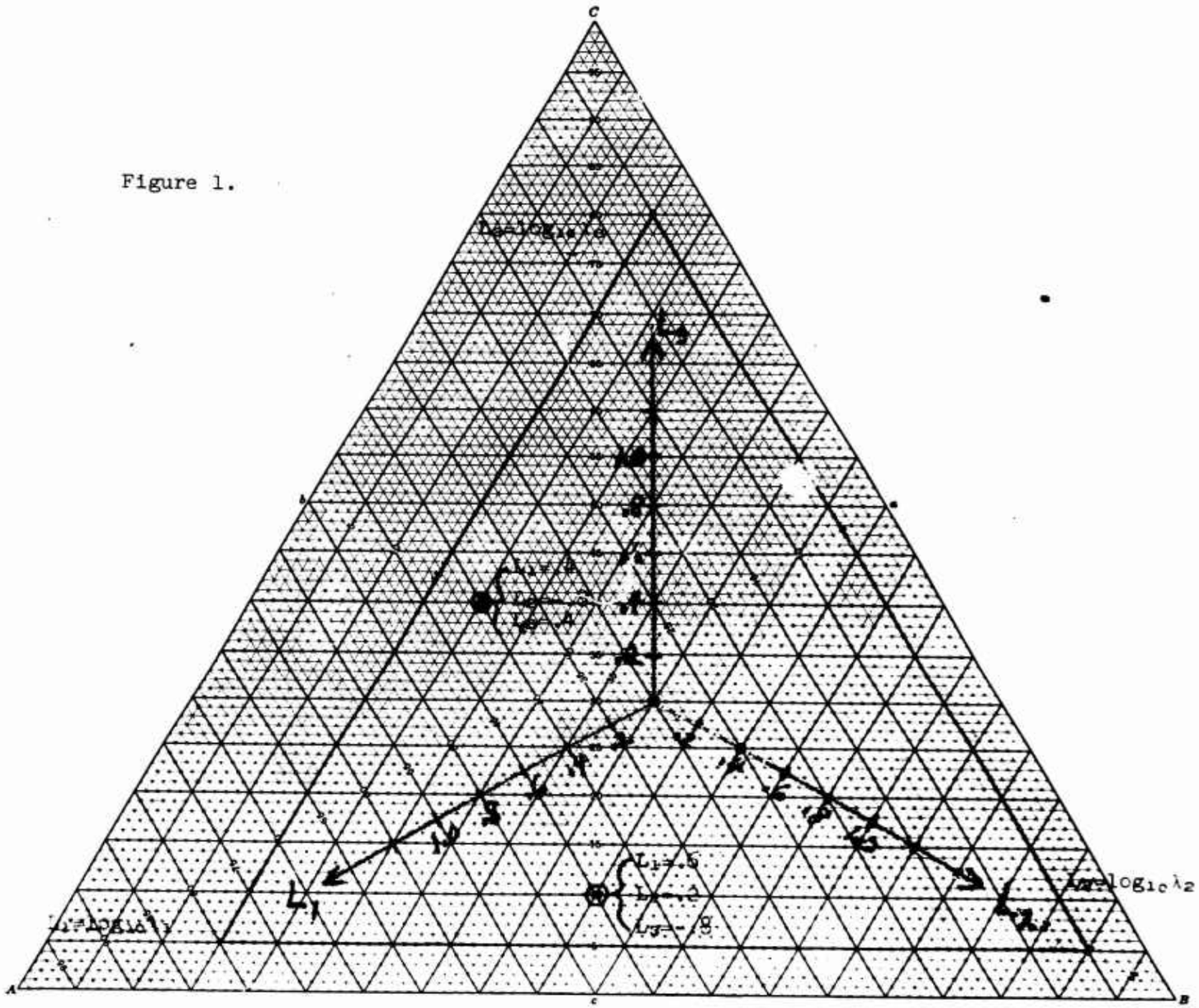
C
A
B
$L_3=\log_{10}\lambda_3$
$L_2=\log_{10}\lambda_2$
$L_1=\log_{10}\lambda_1$
$L_1=b$
$L_2=a$
$L_3=g$

Figure 2.
Strain-energy
Contour Lines

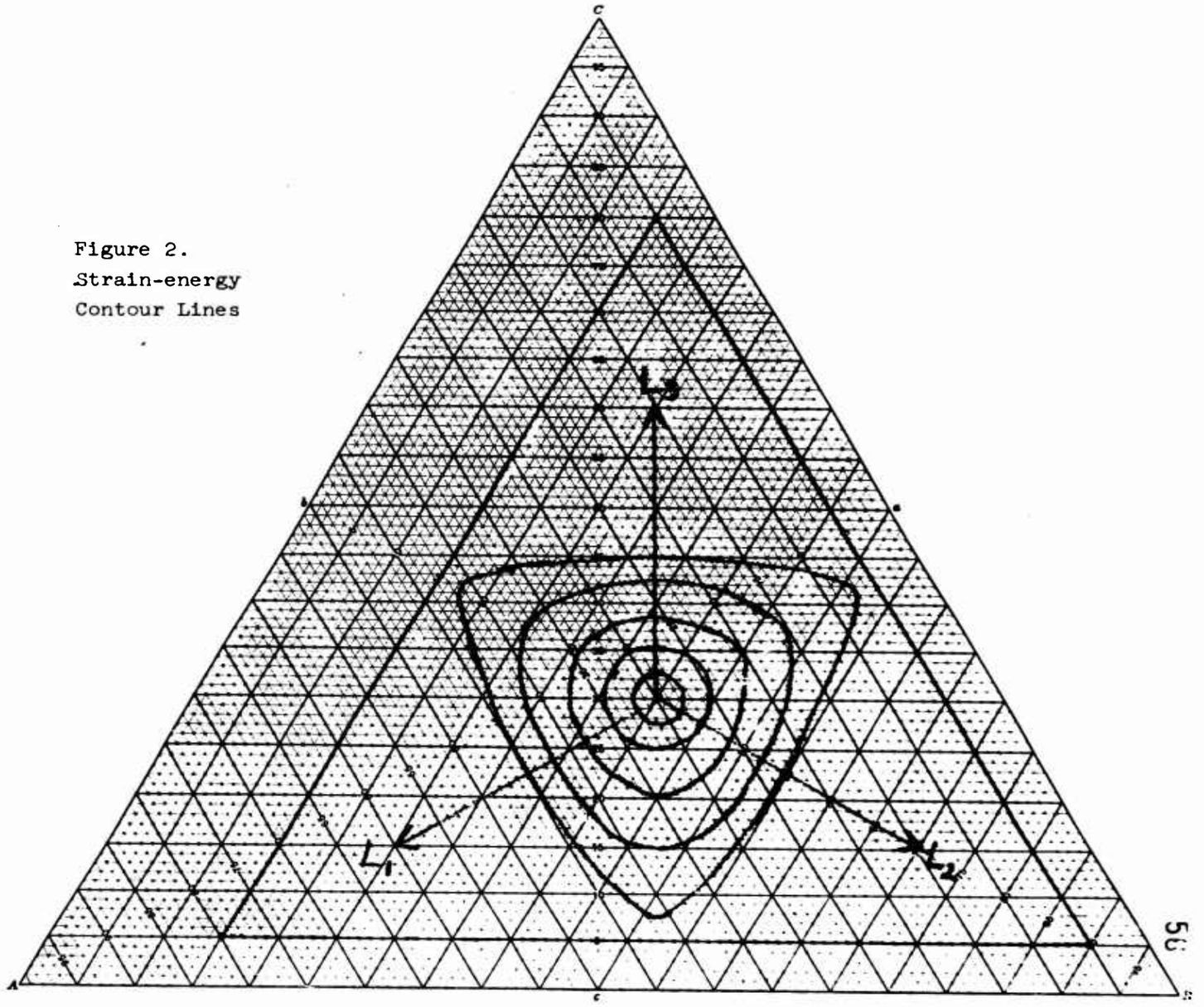

Figure 3
Polar Coordinates
on Triangular Diagram

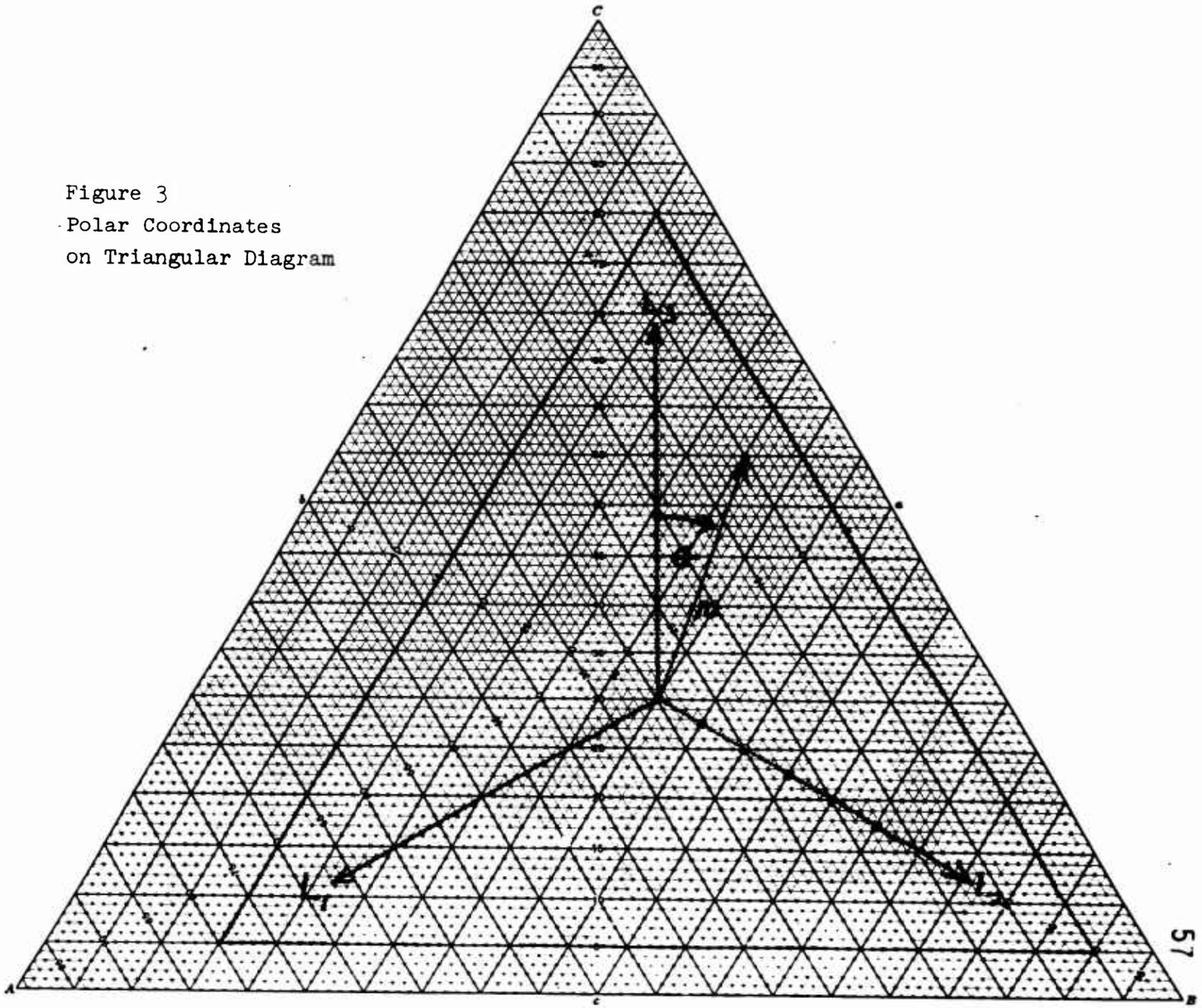

PART II. VERY LARGE STRAINS

INTRODUCTION:

This section deals with the equation of state for elastic materials, for arbitrarily large strains and for arbitrary multiaxial character of the stress and strain. The material will be assumed to be incompressible, and to exhibit equilibrium elastic response (no hysteresis), relatable to a unique scalar strain-energy-density W which depends upon the strain state. Our problem is thus the construction of a suitable strain-energy function, $W(\lambda_1, \lambda_2, \lambda_3)$ to represent the elastic behavior over the entire range from zero strain to failure, for simple tension, shear, biaxial tension, or any intermediate type of multiaxial stress.

MATHEMATICAL FORMULATION OF A STRAIN-ENERGY FUNCTION:

The considerations developed earlier lead us to consider a strain-energy function of the form:

$$W_I = \frac{A_2 r^2 + B_3 r^3 \cos 3\theta + A_4 r^4 + B_5 r^5 \cos(3\theta) + \cdots}{\left(1 - \frac{r}{r^*}\right)} \qquad (1)$$

where r*, the "ultimate limit" of deformation, is some trigonally symmetric function of θ.

However, if we merely write

$$r^* = M + N \cos 3\theta + P \cos 6\theta + \cdots \qquad (2)$$

we will obtain a function which has lost the quality of smoothness in the region $(r \to \infty)$.

We are therefore led to search for some modification of Equation (1) which goes to infinity at some boundary $r^*(\theta)$, but retains smoothness at the origin. The ratio of two smooth functions should be smooth, so let us consider the function:

$$W_{II} = \frac{A_2r^2 + B_3r^3 \cos 3\theta + A_4r^4 + B_5r^5 \cos 3\theta + ---}{1 - (Mr^2 + N\, r^3 \cos 3\theta + Pr^4 + ----)} \qquad (3)$$

If we expand W_{II} as a power series in r, we obtain:

$$W_{II} = A_2r^2+B_3r^3 \cos 3\theta + (A_4+MA_2)r^4 + (B_5+MB_3+NA_2)r^5 \cos 3\theta + ---(4)$$

As anticipated, all terms which appear meet the requirements for smoothness at the origin, and trigonal symmetry.

It is my contention that the function W_{II} (r, θ) should provide a better approximation to the multiaxial stress-strain behavior over the entire range, with a smaller number of adjustable parameters used, than any previously suggested specific equation (e.g., expansion in terms of strain invariants, or Landel's expression in terms of the principle strains). The expression reduces to linear elasticity as $r \to o$; it reduces to Landel's equation for moderate strains; and it captures the rapid upturn in stress as the limit of extension is approached.

The importance of including the denominator in W_{II} (r, θ) is that it permits good fitting in the very large strain region with a minimal total number of adjustable parameters. The numerator expression alone can be made to fit any possible strain-energy function over the entire range, but it would converge very slowly near the limit of extension, and thus require very many terms. This advantage of W_{II} (r, θ) is only realized if we cut off the series as polynomials. Let us therefore propose three specific polynomial versions of this function, one having three arbitrary constants, one having four, and one having five:

$$W_{III}(r,\theta) = \frac{A_2r^2}{1 - (Mr^2 + Nr^3 \cos 3\theta)} \qquad (5)$$

$$W_{IV}(r, \theta) = \frac{A_2 r^2 + B_3 r^3 \cos 3\theta}{1 - (Mr^2 + Nr^3 \cos 3\theta)} \qquad (\cdot)$$

$$W_V(r, \theta) = \frac{A_2 r^2 + B_3 r^3 \cos 3\theta + A_4 r^4}{1 - (Mr^2 + Nr^3 \cos 3\theta)}$$

W_{III} (r, θ) can hardly be expected to fit very well over the entire range, but it illustrates how the parameters can be obtained from experimental data. The constant A_2 is obtained from the limiting shear modulus, G, which hold for infinitesimal strain, and which can be established by standard extrapolation of stress-strain data to zero strain. The constants M and N can be obtained from the limiting extension for uniaxial stretching and for uniaxial compression (or biaxial stretching). These limiting strains must be determined by extrapolation of some kind. It is suggested that the reciprocal of stress be plotted against λ, and extrapolated to zero. Examination of typical stress-strain data in the vicinity of failure leads to the conclusion that a linear extrapolation is probably not very good. Of course, a fit can be forced at the high end of the actual data, but the logic of this approach would favor the use of a well-chosen extrapolation to the (un-reachable) ultimate extension. The question of proper extrapolation method will be further examined in a later report.

As we turn to the more elaborate approximations, W_{IV} (r,θ) and W_V(r,θ), we can continue to use the values of A_2, M, and N which were used in W_{III}(r,θ), since these were obtained from extrapolations to zero and r*. The value of B_3 in W_{IV} (r,θ), and the values of B_3 and A_4 in W_V (r,θ) can now be obtained from the deviations of experimental data from the limiting linear elasticity curve, in the low strain region; or, alternatively, by forcing a fit at chosen points in the intermediate strain region. Still another possibility would be to evaluate B_3 by forcing a fit to the slope of the reciprocal of the stress as r → r* in tension.

T. Alfrey, Jr/crg/10-17-67

PLASTIC YIELD BEHAVIOR OF GLASSY POLYMERS

R. D. Andrews

Department of Chemistry and Chemical Engineering
Stevens Institute of Technology
Hoboken, New Jersey

INTRODUCTION

The plastic yield behavior of glassy polymers is a subject which is becoming of increasing importance at the present time. One reason for this is the desire to understand the stress response of solid polymers in the region of very high stresses. A considerable amount of work has been devoted in the last 20 years to the study of the stress response of polymers at low stresses, and in particular their behavior in the linear viscoelastic region. However, the response of polymers under processing conditions and in many practical use situations involves very high stresses and mechanical behavior which is very non-linear. Plastic yield can be regarded as an extreme form of non-linear behavior, and an understanding of the plastic yield process in combination with an understanding of linear viscoelastic behavior may be the best path to the formulation of a satisfactory theory of non-linear viscoelastic behavior.

The phenomenon of plastic yield has received particular study in the synthetic textile industry, since it is an important part of the fabrication process of synthetic textile fibers. Drawing is required to give such synthetic fibers their maximum strength. This increase of strength comes from a combination of molecular orientation and an improved perfection of morphological order. However, one of the striking characteristics of the drawing or plastic yield behavior of amorphous glassy polymers is the great similarity which is shown to the corresponding drawing behavior of crystalline polymers, despite the great difference in solid state structure. It therefore seemed to us most useful to study the nature of the yield process in glassy polymers, since the changes of crystalline morphology which are produced when a crystalline polymer is drawn, which can be seen clearly from the changes in the X-ray pattern, are not present as a complicating factor in this case.

Our own research work in this area was carried out over a period of about four years, starting in the Fibers and Polymers Division at MIT and continuing during a further contract at Stevens Institute of Technology. This work was sponsored by

the U. S. Army Natick Laboratories, and we are very grateful to them for this continued financial support. The results presented here represent the cooperative work of a number of individuals whose contributions will be more properly credited in future journal publications. Many of the unpublished results have been presented in a preliminary form in a final project report[1].

The phenomenon of plastic yield is a very familiar one in the metals field, and it is a very important component of certain metal forming processes. There is considerable interest at the moment in the possibilities of forming plastics also by such a yield or "cold forming" process. The feasibility of this type of forming process is not yet completely clear. The yield process could also be an important mechanism for energy absorption under impact conditions--perhaps even at ballistic rates.

In addition to such practical applications, the yield phenomenon is of course of great fundamental scientific importance, and a thorough understanding of its nature is highly desirable. Since it is such a fundamental phenomenon, it is of interest from very many different points of view, and many different aspects of it are important to understand. Consequently it is unreasonable to expect that any complete theory of the plastic yield phenomenon can be stated in a few words, since it would be hoped that such a theory would provide the answer to very many different questions. One of the interesting questions in this area, for example, is why the yield phenomenon in polymers is so often accompanied by neck formation in the sample. Despite the fact that this was one of the earliest observations made in connection with the drawing process, the mechanics of the necking phenomenon are still not adequately understood.

STRESS-STRAIN TESTS

Many glassy polymers, such as polystyrene, are regarded as brittle materials. This means that they fracture at small strains in a stress-strain test, without showing any plastic yield. Other glassy polymers, such as polymethyl methacrylate will show plastic yield and drawing behavior in a tensile test in certain ranges of temperature and strain rate. Stress-strain curves of these two types are shown in Fig. 1. When polymers are subjected to high stress, there is a competition between yield and fracture. A general statement can probably be made that all solid polymers will show plastic yield when stressed to a high enough level, provided that fracture does

not first intervene.

It was found very early in our investigations that it was possible to make polystyrene yield in a tensile test, even though it usually fractures in a brittle way. This can be done by first preorienting the material by hot stretching above the glass transition temperature. After this treatment, the stress-strain curve shows yielding behavior, very similar to that of PMMA, at temperatures below the glass transition[1,2]. However, the yield stress does not seem to depend on the degree of molecular orientation (as measured by the birefringence of the oriented sample), indicating that the orientation does not affect the nature of the yield process itself, but rather is effective in raising the fracture strength of the material. This is illustrated in Fig. 2, which plots the yield stress as a function of preorientation birefringence (used as an index of "degree of orientation") for a series of temperatures below the glass transition. The amount of strain obtained in the yield process decreases markedly with increasing preorientation, however, as illustrated in Fig. 3.

From the data in Fig. 2, it can be seen that the yield stress for polystyrene decreases linearly with increasing temperature, as indicated in Fig. 4. This straight line extrapolates to zero stress near the glass transition temperature of the polymer. The fracture strength of a polymer shows much less dependence on temperature, as sketched also in Fig. 4. The crossing of these two curves shows why a polymer may be ductile at higher temperatures and brittle at lower temperatures, in the glassy state. This interpretation of the brittle-ductile transition has also been discussed by Vincent.

The time dependence of drawing under constant strain rate conditions has been investigated[1,3] for unoriented PMMA and the results are shown in Fig. 5, in which yield stress is plotted vs. temperature. At each strain rate a linear relation between yield stress and temperature is obtained, as in the case of polystyrene. The magnitude of the yield stress increases with increasing strain rate and the slope of the straight line vs. temperature also increases. These curves extrapolate to zero stress at temperatures which are not quite identical, but which are again near the glass transition temperature of the polymer.

Other molecular and structural parameters which are of interest in the case of amorphous glassy polymers are the molecular weight of the polymer and the possible presence of cross links in the structure. The effects of molecular weight and cross linking on the yield process have also been

investigated[1,3] for PMMA with results as shown in Fig. 6. The straight line relation between yield stress and temperature persists in all cases. Polymers showing a six-fold variation in molecular weight (200,000 to 1,200,000) show essentially the same yield stress, indicating that the yield stress is not dependent on molecular weight. The crosslinked polymer also shows very little difference in behavior from that of the polymer which is not crosslinked.

The yield phenomenon is often referred to as "solid-state flow". The above results suggest that the yield phenomenon cannot be regarded as a flow process in the normal sense, since viscoelastic flow of a polymer (i.e., the viscosity of a polymer melt) is known to depend on the 3.4 power of molecular weight, and no such relation is seen here. Crosslinking also effectively prevents any long range molecular flow but obviously produces very little effect on the yield phenomenon. These results thus provide some very relevant data in any discussion of the yield or drawing phenomenon in terms of a flow theory. This of course does not rule out the use of some modified form of a liquid flow theory if attention is focused only on a very localized relative motion of molecules rather than true flow in the usual sense. It is also observed that the deformation produced when a polymer is drawn can be completely recovered if the sample is heated above its glass transition temperature. This total shrinkage illustrates again the fact that no genuine intermolecular flow has occurred.

DRAWING UNDER DEAD LOAD

Although the yield process has customarily been studied by the use of stress-strain tests at constant strain rate, it can also be observed in creep experiments carried out under constant load. This latter type of experiment has certain advantages; in particular, the time effects associated with the yielding process are seen in a magnified way. A detailed investigation of the drawing behavior of preoriented polystyrene has been carried out[4] using this technique. The drawing phenomenon is observed in an interesting way in these experiments: After a period of apparently normal viscoelastic creep, neck formation takes place fairly abruptly, followed by the usual type of neck propagation. Fracture may also take place at various stages of this process. The time elapsed between the beginning of the creep experiment (when the load is applied to the sample) and the time when neck formation takes place has been designated as the "delay time" for yielding (t_d). Since the neck formation is not completely instantaneous,

an arbitrary method has been used for defining the delay time as illustrated in Fig. 7. The straight line regions of the creep curve before neck formation and during neck propagation are extrapolated by dashed lines and the intersection point of these dashed lines is taken as the delay time.

Creep measurements of this type were made as a function of temperature and stress level. One of the major results of this investigation was that drawing was found to take place only in a limited region of stress and temperature. That is, at each temperature in the glassy state, there existed a critical stress level above which yield and drawing by neck formation would take place, but below which yielding would never take place--presumably even at infinite time. The critical drawing stress divides the stress-temperature plane into two regions as shown in Fig. 8. This critical stress boundary curve extrapolates to zero stress near the glass transition temperature, but seems not to be exactly a straight line. Above the critical stress level the delay time is a function of the applied stress and decreases with increasing stress level. The type of relationship obtained is shown in Fig. 9: the logarithm of delay time is a linear function of stress level. The delay time also decreases progressively with increasing temperature, as would be expected of any temperature-dependent rate process. The straight lines in Fig. 9 end abruptly at the critical stress level--a very interesting and unusual sort of relation.

Similar measurements have been made on unoriented PMMA, with very similar results[5]. A critical stress boundary as a function of temperature was also observed for this polymer. Effects of quenching and annealing, and of absorbed moisture were also investigated for PMMA. The effect of rapid quenching of the polymer from above the glass transition temperature was to decrease the delay time and increase the diffuseness of the neck which formed. Annealing at elevated temperature had the opposite effect of increasing the delay time. Absorbed moisture decreased the delay time in a very striking way, indicating a very large effect of plasticizer on the yield process.

TIME EFFECTS

Another very useful way of studying the time effects associated with the yield and drawing process is by means of interrupted drawing experiments. This type of experiment was first carried out by Vincent[6] and we have followed out his method somewhat further. In this experiment a normal stress-strain curve is carried out up to the point where neck forma-

tion takes place and steady-state neck propagation has begun. At that point, the experiment is interrupted by suddenly stopping the strain. The interruption may be produced in two ways. The first is by holding the strain constant and allowing the stress to relax for a period of time, and then resuming the drawing experiment by resuming the constant strain rate. The other method of interruption is to reverse the elongation of the specimen until the load is completely removed, and then to allow a time of resting in that state before the forward elongation of the sample is begun again. The results obtained in these two cases are significantly different. After a period of stress relaxation at fixed strain, when the straining is resumed a new stress peak or yield peak is observed, after which steady state drawing is resumed. This peak is observed even though neck formation has already taken place in the first phase of the experiment. In the experiment in which the sample is unloaded, when the extension of the sample is resumed no new yield peak is observed; the stress level simply rises to the original steady-state drawing stress and remains constant at that value. The initial slope of the reloading curve, which corresponds to something like an elastic modulus, is also lower after the interruption by unloading. These results are illustrated schematically in Fig. 10.

The simplest interpretation of these results is that a "hardening" of the sample takes place during the interruption by stress relaxation, whereas a "softening" of the sample takes place when the drawing is interrupted by unloading. The reason for these effects is not completely clear, but they indicate that hardening and softening of the material may be playing a significant role in the yield process.

In our experiments, the effect of the length of the interruption period was examined and it was found that the yield peak gradually builds up as a function of time in the interruption by stress relaxation. The apparent softening during the interruption by unloading also disappears gradually with time and the material regains its normal rigidity when the sample is allowed to remain unloaded for a prolonged time. Effects of this sort are known also in metals and other crystalline materials, where the behavior is believed to be related to dislocation multiplication and decay. Some hypotheses could be formulated on the possible role of some type of solid state defect or the possible breakdown of intermolecular secondary bonding as the corresponding phenomena in the case of glassy amorphous polymers, but this line of speculation will not be pursued here.

GEOMETRY OF YIELD

In addition to the well-recognized phenomenon of neck formation in the case of yield of polymers, some other types of localization of the yielding process are also observed. In particular, what may be referred to as "deformation bands" have been observed in polystyrene and many other polymers[7,8]. The bands observed in polystyrene are extremely thin sheets (a few microns thick) which form at an angle approximately 45° to the direction of stress in a sample subjected to tension or compression. Electron microscope studies have indicated that the material in these bands has undergone a shear strain of approximately unity and the molecular orientation which results gives the bands a strong birefringence. In samples undergoing dead load creep, these bands have been observed to form prior to neck formation but seem to lead directly to the formation of the macroscopic neck. When neck formation and propagation have taken place these bands have been absorbed and disappear. How essential a role these deformation bands play in the formation of the macroscopic neck has not yet been demonstrated, but this is a phenomenon which must be kept in mind in any consideration of the detailed geometry of the yield process.

Photographic studies of the shape of the neck[9] have indicated a complicated dependence of neck sharpness on strain rate and temperature, since neck sharpness seems to go through a maximum when each parameter is varied--at least in the case of PMMA. Such photographic studies of neck profile geometry also allow the derivation of a true stress-strain curve for a polymer as a material, independent of the complications in stress distribution produced by neck formation when the apparent stress-strain curve of an overall specimen is measured.

In addition to the localization of the yield process in a geometric sense, another interesting aspect of the process is the volume effects associated with it. Some preliminary measurements of volume changes associated with yield in compression have been carried out by the use of a mercury dilatometer combined with a conventional testing machine[10]. The results for several polymers indicate that a significant volume increase accompanies the yield process. This volume increase decays when drawing or yield is interrupted by stress relaxation and reappears when drawing is resumed and the new yield peak is produced. This leads to the formulation of a yield criterion in which the critical factor is not simply a certain value of shear stress, but also involves a significant volumetric component in the yield condition[10].

DISCUSSION

One of the basic problems associated with the yield behavior in solid polymers has been to explain how strains of the order of hundreds of percent could be produced in a polymer below its glass transition temperature, where it is generally believed that chain segment motion and long range changes of molecular conformation are impossible because of the rigidity of the glassy structure. It seems necessary to assume that the material is actually going through a glass transition as part of the yield process. One of the first theories of the yield process, proposed by F.H. Müller in Germany several years ago, was that neck formation led to localized heating which raised the polymer above its glass transition temperature. This hypothesis was proved to be incorrect by very slow drawing experiments carried out by Vincent[6], and also by more detailed calorimetric measurements carried out by Müller himself. It seems more reasonable to assume that the glass transition effect can be produced by stress itself or more exactly by a combination of stress and temperature. The yield phenomenon might therefore be reasonably described as a "stress-induced glass transition". Examination of the literature shows that this idea was also proposed earlier by Bryant[11]. This type of theory would provide a logical explanation of the yield stress decreasing linearly with increasing temperature and extrapolating to zero at the (thermal) glass transition of the polymer. However, the magnitude of the strains obtained in the yield process and also the recoverability of the strain on heating above the glass transition temperature suggest that this is only a marginal or partial glass transition, giving a partially softened structure equivalent to that obtained thermally at temperatures at the lower limit of the glass transition range.

Some recent experiments[12] on the drawing of PVC under dead load creep conditions provide some further insight into the equivalent effects of stress and temperature in producing the glass transition. Creep experiments were carried out at a series of stresses at a constant temperature, and at a series of temperatures at a constant stress level. The results, plotted as log compliance vs. log time, are shown in Figs. 11 and 12. The pattern of the family of curves obtained seems essentially identical in both cases. The rapid-rise region of the creep curve can be taken as an indication of the drawing process. At a series of temperatures in the glassy state the stress was adjusted so that the inflection point of the creep curve was always at a time value of ten minutes. With the time parameter standardized in this way, a plot of corresponding values of stress vs. temperature gave the usual straight

line relation, extrapolating to zero at the glass transition temperature. The conclusion can therefore be drawn from these results that the glass transition is in fact not simply a temperature but can better be regarded as a phenomenon which is a function of stress, temperature and time. This opens up interesting new avenues to the exploration of the yield and glass transition phenomena since temperature is a homogeneous and isotropic property, whereas stress can be applied in a directional way and in various multiaxial forms. The relation between temperature and stress in producing yield under these conditions would be of great interest to explore.

References

1. R. D. Andrews, S. W. Allison, D.H. Ender, R. M. Kimmel and W. Whitney, "Research Study on Cold Drawing Phenomena in High Polymers", Technical Report 67-10-CM, Clothing and Organic Materials Div., U. S. Army Natick Laboratories (August, 1966).

2. S. L. Cooper, W. Whitney, N. S. Schneider and R. D. Andrews, paper presented at Society of Rheology meeting in Pittsburgh, Pa. (Nov., 1963).

3. S. J. Kurtz, G. Langford, R. D. Andrews and N. S. Schneider, paper presented at Society of Rheology meeting in Pittsburgh, Pa. (Nov., 1963).

4. D. H. Ender and R. D. Andrews, J. Appl. Phys. 36, 3057 (1965).

5. D.H. Ender and R. D. Andrews, Bull. Am. Phys. Soc., Ser. II, 11, 198 (1966).

6. P. I. Vincent, Polymer 1, 7 (1960).

7. W. Whitney, J. Appl. Phys. 34, 3633 (1963).

8. A. S. Argon, R. D. Andrews, J. A. Godrick and W. Whitney, paper to appear in Feb., 1968 issue of J. Appl. Phys.

9. S. W. Allison and R. D. Andrews, J. Appl. Phys. 38, 4164 (1967).

10. W. Whitney and R. D. Andrews, J. Polymer Sci. C16, 2981 (1967).

11. G. M. Bryant, Textile Res. J. 31, 399 (1961).

12. R. D. Andrews and Y. Kazama, J. Appl. Phys. 38, 4118 (1967).

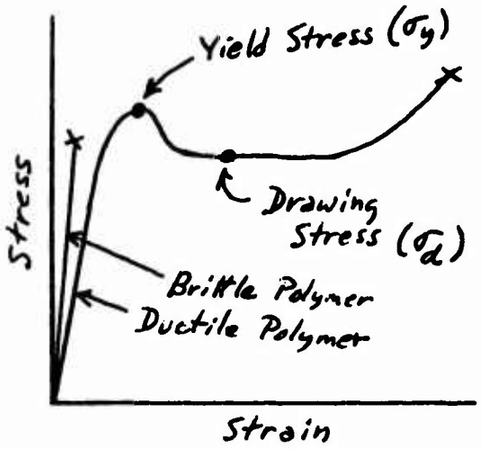

Figure 1.

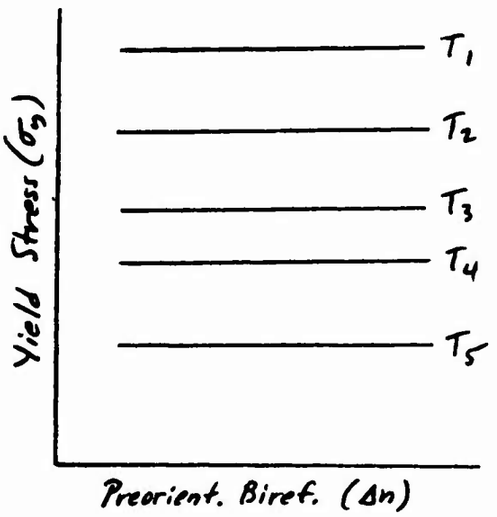

Figure 2.

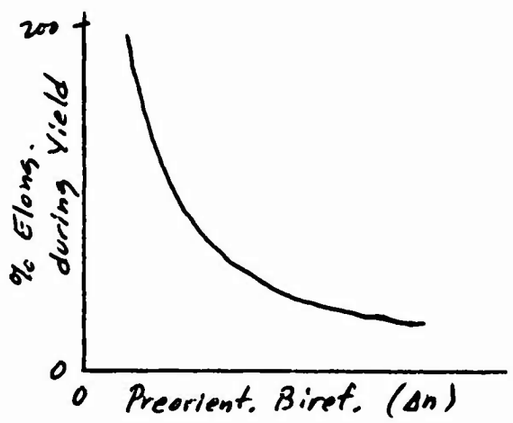

Figure 3.

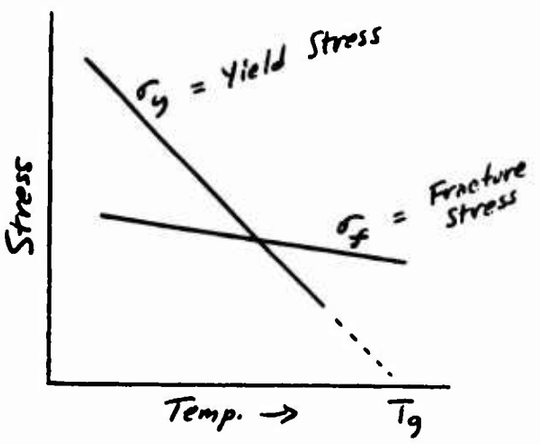

Figure 4.

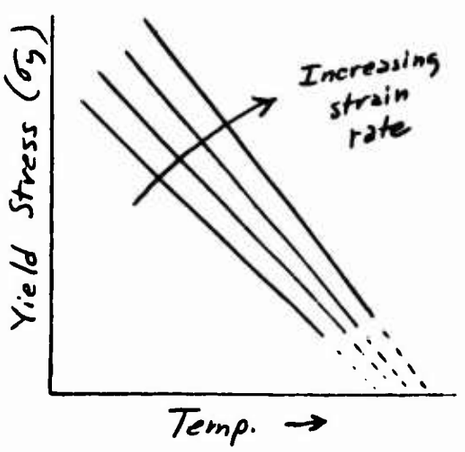

Figure 5.

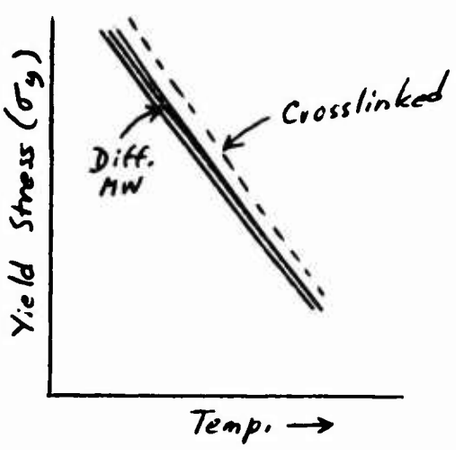

Figure 6.

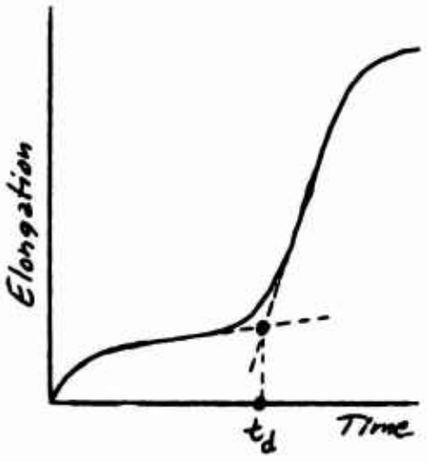

Figure 7.

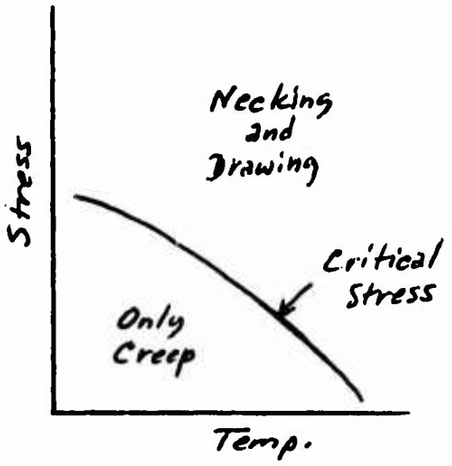

Figure 8.

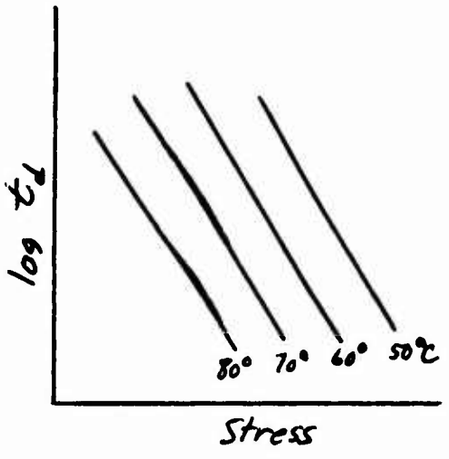

Figure 9.

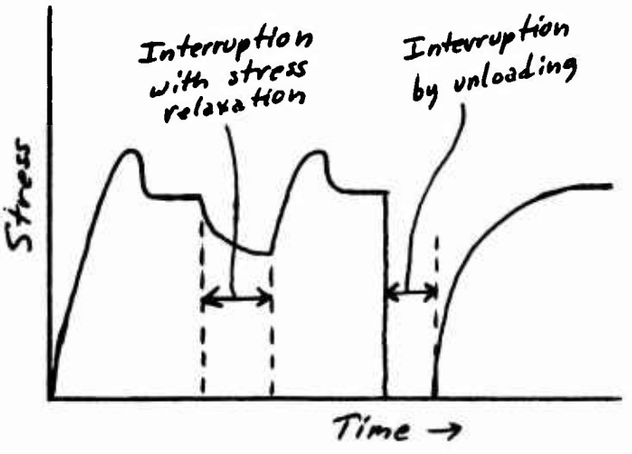

Figure 10.

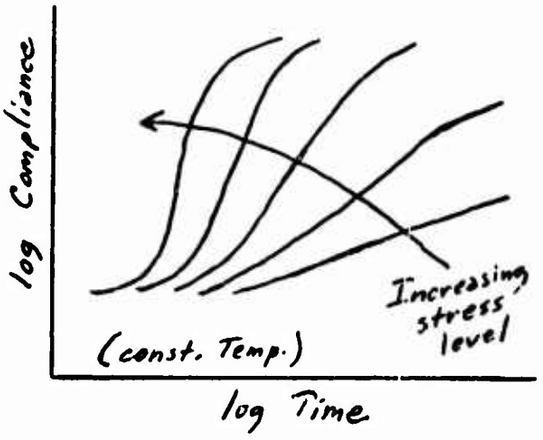

Figure 11.

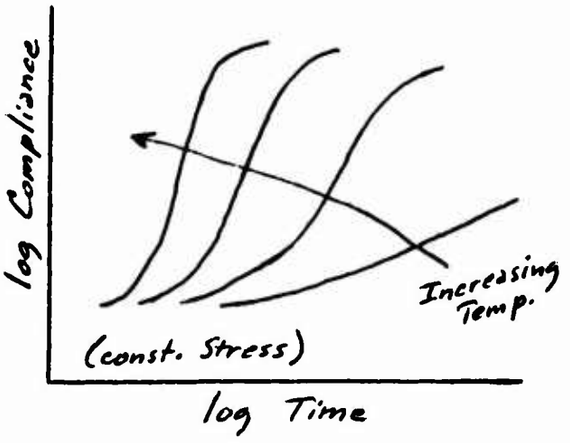

Figure 12.

DISCUSSION ON PAPER NO. 4

Associate Professor Allan S. Hoffman:
Massachusetts Institute of Technology

There are many published studies of the effects of high energy radiation on polymers; generally, property measurements are made before and after exposure to the radiation. Recent work in our laboratories has indicated that there are significant "temporary" effects of radiation occurring during exposure of polymers to high intensity radiation fields. For example, creep rates of many diverse polymers are greatly accelerated during irradiation; when the samples are removed from the radiation field, they soon return to a much lower creep rate. This effect has been noted in our studies for polystyrene, polymethylmethacrylate, polyvinyl, chloride-vinylacetate copolymer and polycarbonate. The samples are also noted to expand during irradiation (after correction for thermal expansion) under no stress; this expansion has been directly related to the acceleration in creep during irradiation under stress. The samples are water-cooled and the maximum temperature rise due to the radiation is never more than a few degrees. We believe that the cause of both the expansion and accelerated creep is related to the generation of gases within the specimen during irradiation. The evolved gases could generate local free volume, thus promoting local molecular slip. Calculations show that the average temperature rise which could effect the expansions noted under no stress is not enough to bring any of the samples even close to its glass transition region. Therefore, the sudden acceleration of flow in these polymers upon irradiation does not

appear to be caused by the same mechanism as is the sudden onset of flow, i.e., cold-drawing in glassy polymers. We are continuing our investigations of this unusual radiation effect.

Professor A. V. Tobolsky:
Princeton University

The concept has been put forward by several workers that the yield point is a point at which the polymer attains a certain value of fractional free volume, close to the value of fractional free volume at T_g. The key concept is that extra free volume is introduced by strain. Using a new definition of fractional free volume, Litt and I were able to compute the yield strain of BPA polycarbonate from room temperature to 150°C. with fair success.

Dr. I. M. Ward:
University of Bristol, U.K.

I was particularly interested in Professor Andrews' remarks on the possible existence of a similarity between cold drawing and the extension of a molecular network. The postulate of a network in a glassy polymer has recently proved useful in two different connections. 1. It is well known that the natural draw ratio of a polymer is very dependent on the degree of pre-orientation prior to drawing, as determined by birefringence measurements. Dr. Pinnock and I combined stress-optical and shrinkage measurements on pre-oriented filaments of polyethylene terephthalate at temperatures above the glass transition[1]. The behavior was consistent with that of stretched rubber network. It

was then shown [2] that subsequent cold drawing appears to extend on initially isotropic network (i.e. the shrunk zero birefringence state) to a fixed limiting extensibility which is independent of the division of stretching between the pre-orienting extrusion stage and the cold drawing stage. This explains why a comparatively low birefringence, which corresponds to high shrinkage, gives rise to a low natural draw ratio.

It may well be, of course, that the limiting extensibility of the network is not a geometrical factor per se, but that it is due to a sudden increase in strain-hardening.

2. Professor Norman Brown and I have recently studied the nature of deformation bands in oriented polyethylene terephthalate[3]. One feature which we studied in detail was the molcular re-orientation of the deformation band, as determined by the rotation of the extinction direction between crossed polarisers. This rotation was compared with the macroscopic deformation of a scratch parallel to the initial draw direction (which is, of course, the initial extinction direction). A paradox was obtained in that this scratch rotated in the opposite sense to the extinction direction. An explanation was obtained for this paradox, in terms of the shear of a molecular network. Although the junction parts of the network deform affinely, the individual chains do not. Thus the macroscopic strain gives rise to a rotation of the scratch in one sense, whereas the direction of the major refractive index rotates in the opposite sense.

REFERENCES

1. Pinnock, P.R. & Ward, I.M., Trans. Faraday Soc., 62, 1308, (1966).

2. Allison, S.W., Pinnock, P.R. & Ward, I.M., Polymer 7, 66, (1966).

3. Brown, N. & Ward, I.M., (to be published).

Comment Submission from Dr. R. F. Landel

Journal of Applied Physics Volume 38, Number 7 June 1967

The Strain-Energy Function of a Hyperelastic Material in Terms of the Extension Ratios

K. C. Valanis and R. F. Landel

Iowa State University, Ames, Iowa, and Jet Propulsion Laboratory, California Institute of Technology, Pasadena, California
(Received 22 November 1965; in final form 13 March 1966)

Abstract:

A simple form of the strain-energy function of natural rubber results if the latter is expressed in an analytic function of the extension ratios rather than the invariants. For incompressible isotropic materials it is postulated that this is a separable symmetric function of the extension ratios, i.e., $W=w(\lambda_1)+w(\lambda_2)+w(\lambda_3)$. This form has been substantiated by critical plots using uniaxial and biaxial data reported in the literature by several investigators. The above form appears to be valid over a wide range of deformations ($0.2 \leq \lambda \leq 3.5$). An explicit representation of W for this range is given in graphical form. In the more limited range ($0.6 \leq \lambda \leq 2.5$) $w(\lambda)$ has the analytic form $w=2\mu\lambda(\ln\lambda - 1)$.

A working hypothesis of polymer fracture

P. I. VINCENT

Imperial Chemical Industries Limited, Plastics Division, Welwyn Garden City, Herts., England

Abstract. It is proposed that many observed trends in the probability of fracture of polymers can be understood if the fracture process is treated as an instability in deformation. A table summarizes the effects of many variables and, in order to explain the approach, a few examples are treated in greater detail:

(i) The inverse relation between maximum attained impact strength and tensile yield stress.

(ii) Cracking of low molecular weight samples during solidification.

(iii) Reduction in the rate of orientation hardening at high temperatures.

(iv) Localized temperature rises during high speed deformation.

(v) Differences in behaviour in tension, flexure and compression.

(vi) The effects on the true stress–strain curve of changes in plasticizer concentration, molecular weight and pre-orientation.

It is concluded that the mechanism of polymer fracture is a competition between localized hardening by molecular orientation and localized softening. The softening is partly of the normal type which leads to yielding and partly caused by a rise in temperature in adiabatic deformation at high straining rates.

1. Introduction

The study of polymer deformation involves measuring the relation between stress, strain, time and temperature as a function of all the relevant material variables and explaining the effects found in terms of the material structure. The study of polymer fractures goes one step beyond this and involves determining the probability of fracture at any point on the stress–strain–time–temperature 'map'. The primary objective of this paper is to consider how far changes in the probability of fracture can be explained as consequences of changes in deformability and so to discover what additional considerations are necessary. The following reasons are given for believing that this is a particularly useful approach to the problem of polymer fracture.

(i) Fracture is inevitably preceded by some deformation and so it seems likely that one cannot ignore deformability when thinking about fracture.

(ii) Many observed changes in the probability of fracture can be at least partly explained as consequences of changes in deformability. Examples will be given below but, to take an extreme case, it seems clear that the great difference between the tensile breaking strains of natural rubber and polystyrene at room temperature is largely a consequence of the great difference in their deformabilities at this temperature.

(iii) During investigations of the mechanical properties of polymers, it is frequently desirable to be able to discover the reason for observed changes in the probability of fracture. It has been found in practice that it is a helpful first step to decide whether or not the change in the probability of fracture is related to a change in deformability. This decision directs attention to different classes of structural feature as possible explanations. As a specific illustration, suppose that a sample of polyvinyl chloride (PVC) pipe were found to be more brittle in impact than a normal control sample.

Then, if there were an accompanying reduction in deformability, such as an increase in a modulus or a yield stress, one would concentrate on the possibility that the brittleness was caused by a change in formulation; there might perhaps be an unusually large proportion of a soluble stabilizer or lubricant. If, on the other hand, there were no parallel change in deformability, it would be more likely that the brittleness was a consequence of inferior fabrication conditions or of contamination.

(iv) The ultimate aim of fracture studies is the computation of the probability of fracture from the known material structure; this problem is extremely complex and full solution is hardly to be expected. It seems more hopeful that fracture probability could be deduced, at least partly, from a knowledge of deformability. One could then rely on deformation measurements as basic data and hope that they will eventually be deduced from the material structure. Calculation of deformability, though still complex, is somewhat more tractable than direct calculation of fracture because fewer variables demand consideration.

(v) Fracture measurements are notoriously subject to more error and scatter than measurements of deformation. It is useful to be able to take advantage of the greater reliability of measurements of deformation when trying to improve practical and theoretical understanding of fracture.

2. Hypothesis

A large number of changes in experimental conditions, material variables and sample fabrication conditions are known to have an effect on the probability of fracture. Many of these effects can be understood or qualitatively explained on the basis of the following three principles:

(i) If the experimental conditions or the material are changed in such a way that the stress is greater at a given strain, then the probability of fracture at that strain is increased. To put it much more crudely, harder materials tend to be more brittle than softer materials.

(ii) The probability of fracture increases when there is an increase in the severity of stress concentrations. The stress concentration may be a consequence of the shape of the test specimen or of an irregularity in the structure of the material.

(iii) The probability of fracture is increased by factors which tend to make deformation more unstable and decreased by factors which tend to make deformation more stable.

The working hypothesis referred to in the title of this paper is that these three principles are adequate to explain the known trends in polymer fracture. The significance and application of these principles is most readily explained by means of examples.

3. Examples

Some trends in the probability of fracture can be explained on the basis of a single one of the three principles but in other cases two or all three of the principles may combine or compete to produce more complex behaviour. Shortage of space prohibits detailed consideration of all the factors known to affect the probability of fracture in polymers and their explanation in terms of the three principles. To overcome this, a table has been constructed to provide a summary of many effects. Naturally the points made in the table can only be brief and dogmatic. Much more extended treatment would be needed to prove them and to examine apparently anomalous or paradoxical instances of behaviour. In order to explain the approach, a few examples will be treated in greater detail.

3.1. *Application of the first principle*

For all polymers there is a region of behaviour where the tensile elongation to break and the impact strengths decrease as the ambient temperature is decreased. For amorphous polymers this region is below a temperature which is close to the glass transition; for crystalline polymers the region may be below a temperature between the glass transition and the melting point. Such a decrease in temperature always causes a decrease in deformability—an increase in moduli and yield stresses. Thus, when investigating the mechanical properties of polymers, it is commonly observed that the breaking strains and impact strengths decrease when the moduli and yield stresses increase. This is not only observed when the temperature is varied but also with changes in crystallinity, concentration of plasticizers and other additives, and with many changes in the chemical structure of the polymer.

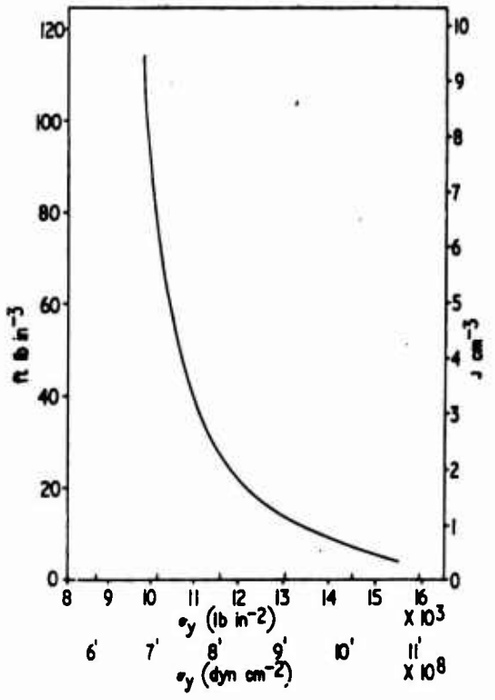

Figure 1. Relation between the maximum attained impact strength and the yield stress.

Figure 1 gives a more specific illustration of this commonly observed inverse relation between, speaking approximately, hardness and toughness. The abscissa of figure 1 is the tensile yield stress measured at +20 °C and an initial straining rate of 50% per minute. The ordinate is the Charpy impact strength at the same temperature (the energy lost by the pendulum was divided by one ninth of the product of span, width and residual thickness); the specimens contained sharp, deep notches giving an elastic stress concentration factor of about 7·6. The results are quoted in J cm^{-3}; if they are divided by 1·25 they give a reasonable approximation to the A.S.T.M. impact strength in the traditional ft lb/in. of notch). Samples of hundreds of different thermoplastics have been subjected to this combination of tests and it has

Factor affecting the probability of fracture	First principle	Second principle	Third principle
Temperature	At lower temperatures, moduli and yield stresses are higher, breaking strains are lower.		Above the ductility peak, orientation hardening and breaking strains decrease.
Straining rate	At higher straining rates, moduli and yield stresses are higher, breaking strains are lower.		At high straining rates, the specimen heats up locally, stability and breaking strains decrease.
Notches, holes, cracks etc.		Produce stress concentrations and increase the probability of fracture.	Reduce stability.
Flexural strength is greater than tensile strength			Deformation is more stable in flexure because of the stress gradient.
Greater ductility in compression than in tension			Deformation is more stable in compression because the area increases with tne strain.
Low compression moulding temperature or pressure, rough machining, weld lines etc.		Produce structural irregularities and stress concentrations which increase the probability of fracture.	
Molecular orientation	At very high orientation, moduli and yield stresses are high, breaking strains are low.	Perpendicular to orientation, fibrillation or de-lamination is often easy and oriented faults are observed.	At moderate orientation, deformation is more stable and the probability of fracture is reduced.
Molecular weight		Very low molecular weight samples crack on solidification.	Decreasing molecular weight reduces orientation hardening and increases the probability of fracture.
Crystallization	Increases moduli and yield stresses and generally increases the probability of fracture at a given strain.	Over-crystallization leads to voiding and cracking which introduce stress concentrations and decrease breaking strains.	Strain-induced crystallization can increase orientation hardening and resistance to fracture.

Cross linking	Can increase moduli and yield stresses and reduce breaking strains.	Too much cross linking can cause cracking and stress concentrations and reduce breaking strains.	Can increase orientation hardening and resistance to fracture.
Plasticizers and other soluble additives	Usually decrease moduli and yield stresses and increase breaking strains.	Can improve processability and so reduce structural irregularities.	Can decrease orientation hardening and reduce breaking strains.
Added powders	Can decrease yield stresses and improve resistance to brittle fracture.	Can create stress concentrations and so promote fracture.	Can increase orientation hardening and resistance to fracture.
Added glass fibres	Can increase moduli and yield stresses and decrease breaking strains.	Can create stress concentrations and initiate fracture.	
Blending soft polymers with hard polymers	Deformability and resistance to fracture of the blend are generally intermediate between those of the components.	The added polymer can create stress concentrations in the matrix.	
Copolymerization	The probability of fracture changes as the moduli and yield stresses change.		
Plasticizing environments	Can soften the surface of the test specimen and slightly improve the resistance to fracture.		Can reduce orientation hardening and increase the likelihood of cracking.
Side group structure	As side group length increases, moduli and yield stresses decrease and breaking strains increase. Branched side groups and rings have the opposite effects.	Bulky side groups apparently introduce structural irregularities and promote brittle fracture.	
Glass transition temperature	The position of the glass transition has an inverse effect on moduli and breaking strains.		
Secondary transitions	Large secondary transitions often have an inverse effect on moduli and breaking strains.		

been found that it is comparatively easy to obtain a sample with a combination of yield stress and impact strength which lies below and to the left of the curve but extremely rare to find an isotropic sample which gives results which lie above and to the right. (It is necessary to make the proviso that the sample should be isotropic since molecular orientation can cause very high results in impact tests. This aspect will be discussed later.) Naturally one cannot say from this evidence that it is impossible to produce an isotropic thermoplastic sample with, say, a yield stress of 10^9 dyn cm^{-2} and an impact strength of 10 J cm^{-3}, but it is clearly difficult.

The question of what can be deduced from this well-established relation now arises. If it is accepted that ease of deformation and resistance to fracture are frequently correlated, can we say that ease of deformation causes resistance to fracture or should we say that they are independent effects of the same underlying change? Or, to revert to the extreme example given earlier, does rubber have a higher breaking strain than polystyrene at room temperature because it is softer? It is difficult to obtain definite evidence on this point but, when the complete picture is discussed later, it will be seen that there is an indication that the relation is one of cause and effect.

3.2. *Application of the second principle*

The most straightforward method of demonstrating the influence of stress concentrations on the probability of fracture is to perform tests on specimens of different shapes. It is well known that the impact strength of specimens with machined notches can be very much less than that of unnotched specimens; the impact strength decreases as the elastic stress concentration factor increases.

In addition to such deliberate changes in the shape of the test specimen, numerous examples have been noted where the fracture of plastics under given test conditions has been made more probable by the existence of irregularities in the structure. Some of these are mentioned in the table and include bubbles, cracks, contamination, machined surfaces and weld lines. Similar effects can be found in compression mouldings when the temperature or pressure is too low.

Structural irregularities which cause stress concentrations and increase the probability of fracture can also be created by altering the molecular structure of the polymer. In an experiment to study the effect of molecular weight changes of the fracture of polymethylmethacrylate, a polymer was made with an unusually low molecular weight (reduced viscosity in chloroform 0·2; weight average molecular weight 36 000 $\mp$ 1000). When this sample was compression moulded, it cracked during cooling. Attempts were made to produce crack-free samples by careful casting from chloroform and dichlorethane solutions but figure 2 (plate XIV) shows the type of result obtained. In this case at least, reducing the molecular weight gives low strength because the sample contains structural irregularities. Later, a suggestion will be made to explain why such samples crack on solidification.

Clearly it is well established that the presence of stress concentrations increases the probability of fracture. It is only necessary to make the point that they may be deliberate, like machined notches, or accidental, like contamination, or inherent in the material, as with the low molecular weight sample discussed.

3.3. *Applications of the third principle*

One of the most striking differences that can be observed during tensile tests on thermoplastics is the difference between the specimens which first neck and then cold draw to large extensions and those specimens which neck and then break at much lower extensions without cold drawing. It can be shown (Vincent 1960) that necking is an instability of deformation which is caused by softening of the material

as the strain increases and that cold drawing is a restabilization of the deformation which is caused by hardening of the material at high strain. This hardening has only superficial affinities with strain hardening in metals; since it is primarily caused by molecular orientation it may be preferable to call it orientation hardening.

In the study of ductile metals necking is a plastic instability. Since polymers are not plastic in the same way as metals, it may perhaps be better to say that necking in polymers is a pseudo-plastic instability and that cold drawing is a pseudo-plastic restabilization caused by orientation hardening. There are disadvantages in using nomenclature of this type but it seems necessary to emphasize the point that the mechanisms are different from those in metals.

It is now possible to re-state the third principle to read as follows: the probability of fracture is increased by factors which tend to cause pseudo-plastic instabilities and decreased by factors which tend to cause pseudo-plastic restabilization.

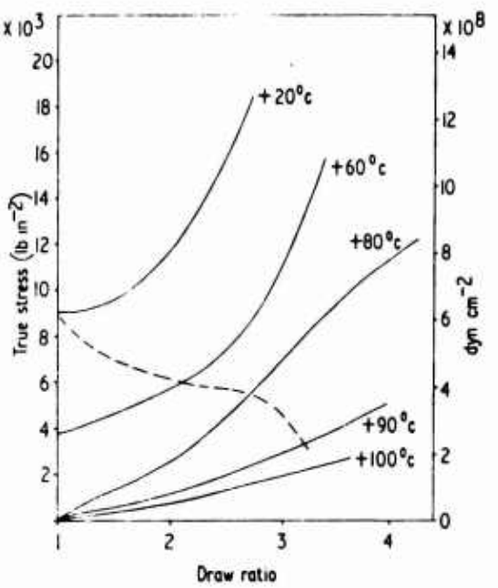

Figure 3. Isothermal true stress–strain curves of a sample of rigid PVC with an estimated adiabatic curve (broken curve) from +20 °c.

As a first illustration, consider again the effect of changes in the temperature of test. Figure 3 shows true stress–strain curves of a sample of rigid PVC at various temperatures. (They were obtained by photographing the specimens during extension after necking and then, from the negatives, measuring the minimum cross-sectional area. Assuming no change in density, it is then possible to compute the true stress and the draw ratio at various loads and so to construct the true stress strain curves.) It can be seen that, as the temperature is decreased below +80 °c, the stress at a given strain increases and the breaking strain decreases; this is a simple illustration of the first principle. However, when the temperature is increased to +100 °c, the breaking strain again falls, in spite of the reduced stresses. Clearly this cannot be a consequence of the first or second principle but it can readily be explained from the third principle; the reduced slope of the true stress–strain curve demonstrates that the rate of orientation hardening is decreased at +100 °c.

A second example of an application of the third principle comes from a consideration of the effect of changes in rate of extension. It is well known that increasing the rate of extension can decrease the breaking strain. For example, the specimens of rigid PVC which were used to provide the true stress–strain curves in figure 3 were extended at 0·02 cm sec^{-1} (initial straining rate about 50% per minute); even at +20 °c, the deformation stabilized after necking and the specimen cold drew. Similar specimens extended at higher speeds, say 0·7 cm sec^{-1}, do not restabilize but break in the neck without cold drawing. It is true that the tensile yield stress is increased by increasing the straining rate but the effect is not so large that the first principle gives an adequate explanation of the change from cold drawing to necking rupture. It is more likely that the explanation lies in the marked local rise in temperature, easily verified by touching the specimen, which accompanies necking in specimens drawn at straining rates above a few hundred per cent per minute (Vincent 1960). This temperature rise must reduce the yield stress of the material in the neck. Using simplifying assumptions—constant specific heat, all pseudo-plastic strain energy converted into heat—it is possible to estimate the shape of the adiabatic true stress–strain curve from a knowledge of the isothermal true stress–strain curves at various temperatures. For the sample of rigid PVC starting at +20 °c, this gives the broken line in figure 3. The detailed shape of this curve is probably inaccurate because of the simplifying assumptions but it is clear that the adiabatic true stress–strain curve has a negative slope. It follows that, under adiabatic conditions, the deformation is much less stable than under isothermal conditions. From the third principle, the probability of fracture increases as the conditions become more adiabatic and less isothermal. The drop in fracture energy which occurs for several polymers between 0·02 and 0·7 cm sec^{-1} may be considered to be an isothermal–adiabatic transition.

When computing an adiabatic true stress–strain curve, the slope of the computed curve depends on the magnitude of the yield stress and its dependence on temperature and on draw ratio (strain). The slope will tend more to be negative with increase in the yield stress and its temperature dependence and with decreased orientation hardening. It follows that, as the yield stress increases, there is more chance that the deformation beyond yield will become unstable and not restabilize. In other words, high yield stresses tend to cause low extensions. This, then, is the clue, promised above, suggesting that the relation between high stresses and low breaking strains is one of cause and effect; when the stress is higher at a given strain, there is a greater probability of unstable adiabatic deformation leading to fracture at lower extensions.

Williams and Turner (1964) have shown how the conditions for necking of a tensile specimen may be generalized to a volume element subjected to the more complex stress at the tip of a crack. They suggest that "in many, if not most, problems of fracture of interest to the engineer, a plastic instability precedes separation of the material". Williams (1965) has extended their approach to take account of the temperature rise at the tip of a crack in fast crack propagation. Williams and Turner (1964) also point out that this view of fracture throws light on the increased ductility of materials when they are tested in tension with a superimposed hydrostatic pressure.

In the same way, one can understand why specimens are more ductile in compression than in tension. Plastic instabilities are less likely in compression because the area of the specimen increases as the strain increases. Further, a tensile specimen with a machined notch or other stress concentration will be less stable than an unnotched specimen. It may be, therefore, that the second principle is a special case of the third principle. Because stress concentrations promote instabilities, it follows from the third principle that they promote fracture.

The flexural strength of brittle specimens is generally greater than their tensile strengths. This can sometimes be associated with increased stress concentrations caused by irregularities on the surface of the tensile specimen and so derived from the second principle. However, this explanation is incomplete (Vincent 1962). It is probable that the basic cause of the difference is that cracks develop more slowly in the flexural specimens in the direction where the stress is decreasing. That is, instability is delayed by the stress gradient.

Thus a third general example of the application of the third principle is the dependence of fracture on the type of applied stress. Fracture is delayed if plastic deformation tends to decrease the applied stress, as in flexure or, more so, in compression. Fracture is promoted if plastic deformation tends to increase the applied stress, as in tension or, more so, in tensile tests on notched specimens.

Three more examples of the applications of the third principle may be found by considering changes in the nature of the sample under examination.

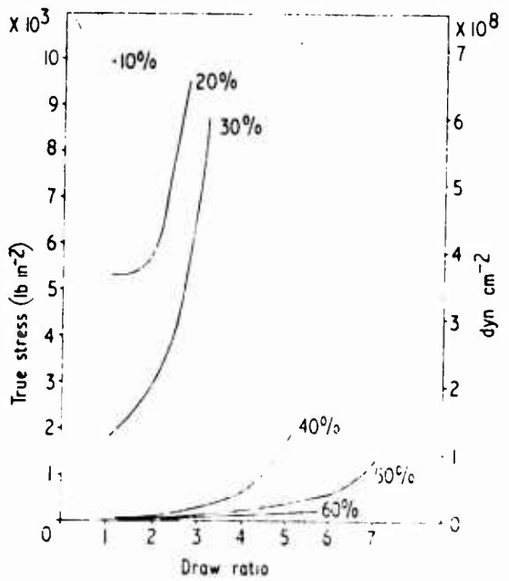

Figure 4. True stress–strain curves of samples of polymethylmethacrylate with different concentrations of di-butyl phthalate.

3.3.1. *Plasticizers.* Figure 4 shows the true stress–strain curves (at +20° c, 0·02 cm sec^{-1}) of samples of polymethylmethacrylate plasticized with various concentrations of di-butyl phthalate. By comparison with figure 3, it can be seen that changing the plasticizer concentration has a similar effect on the true stress–strain curves to changing the temperature. At low plasticizer concentrations, the material has high stresses and low breaking strains—a simple application of the first principle. At high plasticizer concentrations, the breaking strains decrease again although the stresses are low. As with PVC at high temperatures, the rate of orientation hardening is low and so the breaking strain is decreased, by the third principle.

3.3.2. *Molecular weight.* Reductions in the average molecular weight of the sample are frequently observed to increase the probability of fracture. It was pointed out

above that a very low molecular weight sample of polymethylmethacrylate cracked on solidification and that its low strength, therefore, follows from the second principle. However, there is no evidence that this explanation completely covers the effects of molecular weight and, in any case, cracking on solidification does itself require explanation. A more complete understanding of the effect of changes in molecular

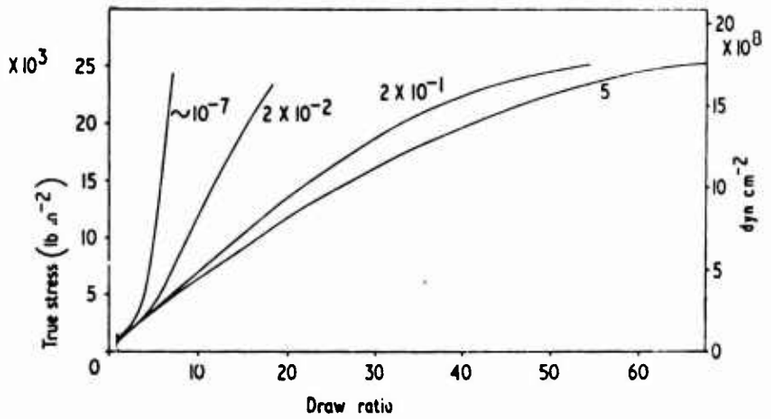

Figure 5. True stress–strain curves at +100 °c of four samples of high density polyethylene with different melt-flow indices.

weight can be obtained from a consideration of figure 5, which shows the true stress–strain curves of four samples of high density polythene at +100 . It is clear that the rate of orientation hardening decreases as the molecular weight decreases (melt-flow index increases). A similar trend can be demonstrated with other polymers and was found by Flory (1946) in his work on butyl rubber fractions. Assuming, now, that it is generally true that orientation hardening depends on molecular weight, one can understand why the probability of fracture, in impact tests, tensile tests and stress-cracking tests, should depend on molecular weight; it follows directly from the third principle. It can also be seen that cracking during solidification could be a consequence of the third principle. At very low molecular weights there is little or no orientation hardening so that contraction stresses set up during solidification create instabilities which, being unopposed by orientation hardening, lead to cracking.

3.3.3. *Molecular orientation.* The effects of molecular orientation on fracture are too complex to be encompassed in a small space. However, one feature can be discussed which appears to give a clear relation between the shape of the true stress–strain curve and the probability of fracture. Consider the isothermal true stress–strain curve at +20 °c given in figure 3 for a sample of rigid PVC. That curve was obtained on an isotropic sample. A similar sample was rolled at room temperature so that its length was increased by 23% in each direction and its thickness was reduced by 31%. The true stress–strain curve beyond yield for the anisotropic sample was found to be the same as for the isotropic sample, provided allowance was made for the pre-orientation by multiplying the draw ratio of the anisotropic sample by 1·23. This necessarily implies that the tensile load–extension curves for the isotropic and anisotropic samples must be different and figure 6 shows this difference. It can be seen that the drop in load after yield is much smaller for the anisotropic sample and this implies greater

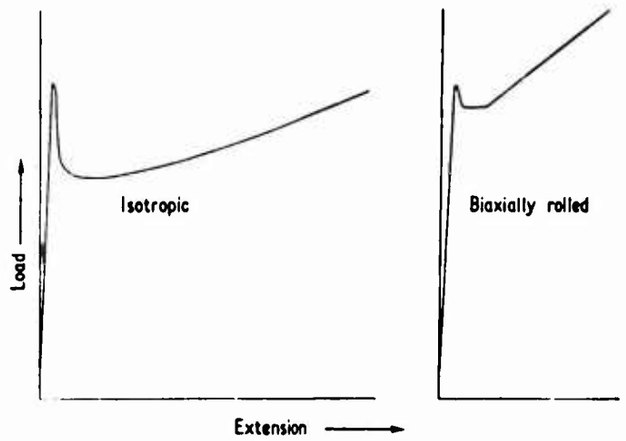

Figure 6. Tensile load–extension curves of two samples of rigid PVC: initially isotropic, and biaxially rolled.

stability of deformation. From the third principle it follows that greater resistance to fracture is to be expected and this is confirmed by the fact that the impact strength of sharply notched specimens at +20 °C was 38 times greater for the anisotropic sample than for the isotropic sample. This explains the proviso mentioned in the discussions of applications of the first principle.

Although this point has been made in terms of a single pair of specimens, it is a general finding that pre-orientation reduces the drop in load after yield in tensile tests and increases the impact strength and the resistance to fracture in other tests.

4. Conclusions

The examples given above show that many known trends in the probability of fracture become more comprehensible when fracture is regarded as either consisting of, or inevitably preceded by, a pseudo-plastic instability. This leads to the following picture of the mechanism of polymer fracture:

(i) As the strain increases, the local strain at a notch, crack or other structural irregularity increases more rapidly.

(ii) The material subjected to the highest strain tends to become softer than the remainder either naturally or because of a local temperature rise or for other reasons.

(iii) The material subjected to the highest strain may tend to become harder than the remainder because of orientation.

(iv) When the hardening is more effective than the softening, the highly stressed material is stable and does not break.

(v) When the softening is more effective than the hardening, the highly stressed material is unstable and either breaks or begins to break and then restabilizes.

On this basis, the study of polymer fracture can be divided into three parts.

(i) It is necessary to have complete knowledge and understanding of polymer deformation.

(ii) It is necessary to have complete knowledge of the stress-concentrating effect of structural irregularities.

(iii) It is necessary to be able to calculate the behaviour of a specimen with known deformability and known stress concentrations.

Although this is still a formidable programme, it does seem rather more tractable than the problem of calculating the probability of fracture ignoring the detailed shape of the true stress–strain curves. So we can answer the initial question by saying that many changes in the probability of fracture can be explained as consequences of changes in deformability.

References

FLORY, P. J., 1946, *Industr. Engng Chem.*, **38**, 417.
VINCENT, P. I., 1960, *Polymer*, **1**, 7.
—— 1962, *Brit. J. Appl. Phys.*, **13**, 578.
WILLIAMS, J. G., 1965, *Appl. Mater. Res.*, **4**, 104.
WILLIAMS, J. G., and TURNER, C. E., 1964, *Appl. Mater. Res.*, **3**, 144.

N.B. Discussions will be found on p. 288 ff.

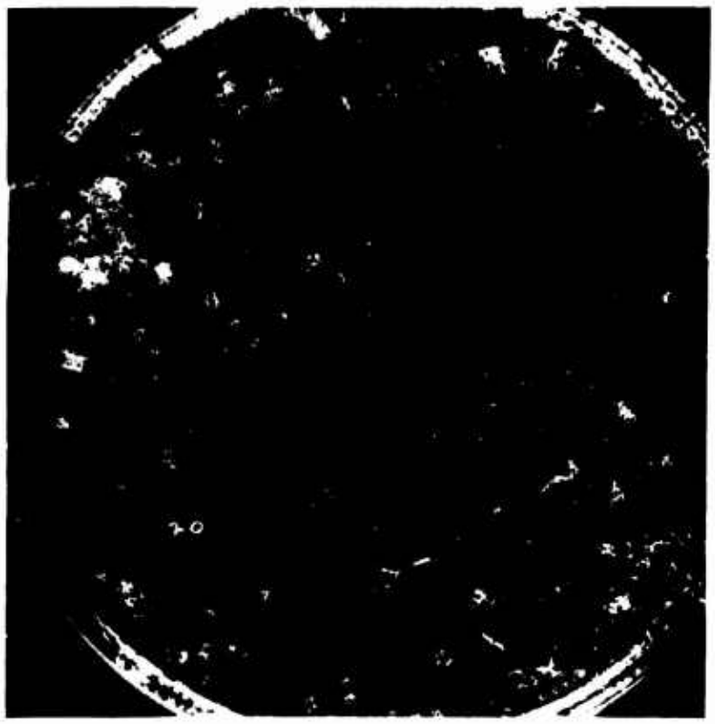

Figure 2. A sample of low molecular weight polymethylmethacrylate cast from dichlorethane solution.

DISCUSSION ON PAPER NO. 5

Assistant Professor I. V. Yannas:
Massachusetts Institute of Technology

The paper presented to us by Dr. Vincent affords me with the opportunity to recall previous equally stimulating work reported by the speaker (Polymer, 1, 7, 1959). Recently, in our laboratory, Dr. Vincent's proposition that necking in polymers is preceded by "strain-softening" was taken literally and put to the following test: Polymethyl methacrylate was subjected to stress relaxation at 80°C. and at different steps of tensile strain ranging up to the strain level requisite for necking approximately 5.5% (under the conditions employed). We found that the isochronal and isothermal relaxation modulus of the glassy polymer was independent of strain up to (approx. 1% strain apparent upper limit of linear viscoelastic behavior); thereafter, the modulus decreased by more than a factor of two as the strain increased from 1.0 to 5.0%. This preliminary finding is currently under our scrutiny.

CYCLIC STRESS-STRAIN BEHAVIOR OF THE DRY POLYCARBONATE CRAZE

R. P. Kambour and R. W. Kopp

General Electric Research and Development Center,
Schenectady, New York

Abstract

Equipment and methods have been developed that allow photomicrographic determination of the stress-strain properties of the individual craze. Serial cyclic tensile tests on polycarbonate crazes are described.

Under stress the typical dry polycarbonate craze thickens solely by straining; no adjacent polymer of normal density is converted to craze material. The craze exhibits a yield stress followed by a recoverable flow to roughly 40-50% strain at 6-8000 psi. Returned to zero stress the craze exhibits creep recovery at a decelerating rate. The yield stress and loss factor of each cycle decrease with increasing initial strain and cycles initiating at 50% strain or more show completely Hookean behavior. Creep recovery results in recovery of yield stress and loss factor also.

Craze tensile behavior is suggested to be essentially an extension of the craze formation process. Decrease in elastic modulus and yield stress with increasing strain are rationalized in terms of strain-produced decrease in density and resultant increase in stress concentration factor on the microscopic polymer elements of the craze. Polymer surface tension and the large internal specific surface area of the craze are suggested to be important factors in the large creep recovery rates of the craze.

CYCLIC STRESS-STRAIN BEHAVIOR OF THE DRY POLYCARBONATE CRAZE

R. P. Kambour and R. W. Kopp

General Electric Research and Development Center,
Schenectady, New York

I. Introduction

The fact that crazes can have considerable strength has been known for some time. In a 1949 landmark paper Sauer, Marin and Hsaio noted that polystyrene specimens that were crazed throughout their cross sections exhibited tensile strengths of 4000 psi.[1]

It has also been observed by Spurr and Niegisch[2] and also in this laboratory[3] that crazes in polycarbonate can exhibit tensile strengths greater than the yield stress of the bulk polymer, 8000 psi. For example, in the case of one specimen extended in an Instron tensile tester at a constant rate of elongation, cold drawing initiated in an uncrazed portion of the bar and the shoulder of the neck propagated through several crazes before fracture. Moreover fracture finally occurred in an uncrazed portion of the specimen.

These observations on the strength of crazes were often rationalized in terms of the known orientation of craze material in the original stress direction since plastically-deformed polymer specimens generally have greater strengths in the orientation direction than do unoriented ones. The enhancement of strength due to orientation was presumed to offset the strength reduction inherent in the presence of large numbers of microcracks or voids. If true, the craze might be expected at first thought to have a tensile modulus and a loss factor also approximating those of bulk polymer or even those of oriented polymer. It was surprising therefore to observe that the craze

at the crack tip in polymethyl methacrylate appeared to be highly deformable in a reversible manner under stress.[4]

On the basis of this observation and the likelihood that such deformability contributed substantially to the energy of crack propagation in polymers, a crude apparatus was built to measure stress-strain properties of the craze. The results, reported briefly elsewhere,[5] were unsatisfactory in many respects but did confirm that the craze is markedly more compliant at low stresses than is the bulk polymer. On the strength of these data the apparatus described herein was designed and built.

II. Experimental

The measurement of polycarbonate craze tensile properties rests on the ability to grow well-separated solvent crazes through the entire cross sections of tensile specimens. At the specimen surface the craze edge is associated with a shallow indentation having reasonably sharp boundaries. After drying application of stress causes the distance between the boundaries to increase due solely to extension of material in the craze rather than conversion of more bulk polymer to craze material. Thus measurement of this distance as a function of force applied to the ends of the specimen makes possible calculation of a stress-strain curve for the craze. This should be the case as long as the force is supported uniformly by all areas of the craze, which in turn requires that the craze be well-separated from other crazes and have a reasonably uniform thickness (Fig. 1).

Strain measurements are made more complicated, however, by two nonidealities. First the actual craze surface indentation, as shown in Fig. 2a at the edge of the bar, has been found to be

generally wider than the true craze thickness. This is clearly demonstrated by Fig. 2b which shows the same craze at the same bar edge but on the adjacent bar face. The face shown in Fig. 2b has been ground down approximately 0.01" and polished using slow speed and wet abrasives. With the groove gone the craze is seen to reflect light more strongly than the surrounding bulk polymer. The craze/bulk polymer boundary is sharp but the craze width exhibited is significantly smaller than that shown by Fig. 2a. Further in Fig. 2b the profile of the still-intact groove on the adjoining face can be seen; it is clearly wider than the true craze. The surface groove is wider than it would otherwise be because of the drawing into the craze during its formation of surrounding surface material.

Second, at high stresses during tensile testing the surface groove sometimes enlarges partly by drawing in of more surrounding surface material.

Both effects must be compensated for in strain calculations. Such compensations are discussed below.

Specimen and Craze Preparation

The specimens used here were standard dumbbell tensile bars 8-1/2 inches long, 1/8 inch thick and of 1/2 inch wide test section, injection molded from Lexan® polycarbonate resin of $\bar{M}_w$ = 35,000. They were annealed at 170°C in vacuum for 24 hours, which resulted in roughly a 1/2 inch decrease in length and a consequent increase in thickness due to release of molding orientation. They were cooled over one hour or so to 140°C (polycarbonate T_g) and then quenched to room temperature.

® Registered trademark of the General Electric Company.

The general craze preparation procedure was as follows. Each specimen was mounted in a tensile jig, immersed in 95% ethanol liquid and subjected to stress using a lever arm and weights. Experience showed that the best chances of success obtained if the initial load was in the range of 2000 psi. If no crazes were seen to initiate after five or ten minutes, the load was increased by a few hundred psi and so forth. Once craze initiation was observed (usually in the range of 3000 psi), the load was usually held constant and over a period of a few hours craze growth progressed through the bar. When growth was judged complete enough, the ethanol bath was removed and the bar allowed to dry out under strain. When clamped under strain most of the alcohol evaporates out of the craze in a few minutes[3] and drying in this way for a few days suffices to prevent craze healing upon release of stress. Nevertheless because even a small residue of alcohol might markedly affect subsequent tensile properties, specimens to be tested were left usually to dry under strain for one to six months. In some cases the strain was that existent under the crazing force at the finish of craze growth; in other cases the stress on the bar was reduced to 1300 psi and the bar clamped at the corresponding strain. One specimen received a rather more complex treatment which is detailed in an appendix.

Crazes suitable for testing were selected with the aid of a microscope. Sometimes a craze which met the aforementioned criteria on one side of the bar only, could be made useful by cutting away the other wide of the bar selectively. In all cases, however, the bar was reduced in width at the test section to 1/4 inch or less using a router and a cutting jig.

Craze Tensile Tester

The stressing apparatus described below was built to allow the taking of photomicrographs of the craze edge under controlled stresses and strain rates. It was designed to allow testing at constant strain rates or, alternatively, at constant force (i.e. creep test). Experience with the first tester revealed the necessity of being able to readjust continually the longitudinal position of the test specimen caused by the fact that the test craze is virtually never in the strain center of the system and thus tends to translate from the field of view of the microscope as the stress is changed. It was also evident that control of the position of the craze in the two directions orthogonal to the stress direction was required since under stress small vertical and lateral movements tend to take place. Lateral movement must be prevented so that the photographs will all be taken of the same location along the craze edge; vertical movement must be controlled in order to keep the bar surface sharply in focus. Sharp focus is a critical requirement since even slight defocussing causes enlargement of the craze image and consequent error in the calculated craze width.

The testing apparatus is shown schematically in Fig. 3. The test specimen is mounted horizontally between two tensile chucks such that the edge of the craze to be studied is in the field of view of a Zeiss GFL microscope. The tensile chucks are attached to two matched hydraulic pistons. The two corresponding cylinders (1-1/2" bore, 1" diameter rod, 2" stroke, made by the Parker Hannefin Co.) are bolted to a rigid frame which is supported via six roller bearings on three horizontal, 3/4 inch diameter, case-

hardened steel rods. Although the pistons are closely matched in size, small differences in cylinder wall smoothness plus the overall level of friction produced by the rubber piston seals (~25 pounds force) prevent the piston system from operating ideally. (If the system were nearly frictionless, any point on the test specimen could be pinned in the field of view of the microscope by a light clamping pressure and the difference in specimen elongation on each side of the pinning point would be compensated for by different amounts of travel of the respective pistons.) As it is the double piston arrangement reduces, but does not eliminate, the tendency for craze translation from the field of view. The residual tendency for translation is compensated for by moving the carriage on the steel rods, which is accomplished by light hand pressure.

Force can be applied from either of two sources: a pneumatic-hydraulic 32:1 pressure booster (Model 4785, Wilton Corp.) which is connected via a reducing valve to the 80 psi laboratory air line. Alternatively a third hydraulic piston which sits under the crosshead of an Instron Universal Tester can be used. The first source permits constant force application and thus creep studies; the second permits roughly constant strain rate studies which are thus similar to conventional tensile tests.

Between one of the tensile chucks and its piston is fixed a Baldwin-Lima-Hamilton U-1 500 lb. tensile load cell the output of which is connected directly to the Instron load recording system. (Force recorded from the Instron compression load cell, when the third piston sits upon it, is in error due to the frictional losses in the three pistons.)

The positioning of the craze in the two directions orthogonal to the stress direction is accomplished via a clamping frame mounted on the microscope stage. Two opposed, sharpened steel screws are tightened by hand against the specimen edges thus controlling the horizontal location of the craze. The fine adjustment of focus on the Zeiss GFL microscope is accomplished by movement of the stage rather than the microscope limb; thus the pinning screws couple the bar to the stage sufficiently to permit adjustment of focus. During a test the position and focus of the craze are observed by viewing through the beam splitter of a Bolex 16 mm movie camera used for taking the photomicrographs.

In the experiments reported here force was applied via the Instron crosshead. Typically the force-time relationship is not completely linear (Fig. 4). The deviations from linearity are associated with deformation of the rubber cup seals on the pistons and are thus unavoidable with this equipment. Fortunately these deviations are confined to the low stress region where time effects are expected to be less important than at high stress.

Craze Stress-Strain Calculations

The vertical marks on the curve in Fig. 4 are points at which individual photographs were taken. The marks were produced by a microswitch activated by the camera release. Using the force at each mark and the corresponding craze photo, the craze stress-strain curve was constructed. Craze width measurements were made by projecting each photographic negative onto a flat white surface and measuring distances thereon with the aid of a centimeter scale.

Craze strains, corrected for the nonidealities described earlier, were determined as follows. The apparent craze thickness ℓ_a (i.e. the width of the surface groove) was measured from each photo. The determination of true craze thickness ℓ_t was made possible by the observation that under stress the surface groove usually undergoes a change of profile, becoming flat over the central region but leaving the satellite bands of cold drawn material tilted and thus dark in reflected light. The central region of the groove image is thus now sharply bounded, has the same reflectance as does the craze in Fig. 1b, and is thus considered to indicate the true craze thickness at that stress and time $\ell_{t,\sigma}$. The combined width of the two satellite bands, $\Delta\ell = \ell_{a,\sigma} - \ell_{t,\sigma}$ is usually unchanged by stress; it can thus be subtracted from $\ell_{a,o}$ to obtain $\ell_{t,o}$ the original true craze thickness for the calculation of craze strain $\epsilon = (\ell_{t,\sigma} - \ell_{t,o})/\ell_{t,o}$. Typically $\ell_{a,o}/\ell_{t,o} = 1.4$ to 1.6 indicating the importance of such a correction procedure.

In some cases it became apparent that under stress the satellite bands were enlarging by engulfing more of the adjacent surface material so that $\ell_{a,\sigma} - \ell_{a,o}$ was no longer equal to $\ell_{t,\sigma} - \ell_{t,o}$. Craze thickness changes however could still be determined by measuring the change in distance between any two surface blemishes, one on each side of the groove and located far enough away from the groove so that they did not become engulfed. This procedure was not usually necessary.

It is also possible to determine true craze thickness by grinding and polishing down the appropriate part of the bar

surface subsequent to the conclusion of testing and taking a micrograph similar to that of Fig. 2b.

III. Results

In Figure 5 are displayed four craze tensile cycles of a series run on a craze which had been grown at 4100 psi, after which the load was reduced to 1300 psi and the specimen left in this condition for seven months. It was then left completely unloaded for seven weeks prior to testing. In the first through the fifth cycles the delay between the end of one cycle and the beginning of the next was one minute or less. Between the fifth and sixth cycles the delay was ten minutes, between the sixth and seventh three hours, between the seventh and eighth two and one-half days, and between the eighth and ninth one month. In Fig. 5 there is also displayed a conventional stress-strain curve for normal polycarbonate up to 6200 psi and return for comparison purposes.

In the first cycle the craze exhibits an initial high modulus region followed by a yield stress at about 2200 psi and a region of largely ductile deformation out to 44% strain at 6200 psi. Upon reversal, drop in stress is accompanied by almost no change in strain down to very low stresses where creep recovery appears to accelerate. The second cycle, begun at a residual strain ϵ_R = 24%, shows a marked reduction in initial slope and in yield stress but an increase in slope of the ductile region. Finally, the fifth cycle shows almost completely elastic behavior; the strong tendency here for creep recovery upon unloading, in addition to slight differences between rates of loading and unloading, cause the return curve to cross over the ascending

branch. Creep recovery at zero stress is rapid at first but decelerates markedly; nevertheless in one month recovery back to ϵ_R = 7% has occurred and a ninth cycle exhibits once more a marked yield stress and hysteresis loop.

Under the best of experimental circumstances the precision in craze strain determination is ± 1-2% which precludes accurate determination of elastic modulus in the initial part of the ascending branch of cycles exhibiting yield stresses. In the case of Cycle #1, $E_{initial} \sim 100,000$ - 150,000 psi is the best estimate possible. Furthermore, in general tne yield stress itself seems to vary from one cycle to the next in a somewhat irregular way, perhaps because the onset of yielding may vary in stress and time from one part of the craze plane to another. Experience shows that the total strain energy $U_{6200} = \int_0^{6200} \sigma d\epsilon$ up to the maximum stress and the loss factor, calculated as the percentage of strain energy contained inside the hysteresis loop, are much more consistently varying quantities. These functions, determined graphically, are plotted for this series of cyclic tests vs. residual strain at the start of each cycle ϵ_R in Figs. 6 and 7 (Specimen #1). Both functions show a recoverable decline with increasing ϵ_R. It is noteworthy that these cyclic fatigue tests have not, to a first approximation, damaged the craze at all, if one may take as evidence that recovery to a given value of ϵ_R confers a quantitative reattainment of corresponding tensile properties.

Shown also here are similar data for two other specimens. The history of Specimen #3 is detailed in the appendix. Specimen #2 was crazed at 3500 psi, strain-dried (1300 psi initial drying

stress) for three and one-half months and testing commenced twelve hours after release from the jig.

The relationships in Figs. 6 and 7 are similar in shape to those for Specimen #1 but are not coincident. It seems likely that such is the case because the strain scales are not necessarily the same for all specimens. That is, differences in craze history prior to testing leave each craze with more or less different degrees of absolute strain (taking $\epsilon_{absolute} = 0$ to correspond to unoriented polycarbonate of normal density). In general it has not been possible to determine craze index of refraction on these crazes accurately enough to calculate $\epsilon_{absolute}$ to within 10 or 20%.[3] However with Specimen #3 the craze was clear enough and of high enough index to make accurate measurement possible and a void content of 39% was calculated for $\epsilon_R = 0$. Since void content = $\epsilon_{absolute}/(1 + \epsilon_{absolute})$, an absolute strain scale could be generated for Specimen #3 craze; it is displayed at the top of both figures.

Then, on the likelihood that the discrepancy between the behavior of Specimen #1 craze and of Specimens #2 and 3 crazes is apparent rather than real, due to differences in absolute strain values at which each test series was begun, an iterative procedure based on shifting ϵ_R for Cycle #1 was used to recalculate values of ϵ_R for all other cycles. Simultaneously the required new values of U_{6200} were calculated. The procedure was repeated until the fit shown by the crossed squares in Figure 6 was obtained ($\epsilon_{R\blacksquare} = 1.15\ \epsilon_{R\square} + .15$). The corresponding loss factor data were also shifted by the same amounts. (Only a horizontal shift is required here since loss factor is a simple percentage having no

dimensions.) The shifts in loss factor are not as successful in making data for these specimens coincident; the improvement in fit is substantial however.

It will be noted that a point for Specimen #3 exists at a negative value of ϵ_R. This point serves to illustrate one of the initially confusing features of craze behavior. In the first cycle of this series ($\epsilon_R = 0$) stress was raised to 6050 psi at which point the specimen fractured at a craze some distance away from the test craze. After fashioning a new grip section for the specimen, testing recommenced at the point $\epsilon_R = -17\%$, the contraction in the test craze having been produced by the sudden release of stress upon fracture which exerts enough of a compressive impact on the craze to produce a significant retraction and density increase. (Indeed in an Instron compressive test most of the reflectivity of a craze will disappear in a few minutes or so under 3000 - 4000 psi pressure.) This behavior is not surprising once understood. It is most disconcerting at first however that, after having applied a programmed tensile stress, one subsequently finds the craze in a state of negative residual strain.

Finally, two partially open points are to be noted at the bottom of the Specimen #3 line. These denote incomplete cycles, as in Fig. 8, which begin and end at about 1000 psi. They were run in this fashion in order to begin at a higher value of ϵ_R than can otherwise be obtained, due to the rapid rate of creep recovery at stresses below 1000 psi. It is clear from these data and the trends displayed in Figs. 6 and 7 that, on this time scale, polycarbonate crazes behave in a very nearly Hookian fashion above absolute residual strains of about 160-170%. From this curve an

elastic modulus E = 47,000 psi is calculated which is 15% of the elastic modulus of unoriented polycarbonate of normal density.

IV. Discussion

Results of low angle x-ray scattering and electron microscopy may be interpreted to suggest that the void content of the craze is dispersed in the form of interconnected spheroidal holes having a common dimension of 100-200 Å, in an oriented polymer matrix.[4,6] On this basis we consider here, as a mechanical model for the craze, a polymer foam of density equal to that of the craze. We consider furthermore that the holes of the foam nucleate at a finite number of sites when the local stress reaches a critical value and grow to a fixed size, further rarefaction taking place by the opening up of new holes.

Of use in testing this model is the relationship between the ratio of foam tensile modulus E_f to bulk polymer tensile modulus E_o and polymer density developed by Gent and Thomas.[7] It is the contention of these authors, successful in terms of comparison with experimental data, that rubber foams may be represented by webs of interconnected filaments of polymer and that neither the specific geometry of the filament nor that of the filament junction has much influence on the ratio E_f/E_o. The cycle shown in Fig. 8 begins at $\epsilon_{absolute}$ = 170% which corresponds to a craze void content of 63%. From Gent and Thomas we have for this density E_f/E_o = .13 and thus a calculated craze modulus of 42,000 psi which is in excellent agreement with the experimental value 47,000 psi aforementioned.

There are, however, two somewhat uncertain factors which cast a cloud over this agreement. First, in the craze formation process the polymer has undergone some degree of molecular orientation as

evidenced by high angle x-ray data[1,6] and by craze birefringence;[8] such orientation is possibly as much as is developed by a corresponding degree of cold drawing. Molecular orientation increases the tensile modulus of bulk polycarbonate and should likewise raise the true modulus of the hypothetical craze filament. By an admittedly long extrapolation of the relationship of Robertson and Buenker[9] for polycarbonate tensile modulus to 170% strain, we calculate a "strain hardening" factor of 2.2. Application of this factor raises the calculated craze modulus to a maximum possible value of 90,000 psi.

On the other hand, we have been forced unavoidably to make comparison of a modulus calculated using the normal polymer modulus E_o determined at small stresses, with a craze secant modulus measured at large stresses. At 6000 psi for example the secant modulus of normal polycarbonate is 190,000 psi. If we use this value instead of E_o together with the strain hardening factor 2.2 we obtain:

$$E_{craze} = \frac{E_f\ (320,000)\ (2.2)}{E_o\ (190,000)} = 55,800 \text{ psi}$$

which again agrees well with the experimental value.

Another approach to understanding craze mechanical properties can be made through consideration of craze yield stress. In Fig. 9 the dependence on absolute strain of the yield stress is exhibited. The data shown were taken from only those cycles where such a stress could be reasonably estimated. In spite of the degree of scatter the drop in yield stress with increasing strain is readily apparent. An attempt to calculate this dependence is set forth as follows.

First we assume somewhat arbitrarily that the craze initiation stress under rate conditions similar to those of the testing cycles used here would be close to the conventional shear-deformation yield stress 8000 psi were craze formation to occur in the dry polymer. Craze initiation under dry conditions actually is suppressed by the beginnings of homogeneous orientation at lower stresses so that under these conditions the craze initiation stress cannot be directly determined. That is, homogeneous orientation is somewhat more effective in making crazing more difficult than in so doing to shear deformation. Second we assume that the rarefaction of an existing craze involves microscopically the same value of stress as is required in craze initiation but that again the foam factor causes the apparent craze yield stress to be lower than the microscopic stress. Thus the curves labelled #1 and #2 in Fig. 9 simply represent the reduction in apparent craze yield stress due to rarefaction brought about by multiplying the arbitrary stresses 8000 and 8800 psi respectively by the foam factor E_f/E_o. Agreement appears reasonably good.

According to Robertson, however, preorientation of polycarbonate causes an increase in the yield stress associated with cold drawing σ_{CD} according to the relationship $\sigma_{CD}(\Omega) = \sigma_{CD}(0)\ [1 + b\Omega^{\alpha}]$ where Ω is the degree of orientation defined ultimately by birefringence and the constants b and α are found to equal 1.21 and 1.61 respectively for data up to the maximum value of Ω produced by him ($\sim$ 50%). If with some trepidation we extrapolate this "strain hardening" relationship over the range of Ω from 60 to 140% we calculate a set of strain hardening factors which, when combined with Curve #1 produces Curve #3 in

Fig. 9 which gives a decidedly poorer fit to the data.

At present then it seems fruitless to attempt further speculation about these aspects of craze mechanical properties. Data is needed on: (1) the effects of higher degrees of orientation on bulk polymer modulus and yield stress; (2) quantitative degrees of molecular orientation in crazes; and (3) a better understanding of craze microstructure.

Fig. 10 shows the creep recovery behavior of Specimen #3 after the last cycle and also that of a cold drawn bar. After three and one-half months, craze recovery appears to be continuing still. The linear behavior here also means that $\partial \ln(-d\epsilon/dt)/d\epsilon$ = constant for both bodies; appropriate plotting shows $-d\epsilon/dt$ for the bar dropping much more steeply with decreasing ϵ and the rates cross over at $\epsilon = 106\%$. The continued recovery of the craze implies that it is not only in a higher energy state than that of the unoriented polymer but that its state is apparently not thermodynamically metastable at any strain level. It seems likely that the driving force for craze-creep recovery arises from the molecular configurational entropy and from the free energy of the large specific internal surface area.

We may estimate the stress due to molecular configurational entropy from rubber elasticity. At 160°C which is about 15° above T_g polycarbonate exhibits an elastic modulus at the beginning of the rubber plateau of 800 psi.[11] We suggest then that in the craze at 100% absolute strain and at room temperature the configurational retractive stress is of the order of several hundred psi. (We make no quantitative calculation because of the uncertain temperature correction which would have to be applied

to chain entanglement molecular weight inter alia.)

One way to estimate crudely the internal retractive stresses arising from the surface energy is to consider again that the material in the craze is dispersed in the form of long cylindrical filaments of radius r and greater length h connected to other polymer elements at each end. The volume of the filament is then $V = \pi r^2 h$ and its free surface area $2\pi rh$. Keeping the filament volume constant we may express the filament surface area as

$$A = 2\pi^{1/2} V^{1/2} h^{1/2}$$

and any change in area due to change in length at constant volume

$$dA = \pi^{1/2} V^{1/2} h^{-1/2} dh.$$

The change in total surface free energy of the filament F is

$$dF = \bar{F} dA = \bar{F} \pi^{1/2} V^{1/2} h^{-1/2} dh$$

where $\bar{F}$ is the specific surface free energy of the polymer. Now we may designate the change in energy with decrease in h, dF/dh, as a free energy gradient corresponding to the net force f_h acting in the h direction. Therefore we obtain

$$f_h = dF/dh = \bar{F} \pi^{1/2} V^{1/2} h^{-1/2} = \bar{F} \pi r$$

The net retractive stress then acting in the h direction is

$$\sigma_h = f_h/(\pi r^2) = \bar{F}/r.$$

We set r = 50 Å and $\bar{F}$ = 40 ergs/cm^2 a reasonable estimate of the polycarbonate surface energy (e.g. Ellison and Zisman[12] set the critical surface tension of polystyrene at 33-43 dynes/cm). Consequently,

$$\sigma_h \simeq 1200 \text{ psi.}$$

The estimated total retractive stress is rather low compared,

for example, to the conventional yield stress for polycarbonate. It must be remembered, however, that recovery rate here is much lower than any of the conventional testing rates at which yield stress, which is rate-dependent, has been measured.

It is conceivable, furthermore, that the degree of polym dispersion in the craze also aids chain motion by effectively lowering the glassy state viscosity. In the Nabarro-Herring treatment of the vacancy-limited creep of a crystalline solid, viscosity is considered to increase with δ^2 where δ is the distance between vacancy sinks. Greet and Turnbull[13] discuss such a concept in regard to the glass transition and suggest that in the perfect glass such distance δ may approach body dimensions. If such were the case, the viscosity of a 100 Å diameter oriented craze filament, assuming it to be perfect, would be reduced by a factor as large as 10^{12} from that of the normal polymer glass.

In studies of the glass transition in polystyrene, Braun and Kovacs[14] find no decrease in T_g for particles in the range 1000 to 10,000 Å in diameter. Thus 10^3 Å is probably the upper limit for δ for real glasses and we could therefore expect a reduction in the viscosity of the craze filament of no more than 10^2.

Considerations of this kind are of course highly speculative but nevertheless the influence of free surfaces upon the ease of craze formation is experimentally observable. Crazes are always more easily initiated at the polymer surface than internally; although the importance of surface flaws cannot be denied, the fact that surface initiation is favored even in carefully cast and annealed films implies that molecular motion is enhanced by the presence of a free surface.

Furthermore the reality of surface tension effects is reinforced by the healing record of a bar crazed as were the ones for tensile testing. After completion of craze formation the specimen was unstressed but left in the alcohol bath for nineteen hours during which time craze refractive index rose from 1.46 to 1.475. The bar was then removed and the much faster rate of craze index rise indicated in Fig. 11 observed. Analogous behavior has been observed here with polymethyl methacrylate crazes also. The role of organic agent in craze formation has variously been considered to be that of surface agent or alternatively plasticizer. Were plasticization the only role of alcohol here, then craze healing would have been fastest in the bath where the source of the agent is unlimited. Once the specimen was removed, however, alcohol supply in the craze was finite and diffusion away into the bulk polymer probably resulted in internal surface area no longer covered by liquid and thus the craze now was subject to markedly increased surface retractive forces. But also craze healing in the bath is faster than retraction of the completely dry craze. The combination of these observations and the known 7% solubility of alcohol in the polymer indicates that the role of alcohol in so-called solvent crazing is both that of surface stabilizer and plasticizer.

In general then, we view craze extension as being qualitatively no different from craze formation. The macroscopic yield stress observed appears to correspond to the attainment microscopically of the stress necessary for further hole formation. It is primarily the geometric factors of the type involved in foam properties which cause a lowering of this macroscopic stress

and a reduction in macroscopic modulus. In other words, although the molecular orientation entailed in craze formation and extension probably results in some degree of microscopic "strain hardening," the geometric effect of void formation is overriding and thus microscopically craze formation and extension result in a "strain softened" section of material. One way of some use in quantitatively describing such softening is to define the ratio of the craze initiation stress (i.e. 8000 psi ca.) to the absolute strain produced ultimately at this stress (200% ca.) as a kind of modulus, a craze formation secant modulus, which in this case then has the value 4000 psi. At this level of stress the secant modulus of polycarbonate is roughly 150,000 psi so that in this sense the polymer acts forty times more compliant in full craze formation than it does elsewhere at this stress level.

We expect that observations and considerations of the kind discussed herein will be of use in analyzing craze and crack propagation forces and kinetics. They are also of use in understanding the details of energy absorption during stress whitening of rubber modified polymers. Bucknall and coworkers[15] have shown that massive amounts of craze formation are associated with stress whitening and impact energy absorption in rubber-modified thermoplastics. Inspection of cyclic tensile curves to stresses above the craze formation yield stress reveals both an average secant modulus which drops with increase in craze formation and the presence at low stresses of a recoverable yield stress which we identify as the manifestation of the yielding of crazes previously formed.

Appendix

Specimen #3 was crazed at 3500 psi and unstressed and removed from the alcohol bath simultaneously. Over the following two days craze index of refraction rose from 1.46 to 1.52 indicating a large degree of healing. The specimen was then restressed at 3500 psi in air which caused most of the crazes to develop quickly a low refractive index; raising the stress to 3800 psi caused the remainder similarly to redevelop. Stress was then removed, craze refractive index immediately measured (1.33) and the bar left unstressed for three weeks during which time craze index did not change. Tensile testing was then commenced. With this specimen $\ell_{t,o}$ was determined by grinding and polishing down the surface subsequent to the finish of testing and obtaining a photomicrograph similar to Fig. 1b, at known magnification.

The manner of craze redevelopment under the second stressing is of considerable interest. Rather than gaining high reflectivity by a gradual, homogeneous opening up over the whole craze at once, the process occurred in a heterogeneous way much analogous to craze formation itself. That is, one edge of the craze became "redeveloped" and redevelopment spread out from this point, growing through the particular craze in a matter of seconds to almost an hour depending on the individual craze. The boundary between the growing, highly-reflecting region and the remainder of the partially healed region was sharp at all times. Thus in spite of being "prenucleated" over the whole craze plane by the residue of voids, craze redevelopment occurred by abrupt and more or less complete expansion of each element in its turn. Such a process is understandable by analogy with the reduction in yield

Appendix (continued)

stress of the craze with increase in void content; that is, once the process begins in a region that region becomes more compliant and expansion continues until orientation eventually overcomes the effect of loss of true load bearing cross section through void formation.

Acknowledgments

The authors wish to thank Mr. R. H. Savage for advice concerning photomicroscopy, and Drs. R. E. Robertson and J. M. O'Reilly and Prof. A. N. Gent for fruitful discussions of craze behavior.

References

1. J. A. Sauer, J. Marin and C. C. Hsaio, J. Applied Phys., 20, 507 (1949).

2. O. K. Spurr and W. D. Niegisch, J. Applied Polymer Sci., 6, 585 (1962).

3. R. P. Kambour, Polymer, 5, 107 (1964).

4. R. P. Kambour, J. Polymer Sci., A2, 4, 349 (1966).

5. Winter Meeting, Society of Rheology, Santa Barbara, Calif., Jan. 28-29 (1965).

6. R. P. Kambour, D. G. LeGrand and W. R. Haaf, unpublished work.

7. A. N. Gent and A. G. Thomas, J. Applied Polymer Sci., 1, 107 (1959).

8. G. A. Bernier and R. P. Kambour, unpublished observations.

9. R. E. Robertson and R. J. Buenker, J. Polymer Sci. A, 2, 4889 (1964).

10. R. E. Robertson, General Electric Research Laboratory Report No. 64-RL-3599C, March 1964.

11. J. P. Mercier, J. J. Aklonis, M. Litt and A. V. Tobolsky, J. Applied Polymer Sci., 9, 447 (1965).

12. A. H. Ellison and W. A. Zisman, J. Phys. Chem., 58, 503 (1954).

13. R. J. Greet and D. Turnbull, J. Chem. Phys., 46, 1243 (1967).

14. G. Braun and A. J. Kovacs, Physics and Chemistry of Glasses, 4, 152 (1963).

15. C. B. Bucknall and R. R. Smith, Polymer, 6, 437 (1965); C. B. Bucknall and D. G. Street, Soc. Chem. Industry Monograph No. 26, in press; C. B. Bucknall, British Plastics, in press.

Figure Captions

Fig. 1. Contrast between complete, isolated craze which is useful for testing and an incomplete one which is of no use.

Fig. 2. Photomicrographs of bar surface showing: (a) indentation associated with craze; and (b) the same craze after surface grinding and polishing showing that the groove width is greater than true craze thickness. (Thickness here is 0.01 mm)

Fig. 3. Craze tensile testing apparatus.

Fig. 4. Force-time program in the typical cyclic tensile test of the craze. Vertical marks record stresses at which photomicrographs were taken.

Fig. 5. Four cycles in a series of cyclic tensile tests on a polycarbonate craze. See text for delay times between cycles. Also included is cyclic tensile curve for normal polycarbonate. Stressing rate of the craze in the linear portion of the load-time curve was 500 psi/min approximately.

Fig. 6. Dependence of total strain energy of craze U_{6200} up to the maximum stress upon residual strain ϵ_R for three specimens. See text for definition of absolute strain scale. See text for method of shifting Specimen #1 data.

Fig. 7. Dependence of loss factor of craze upon residual strain ϵ_R at start of cycle. See text for details of Specimen #1 data shift.

Figure Captions (continued)

Fig. 8. Incomplete cycle corresponding to one of the partial circles in Figs. 6 and 7. Minimum stress between preceding cycle and this one was 1000 psi.

Fig. 9. Yield stress of the craze vs. absolute strain for three specimens. Data for specimen #1 are strain-shifted as before.

Fig. 10. Creep recovery of Specimen #3 craze after tenth cycle and of cold-drawn polycarbonate bar vs. log time.

Fig. 11. Rise in refractive index n with time for polycarbonate crazes: (a) for a bar which is unloaded and removed from alcohol simultaneously; and (b) for a bar unloaded but left in alcohol for first nineteen hours before removal.

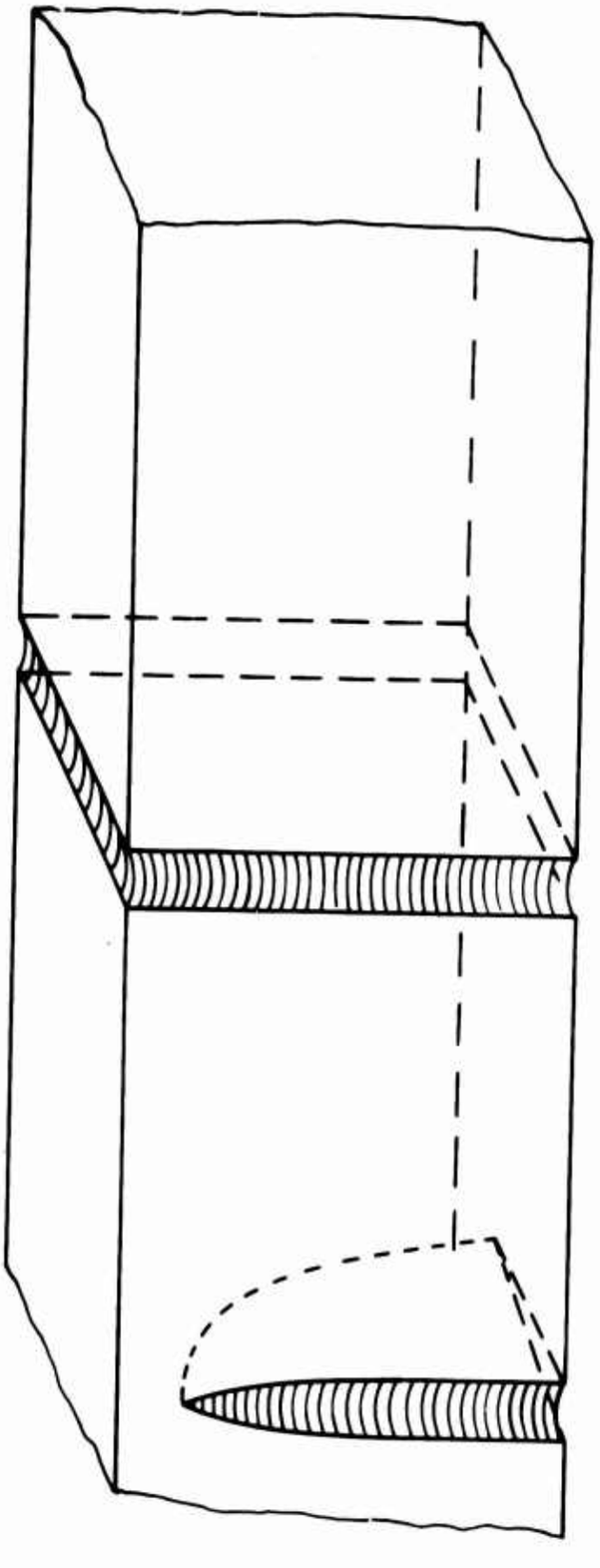

Fig. 1

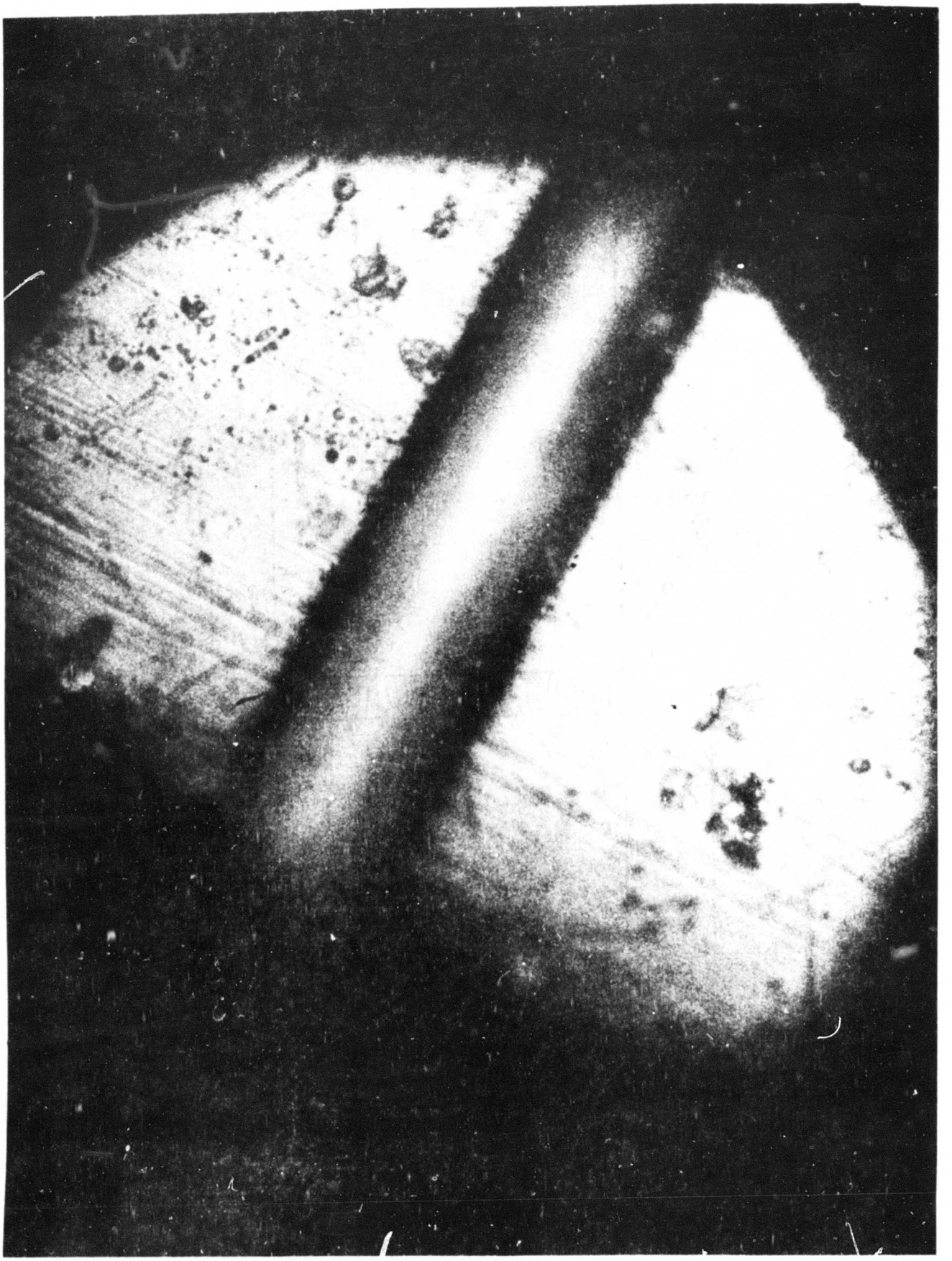

Fig. 2 a

Fig. 2b

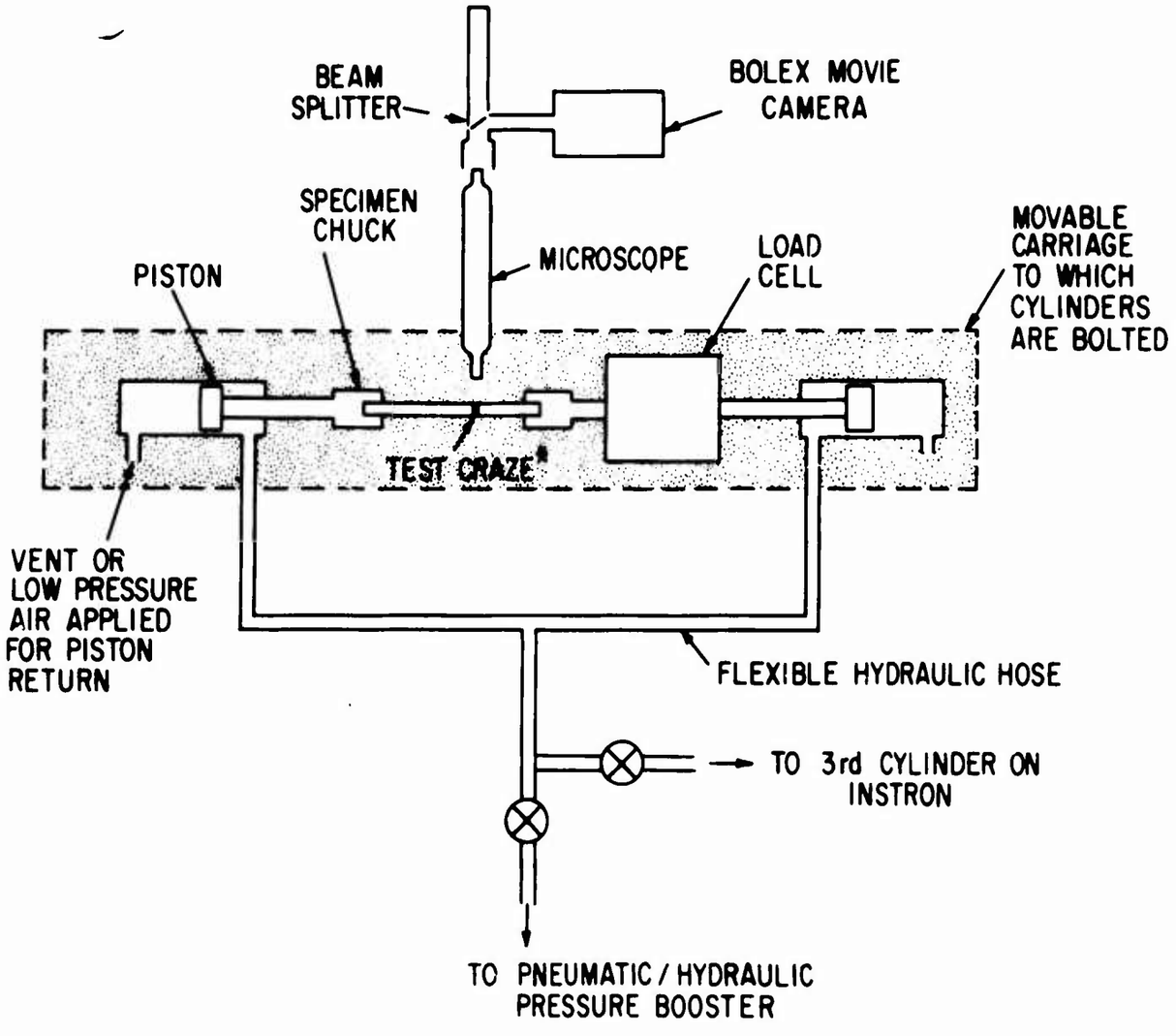

* MICROSCOPE STAGE AND CRAZE PINNING DEVICE NOT SHOWN

Fig. 3

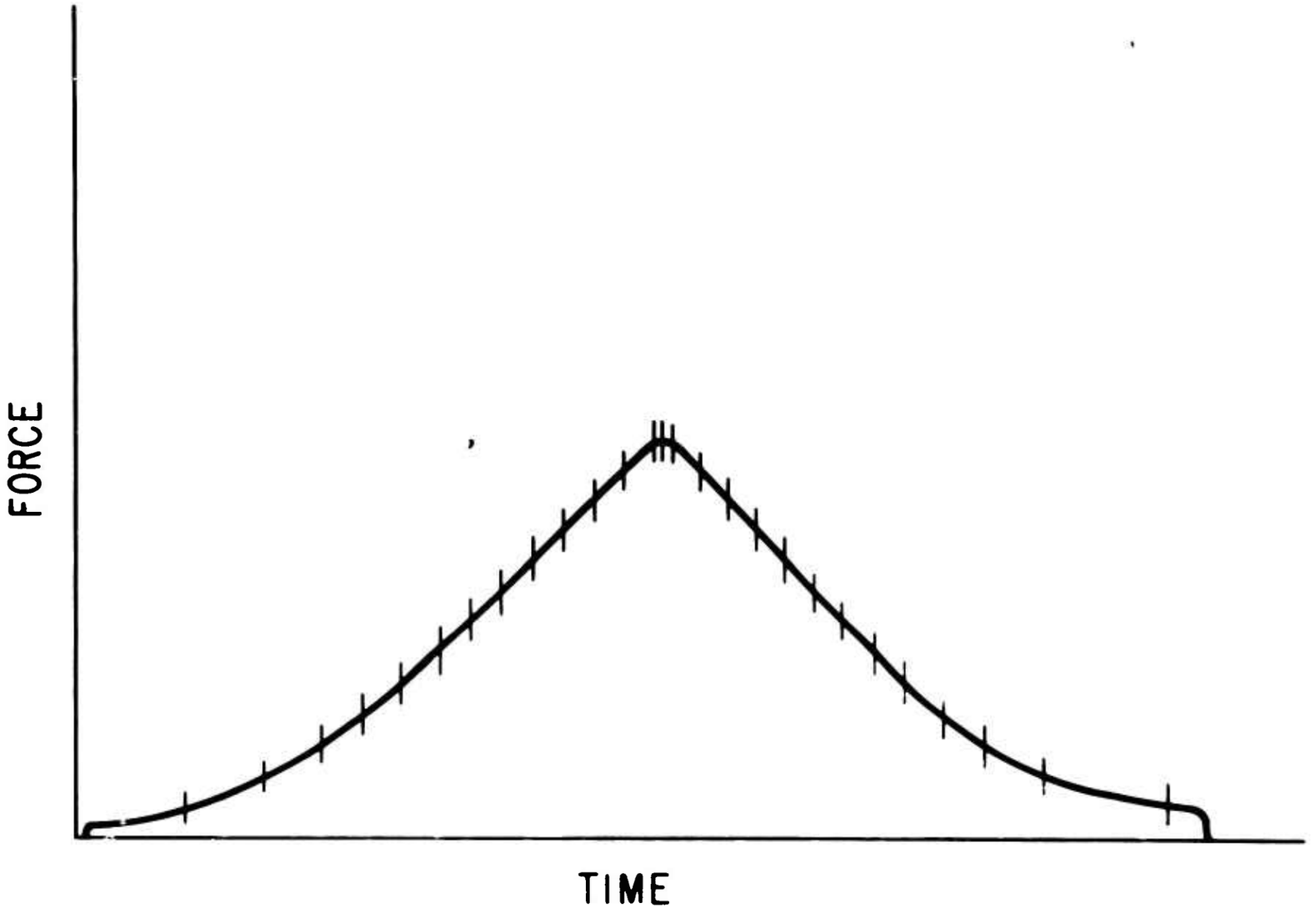
FORCE
TIME

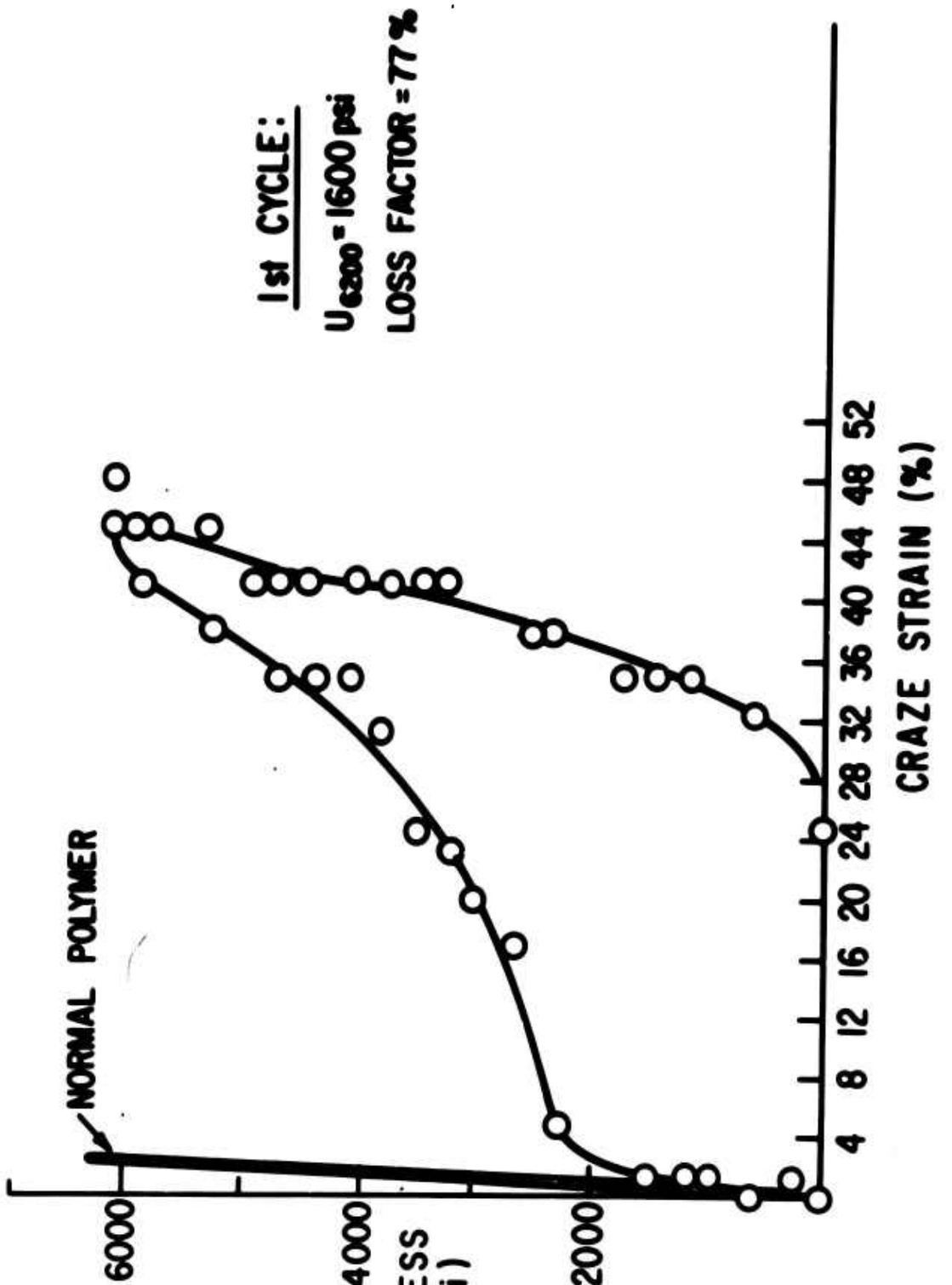
1st CYCLE:
U_{e200} = 1600 psi
LOSS FACTOR = 77 %
NORMAL POLYMER
6000
4000
2000
STRESS (psi)
4 8 12 16 20 24 28 32 36 40 44 48 52
CRAZE STRAIN (%)

Fig. 5a

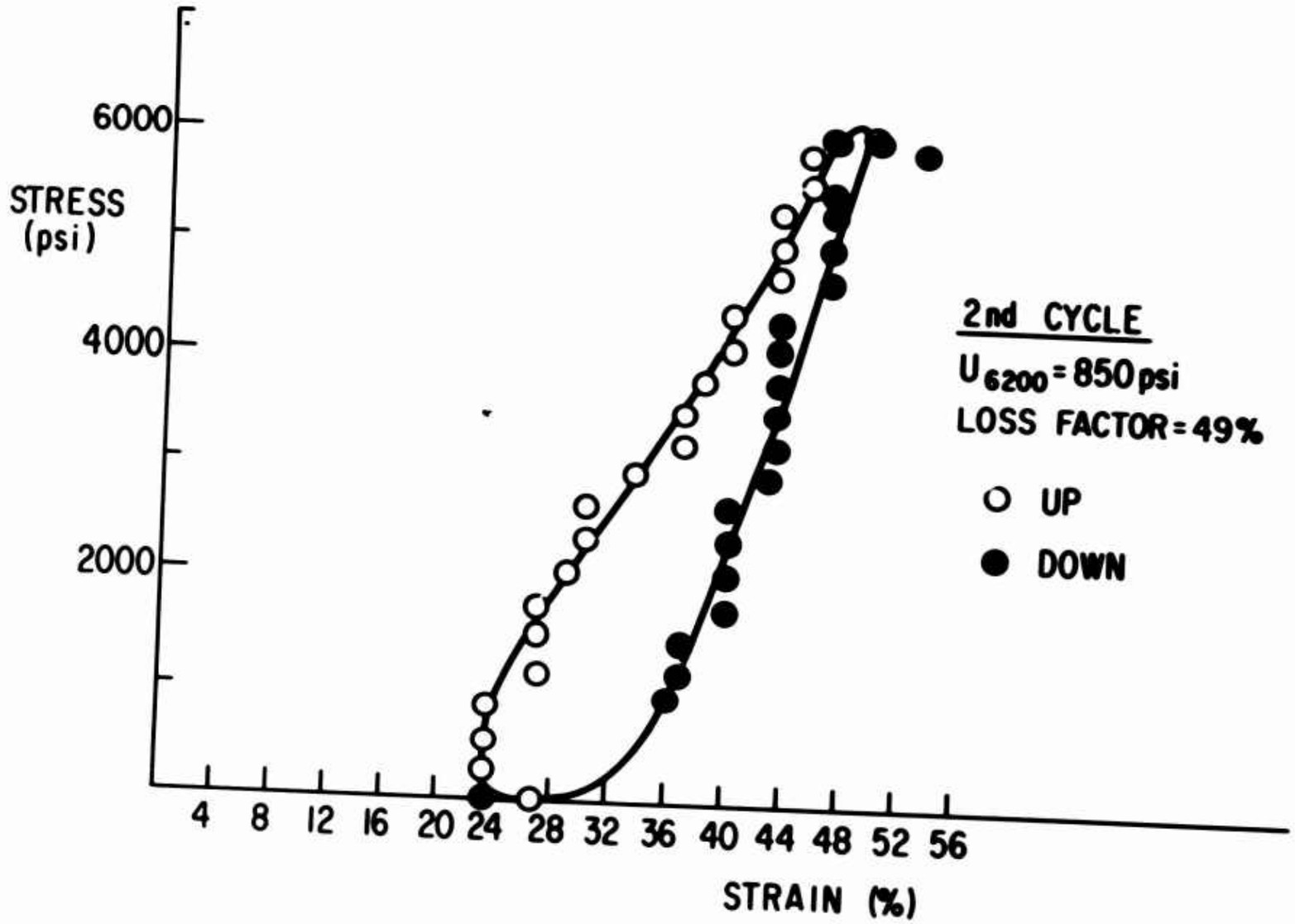
6000
4000
2000
STRESS
(psi)
2nd CYCLE
U6200 = 850 psi
LOSS FACTOR = 49%
UP
DOWN
4 8 12 16 20 24 28 32 36 40 44 48 52 56
STRAIN (%)

Fig. 5b

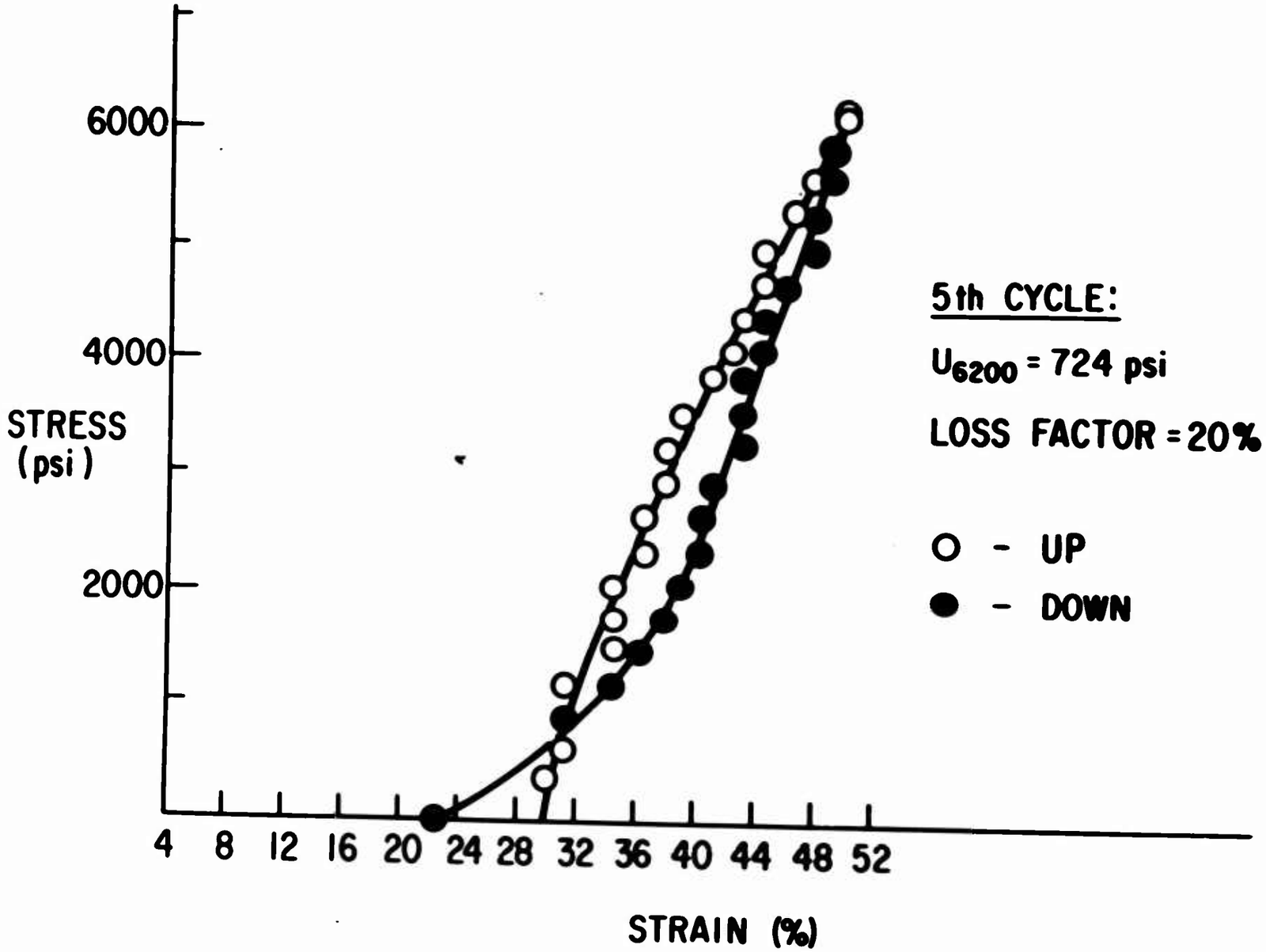
6000
4000
2000
STRESS
(psi)
4 8 12 16 20 24 28 32 36 40 44 48 52
STRAIN (%)
5th CYCLE:
U_{6200} = 724 psi
LOSS FACTOR = 20%
○ - UP
● - DOWN

Fig. 5c

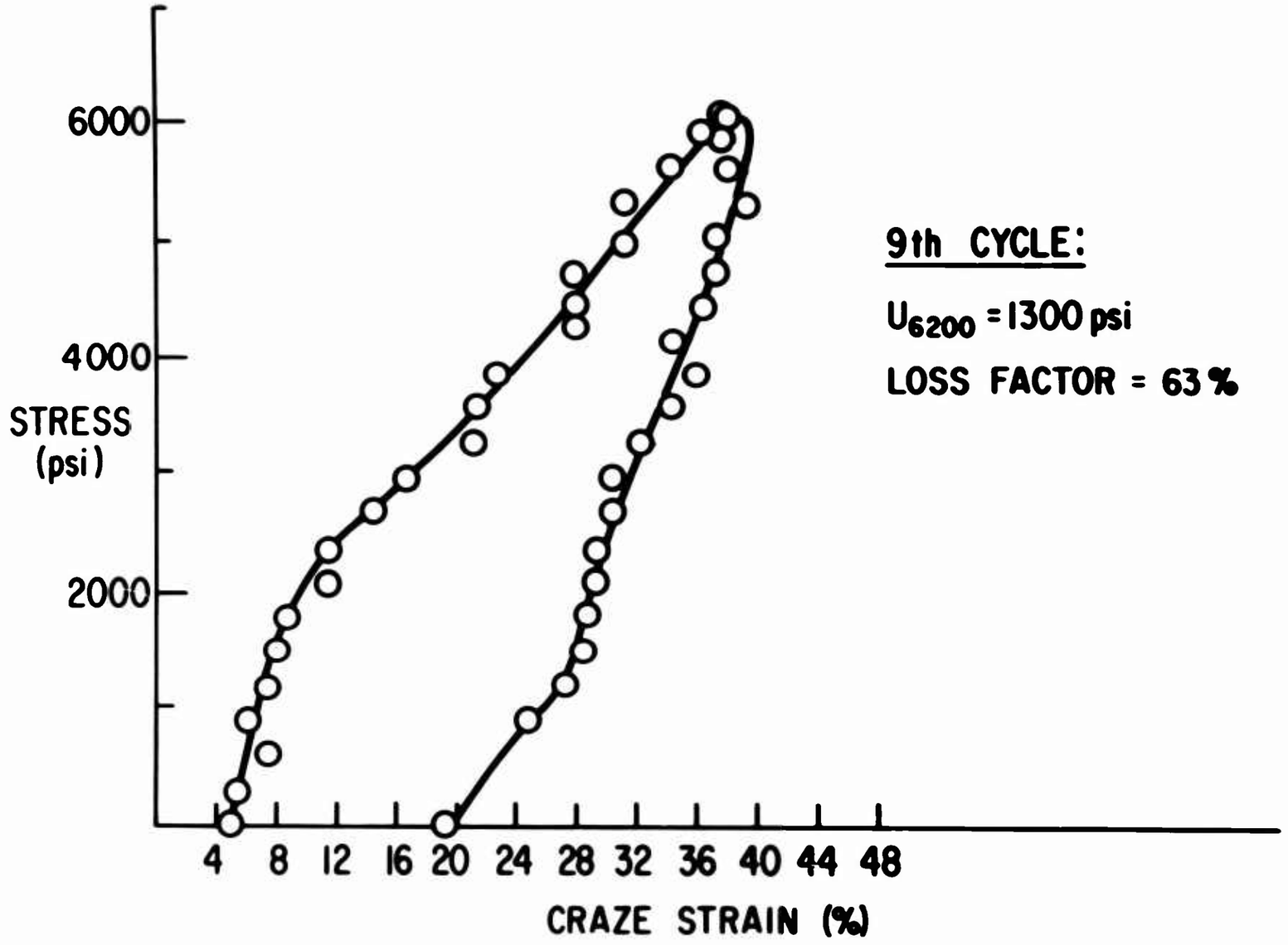
6000
4000
2000
STRESS
(psi)
4
8
12
16
20
24
28
32
36
40
44
48
CRAZE STRAIN (%)
9th CYCLE:
U_{6200} = 1300 psi
LOSS FACTOR = 63 %

Fig. 5d

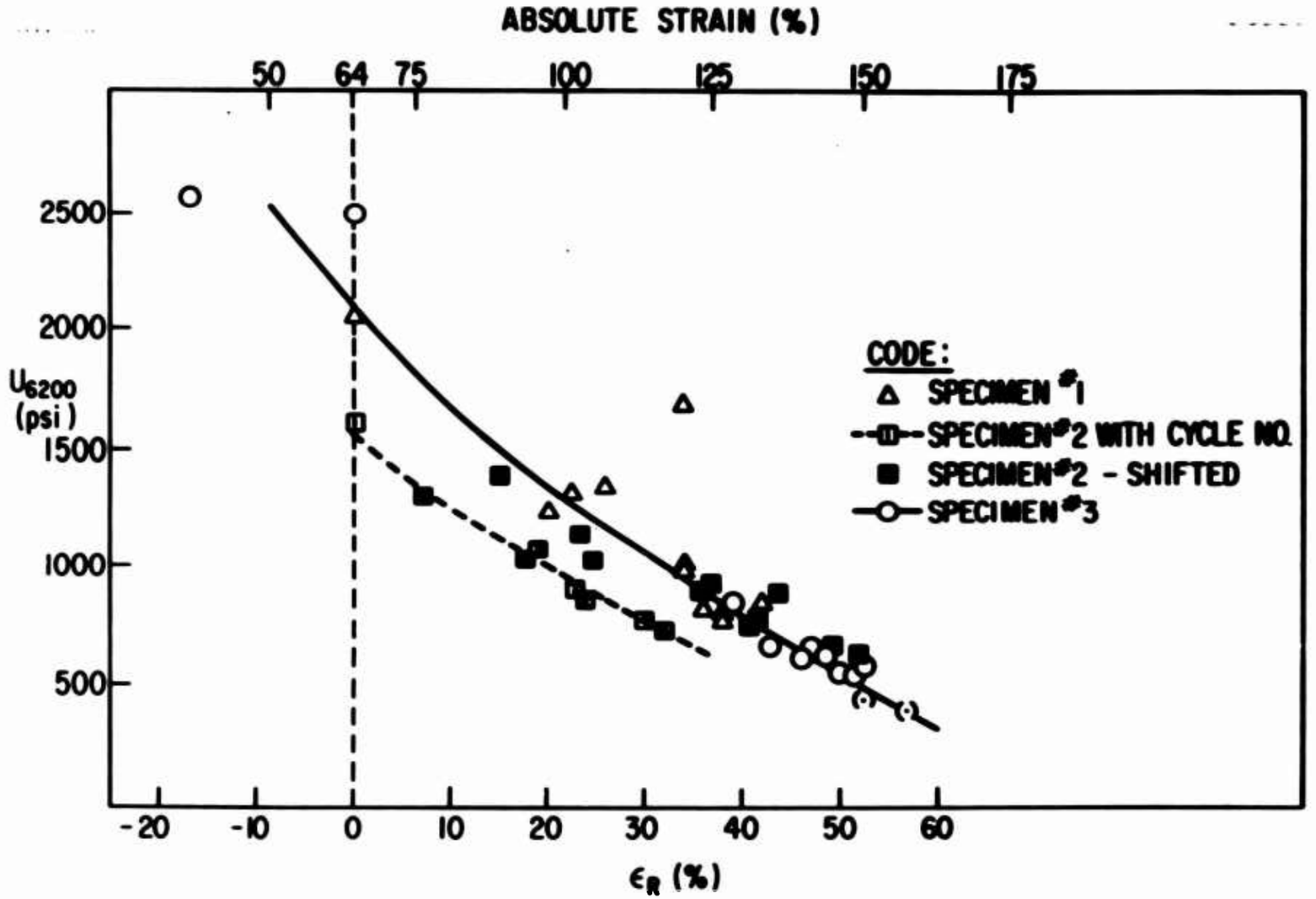
ABSOLUTE STRAIN (%)
50
64
75
100
125
150
175
2500
2000
1500
1000
500
U_{6200} (psi)
CODE:
SPECIMEN #1
SPECIMEN #2 WITH CYCLE NO.
SPECIMEN #2 - SHIFTED
SPECIMEN #3
-20
-10
0
10
20
30
40
50
60
ϵ_R (%)

Fig. 6

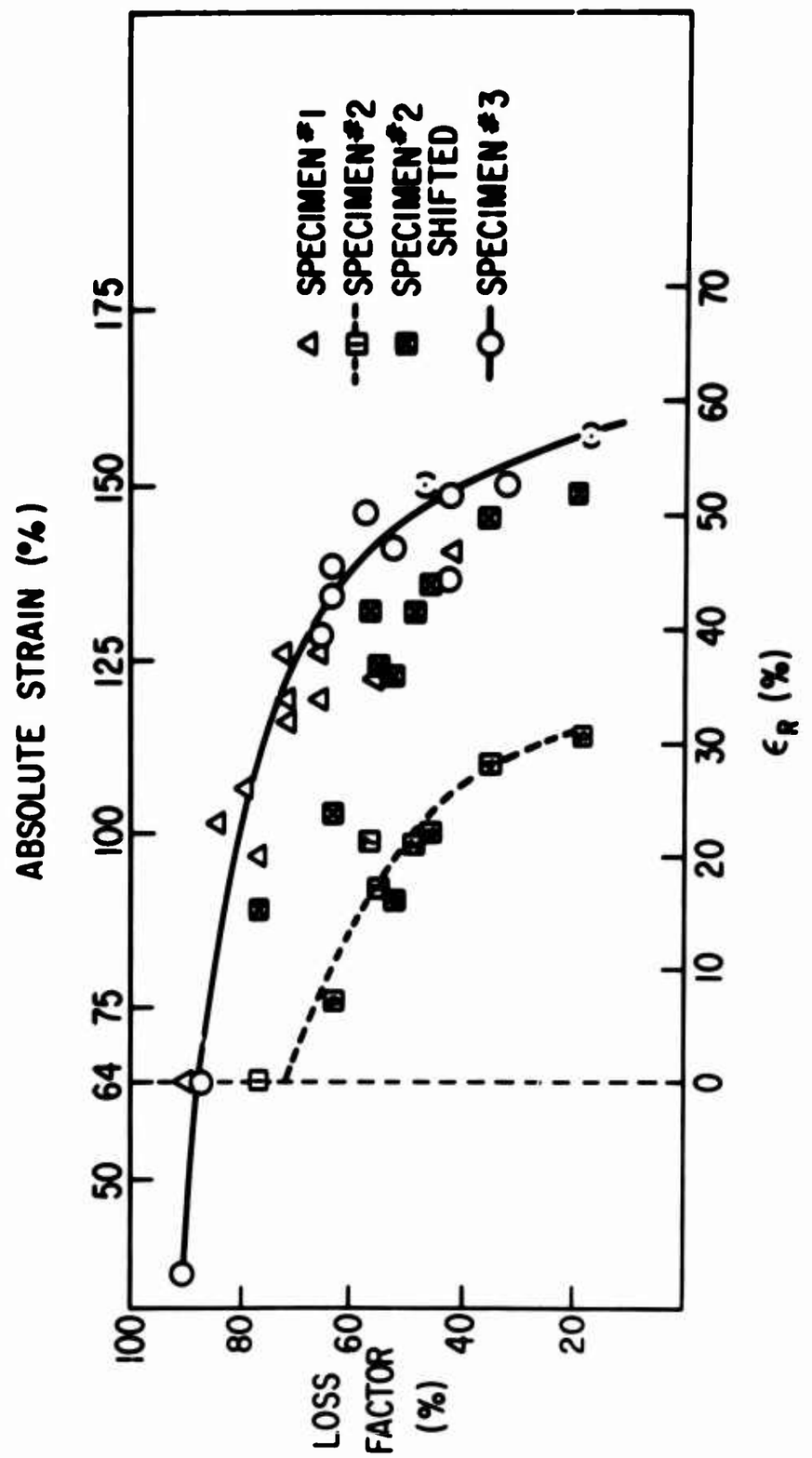
ABSOLUTE STRAIN (%)
50
64
75
100
125
150
175
LOSS FACTOR (%)
100
80
60
40
20
0
10
20
30
40
50
60
70
ϵ_R (%)
SPECIMEN #1
SPECIMEN #2
SPECIMEN #2 SHIFTED
SPECIMEN #3

Fig. 7

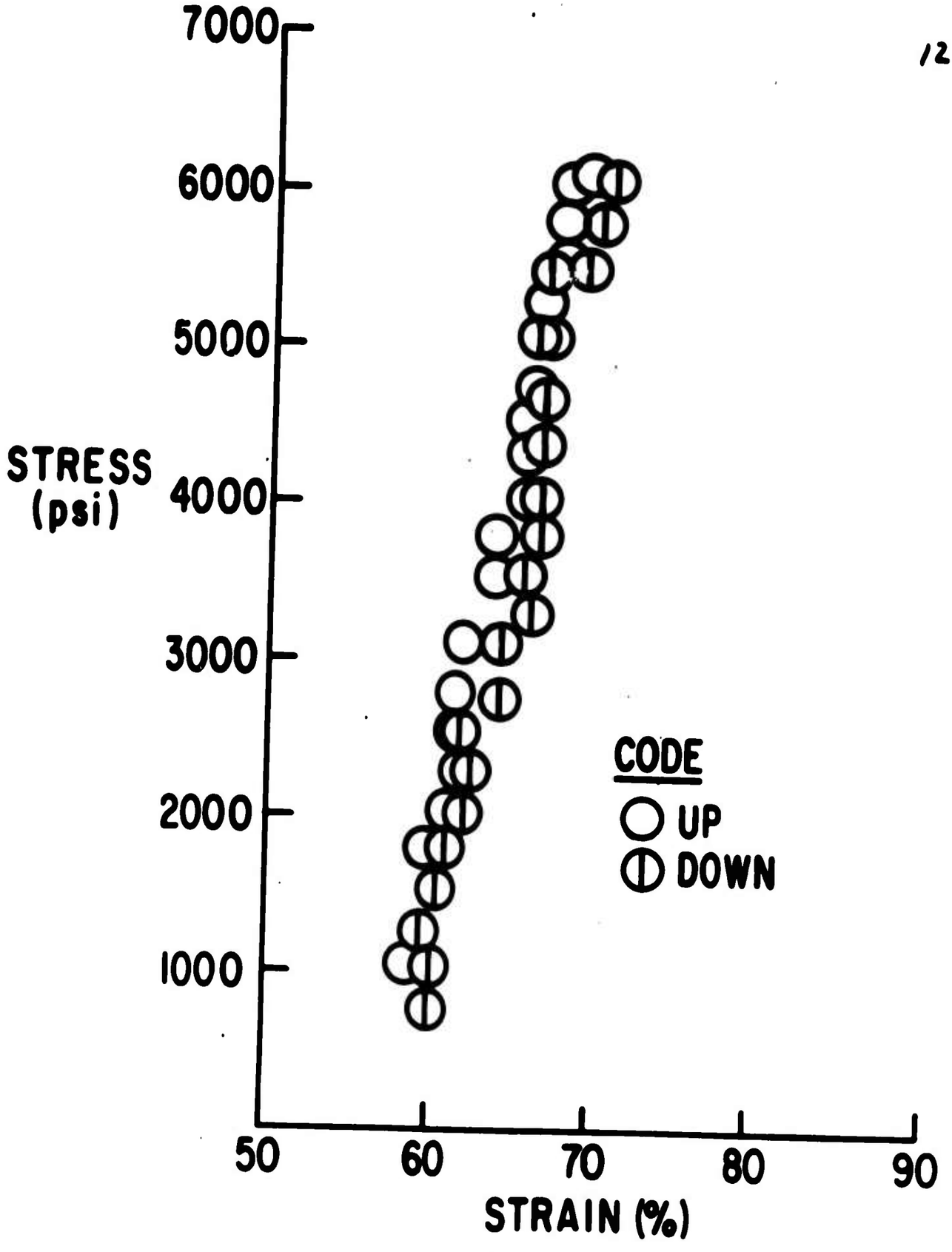
7000
6000
5000
4000
3000
2000
1000
STRESS (psi)
CODE
UP
DOWN
50
60
70
80
90
STRAIN (%)

Fig. 8

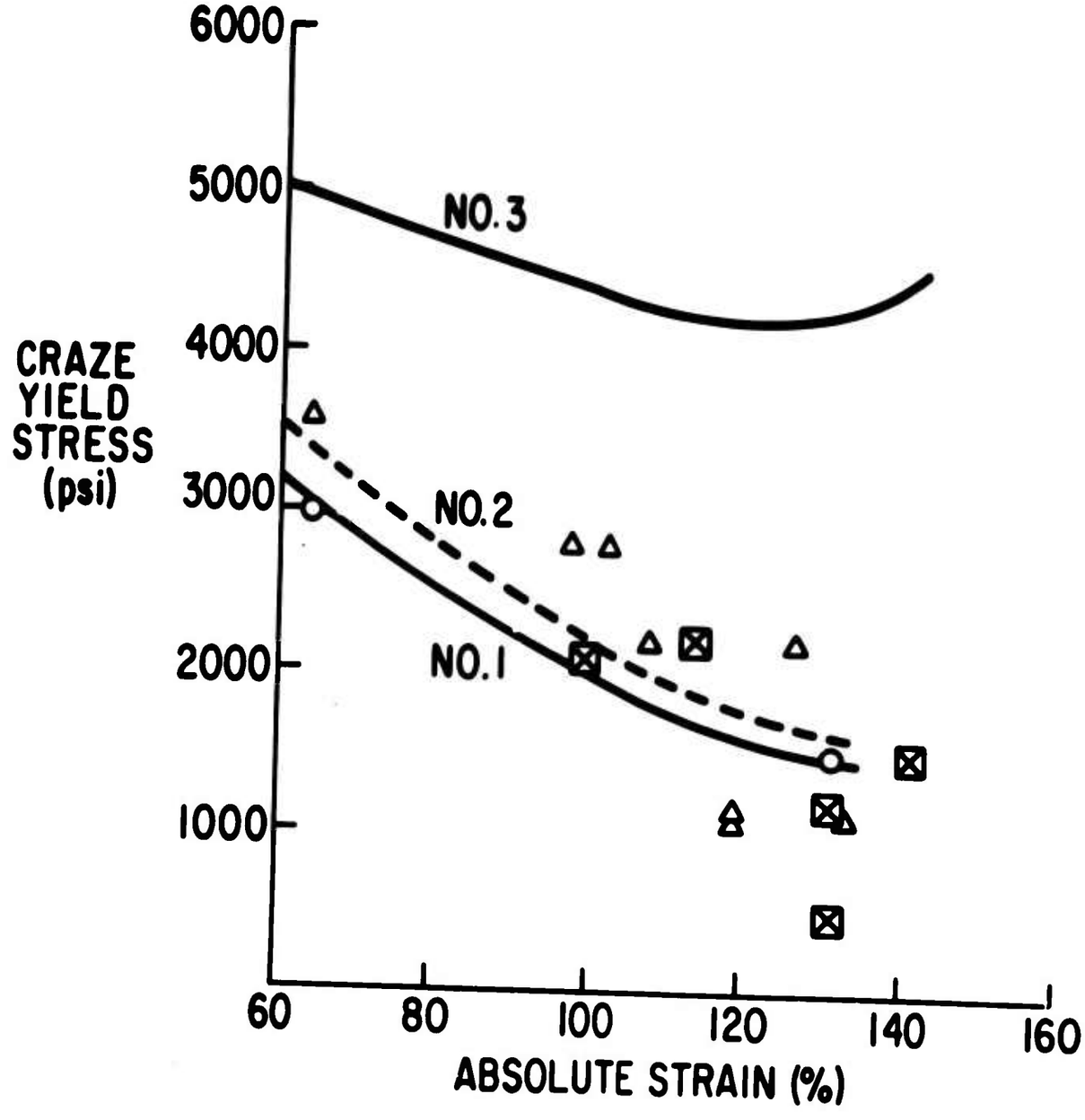
6000
5000
4000
3000
2000
1000
CRAZE
YIELD
STRESS
(psi)
NO.3
NO.2
NO.1
60
80
100
120
140
160
ABSOLUTE STRAIN (%)

Fig. 9

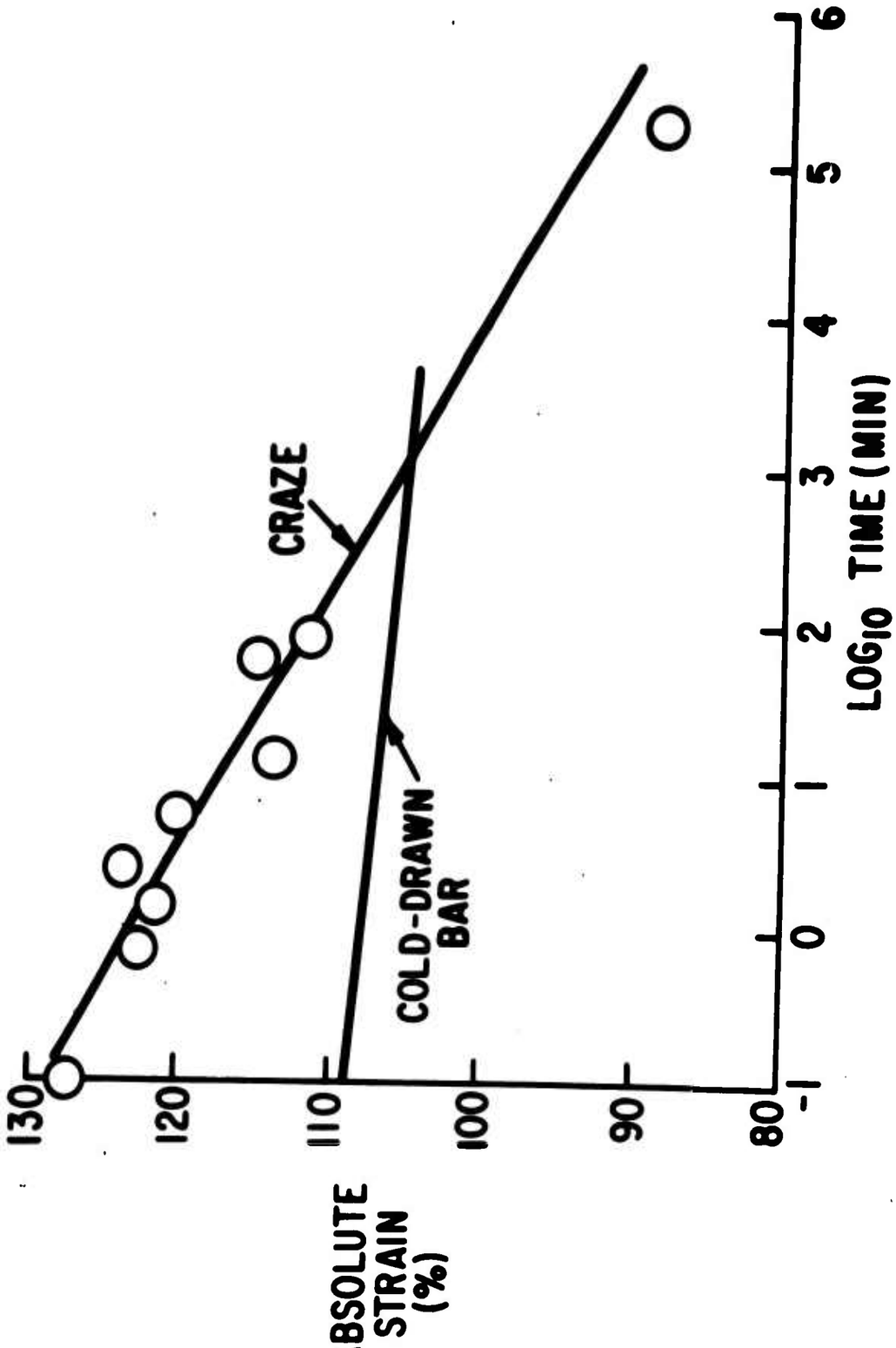
ABSOLUTE STRAIN (%)
130
120
110
100
90
80
CRAZE
COLD-DRAWN BAR
-1
0
1
2
3
4
5
6
LOG10 TIME (MIN)

Fig. 10

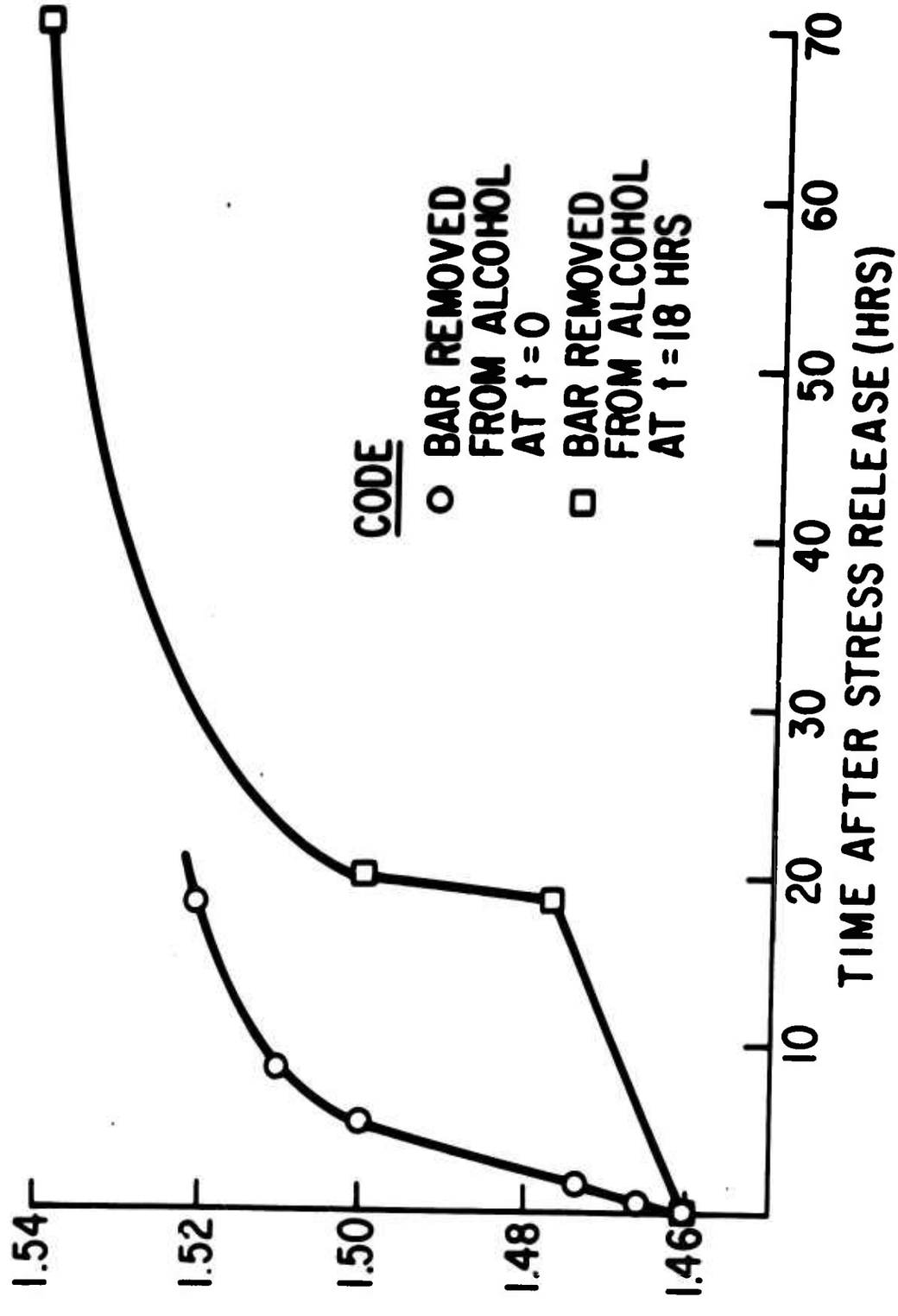
1.54
1.52
1.50
1.48
1.46
n
10
20
30
40
50
60
70
TIME AFTER STRESS RELEASE (HRS)
CODE
○ BAR REMOVED FROM ALCOHOL AT t=0
□ BAR REMOVED FROM ALCOHOL AT t=18 HRS

Fig. 11

"POLYMER CRYSTALS - GOOD AND BAD"

by

H. D. Keith
Bell Telephone Laboratories, Incorporated
Murray Hill, New Jersey

According to the printed program I am supposed to spend 50 minutes presenting a critical review of polymer morphology. Considering the vast literature that now exists it would indeed be easy to consume much longer than this and still cover only a few selected highlights. But what, I wonder, can I possibly tell you that is not already widely and well known? What can I say that would be new and also true? I doubt if the fundamental understanding of the subject is soundly enough based at this point in time for anyone to feel confident that he can discern unassailable truths of interpretation that may not be upset within months.

So with these thoughts, or perhaps I should say misgivings, in mind I have decided to curtail this introductory address. In doing so I am sure I will have your approval; but I also hope that, by leaving additional time for a more general exchange of views, this will add to the value of the session in the spirit in which this conference has been conceived. With the prior agreement of our general chairman, I propose to speak for 25 minutes at most so that we may take the first research paper and questions relating to it before the coffee break, and in this way leave extra time for discussion.

For 10 years we have had in the morphological approach to polymer science a remarkably vigorous and stimulating outpouring of new discovery. We have come a long way and we certainly hope to go much further. But for the moment the pace of advance has slowed. This is therefore an excellent time to take stock; but with programs of most meetings so crowded now with formal presentations it is all too seldom that a goodly number of us have an opportunity to take stock together. What we need above all, I think, is a good "bull session" and the success of this morning's proceedings will be gauged in large measure by the extent to which we profit by the opportunity they afford to have just that.

My function, then, as I see it in this light, is simply to get you in the right mood for discussion and argument, to raise a number of provocative questions for critical inspection and fresh thinking, questions that may also serve as catalysts for the introduction of other topics. Obviously there are many more topics worthy of consideration than those that I intend to emphasize - and my choice is personal, though I doubt if others in my shoes at this moment would exercise a choice that is much different. If I omit someone's favorite topic or do less than justice to another's contribution, no slight is intended; it is inevitable that I must do so.

One point in particular, I think all would agree, is unusually timely for special emphasis. This concerns

details of the folded conformations of linear chain molecules in lamellar polymer crystals. Is there very regular, essentially idealized, folding so that we may have what I choose to call "good crystals", or is there irregular, loopy folding giving rise to what, to emphasize the contrast, I call "bad" crystals? And in either case what happens to the chain ends and what part do they play in the properties of the crystals? Now, what is good or bad depends on your outlook, but there is little point in preferring good crystals to bad crystals merely because the good crystals are conceptually much simpler to describe and analyze. We have to make do with what nature gives us. Our problem above all is to recognize precisely what this is. On one hand, there is unmistakable evidence in the case of chain folded crystals that invites thinking in terms of the ideal state of affairs and, on the other, equally convincing evidence that compels us to turn our thoughts in the opposite direction. Our two principal speakers this morning, Professor Fischer and Dr. Lindenmeyer, will develop these two lines of evidence, to which each in his own sphere is an outstanding contributor. They are not fundamentally in conflict, but presumably will describe different aspects of a subtle but unified underlying reality. The recognition of this reality is one of the most pressing problems of the moment.

In order to set the stage for their papers, let me begin my review in the only fitting way by going back exactly a decade to early 1957 when Till published his paper on lamellar single crystals of polyethylene, to be followed within months by the independent work of Fischer and of Keller. But, in passing, I should pay admiring respects to Jaccodine who had really made the discovery a few years previously and particularly to Storks who had foreseen chain folding as early as 1938. Both, unfortunately, suffered the penalty that is often exacted from those who conceive thoughts out of season.

The first slide shows an electron micrograph of a monolayer single crystal of polyethylene grown from dilute solution in xylene. It is about 100A thick, looks for all the world like a paraffin crystal (apart from a central pleat) and, as electron diffraction shows, has the chain molecules aligned more or less normal to its own plans. From this evidence Keller drew the conclusion that the chains crystallize by folding, a conclusion that has revolutionized our thinking and provided the essential stimulus for so much of the excitement of recent years. The first shock of novelty over, thoughts turned primarily in two directions: first, to elucidating details of the molecular packing and of possible folding schemes and, secondly, to explaining why and how chain molecules adopt this curious but undoubtedly advantageous way of crystallizing. By 1960 or thereabouts

we had reached the point of knowing that, to a good approximation at least, a crystal such as you see here consists of four distinct fold domains, that the molecular folds lie in each sector in (110) planes parallel to the corresponding growth face, that fold period (crystal thickness) varies with crystallization temperature in a specific way, and that the crystals grow as hollow pyramids which collapse on drying to give pleats such as the one you see here. To this we might add without worrying too much about precise chronology that the crystals may also be ridged or may take on warped chair-like forms. These latter observations came later to be rationalized on the assumption that asymmetry and bulkiness of regularly packed folds on the upper and lower surfaces cause too much strain to be supported by a flat crystal, and that the folds therefore take on staggered configurations giving rise to sloping surfaces many of which have been identified with specific crystallographic planes.

By 1960 we also had two essentially different theoretical approaches to explain the fact that the molecules do indeed fold. I would not say that the equilibrium theory is wrong; many of the considerations that it brought into prominence are still germane to a full understanding of the lattice dynamics of polymer crystals, but in terms of the original intent it must be considered not to have been fruitful. The kinetic approach, based conceptually on the

nucleation theory developed in the 20's and 30's by Volmer and by Becker and Doring, on the other hand, has had great success in explaining the known facts (particularly the variation of fold period with supercooling) and in predicting melting behavior, etc, with gratifying reliability. To the well known work of Lauritzen and Hoffman, Price, Frank and Tosi has recently been added the elaborate and elegant generalized treatment by Lauritzen, Di Marzio and Passaglia of sequential addition processes, including the deposition of folded chain molecules on a polymer crystal, that marks a substantial advance in theoretical rigor. The models may yet require refinement, however, and the theory would certainly profit from a better input of more exact experimental data; nevertheless there is little or no reason to doubt that the basis of a sound and lasting interpretation of the causes of chain folding is already well established.

The picture, then, with which polymer physicists were mostly preoccupied after some five years or so was one conceived in a spirit of seeking after idealized behavior describable by the simplest crystal geometry. We thought of polyethylene single crystals as polyhedra with regular, well-smoothed growth faces, with highly regularized folding schemes (the RG I and RG II schemes, etc) and with a staggering of folds which, possibly after some readjustments had taken place, was itself fairly regular. It is true that the papers of the time were not without their perfunctory

words of caution, but I don't think they were meant to be taken too seriously. The thermodynamicists, however, notably Flory and Mandelkern, were not convinced and, while accepting the possibility that chains might well fold at crystal surfaces, they argued that such folding would mostly involve "loose loops". They favored what became known as the "busy switchboard" model. But among the morphologists the pursuit of idealized structure went on apace and the findings were carried over, undoubtedly with more genuine caution, into interpretations of morphology realized by crystallization from the melt where, of course, chain-folded crystallization had also been established as a certainty.

In retrospect, this is not the only instance of unguarded overemphasis. Many of the features I have mentioned were found in other polymers too, as anyone who has even glanced at Prof. Geil's survey book will know. But it is a sobering thought to realize how much of the detailed, the definitive, experimentation has been performed using polyethylene. Even today it is rather painfully evident that studies of annealing and melting behavior, precise measurements of density and so on, using polyethylene, outweigh similar studies of other polymers, both in profusion of number and in detail, in a staggering and disconcerting disparity. The attractions of polyethylene as

a model substance are indeed obvious. It is the simplest of chain molecules, but also the most mobile in the solid state in terms of lengthwise translation and also the fastest and easiest to crystallize. It is not idle to ask ourselves just how generally applicable is the knowledge we gain from its study. It would be all too easy to over-interpret observations made with other polymers by citing seemingly analogous behavior in this better known but possibly exceptional material.

About five years ago the first jarring notes began to sound. People began to measure the densities of polyethylene single crystals. I don't really know who did it first and I asked Prof. Geil recently. He isn't sure either, but thinks that Statton and he did. At all events, the fact that trouble might be brewing first struck me at the American Physical Society meeting in Baltimore in 1962, when Brown and Eby showed that the density of polyethylene crystals is appreciably lower than anticipated and is in fact a linear function of the reciprocal of their thickness, extrapolating at infinite thickness to the theoretical X-ray density. By 1963 Fischer and his colleagues had produced further evidence drawn from density and X-ray measurements, showing again that there are real and disconcerting discrepancies between what one finds in practice and what one would expect to find with crystals having the regularity of structure suggested by earlier morphological observations

alone. This led a number of workers to repeat the density measurements on polyethylene crystals with gradual improvements in technique and reliability. The results were at first subject to unusually large scatter, some finding low values in the range 0.96 to 0.97, others close to 1.0 - roughly the theoretical value. There is fairly general agreement now on values between 0.96 and 0.98 depending on thickness, and the latest number I hear from the Bureau of Standards where the experiment has been done with extreme care and attention to sources of error is 0.98. Prof. Fischer interpreted such low density values as indicating the presence of a disordered "amorphous" layer about 20 A thick at the folded surfaces. I will not steal his thunder, but he arrived at this conclusion only after first considering, and for various reasons rejecting, other possible interpretations. Supporting evidence for his view came more recently from the work of Peterlin and his collaborators in studies of the effect of fuming nitric acid on single crystals of polyethylene. Similar work at Bell Telephone Laboratories by Winslow and his colleagues, and also I understand in Keller's laboratory, leads to essentially the same results. I have no doubt we shall hear about this in the discussion. So it would seem that we have been wrong and that folds are looped and irregular; that all along we have really been dealing with "bad" crystals.

But, while this was going on there were other developments, notably at the Chemstrand Research Center where Holland and Lindenmeyer were carrying out a very beautiful and elegant study of Moiré patterns generated by double diffraction from bilayer crystals of polyethylene. You will hear an account of this presently, and your reaction must surely be to regard the evidence as showing unambiguously that, with these bilayer crystals at least, folds on the surfaces pack crystallographically and with remarkable regularity. Bassett at Reading has also found evidence for a similar view - perhaps he will tell us briefly about that later. Now, where are we?

One could well ask who is right and who is wrong. But, and I stress this, that would, I submit, be altogether the wrong question to put. I suspect that each view is in its own context equally valid. It would seem that the underlying reality, as I called it earlier, is complex; that there is a spectrum of behavior that has been sampled at two different points. What are the details of the spectrum as a whole, and what in any given circumstances decides which sampling we get? This is the first and the principal question that I want to raise. Related to it is the second question. Which sampling of the spectrum (which after all refers to single crystals grown slowly for the most part from dilute solution) is the appropriate one to lean upon for guidance in attempting to interpret the morphology of aggregates of crystals - spherulites and the like - crystallized under less

idealized conditions from concentrated solution and from the melt. Clearly, molecular weight and kinetics bear importantly upon both questions. But let me not inject my own interpretations - I am supposed to be asking questions.

Let me turn now to some other morphological questions. Once we depart from single crystals that are grown slowly so that they have what seem to be smooth outlines, we are involved with stepped growth faces, and thus with microsectorization and with much more complicated folding schemes. Burbank in a little known paper in 1960 raised many interesting points in this connection. One wonders what the situation might be in crystals grown relatively rapidly in the melt; to what extent do our ideas about folding carry over? Let us not forget that it is these crystals that represent the real crystals in bulk polymers of technological interest, just as a piece of hardened steel represents the real metal as distinct from the idealized single crystal of pure iron. In both cases the relevance of the ideal to the real situation is subject for argument. But let me not belabor this; it is food for thought but I don't think we are yet in a position to pursue it profitably.

Before I leave the subject of the morphology of single crystals and of aggregates of such crystals let me pose two further questions. First, in multilayer single crystals grown in solution, or in the melt for that matter,

successive layers are not oriented in precise register with one another. We could scarcely expect otherwise particularly if folding is irregular but, over and above this, the layers diverge or splay quite markedly. Why? Staggered folding or whatever gives rise to pyramidal habits obviously plays a part, but it is not obvious to me that on its own it is sufficient explanation. Secondly, in polypropylene, solution-grown crystals take the form of lathes that are much longer in the "a" direction than in the "b" direction. The ends of these lathes are "squared off"; they appear to be (100) planes and certainly not (110) or some other low index (hko) planes. We would normally say without hesitation, then, that (100) is the fast growing face but, as Morrow and Sauer have indicated, the folding of polypropylene helicies of fixed hand is plausible in the α-crystal structure only if it takes place in (010) planes. They have produced evidence for this type of folding from deformation studies. Now the fast growing plane seems to advance in the same direction as that taken by the loops of the folded molecules. This is definitely a switch from the usual pattern of behavior. Believing that nothing so implausible could possibly be right, Padden and I have had a look at this system but we haven't discovered anything that gives us justification for taking issue with Morrow and Sauer's interpretation. Of course we can all think of one or two obvious ploys to

remove the difficulty but are any of them plausible? Here we have a situation that needs explanation and it may not be unique.

It is time now that I turn to crystallization from the melt - to spherulitic crystallization. But there is not too much that I want to say about this, for here the problems have perforce been primarily concerned with the organization of chain-folded crystals into more complex structures, and have seldom been faced as yet on a truly molecular scale. Thus, the uncertainties about molecular packing, regularity of folding, etc, in bulk polymers have really been the same uncertainties that we encounter with single crystals grown from solution except that, as I have already indicated, they may be aggravated to a bewildering degree.

We think we know, broadly speaking, how spherulites are formed, though only at a level which ignores details both of molecular attachment to growing crystals and of the perfection of those crystals. That there is a fractionization during crystallization and a segregation of low molecular weight material, as Padden and I first suggested in 1961, is, I think, no longer in question - even if the details may still be cloudy. Anderson has shown that this low molecular weight material is capable of forming paraffinoid or extended-chain crystals. What is still lacking, however,

is a good three-dimensional picture of how this material of low molecular weight is distributed between the chain-folded lamellae and how it is connected to them. The problems are mostly ones of technique. The methods available to us are all a good deal less direct than we would like. We can study thin films by transmission microscopy - how representative are these films? We can replicate free surfaces - again how representative are the surface structures? Fracture surfaces are, ipso facto, special surfaces and thus suspect. We can digest solid polymer with nitric acid and look at the "bits" that remain - how much do they tell us? They are largely bits of paraffinoid material by this time, possibly capable of recrystallization and rearrangement since many of the folds are fractured. It is like trying to discern the picture on a jigsaw puzzle given a small fraction of the pieces and knowing that they may have suffered some distortion of shape. We can use the method that we employ at Bell Telephone Laboratories of mixing low molecular weight paraffin with the polymer and then etching it out. The paraffin is probably not too dissimilar in its behavior to the low molecular weight species that are segregated anyway, but we are again faced with the problem of extrapolating from the behavior of very thin films. If there is an obvious question implicit in this discussion it must surely be: does anyone know a way around the difficulties?

There is another point I want to touch on briefly. In our studies of blends of polyethylene and paraffin, Padden and I find that as soon as we approach conditions analogous to those found in true crystallization from the melt, then (except possibly at the very slowest rates of crystallization) the growth faces of the crystals become serrated on a fine scale and so rough that crystallographic facets are difficult to discern at all. Diffraction shows at the same time that the crystals are becoming disordered. I find it difficult to believe that relatively simple folding schemes and staggered arrangements of folds as we meet them in solution-grown crystals have anything like as much significance in the crystals comprising a piece of bulk polyethylene. Others may disagree but, at all events, here is an area of great uncertainty. I would put it in the form of a question if I thought that anyone had a sound answer.

Another pertinent topic in connection with the morphology of bulk polymers, particularly in relation to the interpretation of mechanical behavior, deformation, and recovery after deformation, is the connectivity between crystals, the nature of inter-crystalline links and of the so-called amorphous content. Doubtless you can think of many questions needing to be answered here, and I shall not take time to tabulate the obvious ones.

There are many other questions that I might raise; for example, why does crystallization under pressure apparently induce an extended chain morphology? But I must stop somewhere and there will be time for that later. The principal topic I wanted to get in focus is the one I devoted most time to. How regularly does a molecule fold, how variable is the regularity and what controls it? There should be no lack of interesting points for discussion.

DISCUSSION ON PAPER NO. 7

Professor B. Wunderlich
Rensselaer Polytechnic Institute

To H. D. Keith and E. W. Fischer's question of the density of folded chain single crystals and the connected problem of regularity of folds, I commented that low densities like Passaglia had found, as well as higher ones similar to what one would expect for sharp folding was no contradiction since we had at that time just completed new density measurement on different chain folded morphology.*

* See Contribution page 215

On the structure of disordered regions in polyethylene single crystals and in drawn polyethylene

by E.W. Fischer, H. Goddar and G.F. Schmidt

Laboratorium für Physik der Hochpolymeren am Institut für Physikalische Chemie der Universität Mainz

1) Introduction

The physical properties of polymeric material do not depend only on the chemical nature of the macromolecules but also on the state of order of the chains. In a semicrystalline polymer the physical properties are controlled to a great extent by the structure of the disordered regions. For example fig. 1 shows a model of the disordered regions within annealed drawn polymers[1], which will be elucitated in more detail later on. In addition some properties of polymers are specified depending obviously on the arrangement of the chains in the disordered regions. These properties have been studied intensively in many laboratories. For explanation of the experimental results various models of the structure of the disordered regions have been proposed. The problem involved, however, is not only of interest from a technological point of view, but it is of importance too with regard to the basic question for the reasons of existence of disordered regions in polymeric materials and for the explanation of crystallization and melting behaviour.

The aim of this paper shall be a contribution of some new informations about the nature of disorder in polyethylene. For many reasons this polymer is extremely suitable for structure investigations. It is believed, however, that most results discussed here may also be applied qualitatively to other polymers. Besides the structure of drawn polymers as demonstrated in fig. 1 another interesting case would be the nature of disorder in isotropic, melt-crystallized material. The structure of this state of polymer is very complex, however, and experiments cannot be evaluated without additional assumptions, e.g. isotropic bulk polyethylene exhibits two different long spacings which cannot be attributed definitely to the dimensions of the crystallites[2].

So we confined ourselves to the study of polyethylene single crystals and drawn polyethylene.

One of the most important properties of the disordered regions is their density. This quantity yields a clear insight into the structure of those regions and is extremely valuable for discussing various models of structure. This paper deals with experiments measuring the values of density of disordered regions by means of two methods. The first method consists in determination of the absolute value of the mean square electron density fluctuation in single crystals and drawn polyethylene, the second technique uses the changes of low angle intensity due to staining of the disordered regions by iodine. Additional informations about the structure of these regions can be obtained by measuring the effects of annealing and the temperature dependence of the x-ray small angle intensities.

2) Single crystals

During the last years a variety of experimental observations has indicated that in most cases only 80-85 % of the polyethylene embodied in the socalled single crystals can have the properties required for the crystalline state. Tab. 1 shows various methods applied to this problem by many authors[3)-15)]. The properties of single crystals having been used for measuring their crystallinity include density, enthalpy of fusion, x-ray scattering, infrared absorption and selective oxidation. The table shows too that a broad variety of crystallization conditions have been applied and different materials have been used. All these experiments yielded the results, that 15-20 % of the monomer units have to be assigned to a noncrystallized state or to some kind of defects.

Now the question arises where the disordered regions lowering the crystallinity are located. One group of authors believe that the mentioned results either are falsified by systematic errors[16)] or that they reflect voids or defect structures within the interior of the crystals[17)18)]. Another groop appraises the experimental observations as indication of an amorphous surface layer of the single crystals. Both points of view are supported by selected experimental results.

The assumption of lattice defects within the interior of the crystals accompanied with a regular folded chain surface, is supported by the crystallographic regularity of the boundaries of the crystals[19], by experiments yielding oriented overgrowth of polyoxymethylen on the top of polyethylene single crystals[20] and especially by the beautiful dislocation networks between bilayered crystals described by Holland and Lindemeyer[21]. The latter experiments yield strong evindence for the existence of a regularly folded chain surface of those crystals under investigation. They also proof that a regular fold including only a few monomer units represents one possible conformation of a molecular chain. These results have to be taken into account discussing the surface structure of polymer single crystals. On the other hand, however, the absence of dislocation networks in many kinds of single crystals studied in various laboratories shows that the regularity discovered by Holland and Lindemeyer is not a general feature of these crystals, otherwise it should be observed with the generally used technique of electron microscopy. In addition the properties mentioned in table I, like density or enthalpy of fusion, are unknown for the case of crystals presenting dislocation networks. It is questionable if they will exhibit the same figures as the generally used crystals.

From this point of view the experimental observations seem to indicate that the surface structure of the single crystals depends very sensitively on the crystallization conditions or, more probably, on particularities of the investigated polymers, for example, on the distribution of molecular weight or on number of chain branchings. The reasons for this apparent discrepancies are not yet understood and so we will concentrate our interest to the "normal" single crystals possessing crystallinities of about 80-85 % which are supposed to represent the general case.

As mentioned above experimental results exist indicating that the disordered material belongs to the intercrystalline surface layers[3)7)15)22)]. First indication was yielded by the experimentally established relationship between density ρ and long spacing L of single crystal mats prepared under various conditions[3)]. The results could be explained most definitely by a model

shown in the next slide and consisting of lamellae with an ideal density ρ_c separated by a layer with a smaller density $\rho_c - \Delta\rho$. The model is based on the existence of the discontinous small angle scattering, since the reflections used for determination of the long spacings L can be caused only by an almost periodically fluctuating electron density. The point in question is the value of the density difference $\Delta\rho$. Are the reflections caused by close packed chain folds, or by voids accompaning the regular folded chain surface, or by an amorphous surface layer?

The question can be answered by determination of the mean square fluctuation of the electron density distribution[23)24)]. According to theory[25)] this quantity $\langle \Delta\eta^2 \rangle$ which is also called scattering power, is proportional to the integral

$$\langle \Delta\eta^2 \rangle = K J_o \int \tilde{J}(\theta)\ \theta d\theta \qquad (1)$$

where the proportional constant K can be determined by measuring the absolut value of intensity J_o of the incident x-ray radiation. The scattered intensity $J(\theta)$ is measured by means of a slit camera. The scattering power does not depend on the geometrical arrangement of the scattering units. Assuming a simplified structure consisting of two phases only, e.g. a crystallin-amorphous polymer, the scattering power $\langle \Delta\eta^2 \rangle$ is given by

$$\langle \Delta\eta^2 \rangle = (\eta_c - \eta_a)^2 w_c \cdot w_a \qquad (2)$$

where w_c, w_a are the volume fractions of crystalline, resp. amorphous material.characterized by electron densities η_c and η_a, resp..In the case of bulk polyethylene this quantity was measured by Hermans and Weidinger[26)] and by Kratky and Schwarzkopf-Schier[27)]. These authors obtained $\langle \Delta\eta^2 \rangle = 1{,}5 \cdot 10^{-3}$ and $1{,}02 \cdot 10^{-3}$ $[(\text{mole electron/cm}^3)^2]$, resp..

From the scattering power the volume fractions of the two phases can be calculated assuming a reasonable value for $(\eta_c - \eta_a)$[26)27)28)]. With regard to our problem, however, we are interested in measuring the density difference $\Delta\rho$ between the crystalline cores and the intercrystalline surface layers using

values of crystallinity w_c evaluated by other methods (for example from the enthalpy of fusion). $\Delta\rho$ is calculated from the scattering power by equation

$$\Delta\rho^2 = \frac{\langle \Delta\eta^2 \rangle}{\left(\frac{\sum Z_i}{M_o}\right)^2 w_c(1-w_c)} \qquad (3)$$

with M_o = molecular weight of repeating unit, $\sum Z_i$ = sum of atomic numbers. Instead using crystallinity one also can calculate $\Delta\rho$ on the basis of the measured values ρ of density of the single crystal mats and the well known density ρ_c of the ideal crystal

$$\Delta\rho = \frac{\left(\frac{M_o}{\sum Z_i}\right)^2 \langle \Delta\eta^2 \rangle + (\rho_c - \rho)^2}{\rho_c - \rho} \qquad (4)$$

We studied an isotropic mat consisting of multilayer crystals and yielding a scattering curve shown in the fig. 3. Background scattering has been substracted. Calibrating the scattered intensity by means of a standard sample[29] we obtained a scattering power of

$$\langle \Delta\eta^2 \rangle = 1{,}20 \cdot 10^{-2} \left(\frac{\text{mole electrons}}{\text{cm}^3}\right)^2 \qquad (5)$$

which agrees approximately with the values in the case of bulk polyethylene mentioned above. Using this value and taking into account a degree of crystallinity of $w_c = 0{,}82$ obtained by heat of fusion measurements[11] eq. 3 yields a density difference of

$$\Delta\rho = 0{,}159 \ \frac{g}{cm^3}$$

On the other hand from the density of these samples $\rho = 0{,}970 \ \frac{g}{cm^3}$ and from eq. (4) a value of

$$\Delta\rho = 0{,}160 \ \frac{g}{cm^3}$$

is obtained. The mutual agreement of both these values shows that no detectable amount of voids is present in our sample. Additionally the measurements yields the remarkable fact that the value of $\Delta\rho$ calculated from the scattering power does agree rather well with the generally accepted value of $\Delta\rho = 0{,}142/cm^3$ obtained by extrapolating the specific volume of amorphous polyethylene to room temperature[30].

In order to calculate Q according to eq. (1) the scattering curve has to be extrapolated to angle zero. Since the intensity values are multiplicated by Θ, however, the error resulting from this proceeding is lower than that due to the uncertainties of density and crystallinity measurement. All errors together may not change the value of $\Delta\rho$ for more than 10 %.

In spite of this limitation of accuracy the evaluated value of $\Delta\rho$ yields a significant conclusion. Assuming that the scattering curve in fig. 3 is caused by voids separating crystals with a regulary folded chain surface, see fig. 4a, the mean square electron density fluctuation $\langle\Delta\eta^2\rangle$ has to be expected to amount to a much higher value. Starting from $\rho = 0{,}970\ g/cm^3$ and $\rho_c = 0{,}998\ g/cm^3$ according to eq. (4) one obtains $\langle\Delta\eta^2\rangle = 8{,}83\cdot10^{-3}$ instead of the measured value of $1{,}20\cdot10^{-3}\left(\frac{\text{mole electrons}}{cm^3}\right)^2$. This discrepancy excludes obviously the assumption of voids producing the scattering curve of the single crystal mat under investigation.

Naturally dense packing of crystals has to be achieved by suitable filtration technique. So one also can obtain a loosely packed sample of crystals by using different filtration procedures[31]. Moreover some polymer crystals do not pack closely due to their inflexibility, e.g. polyoxymethylene. Consequently in those cases the scattering power is much higher than the described value. For example, a loosely packed polyethylene sample yields a scattering power of $\langle\Delta\eta^2\rangle = 5{,}34\cdot10^{-3}$*. We believe, however, that the value of $\Delta\rho = 0{,}16\pm0{,}016\ g/cm^3$ calculated from the small angle scattering curve of fig. 3 does agree not only accidentally

---

*) A polyoxymethylene single crystal sample exhibits a value of $\langle\Delta\eta^2\rangle \approx 1\cdot10^{-1}\left(\frac{\text{mole electrons}}{cm^3}\right)^2$

with the generally accepted value of density difference between crystalline and amorphous phase, rather we are convinced of the existence of an intercrystalline disordered layer characterized by the packing density of a molten phase, although the conformation of the chain molecules may be different as it may be concluded from viscoelastic behaviour and NMR absorption.

Fig. 4 shows some models proposed for the structure of single crystal surfaces. From existence of small angle reflexions it must be concluded that the electron density of the surface layer has to be different from that of the crystallites case. The model of fig. 4a characterized by voids surrounded by regularly folded chains must be excluded as mentioned already. A regularly folded chain structure without inclusion of voids would yield a lower scattering power than we observed[24]. In addition the mat of single crystals in this case should possess a density higher than the ideal density calculated from x-ray data. Further arguments for rejection of this model are given by results of small angle scattering studies on iodine stained crystals. The intensity of long spacing reflections decreases continoudly with increasing iodine content until it disappears almost, then it increases again. From this result we may conclude that density of intercrystalline layers must be lower than that of the crystallites.

Our described result can be explained, however, by the assumption of a rough chain folded surface[18], whereby the extruding chain folds are packed together like within an amorphous region of polyethylene. Another possibility is the random re-entry model of Flory[32] characterized by the assumption of a broad distribution of re-entry distance and lengths of loops. Both models may show the same density of the intercrystalline surface layer. Additional informations are required for solving this problem.

These informations can be obtained by investigation of structure changes taking place at higher temperatures. During annealing the small angle scattering pattern is changed, whereas the changes are partly reversibel and partly irreversibel with regard to temperature. These effects can be seen in fig. 5

and Tab. II. After having annealed the crystals at temperatures above 110°C the measurement of the x-ray scattering at room-temperature yielded a scattering power lower than that of an unannealed sample. This observation corresponds to the well known increase of crystallinity observed with other methods, too[3]. Therefore the evaluated value of the density difference Δ_ρ was found to be approximately constant, see table II

On the other hand the scattering pattern measured at higher temperatures exhibits a remakably higher scattering power as it is shown in fig. 5 and tab. II[33]. For example, at 125°C the evaluation yields a scattering power of $2{,}23 \cdot 10^{-3}$ which is more than twice so much as at room temperature. This increase is not caused by an increase of the density difference Δ_ρ as one may suppose. From specific volume of the sample measured at 125°C dilatometrically[34] by using the relations between $\Delta\rho$, $\Delta\eta^2$ and ρ a value of $\Delta\rho = 0{,}174$ g/cm^3 is obtained in excellent agreement with the value calculated from the known expansion coefficients of the crystalline resp. amorphous phase. Therefore the main contribution to the increase of the scattering power at higher temperatures is due to a decrease of crystallinity. From the equation derived above we obtained $w_c = 0{,}65$ at 125°C instead of $w_c = 0{,}88$ at room temperature.

The decrease of crystallinity is a well known effect often called partial melting. In principle it can be achieved in two different manners, either by melting of some crystallites or by an increase of thickness of the intercrystalline surface layers. The latter effect we call boundary melting[35]. Each type of melting is expected to result in a different change of the scattering pattern. Theory of small angle scattering reveals definitely that melting of some crystallites without further changes of the macrolattice will always yield a decrease of intensity of the reflections accompanied by an increase of the background scattering[36]. On the other hand the growth of thickness of the amorphous surface layer enlarges the intensity of the reflections[33] and causes an increase of the scattering power beeing observed. Therefore the temperature dependence of

reflection' intensity enables the decision between the discussed processes. The scattering patterns of fig. 5 and 6 show clearly that the intensity change observed can only be explained by boundary melting.

The observed temperature dependence of thickness of the disordered layers between the crystallites can be explained by theoretical considerations[35] based on the assumption that during annealing a metastable equilibrium between the boundary layer and the crystallites is established. Since the entropy of conformation on the noncrystallized sequences does not depend linearly on the length of the sequences[35)38)], one obtains from the condition of minimalized free energy an average equilibrium length of these sequences. In the case of loops fitted with their ends in a crystal the equilibrium length increases with rising temperature.

The equilibrium length can be calculated using simple statistical models. From these values the temperature dependence of thickness of disordered layers can be revealed and the intensity of small angle reflections can be calculated. The result is plotted in fig. 7. together with the experimentally measured values. In order to get agreement a certain value of the distance of position of the re-entry has to be chosen. The numerical value was about 35 Å, but it depends, of course, somewhat on the statistical model used for calculation. With regard to our problem the most important conclusion from theory consists in the result, that loops with adjacent ends will not increase their length with rising temperature. Therefore the cited results are speaking in favor of a model with random re-entry and distribution of loop length.

3. Structure of Disordered Regions in Drawn Polymers

The presence of electron density fluctuations in drawn polymers is definitely proved by the appearance of meridional and equatorial scattering in the small angle x-ray diagram. For explanation of this well-known effect different models have been developed. For example, fig. 8 shows some proposals for structure of a drawn polymer exhibiting a so-called four point diagram. The

variety of models reflects the ambiguity of scattering effects. For example with the models in the upper line the four point diagram is supposed to be caused by the particle scattering, whereas it is explained in terms of interparticular interferences with the other models.

Looking at the structure of the disordered regions evidently the density again presents the most important property of these regions. In order to evaluate the density difference between crystalline and disordered regions in the case of drawn polymers, one has to take into account the anisotropy of the structure and of the scattering. So for example the intensity distribution in meridional direction $I(0,0, b_3)$ does not depend on the mean square density fluctuation between crystalline and disordered regions, but it does reflect the fluctuation of the projected electron density[40]:

$$\rho_p (x_3) = \int \rho (x_1, x_2, x_3)\, dx_1\, dx_2 \qquad (6)$$

It can be shown that the meridional intensity $I (b_3)$ is proportional to the convolution square of the projected density. Therefore in general an increase of $I (b_3)$ cannot be judged as an increase of density difference.

The only quantity which yields the desired information about the mean square electron density fluctuation $\langle \Delta\eta^2 \rangle$ is proportional to the integral

$$\langle \Delta\eta^2 \rangle = K J_0 \iiint J (b_1, b_2, b_3)\, db_1\, db_2\, db_3 \qquad (7)$$

see also eq. (1)

In the case of rotational symmetrie around the fiber axis this quantity can be evaluated by means of a slit camera. Measuring the scattering curve in direction perpendicular to

the fiber axis (slit parallel to fiber axis) one obtains the intensity integrated with respect to b_3 :

$$J_{sl}(b_r) = \int J(b_r, b_3)\, db_3 \qquad (8)$$

According to eq. (7) the scattering power of the sample can be calculated by integration of $J_{sl}(b_r)$ with respect to b_r:

$$\langle \Delta\eta^2 \rangle \sim \int J_{sl}(b_r)\, b_r\, db_r \qquad (9)$$

For this integration it is necessary to extrapolate the measured intensity $J_{sl}(b_r)$ to the angle $2\theta = 0$. In most cases this can be obtained sucessfully using a Guinier-plot $\log J_{sl}(b_r)$ vs. b_r^2 .

In this manner we obtained from a drawn and annealed low pressure polyethylene (Lupolen 6011 L, drawn 1500 % at 70°C, annealed 1 h at 125°C and quenched) yielding the scattering curve of fig. 9 a value of

$$\langle \Delta\eta^2 \rangle = 6{,}6 \cdot 10^{-4} \left(\frac{\text{mole electrons}}{\text{cm}^3} \right)^2$$

which is considerably less than the value obtained from isotropic meltcrystallized polyethylene or polyethylene single crystals. Since the density of the drawn polyethylene, however, is almost equal to the densities of other types of samples, the density difference between crystallites and disordered regions must be lower than 0,142 g/cm^3 generally used for the value of $\Delta\rho$ in the case of polyethylene[30]. Assuming that the density ρ_c of the crystalline regions in drawn polymers is equal to the ideal value calculated from x-ray data, we can use eq. (4) for calculation of $\Delta\rho$. From $\rho = 0{,}973$ g/cm^3 and the value of $\langle \Delta\eta^2 \rangle$ mentioned above one obtains

$$\Delta\rho = 0{,}109 \text{ g/cm}^3$$

On the other hand $\Delta\rho$ can be determined from eq.(3) using the degree of crystallinity measured by heat of fusion[43]. Then a value of

$$\Delta\rho = 0{,}130 \text{ g/cm}^3$$

is obtained. This discrepancy reflects the well known fact that in drawn polymers the heat of fusion is higher than it would be expected with regard to the density of the sample. This effect was described firstly by Peterlin and Meinel[44] and attributed to a reduction of specific enthalpy of the disordered regions due to the stress of the tie molecules. The discrepancy between the values of $\Delta\rho$ showing up from drawn polyethylene on the one hand and from single crystals and bulk isotropic polyethylene on the other hand may also reflect a better alignment of the molecules in the disordered regions.

More insight into the structure of these regions can be gained by studying the changes taking place during annealing at higher temperatures. It is well known that small angle intensity scattered from drawn polymers increases during heat treatment. For example, Statton[45] reports a fortyfold increase of meridional intensity by annealing Nylon 6,6-fibers. It should be noticed, however, that the meridional intensity $J(b_3)$ is correlated to the projected electron density ρ_p according to eq. (6) and not to the electron density fluctuation $\rho(x_3)$ along fiber axis. Nevertheless Statton's conclusions that density difference $\Delta\rho$ increases during annealing seems to be correct as it is shown for the case of polyethylene in the following considerations.

The exact solution of this problem requires the measurement of the scattering powers of unannealed and annealed samples. Unfortunately in the case of unannealed samples the determination of $\langle\Delta\eta^2\rangle$ is complicated very often by the existence of longitudinal voids causing an intensive equatorial scattering. This was found for the sample discussed above, yielding a value of $\langle\Delta\eta^2\rangle = 6{,}6\cdot10^{-4}$ in the annealed state, see fig. 10 a, b. An information about the $\Delta\rho$-value of the unannealed sample can be obtained, however, by means of iodine staining experiments discussed below.

By special treatment before drawing and by drawing at higher temperatures, however, equatorial scattering can be eliminated at least up to a Bragg value of 360 Å. So for example fig. 10 c shows the x-ray pattern of an unannealed sample drawn 1000 % at 80°C (Lupolen 6011 L). Before drawing, the sample was molten, then quenched in icewater and subsequently drawn at once.

The curve obtained from Guinier-plot could easily be extrapolated to $b_r = 0$. This experiment resulted in

$$\overline{\Delta\eta^2} = 2{,}15 \cdot 10^{-4} \left(\frac{\text{mole electrons}}{\text{cm}^3} \right)^2$$

for the unannealed and

$$\overline{\Delta\eta^2} = 4{,}32 \cdot 10^{-4} \left(\frac{\text{mole electrons}}{\text{cm}^3} \right)^2$$

for a sample annealed 1 h at 125°C.

Further investigations of the dependence of the scattering power of those samples on annealing temperature yielded the result that $\langle \Delta\eta^2 \rangle$ increases continously with arising annealing temperature up to a value of $\langle \Delta\eta^2 \rangle = 5{,}72 \cdot 10^{-4}$ after annealing at 130°C. Table III shows the various values obtained from different temperatures including the density difference values determined by iodine staining.

The experiments yield the remarkable result of a strong increase in $\Delta\rho$ taking place during annealing. One should take into account, however, that $\Delta\rho$ may even be lower in the case of the unannealed sample than measured with the aid of the scattering power. The method of extrapolating the scattering intensity to $b_r = 0$ using a Guinier-plot, includes the possibility of calculating an uncorrectly high value of $\langle \Delta\eta^2 \rangle$ since the existence of equatorial scattering caused by longitudinal voids cannot be excluded for Bragg values greater than 360 Å.

Evidence of still lower values of $\Delta\rho$ is obtained from the results of iodine staining investigation. Before discussing the density difference values determined by this method, another consequence of our staining experiments should be demonstrated. Looking at two different models of drawn polymers shown in fig.11 one states a remarkable difference with regard to the fluctuation

of the projected electron density. In the case of the Hess-Kiessig-model characterized by chains passing through the disordered regions, the projected electron density of the latter ones is higher than that of the crystallites. In the case of a model assuming chain folds at the boundaries of the crystallites, however, the projected density difference possesses an opposite sign. During selective staining by atoms of a higher scattering power in both cases the projected electron density of the disordered regions increases. The effect on meridional intensity will be different, however. In the first case a monotone increase of intensity will be observed, whereas in the second case firstly a decrease, followed by an increase, will occur. From fig. 12 we definitely learn the behaviour which is expected from the second model. The intensities shown here were taken by measuring the intensity distribution along b_3-direction by means of a slit camera, slit perpendicular to fiber axis. By this method we measure

$$J_{sl}(b_3) = \int J(b_r, b_3)\, db_3 \qquad (10)$$

which is proportional to the projected electron density difference on the condition that relative intensity distribution along b_r-direction does not change during iodine staining, as it is shown in fig. 13. In our opinion this result yields an additional and definite proof that chain folding does occur in drawn polymers. Surely not all chains are refolded on the surface of the crystallites, since the mechanical strength of fibers requires some chains passing through several crystallites.

In addition to these qualitative conclusions the staining experiments can be used for determination of the density of disordered regions. The intensity $J_{sl}(b_r)$ of an untreated sample may be written as

$$J_u = F \cdot \Delta\eta^2 = F \cdot \left(\frac{\Sigma z_i}{n_0}\right)^2 \cdot \Delta\rho^2 \qquad (11)$$

if the sample is assumed to consist of two phases characterized by density difference $\Delta\rho$. Under the condition that the relative intensity distribution along b_r remains constant, see fig.13,

and that iodine only penetrates the disordered regions, the intensity of an iodinated fiber is given by

$$J_k = F \cdot [n_c - (\eta a + \eta_k)]^2 = F \cdot (\Delta\eta - \eta_k)^2 \qquad (12)$$

with η_k electron density of iodine in the disordered regions. As it was shown by Marikhin[46], from eq. (11) and (12) we obtain

$$\pm\sqrt{\frac{J_k}{J_u}} = 1 - \frac{1}{\Delta\rho} \cdot \frac{\beta_k}{\beta} \cdot \rho_k \qquad (13)$$

with β and β_k the terms $\frac{\Sigma Z_i}{M_o}$ in the cases of polyethylene and iodine, resp..

From this relations it is possible to calculate $\Delta\rho$ on the basis of measuring the intensity of samples with various iodine contents. The curves used for this evaluation are shown in fig. 14.

For a detailed discussion of the evaluation procedure we must refer to the original paper[47]. The values of $\Delta\rho$ obtained by this method are presented in table III. There is a good agreement between the $\Delta\rho$-values calculated from scattering power or from iodine staining in the case of annealed drawn polyethylene. We may conclude that this method of iodine staining also yields the true valu of the density difference in the case of the unannealed fiber. We state a fivefold increase in density difference between crystalline and amorphous regions taking place during annealing.

In the present state of investigations we cannot definitely decide the question if this increase of density difference is caused by chain refolding or by other processes. From the results of other measurements, as mechanical behaviour, swelling of drawn fibers, and NMR investigations, however, we think that a good explanation can be given by the model of fig. 15[1]. The state of the unannealed fiber is characterized by an almost homogeneous crystalline matrix with a periodical fluctuation of defects involved. During annealing the defects are arranged in layers perpendicular to fiber axis. This process results in a decreasing density of disordered layers accompanied by an increasing

perfection of the crystallites. The activation energy of this diffusion of defects may be estimated from the temperature dependence of the scattering power. We obtained a value of 10 kcal/mol[45]. This value is in rather good agreement with the result reported by Statton in the case of Nylon 6,6[42], although his interpretation is different from ours.

The authors are indebted to the "Deutsche Forschungsgemeinschaft" for financial support of this work.

Summary

In order to obtain additional informations about the structure of the disordered regions in polyethylene single crystals and in drawn polyethylene the density of these regions was determined by means of measurements of the absolute value of the scattered intensity in the small angle range and by measuring the intensity changes due to iodine staining. In the case of single crystal mats experiments yielded the result that the chain molecules are not regularly folded at the surface of the crystallites. The experimental data can only be explained by models assuming a roughly folded chain surface or random re-entry of the chain molecules. A roughly folded chain surface model, however, can be excluded since temperature dependence of small angle intensity indicates boundary melting taking place at higher temperatures. On the basis of present knowledge, this effect can only be explained by a random re-entry model.

Measurements of the scattering power of drawn polyethylene result in a very low density difference between crystalline and disordered regions in the case of unannealed fibres. Comparing the scattering power of unannealed and annealed drawn polyethylene and measuring the x-ray small angle intensity of iodine stained fibres, a fivefold increase of density difference results. In addition, from the experiments on iodine stained drawn polyethylene a definite proof of the existence of chain folds in polymer fibres is obtained.

Literature

1. Fischer, E.W. and H. Goddar, J.Polym.Sci. C, in press
2. Hendus, H., Ergeb.exakt.Naturwiss. 31, 331 (1959)
   Geil, P.H., J.Polym.Sci. C 13, 149 (1966)
3. Fischer, E.W. and G.F. Schmidt, Angew.Chemie 74, 551 (1962)
4. Fischer, E.W. and R. Lorenz, Kolloid-Z. 189, 97 (1963)
5. Jackson, J.B., P.J. Flory, and R. Chiang, Trans.Faraday Soc. 59, 1906 (1963)
6. Nakajima, A., F. Hamada, S. Hayashi, and O. Sumida, JUPAC Tokyo, Kyoto, Preprint No. 4.5.02 (1966)
7. Okada, T. and L. Mandelkern, J.Polym.Sci. B 4, 1043 (1966)
8. Wunderlich, B. and W.H. Kashdan, J.Polym.Sci. 50, 71 (1960)
9. Hendus, H. and K.H. Illers, Kunststoffe 57, 193 (1967)
10. Martin, G.M. and E. Passaglia, J.Research NBS 70 A, 221 (1966)
11. Fischer, E.W. and G. Hinrichsen, Kolloid-Z. 213, 93 (1966)
12. Karasz, F.E. and J.D. Hamblin, Report of National Physical Laboratory, Teddington, May 1963 (1963)
13. Bunn, C.W. unpublished, cited from (12)
14. Hendus, H. and Gg. Schnell, Kunststoffe 51, 69 (1961)
15. Peterlin, A., G. Meinel, and H.G. Olf, J.Polym.Sci. B 4, 399 (1966)
16. Kawai, T and A. Keller, Phil.Mag. 8, 1203 (1963)
    Kawai, T and A. Keller, Phil. Mag. 8, 1973 (1963)
17. Holland, V.F. and P.H. Lindenmeyer, J.Appl.Phys. B 6, 000 (1965)
    Holland, V.F., P.H. Lindenmeyer, R. Trivedi, and S. Amelinckx, phys.stat.sol. 10, 543 (1965)
    Lindenmeyer, P.H., J.Polym.Sci. C 15, 109 (1966)
18. Hoffman, J.D., SPE Trans. 4, 315 (1964)
19. Keller, A., Polymer 3, 393 (1962)
    Keller, A., Kolloid-Z. 197, 98 (1964)
20. Kobayashi, K. and T. Takahashi, Kagaku 34, 325 (1965)

21. Holland, V.F. and P.H. Lindenmeyer, Science 147, 1296 (1965)

22. Fischer, E.W. and A. Peterlin, Makromol.Chem. 74, 1 (1964)

23. Fischer, E.W., H. Goddar, and G.F. Schmidt, J.Polym.Sci. B, in press

24. Fischer, E.W., H. Goddar, and G.F. Schmidt, Kolloid-Z., to be published

25. Debye, P. and A.W. Bueche, J.Appl.Phys. 20, 518 (1949)
Porod, O., Kolloid-Z. 124, 83 (1951)
Kratky, O., O. Porod, and Z. Skala, Acta Physica Austr. 13, 76 (1960)

26. Hermans, P.H. and A. Weidinger, Makromol.Chem. 39, 67 (1960)

27. Kratky, O. and K. Schwarzkopf-Schier, Monatshefte f.Chemie 94, 714 (1963)

28. Brumberger, H., O. Kratky, and P. Mittelbach, Monatshefte f. Chemie 95, 1599 (1964)

29. Kratky, O., Makromol.Chem. 35 A, 12 (1960)
Kratky, O. and H. Wawra, Monatshefte f.Chem. 94, 981 (1963)
Kratky, O., Z.f.Analyt.Chemie 201, 161 (1964)

30. Chiang, R. and P.J. Flory, J.Am.Chem.Soc. 83, 2857 (1961)

31. Salovey, R. and D.C. Bassett, J.Appl.Phys. 35, 3216 (1964)

32. Flory, P.J., J.Am.Chem.Soc. 84, 2857 (1962)

33. Nukushina, Y., Y. Jtoh, and E.W. Fischer, J.Polym.Sci. B 3, 383 (1965)

34. Fischer, E.W. and A. Kajiura, to be published

35. Fischer, E.W., Kolloid-Z. 218, 97 (1967)

36. Fischer, E.W., R. Martin, and G. Strobl, to be published

37. Schmidt, G.F., to be published

38. Zachmann, H.G., Kolloid-Z. 216-217, 180 (1967)

39. Morgan, L.B., J.Appl.Chem. 4, 160 (1954)

40. Bonart, R., Kolloid-Z. 211, 14 (1966)

41. Statton, W.O., J.Polym.Sci. 41, 143 (1959)

42. Seto, O. and T. Hara, Reports on Progr.in Polym.Phys. Japan IX, 207 (1966)

43. Fischer, E.W. and G. Hinrichsen, Kolloid-Z. 213, 28 (1966)

44. Peterlin, A. and G. Meinel, J.Appl.Phys. 36, 3028 (1965)

45. Dismore, P.F. and W.O. Statton, J.Polym.Sci. C 13, 133 (1966)

46. Marikhin, V.A., A.J. Slutsker, and A.A. Yastrebinski, Fizika Tverdogo Tela 7, 441 (1965)

47. Fischer, E.W., H. Goddar, and G.F. Schmidt, Faserforschung und Textiltechnik, to be published

48. Fischer, E.W., H. Goddar, and G.F. Schmidt, to be published

Figures

1. Some physical properties of semicrystalline polymers depending on structure of disordered regions.

2. a) Model of stack of single crystals separated by intercrystalline layers with density ($\rho_c - \Delta\rho$)

   b) Relationship $\rho = \rho_c - \frac{d \cdot \Delta\rho}{L}$ between density ρ and long spacing L of polyethylene single crystals annealed at various temperatures[3].

3. Scattering curve of an unoriented polyethylene single crystal mat[33]

4. Models of structure of surface layer of polyethylene single crystals

   a) Regulary folded chain surface including voids

   b) Closely packed regularly folded lamellae. Electron density fluctuation is caused by the increased number of chain units in the intercrystalline regions.

   c) Roughly folded chain surface (Hoffmann[18]). In densely packed lamellae systems the intercrystalline layer may possess the density of amorphous polyethylene.

   d) Random re-entry model with distribution of loop lengths (Flory[32])

5. Small angle scattering curves of polyethylene single crystals at different temperatures[23]

   a) Unannealed, $\langle \Delta\eta^2 \rangle = 1{,}20 \cdot 10^{-3} \left(\frac{\text{mole electrons}}{\text{cm}^3} \right)^2$

   b) Annealed 20 h at 125°C, measured at room temperature, $\langle \Delta\eta^2 \rangle = 1{,}09 \cdot 10^{-3} \left(\frac{\text{mole electrons}}{\text{cm}^3} \right)^2$

   c) Treated like b), measured at 125°C, $\langle \Delta\eta^2 \rangle = 2{,}23 \cdot 10^{-3} \left(\frac{\text{mole electrons}}{\text{cm}^3} \right)^2$

6. Scattering curves from polyethylene single crystals measured at different temperatures[37]

   a) annealed 4 h at 125°C

   b) annealed 4 h at 130°C

7. Maximum intensity of long period reflection[38]

   o measured during first cooling down

   □ measured during second heating cycle

   (The broken curve represents the calculated change due to the different thermal expansion coefficients of crystalline and amorphous phase, resp.)

8. Models proposed for explanation of four point diagrams

   a) Four point diagram obtained from annealed drawn polyethylene

   b) Spiral fibrils (Morgan[39])

   c) Fibrils with blown up amorphous regions (Dorrt[40])

   d) string model (Statton[41])

   e) oblique crystalline layers (Seto-Hara[42])

   f) oblique layers possessing refolded chains

9. Scattering curves from annealed drawn polyethylene (Lupolen 6011 L, drawn 1500 % at 70°C, annealed 1 h at 125°C and quenched)

   a) $J_{s\ell}(b_3) = \int J(b_r, b_3)\, db_r$ (slit perpendicular to fiber axis)

   b) $J_{s\ell}(b_r) = \int J(B_r, b_3)\, db_3$ (slit parallel to fiber axis)

10. X-ray small angle patterns of drawn polyethylene (Lupolen 6011 L)

   a) Drawn 1500 % at 70°C, unannealed

   b) Drawn 1500 % at 70°C, annealed 1 h at 125°C

   c) Drawn 1000 % at 80°C, unannealed

11. Expected influence of iodine staining on x-ray small angle meridional intensity

    a) Hess-Kiessig-model

    b) model assuming folded chains

12. Relative intensity change vs. iodine content (Lupolen 6011 L)

13. Intensity distribution along b_r-direction (Lupolen 6011 L, drawn 1500 % at 70°C, annealed 1 h at 125°C)

14. Relative intensity change vs. iodine content (According to eq. 13)

15. Models of unannealed and annealed drawn polyethylene[1)]

    a) Unannealed

    b) Annealed

Method	Sample Preparation				Authors
	material	solvent	concentration	cryst. temperature °C	
density (floating methods)	Marlex 50	xylene	0,1 %	80	E.W.Fischer and G.F.Schmidt[3]
	Marlex 50	monochlorobenzene, octane, tetrachloroethylene, xylene	0,1 %	30–80	E.W.Fischer and R.Lorenz[4]
	Marlex 50	tetralin	0,1–10 %	50–96	J.B.Jackson, P.J.Flory and R.Chiang[5]
	fractions	various solvents	–	70–110	A.Nakajima et al.[6]
	fractions	–	0,1 %	85	T.Okada and L.Mandelkern[7]
	Marlex 50	toluene	0,05 %	slowly cooled, 0,2 °C/min	B.Wunderlich and W.H.Kaskan[8]
	Lupolen 6011H	xylene	0,1 %	78	H.Hendus and K.H.Illers[9]
density (pyknometry)	Marlex 50	monochlorobenzene, octane, tetrachloroethylene, xylene	0,1 %	30–80	E.W.Fischer and R.Lorenz[4]
	Marlex 50	xylene	0,75 %	70	M.Martin and E.Passaglia[10]
heat of fusion	Marlex 50, fractions	xylene, tetrachloroethylene, octane	0,05 %	60–95	E.W.Fischer and G.Hinrichsen[11]
	Lupolen 6011L	xylene	0,1 %	78	H.Hendus and K.H.Illers[9]
	Marlex 50	xylene	0,1 %	70–90	E.T.Kiss and T.F.Hamblin[12]
	Marlex 50	toluene	0,05 %	slowly cooled, 0,2 °C/min	B.Wunderlich and L.Mandelkern[8]
x-ray	Marlex 50	–	–	–	C.W.Bunn[13]
	Marlex 50	monochlorobenzene, octane, tetrachloroethylene, xylene	0,1 %	30–80	E.W.Fischer and R.Lorenz[4]
	Lupolen 6011H	xylene	0,1	78	H.Hendus and Gy. Schnell[14]
infrared	fractions	–	0,1 %	85	T.Okada and L.Mandelkern[7]
selective oxidation	Hostaflen GM 6055	xylene	0,1 %	70	A.Peterlin, M.Dole, and A.R.Olpin[15]

Tabl. I

Table II

Crystallization and Annealing Conditions	Long Period [Å]	$\left[\left(\frac{\overline{\Delta\eta^2}}{\frac{\text{mole electrons}}{\text{cm}^3}}\right)^2\right]$	Crystallinity (Heat of Fusion)	$\Delta\rho$ [g/cm^3]
Cryst. at 70°C from C_2Cl_4	120	$1{,}20 \cdot 10^{-3}$	0,823	0,159
Annealed 20 h at 120°C	210	$1{,}24 \cdot 10^{-3}$	0,846	0,171
Annealed 20 h at 125°C	240	$1{,}09 \cdot 10^{-3}$	0,854	0,165
Annealed 20 h at 128°C	280	$0{,}87 \cdot 10^{-3}$	0,879	0,158

Sample	$\rho \left[\frac{g}{cm^3}\right]$	w_c (from DTA)	$\langle \Delta\eta^2 \rangle \left(\frac{\text{mole electrons}}{cm^3}\right)^2$	$\Delta\rho$ from $\langle \Delta\eta^2 \rangle$ $\left[\frac{g}{cm^3}\right]$		$\Delta\rho$ from iodine staining $\left[\frac{g}{cm^3}\right]$	
				$\Delta\rho$ from w_c	$\Delta\rho$ from density	$\Delta\rho$ from w_c	$\Delta\rho$ from density
Drawn 1500 % at 70°C, unannealed	0,962	0,82	-	-	-	0,019	0,014
Drawn 1500 % at 70°C, annealed 1 h at 125°C	0,973	0,87	$6,6 \cdot 10^{-4}$	0,130	0,109	0,112	0,093
Drawn 1000% at 80°C	0,960	0,82	$2,1 \cdot 10^{-4}$	0,066	0,056	-	-
Drawn 1000 % at 80°C, annealed 1 h at 125°C	0,968	0,87	$4,32 \cdot 10^{-4}$	0,111	0,074	-	-

Table III

1) Modulus of elasticity, tensile strength
2) Viscoelastic behaviour
3) Thermoelastic behaviour, shrinkage
4) Diffusion, sorption
5) Chemical reactivity, e.g. oxidation

fig.1

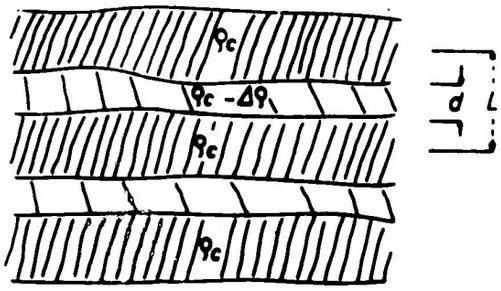

a.)

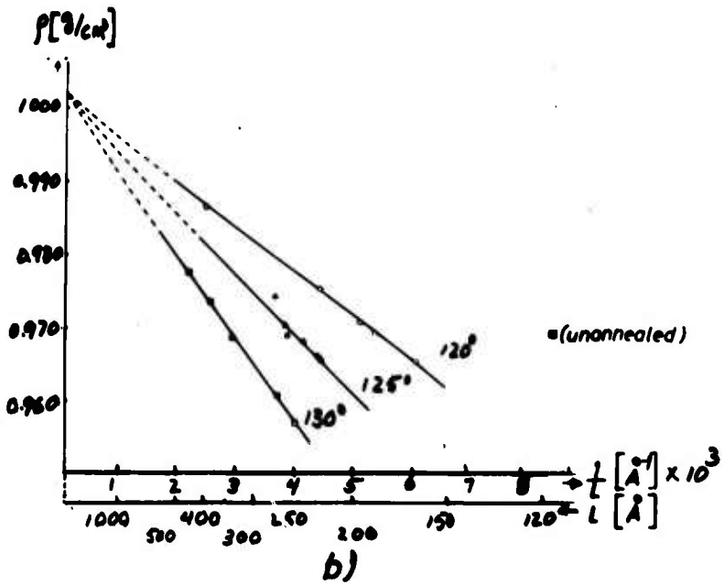

b)

fig.2

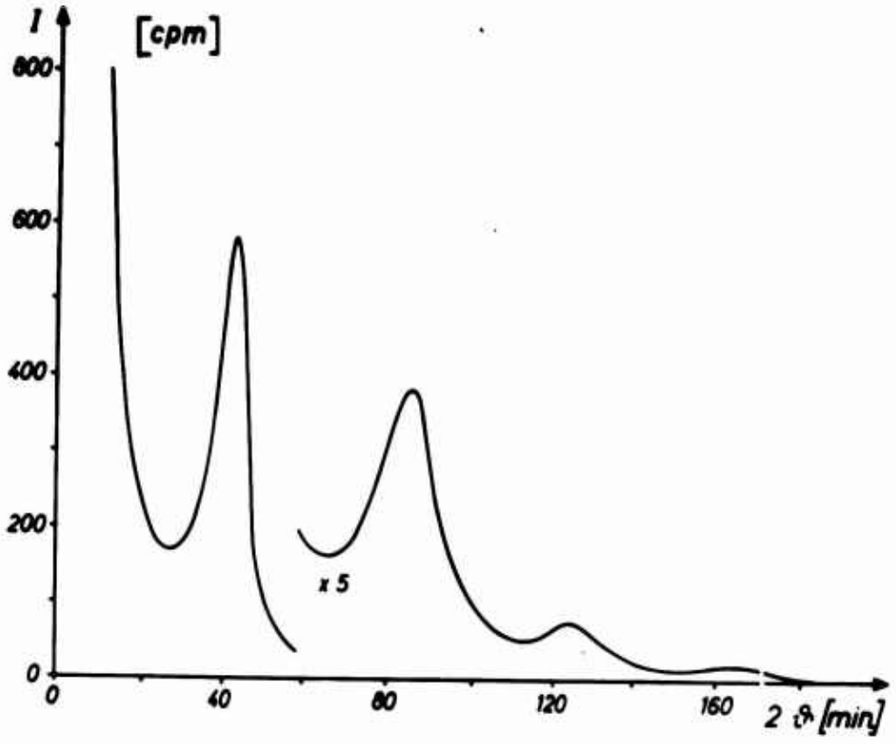

fig. 3

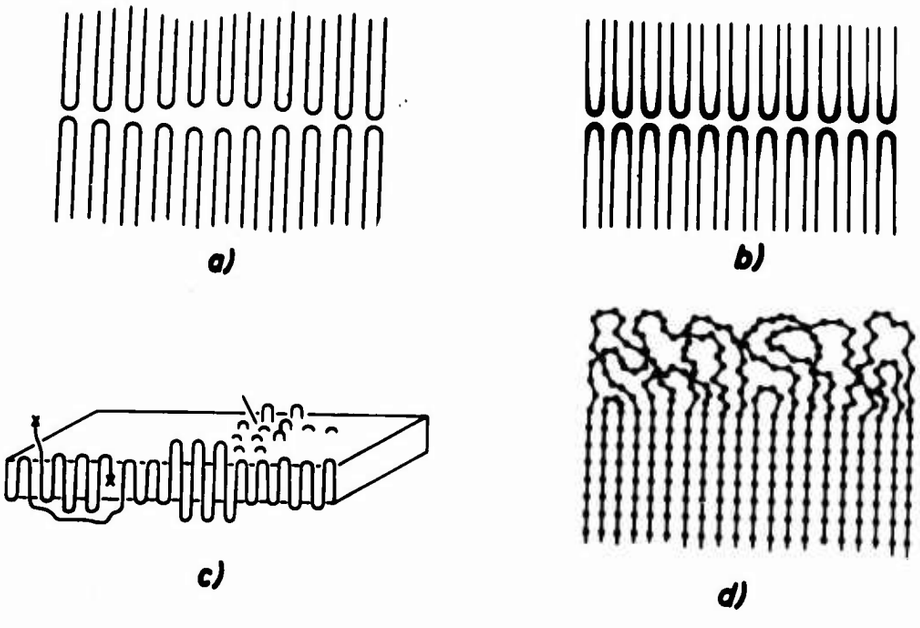

fig. 4

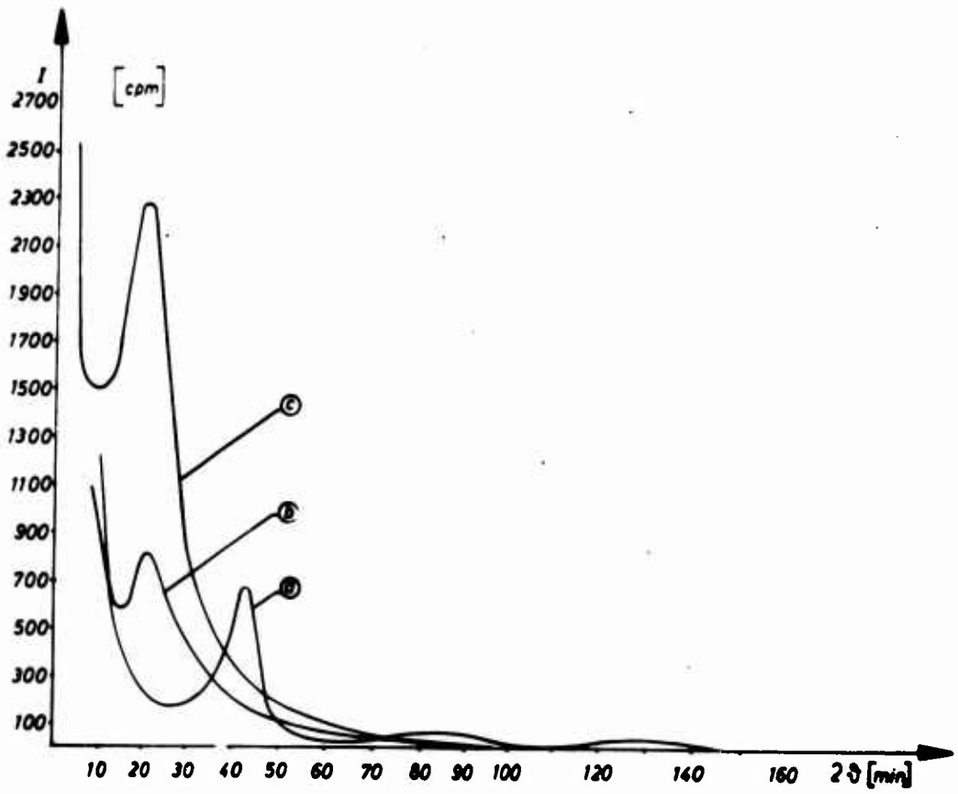
I
[cpm]
2700
2500
2300
2100
1900
1700
1500
1300
1100
900
700
500
300
100
c
b
a
10 20 30 40 50 60 70 80 90 100 120 140 160 2ϑ [min]

fig.5

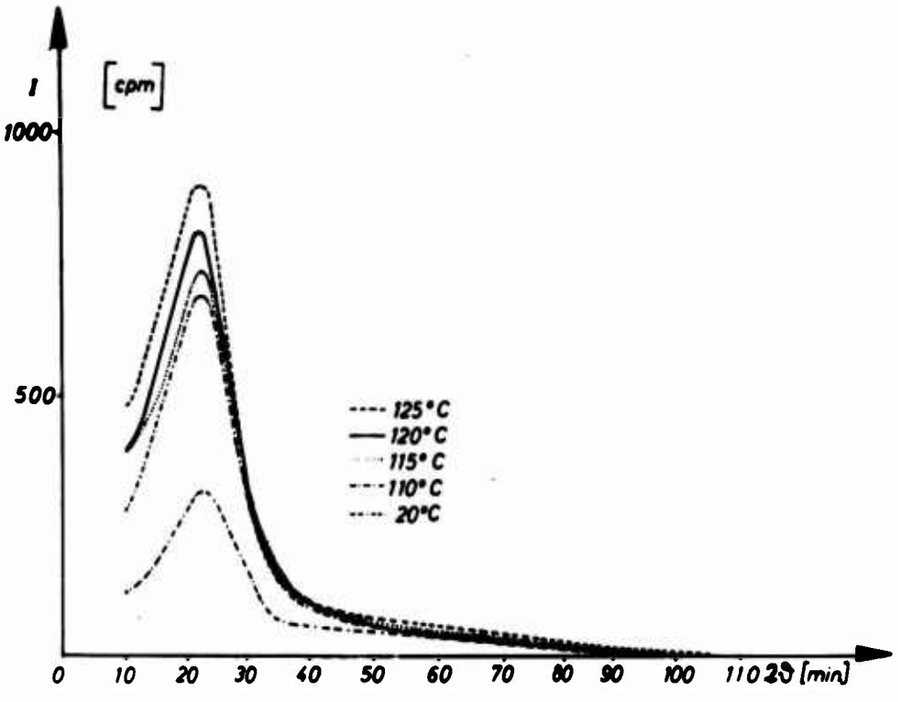
I
[cpm]
1000
500
125°C
120°C
115°C
110°C
20°C
0 10 20 30 40 50 60 70 80 90 100 110 120 [min]

fig. 6a

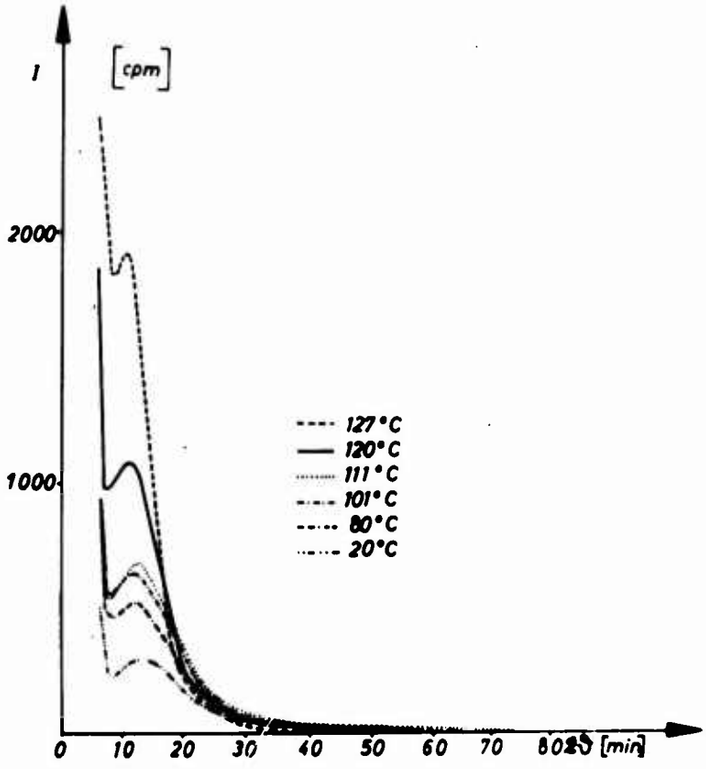
I
[cpm]
2000
1000
127°C
120°C
111°C
101°C
80°C
20°C
0 10 20 30 40 50 60 70 80 90 [min]

fig. 6b

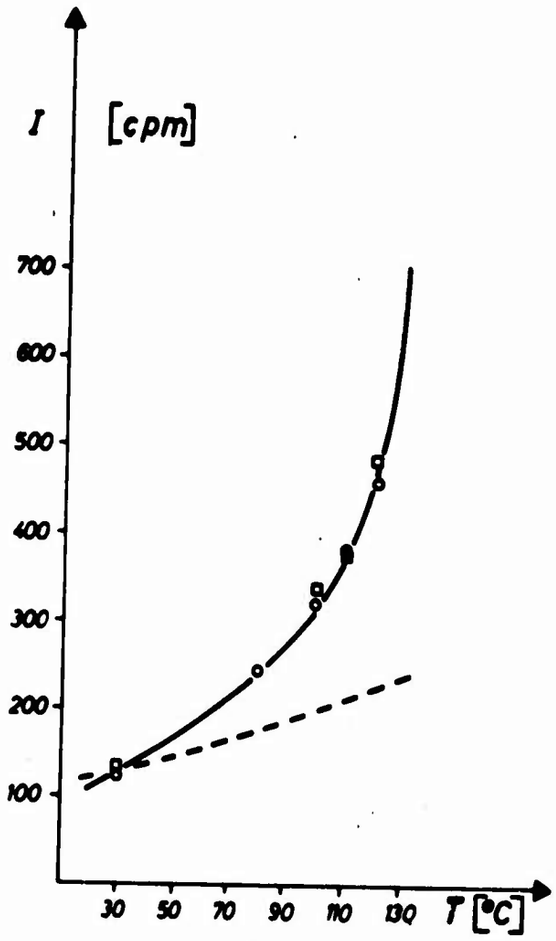

fig. 7

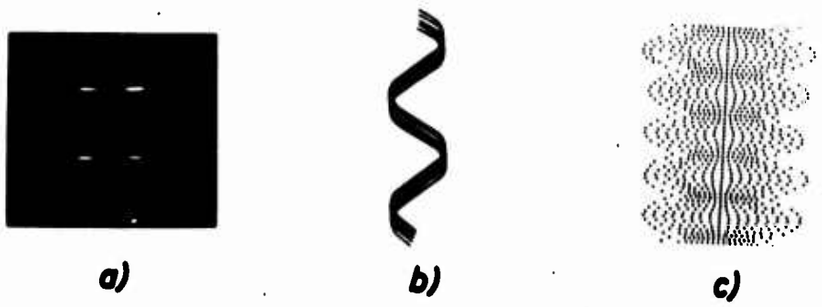

fig. 8

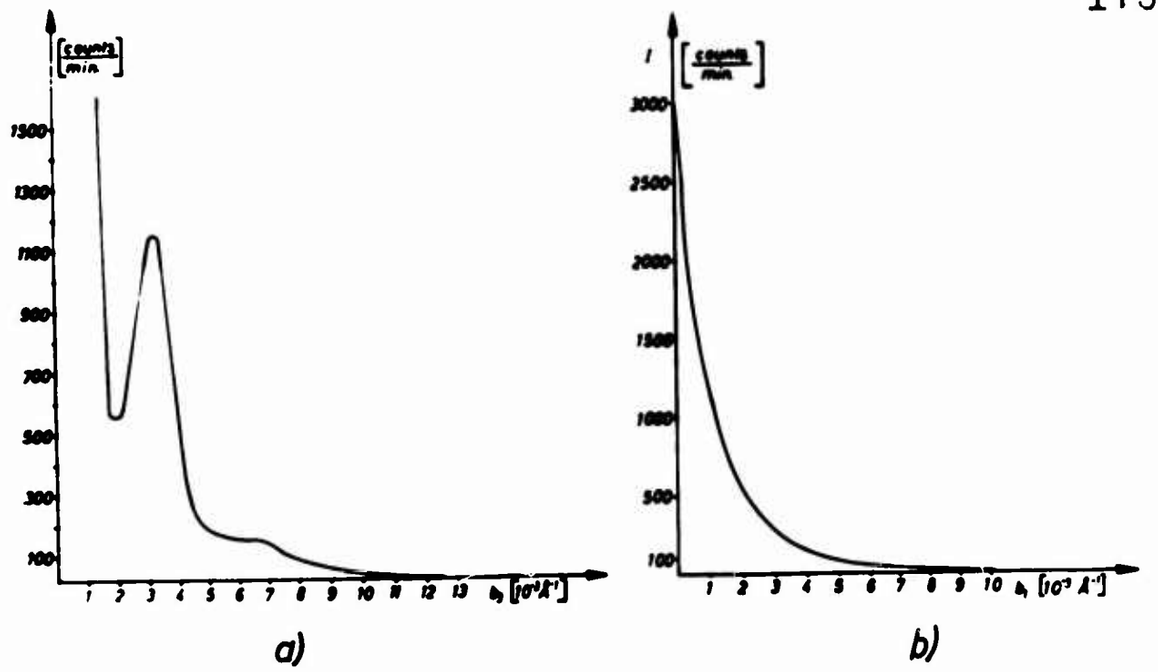

a) b)

fig. 9

a) b) c)

fig. 10

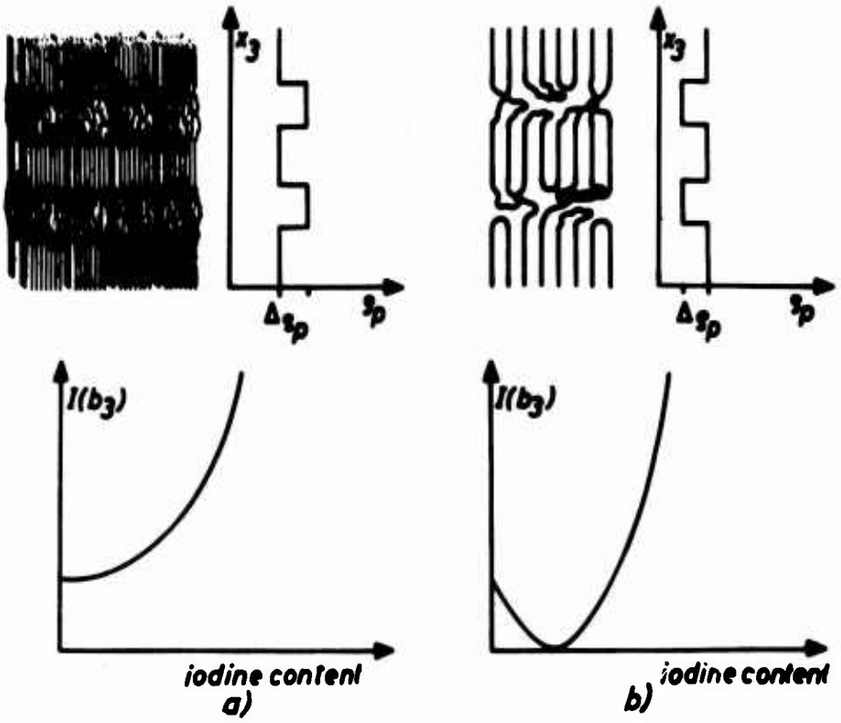
x_3
Δs_p
s_p
$I(b_3)$
iodine content
a)
b)

fig. 11

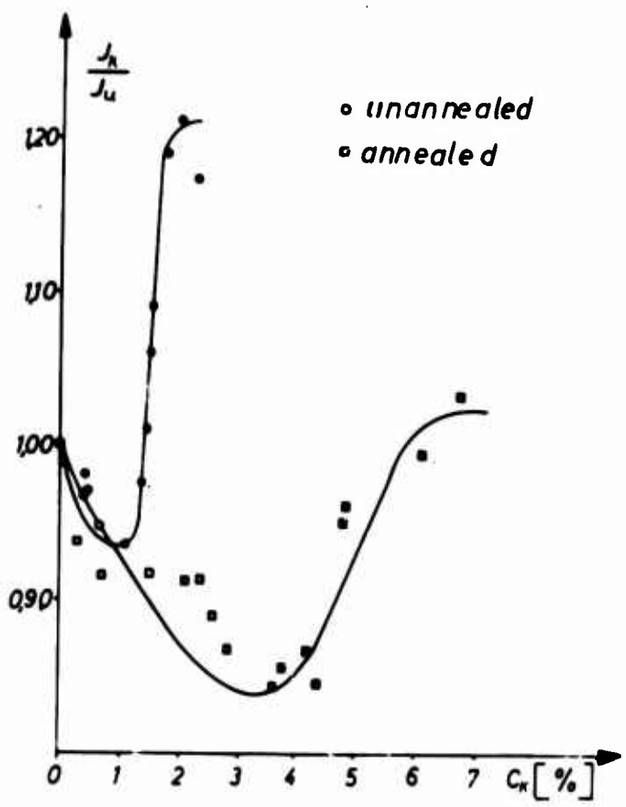
$\frac{J_k}{J_u}$
unannealed
annealed
1,20
1,10
1,00
0,90
0
1
2
3
4
5
6
7
C_K [%]

fig. 12

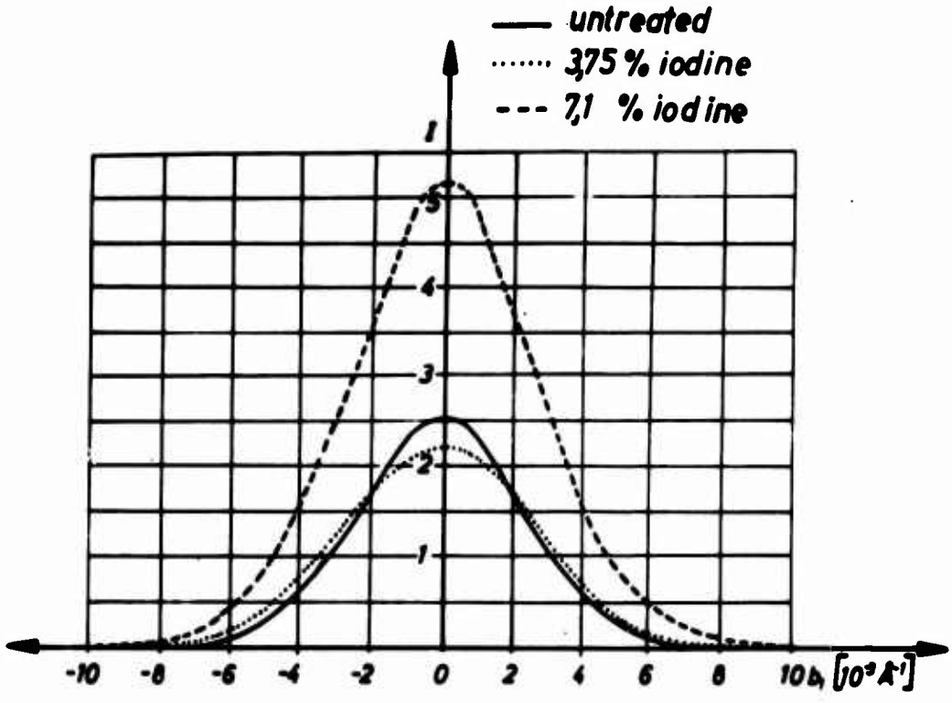
untreated
3,75 % iodine
7,1 % iodine
1
2
3
4
5
-10
-8
-6
-4
-2
0
2
4
6
8
10 h [10⁻³ Å⁻¹]

fig. 13

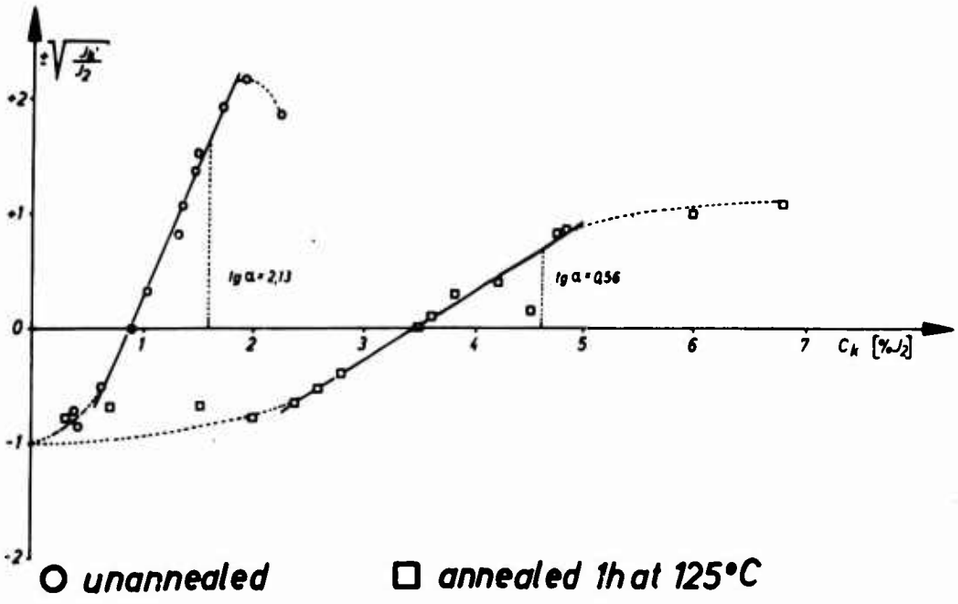
lg α = 2,13
lg α = 0,56
C_k [%-J₂]
O unannealed
□ annealed 1h at 125°C

fig. 14

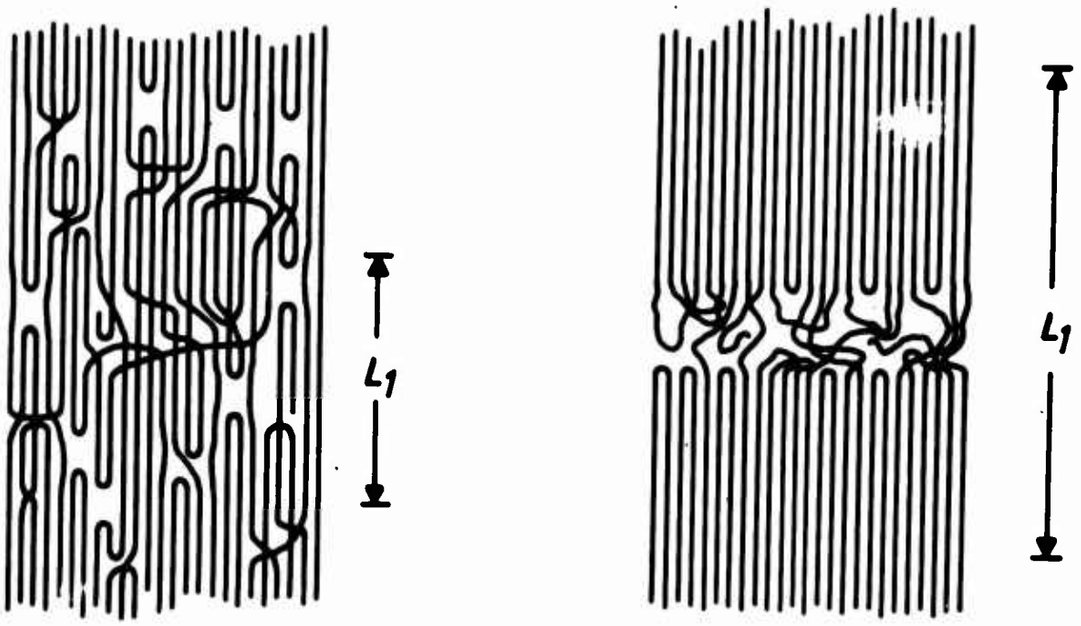

fig. 15

REGULAR CRYSTALLOGRAPHIC CHAIN-FOLDING IN POLYETHYLENE CRYSTALS

P. H. Lindenmeyer, Chemstrand, North Carolina

Ever since the discovery of single crystals of polyethylene there has been a continuing debate about the nature and the regularity of the molecular chain folding which must exist in these crystals. Experimental evidence exists which some of us contend cannot be interpreted in any other way except by a regular crystallographic chain-folding. Likewise other evidence exists which people have interpreted as conclusively precluding a regular chain folding and requiring the existence of an amorphous or disordered layer on the surface of these crystals. Obviously either one or the other of these two groups of people are in error as to their interpretation of the data or else there exists a misunderstanding or lack of communication on the meaning of terms. Although I cannot pretend to an unbiased point of view, it is my opinion that the differences involved are due to a misunderstanding of terms and definitions rather than a basic misinterpretation by either group. Specifically just what are the requirements for "an amorphous or disordered overgrowth layer" and what is required by a "regular crystallographic fold surface"?

The evidence in favor of regular crystallographic folding requires a sufficient amount of such folding to define the crystallographic nature of the fold surface so as to account for (a) the preferential cleavage (b) the pyramidal or other morphological structures and (c) the direct observation of dislocation networks. The evidence opposed to regular chain

folding rests in the contention that quantitative measurements of density, infrared absorption and enthalpy are not consistent with a regular folded chain structure. Likewise the influence of annealing and solvent swelling on NMR mobility as well as certain partial melting phenomena are more readily explained by the presence of an amorphous layer rather than a regular folded surface. The problem in reconciling these two points of view rests in defining more exactly the nature of the "regular crystallographic fold" required to produce the one set of observations and the possible nature of an "amorphous or disordered layer" which might explain the other set of observations.

It is my opinion that one might conceive of a folded chain surface which is sufficiently regular to have the observed properties of preferential cleavage, the pyramidal morphology and the dislocation networks but at the same time exhibit sufficient mobility and disorder to account for the observed density, infrared and enthalpy. Likewise the thermodynamic stability of such crystals must be such as to account for the observed annealing melting behavior.

In the remainder of this talk I hope to, first, summarize the positive experimental evidence in favor of regular crystallographic chain folding. Secondly, I will present some theoretical justification for regular crystallographic chain folding. And finally, I shall present some attempts to rationalize the opposing views.

It is my intention to try to put regular crystallographic chain folding in what I consider its proper prospective, namely -- it is a

metastable state which results under certain crystallization conditions as a consequence of the kinetics of crystallization. Since it is at best a metastable state, one would expect deviations from a perfectly regular crystallographic folded-chains under most conditions.

Turning to the first slide we see the now familiar pleats formed by the collapse of the hollow pyramidal crystals. The second slide shows Professor Keller's electron micrograph of pyramidial crystals sedimented on glycerine in which he has pressured much of the pyramidal structure. Note the definite impression of the "chair" structure in the left hand crystal. Slide number three illustrates the preferred cleavage of these crystals. In slide four we show Dr. Holland's morie' pattern with its edge type dislocations. Although this particular moire' effect does not require a regular chain folding, the dislocation network shown in slide five clearly requires a regular packing of regular crystallographic folds. The interpretation of these networks is established beyond any reasonable doubt. Their Burgers vectors were established as shown in slide six and were found to be characteristic of the orthorhombic subcell of polyethylene. Slide seven is a sketch illustrating the type of packing which would be expected to give rise to dislocations of the type observed.

I think we can safely say that at least for these particular crystals there is conclusive evidence that a regular crystallographic chain folding does exist. It is true that these crystals represent a single low molecular

weight fraction. It is conceivable that they represent some unique state. However, it would seem much more reasonable to believe that regular crystallographic folding occurs in most polymer crystallization but only in these particular crystals has it reached the degree of perfection necessary to exhibit dislocation networks. A considerable lesser degree of regular chain folding is required to produce the pyramidal morphology and presumably even less is required to produce the lamella obtained in melt crystallization.

I should like now to address myself to the question of "why do polymer molecules fold when they crystallize?" My answer to this is simply that a polymer molecule folds because it can lower its free energy by folding. Consider first an isolated polymer chain at sufficiently low temperature so that its conformation will be determined by the energy.

In slide eight we illustrate how the increase in energy required to fold a polymer chain is compensated by a decrease in energy due to the crystallographic packing of the straight chain portions. If the chain is long enough the increase in energy of the fold can always be compensated by the packing energy. Thus the lowest energy conformation of a single isolated molecule is a regularly folded chain. This same principle can be applied to an isolated molecule crystallizing on an infinite crystal substrate as shown in slide nine. We can now consider a regularly folded chain crystal as a model for a simple statistical mechanical calculation.

Each folded-chain is considered to be a small system with the various number of folds representing the various energy levels available to the system. The number of arrangements of the molecule with a given energy, the degeneracy of the energy level, is simply the number of ways of arranging the R segments which are not included in the crystal. The equations and the model used are shown in slide ten. Using the partition function shown in equation three we have calculated the free energy as a function of crystal thickness for a monodisperse polymer. The results are shown in slide eleven. Note that although the absolute minimum in free energy occurs at a crystal thickness equal to the chain length, there exist a whole series of subsidiary minima corresponding to various number of folds. If we average over a typical distribution we obtain the results shown in slide twelve.

Thus we see that for a fixed distribution of molecular lengths the folded chain crystal is the most thermodynamically stable form. However, the stability of such a crystal is extremely sensitive to the lowest molecule length species -- if these can be eliminated the free energy of the remaining crystal is reduced. Thus there is a thermodynamic driving force tending to eliminate the lowest molecular length from the crystal and consequently increase the fold period. This is the driving force that is responsible for the physical changes which occur during the aging of crystalline polymer.

One might ask "How far does this molecular species segregation proceed?" My answer is that it would like to go all the way. If only a single molecular length is available in some local area, then the extended-chain crystal is the most thermodynamically stable crystal. Thus there is a thermodynamic driving force toward complete fractionation of the molecular species, however, the extent to which molecular segregation occur depends upon the kinetics of the crystallization and annealing processes.

In my opinion the most important barrier to our understanding of the relationship between structure and physical properties -- which after all is the reason why we are interested in structure -- lies in our understanding the thermodynamics and kinetics of molecular folding and molecular species segregation.

Finally, I would like to speak briefly about some work in our laboratories which was reported briefly by Dr. McMahon at the recent physical society meeting. I want to make clear that the people responsible for this work were Drs. McMahon and McCullough and Mr. Schlegel. They have used a computor to calculate the separation distances between atoms as a function of bond rotation and a Lennard-Jones type potential function to calculate energy. They have been attempting to find those crystallographic defects which have low energies. Such defects include the crystallographic folds as well as various "kinks" and "jogs" which must be involved in the interior of polymer crystals if molecular motion is to occur.

In constructing a crystallographic fold by the rotation about C-C bonds one is faced with the solution of two problems. The first is strictly a problem in geometry. The polymer chain emerging from the crystal must be translated by a crystallographic vector to the point where it re-enters the crystal. This is a three-dimensional vector and it provides three geometrical constants which must be satisfied. In addition the chain must reverse its direction and assume the proper orientation to fit into the crystal. This provides three more geometrical restraints. Thus, in order to solve the geometry of a chain fold by bond rotation we must have at least six bonds which are rotated to satisfy the three orientational and the three translational restraints required to produce a crystallographic fold. The second problem to be solved is the requirement that the fold be a chain conformation which will minimize the energy. Therefore, in order to investigate crystallographic fold structures we must find those combinations of seven-bond rotations which satisfy the six geometrical constraints and which minimize the energy. The problem was a formidable one since the equations involved are non-linear in several different ways. I shall not trouble with details but simply say that after wondering around in seven-dimensional space for a year and a half these gentlemen came up with the solution and have tabulated all the minima in energy which are less than 100 Kcal.

The most interesting and surprising result of this work was the discovery that for these seven bond folds there exists exactly one diagonal fold (i. e. in the (110) plane) and one b-axis fold (in the (100) plane) which were at least 4 Kcal lower in energy than all other minima. These two crystallographic folds are shown in Slides 13 and 14 along with tabulated values of the seven bond rotations. Note that the diagonal fold

involves a crystallographic translation of [½½½] whereas the b axis fold involves a [0 1 0] vector. This is in agreement with the morphological studies which concluded that the diagonal fold must have a slope in the direction of the fold whereas the b axis fold does not.

At this point I must say something about the actual constants used in the potential function. It seems that everyone who works in this field has their own favorite potential function and their own reasons for preferring their function over all others. I shall not attempt to go into the various arguments here except to say that the potential function we have used is perhaps the "hardest" or "steepest" function which can be justified. All other proposed functions would be somewhat less discriminating in the structures they would allow. If we take the minima predicted by our potential function and calculate their energies using much "softer" potential functions as suggested by others we find that the number of solutions within 5 Kcal of the lowest energy structure are indeed increased but not greatly. For example, attributing 70% of the energy to an intrinsic bond potential increases the number of structures within 5 Kcal of the lowest structure from 2 to 12. Using 90% intrinsic bond potential which is certainly near the opposite extreme raises the number from 2 to 31. Thus regardless of the choice of potential function it is clear that entropy cannot play a large role in determining the structure of the seven bond crystallographic fold.

Unfortunately the search for the crystallographic fold is not yet ended. The minimum energy calculated for these seven bond folds turns out

to be 14.5 Kcal for the diagonal fold and 12.5 for the b-axis fold. (This can be reduced to 11 and 9.7 for a softer potential function). However, these results are still substantially higher than current estimates of the end surface energy by kinetic and thermodynamic methods. Three possibilities for reducing or accounting for these high energies exist: (1) the inter-molecular energy of packing these folds might result in a negative contribution to the surface energy, (2) the addition of more rotating bonds into the fold might result in a structure with lower energy and finally, (3) it may be that the comparison of these calculated energies should not be made with other estimates of surface energy since no allowance is made here for interactions with a liquid which is always present in practice.

Some progress has been made in checking the first two of these possibilities inter-molecular energies have been calculated for the packing of some of these seven-bond folds into the proper crystallographic planes [(312) for the diagonal folds and (302) for the b-axis fold]. The calculations made thus far have not yielded any negative contributions -- in fact they have all yielded exceptionally high positive energies. Thus it would appear that the seven-bond crystallographic folds not only have a somewhat higher fold energy than we would like but they also do not pack efficiently into the crystallographic planes required by experimental observations.

We have extended these calculations to eight and nine rotating bonds by observing perturbations in the vicinity of known seven-bond solutions. Although we have not yet completely investigated all the nine bond structures

it is apparent that these solutions differ from the seven-bond structures by relatively minor rotations of the additional bonds. Nevertheless, these minor rotations do permit somewhat lower fold energies and they do result in a substantial lowering of the barriers between the low energy fold structures. Thus nine-bond folds have lower energies and permit a greater possibility of motion between fold structures. Note that one would not expect a continued decrease in energy by the addition of more and more rotating bonds. A compromise must be reached between minimizing the intra-molecular fold energy and increasing the bulk of the fold so that it interferes with the inter-molecular energy of packing the fold into crystallographic planes. We are hopeful that it will be possible to arrive at a fold structure or a limited manifold of such structures which will minimize the sum of the intra and inter molecular energies.

Two important points can be made here concerning this work. (1) Regular crystallographic molecular folds are possible with a minimum of seven rotating bonds. However, they have relatively high energies and do not pack efficiently into the required crystallographic planes. (2) To obtain a crystallographic fold which has a low energy and which can pack efficiently it now appears necessary to allow more bonds to take part in the fold.

This work certainly appears to be moving in the direction of reconciling the differences between the experimental evidence which would require a regular crystallographic fold surface and that which appears to preclude such a surface. If the regular crystallographic fold surface turns out to require as many as eight or nine or even more methylene groups in order to

pack efficiently then the quantitative arguments would have to be re-assessed.

In conclusion, I think we can say that there exists both experimental evidence and theoretical justification for regular crystallographic folding in polymer crystallization. Closely associated with molecular folding is the segregation of molecular species. An understanding of the kinetics and thermodynamics of molecular folding and molecular species segregation is almost within our grasp and ought to go a long way toward providing an understanding of the relationship between structure and physical properties.

REFERENCES

1. P. H. Lindenmeyer, J. Chem. Phys. 46, 1902(1967).

2. P. E. McMahon, R. L. McCullough and A. A. Schlegel, J. Appl. Phys. 38, 4123(1967).

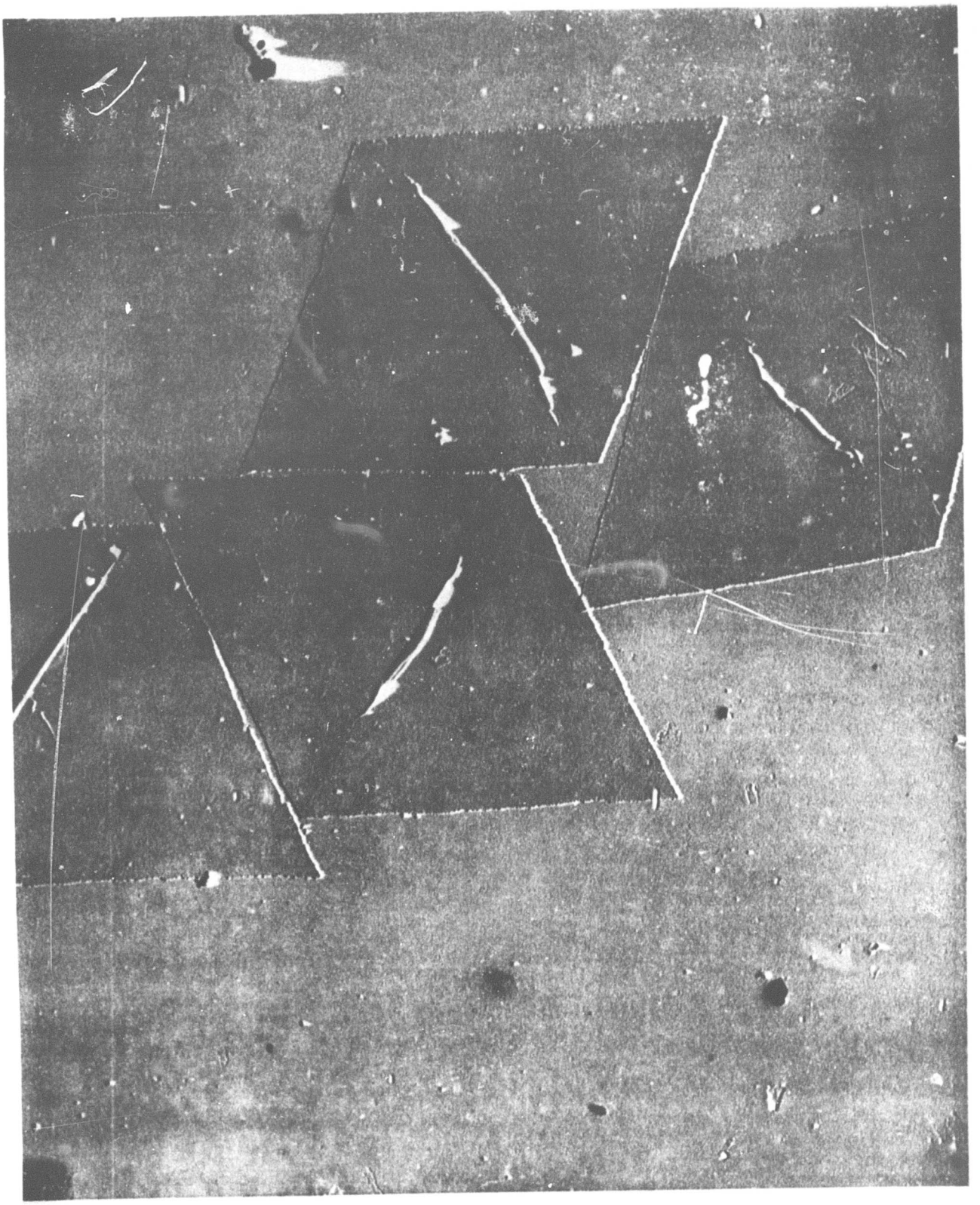

Slide 1

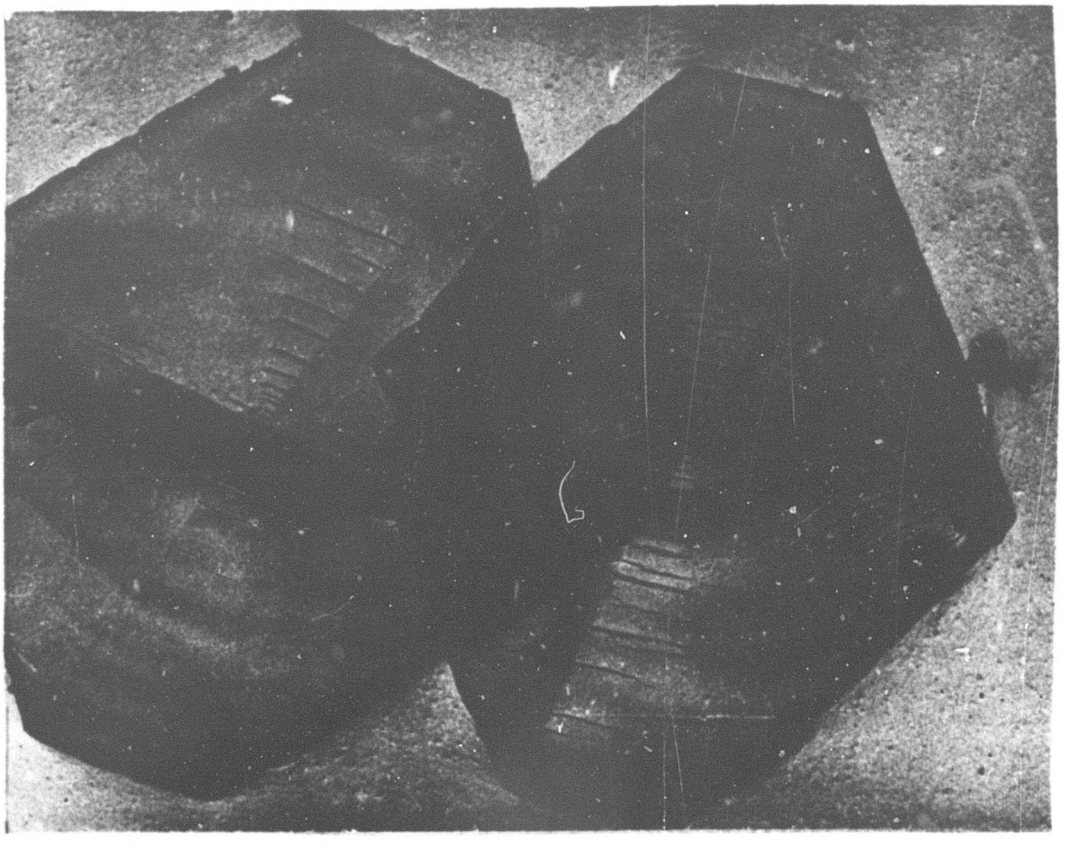

Slide 2

Slide 3

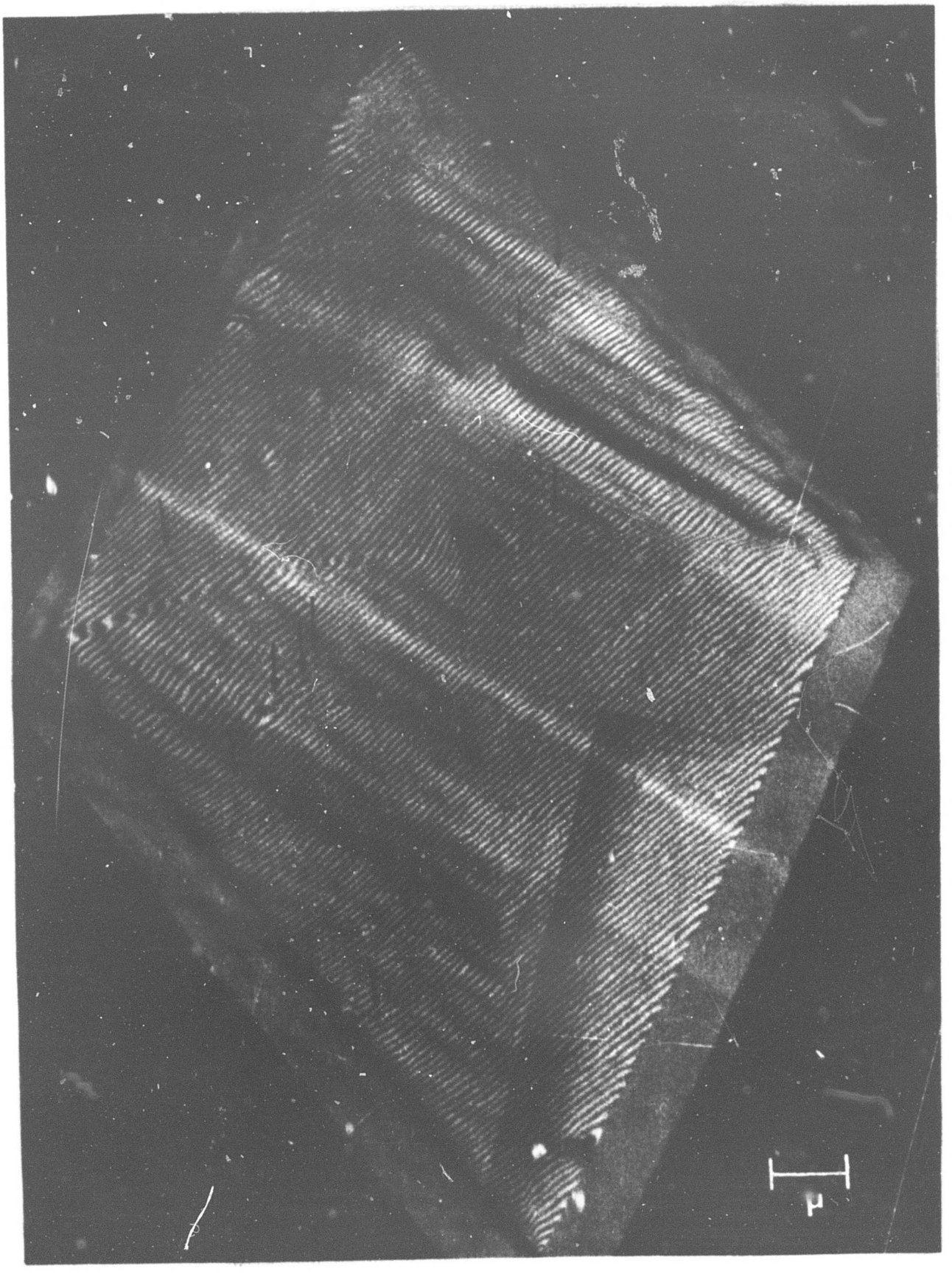

Slide 4

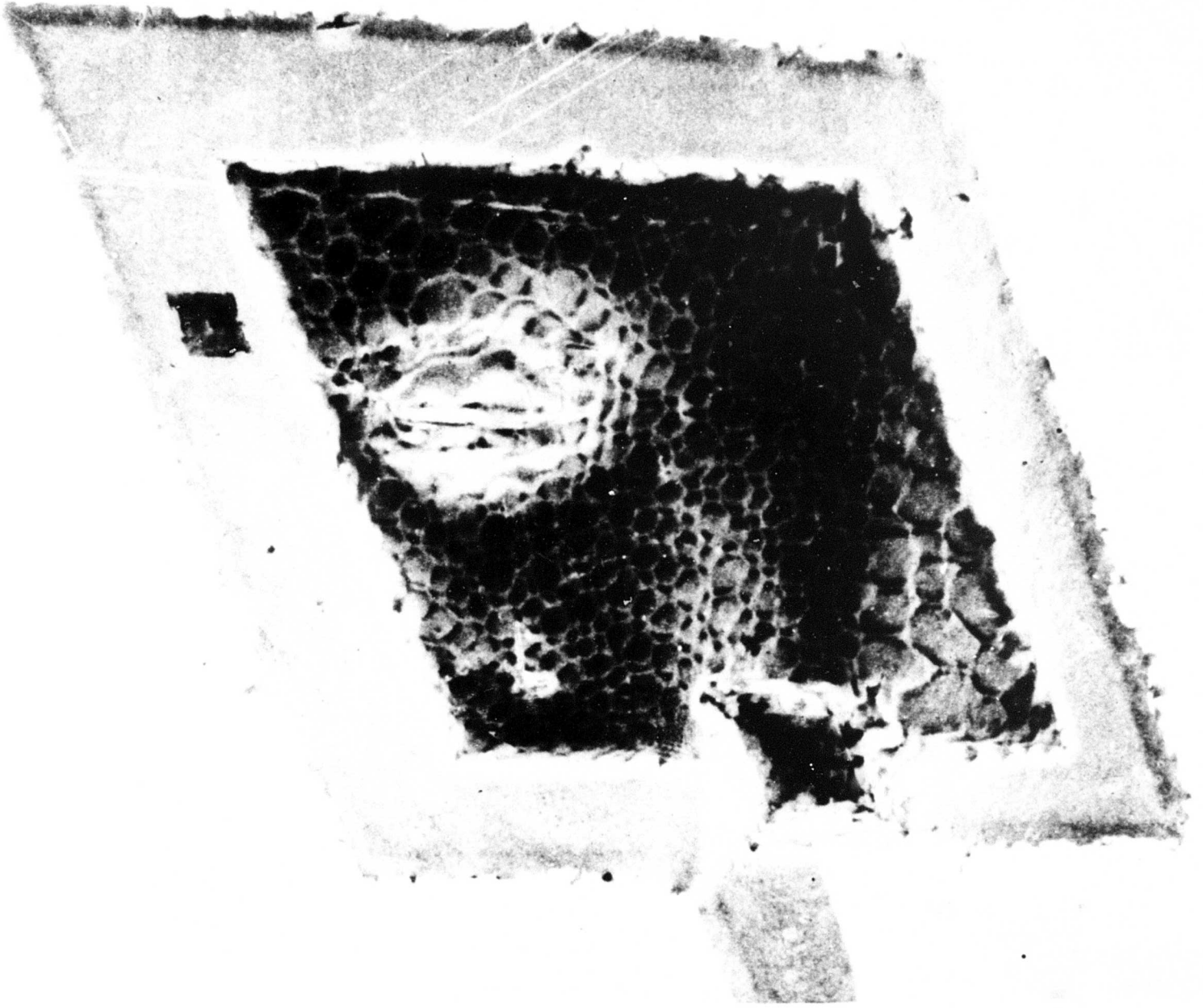

Slide 5

661

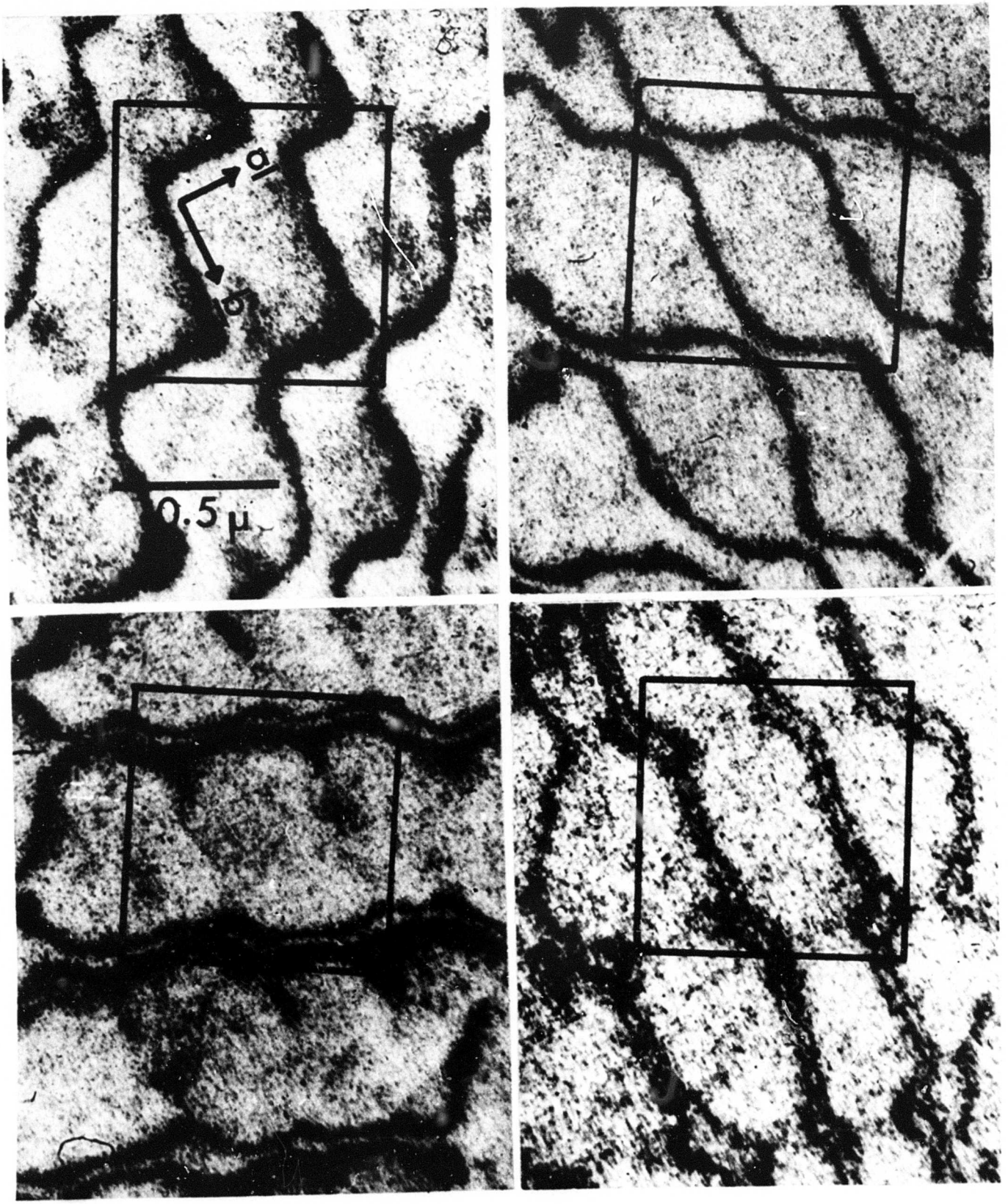

Slide 6

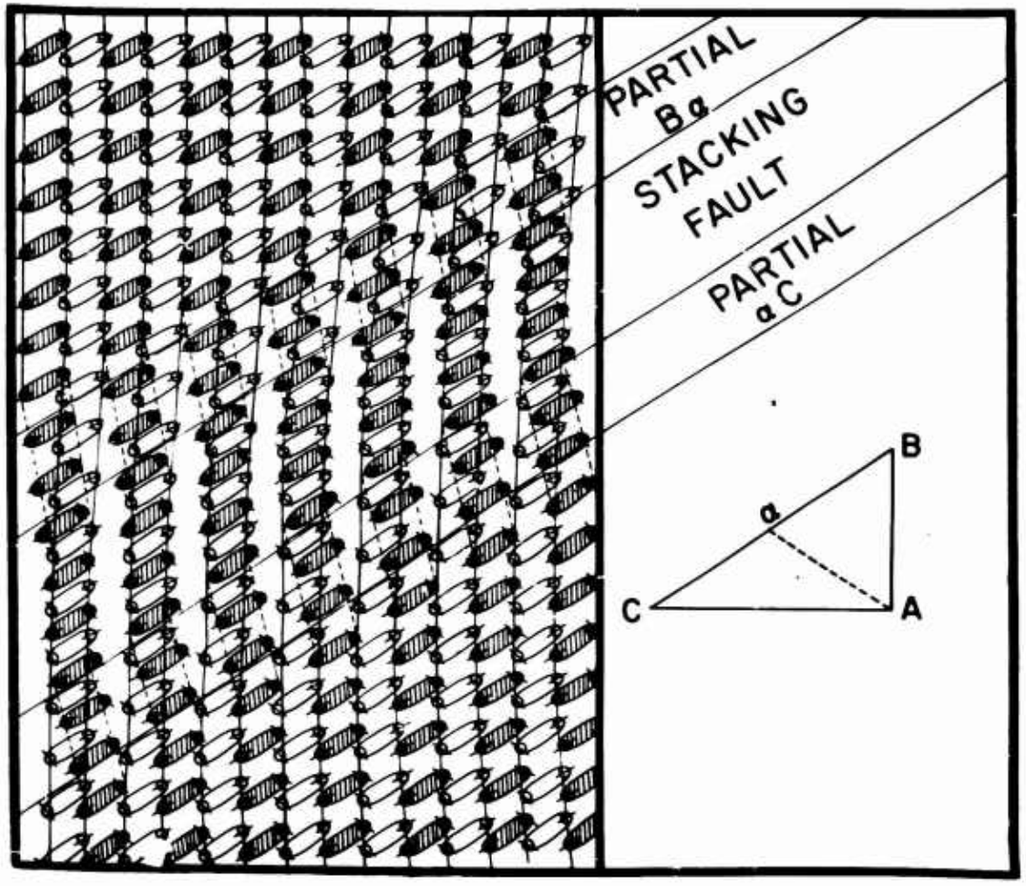

Slide 7

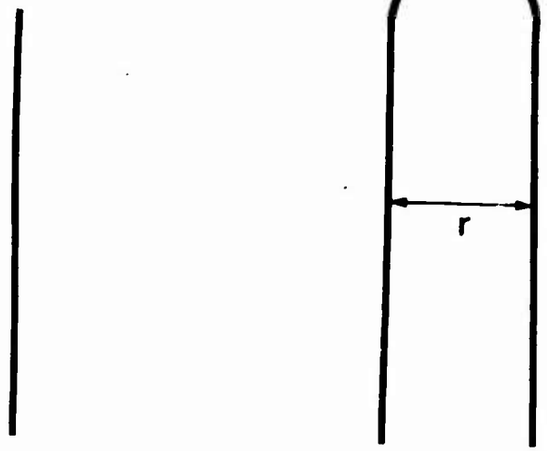

MINIMUM
INTRA-MOLECULAR
ENERGY
EXTENDED CHAIN

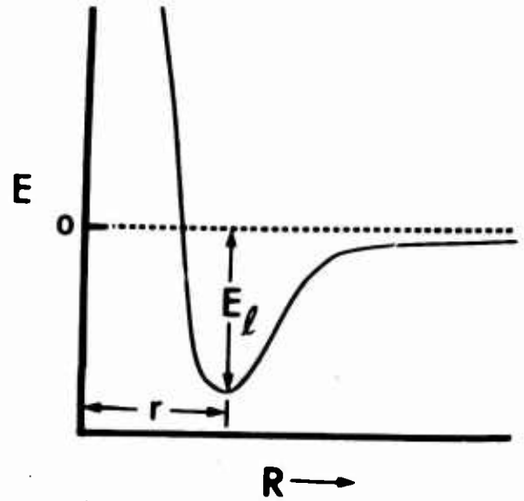

MINIMUM
INTER-MOLECULAR
COHESIVE ENERGY
FOLDED CHAIN

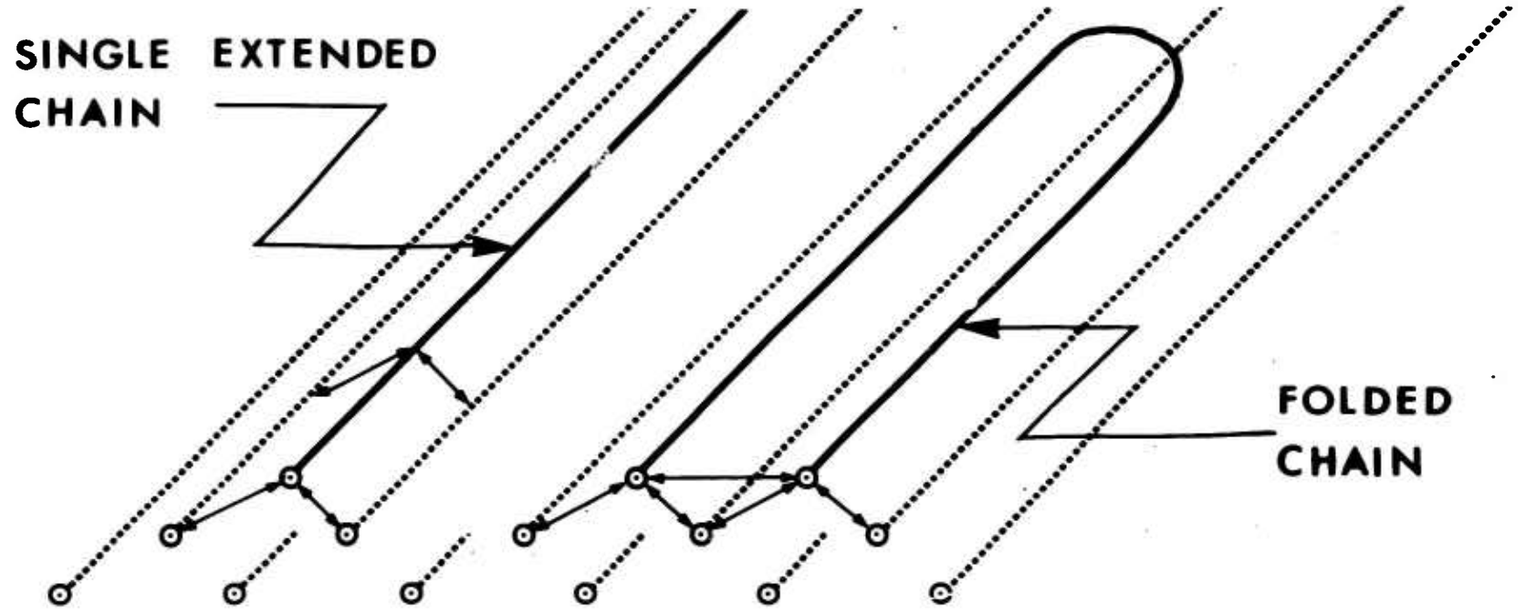

Slide 9

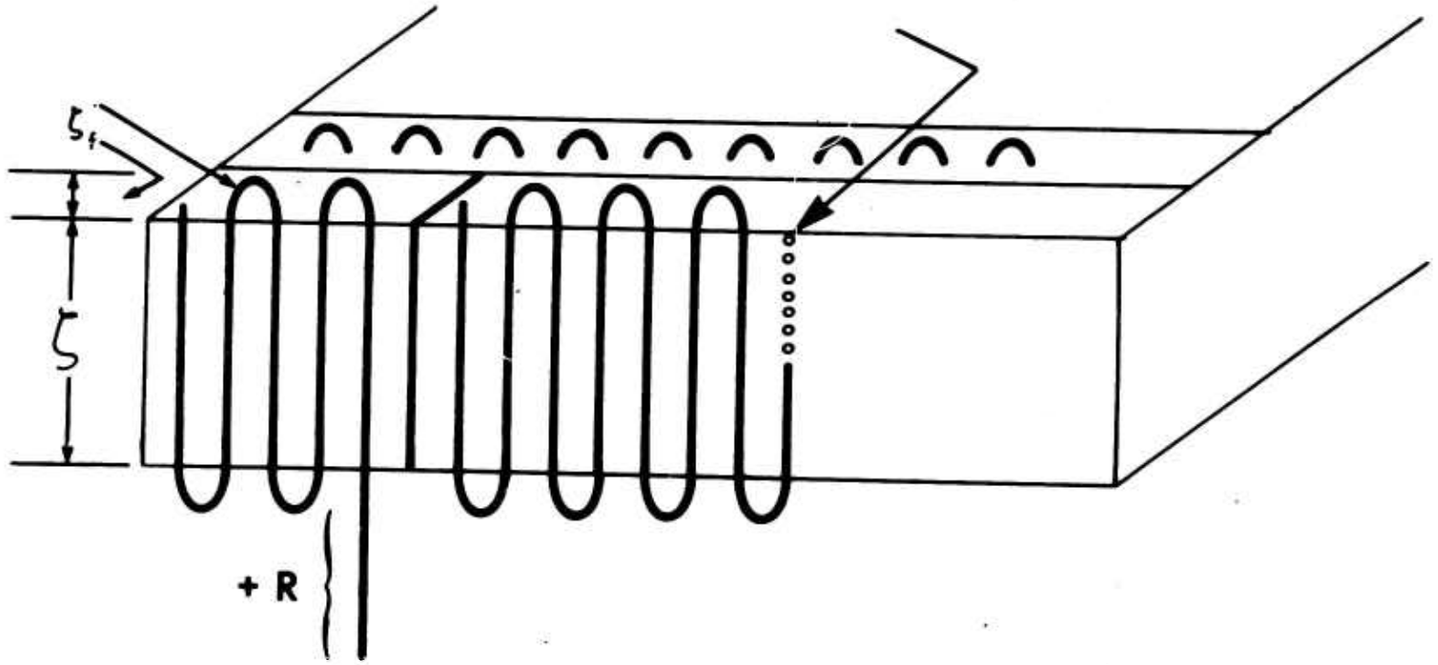

1. $E(x,\zeta,f) = \zeta_f E_f f + \zeta E_\ell (f+1) + 2RE_\ell H(R)$

2. $R(x,\zeta,f) = \chi - \zeta_f f - \zeta(f+1)$

3. $Q(x,\zeta,T) = q_N \sum_f 2[|R(x,\zeta,f)| + 1]\, e^{-\frac{E(x,\zeta,f)}{kT}}$

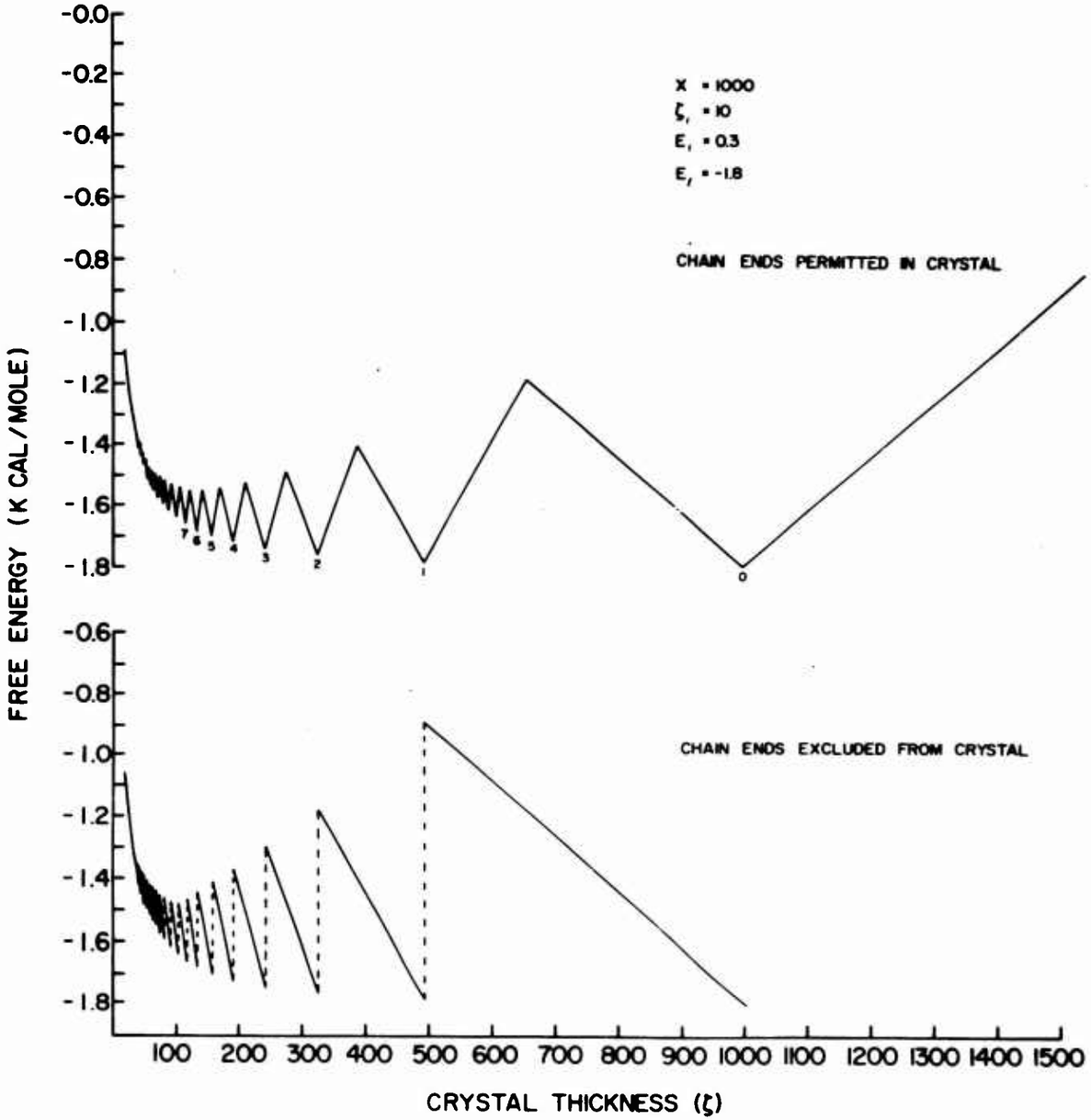
X = 1000
ζ, = 10
E, = 0.3
E, = -1.8
CHAIN ENDS PERMITTED IN CRYSTAL
CHAIN ENDS EXCLUDED FROM CRYSTAL
FREE ENERGY (K CAL/MOLE)
CRYSTAL THICKNESS (ζ)
-0.0
-0.2
-0.4
-0.6
-0.8
-1.0
-1.2
-1.4
-1.6
-1.8
100 200 300 400 500 600 700 800 900 1000 1100 1200 1300 1400 1500
7 6 5 4 3 2 1 0

Slide 11

OMITTED

Pages 206, 207, 208 representing slides 12, 13, 14 of Paper No. 9 by P. H. Lindenmeyer were missing and unfortunately could not be replaced in time for completion of the Proceedings.

Pages 209 through 214, containing a reprint of theory of Polymer-Chain Folding, THE JOURNAL OF CHEMICAL PHYSCIS Vol, 46, No. 5, 1 March 1967, were deleted for lack of permission to reprint.

Contribution by Professor Bernhard Wunderlich

Density and Heat of Fusion of Folded Chain Polyethylene Crystals

by

Fumiyuki Hamada and Bernhard Wunderlich
Department of Chemistry
Rensselaer Polytechnic Institute
Troy, New York

and

Takuji Sumida, Seiichi Hayashi and Akio Nakajima
Department of Polymer Chemistry
Kyoto University, Kyoto, Japan

Abstract

The flotation method of density determination for solution grown crystals of polyethylene is shown to be a reliable method if sufficient care is taken in preparing the crystals for density measurement. With varying crystallization temperature and molecular weight the measured density varied between 0.983 and 0.997 g cm^{-3}. The density is shown to vary with surface structure as well as lamellar thickness. The heat of fusion of solution grown crystals is proportional to specific volume as long as the fold length stays constant. Different fold length crystals show different specific volume - heat of fusion relationships.

1. Introduction

The measurements of density and heat of fusion have been the simplest and most convenient methods for characterizing the crystallinity in melt crystallized polymers. Folded chain crystals grown from solution in contrast have proven to yield conflicting data when standard methods of density determination were used. Many different values have been reported in the literature. One group of authors [1-4] found densities in the region of 0.97 g cm^{-3} by a flotation method. These values are considerably lower than the ideal crystallographic subcell density of 1.00 g cm^{-3} and require an "amorphous content" of about 20%. On the other hand, Kawai and Keller [5,6] obtained a value close to the ideal crystallographic density using the pyknometer method. Martin and Passaglia[7] finally determined the density of polyethylene single crystals from solution also using the pyknometer method and obtained a density value of about 0.98 g cm^{-3}. In addition, Kawai and coworkers[8] recently determined the density of solution grown polyethylene single crystals crystallized at various conditions using the pyknometer method and obtained densities between 0.99 and 1.00 g cm^{-3} which are still higher than the values of the other authors. Table 1 shows a summary of measured values of density of solution grown polyethylene single crystals. The present work was undertaken to find out more about the density of solution grown polyethylene crystals and to reestablish density determinations as a valuable tool in

structure determination. In addition heats of fusion and melting characteristics were measured to elucidate questions of crystal perfection.

Experimental Section

A. Materials

Molecular weight fractions of linear polyethylene were prepared by column fractionation.[9] (Sholex-6009, polyethylene manufactured by Japan Olefin Chem. Co., similar to Marlex-50). The viscosity average molecular weight of these fractions ranged from 8,400 to 280,000. Other samples were: linear polyethylene of the Marlex-50type with an approximate viscosity average molecular weight of 60,000, polymethylene with an estimated molecular weight of 10^7, and n-$C_{36}H_{74}$ paraffin. The paraffin was obtained from Humphrey Wilkinson Co. and was made by coupling of pure alkyl halides.

B. Crystallization

Two methods were used for the crystallization of polyethylene from solution. In one method polyethylene was dissolved in p-xylene under nitrogen, the hot solution was then transferred to the crystallization vessel which was kept at the chosen temperature and contained outgassed p-xylene. The final solution had a concentration of 0.1% polymer by weight. The solution was kept for 48 hours under nitrogen at the given temperature for crystallization. The resulting crystal aggregates were collected at the same temperature on a glass filter . To align the crystal lamellae as much as possible the filtering was slowed down to take about

5 hours for 200 cm^3 of suspension. The crystal mat obtained was removed from the glass filter and then dried in vacuum at 60°C. The dried mat was used for density measurement in a density gradient column, for determination of heat of fusion in a scanning calorimeter, and for the determination of lamellar thickness by small angle X-ray diffraction.

The other method of crystallization was used for sample preparation for the density measurement of single crystal aggregates in suspension. The solution of polyethylene in p-xylene of 0.1% concentration was in this case prepared under nitrogen and the hot solution was then cooled to the given crystallization temperature. After this solution was kept for seven days at the crystallization temperature, the crystal aggregates were removed for density determination in suspension.

C. Density Measurements

Different methods were used for the density measurement of polyethylene crystals differently collected. A density gradient column was used for the density measurement of the dry mats. A modified flotation method was used for the density measurement of crystal aggregates in suspension. All measurements were carried out at 23°C .

(a) Density gradient column method: The liquid for the density gradient column was a mixture of monochlorobenzene and toluene. The pieces of the dry mat and a mixed liquid having a density close to that of the crystals were evacuated

for 5-10 hours in a suitably shaped glass tube. The pieces of the dry mat were then immersed in the liquid mixture under vacuum. After further pumping for 3-4 hours to minimize the air bubbles from the dry mat, the wet crystal mat pieces were transferred to the density gradient column. The density values obtained from any one sample showed only little variation in density (from $\pm$ 0.0001 g cm^{-3} to $\pm$ 0.003 g cm^{-3} for different samples).

(b) Flotation method: A mixture of monochlorobenzene and toluene with its density close to that of the suspended crystals was prepared in a glass tube. This mixture was evacuated to eliminate all dissolved air. The polymer crystals were then transferred from the crystallization flask which was still at the crystallization temperature. The crystals were lifted gently with the help of a wire mesh net from the crystallization flask and then immediately immersed into the liquid mixture. Thus wet crystal aggregates were transferred to a liquid mixture for density measurement with a minimum of disturbance. The liquid mixture with the crystal aggregates was stirred carefully and again set under vacuum to eliminate air bubbles. Monochlorobenzene or toluene was added to the mixture to adjust the density to make the crystal aggregates float. This procedure was repeated for 7 to 30 days until the densities were matched. The density of the liquid mixture was finally determined by Mohr-Westphal balance. Any crystal aggregates which adhered to the wall of the glass tube were eliminated. When the density of the crystal aggregates and liquid mixture was nearly matched, most of the crystal aggregates floated

between the top and the bottom of the liquid mixture. Always a few crystals, however, rose to the top and a few sank to the bottom. This means that the crystals have a distribution of densities and an appropriate average had to be chosen. We tried to determine the width of the distribution of the density of crystal aggregates in suspension, but failed. The estimated width of the density distribution is 0.01 to 0.02 g cm^{-3}. This density distribution is somewhat dependent on the absolute value of the density of the crystal aggregates and is significantly broader than that measured in repeated determinations on the dry mat.

D. Heats of Fusion

The heats of fusion were determined with a Perkin-Elmer Differential Scanning Calorimeter.[10] Sample weights were 3-6 mg determined to one percent accuracy on a Cahn electrobalance. The scanning rate was 5°C min^{-1}. Calibration of the power input into the sample was performed by measurements of the heat of fusion of indium, anthracene, urea, and benzoic acid. The literature values of the heat of fusion of these substances are respectively 6.80, 38.7, 57.8, and 35.2 cal g^{-1}.[11,12] The calibrations were repeated sufficiently often to allow an estimate of the precision. The standard deviation of a single measurement of all calibrations was $\pm$ 1%. The average value of the conversion factor area measured to heat was 13.64 mcal cm^{-2}. Areas of the power-time recordings were evaluated by planimetry. The sensitivity chosen was 4x (about 4 mcal min^{-1}).

The reproducibility of heats of fusion obtained was found to be better than two percent in most cases. Difficulties in drawing the base line existed because of considerable reorganization during heating causing a broad melting peak. These difficulties were minimized by determination of the start of melting on large amounts of substance and drawing the baseline in accordance with the thus predetermined melting range. The typical melting range as determined in this way by the first deviation from pure specific heat recording stretched from 100 to 135°C. All actual areas measured varied between 13 cm^2 and 23 cm^2. No correction[15,16] based on the surface enthalpy of lamella of the crystals is included in the values reported.

Results

A) Paraffins

To have a check on the methods of density measurement, we determined first the density of single crystal aggregates of $n\text{-}C_{36}H_{74}$. The crystals were grown from methyl acetate solution at 43.3°C within two days. The single crystals as observed by interference microscopy were multilayer crystals with an average size of 50μ. First the density was measured in a gradient column made of a mixture of ethyl alcohol and water. The single crystal aggregates were transferred directly to the density gradient using a wire mesh net. In this way the crystals never dried out. The obtained value of density was 0.950 g cm^{-3}, a value lower than the crystallographic density. Next, the density was measured by the flotation method as described above starting with a mixture

of ethyl alcohol and water of density 0.950 g cm^{-3}. Most of the paraffin single crystal aggregates showed a density of 0.960 g cm^{-3} but a few aggregates showed a density of 0.965 g cm^{-3}. The density 0.960 g cm^{-3} corresponds to the known crystallographic density of the orthorhombic form[13] and the density 0.965 corresponds to the crystallographic density of the monoclinic form.[14] The weight of the crystals of density 0.965 g cm^{-3} was too small for X-ray diffraction analysis. Overall the distribution of density was narrow ($\pm$ 0.002 g cm^{-3}) and the agreement of the calculated data from X-ray diffraction with flotation method was good. In contrast the values obtained by the density gradient method were significantly less than the crystallographic density. This lower density might be due to remaining air bubbles on the surface of the single crystal aggregates and/or to the trapped solvent between the lamellae of the crystals. Also the density of single crystal mats was determined by the density gradient column method. The result was 0.942 g cm^{-3}, even lower than the density of the single crystals in suspension in the density gradient column. This added density defect is probably caused by the voids in single crystal mats produced during the filtering operation.

These preliminary experiments show that the density measurement of single crystal aggregates in suspension by the flotation method can give correct answers for small lamellar crystals, while the density gradient column seems to yield too low values.

B) Polyethylene

Table 2 shows the density and low angle spacing of polyethylene crystals grown from solution at various crystallization temperatures and solvents. In Fig. 1, the filled circles mark the average densities of polyethylene crystal aggregates grown from p-xylene solution at different crystallization temperatures for a molecular weight fraction of 42,000. The open circles represent the density of dry mats of identically crystallized polyethylene measured in a density gradient column. Both sets of data show that the density increases with increasing crystallization temperature. The density values of single crystal aggregates measured in suspension are, however, significantly higher than the density values obtained from the filtered dry mats. The difference is bigger at the lower crystallization temperatures. Figure 2 shows a plot of the density of polyethylene single crystal aggregates crystallized from p-xylene at 84.5°C as a function of molecular weight. Filled circles again show the density of crystals in suspension and open circles show the density of dry mats. The density decreases with increasing molecular weight. Also shown in Fig. 2, are a filled triangle and an open triangle which respectively show the density of crystal aggregates in suspension and dry mats of unfractionated Marlex 50. The filled square and the open square show the density of single crystal aggregates in suspension and dry mats of polymethylene, respectively.

To solve the question whether high density crystals also have a high enthalpy of fusion, the heat of fusion of solution-grown polyethylene and n-$C_{36}H_{74}$ single crystals was measured with the differential scanning calorimeter

In Fig. 3 and Fig. 4, some of the observed melting curves are shown. Figure 5 is a plot of the measured heat of fusion of solution-grown polyethylene crystals and n-$C_{36}H_{74}$ crystals as a function of the specific volume at 23°C. Curves 1 and 2 are the results on polyethylene crystals obtained by us, curve 4 shows the heats of fusion of the paraffins, curve 3 reproduces uncorrected data of the heat of fusion of solution grown polyethylene crystals by Fischer,[15,16] and Hendus and Illers.[17] The heats of fusion of n-$C_{19}H_{40}$ and n-$C_{25}H_{52}$ single crystals were adopted from that of the orthorhombic form reported in the literature.[18-20] The heat of fusion of n-$C_{100}H_{202}$ was calculated using the equation given by Flory,[21] modified to fit the extrapolated value (ΔH = 980 cal mol^{-1})[15,16] of heat of fusion of specific volume 1.000 $cm^3 g^{-1}$:

$$\Delta H_n = 980 - \Delta C_p \Delta T - (2150/n)$$

ΔH_n is the enthalpy of fusion per CH_2 group of the paraffin of chain length n, ΔT is the difference between the equilibrium melting temperature of an extended chain polymer crystal of infinite molecular weight (about 142°C)[29] and the melting point of the n-paraffin homolog of chain length n, ΔC_p finally is the difference between the heat capacity of extended chain crystals of polyethylene[23] and the heat capacity of amorphous polyethylene.[24] The densities of n-$C_{19}H_{40}$, n-$C_{25}H_{52}$ and n-$C_{100}H_{202}$ were calculated from crystallographic data of the orthorhombic unit cell in the literature[20] and for the density of n-$C_{36}H_{74}$ the measured density for the orthorhombic unit cell was used. The open square shows the heat of fusion of unfractionated Marlex 50

crystallized under high pressure.[25] The extrapolation of plot 2 to a specific volume of 1.000, which is the ideal crystallographic subcell specific volume of polyethylene, yields a heat of fusion of about 65 cal g^{-1} while the extrapolations of curves 1, 3, and 4, to a specific volume of 1.000 cm^3 g^{-1} yield about 70 cal g^{-1}.

Discussion

A. Flotation Densities

First we shall discuss the reliability of the flotation method as a method of density measurement of small crystal aggregates in suspension. In one set of measurements we compared the density obtained by the flotation method directly with that obtained by the density gradient column method on the identical crystals. When the densities of the crystal aggregates and the flotation liquid were nearly matched and the aggregates floated between the top and the bottom of the liquid mixture, some of the floating crystal aggregates were carefully transferred to a density gradient column of the same liquid pair using a pipette. The density obtained in the density gradient column was often the same as in the flotation method, but occasionally somewhat lower than that obtained by the flotation method. We ascribe this inconsistency in results to the degree of care taken in transfer of the crystal. It is extremely difficult to accomplish the transfer without picking up air. In the case of dry mats, we obtained always nearly the same density by both methods. The transfer in this case is much easier because of the more compact nature of the crystals. Although the density gradient

column method is subject to some error due to the interfacial free energy gradient present in the column,[6] we have shown here that this error is negligible for the toluene-monochlorobenzene liquid pair. A similar conclusion was reached by Fischer for the propyl alcohol-dioxane liquid pair.[15,16] It is noteworthy, however, that unless sufficient care is taken in preparing the sample, the density gradient method may give considerably lower density values in the case of solution grown polyethylene crystal aggregates in suspension. In the case of poor preparation of sample for density measurement, for example by direct transfer of crystal aggregates without intermediate elimination of air by evacuation we observed as much as 0.025 g cm^{-3} lower densities for the same materials. This lower density is probably due to air bubbles added to the surface of the single crystal aggregates and trapped solvent between lamellae of crystals. The trapped solvent caused the density of polyethylene crystals from p-xylene to increase gradually slightly with time until after one to two days a constant value was approached, while the density of polyethylene crystals from tetrachloroethylene decreased slightly rapidly with time so that a constant value was approached after about three hours.

The difference between the density of crystal aggregates in suspension and that of dry mats as shown in Fig. 1 and Fig. 2 is of great importance. This difference seems to be due to the voids in the dry mat. We reached this conclusion because of the following facts: a) The density of a dry mat which was dried very well shows a slightly lower density than that dried poorly. b) The difference between density

values of crystal aggregates in suspension and as dry mats decreases with increasing crystallization temperature.
c) The collapsed crystal aggregates contain voids visible by microscopy. These voids are initially filled with solvent but cannot be refilled when the solvent was once removed by drying. The dry mats of crystals grown at higher crystallization temperature have less voids because of the more regular structure of the crystals and because of the higher temperature used for filtration. Figure 6 is an interference micrograph of a collapsed polyethylene growth spiral covered on both sides with a vacuum deposit of silver.[26] Several areas of irregular collapse can be seen. Similar growth spirals observed by double beam interferometry with transmitted light show none of these voide[27] since the reference beam is carried through air and eliminates thus any phase difference lack due to voids. It may be possible to improve this method by using instead of the weak gravitational force the centrifugal force of a centrifuge. This should increase the sensitivity to a change in density. Lower density values might still be obtained, however, unless similar care as described above is taken in sample preparation.[6]

Another inevitable problem in density determination of small crystals by flotation method is the selective adsorption of one of the measuring liquids. We checked, therefore, the effect of the selective adsorption on the density of crystals. The results are shown in Table 3. The effect is easily measurable, but much smaller than the effect of poor sample preparation. The density is affected only in the third

decimal. In the case of n-butyl benzoate only a single liquid which has the density of 1.000 at 26°C was used in the flotation method. The temperature at which the crystals float between the top and the bottom of the single liquid was measured and then the density at 23°C was calculated using thermal expansion coefficients. The reproducibility of this method was not as good and the density obtained by this method may have some uncertainty.

The last problem to be discussed is the increase in density caused by oxidation during the preparation of polyethylene fractions and during crystallization from solution. According to Hendus and Illers,[17] a small C=O content in polyethylene may significantly affect the density and the heat of fusion of polyethylene crystals. We checked the C=O content of our crystals by determination of I R absorption at 1720 cm^{-1}. The C=O content found was below 0.1%. The effect of C=O content in our crystals on the density and heat of fusion should therefore be small.

In summary it has been shown that the flotation method can give reliable data if adsorbed air is eliminated by careful sample preparation. Remaining systematic errors are solvent adsorption and possible oxidation. In our case (monochlorobenzene-toluene) both of these factors could give slightly too high densities. We estimate this error to be less than 0.5%.

B. Effect of Crystallization Conditions and Molecular Weight on Density.

Figure 1 shows that the density of crystals of polyethylene of molecular weight 42,000 grown from p-xylene

increases with increasing crystallization temperature. This increase in density may be caused by two effects, the decrease in the amount of (001) surface area in a crystal due to the increase of lamella thickness, and the change in the structure of the (001) surface with increasing crystallization temperature, since the sub-cell unit density does not vary significantly. The change of morphology of crystals grown from xylene or tetralin at various temperatures can be seen by interference microscopy[28] and by electron microscopy.[4, 29] At high crystallization temperature single crystals are formed, while at low crystallization temperature dendrites grow. In accord with this change in morphology the melting curves as determined by the differential scanning calorimeter change as can be seen from Fig. 3. The melting curves of crystals grown from xylene solution at higher temperature show two peaks while the melting curves of crystals from xylene grown at lower temperature show only the higher temperature peak. The interpretation can be made in conjunction with previous detailed analyses of time dependent melting in our laboratory.[30,31] The dendrites grown at lower temperature are less stable thermodynamically, but can recrystallize faster into crystals of larger fold length than the single crystals grown at higher temperature which are somewhat more stable, but less mobile. The single peak at higher temperature indicates thus only the melting of reorganized crystals and the double peaks show melting of crystals with less reorganization besides a portion which has reorganized more. Figure 2 shows that the density of crystals grown at 84.5°C from p-xylene decreases with increasing molecular

weight. The morphology of crystals grown from xylene changes also somewhat with increasing molecular weight.[28,29] It is easy to form orthorhombic single crystals from polyethylene fractions of lower molecular weight, while dendrite or complicated crystal are obtained from polyethylene of high molecular weight. The fold length, however, is largely independent on molecular weight,[29] so that the low density in crystals of high molecular weight polyethylene must be mainly due to a change in surface structure and a possible presence of tie molecules. The effect of the molecular weight is also shown in the melting curves of polyethylene crystals grown at 84.5°C from p-xylene in Fig. 4. The melting curves of lower molecular weight crystals show two peaks, while the melting curves of crystals of polyethylene of higher molecular weight show only one peak at the higher temperature. This indicates again that the crystals of high molecular weight of less perfect crystal structure can recrystallize faster into lamellae of larger thickness than those of low molecular weight which have a more perfect crystal structure.

In summary the density of crystal aggregates in suspension was found to vary between 0.983 and 0.997 g cm^{-3} according to the conditions of crystallization and the molecular weight of the sample. Most of these values are significantly higher than the values obtained by authors other than Kawai and Keller.[5,8] Crystals grown from solution at lower temperature show lower densities. Crystals of higher molecular weight and unfractionated polyethylene grown from solution also show lower density. This result is consistent with the data by Martin and Passaglia,[7] but is not consistemt with the

result of Kawai and Keller.[5,8] It is noteworthy, that we found in all cases a few crystals having a density of nearly one included in the single crystal aggregates. The densities measured on the dried mats are generally lower and are similar to data obtained by Fischer.[15,16]

C. Heats of Fusion.

In Fig. 5, we can see the effect of crystallization temperature and molecular weight on the heat of fusion of polyethylene. The points plotted in curve 1 show the heat of fusion of crystals of polyethylene having the same molecular weight, but different lamellar thickness because of various crystallization temperatures. The increase in heat of fusion with increasing crystallization temperature must in this case mainly be due to the decrease of the amount of lamellar (001) surface area due to the increase in fold length. The measured heat of fusion of the almost extended chain polyethylene[25] falls nearly on the same curve. The points plotted in curve 2 show the heats of fusion of crystals of polyethylene having various molecular weights but identical lamellar thickness because of identical crystallization temperature. The heats of fusion plotted in curve 2 increase with decreasing molecular weight. This must be due to the formation of more compact crystals with more regular surfaces with decreasing molecular weight. The difference between the extrapolated heat of fusion of curve 1 and 2 to specific volume of 1.000 $cm^3 g^{-1}$ is about 5 cal g^{-1}. This difference is a measure of the decrease in heat of fusion on folding if the folded region of lamellae

has a specific volume of 1.000 $cm^3 g^{-1}$. Our heats of fusion agree with the heat of fusion obtained by Fischer,[15,16] and Hendus and Illers[17] on similar solution grown crystals. The discrepancy between our curves 1 and 2, and curve 3 is due to the discrepancy between our density data and their density data.[15,17] Curve 4 shows the heats of fusion of n-paraffins. The heat of fusion increases with increasing carbon number and approaches the value for the heat of fusion of extended chain crystals of polyethylene of high molecular weight. The difference of this curve to a similar one shown by Hendus and Illers[17] is due to our use of crystallographic specific volume of paraffins.

In summary the heat of fusion measurements support the conclusions drawn from the density measurements: Both (001)-surface structure and surface area must be considered as major factors in interpretation of crystals grown from solution. Each series of polyethylene crystals of constant fold length has a different heat of fusion-specific volume relation displaced from the curve for melt crystallized polyethylene to lower heats of fusion.

Acknowledgements.
The work performed at Rensselaer was supported by
The National Aeronautics and Space Administration.

Authors wish to express their appreciation to Mr. J. Mitchel Jr and Mr. C. E. Day of duPont de Nemours & Co., for their giving the information about the infrared determination of carbonyl content of oxidized polyethylene.
The heats of fusion were determined in cooperation with
Miss C. M. Cormier and Mr. C. L. Gruner.

References

1) B. Wunderlich, and W. H. Kashdan, J. Polymer Sci., 50 71 (1961)

2) E. W. Fischer, and G. F. Schmidt, Angew, Chem., 74, 551 (1962)

3) E. W. Fischer, and R. Lorenz, Kolloid-Z & Z. Polymere, 189, 97 (1963)

4) J. B. Jackson, P. J. Flory and R. Chiang, Trans. Faraday Soc., 59, 1906 (1963)

5) T. Kawai, and A. Keller, Phil. Mag. 8, 1203 (1963)

6) T. Kawai, and A. Keller, Phil. Mag. 8 1973 (1963)

7) G. M. Martin, and E. Passaglia, J. Res. Natl. Bur. Stand., 70A, 221 (1966)

8) T. Hama, T. Goto, T. Kawai and H. Maeda, Paper presented at IUPAC Meeting, Tokyo, Kyoto, Japan (1966)

9. V. Desreux, Rec. Trav. Chim., 68, 789 (1949): P. Henry, J. Polymer Sci., 36, 3 (1959); R. Chiang, J. Phys. Chem. 69, 1645 (1965)

10) M. O'Neill, J. Anal. Chem., 36, 1238 (1964); E. S. Watson, M. J. O'Neill, J. Justin and N. Brenner, Ibid., 1233 (1964)

11) Landolt-Bornstein, Zahlenwerte and Funotionen, Vol.II Berlin, (1961)

12) For the values chosen for indium and benzoic acid see also W. Oelson, O. Oelson and U. D. Thiel, Z. Metallk 46, 555 (1955); G. T. Furukawa, R. E. McCoskey and G. J. King, J. Res. Natl. Bur. Stand., 47, 256 (1951)

13) V. Vand, Acta Cryst., 6, 797 (1953)

14) H. M. M. Shearer and V. Vand, Acta Cryst., 9, 379 (1956)

15) E. W. Fischer and G. Hinrichsen, Polymer (London), 7, 195 (1966)

16) E. W. Fischer and G. Hinrichsen, Kolloid-Z. & Polymere 213, 93 (1966)

17) H. Hendus and K. H. Illers, Kunststoffe, 57, 193 (1967)

18) A. A. Schaerer, C. J. Busso, A. E. Smith and L. B. Skinner J. Am. Chem. Soc., 77, 2017 (1955)

19) F. W. Billmeyer, Jr., J. Appl. Phys., 28, 1114 (1957)

20) M. G. Broadhurst, J. Res. Natl. Bur. Stand., 66A, 241 (1963)

21) P. J. Flory and A. Vrij, J. Am. Chem. Soc., 85,

22) T. Arakawa, Ph.D. Thesis, Department of Chemistry, Cornell University, Ithaca, N.Y. (1964)

23) B. Wunderlich, J. Phys. Chem., 69 2078 (1965)

24) B. Wunderlich, J. Chem. Phys., 37 1203 (1962)

25) B. Wunderlich and C. M. Cormier, J. Phys. Chem. (in press)

26) P. Sullivan and B. Wunderlich, SPE Transactions, 4, (1964)

27) See for example Fig. 7 in B. Wunderlich, J. Polymer Sci., Part C, 1 41 (1963)

28) B. Wunderlich, E. A. James and T. Shu, J. Polymer Sci., A2, 2759 (1964)

29) V. F. Holland and P. H. Lindenmeyer, J. Polymer Sci., 57 589 (1962)

30) B. Wunderlich, P. Sullivan, T. Arakawa, A. B. DiCyan, and J. F. Flood, J. Polymer Sci., Part A, 1, 3281 (1963)

31) E. Hellmuth and B. Wunderlich, J. Appl. Phys. 36, 3039 (1965)

Figure 1. The effect of crystallisation temperature on the density of polyethylene crystals of the same molecular weight (42,000) grown from p-xylene at various temperatures. Filled circles represent measurements of crystal suspension by the flotation method. Open circles are the same crystals measured in the density gradient column after filtration to a dry mat.

Figure 2. The effect of molecular weight on the density of polyethylene crystals grown from p-xylene at 84.5°C. Meaning of circles as in Fig. 1. Triangles represent unfractionated Marlex 50, squares represent polyethylene.

Figure 3. Melting curves for polyethylene crystals grown at 70°C, 84.5°C, and 89.1°C of the same molecular weight (42.000) (heating rate 5°C min^{-1} normalized to equal weights, not corrected for instrument lag).

Figure 4. Melting curves for polyethylene crystals of MW 8,400. 42,000 and 280,000 crystallized at 84.5°C (heating rate, 5°C min^{-1}, normalized to equal weights, not corrected for instrument lag).

Figure 5. Plot of the measured values of the heat of fusion of polyethylene crystals, from solution and n-paraffins as a function of the specific volume at 23°C.

Curve 1: Polyethylene crystals of same molecular weight (42,000) grown from p-xylene at various temperatures; from bottom to top, 60°C, 70°C, 84.5°C and 89.1°C.

Curve 2: Polyethylene crystals of various molecular weight grown from p-xylene at 84.5°C; from bottom to top, MW 60,000 (broad distribution), 280,000, 10^7 polyethylene, 140,000, 42,000 and 8,400.

Curve 3: Data on polyethylene crystal grown from solution obtained by Fischer,[15,16] and Hendus and Illers.[17]

Curve 4: n-paraffin crystals of orthorhombic form.

Figure 6. A top and bottom silvered polyethylene growth spiral viewed with transmitted light. The illumination is from an unfiltered mercury lamp. The long side of the photograph corresponds to 0.19mm. The contrast is caused by interference at the top and bottom silver layer.[26]

Table 1

Density of Polyethylene Single Crystals from Solution

Method:	Author	Density
SUSPENSION:		
A. Centrifuge Flotation	Fischer (1963)	0.96~0.97
	Flory (1963)	0.970~0.97
B. Flotation	Wunderlich (1961)	0.965
DRY MAT:		
C. Density Gradient Tube	Fischer (1963)	0.96~0.97
	(1966)	0.96~0.98
D. Flotation	Wunderlich (1961)	0.965
PYKNOMETER METHOD:		
	Fischer (1963)	0.96~0.97
	Kawai,Keller (1963	1.00
	Martin, Passaglia (1966)	0.98
	Kawai et al (1966)	0.99~1.00

Table 2

Density of Polyethylene Crystals*

from Solution in g cm^{-3} at 23°C

Solvent used	T_c (°C)	$\langle \bar{l} \rangle$ (Å)	Density Gradient Tube (Dry Mat)	Flotation Method (Suspension)
p-xylene	89.1	151.7	0.993	0.995
	86.0	140.1	0.985	–
	84.5	-	0.984	0.994
	78.1	117.6	0.980	-
	70.0	-	0.976	0.992
	60.0	-	0.974	0.987
decalin	83.9	121	0.981	0.997
	75.4	839	0.976	-
n-hexadecane	106.5	181	0.990	0.992
	95.9	143	0.985	-

* Molecular weight fraction 42,000.

Table 3

Effects of Selective Adsorption of a Solvent in Determination of Density

Solvents used	Density measured
Carbon Tetrachloride + Toluene	0.998
Monochlorobenzene + Toluene	0.997
Butyl Benzoate	0.993
Ethyl Alcohol + Water	0.990

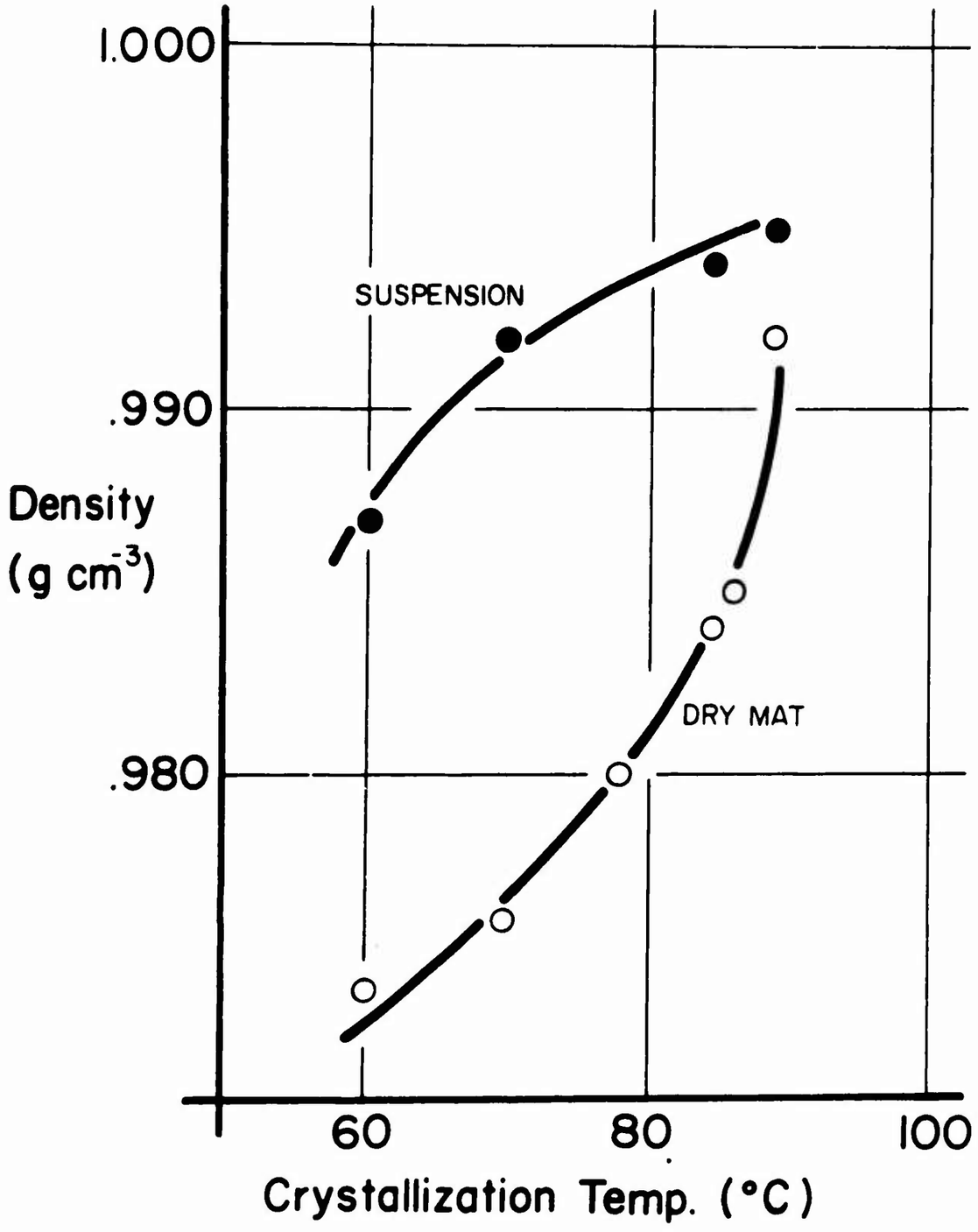
1.000
.990
.980
Density
(g cm^{-3})
SUSPENSION
DRY MAT
60
80
100
Crystallization Temp. (°C)

Figure 1

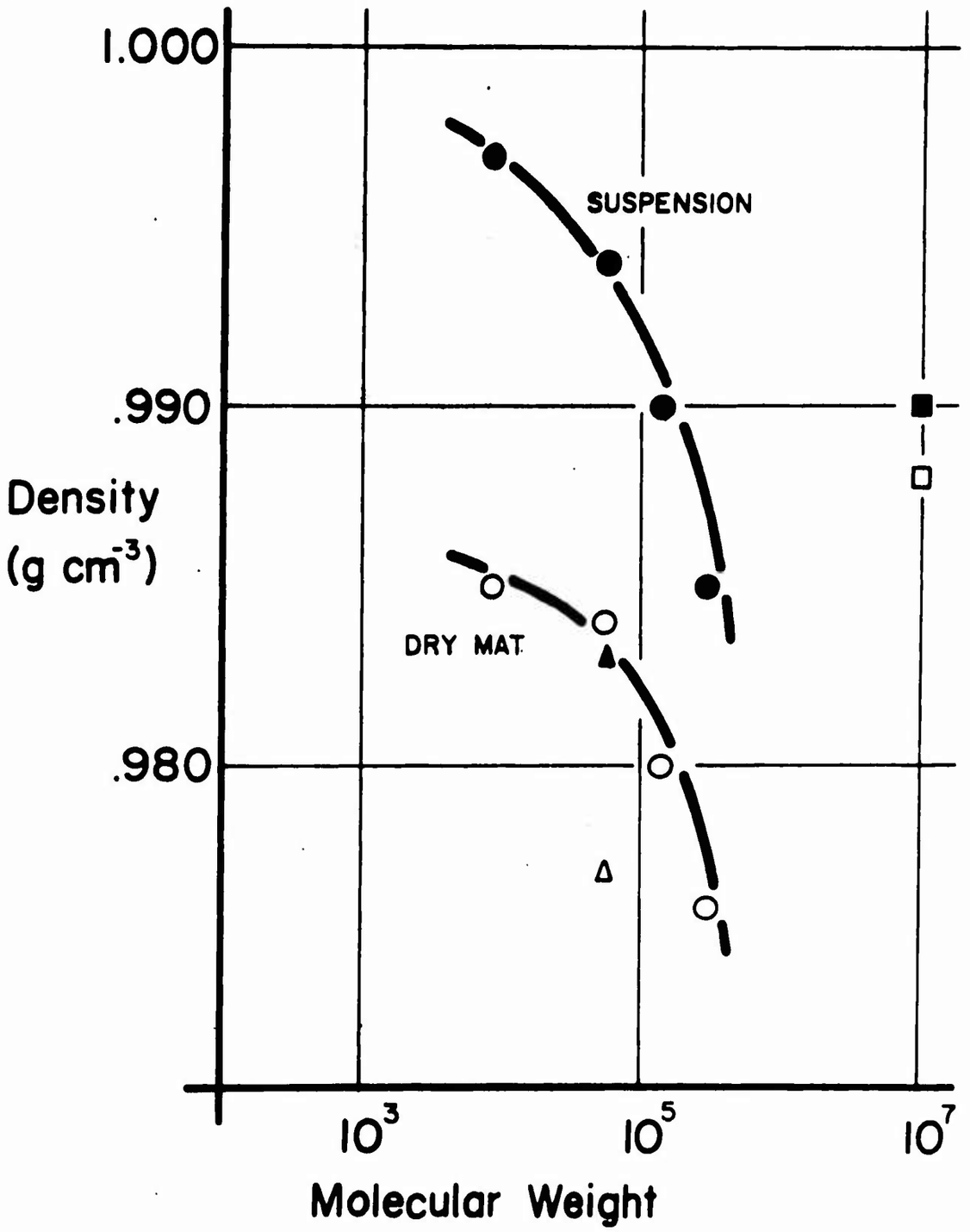
1.000
.990
.980
Density
(g cm^{-3})
SUSPENSION
DRY MAT
10^3
10^5
10^7
Molecular Weight

Figure 2

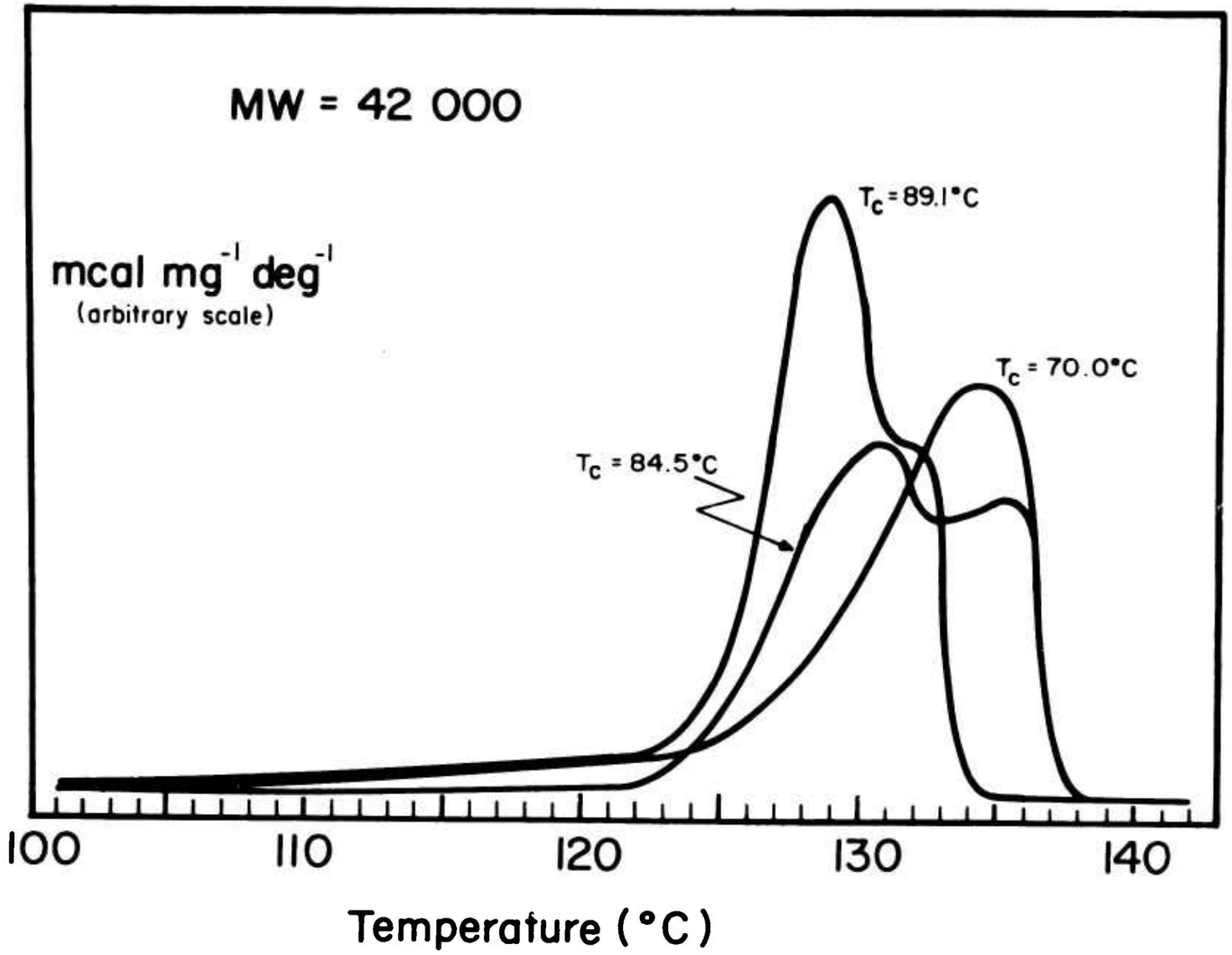
MW = 42 000
mcal mg^{-1} deg^{-1}
(arbitrary scale)
T_c = 89.1°C
T_c = 70.0°C
T_c = 84.5°C
100
110
120
130
140
Temperature (°C)

Figure 3

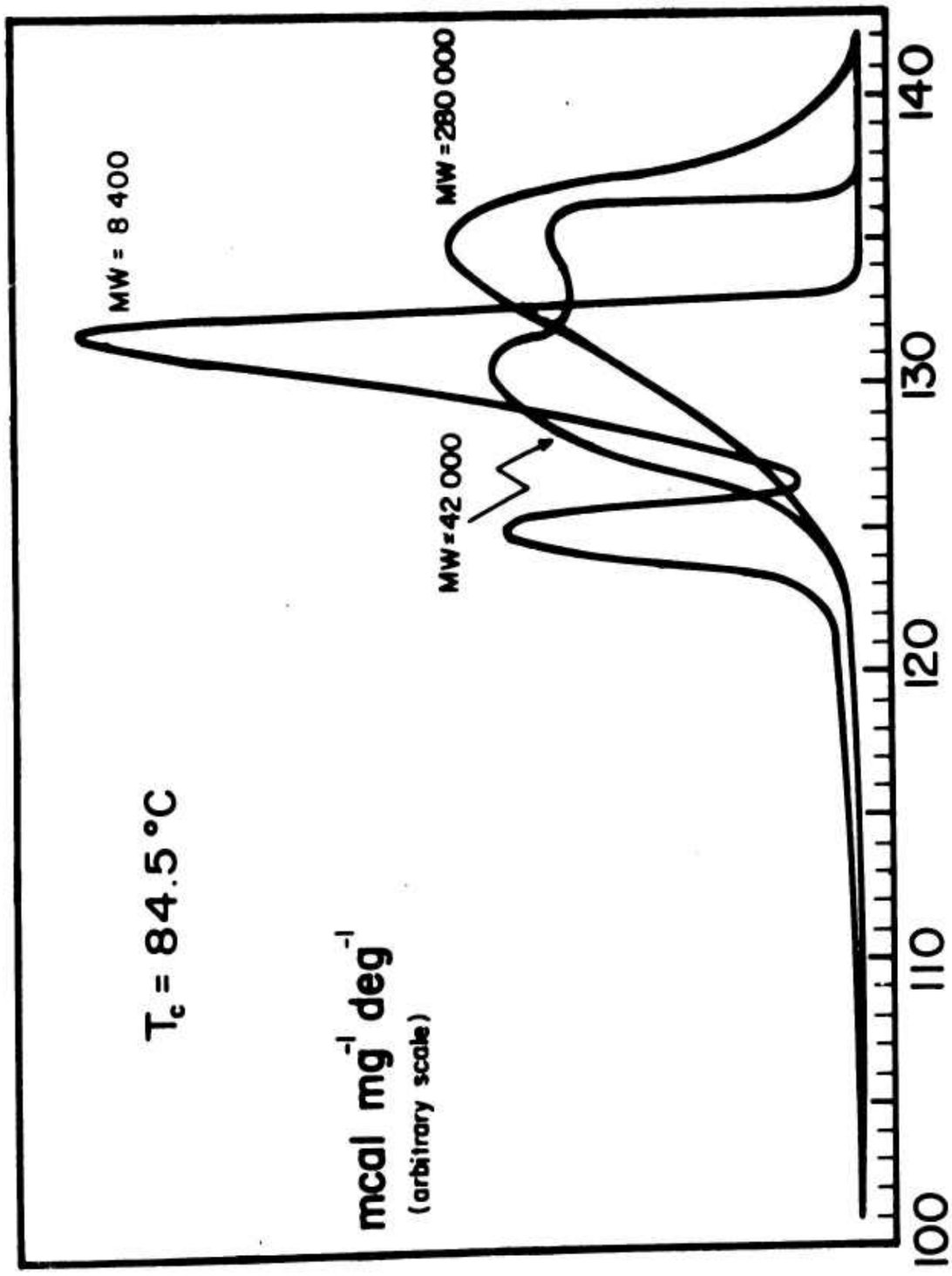
MW = 8 400
MW = 280 000
MW = 42 000
T_c = 84.5 °C
mcal mg^{-1} deg^{-1}
(arbitrary scale)
100
110
120
130
140
Temperature (°C)

Figure 4

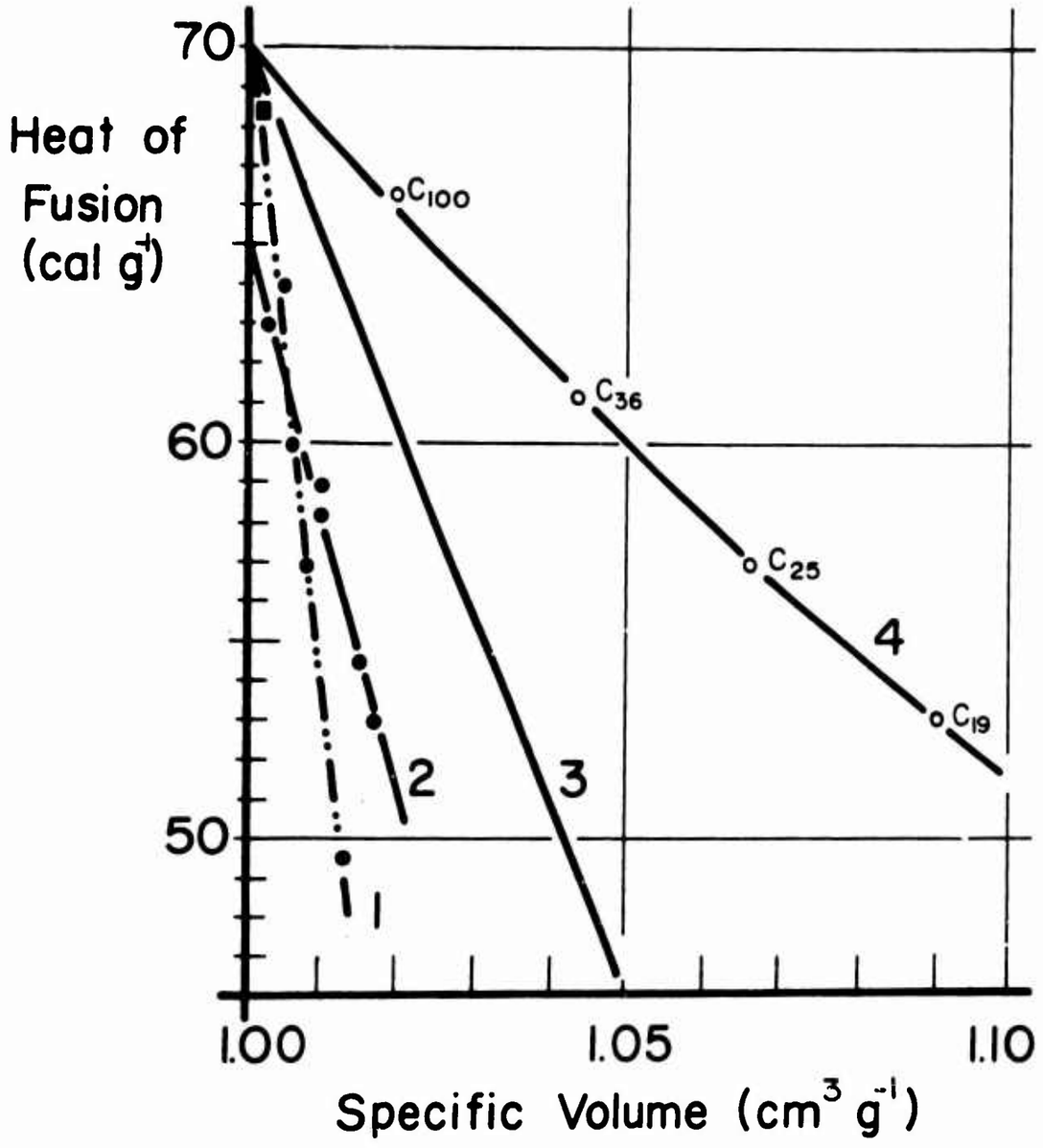
70
60
50
Heat of
Fusion
(cal g⁻¹)
C100
C36
C25
C19
1
2
3
4
1.00
1.05
1.10
Specific Volume (cm³ g⁻¹)

Figure 5

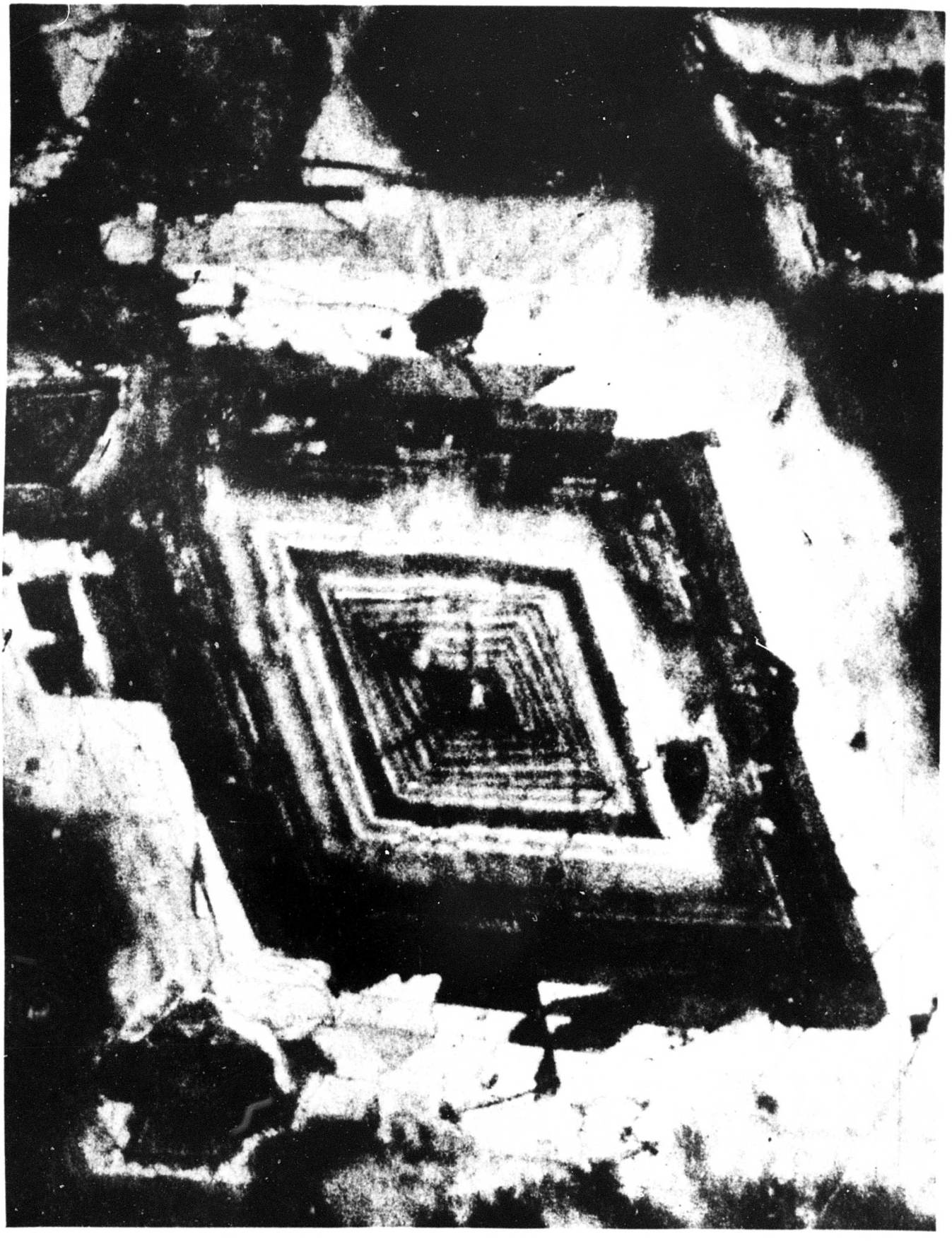

NEW DISCUSSION CONTRIBUTION.

SOME AVENUES IN POLYMER SINGLE CRYSTAL STUDIES

by

A. Keller

H.H. Wills Physics Laboratory, University of Bristol.

It will be clear from the foregoing lectures that we are faced with two diametrally opposed views as regards the surface structure of chain folded single crystals, each of which is based on apparently sound evidence. On the one hand we need to envisage disordered amorphous material on the fold surface, on the other the fold surface should possess crystallographic regularity. The compromise solution which suggests itself is that there is regular folding but this may be superposed by disorder due to loose hairs and loops of varying lengths such as sketched tentatively in Fig. 1. Indeed such disorder types could readily be envisaged as a consequence of chain folded crystal growth under ideal conditions. The amount and type of this disorder is expected to be variable dependant on molecular weight and crystallisation conditions.

It follows that if we are to resolve the existing conflict we have to make sure that our crystals are well characterised and particularly that the same samples are used for the different investigations on which the conflicting experimental findings are based. In particular, electron microscopic evidence relies on individual crystal layers which are seldom representative of the macroscopic sample obtained by isolating the crystalline precipitate

in the usual single crystal suspensions. The need arises therefore of obtaining crystal preparations where the representative crystal elements can be identified by simple sampling. A new method which emerged recently as a result of collaboration between our own laboratory and Dr. Kovacs in Strasbourg, France is a definitive step in this direction. (1) It will be outlined briefly in case of polyethylene although it is applicable also to other polymers.

A new method of controlled crystal growing

The usual polyethylene crystals dissolve at 97°C in xylene as judged by visual clearing and by precision dilatometry. Nevertheless, the rate of subsequent crystallisation was found to depend on the dissolution temperature (T_s) up to about 106°C beyond which further raising of the temperature had no longer any effect. Within this dissolution range the number of crystals which formed on subsequent crystallisation decreased with increasing T_s. The resulting crystals were all of uniform size indicating that they grew from pre-existing nuclei which themselves must consist of the polymer as they are removed irreversibly by appropriately raising T_s. The crystals were much smaller, hence their number much larger (by 2-4 magnitudes) than those which are obtained when the dissolution temperature is high enough for the previous crystallisation memory to be lost. This has the consequence that the crystals have less chance to develop by the usual sheaving and overgrowth processes and consequently will be of simpler types. In fact for a low enough T_s range (97 - 104°C) the

crystals formed subsequently were practically exclusively monolayers, even from concentrations where collection of macroscopic quantities becomes practicable (up to 0.2 - 0.5% although the crystals become gradually more complicated as the concentration is raised). Thus we have a method for growing crystals of uniform size where a randomly selected individual is representative of the total, and where in addition the crystals are essentially simple mono layers. The last feature ensures that any disorder, if present, is restricted to the fold surface and the problem is not complicated by the presence of material associated with multilayers such as tie molecules, material trapped between layers etc.

The number of crystals, hence their size could be varied systematically; higher T_s gives larger crystals (Fig. 2). When in control of all the variables (see below) monolayer crystals can in fact be grown 'to order', all having the same habit, thickness and size (the latter within 5%).[2] This point gives ground for some reflection. Polymer crystals may well be complicated and contain disorder. Nevertheless, it is possible to control their growth and habit to an extent hardly realizable amongst the simplest organic and inorganic substances.

Direct examination of crystal surfaces

Direct visual observations have often been decisive in the field of polymer crystals. One may therefore look for methods for exploring the surface topograph directly. A very sensitive method, the so

called decoration technique, due to G.A. Bassett has been in use for some time in the field of inorganic crystals. It relies on the vacuum deposition of a mobile metal (usually gold) on the surface in quantities insufficient to coat the surface uniformly. The metal atoms will form small grains by means of the usual nucleation processes as a result of which the crystal surface will appear dotted. In places which favour nucleation the dot density will be higher. Such are re-entrant edges which will appear as densely dotted lines on a more lightly and randomly dotted background. In this way atomic steps could be shown up in alkali halides.

The decoration technique is now being applied to polymer crystals [3][4]. It provides information of two kinds: i) on edges and steps ii) on the texture of uniform surfaces.

i) Edges and steps As in alkali halides edges and steps could be decorated also in polymer crystals [3] (Fig. 3). Steps in single layers were produced deliberately by changing the crystallisation temperature during growth. Known step heights down to 8A could be identified and steps even smaller than this (but not assessed precisely) could be shown up by decoration. The distinctness of straight steps commensurable with the unit cell dimension suggests an ordered surface. The amount of disorder compatible with the observed distinctness and straightness of the steps would, however, require quantitive assessment. The steps and edges are manifest as denuded, decoration free zones of 50 - 100A width (Fig. 3), at the edges at any rate the zones being

on the upper side of the step. This is a general and unique feature of polymers; in other substances including paraffins[3] the steps are shown up by a single dotted line only. The effect indicates a difference in texture within these zones, which gives rise to higher metal mobility there. The molecular origin of this texture difference which must reside in the macromolecular nature of the crystal is now being investigated.

ii) Texture of uniform surfaces As seen in Fig. 3 the overall density is lower on the polymer crystal than on the surrounding carbon substrate which in itself makes the crystal appear as distinct. This is the consequence of the chemically different nature of the surfaces (the polymer is essentially a hydrogen surface)[3]. Of greater significance is the fact that the decoration density can vary within the same crystal layer. With the aid of uniform monolayer crystal preparations it could be established that the decoration was representatively coarser in the crystal interior. The extent of the difference in decoration density, however, was small and was variable from sample to sample. A more definitive effect was obtained by flooding the previously decorated crystal with, say xylene [5, 4]. This greatly enhanced the coarseness of the decoration pattern in the interior, while leaving the finer pattern along the exterior rim unaltered (Fig. 3). This in itself shows that a) even within a given monolayer the surfaces can be of different kinds, variation occuring during growth, b) portions of the surface are mobilizable by swelling agents. As the mobilization

would not be expected with the crystal proper it must be associated with amorphous material.

The origin of the mobilizable material is being investigated. It is seen from Fig. 3 that the change in texture type need not be associated with the growth step. Conditions responsible for the mobilizable surface are rather intricate. It appears that it is favoured both by long molecules and high concentration (The fact that it occurs in the crystal interior is a reflection of this: the longer molecules are expected to deposit first from a solution where the concentration is comparatively higher). This trend is at least in accord with the picture in Fig 1. As already stated, the defect structure there is more likely when the molecules are longer and the solution is more concentrated.

The difference in decoration density and the associated mobilization effects cannot be interpreted quantitatively at present. Nevertheless the effect should serve to divide crystals into mobilizable and non-mobilizable categories as a preliminary characterization prior to other measurements. If grown by self seeding [1] a single sampling can characterize the whole preparation. It would remain to be seen how other properties invoked in favour of order or disorder respond to such a classification.

It is instructive to point out that crystals such as in Fig. 2 which is well characterized as regards thickness, habit and size, and is essentially a monolayer is in itself not uniform as regards the fold surface. Even when such a crystal is representative of the whole

preparation, a property measured on an aggregate of such crystals would still only represent an average given by the two kinds of fold surfaces. Even if the effects this averaging would have on the macroscopic properties is unknown at present, it is worth reflecting on the subtle distinctions which may have to be invoked in the characterization of a crystal before far reaching generalizations can safely be made from macroscopic measurements on collected aggregates.

Molecular weight distribution of selectively degraded crystals (joint contribution with I.M. Ward)

When polyethylene single crystals are subjected to the oxidising effect of fuming nitric acid then after long enough treatment the folds are cut and the fold surface is removed in some appreciable depth.[6, 7, 8] Peterlin and Meinel [6] inferred this from the length of the remaining molecular fragments as assessed viscometrically, and ourselves arrived at this conclusion from the fact that the residual segments crystallized as paraffins do with unalterable long period [7]. However, more and possibly decisive information should be obtainable from the changes in the molecular weight distribution in the course of degradation.

Preliminary results have already been reported [9] and more detailed work is in progress [10]. The approach is based on the comparatively new technique of gel permeation chromatography (G.P.C) enabling the rapid characterization of the whole molecular weight spectrum on a small amount of material. On testing polyethylene in

progressive stages of degradation with nitric acid it was found that the molecular weight did not decrease uniformly but through the development of discrete peaks at the low molecular weight end (between 4000 and 1000) as shown by Fig.4. The peak positions changed only little during degradation but relative peak heights varied largely. The peaks at the lower molecular weight end became more pronounced, and finally only one peak that corresponding to the lowest molecular weight remained (Fig.4b). This final peak corresponds to a paraffin of a length which is also in good agreement with the corresponding long period obtained on the fully degraded material [7]. This was to be expected. The discreteness and multiplicity of the peaks in the intermediate stages, however, was novel.

The existence of peaks must mean that there are different chain traverse lengths through the crystals which remain uncut. In view of the fact that the crystals are lamellar and that in the case of Fig.4 in particular they were all monolayers, as obtained by the self seeding technique [1] these characteristic lengths must be accommodated within the same layer. As the last peak corresponds to the original layer thickness (slightly reduced [7] owing to the removal of some fold surface material) the others to chain lengths which are longer than this by about a factor of two or more, it follows that the molecules must be folded. This conclusion may not appear surprising from what we know by now through gradual accumulation of evidence. It is worth recalling nevertheless, that the existence of multiple peaks from monolayer preparations is the only direct molecular evidence, hence perhaps the most intrinsic support

for chain folding.

It follows, that the three peaks detected so far ought to correspond to single, double and triple traverses of the chains. The fact that they are discrete, implies that the fold structure cannot be random. In addition the position of the peak maxima should tell us whether the folds present in largest number are loose or sharp, and permit an assessment of the amount of looseness involved if any. Namely, if the amount of material within the fold is negligible compared to that forming the stems (sharp fold) the molecular weights associated with the peaks should be close to 1: 2: 3. Deviations from these integer values should give a measure of the average looseness involved. The width of the peak on the other hand should relate to the uniformity of the folds. The analysis is complicated by two factors: calibration of the chromatograph, as no standard in the corresponding molecular weight range of the same chemical composition is available, and secondly by the problems of instrumental broadenings and separation of peaks. Nevertheless work in progress shows much promise [10]. Reporting of results will be deferred to the publication specifically devoted to the subject. At this stage merely the following will be stated.

With the aid of a special calibration procedure [11] it is now being found that the ratio of the peak positions of the two lowest peaks is 1: 2 within 5%. According to the foregoings this requires tight folds. The peaks have appreciable width (fractional standard deviation 0.1 - 0.18) which could permit a certain amount of additional fold

looseness. However, in view of the various uncertainties no value can be uniquely assigned to this looseness at the moment. In addition the molecular weight corresponding to the different peaks reflect the original fold length, i.e. crystals which possess longer fold lengths initially, yield peaks which are at a higher molecular weight than those corresponding to crystals with shorter folds. Finally, discrete multiple peaks appear also in nitric acid digested bulk samples both random and oriented (c axis fibre type) indicating distinctness and regularity of the molecular traverse lengths within the crystals which in analogy with deductions from solution grown crystals would be a reflection of chain folding [12].

To conclude with, we now possess means of exploring the texture of crystalline polymers on the level of molecular detail. This coupled with improved control over the growing of crystals and over their characterisation should in the foreseeable future contribute to the resolution of the present conflict and largely enhance our existing knowledge and understanding.

REFERENCES

1. Blundell, D.J., Keller,A., and Kovacs, A.J., J. Polymer Sci.B4, 481 (1966)

2. Blundell D.J. and Keller A, to be published.

3. Bassett, G.A., Blundell, D.J., and Keller, A., J. Macromol. Sci. (Physics) B1, 161 (1967).

4. Blundell, D.J., Keller, A and Saddler, D. Unpublished.

5. Blundell, D.J. Ph. D. Thesis, University of Bristol 1967.

6. Peterlin, A., and Meinel, G., Polymer Sci., B, 3, 1059 (1965).

7. Blundell, D.J., Keller A., and T. Connor (partly) J. Polymer Sci. A. in the press.

8. Winslow, F.H., Hellman, M.Y., Matreyek, W. and Salovey, R., J. Polymer Sci. B, 5, 89 (1967).

9. Blundell, D.J., Keller A., Ward, I.M., and Grant, I.J., J. Polymer Sci. B. 4, 781 (1966).

10. Williams, T., Blundell D.J., Keller,A., and Ward, I.M., and F. Willmouth to be published.

11. Frank, F.C., Williams, T., and Ward, I.M., to be published.

12. Williams, T., Keller, A., and Ward, I.M., to be published.

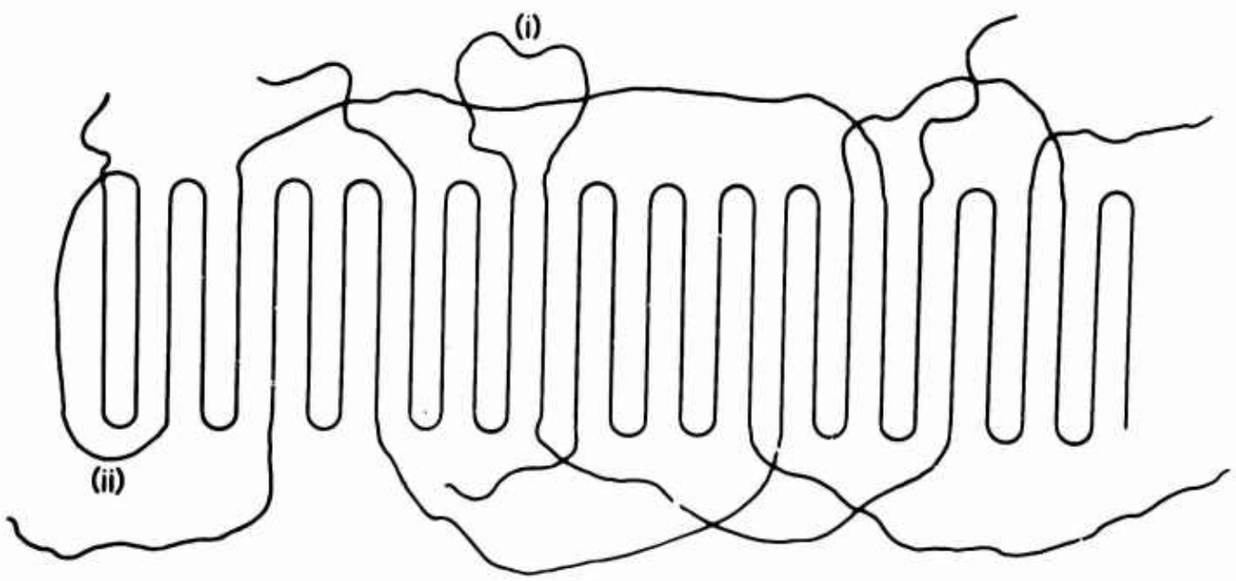

Fig. 1

Fig. 1. Schematic representation of a composite fold surface consisting of adjacently re-entrant sharp folds and various elements of surface looseness.

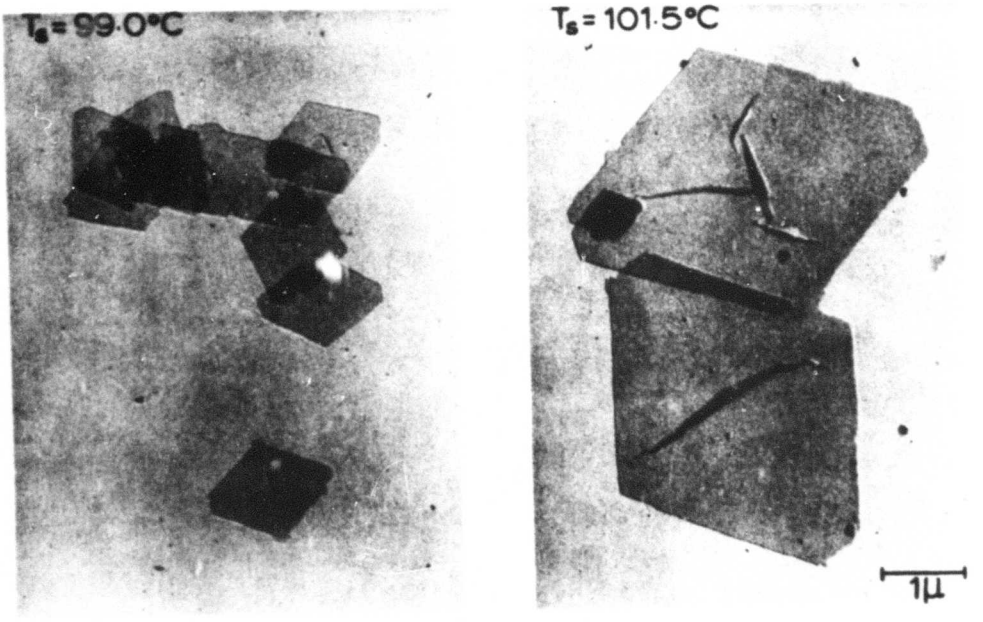

Fig. 2. Electron micrographs of monolayer polyethylene crystals grown at 80°C from 0.1% solution by means of the self seeding technique for two dissolution temperatures, T_s [1].

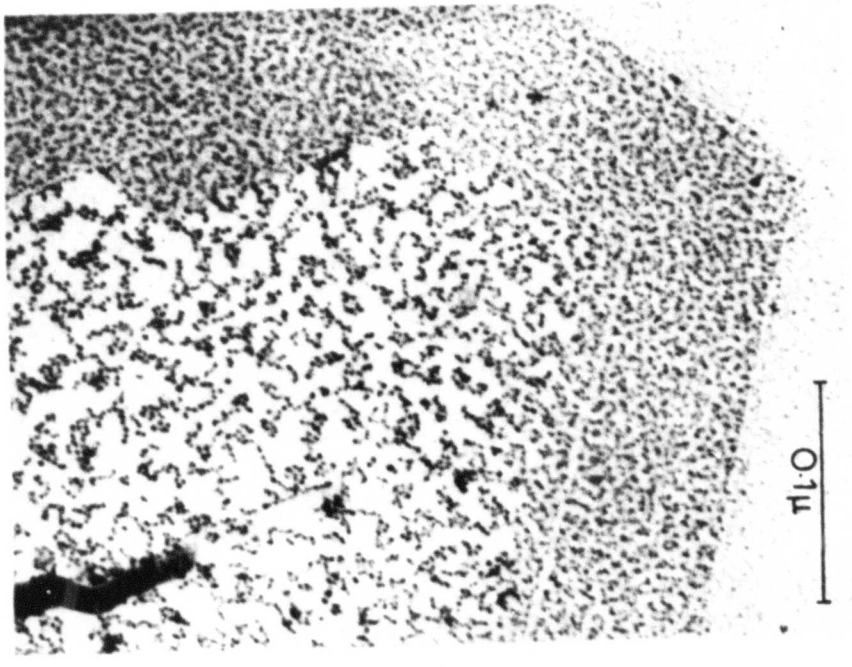

Fig. 3. Electron micrograph of a polyethylene crystal portion. The crystal was grown by self seeding, with a deliberate change in temperature during growth. The crystal was decorated with gold, and subsequently flooded with xylene revealing mobilisation of the fold surface in the crystal interior. [4,5]
(The finely decorated portion on the left is due to the edge of another overlapping crystal.

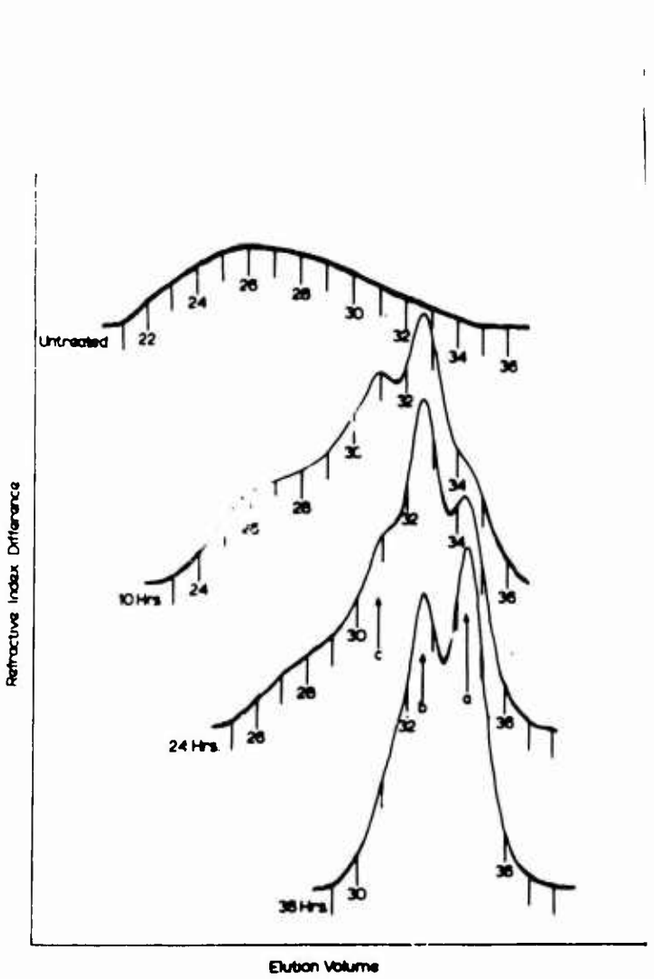

Fig. 4a

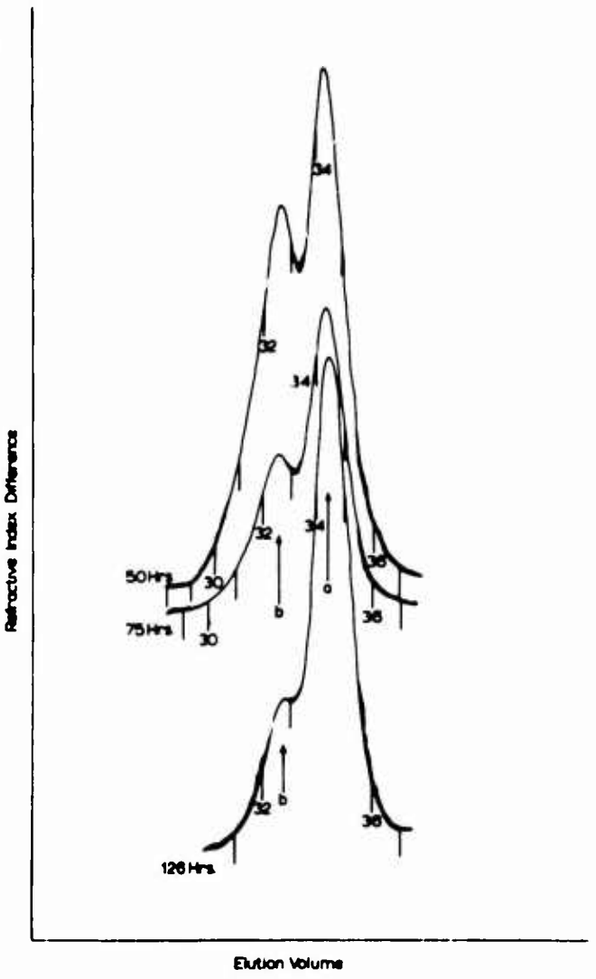

Fig. 4b

Fig. 4. Superposition of results from gel permeation experiments on nitric acid degraded monolayer crystals. The detected refractive index difference is plotted as a function of elution volume for crystals after various times of treatment (larger elution volume corresponds to lower molecular weight; the number are measures of the elution volume, a) treatment times up to 36 hours. b) treatment times 50 - 126 hours. Based on the work in ref. 9.

Contribution by Dr. D. C. Bassett

ON THE REGULARITY OF POLYMER FOLD SURFACES

by

D.C. Bassett,
J.J. Thomson Physical Laboratory,
University of Reading, U.K.

1. Introduction

The nature of fold surfaces in polymer crystals is still a controversial topic, views varying through the entire spectrum from order to complete disorder. Many of the observations, such as density measurements underlying these views are not only somewhat indirect but use crystal aggregates. However, the most direct methods, those of microscopy of individual crystals have always favoured regular folding, a conclusion which is supported by study of moiré patterns.

2. Observations and Interpretation

2.1. Material

Moiré patterns observed in the electron microscope have been compared and contrasted for three polymers, polyethylene (PE), polyoxymethylene (POM) and isotactic poly(4-methylpentene-1) (P4MP). The bilayer crystals necessary for moiré work were all grown by crystallization of supersaturated dilute solutions. MMW polymer was used for P4MP and POM,[1] but to obtain {001} fold surfaces in PE and hence more extensive moirés of strong hk0 reflexions, LMW polymer was taken.[2]

2.2. Moire Patterns

Dark field electron microscopy of two overlying lamellae having a slight relative rotation about their common normal, the $\underline{c}_s$ axis

reveals, ideally, line fringes perpendicular to the selected diffracting planes. However, the detail of these fringes depends upon the nature of contact in the common interface. Undeformed crystals give $\cos^2$ fringes whose location varies if the phase of the pattern is altered e.g. by slight tilting of the crystals. This is appropriate to fig.1(a); corresponding double diffraction moirés are seen in fig.2(a).

Mutual deformation of lamellae is sketched in fig.1(b), indicating a relaxation of molecular positions so that matching occurs over wide areas separated by narrow regions, dislocations, in which the relative twist is concentrated. Moiré fringes, which may, as in the present cases, also involve double diffraction are necessarily confined to the deformed regions, which they thus image. Fig.2(b) is a deformation moiré of this type (first identified as such by Holland and Lindenmeyer)[3] in which the character is evident from the reversal of fringe contrast in regions where the crystal is accidentally tilted. Strictly this criterion is necessary to assign deformation character to a moiré, however, it is usually much simpler to do so on the basis of the associated secondary criteria of narrow dark fringe profile (at normal beam incidence) and especially the characteristic fringe kinking, as is appropriate for dislocations in a network. Deformation moirés identified in this way have provided the experimental basis of this work.

2.3. Fold-Surface Lattices

The importance of deformation moirés is that the dislocations imaged in them are dislocations of the fold surfaces (not of the subcell) representing the interval between successive matching positions of two

surfaces. By considering the observed translations in terms of possible surface models it is possible to draw conclusions concerning fold geometry and packing.

2.3.1. Polyethylene

The fold surface lattice of PE has base vectors $\langle a00 \rangle_s$ and $\langle 0b0 \rangle_s$ [4] These are compatible either with an ordered surface of types RGI or RGI′ [5,6] (fig.3) or with mixed stacking and adjacent re-entry provided that folds in the two possible subcell positions have sufficiently different geometries. Other ordered structures and all disordered surfaces (i.e. including non-adjacent re-entry) are excluded. For both the two possible alternatives, folds must have rather restricted geometries and in that sense be regular.[7]

2.3.2. Polyoxymethylene

The fold lattice of POM has base vectors equal to those of the subcell in $\underline{c}_s$ projection i.e. $^a/_3 \langle 11.0 \rangle_s$.[7] All ordered structures would involve greater dimensions. The surface structure is most probably one with mixed stacking and adjacent re-entry.

2.3.3. Poly(4-methylpentene-1)

Few deformation moirés are observed in P4MP, although the proportion of crystals showing indications of fringe kinking and narrowing increases after heating. All observations are consistent with the likely situation of a network of $^a/_2 \langle 110 \rangle_s$ dislocations in which case the implications for folding would be as for PE. However, the evidence is much weaker than for PE and POM so that the situation remains rather open.

2.4. Edge Dislocations

Deformation moirés indicate that good surface packing can be achieved at the expense of deforming lamellae. This principle may well explain the curious paradox revealed by earlier work on dislocations (probably in edge orientation) indicated by terminating moiré fringes. In as-grown POM and P4MP crystals such dislocations conform to predictions based on sub-cell structure[1] while in PE they do not,[8] but without exception are isolated $\frac{1}{2}\langle ab0\rangle_s$ partials.

Consider matching RGI surfaces in PE and suppose that in one, an odd number of RGII sequences intervenes so that further sequences are RGI′. Then, provided that fold-fold positions for matching of RGI/RGI and RGI/RGI′ surfaces are similar, it follows that matching positions of the RGI′ portion of the surface will be displaced from those of the RGI by $\frac{1}{2}\langle ab0\rangle_s$ parallel to the growth face, plus a fold lattice translation, i.e. by either $\frac{1}{2}\langle ab0\rangle_s$. The observed preference for the radial vector[8] in as-grown crystals is readily accounted for if it is considered that lamellae do not grow in contact, but are pressed together during sedimentation on a substrate, when the predominantly radial stresses will tend to select radial displacements.

This argument is not relevant to mixed stackings as such because a single change of stacking sequence has no special effect in them. Thus, on this hypothesis, as-grown PE crystals would have fold surfaces with substantial ordering. In all three polymers ordering would increase on heating, by a combination of fold smoothing and change of stacking sequences, leading to more terminating fringes (e.g. fig.4) and especially

to dislocations,[1,8,7] including isolated partials, having Burgers vectors equal to the inter-chain separation in the growth face.

3. Discussion

Two aspects of this work will be discussed, firstly how much disorder is compatible with observed deformation moirés and secondly whether these results are in any way special.

The disorders especially relevant to density deficits are those of non-adjacent re-entry on one hand and chain ends and loose folds on the other. Completely random non-adjacent re-entry[9] is incompatible with deformation moirés because such surfaces would not have the marked directionality required to match surfaces. Yet if randomness is restricted so as to overcome this limitation, then, correspondingly, there would be little contribution to a density deficit. As for chain ends, of length l, or loose loops, of length 2l, their maximum proportion cannot be more than $\sim\left(\frac{d}{l}\right)$ where d is the interchain distance or they could cover the fold surface and prevent fold contact. Taking $l \sim 100$A (the lamellar thickness), would limit this proportion to at most a few per cent. Thus folding of crystals showing deformation moirés must be good.

Although deformation moirés indicate good folding, their absence does not necessarily imply the converse. Folding may be very regular but there may still be insufficient reduction in free energy from better surface packing to compensate the energy required to deform lamellae. This appears to be so for P4MP. On the other hand, poor lamellar contact may mask

regular folding and indeed it is possible to see the character of a moiré pattern change where lamellae are deformed.[7] Poor lamellar contact may also lead to apparently deficient densities of crystals and, indeed, on the basis of this common origin, the absence of deformation moirés and low densities might well correlate. The converse might well be especially marked for LMW polymers whose crystals collapse most easily.[10,2] However, such a correlation would have no significance for fold geometry. It would certainly not imply that regular folding is confined to LMW polymer, on the contrary, it seems to be general for solution-grown crystals.

The groundsfor saying this are, firstly, that POM and P4MP crystals showing deformation moirés were prepared from MMW polymer and there appears to be little degradation during crystallization. Secondly, the POM and PE crystals studied, being grown very rapidly would be expected to lead to less regular folding than occurs at smaller supercoolings. Thirdly, there is a great deal of evidence that crystals of MMW polymers, including PE, have regular, uniform shapes[e.g.11,12], and, on the basis of sectorisation, that fold shapes are determined by the growth face on which molecules were added to the crystal. Such observations are inconsistent with fully disordered surfaces and indicate a certain regularity in folding.

In summary, the main conclusions of this work are (1) that mixed stacking with adjacent re-entry occurs in POM and P4MP, (2) that PE folds have regular geometries - the evidence is consistent with ordered

or mixed stacking with adjacent re-entry and (3) that the occurrence of isolated partial dislocations in PE and P4MP and terminating moiré fringes in POM can be explained in terms of fold packing.

References

1. Bassett, D.C., Phil. Mag. 10, 595, 1964.
2. Bassett, D.C., Phil. Mag. 12, 907, 1965.
3. Holland, V.F., and Lindenmeyer, P.H., J. Appl. Phys., 36, 3049, 1965.
4. Holland, V.F., Lindenmeyer, P.H., Trivedi, R. and Amelinckx, S., Phys. Stat. Sol. 10, 543, 1965.
5. Reneker, D.H., and Geil, P.H., J. Appl. Phys., 31, 1916, 1960.
6. Bassett, D.C., Frank, F.C. and Keller, A., Phil. Mag. 8, 1753, 1963.
7. Bassett, D.C., Phil. Mag. (in press).
8. Holland, V.F., J. Appl. Phys., 35, 3235, 1964.
9. Flory, P.J., J. Am. Chem. Soc., 84, 2857, 1962.
10. Keith, H.D., J. Appl. Phys., 35, 3115, 1964.
11. Bassett, D.C., Frank, F.C. and Keller, A., Phil. Mag. 8, 1739, 1963.
12. Bassett, D.C., Dammont, F.R. and Salovey, R., Polymer 5, 579, 1964.

Legend to Figures

Figure 1. Traces of diffracting planes contributing to a rotational moiré pattern from overlying crystals. In (a) the crystals are undeformed while in (b) the relative rotation has been resolved into a series of dislocations.

Figure 2. (a) 200 dark-field moiré in P4MP of double diffraction type.
(b) 110 dark-field moiré in PE exhibiting deformation character.

Figure 3. Ribbon stacking structure for an $\{001\}_s$ fold surface of PE. Folds are indicated conventionally by straight lines at the same Z level, without attempt to represent their actual geometry. Continuous thin lines are folds at the top surface and broken lines fold- at the bottom surface of a layer.
(After Bassett et al. 1963b).

Figure 4. 10.0 dark-field moiré of a POM bilayer which had been heated on mica by placing on a hot bar at 150°C for 2 minutes.

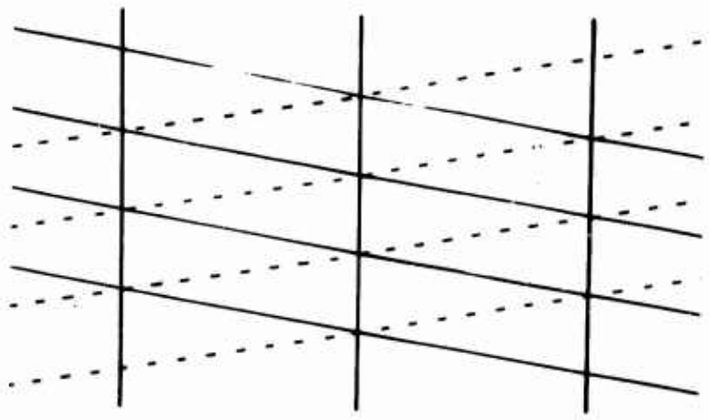

(a)

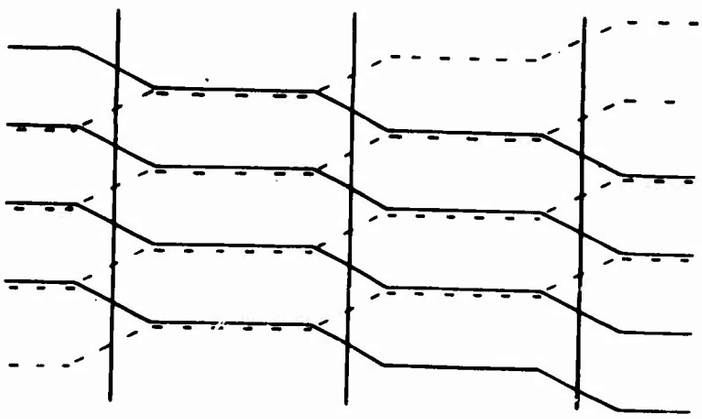

(b)

FIGURE 1

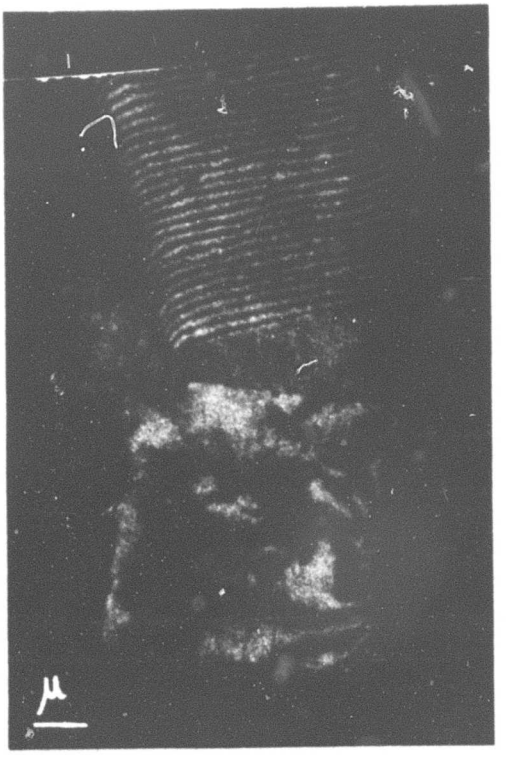

FIGURE 2a.

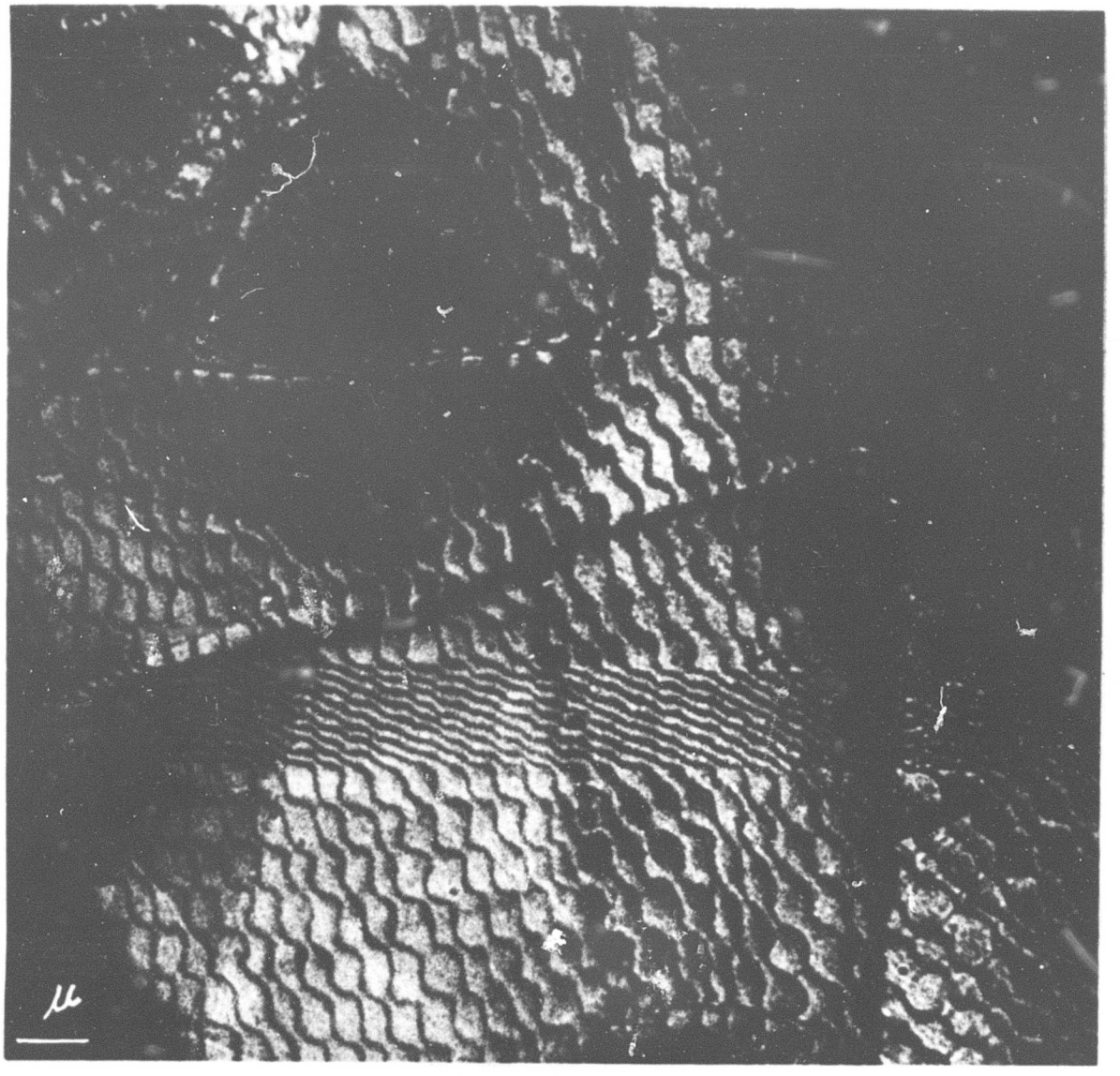

FIGURE 2b

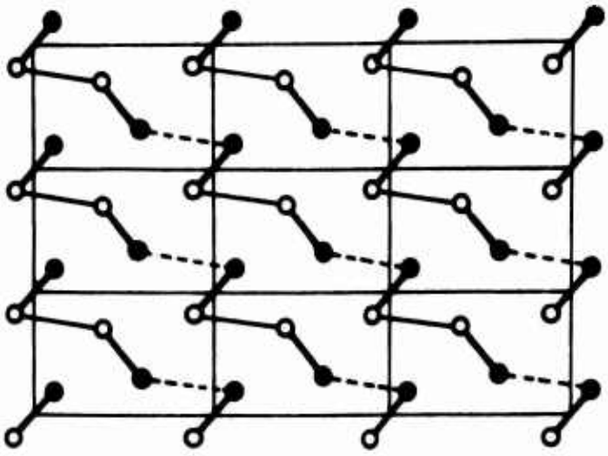

RG I

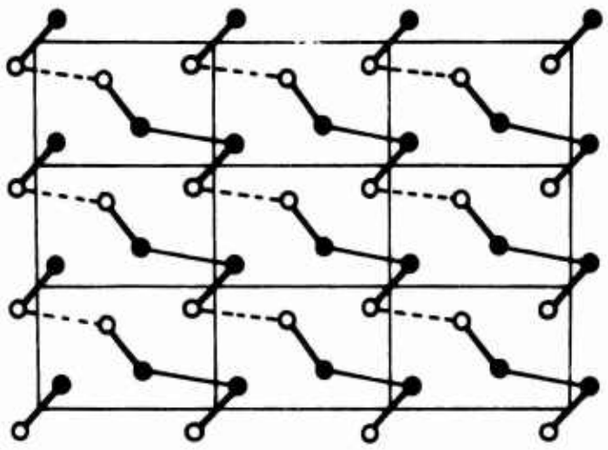

RG I'

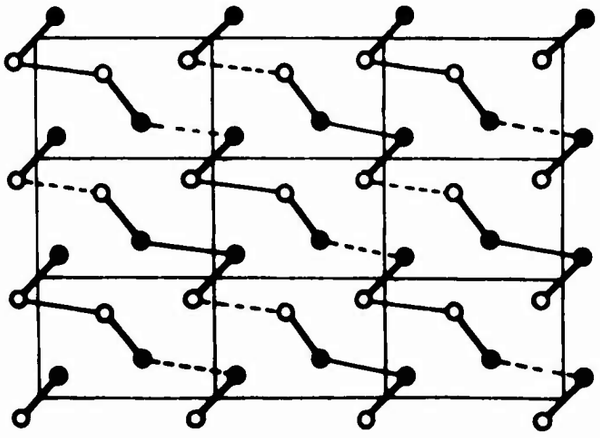

RG II

FIGURE 3

FIGURE 4

Contribution by Dr. T. G. Fox

CHARACTERIZATION OF CHAIN FOLDS IN CRYSTALLINE POLYMERS. A STATISTICAL PROBLEM

(Remarks submitted by T. G Fox and Hershel Markovitz as an addendum to the discussion on crystalline polymers at the April 1967 Natick Meeting)

It appears to us that more quantitative description of the nature of chain folding in any given polymer single crystal requires conceptual and experimental approaches capable of describing the entire spectrum of models from the limit of regularly folding through structures representing small or large deviations from it. It is our purpose here to present some initial suggestions of means to this end though the use of appropriate probability distributions. We believe these remarks and suggestions are in accord with the spirit of the discussion at this meeting and particularly with the comments of Fraser Price.

(We remark that it is not our intention here to consider imperfections within the single crystal such as the inclusion of chain ends, loops, twisted chains, vacancies, and the like.)

Conceptually, it is useful to consider a single crystal grown from dilute solution as <u>ideally</u> a regularly ordered array. Since the long chains in such a crystal clearly must "fold" and traverse the crystal many times, a convenient model for a regularly ordered structure is one in which the molecules enter the crystal one at a time with

crystallization proceeding from one end of the molecule and with the chain folded neatly and regularly at the lattice surface as the turn is made for the next passage through the crystallite.

However, as has been emphasized in the discussion at this meeting and by several workers some years ago, for the most real polymer single crystals, deviations from the ideal of a regularly folded structure must be expected, and in fact are evidenced by various physical measurements of the properties of such materials. Thus, the middle of the chain may enter the crystal first, and impose some irregularities in the "loop" lengths and re-entry pattern since both ends of the initial crystalline segment cannot re-enter the neighboring position in the lattice simultaneously. Of course, chain ends may dangle as irregularities at the interface. In general, the chain segments or "loops" between exit and re-entry of the crystal face need not be all of the same length, and may enter distant rather than neighboring lattice points. Such deviations from regularity may be minor or they may reach such proportion that the chains at the interface constitute a markedly irregular noncrystalline phase. Obviously, if the loops are sufficiently long, their conformation and packing could approach that characteristic of the normal amorphous liquid phase.

In recent years, workers in this field have been handicapped, in their characterization of specific single crystals and in communication of their findings, by the lack of precise language for characterization of the deviations from chain folding. Thus, some have described real crystals as having a regularly folded structure when in truth they meant only that regular folding was a predominate or major habit

without meaning to exclude the possibility of some variation in, for example, loop lengths. Others have suggested that "loose loops" may be present in some materials. The language used has been qualitative at best, and frequently subject to misinterpretation and fruitless controversy.

We believe the description in molecular terms of the chain "folds" or "loops" on the surface of a single crystal requires first, as a minimum, definition of the parameters which describe the length and position on the crystal face of the ends of a given loop and recognition that we require evaluation of a distribution function specifying the probability of occurrence of loops of different lengths and orientations relative to the crystal lattice.

Such a chain fold can be characterized by its length ℓ (in chain atoms) and a vector $\underset{\sim}{r}$ on the face of the crystal joining the points of exit and re-entry into the crystal. Then, specifying $\underset{\sim}{r}$ in terms of some lattice vectors $\underset{\sim}{a}$ and $\underset{\sim}{b}$, we can write

$$\underset{\sim}{r} = (\Delta n_a)\underset{\sim}{a} + (\Delta n_b)\underset{\sim}{b} \; . \qquad (1)$$

To describe completely the loop structures on the face of a given single crystal would require, of course, the specification of the values of ℓ, Δn_a and Δn_b of each loop, and even of the coordinates of the two ends of each loop relative, say, to one edge of the crystal face. Unless the structure possesses a highly regular pattern, with very few imperfections, such a description is impractical, if not

impossible. As is usual in such instances, its very complexity, involving large numbers of chains, may be a saving feature, e.g., permitting the use of statistical representation of the population of loops of various structures.

Thus we should ask, if we choose a fold at random what is the probability $P(\ell,\underset{\sim}{r})$ that the fold is ℓ chain atoms long and that the vector joining the points of leaving and entering the crystal is $\underset{\sim}{r}$. From Eq. (1) we can write this probability as

$$P(\ell,\underset{\sim}{r}) = P(\ell,\ \Delta n_a,\ \Delta n_b) \quad . \tag{2}$$

It is likely that, except in some limiting cases, the evaluation of $P(\ell,\ \Delta n_a,\ \Delta n_b)$ will be extremely difficult, but it might still be possible to determine the one-parameter probability, $P_\ell(\ell^*)$, that a loop chosen at random has ℓ^* chain atoms, irrespective of the values Δn_a and Δn_b; $P_a(\Delta n_a^*)$ and $P_b(\Delta n_b^*)$ can be defined similarly.

It is instructive to illustrate the meaning of these concepts by application to some special cases. As is indicated in Figure 1, we take $\underset{\sim}{a}$ to be the vector joining adjacent positions in the (110) plane and $\underset{\sim}{b}$ to be that in the (100) plane. For the regularly folded model (indicated by I in Figure 1) with every fold ℓ_0 chain atoms long, the probability $P(\ell,\ \Delta n_a,\ \Delta n_b)$ is zero except for the case when $\ell = \ell_0$, $\Delta n_a = 1$, and $\Delta n_b = 0$ simultaneously. Thus, we write

$$P(\ell_0,\ 1,\ 0) = 1 \quad .$$

In this case, P can be expressed in terms of the one parameter probabilities:

$$P(\ell, \Delta n_a, \Delta n_b) = P_\ell(\ell) P_a(\Delta n_a) P_b(\Delta n_b)$$

See Fig. 2A.

In one type of crystallite that may conceivably exist Δn_a is unity and Δn_b is zero for all folds, but the length ℓ varies according to some specific distribution (Loop II in Fig. 1). In such a case, the only additional specification required is $P_\ell(\ell)$. An example is illustrated schematically in Fig. 2B.

Another deviation from the regularly folded crystal is one in which Δn_b is zero for all folds, but Δn_a varies from fold to fold (Loops I vs. III in Figure 1). For such a crystallite, knowledge of the description of fold types would be given by the probability

$$P(\ell, \Delta n_a, 0) = P_{\ell a}(\ell, \Delta n_a)$$

In general, of course, all three parameters ℓ, Δn_a, and Δn_b may vary independently and knowledge of fold characteristics requires the knowledge of $P(\ell, \Delta n_a, \Delta n_b)$ for all values of the three parameters.

In addition to the probabilities expressed above, we need also to know the probability $P_E(\ell)$ that a given chain emerging from the crystal is a chain end (of length ℓ) which does not re-enter the crystal face.

Patently, the distribution of fold characteristics for a given single crystal would depend not only on the composition of the material but on the crystallization procedure, i.e., upon the parameters affecting the thermodynamics and kinetics of crystallization. Thus, a single crystal of a given material may characteristically tend to follow a certain regular pattern under optimum conditions, but may deviate from this if crystallization is conducted at high concentrations or with changing temperature, etc.

In the case of polymers crystallized from the bulk material or from a concentrated solution, an additional description is the frequency of a chain leaving one lamellar crystal and entering an adjacent crystallite. In addition to the probabilities discussed above, it is then necessary to ask the probability Q_t that a given non-crystalline chain makes such a transition and further to designate the probability $Q(\ell, \underline{r})$ that its length is ℓ and that $\underline{r}$ is the vector which joins the points of leaving and entering crystalline regions. Again, it would be required to find experimental techniques for measuring the distribution functions implied.

A central research objective today is, it seems to us, the devising of experimental and/or theoretical approaches to the determination of the probability distributions of fold lengths and fold geometries as discussed above. Conceivably knowledge of $P_\ell(\ell^*)$ may be obtained by chain degradation or light crosslinking of the loops in single crystals or interfacial chains in bulk crystalline polymers with subsequent precise examination of the distribution of chain lengths

and molecular sizes by dilute solution techniques. Determination of the conformations, the packing, and the motions of the polymer chains in the loops may also be deduced from data on the IR and NMR spectra, densities, heat capacity, and other properties of the different regions of crystalline polymers. Various workers have employed certain of these techniques, of course, but it is not our purpose to present a bibliography here.

We realize that even all of this information does not provide a complete description of the conformations of the chain folds in the interfacial regions. However, it would provide a useful reasonable next step. Finally, we would like to emphasize that although we have not presented here any new ideas or information, we believe it useful to emphasize this approach through these remarks in the present form.

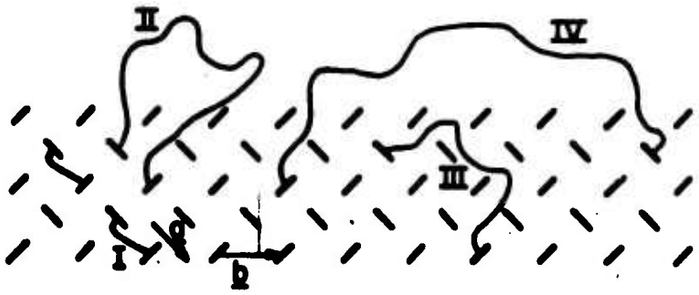

Figure 1

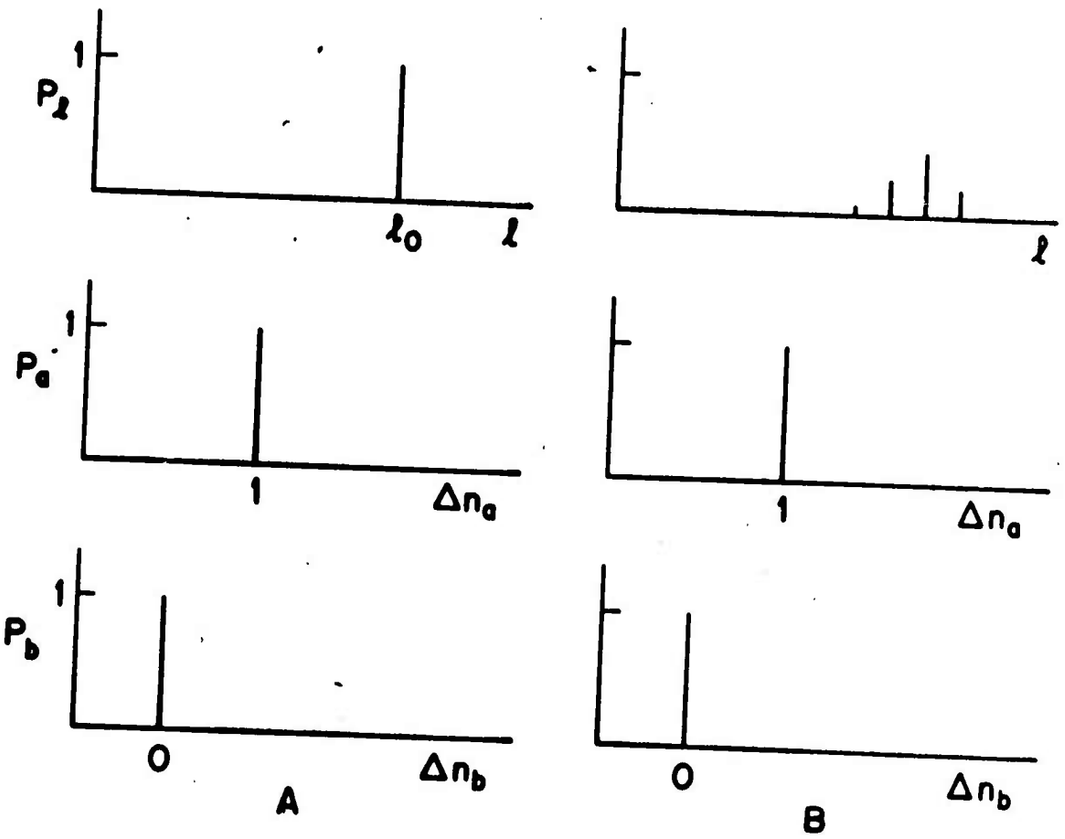

Figure 2

Mechanical Propertie, of Polymer Single Crystals and Extended Chain Crystals ——— Discussion of Defect Region and Loose Chains Attached to Them

Motowo Takayanagi

(Faculty of Engineering, Kyushu University, Fukuoka, Japan)

Polymer single crystals have high degree of crystallinity and their super-structure can be defined more definitive than those of the bulk crystallized samples of the same polymer. Their mechanical properties can, therefore, be more clearly correlated to their structure.

Crystalline absorption of polyethylene single crystals is affected by geometical factor (long period L) and defect region apart from chemical structure. Single crystals with different long period L prepared by regulating isothermal crystallization conditions (Type A samples) and annealed single crystals with different L (Type B samples) were compared in their behavior in the crystalline absorptions. Absorption temperature $T(\alpha_c)$ of both samples A and B are expressed by an one-valued function of L, as in the melting temperature. On the other hand, the absorption manitude $\Delta E = \Delta H^* \cdot E''_{max}$ of samples A increases with increasing L, while that of samples B decreases with increasing L. These difference was attributed to the effect of introduction of defect regions into lamellae by annealing for samples B.

Sinnott[1] found that the relationship between ΔE and $1/L$ can be expressed by a positive slope linear relation and presented the loop hypothesis that the crystalline absorption is associated with the orientation of loops attached to the crystal surface.

We have had a view against Sinnott's one from the concept that the crystalline absorption is associated with the crystal itself (call here "crystal hypothesis") since 1960. If so, the value of ΔE should have a linear negative slope relation against $1/L$. The relationship between ΔE and $1/L$ for Type A samples satisfies apparently this relation.

That is,

$$E = K(\infty)\cdot(1 - \ell_a/L) \qquad (1)$$

where ℓ_a is the thickness of loop region.

From these observations we encounter the difficulties in interpreting the dependence of ΔE upon L in the same way both for Types A and B samples, since they show a contradictory relationship with each other. This problem should be solved here.

The fact that the pressure crystallized sample of polyethylene, which is composed of extended chain molecules as evidenced by electron micrograph, show a remarkably strong crystalline absorption at the temperature located higher than those of A samples, seems to support the "crystalline hypothesis", since this sample is composed of almost perfect crystal with lamellar thickness 10,000 Å or more in some fields. We are forced, therefore, to adopt the crystal hypothesis after its

modification by taking the effect of defects in the crystal upon the crystalline absorption into account order to interpret the behavior of Type B samples.

Figure 1 shows a schematic representation of our "Mosaic hypothesis". Single crystal composed of mosaic crystals of $a_o^2 \times L_o$ is thickened by annealing into the aggregation of mosaic crystals of $a^2 \times L$. Magnitude of crystalline absorption ΔE is assumed to be proportional to the volume fraction of the perfect crystal region (C), which corresponds to the core region of the mosaic crystal. The surrounding zone of the mosaic crystal corresponds to the defect region (A'), which gives rise to the low temperature secondary absorption. Under these assumptions, we can obtain the relationship between ΔE and L as follows:

$$\Delta E = \Delta E^\circ + \alpha - \beta L^{1/2} \qquad (2)$$

where ΔE is expressed by $(2\ \Delta H^*/\pi R) \cdot \int E'' \cdot d(1/T)$ or $\Delta H^* \cdot E''_{max}$ as its substitute. The plot of ΔE against $L^{1/2}$ for Type B samples actually showed a linear negative slope relationship. Tables I and II list the data of Type A and Type B samples respectively.

This concept was extended to interpret the low temperature secondary absorption (β_{sc}) of isotactic poly-4-methyl-pentene-1, which is composed of two peaks, β_{sc}-A and β_{sc}-C. The β_{sc}-A absorption is located at the high temperature side of β_{sc}-C and at the same temperature as that of atactic amorphous sample. By comparing the absorption area of β_{sc}-A of isotactic sample

with that of atactic one, we evaluated the frozen amorphous region, A, and by comparing the absorption area of β_{sc}-A with that of β_{sc}-C for isotactic sample, we evaluated the defect region, A', within lamellar phase. Figure 2 shows the result of analysis of β_{sc} absorption of P4MP1. The edge length of mosaic crystal of P4MP1 single crystal was evaluated as ca 150 Å. Thus we are considering that the mosaic hypothesis of lamella is usable for interpretation of dispersion behavior of crystalline polymer.

The state of molecular aggregation in the amorphous region of the crystalline texture is difficult to understand only from the structural method. The relaxation spectrum of the primary absorption of the crystalline polymer is broader than that of the corresponding amorphous polymer. This will be caused by the circumstances that amorphous molecular chains are affected by different degree of restraint from the crystalline lamellae. The study of this problem by use of single crystals seems to be effective in this case.

Single crystal of trans-1,4-polybutadiene (PBD) were prepared from benzene solution at 18°C. Single crystal mats of PBD displayed a remarkable primary absorption at about -10°C (110 c/s), which is comparable with that of bulk crystallized PBD. Lamellar thickness of this crystal was evaluated as 100 Å by X-ray small angle scattering and its crystal phase thickness evaluated by X-ray line profile method is 72 Å. Dynamical degree of crystallinity evaluated by NMR method is 76%, which agrees

with the value evaluated by structural method. Average thickness of loop region of PBD single crystal as it is formed from the solution amounts to average 30 Å. When we anneal this single crystal at the temperatures above the crystal transformation temperature, 55°C, the primary absorption of the mat suddenly disappears and storage modulus E' increases corresponding with the increased lamellar thickness (150 Å) or degree of crystallinity. Figure 3 schematically represents the structural changel in this process. The NMR degree of crystallinity of the annealed PBD single crystal is 91 %, which corresponds with the thickened lamella with tightened loops. The amorphous region of the bulk crystallized PBD is assumed from these observations to be composed of diffusable chains with length of average 30 Å or the value not so much different from 30 Å. It is noticeable that the primary absorption of the bulk crystallized PBD did not disappear by annealing at 100°C, due to the restraint applied to the amorphous chains by the crystalline lamellae. The single crystals and bulk crystallized sample of highly crystalline polymers with degree of crystallinity of 80~90%, such as high density polyethylene and polyoxymethylene, usally are absent from the primary absorption. The state of surface of PE and POM single crystals is considered to be in a similar state as that of thickened PBD single crystal and composed of tightened loops.

At the end polytetraoxane crystal polymerized by the solid-state gamma-ray irradiation was discussed by its viscoelastic dispersion behavior. The loss peak at about -70°C (110 c/s)

found for drawn polyoxymethylene and mats of single crystals could not be found in ~~contrary to~~ the case of polytetraoxane. This fact means that defect region is almost absent in polytetraoxane. In contrast to polytetraoxane the normal drawn fiber of POM includes many defect regions, which have a strong influence on the mechanical properties of fiber.

We conclude from these observations that information from dispersion behavior is useful to approach the true features of the crystallized polymers by combined use of the morphological and structural methods.

References

1. K. M. Sinnott, J. Appl. Phys., 37, 3385 (1966).

TABLE I Long Period of Single Crystal Mat of Linear Polyethylene Prepared by Isothermal Crystallization (Å)

Sample	Crystallization Temperature (°C)	Crystallization Time (hrs.)	Long Period, L (Å)
1	33.0	24	94
2	49.5	24	104
3	68.5	24	114
4	80.0	72	137
5	85.0	144	167

TABLE II Lamellar Thickness of Annealed Single Crystals of Linear Polyethylene

Series B-I

Sample	Annealing Temperature (°C)	Annealing Time (hrs.)	Long Period, L (Å)
Original	40.5*	-	101
1	70.0	24	102
2	81.0	24	110
3	90.0	24	127
4	100.0	24	156
5	115.0	24	247
6	128.2	72	473

Series B-II

Sample	Annealing Temperature (°C)	Annealing Time (hrs.)	Long Period, L (Å)
Original	74*	-	124
1	115.0	24	210
2	120.0	24	239
3	125.0	24	324
4	128.2	72	436

* Isothermal Crystallization Temperature

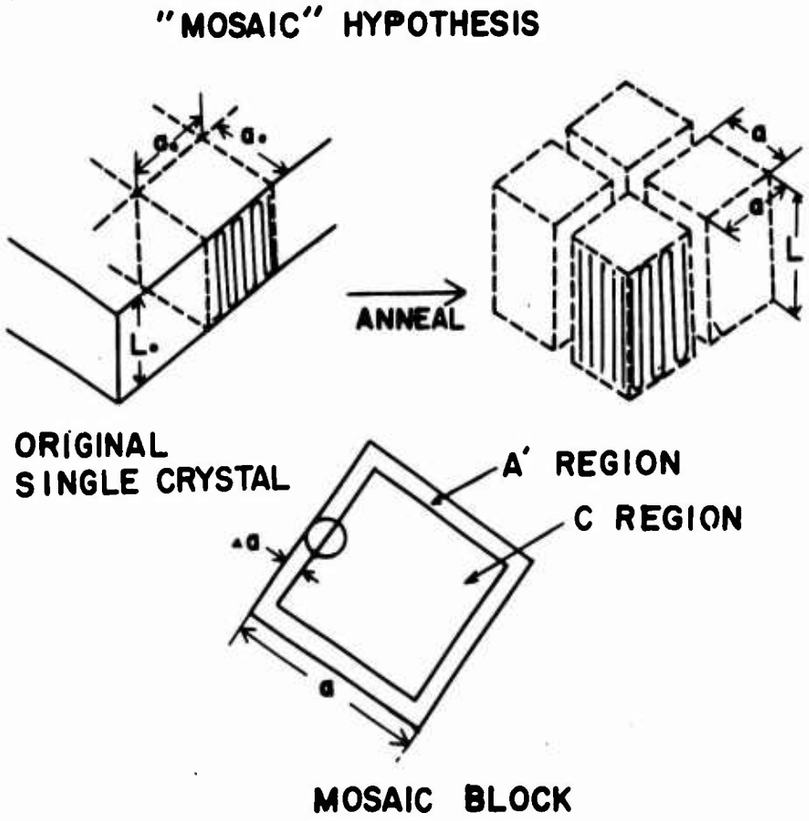

Figure 1. Schematic representation of the "mosaic hypothesis". The isothermally crystallized single crystal (original) has latent defects and has the possibility of generating mosaic structure by annealing. Mosaic blocks affect the viscoelastic absorption. The lower figure is an end view of the mosaic block. a is the edge length of the mosaic crystal and Δa is the width of the defect region surrounding the C region.

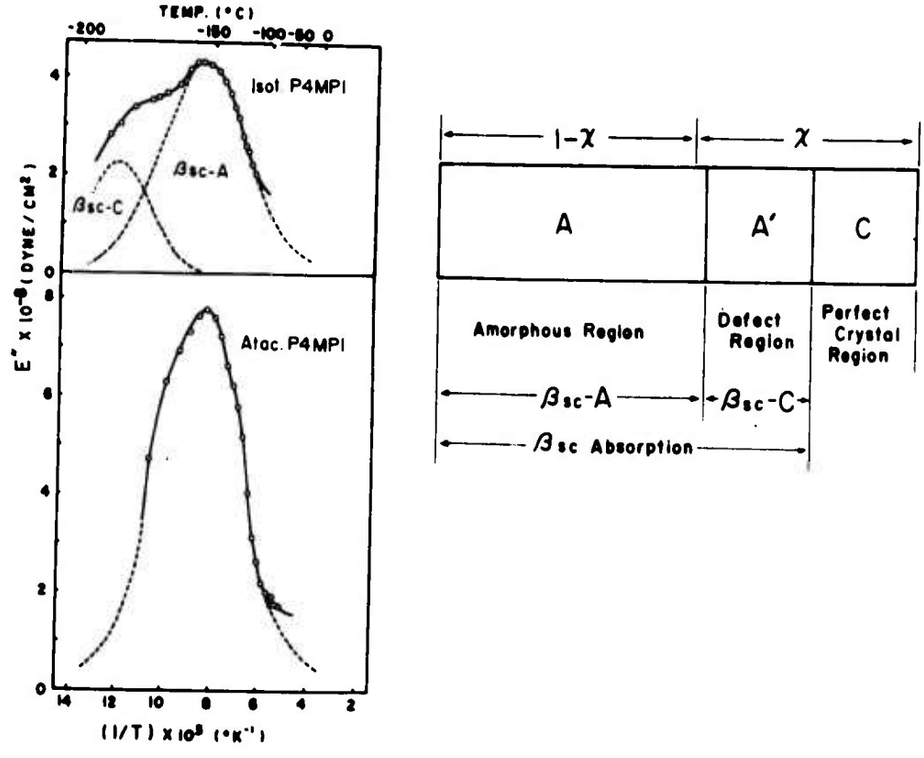

Figure 2. Separation of the β_{sc} absorption into the β_{sc}-A and the β_{sc}-C absorptions. Upper curve is for the isotactic P4MP1 and lower curve is for the atactic P4MP1 (left side). The band spectrum (right side) shows the schematic representation of the relationship among the degree of crystallinity determined by X-ray, the regions of A, A' and C and the contributions of the β_{sc}, β_{sc}-A and β_{sc}-C absorptions.

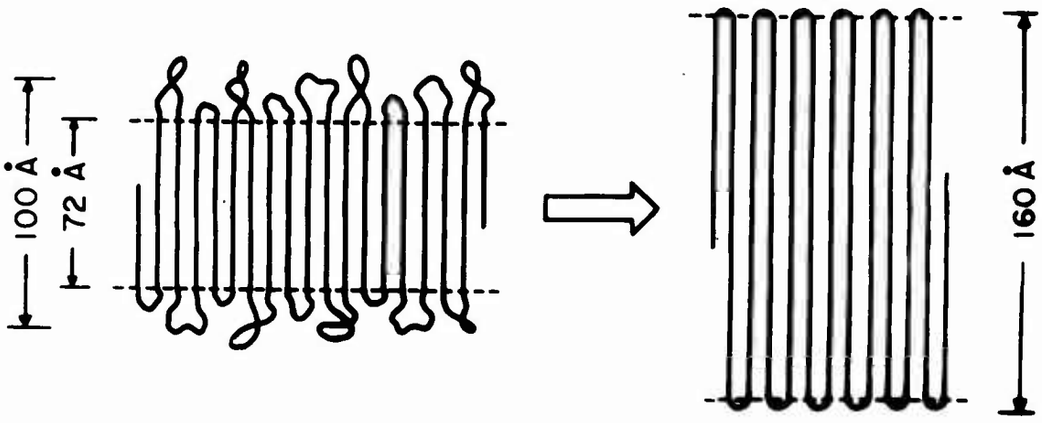

Figure 3. A schematic diagram showing the tightening of loose loops during annealing for single crystal of trans-1,4-polybutadiene.

SESSION 4: Contribution by Professor Roger Porter
University of Massachusetts

partially presented at Conference

HIGH SHEAR FLOW OF PARTIALLY CRYSTALLINE POLYMERS

Few experimental studies have been made concerning the mechanical properties and rheological mechanisms associated with the high-shear steady flow of partially crystalline polymers. The study discussed here differs from they systems and measurement techniques used in previous presentations. These experiments involve steady flow viscosity measurements made under pressure in steel capillaries using an Instron Tester. The choice of test systems has aided substantially the data interpretation. The polymers tested were three low density, low molecular weight polyethylenes. The polymers differed principally in molecular weight which was in the range from 2,800 to 10,000. The steady flow viscosity measurements on these systems at temperatures in the amorphous range, that is above their crystalline melting points, are shown in Figure 1. The data indicate that the flow properties of the two molecular weight materials are entirely Newtonian; that is, their viscosities are independent of shear over a broad shear rate range. There are no indications of thixotropy or shear heating effects with the measurements being entirely reproducible within the test series proceeding from high to low and low to high rate of shear. These data have previously been interpreted in detail[1].

The point to make here is that there is a dramatic difference in Figure 1 between the properties of the highest and lowest molecular weight

polymer. The low molecular weight material is below the characteristic entanglement molecular weight. The high molecular weight material, that exhibits a large non-Newtonian viscosity effect, is above the characteristic entanglement molecular weight. This characteristic entanglement molecular weight for polyethylene is in the range of 4,000 molecular weight as established by a variety of techniques[2].

The salient experiments were viscosity measurements as a function of shear rate with tests at a series of successively lower temperatures extending to 50°C below the nominal melting point for the three polymers involved. The results provide insight into the generation of structure within the polymer with decreasing temperature and the orientation and destruction of structure with increasing rate of shear.

Figures 2 and 3 show these viscosity measurements on two of the three polymers. Figure 2 provides information on the polymer that is entirely Newtonian at temperatures above its melting point. The results reveal profound non-Newtonian effects due to molecular aggregation in crystals at temperatures below the melting point. The viscosity at any shear rate is entirely reproducible within the time period of a few seconds required for varying the shear rate and establishing uniform conditions. The flow curve then is entirely reversible with structural and orientation effects occurring within seconds. The large viscosity effects involved can be attributed exclusively to orientation and destruction of the crystalline aggregates since the melt is entirely Newtonian. Therefore, a method is provided for measuring the concentration and anisotropy of crystalline

aggregates. A discussion in detail of the interpretation of these prominently non-Newtonian flow curves for partially crystalline polymers in steady flow has been recently given at a West Coast Gordon Conference on Polymers[3].

Figure 3 provides entirely new information on the flow characteristics of the partially crystalline polyethylene which has a molecular weight above the characteristic entanglement molecular weight. The general rheological characteristics of the low molecular weight polymer given in Figure 2 are revealed in Figure 3. In addition, at the higher rates of shear there is an additional non-Newtonian effect due to orientation of amorphous chains through entanglement couplings, see Figure 1. The curves in Figure 3 are a graphic display of a dual mechanism for flow orientation within a single polymer. The two mechanisms, by the experience on low molecular weight materials discussed above, are revealed to be the orientation and destruction of crystallites; and separately, at higher shear, the contribution due to deformation through entangled, amorphous polymer chains. Each mechanism can potentially contribute a change of several magnitudes in apparent viscosity with rate of shear. Polymer compositions may be tailored for further investigation of these mechanisms and for advantage in processing of partially crystalline polymers. It is our contention that ever increasing research must be undertaken in this direction. Ever less tractable polymer systems are being devised and utilized on a commercial scale. Thus new information must be developed concerning the fabricating and use of high melting or non-melting polymers. Fundamental characteristics for the flow properties of partially crystalline materials must be defined

by experiment. The results described here reveal information in a particular case using incisively chosen samples. The results reveal two distinct mechanisms responsible for polymer flow orientation in different temperature and shear rate ranges.

REFERENCES

1. R. S. Porter and J. F. Johnson, J. Appl. Polymer Sci. 7, S33 (1963).

2. R. S. Porter and J. F. Johnson, Chem. Rev. 66, 1 (1966).

3. R. S. Porter and J. F. Johnson, Trans. Soc. Rheology, submitted.

Figure 1

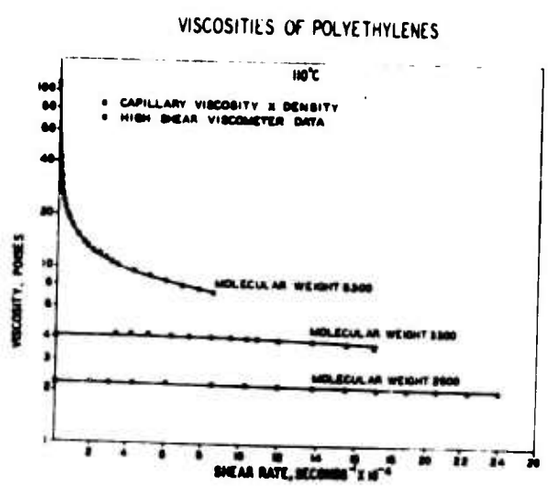

Figure 2

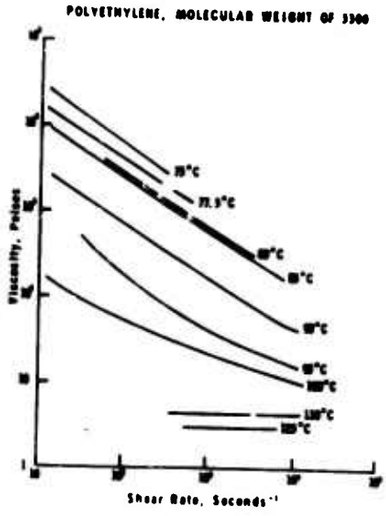

Figure 3

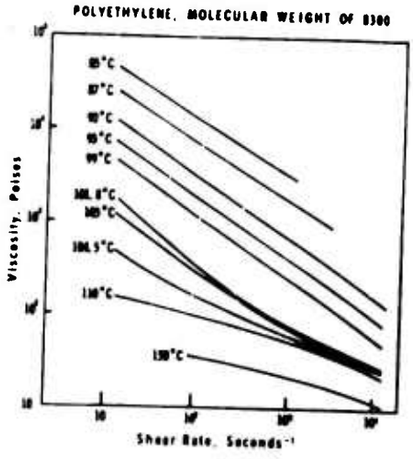

MULTIPLE TRANSITIONS AND RELAXATIONS OF POLYMERS IN RELATION TO MECHANICAL PROPERTIES

Raymond F. Boyer
Plastics Department
The Dow Chemical Company
Midland, Michigan, U.S.A.

PART I. Introduction

A recently published symposium (1) emphasized the fact that most high polymers exhibit several transitons and/or relaxations in addition to the glass temperature, T_G, and the crystalline melting point T_m. This symposium was concerned with the phenomena and their molecular origins but not with mechanical properties associated with these multiple transitions and relaxations. Today's paper is concerned predominantly with this latter topic, and especially with the dependence of mechanical behaviour on transitions other than T_G and T_m.

Figure 1 shows typical multiple transitons and relaxations for polytetrafluoroethylene (PTFE), polyethylene-glycol terephthalate (PET) and branched polyethylene (PE) (2). The issue is simply this: Physical properties of polymers change dramatically at T_G and T_m, as illustrated in Figure 2, taken

from Tobolsky (3), for the shear modulus of atactic and isotactic polystyrene. What changes in physical and mechanical properties can be associated with secondary transitions and relaxations? Are these changes significant enough to affect end use properties? A corollary type of question could be: What is the true T_g of a polymer such as polytetrafluoroethylene?

I was asked to present a critical survey of this field. However, starting from Nielsen's hint (4) that these secondary transitions might be important, there are still relatively few published results from which to choose. Hence, I shall be mainly concerned with calling attention to some widely scattered papers and to emphasizing the available strong indications that secondary transitons are important. In making this survey, I must pay especially tribute to Dr. J. Heijboer who provided me with an unpublished manuscript containing both original data and significant literature references (5).

One very serious problem which inhibits a survey of the type we are considering is the fact that our knowledge of transition and relaxation spectra are circumscribed by one or more of the following facts:

1. Such spectra are available as a function of temperature generally at one or several frequencies but only rarely over a very wide frequency range at a given temperature.*

2. The test method involves essentially zero deformation (thermal expansion, heat capacity, DTA, dielectric) or very small deformation as with dynamic mechanical testing.

On the contrary, important physical properties such as tensile and impact strengths will involve large deformations and may also, as with impact strength, involve a relatively high frequency ($\sim$1000 cps.). One might therefore conclude, a priori, that little correlation should exist between 1 cps. dynamical mechanical relaxation spectra and significant physical properties, or alternately, that correlations which do exist are largely fortuitous.

On the positive side, all transitions and relaxations observed by small deformation and/or low frequency methods arise from specific molecular motions of part or all of polymer molecules. One feels intuitively that such motion may be

---

* Schwarzl (6) was able to calculate (from a wide variety of rheological data) the shear modulus and mechanical loss of polyisobutylene as a function of frequency and show the existence of three loss peaks.

Reddish has published the temperature - frequency of dielectric loss in polyethyleneglycol terephthalate (7). It indicates the usual result: The low frequency plot of loss against temperature gives better resolution for multiple loss peaks than does the plot against frequency at constant temperature.

reflected in mechanical behaviour of the polymer. We will return to this point in discussing specific polymer systems such as polycarbonate (See Figure 5). See also Appendix B.

We have been somewhat inconsistent in nomenclature, frequently following that used by the original authors, as in Figure 1, but occasionally lapsing into a system which we previously proposed. (Ref. 2, page 1339), i.e., $T_{\ell,\ell}$, for $T > T_g$ and $T_{g,g}$ for $T < T_g$. We have tried to make the meaning clear in each case.

PART II. Specific Materials

The materials which I will be reviewing are as follows:

1. Polycarbonate (PC)
2. Polytetrafluoroethylene (PTFE)
3. Polyethylene (PE)
4. Polyvinylchloride (PVC)
5. Polymethylmethacrylate (PMMA)
6. Polyphenylene Oxide (PPO) and Polycyclohexylmethacrylate (PCHMA)
7. Polystyrene (PS)

1. Polycarbonate (PC)

Figure 3 shows schematically the dynamic mechanical loss of bisphenol polycarbonate at 1 cps after Heijboer (5). (See also Nielsen (Ref. 4, Figure 7.26).) In spite of a high T_g of 150°C, this polymer is remarkably tough at room temperature. Nielsen ascribes this toughness to in-chain motion of the carbonate group. Since this is quite pertinent to our theme, we shall examine in some detail the polycarbonate system. Heijboer (5) confirms the general correlation between impact strength and the low temperature loss peak.

A recent paper by Miller (8) reported load-elongation curves on a variety of polymers over a very wide temperature range. He found abrupt decreases in tensile strength and increases in elongation in the region of low temperature relaxations normally designated as γ regions where $T_\gamma < T_G$. Further discontinuities in tensile strength and elongation occur in the region of T_G.

Miller suggested that these lower temperature points are indeed the glass temperature. I consider that the really significant part of the Miller paper is the demonstration of multiple dislocations in load-elongation curves at temperatures corresponding to multiple loss peaks in mechanical spectroscopy at 1 cps and very low deformation. Figure 4 is a plot of the ultimate yield strength data for polycarbonate showing two characteristic breaks at around -120°C and +150°C, using Miller's data.

Figure 5 is a composite plot showing five different types of physical measurements, all indicating the low temperature relaxation and all but one of which are related to T_g = 150°C. The testing frequency of these various test methods range over a factor of 10^5 cps. The low temperature relaxation with an activation energy of 7.7 K Cal. changes dramatically with frequency while the T_g peak with an activation energy of 115 K Cal. is somewhat less sensitive to frequency.

First are the NMR results of Matsuoka and Ishida (9) which allowed them to conclude that the relaxation at -80°C resulted from restricted motion of phenyl groups in the chain. They also had dielectric data (not shown). Instead, we used the dielectric loss data of Krum and Müller (10). The dynamic mechanical loss and impact data are from the paper by Heijboer (5) cited in the introduction. The strength data are by Miller and repeat Figure 4.

Thus we have NMR and dielectric loss demonstrating that molecular motion is involved and even something about the nature of the motion. At the same time we see that this motion is reflected not only in the small amplitude, low frequency non-destructive dynamic mechanical results but also in the large deformation, destructive yield strength and impact strength data.

Finally, Bussink and Heijboer (11) have shown that ring methyl groups ortho to the carbonate linkage restrict rotation of the carbonate group, raise the temperature of the low lying β transition, and impair the room temperature impact strength of polycarbonate.

We shall see from what follows that polycarbonate is probably an ideal illustration of what we were seeking and that many exceptions can be expected on going to different types of polymers.

2. Polytetrafluoroethylene (PTFE)

Figure 1 showed the 1 cps dynamic mechanical loss spectrum for PTFE, taken from McCrum (12). There are four transitions observed: The melting point, two glass transitions and a first order phenomenon around room temperature. What changes in mechanical properties can be associated with these energy loss peaks?

Figure 6 is material taken from an ICI technical bulletin on Fluon, their PTFE polymer (13). Here the modulus in psi is plotted as a function of temperature. It is normal for the modulus to drop in traversing a transition and these drops occur at the temperatures corresponding to the four cited transitions in Figure 1. (McCrum likewise showed such results.) It is obvious that a design engineer who

intends to use this polymer over a wide range of temperatures, especially down into the cryogenic region, must be aware of the dramatic changes in the modulus of elasticity. This is a simple and obvious example.

There is still considerable speculation as to the glass temperature of PTFE: Is it the glass I or the glass II of McCrum or is it still some different value? Table I summarizes these three divergent points of view.

We have previously suggested (Ref. 2, p. 1401 ff) a set of criteria useful in selecting T_g. These are precisely among the criteria employed by the several authors in Table I. This indeed complicates the choice of a T_g. We have previously argued (Ref. 2, Table XV) that the 400°K relaxation could not be T_g. Unfortunately, the specific heat data cited by O'Reilly and Karasz stopped at an upper temperature of 365°K and hence could not clarify the nature of the glass I transition.

Figure 7 is a simple linear extrapolation of the Durrell, Stump and Schumann copolymer data (17). This seems quite convincing for a T_g of -50°C although this would be the T_g of a hypothetical substance, amorphous PTFE. Crystallinity would presumably change T_g to some higher value.

Figure 8 is a plot of impact strength against temperature from the review paper of Sperati and Starkweather (19). A vertical line at -70°C indicates where the glass II peak should be at a frequency of 1000 cps.

We are still in a dilemma: Is T_g the glass II peak of Figure 1 with impact rising in a normal fashion above T_g ? Or is PTFE analogous to PC with a high glass temperature, i.e., glass I, but good impact strength in the glassy state because of the low lying secondary relaxation, i.e., glass II?

PTFE is more difficult than PC to analyze for several reasons such as higher crystallinity and only one type of group, $-(CF_2)-$, along the polymer chain.

We previously argued (page 1350-51 of ref. 2) for ascribing the glass II transition to crankshaft motion. Additional reasons for this are:

1) Reddish, Powles and Hunt (20) have compared the variation of the glass II peak with frequency for dielectric measurements as against mechanical and NMR. The dielectric points lie on a parallel curve, suggesting a common origin. A crankshaft is the most likely explanation of dipole loss in an essentially non-polar polymer (ref. 2, pg. 1351).

2) Matsuoka and Ishida (p. 257 of Ref. 9) found that the ratio T_β/T_g (at 100 cps) is about 0.75 for simple polymers and, except for PC, ranges from .55 to .87 for all polymers in their table.* 0.75 X 400 gives a T_β of 300°K whereas the glass II temperature is 176. If T_g = -50, then we have 176/223 = 0.79 (using the 1 cps values).

3) We previously overlooked the paper by Eby and Sinnott (21) which showed that the glass II process corresponded to about 5 CF_2 groups which is about right for a crankshaft.

4) Finally, as shown by McCrum (22), the temperature of the glass II peak does not change on adding up to 14 mole % of a comonomer, hexafluoropropylene, but the peak height decreases. Copolymerization invariably changes T_g even when the two homopolymers have the same T_g. (See Figure 36 of Ref. 2 as well as Illers (23.)

*Haldon and Simha (46) found a similar ratio in the range of 0.7 to 0.85 and averaging about 0.75 for the polyalkylmethacrylates.

Hence, we conclude as follows:

1. The glass II transition is crankshaft motion.

2. The T_g of amorphous PTFE is about -50°C but the glass process is suppressed by the crystallinity and the stiffness of the backbone chain.

3. The good impact of PTFE at room temperature can be ascribed both to crankshaft motion and to the latent motion inherent in a T_g of -50°C.

4. The glass I transition is an amorphous one and would be classified by us as $T_{\ell,\ell}$ (2).

5. It should be noted from Figure 8 that PTFE is still tough at -70°C. compared with PS or PMMA. In fact, Vincent (54) reports it to be tough at 77°K. Since McCrum's measurements went to 4.2°K, with no sign of a loss peak below glass II, some other energy loss mechanism than glass II must be involved.

We have not commented about the effect of the room temperature transitions on physical properties. Aside from the obvious changes in modulus and thermal expansivity, there is some evidence that the coefficient of friction drops abruptly on cooling through the 19°C transition. (pg. 485 of ref. 19)

TABLE I

REPRESENTATIVE VIEWS ABOUT T_g OF PTFE

Proponents	T_g °K	Reasons
A. T_g = 400°C, i.e., Glass I of McCrum		
Tobolsky et al (14)	383	Obeys WLF Equation
Araki (15)	400	T_g/M_M = 0.66
		$\Delta\alpha T_g$ = 0.12
B. T_g 200°C, i.e., Glass II of McCrum		
O'Reilly and Karasz(16)	160°	There is a discontinuity in specific heat at 160°K.
Simha and Boyer*	160°	$\Delta\alpha T_g$ = 0.112
C. Neither		
Durrell et al (17)	223	Copolymer data (See Fig. 7)
Ohzawa and Wada (18)	208-238	Thermal expansion and mechanical loss

*R. Simha and R. Boyer, J. Chem. Phys., 37, 1003 (1962)

3. Polyethylene

Polyethylene is much better understood than is PTFE, partly because it has been studied more extensively, partly because its solubility permits easier characterization, including preparation of single crystals, and partly because considerably more copolymer information is available. Figure 1 shows four transition regions for branched PE. We have discussed the PE system previously in great detail (Ref. 2, pages 1341-50, 1403-10), showing that T_g of the hypothetical substance, amorphous PE, is about -80°C (Ref. 2, Fig. 20). Independent studies by Illers (23) and Bohn (24) lead to the same conclusion. We also summarized data indicating that amorphous ethylene-propylene copolymers had a γ transition in addition to a T_g (Fig. 22 of Ref. 2).

Schatzki (Ref. 1, pg. 139) has proposed a crankshaft model to explain the γ loss in the amorphous regions while Andrews and Hammack (25) ascribe it to a loosening of a special type of hydrogen bond in the amorphous regions. Sinnott, among others, has demonstrated that single crystals of PE also show the γ transition, as well as the α transition (Ref. 1, pg. 141 ff). Neither the Schatzki nor the Andrews-Hammack mechanism would hold for a highly crystalline material.

Illers has clarified the reason why the γ transition can exist in single crystals, melt crystallized linear PE, branched PE and amorphous E-P copolymers: The γ transition can be resolved into three distinct peaks at about -110°, -140 and -170°C (26). Illers calls these respectively γ_I, γ_{II} and γ_{III} and has proved the γ_I is an amorphous peak while the other two are crystalline peaks (27).

Matsuoka, Ishida and Aloisio noted two peaks by dynamical mechanical methods: one at -110°C which they ascribed to amorphous regions, and one at -140°C which appear to arise from crystalline defects (28).

A study of linear thermal expansion of PE by Zakin and Simha (29) clearly reveals discontinuities in $1/L_o$ (dL_o/dT) at about -170°C, -125°C and several higher temperatures. They show, for example, a quite pronounced change in expansion coefficient at about -22°C which is most likely the Tg of this sample (density, 0.929 and 54% crystallinity by X-ray).

Finally, it should be recalled that McCrum (22) finds two glassy peaks in linear PE: a Glass I peak at 60°C and a Glass II peak at -117°C, in analogy with PTFE.

Putting together these various facts, we show schematically in Figure 9 a transition map for PE, PP and all E-P

copolymers. The γ transition shown is that for the amorphous region. Now we ask how the mechanical behaviour of PE depends on transitions other than T_g.

Heijboer (5) found that the unnotched impact strength of linear PE begins to increase dramatically as low as -150°C. We show in Figure 10 some dart drop data by Turley (30) which indicates a sharp rise in impact values at about -125°C. We have noted by vertical lines on this plot three characteristic temperatures

T_g (crystalline PE)	-30°C
T_g (amorphous PE)	-80°C
T_γ	-125°C

The latter might be as high as -100°C at 1000 cps. It would appear from the data of both Heijboer and Turley that even the usual γ transition (-125°C) cannot explain their results and that we must rely on loss mechanisms in the crystallites such as γ_{II} and γ_{III} of Illers. Miller(8) did not give the detailed data but stated that PE is glassy at -150°C.

One might ask if the creep characteristics of linear polyethylene are not enhanced by the three γ transitions, and especially the two γ transitions in the crystalline regions which are normally supposed to prevent a polymer above its T_g from cold flow.

Next, we consider the α transition. McCrum (22) clearly defines it as a glassy transition. Sinnott describes it as "the reorientation of folds at the surfaces of lamellae." Illers (26) refers to it as "an intermolecular hindered rotation of the length of fold about the longitudinal axis of the molecule within the crystal lattice."

Figure 11 shows four characteristic features of linear PE which change in the region of the α transition.* These are more in the nature of characterization parameters (31)(32)(33)(34)(35). In addition, Nakayasu, Markovitz and Plazek (36) have measured both mechanical creep and dynamic loss from -29 to +80.8°C and find evidence for the α transition.

Finally, we should call attention to the work of Retting (37) who measured the tearing energy of PE (and other polymers) as a function of tearing velocity. He found several well pronounced maxima and minima in the tearing energy. He associated these with maxima in dynamic mechanical loss plots as a function of temperature. Retting believed that the maxima in tearing energy correspond to minima in mechanical loss, and vice versa. However, after private discussions with Dr. E. H. Andrews and after the lecture by

*It has been suggested to me privately by several experts on radiation chemistry that the use of radiation cross-linking in polyethylene structure studies is likely to be erroneous because the site of the cross-linking action is not fixed. This criticism might apply if one tried to fix the locus of the α transition. However, in Fig. 10d only the amount of cross-linking at fixed dose is being used.

Gent at this symposium, it now appears to me that the maxima in tearing energy should go hand in hand with maxima in dynamic loss.

The important thing for the purpose of today's symposium is the fact that tearing energy versus velocity and dynamic loss versus temperature both show several processes different in activation energy with a strong indication that the same activation energy obtains for the same process by both mechanisms.

Finally, we conclude this section on PE with Table II which is a comparison of PE and PTFE.

Incidentally, Illers (26) has shown that the α transition in PE contains three components. The phenomenon shown in Fig. 11 are probably all dependent on the crystalline regions but there are presumably amorphous area effects too.

TABLE II

COMPARISON OF SEVERAL TRANSITIONS AND RELAXATIONS IN PE AND PTFE

	PE	PTFE
T_m	137 °C.	327 °C.
Glass I	60	127
ΔH_a K Cal	32	115
T_g (100% amorphous)	- 80	-50
ΔH_a K Cal	18	--
T_g/T_m	0.47	0.37
Glass II, or T_γ (amorphous)	-110°	-97
ΔH_a K Cal	7.6 K Cal.	18 K Cal.
T_γ/T_g	0.84	0.79
Lowest observed transition	-170	-97
Temperature at which impact strength starts to increase	-150	-70
Nature of Polymer at 77°K.	Tough	Tough

4. Polyvinylchloride (PVC)

It has long been known that both dielectric and dynamic mechanical tests revealed two loss peaks in PVC: T_g at about 65°C to 85°C and a low broad one at about -30°C which moved to higher temperatures rapidly with increasing frequency and which disappeared on the addition of plasticizer. Recent studies by Oberst (38) and Bohn (39) have clarified the impact behaviour of PVC by considering the lower or β peak.

Oberst studied the correlation between impact strength (by five different methods) and dynamic properties at 100 and 1000 cps for a variety of materials, both as a function of temperature. Figure 12 is a plot of one set of his results for PVC using Charpy impact values and dynamic loss at 1000 cps. There is a strong indication that good room temperature impact of PVC arises because of molecular motion in the so-called β process.

Bohn has extended these results by combining two well-known facts about PVC:

a) The impact strength of PVC will drop from 3.0 to 0.3 ft. lbs. on adding up to 10% of DOP.

b) The β peak disappears on addition of PVC.

He postulates that the loss of impact strength on adding plasticizer results from the disappearance of the β peak.

Figure 13 shows a crude correlation which we made from Bohn's paper: We measured the peak height of the β process at different plasticizer content of DOP and then plotted impact strength against peak height. Area under the β peak might have been more meaningful but would not have altered the character of the conclusions.

Bohn speculated about molecular mechanisms involved in the lowering of the β peak height by plasticizer, without seeming to reach any definite conclusions. For our purpose today, the important point is the direct correlation between β peak height and impact strength.

Vincent (40) showed curves for PVC in which he had plotted true stress against draw ratios for different temperatures. In the temperature interval between -20°C and +60°C, the curves all coincided, but at 70°C, and higher, each temperature required its own curve. It would thus appear that between T_g and the β relaxation, only one molecular process prevailed.

Thus far we have discussed polymers which naturally contained several energy absorption peaks. Oberst and his collaborators (41) have been examining lossy polymers as the core material in metal skin sandwich panels for use in

sound deadening. Since such panels must serve over a wide temperature range (i.e., jet planes going from the desert to the arctic), they need to absorb energy over a wide range of temperatures, as well as in the frequency range of 100 to 1000 cps.

One means of achieving the desired width of energy absorption is by copolymerization of a monomer like vinyl-chloride whose homopolymer has a high T_g with a "soft" monomer like 2-ethylhexyl acrylate whose homopolymer has a low T_g, while causing the ratio of the two monomers to drift during the copolymerization. Bohn (42) describes dynamic mechanical loss on such copolymers. Figure 14 shows schematically the loss curves for Polymer A, Polymer B, random AB copolymer, and a drifting AB copolymer. The drifting composition copolymer contains a multiplicity of energy absorption peaks, none of which is as high as that obtainable from a homopolymer or random copolymer.*

---

*Polymers which naturally contain several energy absorption peaks might be better for use in sound absorption than those with a single peak. Polyisobutylene absorbs appreciable energy at 1000 cps from -40°C to at least +40°C with two loss peaks at -30°C and +10°C (data by Fitzgerald, Grandine and Ferry, J. Appl. Physics, 24, 650 (1953)). This probably explains the good energy absorbing characteristics of butyl rubber.

Finally, we add this note about PVC: At the energy loss peaks for T_g and the β process, there will be concomitant changes in modulus (38) (39) (42) and also in thermal expansion and compressibility as shown by Heydemann and Guicking (43). The changes at the β transition are only 1/7 as great as at T_g, but could still be significant in precision engineering design.

5. Polymethylmethacrylate (PMMA)

Figure 15 shows dynamic mechanics loss data by Wolf (44) for PMMA, with the very prominent T_g peak at 111°C. The $T > T_g$ peak at 200°C is presumably the one we refer to as $T_{\ell,\ell}$. The peak at 51°C is the well-known β peak which appears to start as low as -50°C. Figure 16 is the thermal expansion data by Heydemann and Guicking (43) which suggests the possibility that the β peak involves two processes. Their compressibility results also show several breaks.

Much earlier, Martin, Rogers and Mandelkern (45) had shown a specific volume-temperature plot with change in slope at -40 and +90°C. Haldon and Simha (46), using linear expansion, found breaks at -130°, 15 and 103. We also saw evidence, in examining the Haldon-Simha data, for a break centering around -50°C. Thus all three groups agree on T_g and agree on the existence of several other breaks while disagreeing

on the temperature at which these breaks occur. From Table III, it would appear that going to lower starting temperatures brings out more relaxation regions and lowers the temperature at which they seem to appear. Also included in Table III is the dynamic data of Wolf obtained by estimating on Figure 15 the existence of minor peaks at -75°C and 0°C. The Wolf results agree completely with those of Haldon and Simha, lying at a higher temperature, with the difference decreasing as T increases while apparent activation energy increases.

We wish now to discuss several instances in which observed mechanical properties show sensitivity to the β transition.

Roetling (47) observed the yield stress behaviour of PMMA from 30° to 90°C over six decades of rate. At first he tried to fit the yield stress behaviour by an Eyring viscosity equation with one activation energy. This did not work. Instead he had to use a Rhee-Eyring equation with two activation energies. With a choice of the activation energies as 20 and 100 K Cal., he could fit all of the data by a single equation. The first is the activation energy associated with the 50°C β peak as obtained from dynamic data and the second is the activation associated with T_g. Here is one definite case where creep experiments being carried out at

temperatures which include the secondary transition, require that it be recognized. Roetling has provided one method of doing so.

Roetling (48) subsequently studied yield stress for polyethylmethacrylate through the glass region (T_g = 65°C) from 30 to 80°C. The β transition is at about 25°C. Here again he had to use the Rhee-Eyring approach with activation energies of 32 and 98 K Cal., respectively.

Next, we refer to some old work of McLaughlin and Tobolsky (49) who studied creep of PMMA at 80°C for samples quenched by varying amounts. We reproduce their results in Figure 17. It seems probable, in view of Roetling, that the β transition provides molecular motion which makes creep between T_β and T_g possible, while quenching probably enhances the β peak by increasing free volume in the glass state.

Morris and McCrum (50) observed creep of PMMA between -30°C and +40°C and were able to rationalize their creep data with dynamic loss data by assigning to the β process an activation energy of 19 K Cal.

Again, referring to Dr. Vincent's lecture from this symposium, he reported that plots of true stress against draw ratio for PMMA would be on one curve in the temperature interval from 60° to 110°C; but at 115°C and higher

temperatures, a specific curve was needed at each temperature. As with PVC, one mechanism appeared to prevail between the β peak and T_g.

Finally, we will call attention to data of Maxwell and Harrington (51) on energy required for the tensile breaking of PMMA as a function of temperature (30°-90°C) and strain rate (.001-200"/sec.). Their results appear in Figure 18. We suggest that the seeming complexity of these results may arise because of multiple relaxations, i.e., T_g, the β transition in this polymer which can be as low as 15°C for a very slow test (see T ble III), and possibly a still lower transition (-30° to -50°C by thermal expansion, 0°C by 1 cps dynamic). See also Appendix A*.

The mechanism of the β relaxation is still in doubt. Heijboer has at present quite strong evidence to suggest that it arises from motion of the ester side group (52). Roetling (47), however, quotes some unpublished studies by Havriliak indicating that the β transition could not be due to side chain rotation relative to the main chain but is probably due to either a twisting or rotation of the main chain about its longitudinal axis. The strong role played by β transition in creep properties suggests to us that Havriliak's view may be more nearly correct.

* Vincent (Ref. 54, p 428-9) has discussed this same data in some detail.

TABLE III

MULTIPLE TRANSITIONS BY THERMAL EXPANSION DATA ON PMMA

Workers	Lowest Temp. Used	Location of Breaks, °C, in Order of Decreasing Temperatures Start with T_g at the Right				Ref.
Heydeman and Guicking	- 60	--	7	62	103	(43)
Martin, Rogers and Mandelkern	-140	--	-30	15	105	(45)
Haldon and Simha	-180	-130	-50[a]	15	103	(46)
Wolf (Dynamic Data)	-160	- 75[b]	0[b]	51	111	(44)

(a) Midpoint of a slow linear increase in thermal expansion.

(b) Obtained by inspection of the curve in Fig. 15.

6. Polyphenylene Oxide (PPO) and Polycyclohexylmethacrylate (PCHMA)

Thus far we have been talking about systems in which a transition lying below T_g makes itself felt in mechanical properties. We now wish to report on two systems which clearly defy any previous generalization.

Heijboer (5) has studied 2,6-dimethylpolyphenylene oxide in the range from -200 to +100°C. As indicated in Figure 19, impact strength remains remarkably high and there is no pronounced maximum in the dynamic loss data. Indicated on the left top of Figure 19 are the impact strengths of PE and PC at -200°C. I speculated that there might be some major relaxation process below -200°C, but Dr. O'Reilly of General Electric commented during the discussion period that none existed down to liquid helium. It is possible that a large excess of free volume or the flexibility of the ether linkage is responsible for this unusual behaviour of PPO.

Polycyclohexylmethacrylate (PCHMA) affords exactly the opposite case. Figure 20 is data by Turley on this material. The pronounced secondary maximum at -80°C has been extensively studied by Heijboer (53) who ascribes it to a chair-chair transition of the cyclohexyl ring. One might expect this polymer to exhibit high impact values at room temperature. However, as Vincent (54) pointed out, it is

extremely brittle at room temperature. This and other facts lead Heijboer to the tentative conclusion that motion in a side group of a polymer chain may not contribute to the impact strength of that polymer (5).

Vincent (54) has warned about trying to generalize on the effect of low lying transitions on impact strengths at room temperature. He reports on finding PE, PTFE and PC all tough at 77°K, well below any observed transition.

7. Polystyrene (PS)

Atactic polystyrene shows transition and relaxation phenomena by dynamic mechanical methods at a variety of temperatures which are listed in Table IV in descending order of temperature. To these should be added an artificial loss peak which can be induced in the region of -50 to -100°C on incorporating a rubber in polystyrene. As pointed out by Nielsen (59), the rubber exists as a separate phase and therefore causes a distinct loss peak whose height is proportional to the amount of rubber phase and whose temperature is approximately the T_g of the rubber. Turley has discussed this further (60).

TABLE IV

DYNAMIC MECHANICAL TRANSITIONS AND
RELAXATIONS IN POLYSTYRENE

Temp. °C.	Designation	Reference
160	$T_{\ell,\ell}$	Boyer (55)
100	T_g	Schmieder and Wolf (56)
25-60	β, $T_{g,g}$	Schmieder and Wolf (56)
-140	?	Schmieder and Wolf (56) Illers (57)
-228	?	Woodward (58)

Since PS is normally quite brittle at room temperature, it follows that neither the -140 nor the -228 relaxations contribute significantly to impact strength. Addition of 5% of rubber in the proper manner can triple to quadruple the room temperature impact of PS. The loss mechanism is neither an in-chain or side-chain motion but a separate phase which may be chemically coupled to PS.

The β peak has been studied by a number of investigators. Martin, Rogers and Mandelkern found evidence of it at -30°C by thermal expansion (45). Wunderlich and Bodily(61)detected it by DDTA as covering the range from -25 to +70°C, but centering around 27°C (61). Illers (57) investigated this loss in PS and its derivatives, finding a dynamic loss peak for PS in the region of 25-60°C as the frequency changed from 0.05 to 40 cps, with an apparent activation energy of 35 K Cal. It is thought that this process involves the lib rational motion of phenyl rings, although we tend to consider it as a $T_{g,g}$ crankshaft type of motion.

We have one example where the β transition appears to affect mechanical property measurements. Seitz and Balasz (62) were studying the creep of PS at several temperatures below T_g. They planned to extrapolate to room temperature by the superposition principle so that long term creep properties could be predicted. They quickly discovered

that their data was not suitable for extrapolation. At first they doubted their experimental results until I pointed out the existence of this secondary loss peak and the experience of Roetling with PMMA. Fig. 21 shows schematically the problem which they faced.

Both Illers (57) and Turley (63) found that the height of this β peak increased with quenching. One might expect that creep data obtained below T_g and above T_β would depend on prior thermal history in much the same manner as for PMMA [illegible] in Fig. 16.

Above T_g is an apparent transition or relaxation in the region of 160°C which we labeled variously as $T_{\ell,\ell}$, or $T > T_g$. We recently reviewed the thermal and rheological data pertaining to this transition (55). These data indicated some discrepancies which have not yet been resolved. We propose now to up-date our previous review.

A quite different approach to the $T = T_{\ell,\ell} > T_g$ transition in polystyrene is offered by Colborne (64) who studied polystyrene-plasticizer systems by two different techniques. In one case he measured melt viscosities by a falling ball method as a function of temperature and concentration. Plots of $\log \eta_{melt}$ against 1/T consisted of two straight line portions whose intersection was at a lower temperature

the greater the amount of diluent. In the second method, plasticized films were placed on a hot stick and the lowest temperature at which tackiness developed was noted. Figure 22 is a plot of adhesiveness temperature and T_g both as a function of weight percent tricresylphosphate.

Both Plazek and Fox commented during the discussion period about the $T > T_g$ transition in polystyrene. Dr. Plazek presented melt viscosity data which failed to show any evidence for some transition in the region of 160°C. Fox suggested that the Colborne data shown in Figure 22 might be a manifestation of an isoviscous state. Since Plazek's remarks and data will appear in the discussion section, and since Dr. Fox raised a fundamental question, I wish to comment on both points.

Of greatest relevance to this symposium is a study by Duda and Vrentas (65) on the solubility and diffusion of n-pentane in polystyrene at elevated temperatures. The diffusion results are shown in Figure 23. The dramatic change in slope at 150°C is unmistakable while the numerical values of the two activation energies agree rather well with values we previously calculated from melt viscosity (55). Solubility values are not shown but also went through an abrupt change at 150°.

Secondly, Plazek (66) has recently presented an extensive review on melt viscosity in which he gave the remarkable set of curves shown schematically in Figure 24.

This is a log-log plot of the reduced viscosity, η_r, against the viscosity average molecular weight, $\bar{M}_v$. The data at 160 and 217°C show the characteristic increase in slope from unity below the critical entanglement molecular weight ($\sim$ 35,000) to a slope of 3.4 above this molecular weight. However, the two curves obtained at 100 and 119°C have the slope of about 3.4 on either side of the critical M.W. which might indicate entanglement at all molecular weights. In any event, there is an abrupt change in character on going from 119°C, which is well above T_g, to the temperature of 160°C. I believe this new experimental data is consistent with my proposed explanation of the $T > T_g$ transition being the temperature at which entire polymer chains can change centers of gravity.

Finally, a colleague of mine has supplied some unpublished melt viscosity data on polystyrene in which he calculated the Rabinovitch number (67). This number is simply the slope of the double logarithmic plot of shear stress against shear rate. Figure 25 is illustrative of his results. The Rabinovitch number is essentially independent of shear stress at 160°C but decreases monotonically at 170°C. Data at 180 and 190°C follow the same pattern as the 170°C curve.

Dr. Fox was asking, as I interpreted him, the basic question: Is this $T > T_g$ phenomenon simply some manifestation of an isoviscous state, especially in the Colborne data, and

therefore possibly an artifact of the measuring method rather than an inherent property of polystyrene? This problem had concerned me while thinking about the variation of $T_{\ell,\ell}$ with molecular weight (Table 1 of Ref. 55). Some elaboration of this point may be pertinent now.

One very simple method of getting numerical values for an isoviscous state in molten polystyrene was to take the experimental plots of Allen and Fox (68) of log melt viscosity against linear temperature at various molecular weights and draw a horizontal line corresponding to $\eta = 10^4$ poise. (Actually, we had an 8-1/2 X 11" plot from a manuscript which Dr. Fox had sent us.) One could then read off, simultaneously, values of molecular weight and temperature for which $\eta = 10^4$ poise. The results are shown in Figure 26 where there is a characteristic change at the critical molecular weight for chain entanglement.

The choice of $\eta = 10^4$ as the value to use for an isoviscous state was arbitrary but was selected for two reasons: it permitted the largest number of datum points, and the temperatures which resulted were not too different from $T_{\ell,\ell}$ values. A partial check at other values of η = constant indicated similar results. Figure 27 compares $T_{\ell,\ell}$ and isoviscous state temperatures as a function of molecular weight. There is strong indication that $T_{\ell,\ell}$ is not an isoviscous state, especially in the high molecular weight range, although additional data are needed to settle this point.

Theoretical consideration of how melt viscosity depends on molecular weight, temperature and activation energy, and how the activation energy itself decreases with temperatures above T_g would further indicate that the results of Figure 26 are what should be expected.

The Colborne data are for a solvent-diluent system. In this case, in order to get numerical values for an isoviscous state, we have used the data of Fox, Gratch and Loshaek (69) for the system Polystyrene-Dibenzylether with a polystyrene of M = 70,000. Once again $\eta = 10^4$ poise was chosen for the isoviscous state. The calculated temperatures against weight fraction of polymer are shown in Figure 28, yielding a good straight line. A straight line also results for $\eta = 1$ poise. It lies above and has a higher slope than the curve for $\eta = 10^4$. Because of difference in diluents, one cannot be certain about the comparison: the Colborne temperature drops with diluent much faster than does the $\eta = 10^4$ temperature but Colborne's results may still signify an isoviscous state.

Finally, in the sense of this symposium, some molecular event occurs in polystyrene at about 160°C which affects important physical properties such as diffusion, melt flow and tackiness. The fact that an isoviscous state may be involved does not detract, in our opinion, from the significance of the observations.

PART III. Summary

We have attempted in this admittedly superficial survey to review instances where physical properties of a few key polymers showed some change which might be associated with secondary transitions and relaxations (i.e., those other than T_g and T_m). In general, one or more of the following properties, which could be of interest to the design engineer concerned with the intelligent use of plastics, were noted to change. See Table V.

We assumed for the most part that dynamic mechanical spectroscopy at about 1 cps was the tool which indicated the existence of a secondary loss mechanism while dielectric loss and NMR were auxiliary tools to aid in understanding the phenomenon.

We also recognize that certain basic laws of physics require certain relationships, i.e.,

a drop in modulus will accompany an energy loss maximum

creep and dynamic mechanical loss have a common molecular basis.

TABLE V

Some Physical Properties Which Change at Secondary Transitions

Modulus of elasticity

Coefficient of thermal expansion

Impact strength

Tensile strength

Toughness

- Tearing energy
- Tensile breaking energy

Creep rate

Heat content (C_p, DTA, etc)

Rheological properties

- Apparent activation energy
- Non-Newtonian flow
- Chain entangelement

Coefficient of friction

Dielectric loss

Tackiness temperature

Solubility and diffusion of solvents

Finally, in Table VI we summarize the various specific instances in which we sought a correlation between room temperature impact strength and a low temperature secondary transition or relaxation.

One might conclude from these examples that a low temperature absorption peak is neither a necessary nor a sufficient condition to give good room temperature impact, but that it is helpful in more cases than not.

It seems quite probable that awareness of possible relationships between secondary transitions and physical properties will result in many new examples being found. In some instances, more sensitive tests may have to be devised.

TABLE VI

EFFECT OF SECONDARY LOSS PEAKS ON ROOM TEMPERATURE IMPACT

Material	Existence of Low Temp. Loss Peak	Room Temp. Impact
Polycarbonate (a)	yes	tough
o-Methyl subst. Polycarbonate	no	brittle
PTFE (a), (b)	yes	tough
PE (a), (b)	yes	tough
PMMA	no	brittle
PVC	yes	tough
PVC + 10% plasticizer	no	brittle
Polystyrene	no	brittle
Polystyrene + 5% rubber	yes	tough
PCHMA	yes	brittle
PPO	no	tough

(a) Also tough at 77°K which is below lowest low temp. peak

(b) Above T_g at room temperature.

APPENDIX A

The energy absorption data of Maxwell and Harrington for PMMA shown in Figure 18 are sufficiently intriguing as to provoke the following ad hoc interpretation in terms of multiple transition phenomena.

We suppose three transitions, $\alpha = T_g$, β and γ as suggested by the data in Table III. Figure 29 is a log frequency linear temperature plot in which we postulate constant activation energies for the β and γ transitions (see page 1368 of Ref. 2). We suggest further that the activation energy for T_g is quite low until the glass temperature is approached. This follows the finding of McLqughlin and Tobolsky (J. Colloid Science, 7, 55 (1952), specifically Fig. 9) for PMMA.

Now, at point a on Fig. 29, namely, 30°C and a rate of 0.001"/sec., the sample is above its γ transition and will be relatively tough. Increasing the rate to point b takes the sample below its γ transition and one mode of molecular motion is effectively lost. Hence the energy absorbtion drops from A to B in Fig. 30, which is the equivalent of traversing the γ transition.

Starting next at point c on Fig. 29 and increasing the rate of straining takes the sample through the β and the γ transitions, corresponding to points C to D to E on Fig. 30.

At point f, it is assumed in effect, that T_g has been lowered by the applied stress so as to be effective at 70°C. We further presume that the β and γ transitions have effectively merged. This then gives the regions F to g and g to H to I in Fig. 30. F to g is the largest drop thus far, in keeping with the importance of T_g.

The 90°C data are not indicated on Fig. 30 although their course is similar to the 70° data. The decreased energy absorption for 0.001"/sec. at 90°C, presumably arises from the fact that tensile strength is approaching zero rapidly at T_g.

It should be mentioned that an analysis similar to that in Fig. 29 and 30 will result by assuming only two transitions, namely, T_g and β, although the fine details do not agree as well with Fig. 18.

APPENDIX B

It seems fitting to conclude this survey with brief recognition of some of the key individuals who first noted the correlation between mechanical properties of polymers, such as impact strength, and dynamic mechanical loss curves. We have not attempted a definitive literature study but believe we have covered the key references.

It is quite certain that as early as 1950 Buchdahl and Nielsen (J. Appl. Phys. 21, 482 1950) had studied the dynamic loss behaviour of rubber modified, or impact, polystyrenes and shown a low temperature loss peak which could be ascribed to the presence of rubber as a separate phase, in addition to the main glass peak of polystyrene.

We also know from private sources that as early as 1955 Wolf and his collaborators at Badische were using dynamic mechanical loss to characterize a wide variety of rubber modified polystyrene type materials.

However, Bohn and Oberst (Acustica, 1, 191 1959) presented a more formal study of the subject in which they measured dynamic modulus and loss at frequencies in the range of 10 to 1, 000 Hz, and impact strength, all as a function of temperature, for polypropylene and polytrifluorochloroethylene (PTFCE). They showed that impact

strength increased exponentially starting at temperatures not too far below the maximum in the dynamic loss curves. They further emphasized that a secondary loss peak (T< Tg) in PTFCE around 0°C. seemed to be decisive for the good impact strength of this material at room temperature. In their final paragraph they suggest the possibility of introducing secondary loss peaks through mixtures or copolymerization which will improve impact strength without an appreciable sacrifice in modulus.

A year later, and presumably completely independent of Bohn and Oberst, Staverman and Heijboer (Kunststoffe, 50, 23 1960) discussed the general connection between scientific tests such as dynamic spectroscopy and many of the practical tests on plastic materials. Their Figure 7 shows a complete parallel between impact strength and compliance at 1,000 Hz, both as a function of temperature, for polypropylene.

Next, three references appearing in 1961 might be noted: Nielsen (Ref. 4, p. 180), in one concise paragraph, sums up most of the substance of our current review. His only reference is to a paper by Bobalek and Evans (SPE Transactions, 1, 93, 1961) who studied aspects of dynamic mechanical loss curves that could be related with impact strength. They made the generalization that non-impact polymers have damping curves which are "low and flat below the main glass

transition," whereas impact resistant polymers have "high damping either with several sharp peaks or one or two broad wide peaks." Thirdly, Illers, Kilian and Kosfeld (Ann. Rev. of Phys. Chem., Vol. 12, p. 60, Scht. 1961) ascribes the good flexibility of polycarbonate at low temperature to a "second definite relaxation process at low temperature." No prior reference or elaboration of this point is given at this specific point in their paper although later, on page 64, they state: "There is a general tendency to replace the technological testing process to a great extent with scientific methods. The extent to which this is already possible today is convincingly demonstrated by Bohn and Oberst (l. c.) and Staverman and Heijboer (l. c.)."

CAPTIONS FOR FIGURES

Figure 1 Examples of multiple transitions and relaxations, using the original designations of the authors. (Ref. 2, Fig. 1).

Figure 2 Change in shear modulus at the glass temperature, T_g, for atactic polystyrene and at T_g and T_m for isotatic polystyrene (Ref. 3, Fig. II-20).

Figure 3 Dynamic mechanical loss at 1 cps for bisphenol polycarbonate. Schematic after Heijboer (Ref. 5).

Figure 4 Variation of ultimate yield strength with temperature for bisphenol polycarbonate, after Miller (8).

Figure 5 Variation of NMR line width (9), dielectric loss (10), dynamic mechanical loss (5) ultimate yield strength (8) and impact strength (5) for bisphenol polycarbonate.

Figure 6 Dynamic modulus of Fluon PTFE (13).

Figure 7 Linear extrapolation of T_g values for tetrafluoroethylene copolymers to a value for amorphous PTFE. Data from Ref. 17.

Figure 8 Impact strength of PTFE as a function of temperature. (19).

Figure 9 Variation of the α, $\beta = T_g$ and γ transitions in ethylene propylene copolymers. Schematic based on numerous sources

Figure 10 Dart drop impact strength of linear PE against temperature. The three vertical lines are left to right T_γ at 1 cps; T_g for completely amorphous sample; T_g for highly crystalline PE.

Figure 11 Four physical properties reflecting the α transition in linear polyethylene. (a) b axis from X-rays (31); (b) refractive index of single crystals (32); (c) NMR line width of single crystals (33), (34); (d) radiation cross-linking of well crystallized specimen (35).

Figure 12 Correlation of Charpy impact strength with 1000 cps dynamic loss data for pure PVC after Oberst (38).

Figure 13 Correlation of impact strength of PVC plasticized with DOP with peak height of β transition by dynamic mechanical loss, using data by Bohn (39). The numbers on the curve are the ratios of PVC to plasticizer.

Figure 14 Schematic representation of dynamic mechanical loss plots for a hard polymer, A; a soft polymer, B; a random copolymer, AB; and a copolymer of A and B whose composition is allowed to drift. (Based on Ref. 41, 42).

Figure 15 Dynamic mechanical loss curve for PMMA according to Wolf (44).

Figure 16 Coefficient of thermal expansion of PMMA according to Heydemann and Guicking (43).

Figure 17 Stress relaxation of PMMA at 80°C as a function of rate of quenching. McLqughlin and Tobolsky (49).

Figure 18 Energy for tensile failure for PMMA as a function of strain rate and temperature. Maxwell and Harrington (51).

Figure 19 Impact strength and dynamic loss of PPO after Heijboer (5). The arrows indicate impact strength of PC and PE at -200°C.

Figure 20 Dynamic mechanical loss of Polycyclohexylmethacrylate at 1 cps after Turley (63).

Figure 21 Suggested variation of creep rate of polystyrene with temperature in the region of T_β and T_g after Seitz and Balˆasz (62).

Figure 22 The adhesiveness of polystyrene - tricresyl-phosphate systems after Colborne (64). The T_g plot is shown for comparison.

Figure 23 Diffusion constant for n-pentane in polystyrene according to Duda and Vrentas (65).

Figure 24 Schematic representation of Plazek data for variation of the melt viscosity of polystyrene with molecular weight at four different temperatures.

Figure 25 Variation of the Rabinowitch number for polystyrene melts at 160°C and at 170°C. Higher temperatures follow the 170°C line.

Figure 26 Definition of an isoviscous state for polystyrene against molecular weight. The ordinate is the temperature at which a polystyrene sample of a given molecular weight will have a zero shear melt viscosity of 10^4 poise. Points shown are calculated from data by Allen and Fox (68).

Figure 27 Plot from Figure 25 compared with the $T_{\ell,\ell}$ $(T > T_g)$ amorphous transition in polystyrene, both as a function of molecular weight.

Figure 28 Isoviscous state for polystyrene-dibenzyl ether systems. Ordinate is the temperature at which an indicated composition has a viscosity of 10^4 poise. Points are calculated from data of Fox, Gratch and Loshalek (69).

Figure 29 Attempt to explain strain energy results of Figure 18 for PMMA based on three loss mechanisms having the indicated temperature - frequency dependence.

Figure 30 Predicted energy - strain rate curves based on Figure 29. The 90°C results are not plotted to avoid overcrowding. Compare with Figure 18.

REFERENCES

1. R. F. Boyer, Editor, J. Poly. Science, Part C, Polymer Symposia No. 14, 1966, Interscience Publishers

2. R. F. Boyer, Rubber Chem. Technology, 36, 1303 (1963)

3. A. V. Tobolsky, Properties and Structure of Polymers, John Wiley and Sons, N.Y.C., 1960. Fig. II-20. See also, Ref. 4, Fig. 7.27.

4. L. E. Nielsen, Mechanical Properties of Polymers, Rheinhold Publishing Co., N.Y.C., 1962, p. 180

5. J. Heijboer, "Dynamic Mechanical Properties and Impact Strength," in press

6. F. Schwarzl in Houwink/Staverman, "Chemie und Technologie der Kunststoffe" Vol. I, p. 633 ff, 1963. See specifically Fig. 33, p. 673

7. W. Reddish, Trans. Faraday Soc., 46, 459 (1950)

8. G. W. Miller, Polymer Preprints, 8, 1072 (1967)

9. S. Matsuoka and Y. Ishida, Ref. 1, p. 256, Fig. 5.

10. F. Krum and F. H. Müller, Kol. Zeit., 164, 6 (1959)

11. J. Bussink and J. Heijboer, Physics of Non-crystalline Solids, North Holland Publishing Co. Amsterdam, 1965, p. 388 ff.

12. N. G. McCrum, J Poly. Science, 34, 355 (1959)

13. The Character of 'Fluon' PTFE, Imperial Chemical Industries, Plastics Div., Welwyn Garden City, Herts, England, 1963, Graph 7.

14. A. V. Tobolsky, D. Katz and M. Takahushi, J. Poly. Sci., A 1, 483 (1963)

15. Y. Araki, J. Applied Poly. Sci., 9, 421 (1965)

16. Ref. 1, page 53

17. W. S. Durrell, E. C. Stump, Jr. and P. D. Schumann, J. Poly. Sci., B, 3, 831 (1965)

18. Y. Ohzawa and Y. Wada, Japanese J. Appl. Physics, 3, 436 (1964)

19. C. A. Sperati and H. W. Starkweather, Jr., Fortschr. Hochpolym.-Forsch., 2, 465 (1961)

20. W. Reddish, J. G. Powles and B. I. Hunt, Polymer Letters, 3, 671 (1965).

21. R. K. Eby and K. M. Sinnott, J. Applied Physics, 32, 1765 (1961)

22. N. G. McCrum, Die Makromol. Chemie, 34, 50 (1959)

23. K-H. Illers, Kol. Z., 190, 16 (1963)

24. L. Bohn, Kol. Z., 194, 10 (1964)

25. R. D. Andrews and T. J. Hammack, Poly. Letters, 3, 659 (1965). See also Ref. 1, p. 261.

26. K-H. Illers, Rheol. Acta, 3, 211 (1964)

27. K-H. Illers, personal communication, June, 1967.

28. Personal communication from S. Matsuoka, May, 1967

29. J. L. Zakin and R. Simha. I am indebted to Prof. Simha for sending me this manuscript prior to publication.

30. S. G. Turley, The Dow Chemical Co., unpublished observations

31. M. Takayanagi, T. Aramaki, M. Yoshino and H. Hoashi, J. Poly. Sci., 46, 531 (1960)

32. A. Peterlin and G. Meinel, Polymer Letters, 2, 751 (1964): J. Applied Physics, 35, 3221 (1964)

33. J. A. E. Kail, J. A. Sauer and A. E. Woodward, Polymer, 4, 413 (1963)

34. Reference deleted

35. R. Kitamaru and L. Mandelkern, J.A.C.S., 86, 3529 (1964)

36. H. Nakayasu, H. Markovitz and D. J. Plazek, Trans. Soc. Rheology, 5, 261 (1961)

37. W. Retting, (a) Materialprüf., 5, 101 (1963); (b) Kol. Zeit., 210, 54 (1966); (c) ibid, 213, 69 (1966)

38. H. Oberst, Kunststoffe, 53, 3 (1963)

39. L. Bohn, Kunststoffe, 53, 826 (1963)

40. P. I. Vincent, this conference, lecture No.

41. For a review in English see H. Oberst and A. Schommer, Chap. 29,"Acoustical Fatique in Aerospace Structures," Syracuse University Press, Syracuse, N.Y., 1965, p. 599-616; or by these same authors, Kunststoffe, 55, 2 (1965)

42. L. Bohn, Kunststoffe, 53, 93 (1963)

43. P. Heydemann and H. D. Guicking, Kol. Z., 193, 16 (1964)

44. K. Wolf, Physikertagung, München, Fig. 11, p. 153 (1956)

45. G. M. Martin, S. S. Rogers and L. Mandelkern, J. Poly. Sci., 20, 580 (1956)

46. R. Haldon and R. Simha, this Symposium. The authors kindly supplied me a manuscript prior to publication.

47. J. A. Roetling, Polymer, 6, 311 (1965)

48. Ibid, ___, 619

49. J. R. McLoughlin and A. V. Tobolsky, J. Poly. Sci., 7, 658 (1951)

50. E. L. Morris and N. G. McCrum, Poly. Letters, 1, 393 (1963)

51. B. Maxwell and J. Harrington, Trans. Am. Soc. Mech. Engrs., 74, 2579 (1952)

52. J. Heijboer, in "Physics of Non-Crystalline Solids," North Holland Publishing Co., Amsterdam, 1965, p. 237 ff.

53. J. Heijboer, Kol. Zeit. 148, 36 (1956); 171, 7 (1960)

54. P. I. Vincent, Polymer, 1, 425 (1960), esp. page 431.

55. Ref. 1, page 267 ff. This reviews most of the literature data.

56. K. Schmieder and K. Wolf, Kol. Zeit., 134, 149 (1953) Fig. 3 and Fig. 8.

57. K-H. Illers, Z. Elektrochemie, 65, 679 (1961)

58. A. E. Woodward, Ref. 1, p. 89 ff.

59. Ref. 4, p. 174.

60. S. G. Turley, J. Poly. Sci. C 1, 101 (1963)

61. B. Wunderlich and D. M. Bodily, J. Poly. Science, C, 6, 137 (196), specif. Fig. 8.

62. J. T. Seitz and C. F. Balˆasz, SPE reprints, Vol. 13, p. 963, May, 1967

63. S. G. Turley, private communication.

64. R. S. Colborne, J. Macromolecular Science (Physics), In press.

65. J. L. Duda and J. S. Vrentas, J. Poly. Science, A-2, p. 202, In press.

66. D. J. Plazek, Wayne University lecture, May 1967. Dr. Plazek's permission to use this data is gratefully acknowledged.

67. H. J. Donald, The Dow Chemical Company, Midland, Mich.

68. V. R. Allen and T. G. Fox, J. Chem. Physics, 41, 337 (1964). Especially, Fig. 1.

69. Rheology, F. R. Eirich, Editor, Academic Press, New York, 1956, Vol. 1, Chapter 12, by T. G. Fox, S. Gratch and S. Loshaek, particularly Fig. 9.

EXAMPLES OF MULTIPLE TRANSITIONS IN POLYMERS

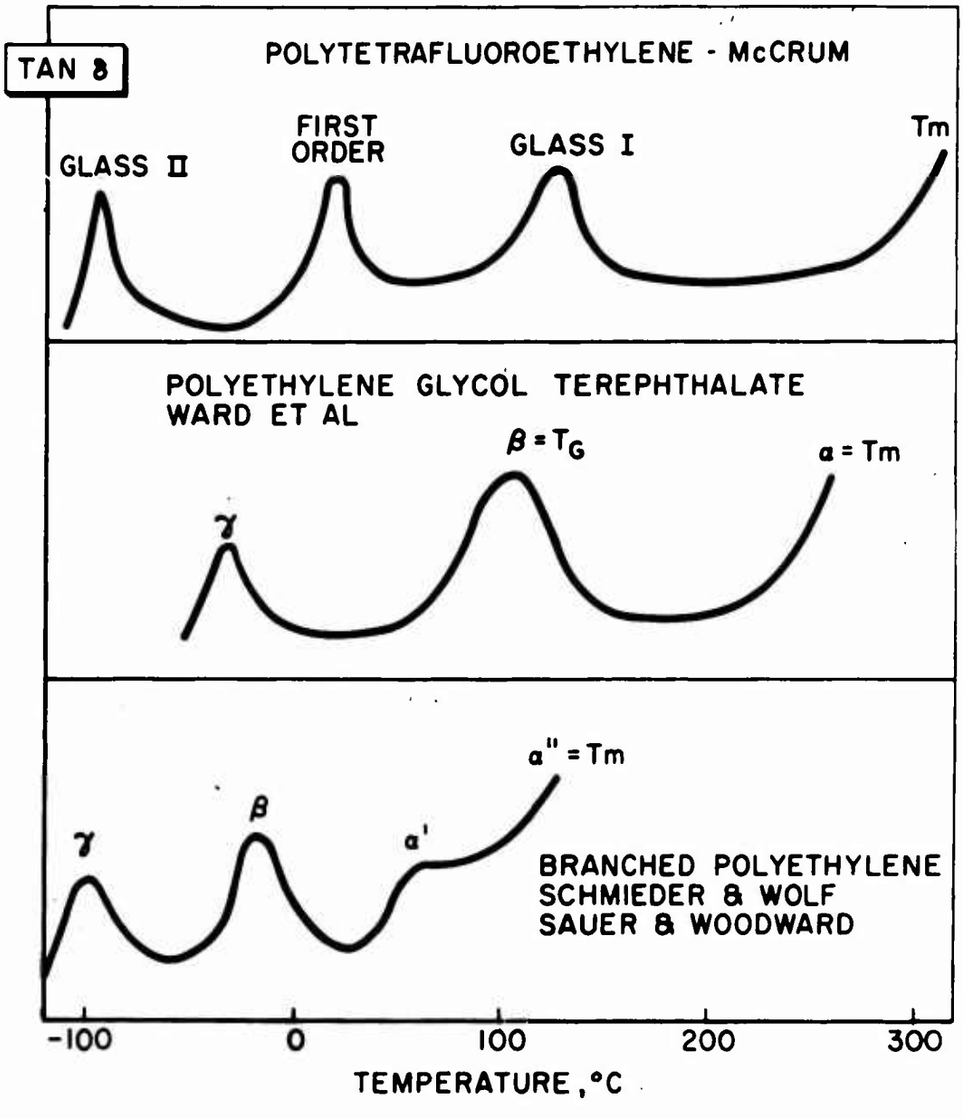

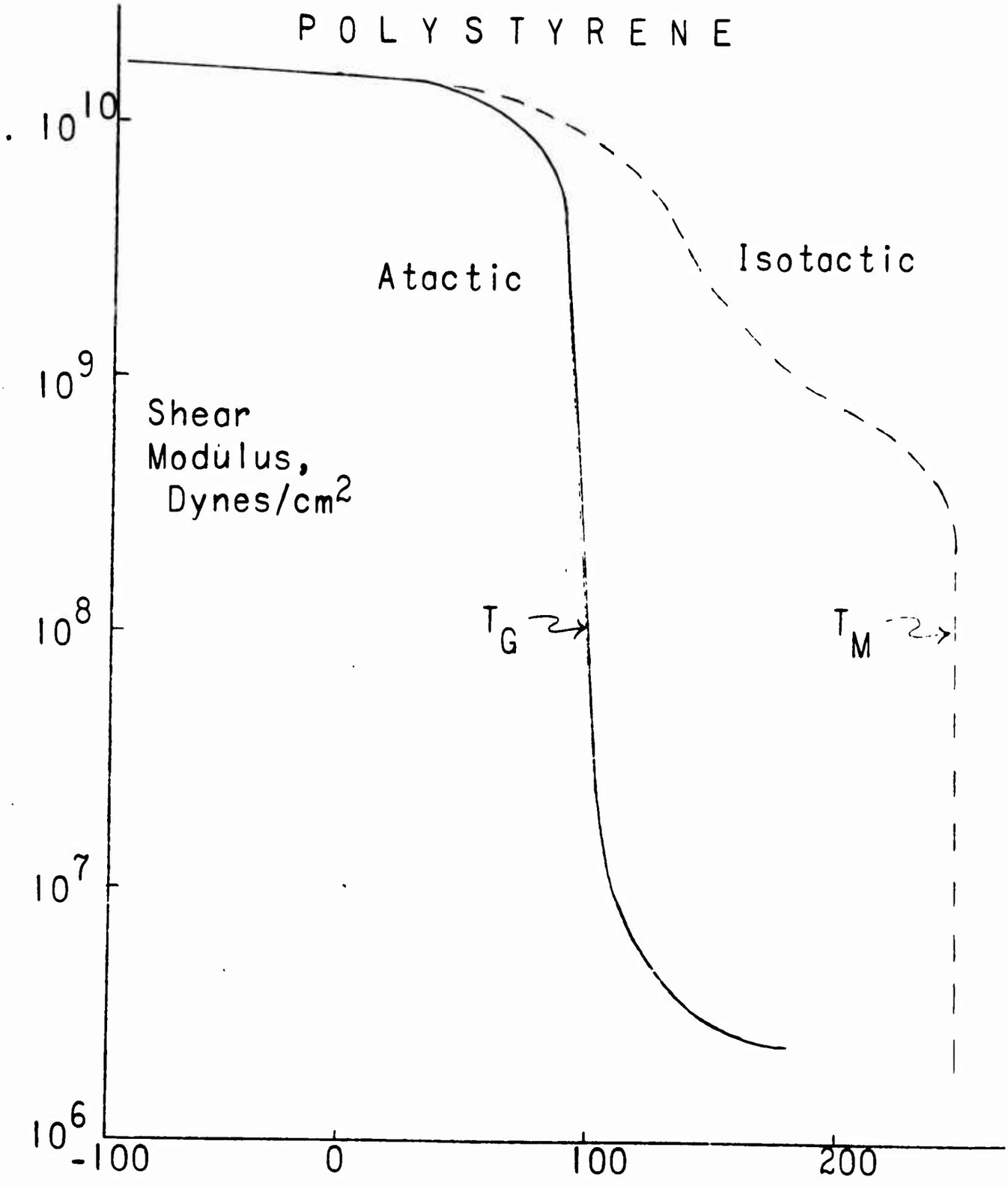
POLYSTYRENE
10^{10}
10^{9}
10^{8}
10^{7}
10^{6}
Shear
Modulus,
Dynes/cm^2
Atactic
Isotactic
T_G
T_M
-100
0
100
200

DYNAMIC MECHANICAL PROPERTIES OF POLYCARBONATE

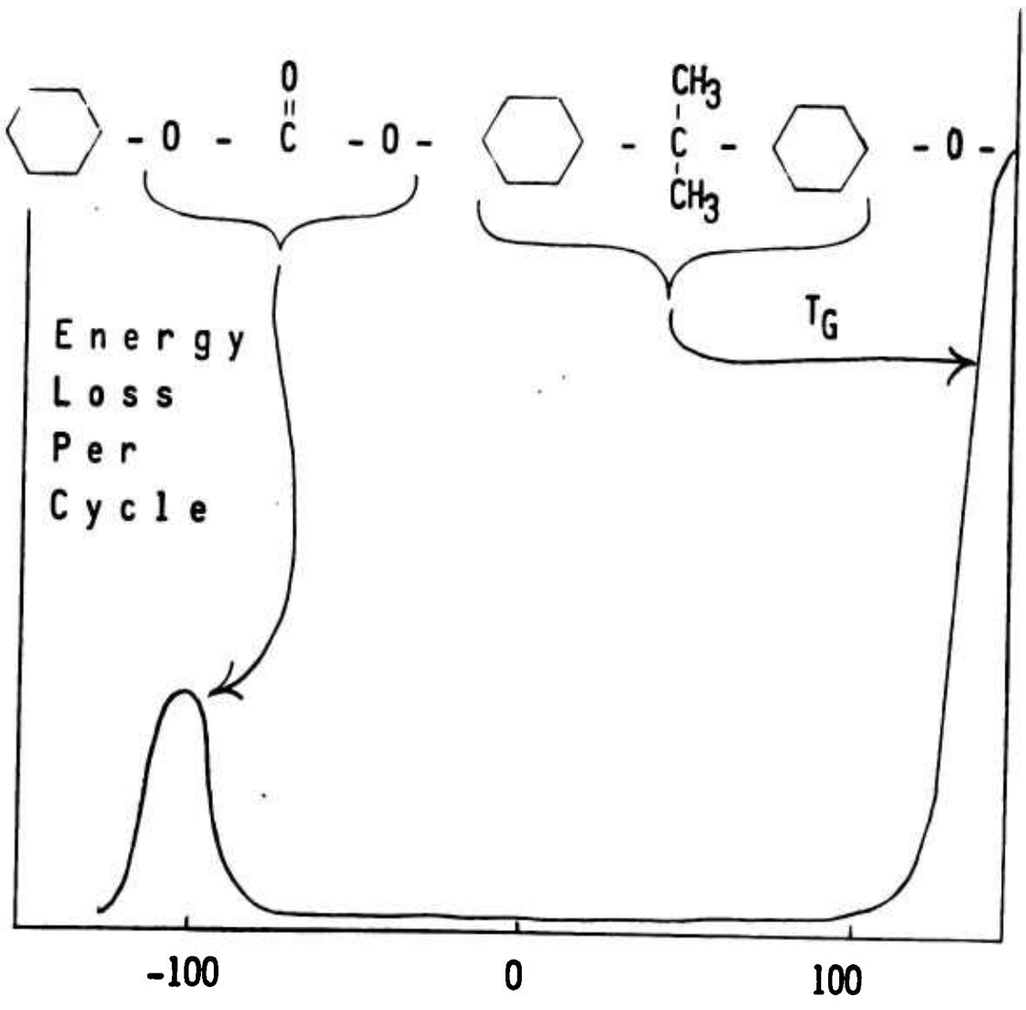

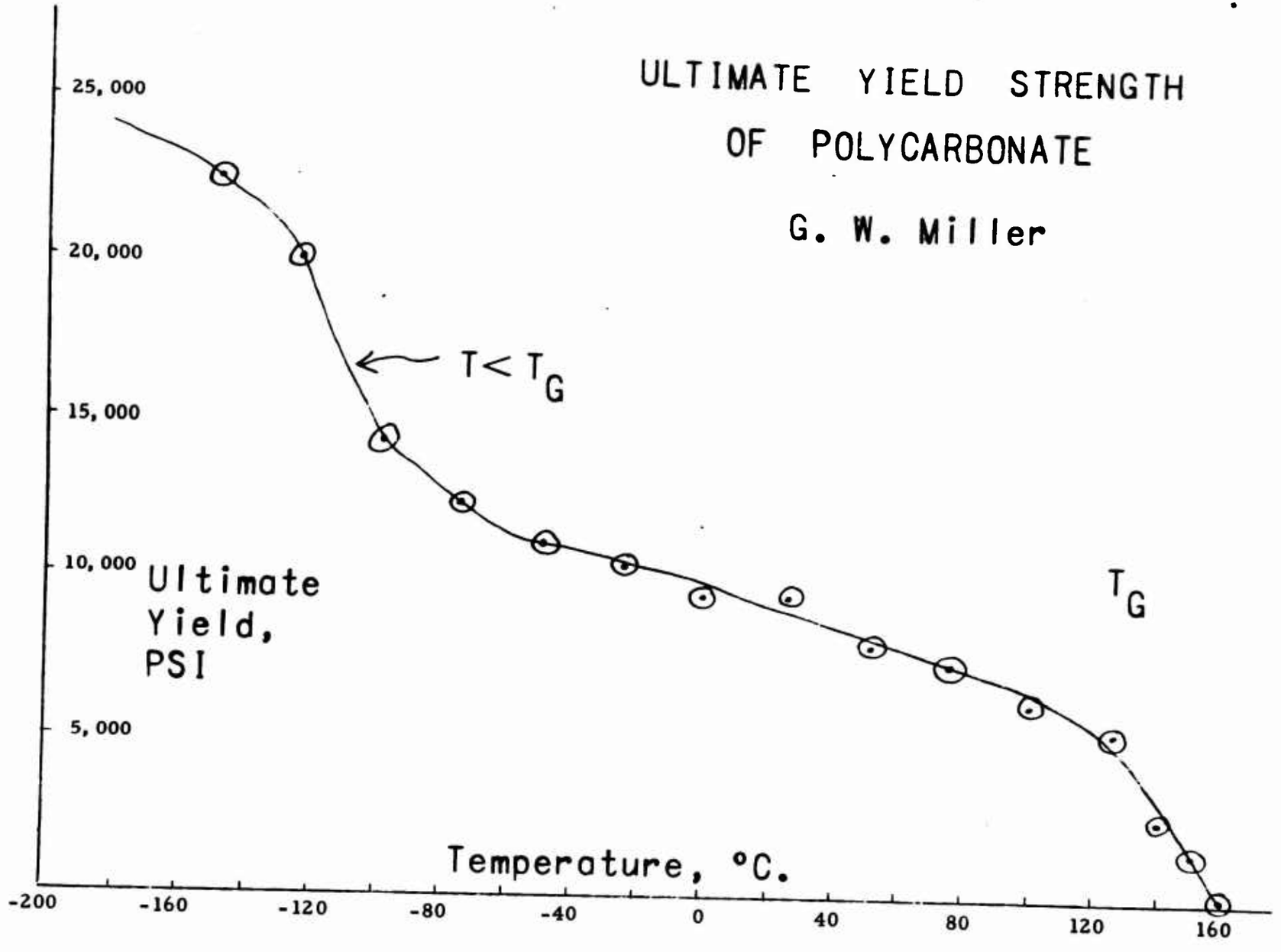
ULTIMATE YIELD STRENGTH
OF POLYCARBONATE
G. W. Miller
25,000
20,000
15,000
10,000
5,000
Ultimate
Yield,
PSI
T< T_G
T_G
Temperature, °C.
-200
-160
-120
-80
-40
0
40
80
120
160

MULTIPLE TRANSITIONS IN POLYCARBONATE

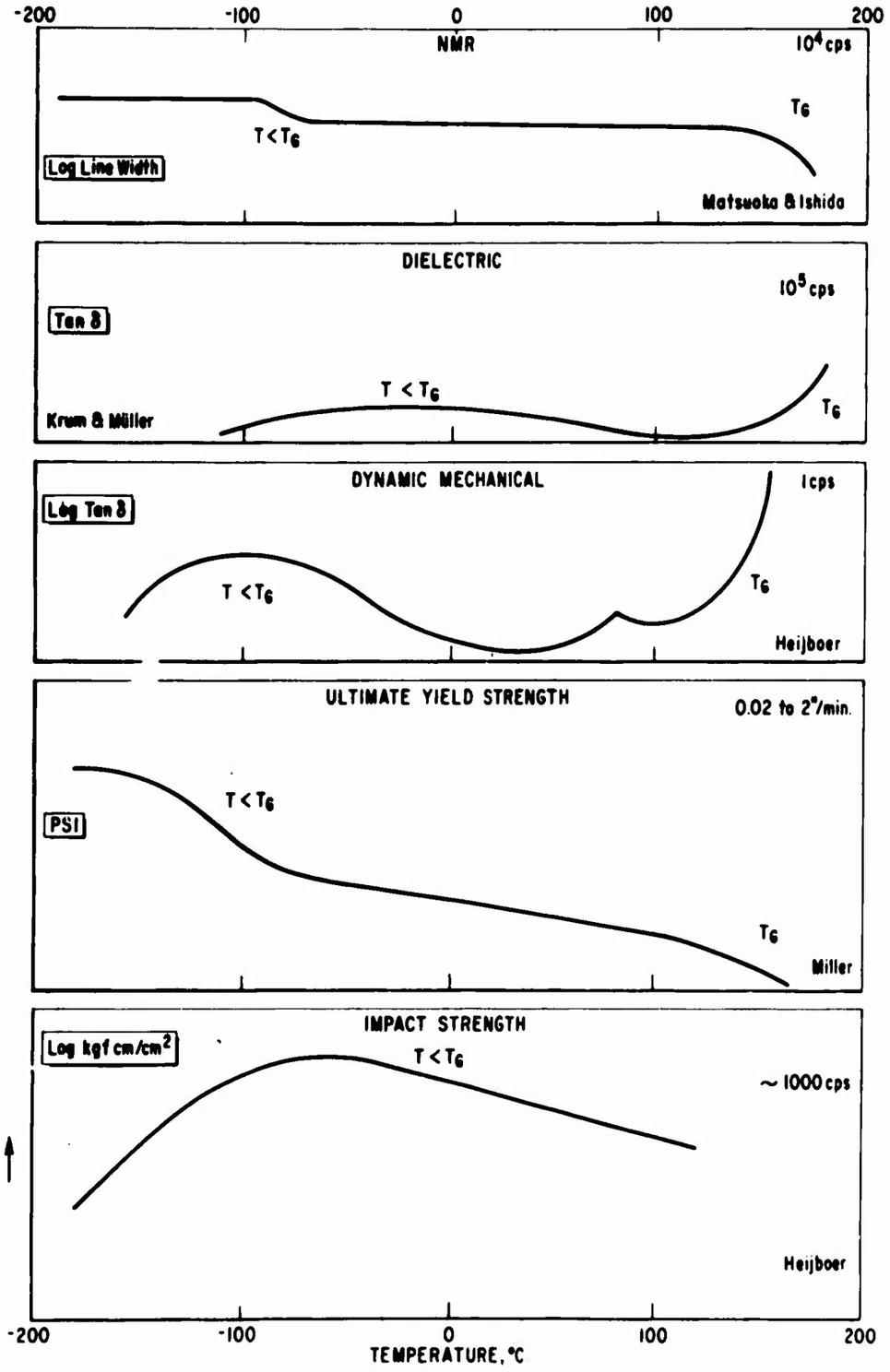

POLYTETRAFLUOROETHYLENE

VARIATION OF DYNAMIC

MODULUS WITH TEMPERATURE

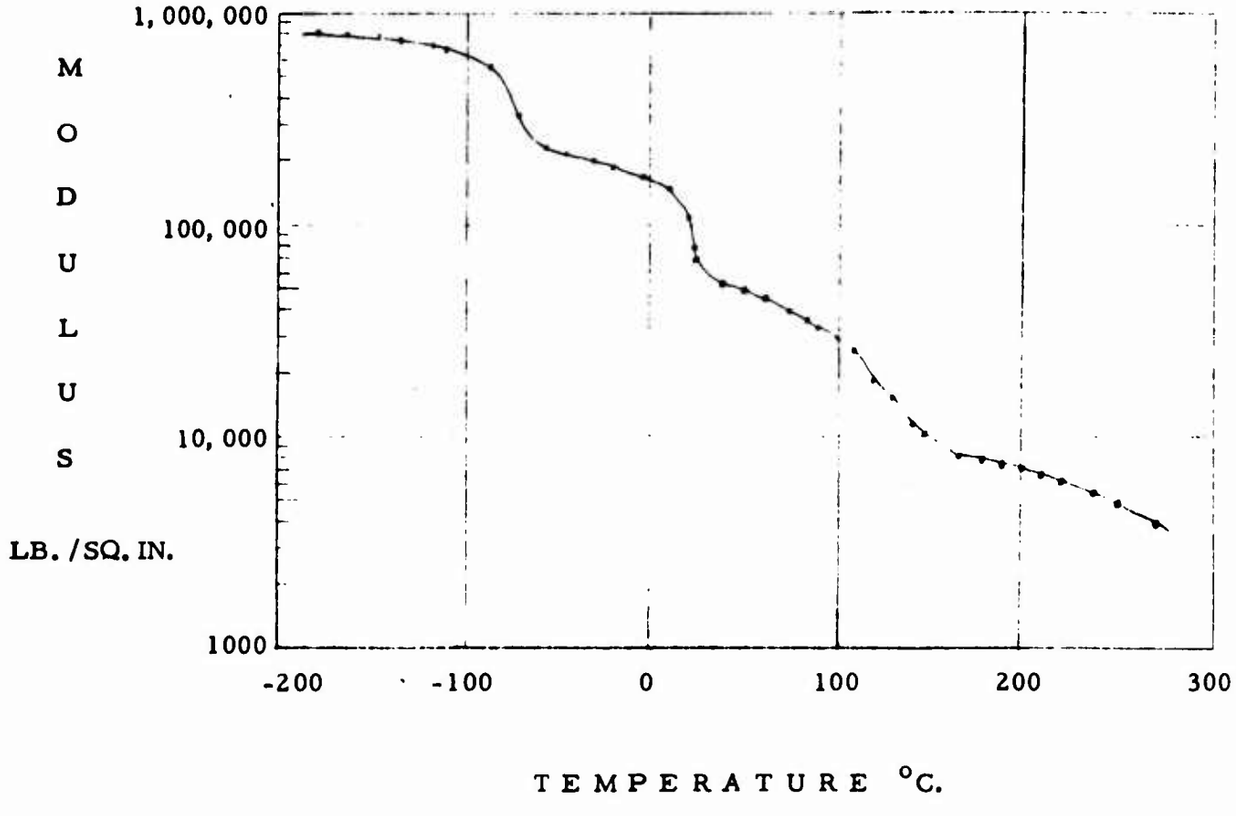

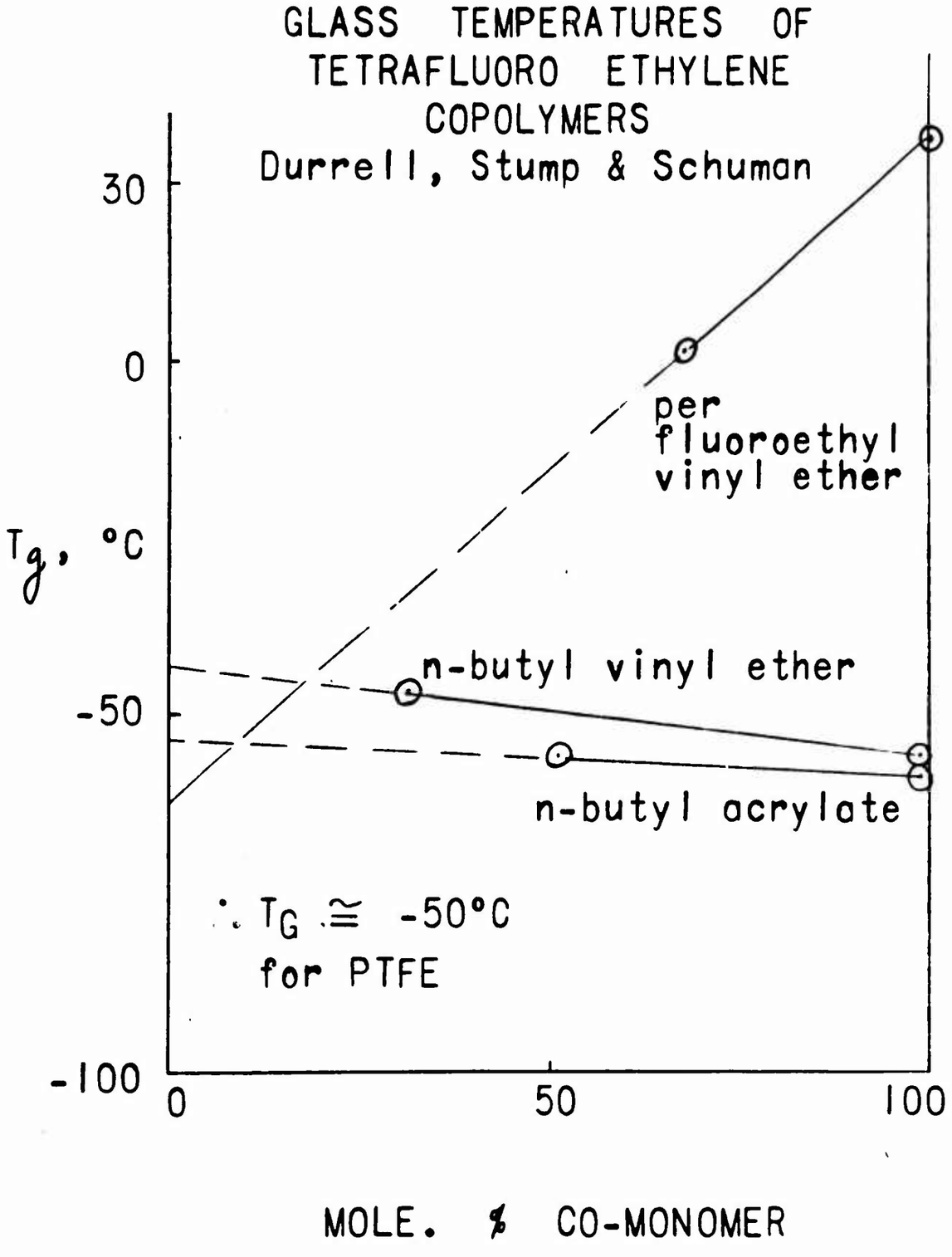
GLASS TEMPERATURES OF
TETRAFLUORO ETHYLENE
COPOLYMERS
Durrell, Stump & Schuman
30
0
-50
-100
T_g, °C
per
fluoroethyl
vinyl ether
n-butyl vinyl ether
n-butyl acrylate
$\therefore T_G \cong -50°C$
for PTFE
0
50
100
MOLE. % CO-MONOMER

IMPACT STRENGTH OF PTFE

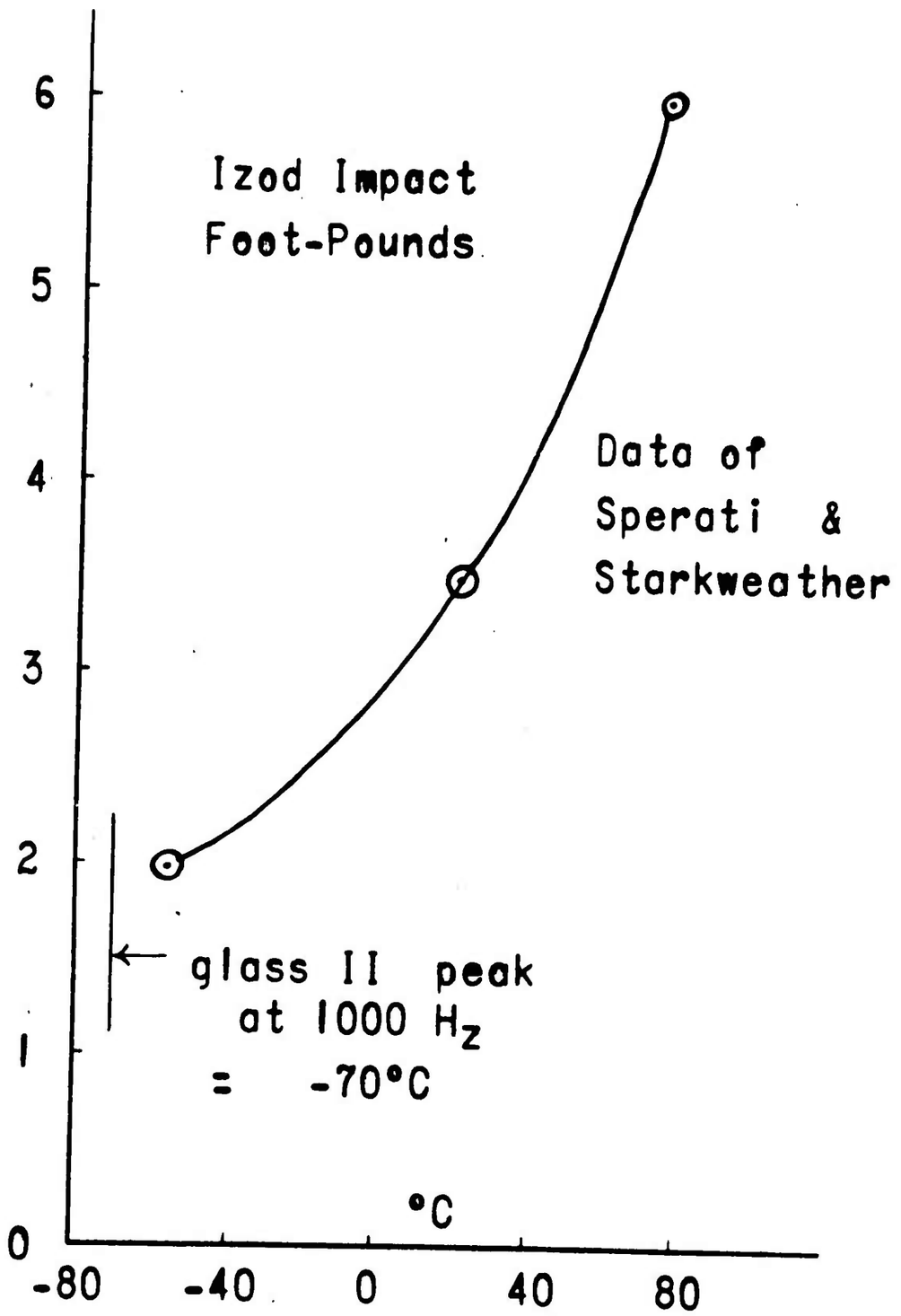

TRANSITIONS IN ETHYLENE-PROPYLENE COPOLYMERS

(Schematic)

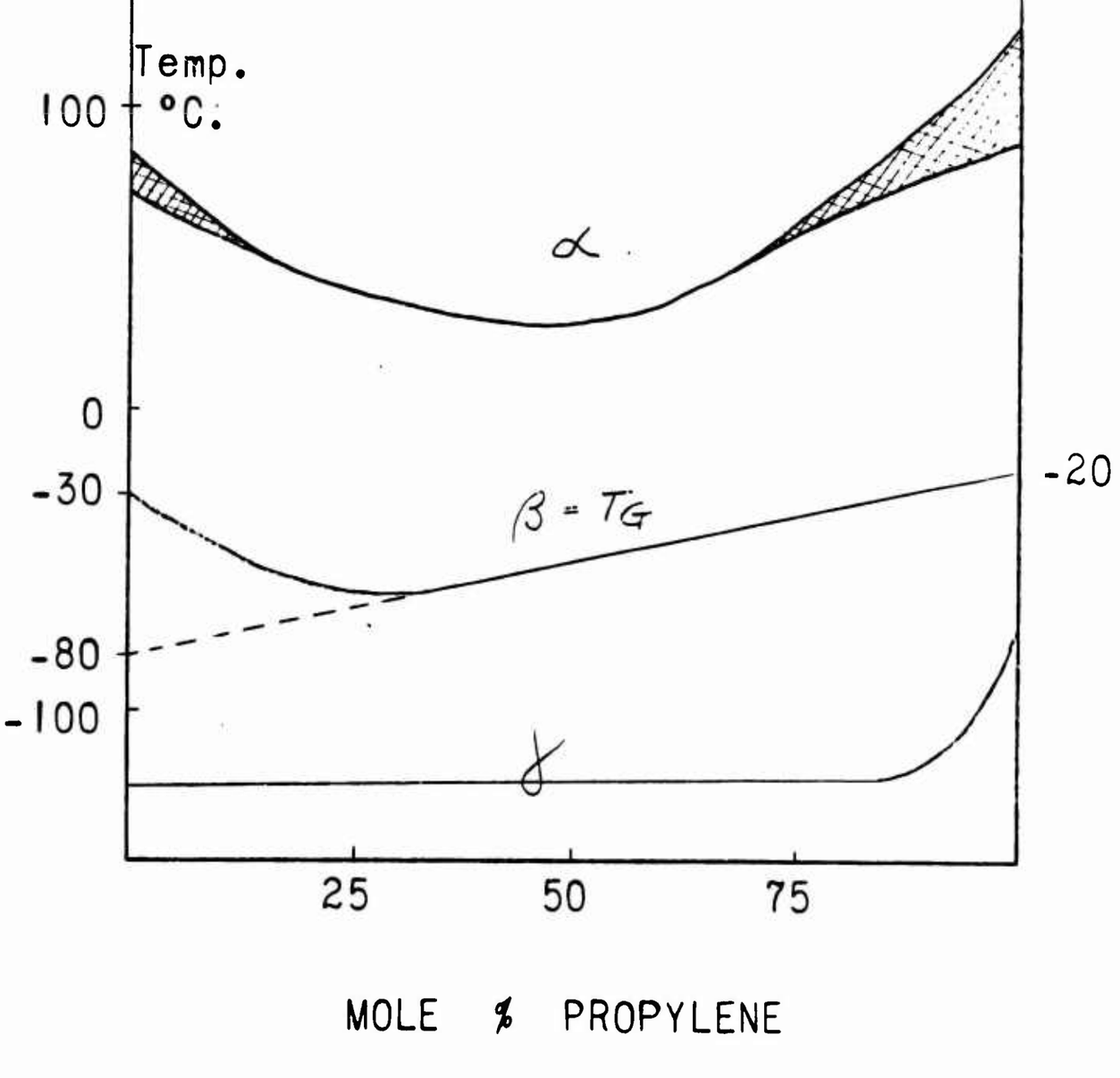

Dart Drop Impact of High Density (0.955) Polyethylene (Data of S. G. Turley)

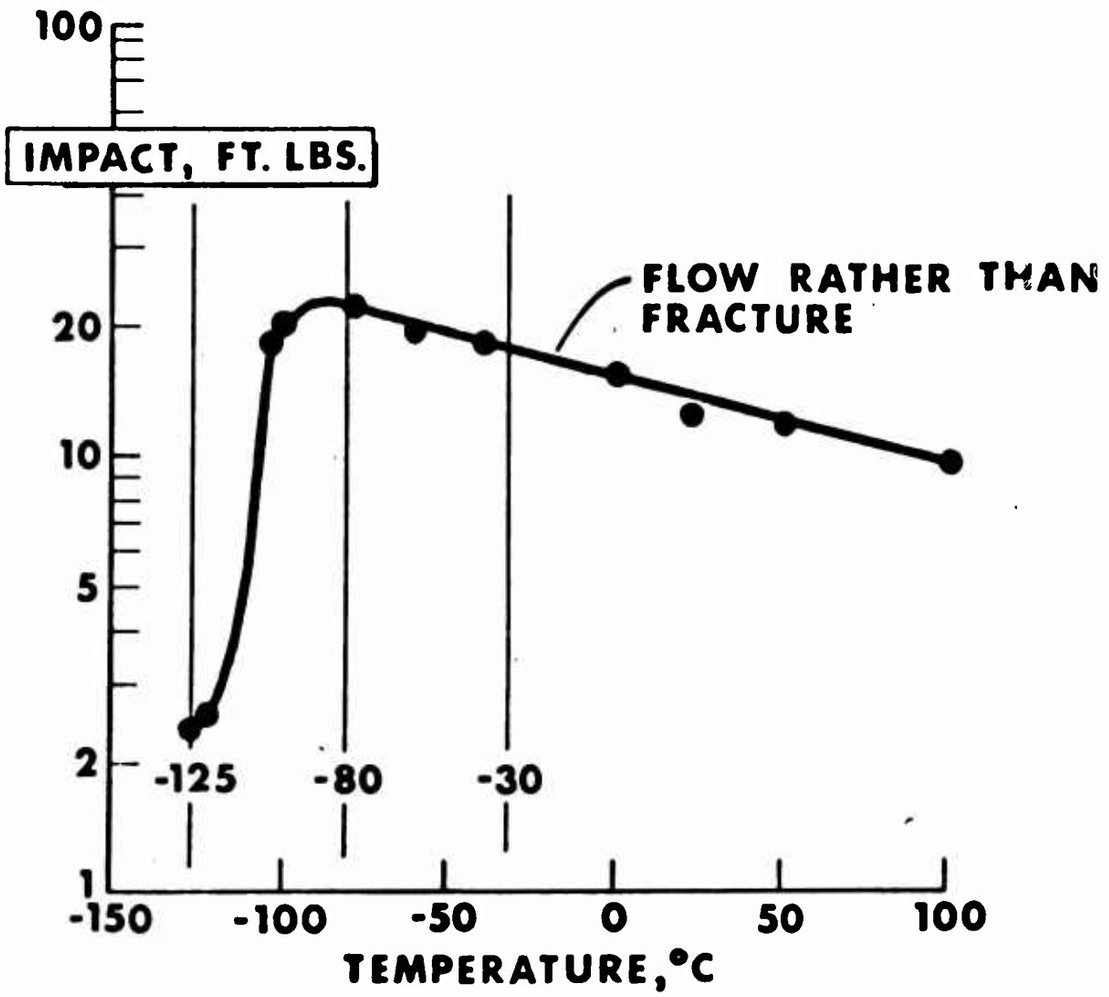

THE α TRANSITION

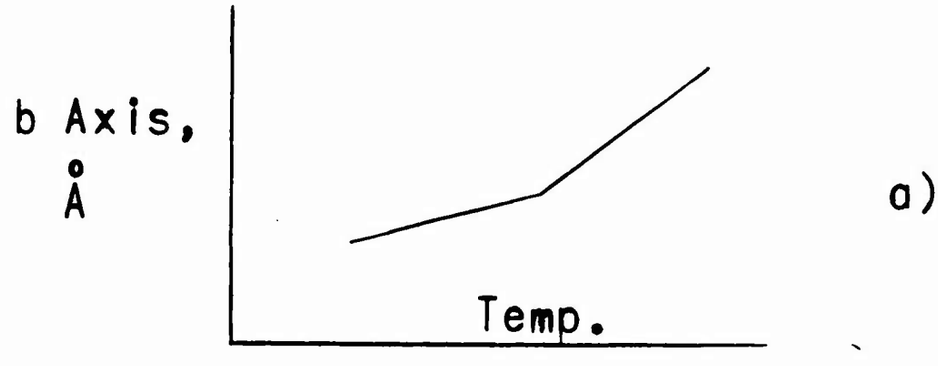

a)

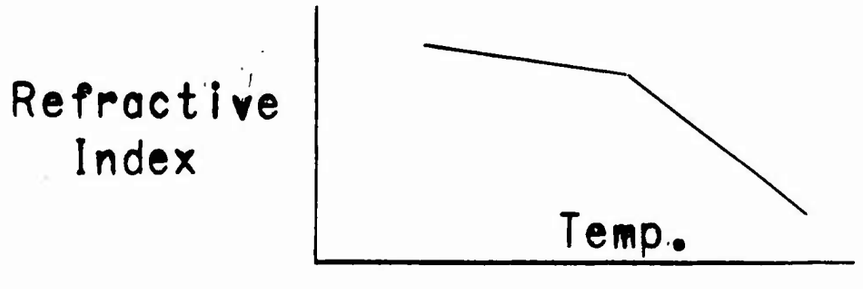

b)

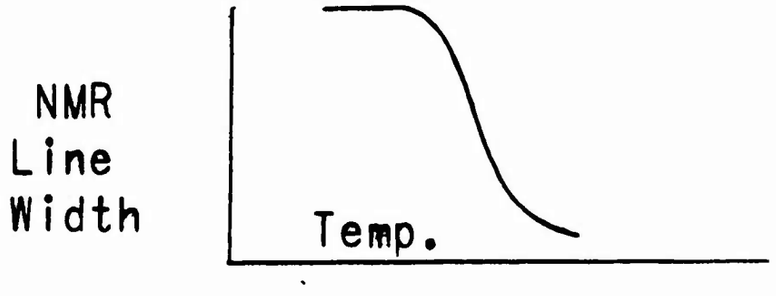

c)

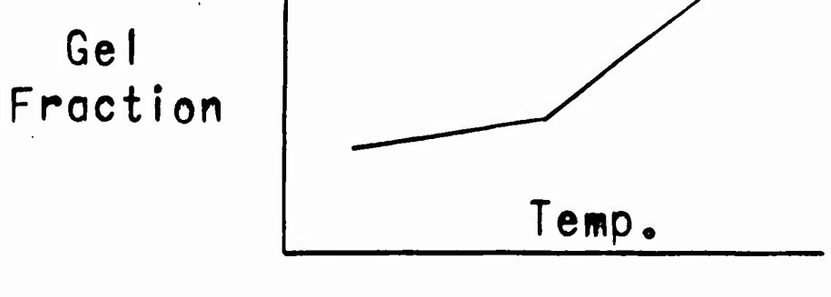

d)

P V C

H. Oberst

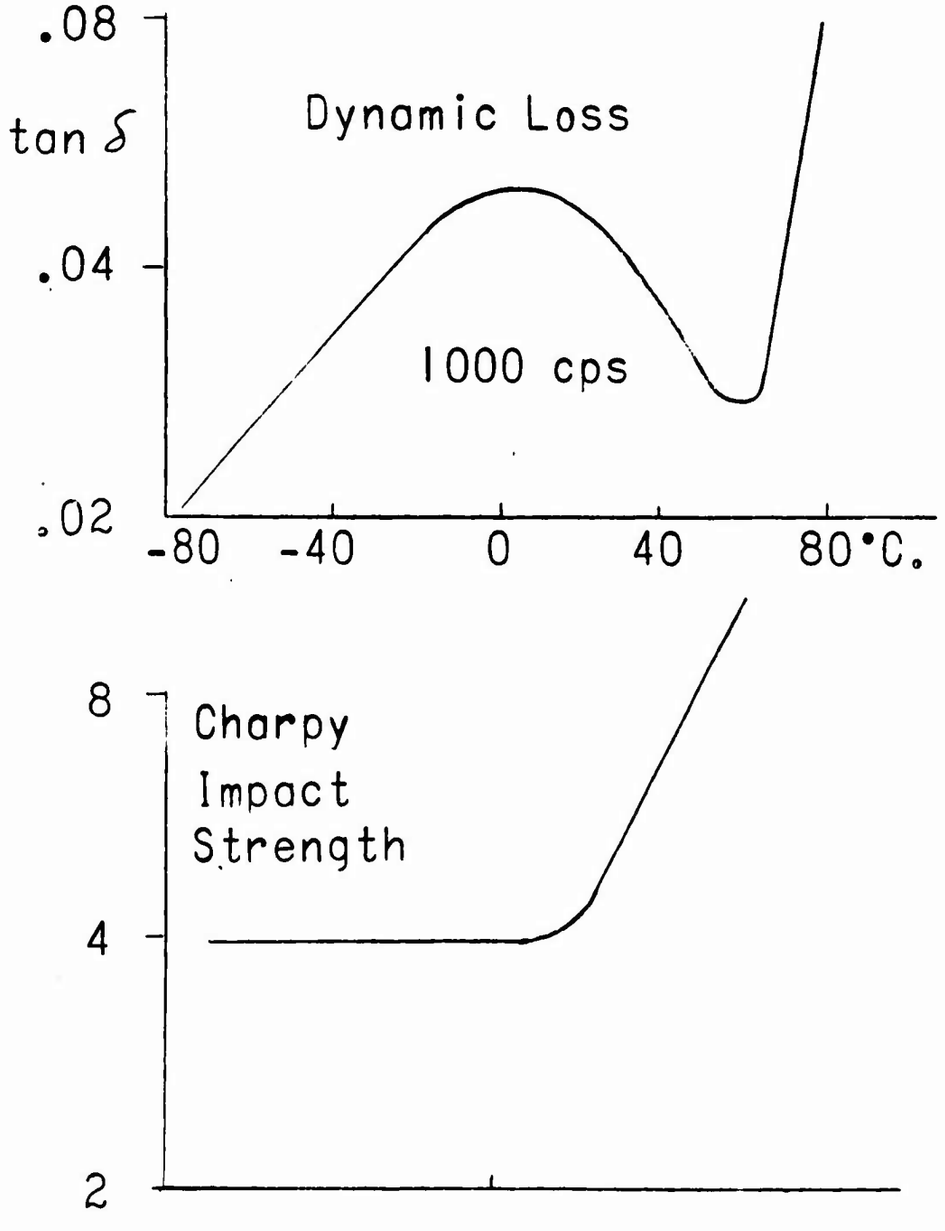
.08
tan δ
.04
.02
Dynamic Loss
1000 cps
-80
-40
0
40
80°C.
8
Charpy
Impact
Strength
4
2

PLASTICIZED PVC

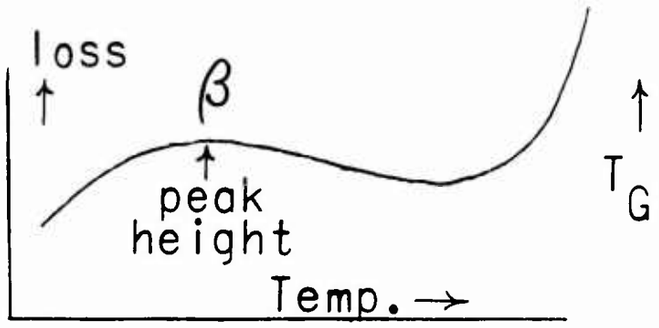

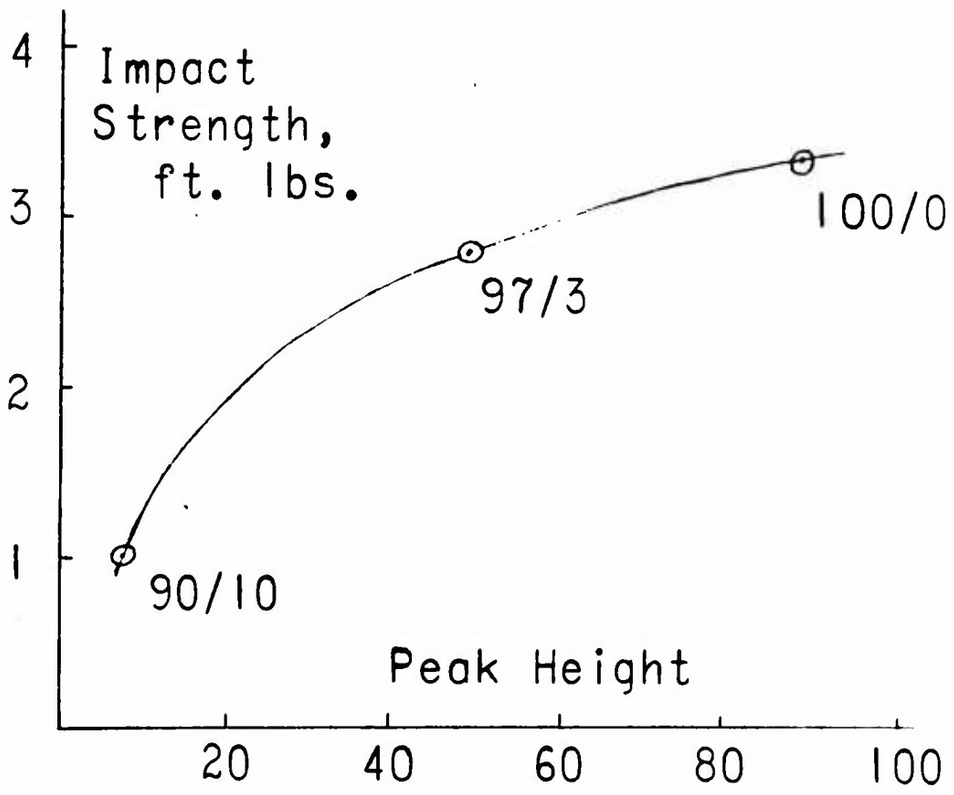

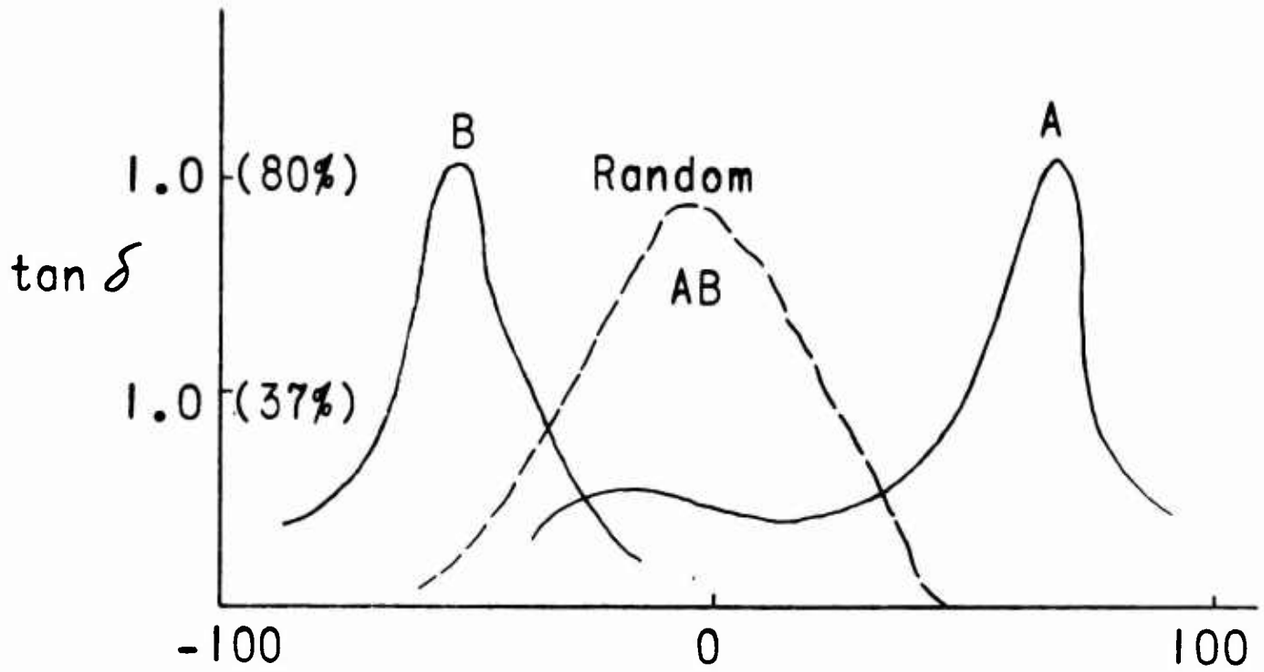
B
A
1.0 (80%)
Random
tan δ
AB
1.0 (37%)
-100
0
100

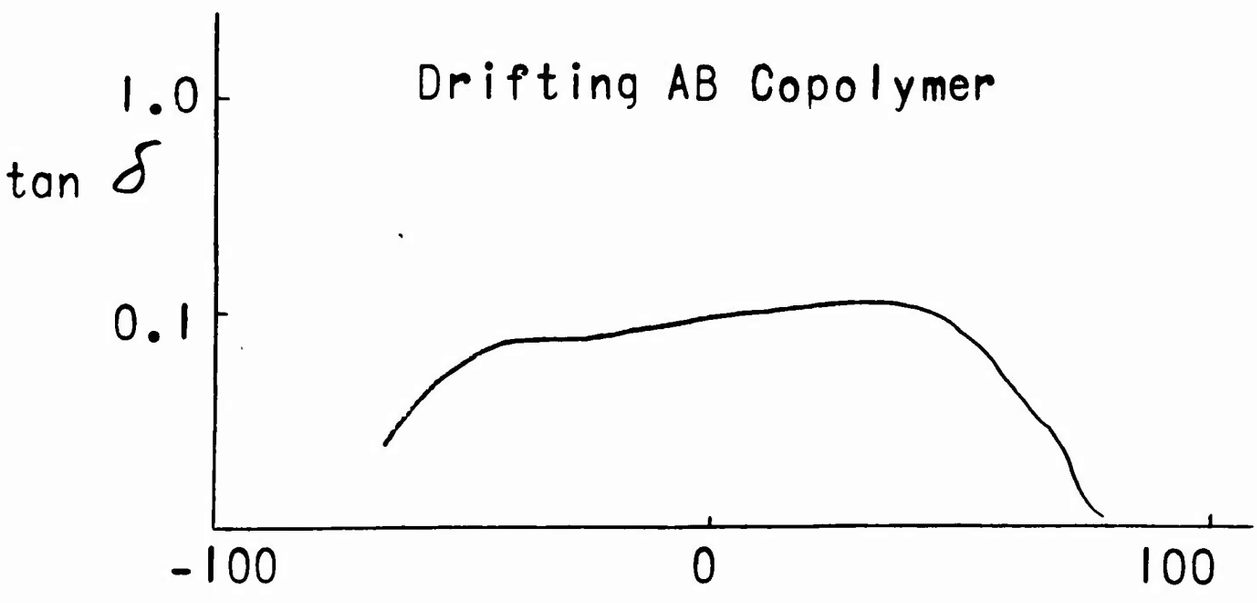
Drifting AB Copolymer
1.0
tan δ
0.1
-100
0
100

LOSS IN PMMA AT 1 CYCLE / SECOND

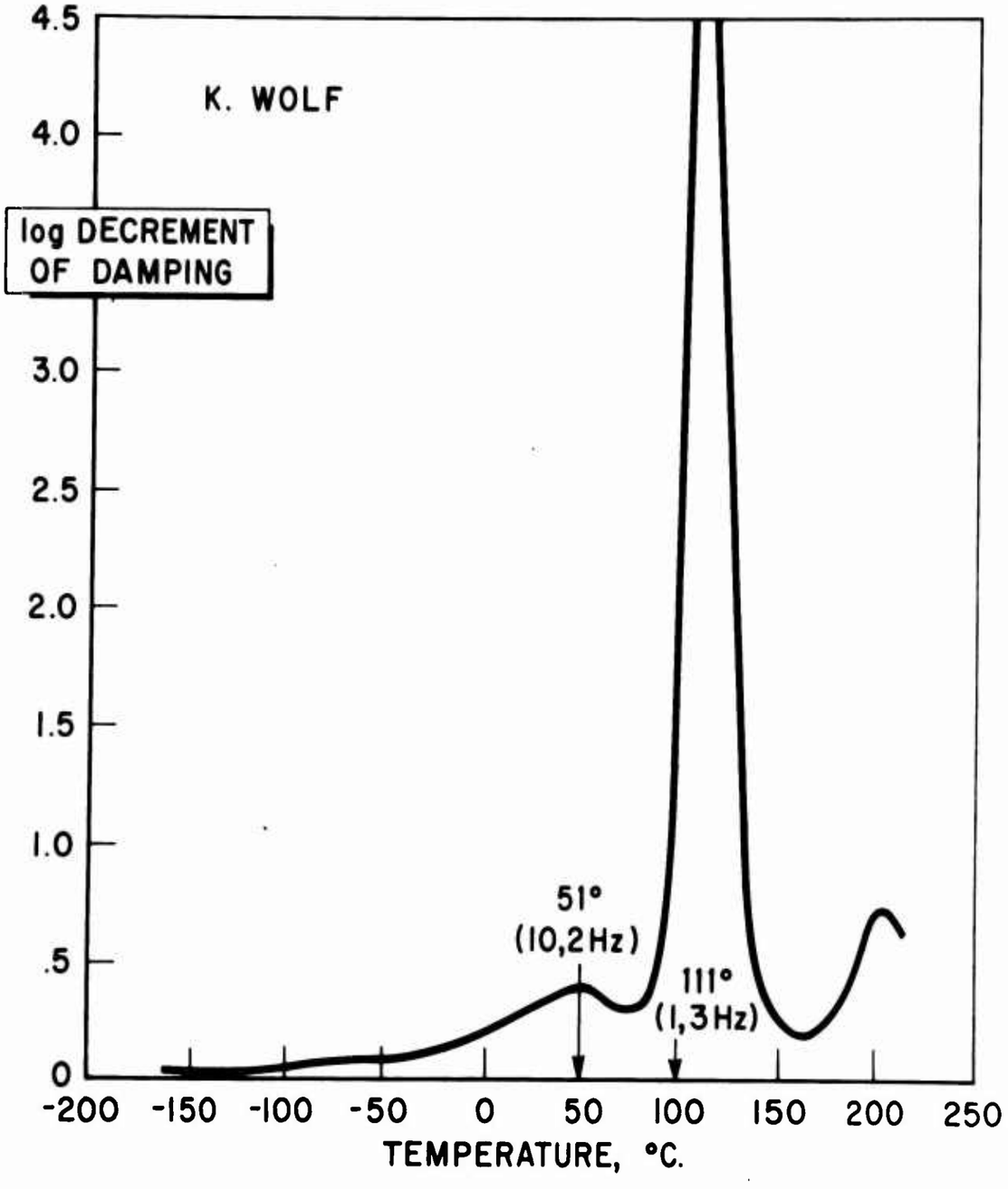

PMMA

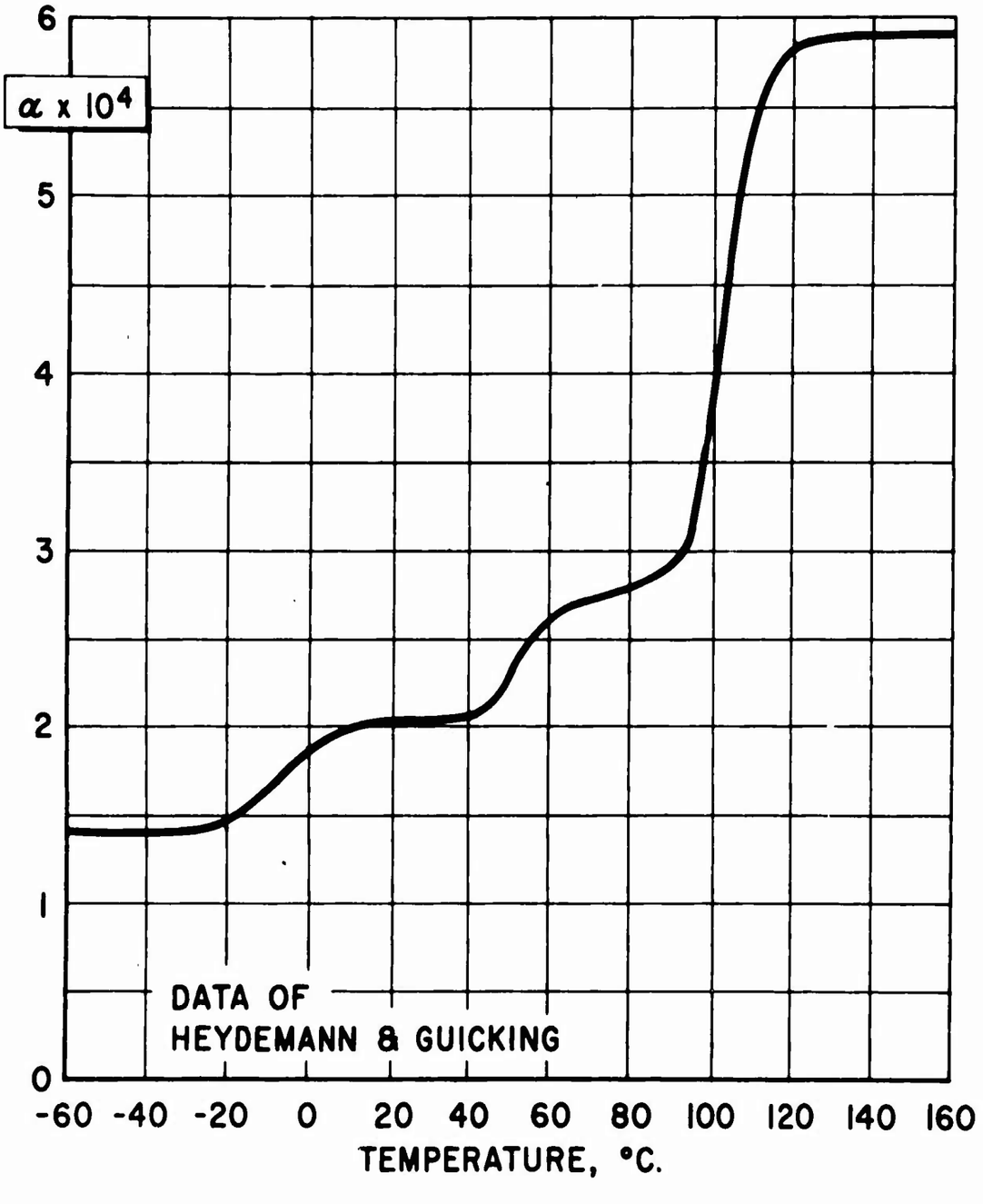
α x 10⁴
6
5
4
3
2
1
0
DATA OF
HEYDEMANN & GUICKING
-60 -40 -20 0 20 40 60 80 100 120 140 160
TEMPERATURE, °C.

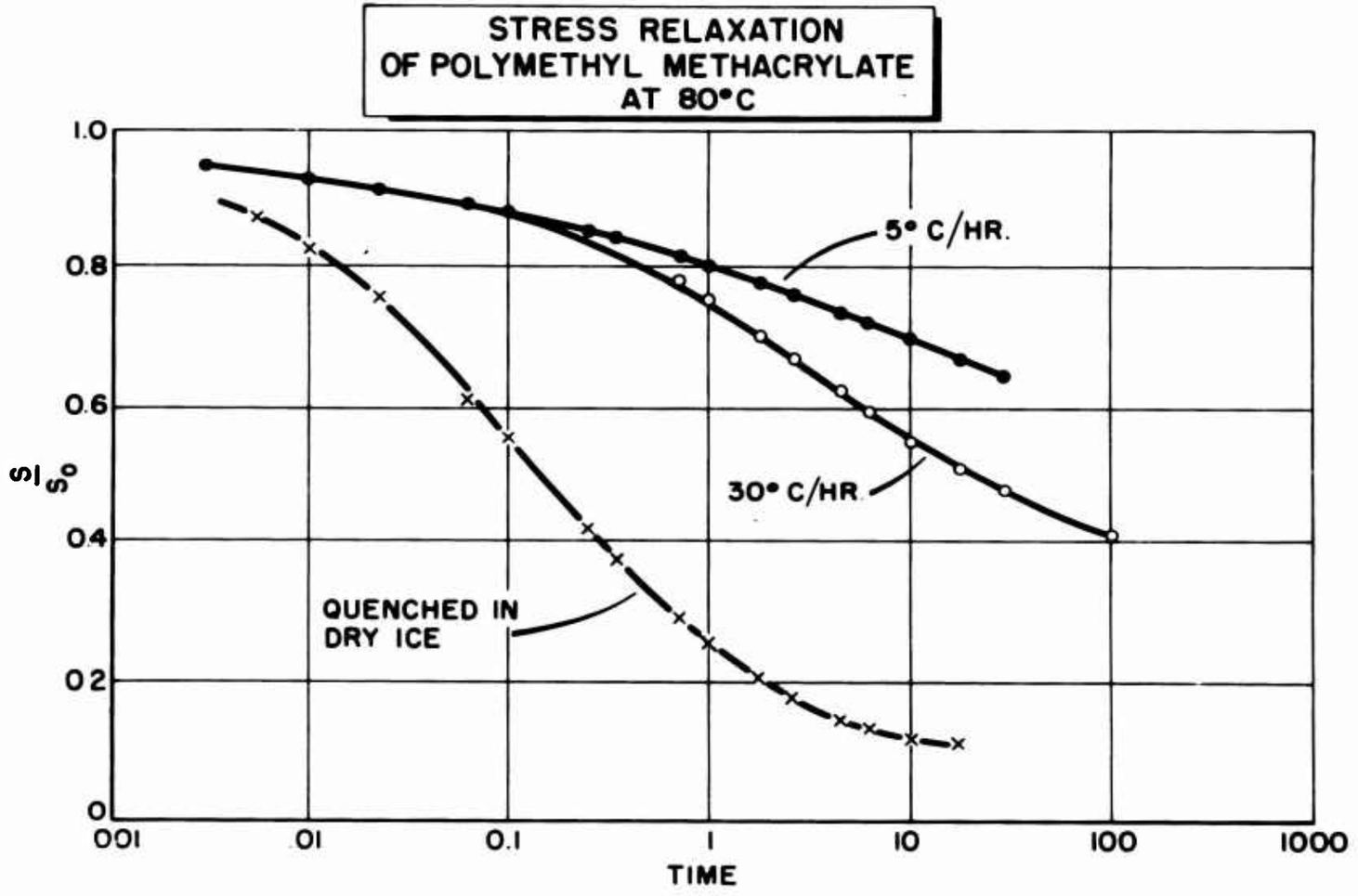
STRESS RELAXATION
OF POLYMETHYL METHACRYLATE
AT 80°C
1.0
0.8
0.6
0.4
02
0
S/S0
5° C/HR.
30° C/HR
QUENCHED IN
DRY ICE
001
01
0.1
1
10
100
1000
TIME

PMMA

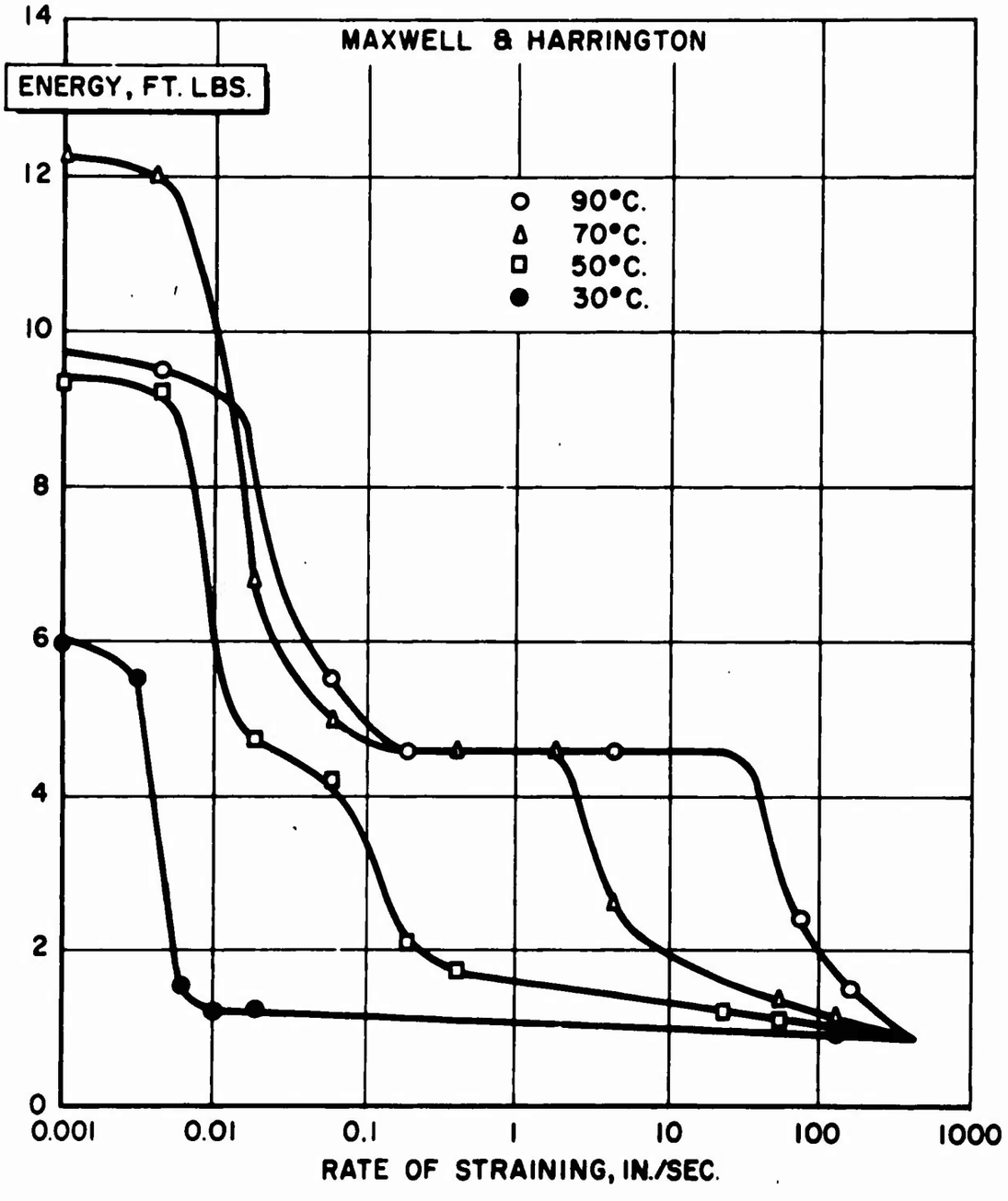
MAXWELL & HARRINGTON
ENERGY, FT. LBS.
90°C.
70°C.
50°C.
30°C.
14
12
10
8
6
4
2
0
0.001
0.01
0.1
1
10
100
1000
RATE OF STRAINING, IN./SEC.

POLYPHENYLENE OXIDE

Heijboer

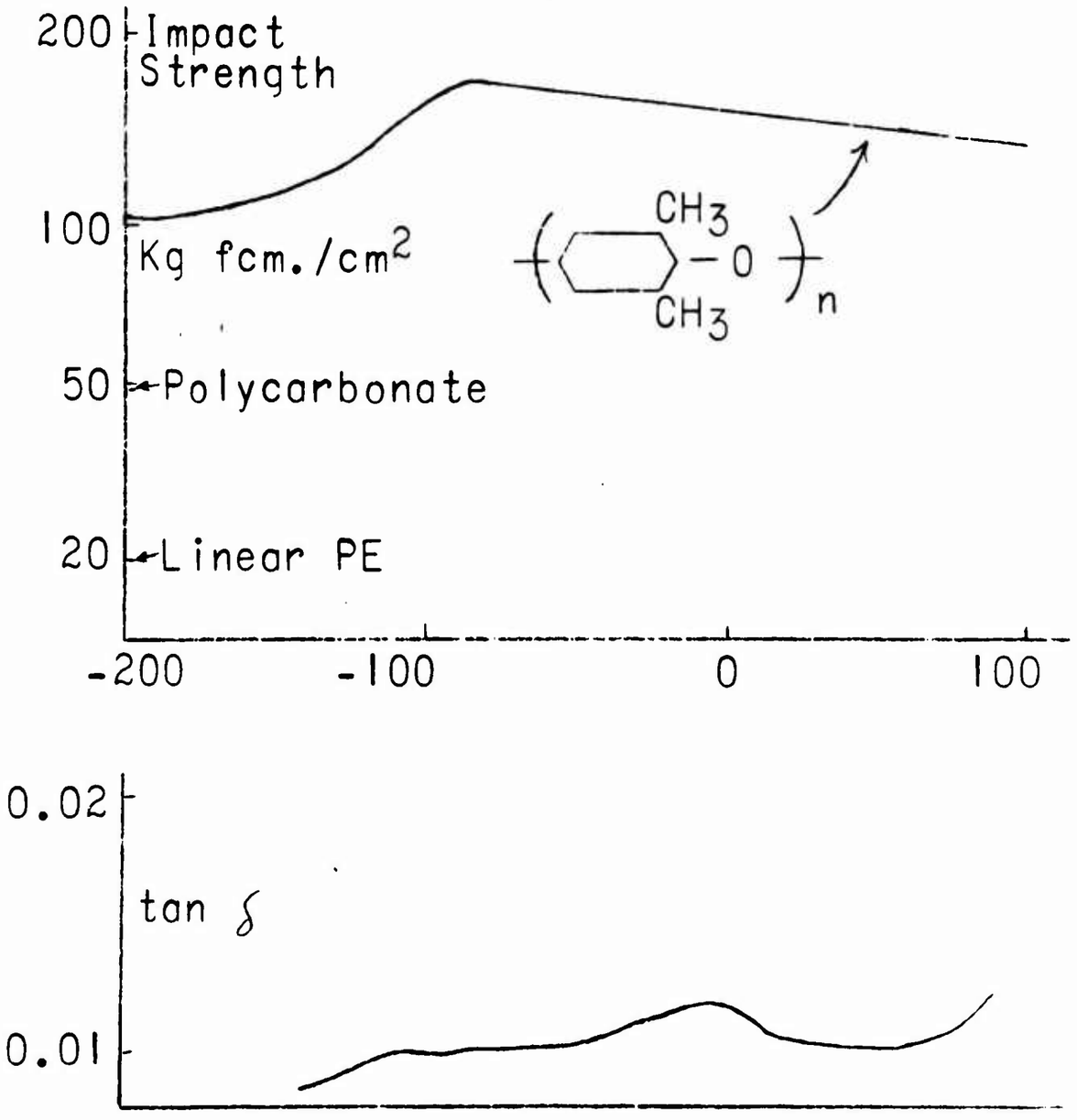

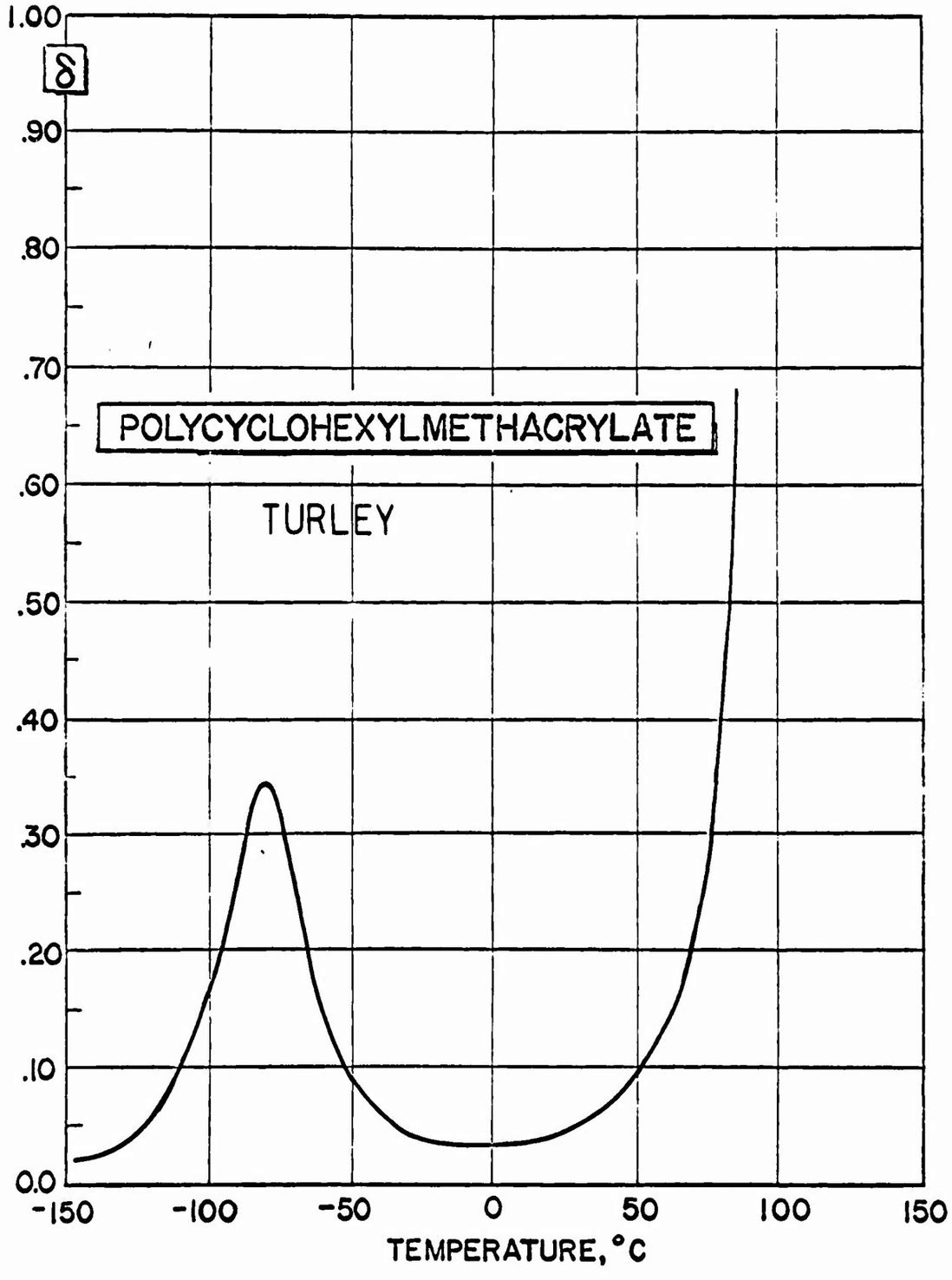
1.00
δ
.90
.80
.70
POLYCYCLOHEXYLMETHACRYLATE
.60
TURLEY
.50
.40
.30
.20
.10
0.0
-150
-100
-50
0
50
100
150
TEMPERATURE, °C

CREEP DATA ON POLYSTYRENE - SCHEMATIC

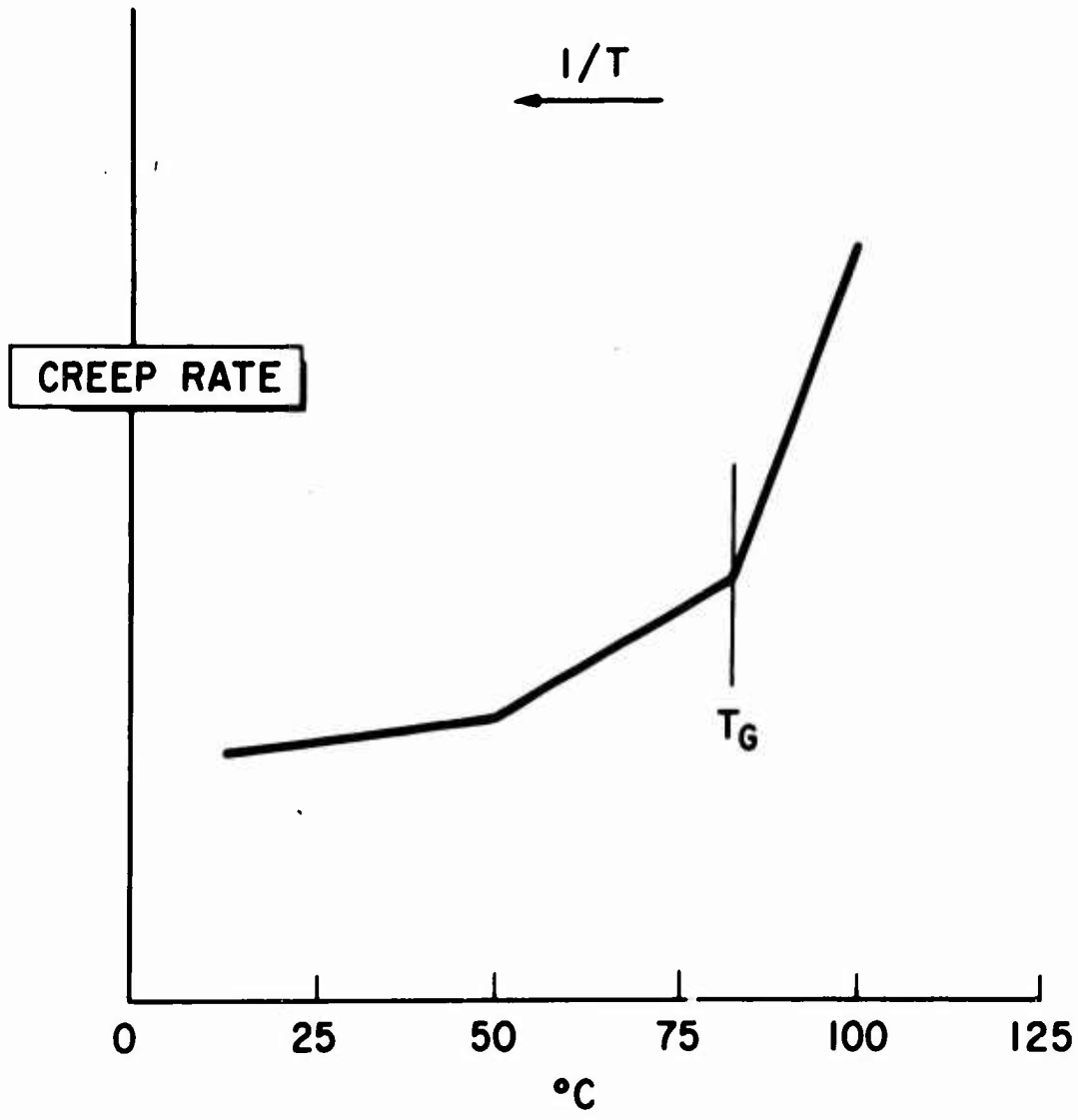

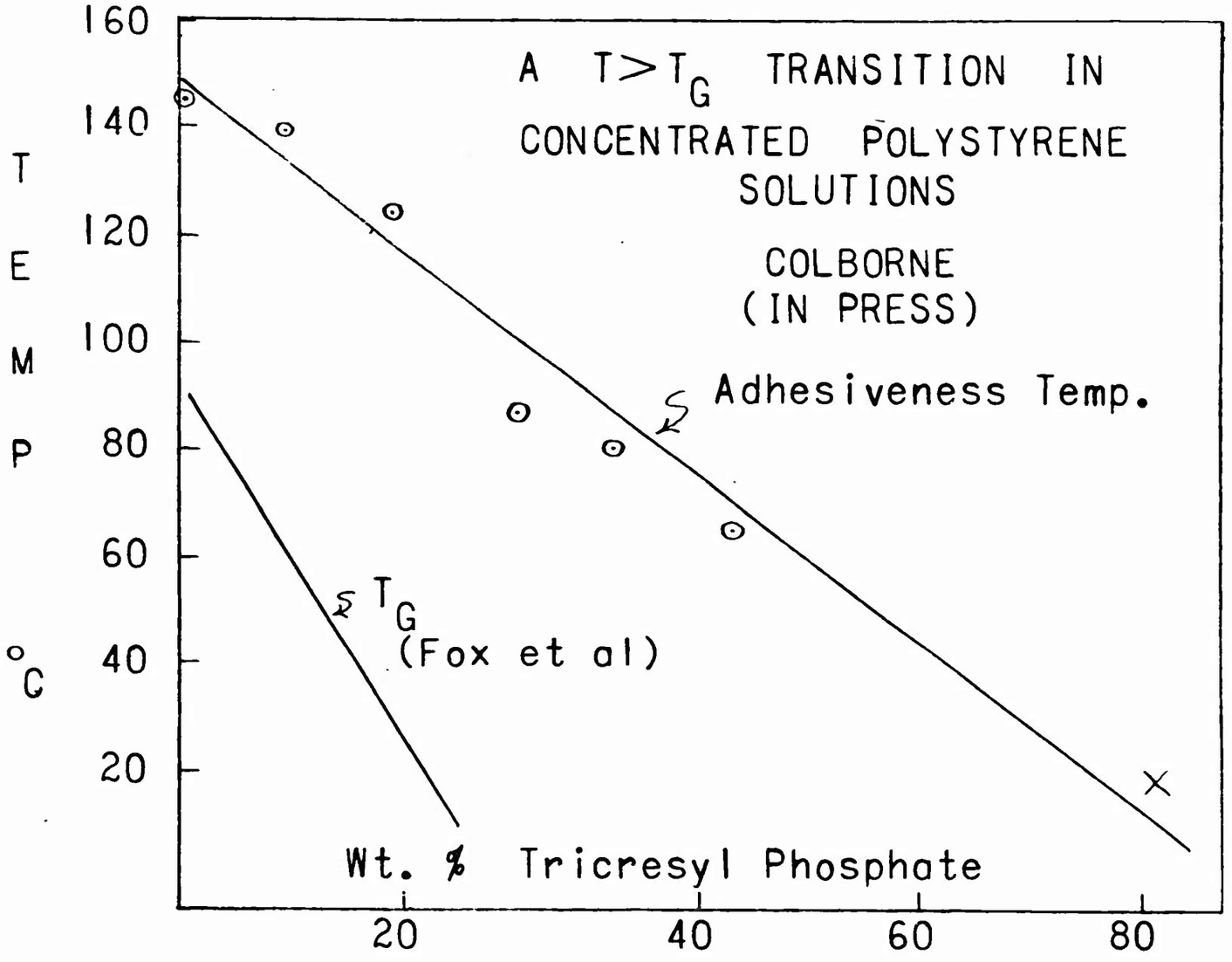
A T>T_G TRANSITION IN
CONCENTRATED POLYSTYRENE
SOLUTIONS
COLBORNE
(IN PRESS)
Adhesiveness Temp.
T_G
(Fox et al)
TEMP °C
160
140
120
100
80
60
40
20
Wt. % Tricresyl Phosphate
20
40
60
80

DIFFUSION OF n-PENTANE IN POLYSTYRENE

Data by Duda

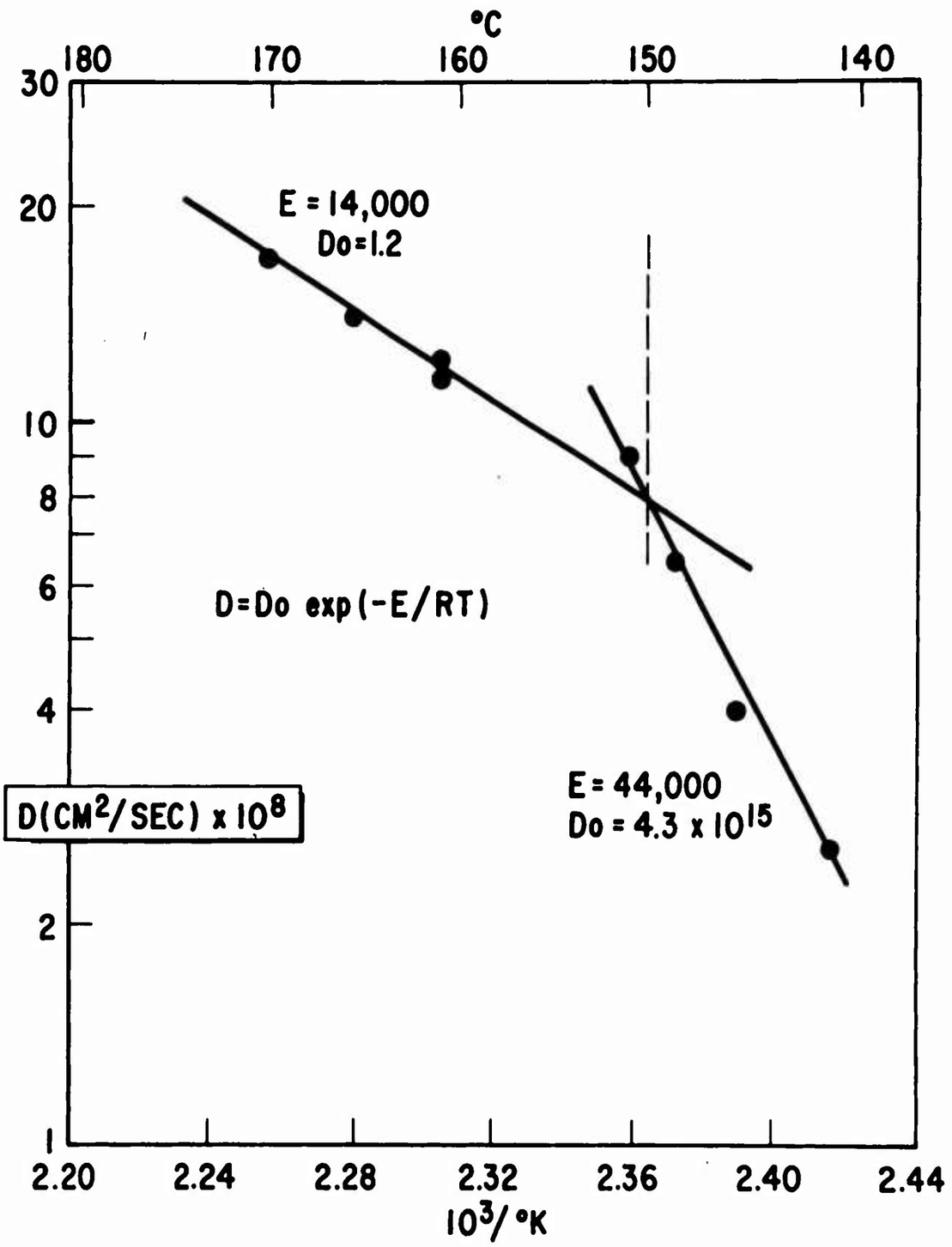

MELT VISCOSITY OF POLYSTYRENE
SCHEMATIC BASED
ON DATA OF PLAŻEK

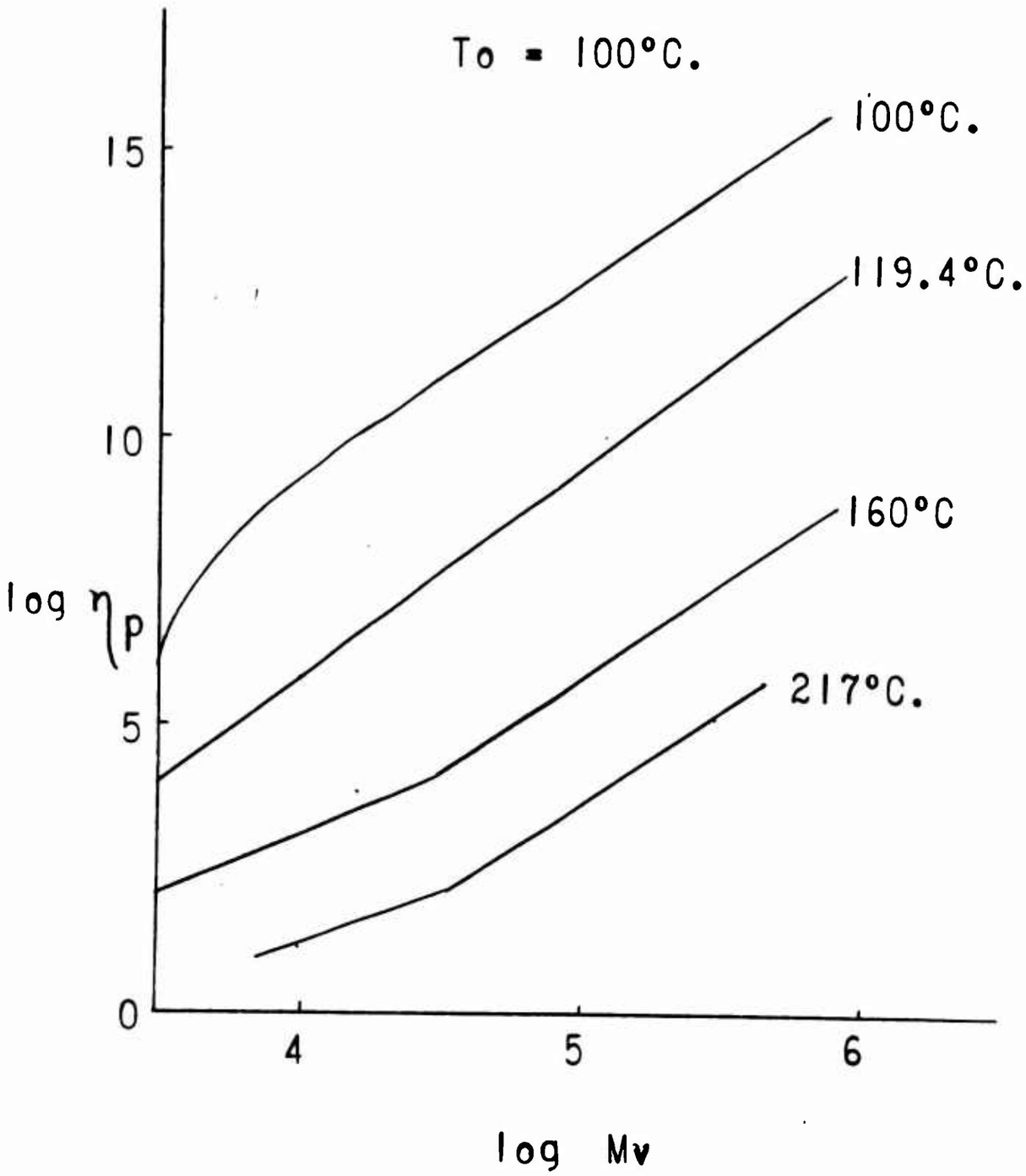

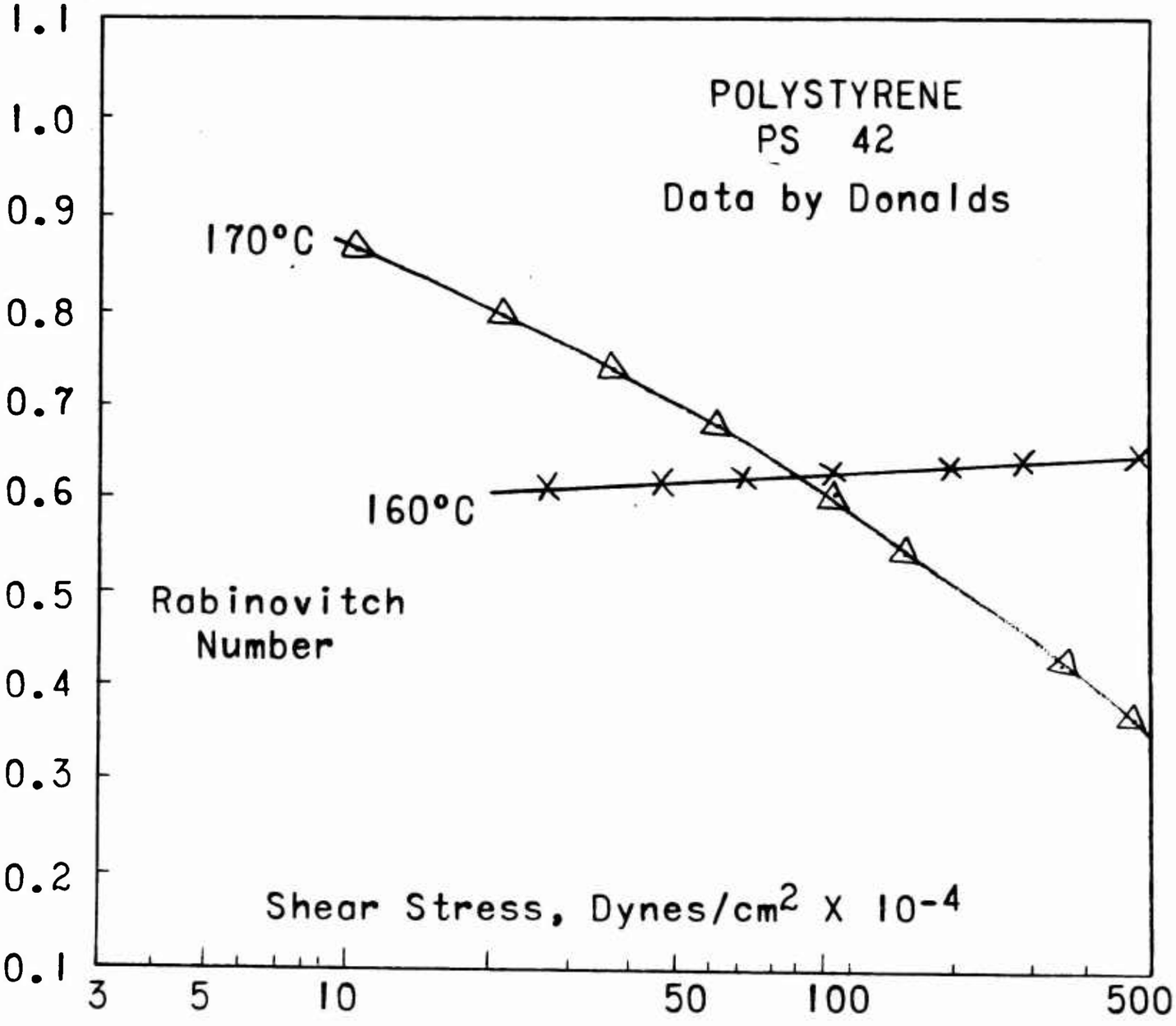
POLYSTYRENE
PS 42
Data by Donalds
170°C
160°C
Rabinovitch
Number
Shear Stress, Dynes/cm² X 10⁻⁴
1.1
1.0
0.9
0.8
0.7
0.6
0.5
0.4
0.3
0.2
0.1
3
5
10
50
100
500

TEMPERATURE FOR $\eta_{MELT} = 10^4$ POISE VS MOLECULAR WEIGHT FOR POLYSTYRENE

Data of Allen & Fox

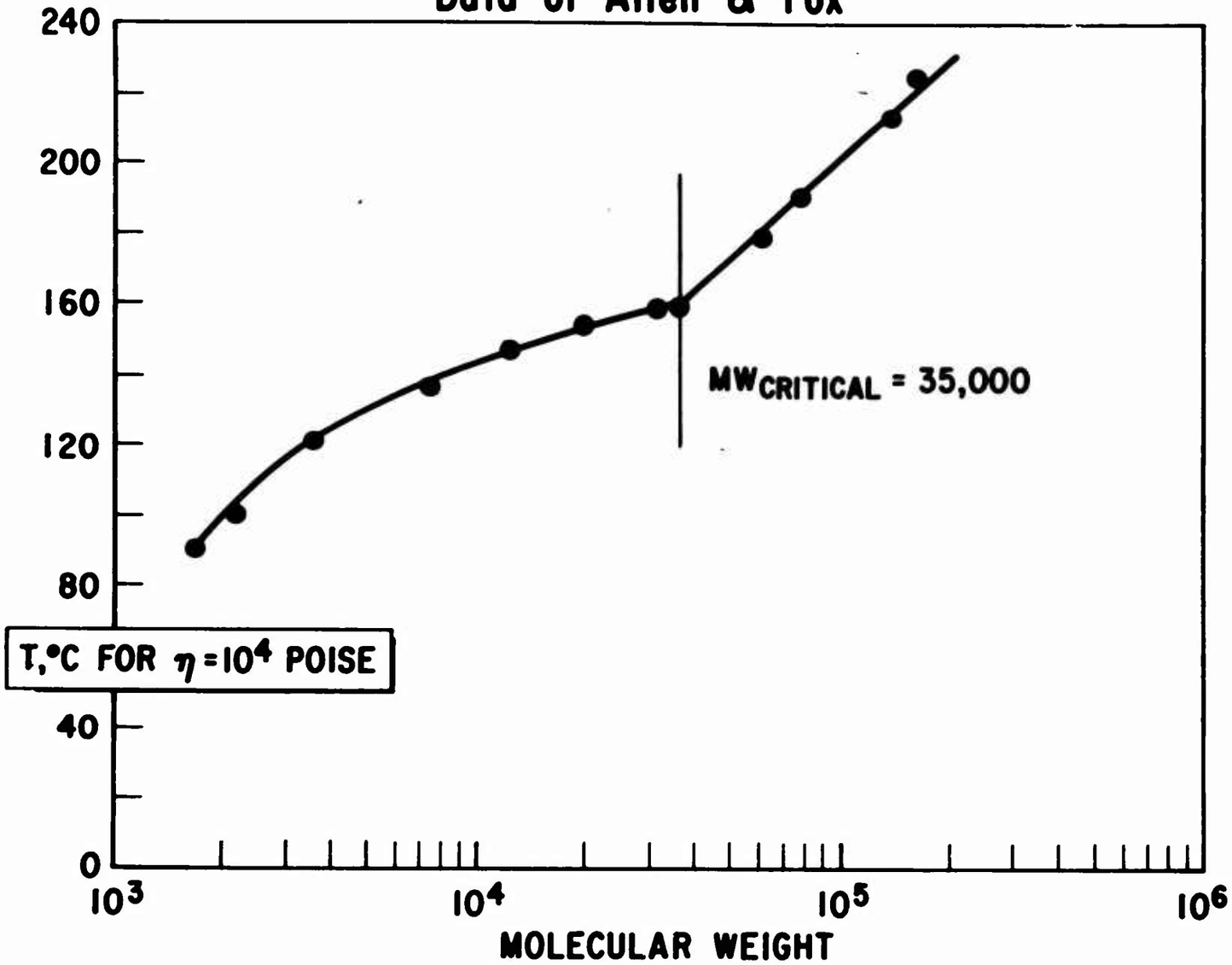

COMPARISON OF $T_{l,l}$ WITH AN ISOVISCOUS STATE FOR POLYSTYRENE

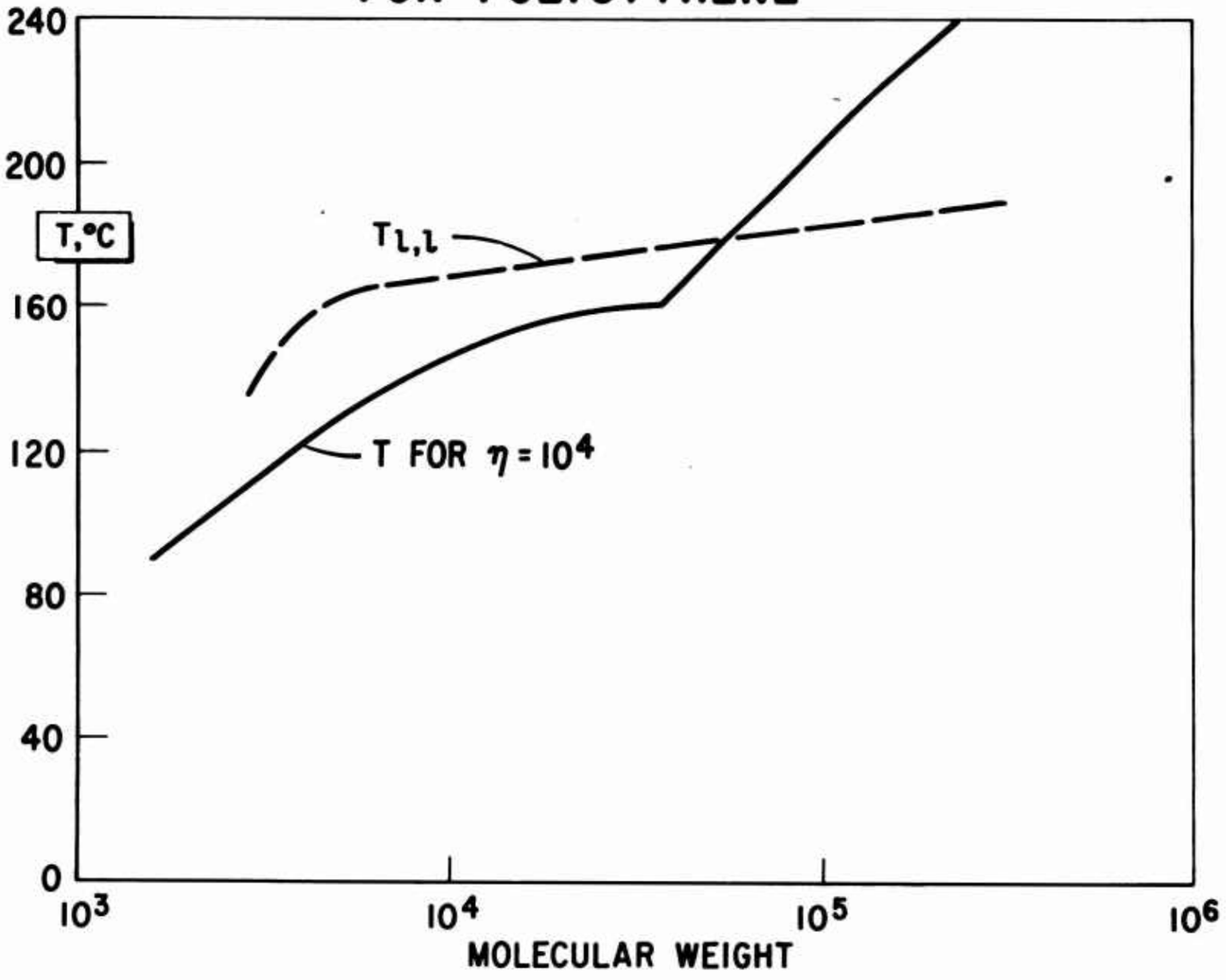

POLYSTYRENE – DIBENZYLETHER

$M_V = 70{,}000$

Data of Fox, Gratch & Loshaek

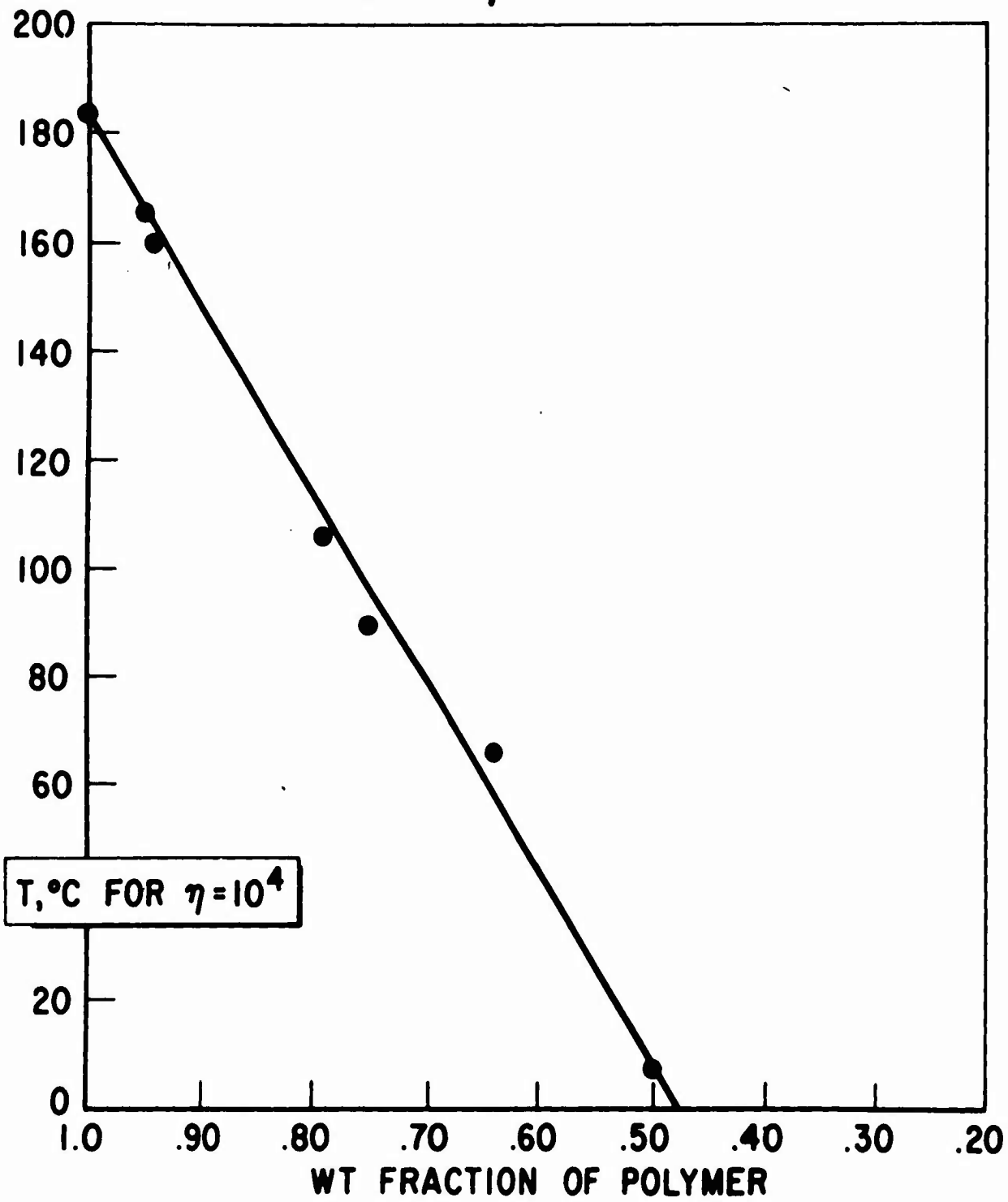

3796

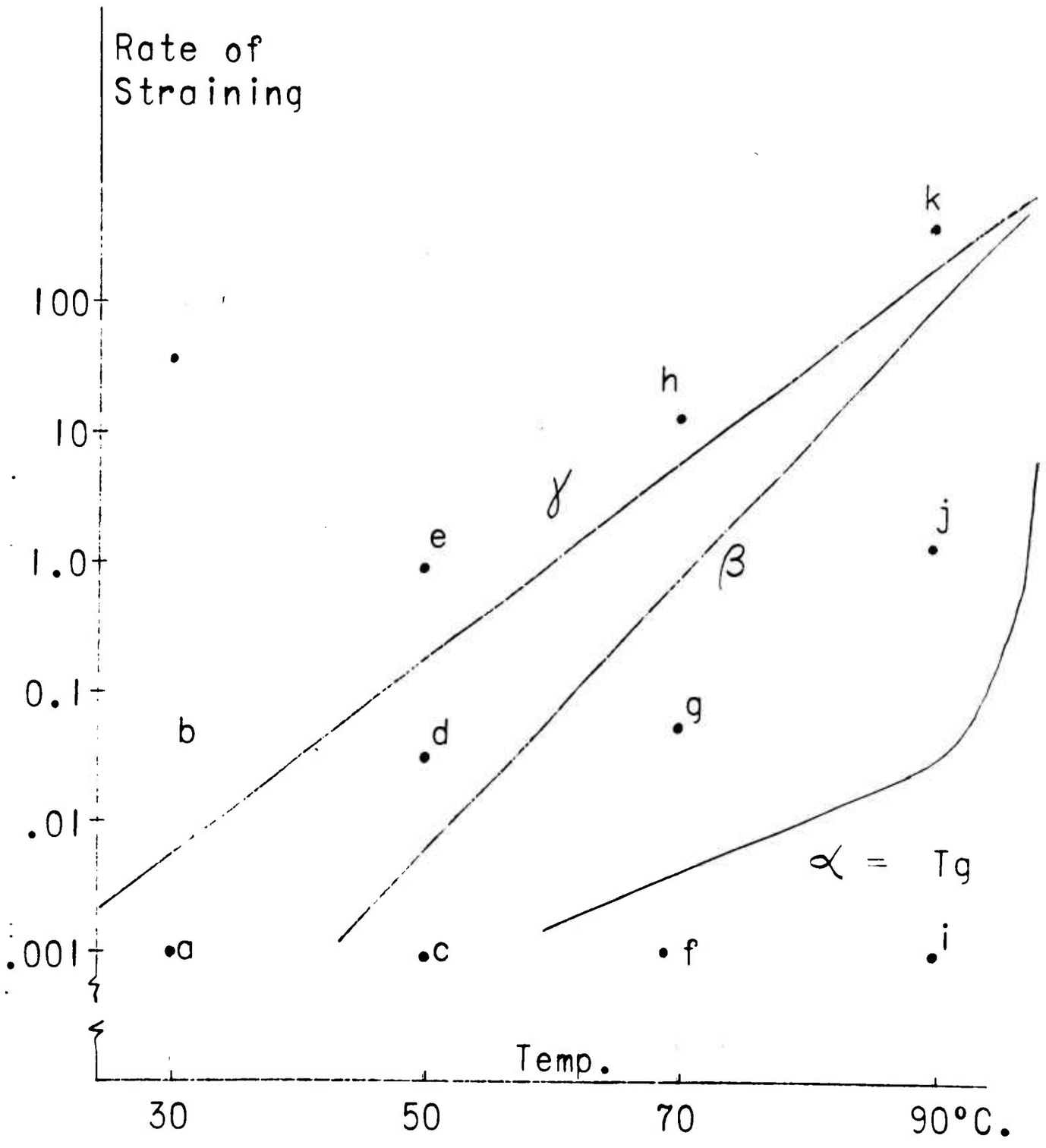
Rate of
Straining
100
10
1.0
0.1
.01
.001
k
h
e
j
b
d
g
a
c
f
i
γ
β
α = Tg
Temp.
30
50
70
90°C.

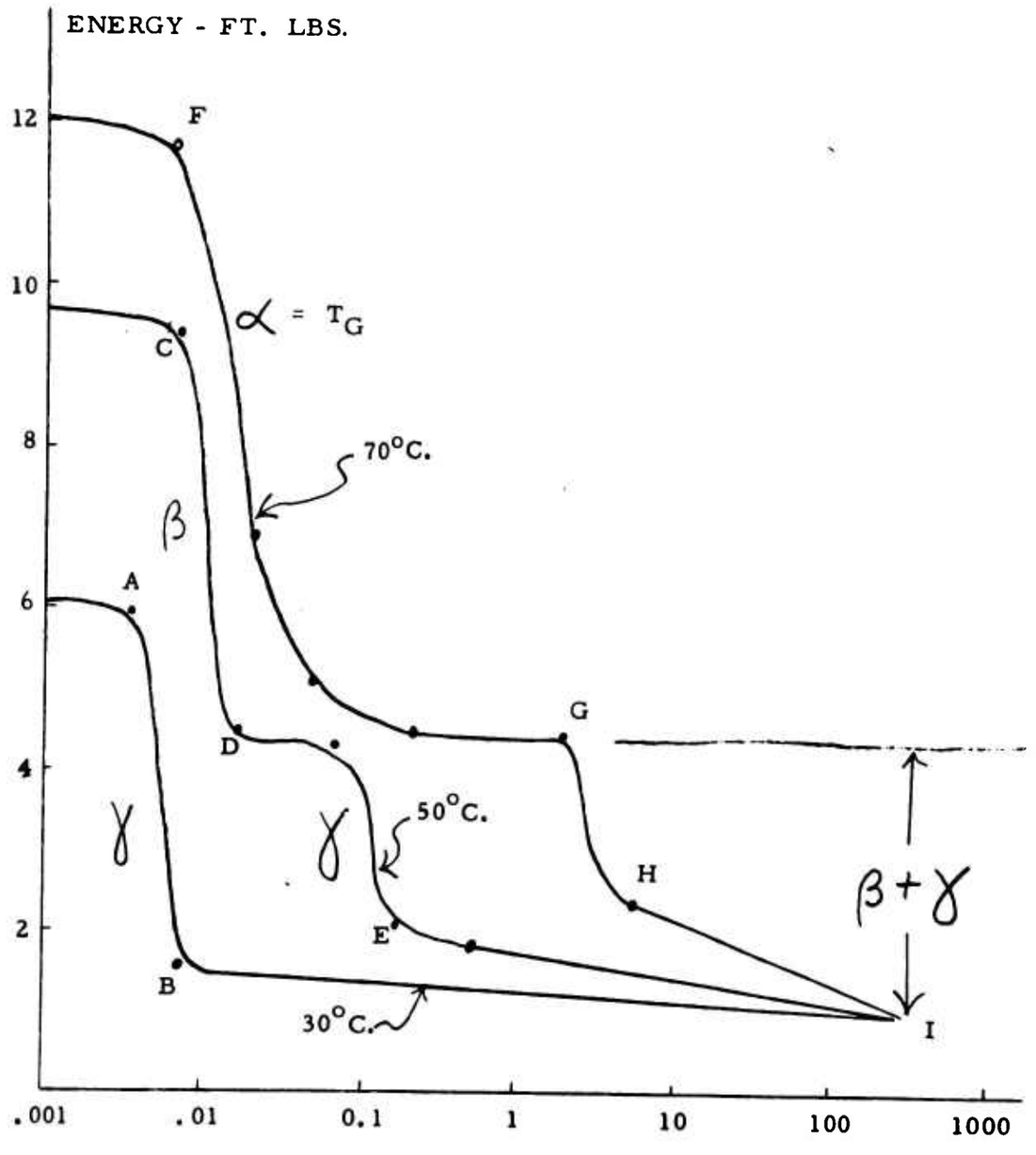
ENERGY - FT. LBS.
12
10
8
6
4
2
F
C
A
B
D
E
G
H
I
α = T_G
70°C.
50°C.
30°C.
β
γ
γ
β+γ
.001
.01
0.1
1
10
100
1000
RATE OF STRAINING IN."/SEC.

MULTIPLE TRANSITIONS IN POLYALKYL METHACRYLATES*

Robert A. Haldon and Robert Simha†

Department of Chemistry, University of Southern California

Los Angeles, California 90007

ABSTRACT

A series of polyalkyl methacrylates, two hydroxylated methacrylates, polymethoxy ethyl methacrylate and polymethyl acrylate have been studied by linear expansion and torsion pendulum measurements, in the temperature range from -180°C to just above the respective glass transition temperatures. The length - temperature (L-T) data were analyzed by a least squares differentiation procedure, based on moving arcs, to give directly the thermal expansion coefficients as a function of temperature.

The L-T measurements suggest the existence of two T_{gg} transitions (T_g - 100 < T_{gg} < T_g) in the polymers with the more flexible side chains, and one transition for polymers with bulky side groups. There is also evidence of a third T_{gg} transition at about -120 to -90°C, which may be associated with adsorbed water molecules. In similar fashion to that of T_g, the location of the T_{gg} transitions decreases upon increasing the length of the n-alkyl side chain. The hydroxylated polymers have higher T_g's than the corresponding alkyl samples, and have thermal expansion coefficients only about one half as large, both features being a result of interchain hydrogen bonds.

Torsion pendulum measurements indicate only one clear cut T_{gg} transition region;

---

* This work was supported by the National Aeronautics and Space Administration under grant NsG-343, to the University of Southern California.

† J. F. Kennedy Memorial Foundation Senior Fellow, The Weizmann Institute of Science, Rehovoth, Israel, 1966/67.

Abstract - 2

hence it seems that the two T_{gg} transitions observed in the expansion studies cannot be unequivocally resolved by dynamic measurements.

Expansion coefficients of the n-alkyl series suggest the retention of some excess free volume below T_g for side chains larger than ethyl. Substitution of $3\alpha'_{g''}$, the expansion coefficient below our second T_{gg} transition, into the Simha-Boyer equation, $(\alpha_\ell - \alpha_g)\cdot T_g$, gives a value close to their empirical constant. This supports their suggestion that polymers with pronounced sub-group motions exist in an iso-free volume state below the sub-group transition temperature.

MULTIPLE TRANSITIONS IN POLYALKYL METHACRYLATES*

Robert A. Haldon and Robert Simha†

Department of Chemistry, University of Southern California

Los Angeles, California 90007

INTRODUCTION

Simha and Boyer[1] have proposed a simple method of calculating a free volume of polymeric materials at their glass transition temperatures, using thermal expansion data. If α_l and α_g are the cubical expansion coefficients above and below the glass transition temperature, T_g, then,

$$(\alpha_l - \alpha_g)\cdot T_g = \Delta\alpha\cdot T_g = K \qquad (1)$$

may be interpreted as a fractional free volume. Values of K are observed[1] to fluctuate around 0.113 for polymers free from pronounced sub-group motions below T_g. One type of system found not to obey the above relationship was a series of poly n-alkyl methacrylates,[2] in which K decreased on lengthening the side chain, at least up to n = 12. Polyalkyl methacrylates are known to have sub-group transitions below T_g,[3] and Simha and Boyer proposed that the side chains retain excess free volume on cooling below T_g, leading to an unusually high value of α_g, and that the relevant free volume quantity should be $(\alpha_l - \alpha_{g'})\cdot T_g$, where $\alpha_{g'}$ is the expansion coefficient below the side group transition temperature.

Other polymers with long flexible side chains show abnormally high values of α_g and correspondingly low values of the product $\Delta\alpha\cdot T_g$. Such systems include the poly n-alkyl acrylates[4,5] and the polyvinyl n-alkyl ethers.[6] Dannis[7]

---

* This work was supported by the National Aeronautics and Space Administration under grant NsG-343, to the University of Southern California.

† J. F. Kennedy Memorial Foundation Senior Fellow, The Weizmann Institute of Science, Rehovoth, Israel, 1966/67.

observed very high values of the glassy state linear expansion coefficient, $(1/\ell)(d\ell/dT)_g$ for a series of poly α-olefins, but did not report his data above T_g. The expansion coefficient increased four times on changing the pendent group from methyl to hexyl.

The purposes of the present study are to measure the expansion coefficients for a series of poly n-alkyl methacrylates, to look for $T < T_g$ transitions, and to examine the suggestion of Simha and Boyer.[1] We shall also attempt, by studying additional methacrylates, to assign molecular motions to the observed minor transitions. Both dilatometry and low frequency dynamic measurements are used to allow a comparison of the two techniques. The temperature range investigated varies from -180°C to above the glass transition temperature of the respective polymer.

EXPERIMENTAL

Materials

The polymer samples studied are listed in Table I.

Preparation of Test Specimens

a) for Length-Temperature Measurements

The PMMA was molded in a compression mold at a temperature about 165°C and a pressure about 5,000 lbs/sq. in. The remaining samples were obtained as transparent sheets and were cut to shape from this, except for PnHMA, PnOMA and PnDMA. These latter three materials were in 30% benzene solution. The solvent was evaporated and the samples cut from the cast polymer. The test specimens were in the form of a cylinder about 1 inch long and 1/4 inch in diameter. The ends of the cylinder were filed flat and carefully sanded before use. Since polymethacrylates adsorb moisture,

the prepared specimens were stored in vacuum. The sample lengths were measured at room temperature with a micrometer reading to 0.0001 inches.

b) for Torsion Pendulum Measurements.

All polymers were compression molded at 100-165°C and a pressure of 5,000 lbs/sq. in., to a thickness of 20 mils. Specimens about 5 cm. long and 1-1.5 cm. wide were cut from the molded material.

Procedures

a) Length-Temperature Measurements.

These were obtained in an automatic device similar to that described by Eisenberg and Sasada.[8] The cylindrical sample is placed in a flat bottomed quartz tube to which is also attached the coil assembly of a Linear Variable Differential Transformer (LVDT). Sample dilation is transferred to the LVDT by a second quartz tube, within the first, resting on top of the sample and carrying the LVDT core. The excitation frequency of the primary coil is 3,000 cycles per second and the secondary output passes via an indicator - amplifier to one input of a two point recorder. The quartz tube assembly is housed in an aluminum block, used as the heating or cooling unit, and which in turn rests in a Dewar flask. This block has a cartridge heater in a central well. Temperature is measured by a 30 gauge copper - constantan thermocouple placed in an identical position to the sample, and connected to the second input of the recorder.

The transformer output is approximately 13 millivolts for full scale deflection and is linear, within ±0.25%, in the range 1×10^{-4} to 1×10^{-1} inches, where zero corresponds to the zero induction point of the transformer. The maximum usable sensitivity was about 4×10^{-5} inches of sample expansion per inch of recorder deflection and that generally used was about 8×10^{-4} inches per inch. The recorder chart could be read to ±0.01 inches

corresponding to a length change of 8×10^{-6} inches. The thermocouple output was read in 0.1 mv. increments, corresponding to 2.5°C at room temperature and 5.6°C at liquid nitrogen temperatures.

The LVDT was calibrated by applying a length change with a micrometer reading to 0.0001 inches.

The runs reported here were performed by heating the samples up from liquid nitrogen temperature to the glass transition. The aluminum block and sample were cooled down to liquid nitrogen temperatures over a period of about an hour, by pouring liquid nitrogen into the surrounding Dewar. The sample was then stabilized at the lowest temperature (about -185°C) for about 1/2 - 1 hour while the liquid nitrogen surrounding the block boiled off, and then allowed to heat up. The natural heating rate was about 1°C/min. at the lowest temperature and at about -140°C the rate was controlled at 0.2 to 0.3°C/min. by increasing the voltage to the cartridge heater. The heating cycle was chosen because it was easier to reproduce slow warming rates than slow cooling rates. Increasing the heating rate to 1°C/min. gave no observable differences in the length-temperature curves.

b) Torsion Pendulum Measurements.

Mechanical loss maxima were determined with a freely oscillating torsion pendulum similar to that described by Cuddihy and Moacanin.[9] The torsion bar and upper clamp are suspended from a supporting structure by a thin piano wire. The lower clamp is fixed and the specimen is held between the two clamps and surrounded by a Dewar flask. Heating is provided by compressed air and cooling by liquid nitrogen, using dry nitrogen as the exchange gas. A copper - constantan thermocouple placed close to the sample measures the temperature. The oscillations are started by twisting the torsion bar through a small angle, and are recorded by an electric sparkover between

a tungsten needle and a rotating drum, provided with electro-sensitive paper.

The frequency range used was 0.3 to 1.5 Hz., and damping is expressed as the natural logarithm of two successive amplitudes, i.e.,

$$\delta = \ln A_i/A_{i+1}$$

Analysis of L-T Data

Volume or length versus temperature data are conventionally analysed by passing a series of straight lines through the points. This procedure, although adequate usually to determine the major glass transition temperature, is generally unsatisfactory for minor transitions where the changes in slope can be very small. Zakin, Simha and Hershey[10] have shown that differentiating the data will more clearly locate minor transitions and, particularly for a polyurethane sample, showed that a minor transition can be "missed" by simply drawing straight lines through the data.

The derivatives of the L-T data were therefore obtained directly by a moving arc method[10,11] previously described.[10] In this method local data points are fitted with least square polynomials, and the method can be used conveniently on data points equispaced in one variable. As before, a seven point parabola was chosen. The equispaced variable was the thermocouple voltage. The relation between thermocouple EMF and temperature is not linear and the derivatives were obtained using a 5-point moving arc parabola. The output voltage of the LVDT is directly proportional to changes in the sample length and thus the linear expansion coefficient, α', can be computed as:

$$\alpha' = \alpha/3 = (1/\ell_o)(d\ell/dT)$$

$$\text{i.e., } \alpha' = (C/\ell_o)(dE_{LVDT}/dE_{Thermocouple})(dE_{Thermocouple}/dT)$$

where ℓ and ℓ_o represent the instantaneous and initial sample lengths respectively, and C is a proportionality factor between changes in sample length and LVDT voltage. ℓ_o was not corrected for the decrease in sample length at low temperature and this seemed justifiable as the contribution to α' would be a maximum of 2% at the lowest temperature. The data were taken from the recorder chart in 0.1 mv. increments of thermocouple voltage. The computations were programmed on a Honeywell 800 computer and the smoothing subroutines used in ref. 10 were not necessary.

A transition was indicated by a step in the α' vs. T plot. At $T < T_g$ the magnitude of such a step indicating a minor transition was usually about 0.1×10^{-4} and occurred over about 20-30°C. Smaller, flatter steps, in which the change is less than 5% in this temperature range are evident from the data but these are discounted because of the instrument's repeatability limitations. Use of a quartz rod to transfer sample dilation causes α' to drop in the vicinity of T_g. This is due to the rod's weight upon the sample, whose modulus is considerably reduced on passing through the transition region. Even after careful annealing and slow cooling of the polymer sample, reliable and reproducible values of α' above T_g could not be obtained. Reduction of the weight of the rod led to better results, and with use of a very thin wooden rod with a foot to rest on the sample, values of α_ℓ' were obtained which compared favorably with literature data, although there was greater scatter above T_g than below. For both T_g and T_{gg} transitions, the transition temperature is chosen by drawing tangents on either side of the step and choosing the mid-point of the step on the temperature axis. For the glass temperature this was found to coincide with that obtained by drawing straight lines through the L-T data points.

Reliability of the measurements

Reliability was gauged by the repeatability of the data for the same sample and by a comparison with the literature values of the dilatometric expansion coeffi-

cients. The first point is illustrated by Fig. 1 which shows repeat runs for PMA of similar thermal history. We note that the maximum difference between runs at low temperatures does not exceed 10%.

We observe for PMA, Fig. 2, $\alpha_g' = 0.75 \times 10^{-4}$ degree^{-1}. The literature values of $\alpha_g/3$ range from 0.65 to 0.83. Furthermore, $\alpha_g' = 0.83 \times 10^{-4}$ obtained for PMA agrees well with the value of 0.90 quoted by Wood,[4] and the value for PEMA, Fig. 2, of 1.14 agrees well with the 1.04 calculated from the published graph of Rogers and Mandelkern.[2] Finally for a polystyrene sample, an α'-T plot in the temperature range -180 to 0°C was obtained, which is almost identical to that previously published,[10] with α' increasing from about 0.55 to 0.65×10^{-4} deg.$^{-1}$ over this temperature interval. The maximum discrepancy between the two graphs does not exceed 5%.

Greatest difficulty with reproducibility occurs with the longer side chain n-alkyl polymers, where T_g is below room temperature. The values of the expansion coefficients were found to depend on thermal history and so these samples were carefully annealed at about 20°C below the glass transition temperature prior to measurements. The g-g transitions for a series of repeated runs appeared at the same temperatures but the expansion coefficients varied up to 10%. This aspect is further discussed later with respect to the effects of thermal history on poly n-butyl methacrylate.

RESULTS AND DISCUSSION

a) L-T Measurements.

Expansivity results for the polymers given in Table I are exhibited in Figs. 1-7, and summarized in Tables II and III.

It is well known that the glass transition temperature decreases as the

n-alkyl side chain lengthens.[2] We note in Table II that T_g increases in the butyl isomer series by about 60°C from n-butyl to the bulky tertiary butyl polymer. Furthermore PHEMA (86°C) and PHPMA (76°C) have higher glass temperatures than the corresponding alkyl polymers, i.e. PnPMA (35°C) and PiBMA (54°C). This can be attributed to strong hydrogen bonding between chains, which is more effective when the side chain is linear. PMPMA (20°C) has a T_g similar to PnBMA (18°C) and so the methoxy oxygen in the side chain appears to be equivalent to the corresponding methylene group in the n-butyl side chain. Lal and Trick[6] observed a similar effect with the ether oxygen in polyvinyl n-alkyl ethers, as compared with poly α-olefins.

We are inclined to locate two glass-glass transitions (T_{gg}) for the n-alkyl polymers beyond PMMA, except PnDMA, and these transition regions also move to lower temperatures on increasing the side chain length. There is also evidence of a third transition around -120°C to -100°C for the higher n-alkyl homologues, and this region shifted to about -80°C after prolonged vacuum drying. It is probable that this transition occurs in PMA, PMMA, Pt-BMA and PMEMA as well at about -120°C, but is less obvious. It is located at too high a temperature to be the motion ascribed by Willbourn,[15] on the basis of high frequency measurements, to a $-(CH_2)_n-$ chain, where n = 3 or 4. We would expect to observe this motion at about -180 to -160°C, near the limit of our temperature range, and indeed we observe generally a decrease in α' in this region, particularly for the less bulky polymers. Shen, Strong and Matusik[16] have shown that the dynamic loss peak, given by Hoff, Robinson and Willbourn[3] at about -150°C for poly n-alkyl methacrylates is displaced upwards by about 50° on substituting a hydroxyl group for the terminal methyl of the side chain. We see no corresponding evidence of this in PHEMA and PHPMA. However the expansion coefficients are

very small, less than one half of those for the n-alkyl polymers, and the change may be too small to be detected. The observation that α' does increase about 30% in the range from -120 to -70°C, may be pertinent in this connection. The assignment of a $T_{gg}(2)$ transition for PHPMA and PMPMA appears somewhat tenuous but seemed justified in the light of repeat runs and the general trend.

Gall and McCrum[17] found a dynamic loss peak (~1 Hz.) at -100 to -80°C for PMMA and this peak moved to lower temperatures on conditioning the polymer in a progressively more humid atmosphere. Our $T_{gg}(3)$ transition persisted even after vacuum drying, but it is possible that the samples picked up water during the measurements.

Apart from this low temperature transition, two T_{gg} transitions were observed for all polymers except PMA, PEMA, Pt-BMA and PnDMA. The literature presents evidence for only one transition in our $T_{gg}(1)$ - $T_{gg}(2)$ range but the low frequency data are confined to PMMA, and Hoff, Robinson and Willbourn's measurements at higher frequency show that even the β transition merges with T_g on lengthening the side chain so that resolution of two T_{gg} transitions would be impossible. Dilatometric results usually do not cover a large enough temperature range below T_g to detect sub-group motions and in this case are confined to PMMA and PEMA. Rogers and Mandelkern[2] show a break below T_g at 40°C for PMMA and 15°C for PEMA. These, they suggest, could be evidence of secondary transitions, or could simply be curvature as a consequence of the Third Law of Thermodynamics. However, other evidence locates the PMMA T_{gg} transition anywhere between -20°C and 62°C. Martin, Rogers and Mandelkern[12] studied PMMA to liquid nitrogen temperatures by an interferometric technique and suggest a break at 0°C. The fact that Boyer[18] interprets this break at -20°C suggests an examination of the derivatives. By dilatometry Holt and Edwards[19] located a transition at 23°C and Heydemann and Guicking[20] two, at -7°C and 62°C.

Heijboer[21] found that the secondary dynamic mechanical loss peak in PMMA disappeared on increasing the methyl acrylate content of a methyl methacrylate - methyl acrylate copolymer and therefore assigned the sub-group motion to rotation of the carbomethoxy group, hindered by the main chain methyl group. Deutsch, Hoff and Reddish,[22] by dielectric measurements, assigned it also to this motion. The $T_{gg}(2)$ transition which is present in all our polymers must be associated with this same motion. $T_{gg}(1)$ is dependent on the side chain flexibility and is possibly a crankshaft type motion (around the main chain) described by Boyer,[18] and first proposed by Schatzki[23] for polyethylene. Such a motion would merge with T_g on making the side group bulkier. PnDMA showed only one obvious g-g relaxation and this may be due to the side chain becoming more ordered, restricting motion somewhat, and perhaps merging the other glass-glass motion with the glass temperature. We note an upswing on the α'-T plot on the low temperature side of T_g.

The effect of structure on the sub-group transition temperatures was similar to the effect on T_g, namely a decrease with increasing side chain length and an increase in the butyl isomer series as a function of the bulkiness of the butyl group. The ratio $T_{gg}(i)/T_g$, (i) = 1, 2, is approximately constant (see Table II), a relationship which also holds for the poly α-olefins.[7] This suggests that the corresponding mechanisms are related and similarly affected by structure as T_g.

b) Torsion Pendulum Measurements.

The mechanical damping versus temperature plots are exhibited in Fig. 7, and T_g and T_{gg} values are listed in Table II.

PMMA shows two distinct maxima, one associated with T_g occurring at about 116°C, and the secondary at about 25°C. The shape of the curve is almost identical to that of Heijboer,[21] and very similar to those of Schmieder and Wolf,[24]

Turley and Keskkula[25] and Gall and McCrum.[17] The lower maximum is very broad, the increased damping beginning as low as -30°C.

Similar results were obtained for PEMA and PnPMA with the two maxima moving closer together. In each case the lower maximum is still broad with the location varying very little. In PnBMA the two cannot be resolved, the lower peak appearing as a shoulder on the glass transition maximum. The lower peak also appeared as a shoulder in PiBMA. Other polymers were not investigated due to molding difficulties with the cross-linked materials. We observed no evidence of a transition in the range -100 to -80°C ascribed to motion of adsorbed water molecules,[17] even after treatment of the sample in a water atmosphere for one week. However for both PnPMA and PnBMA a slight increase in δ occurs around -170°C, which is the limit of our temperature measurements. A similar increase was noted by Reding, Faucher and Whitman[26] for poly n-butyl acrylate, and assigned to motion of the butyl side groups. Such a low temperature peak would be consistent with the -150°C loss peak of Hoff, Robinson and Willbourn,[3] at higher frequencies.

On comparing the transition regions obtained by the two techniques of dilatometry and the torsion pendulum, we note that T_g obtained by the latter is higher than that obtained by dilatometry, which is consistent with the higher frequency of the dynamic mechanical technique. The very broad secondary transition peak certainly spans the temperature range covered by the two corresponding T_{gg} transitions observed by the LVDT measurements. Thus it appears that better resolution is obtained from the length-temperature measurements.

Expansion Coefficients

The linear expansion coefficients below T_g increase on lengthening the n-alkyl side chain, but decrease in the butyl isomer series with:

n-butyl > sec-butyl ≈ iso-butyl > tertiary-butyl

It is unlikely that the bulky t-butyl chains would pack more efficiently than PnBMA with its very flexible side chains, so more free volume must be retained by motion of these flexible side chains on cooling below T_g. The hydroxy substituted polymers have interchain bonding, which results in relatively low values of α'_g, about one half of those for the corresponding non-hydroxylated samples. The expansion coefficients just below the glass temperature increase markedly, from a value for PMMA of 0.75×10^{-4} deg.$^{-1}$, similar to that observed for essentially linear polymers, to values for PnBMA and PnOMA in excess of twice that value. This represents fairly vigorous motion in the glass of the longer side chain polymers and the change in expansion coefficient at T_{gg} for PnBMA is about half of that occurring at the glass temperature.

Comparing α'_g's at an arbitrary reference temperature of -140°C, there is a much larger increase going from methyl to ethyl than from ethyl to n-propyl or n-propyl to n-butyl. This must reflect some motion associated with the n-alkyl side chain, starting with ethyl, still occurring below -120°C. On the other hand the assignment of the -150°C (at ~500 Hz.) dynamic loss peak to motion of the alkyl side chain,[3] referred to polymers with three or more carbons in the side chain. Woodward, Sauer and Wall,[27] however, obtained a loss peak for poly 1-butene which has only two side chain carbons. PsBMA and PiBMA both are flexible enough to exhibit motion below -120°C and PMA has a higher α'_g than PMMA but here the difference can be ascribed to a reduction in chain stiffness.

Effect of Thermal History on Poly n-butyl methacrylate.

PnBMA samples were subjected to various treatments designed to alter the

free volume content of the glass. These treatments are summarized in Table IV, along with the expansion coefficients at two arbitrarily chosen reference temperatures, -140 and -70°C.

The sample annealed at 0°C and that cooled from the glass temperature to -190°C over a period of about one hour were very similar and gave better reproducibility than quenched samples. The annealed sample has the lowest expansion coefficient at the lowest temperatures (i.e. at -140°C), and that quenched from 100°C to -190°C has the highest. This is consistent with excess free volume being frozen in on quenching. Quenching from 100°C yields only a slightly different value of α' than quenching from 55°C. However by the time the quenched samples had warmed to about -70°C, their expansion coefficients were much closer to the values for the annealed sample, suggesting that there is enough molecular motion at these low temperatures to allow the excess free volume to diffuse out. This conclusion is strengthened by Run 2.8 in which PnBMA was quenched from 55 to -78°C. Here α' at -70°C is considerably higher than that of the sample quenched to -190°C and slowly warmed up. Holding the polymer at -78°C for 18 hours after quenching to this temperature gave an expansion coefficient similar to that observed on slow heating from -190°C.

The locations of transitions $T_{gg}(1)$ and $T_{gg}(2)$ varied by no more than ±3° from run to run but with no obvious pattern with respect to thermal history. $T_{gg}(3)$ was about -90°C for all samples. On the other hand, the magnitude of the expansivity changes depended on the treatment. $\Delta\alpha'(1)$ increased and $\Delta\alpha'(2)$ decreased on shock cooling. It will be interesting to compare in detail the effect of thermal treatment on the main and minor transitions.

T_g as an Iso-free Volume State.

Simha and Boyer[1] showed that the product $\Delta\alpha \cdot T_g$ for the poly n-alkyl methacrylate series studied by Rogers and Mandelkern[2] fell on increasing the size of the n-alkyl group. From an expanded plot we have recalculated the latter's data below T_g for PMA and PEMA, both of which show a break in the glassy region covered by these authors, and obtain a higher value of α_g and hence an even smaller $\Delta\alpha \cdot T_g$.

We obtain here a similar result using the product $3(\alpha_l' - \alpha_g') \cdot T_g$. To test the suggestion of Simha and Boyer,[1] we substitute $\alpha_{g''}'$ for α_g' in this product, where $\alpha_{g''}'$ is the expansion coefficient below the second T_{gg} transition, and obtain for the alkyl methacrylate series a value fairly close to that resulting for polymers without bulky pendant groups, as can be seen in Table III. The value obtained for PtBMA appears very large and a similar value was obtained in reference 28. There we note a T_g for this polymer 25° higher than ours and one for PHEMA 30° lower. The lower values of $3\Delta\alpha' \cdot T_g$ found for the hydroxyl polymers is in qualitative agreement with the idea[18] that the free volume is dependent on the amount of cross-linking and will be reduced for cross-linked samples.

Thus it seems that polymers with little sub-group motion below T_g exist in an iso-free volume state at T_g, those with larger sub-groups, particularly flexible ones, such as n-alkyl chains, exist in the iso-free volume state below the temperature at which the sub-group motion becomes possible. These results appear to support the suggestion of Simha and Boyer.[1] It is interesting to note that the products $(\alpha_g' - \alpha_{g'}') \cdot T_{gg'}(1)$ and $(\alpha_g' - \alpha_{g''}') \cdot T_{gg}(2)$ are not constant. In the n-alkyl series they increase with side chain length.

REFERENCES

1. R. Simha and R. F. Boyer, J. Chem. Phys., 37, 1003 (1962).

2. S. S. Rogers and L. Mandelkern, J. Phys. Chem., 61, 985 (1957).

3. E. A. W. Hoff, D. W. Robinson and A. H. Willbourn, J. Polymer Sci., 18, 161 (1955).

4. L. A. Wood, J. Polymer Sci., 28, 319 (1958).

5. K. Illers, Kolloid-Z., 190, 16 (1963).

6. J. Lal and G. S. Trick, J. Polymer Sci., A2, 4559 (1964).

7. M. L. Dannis, J. Appl. Polymer Sci., 1, 121 (1959).

8. A. Eisenberg and T. Sasada, in J. A. Prins, ed., "Physics of Non-crystalline Solids", North Holland Publishing Co., 1965, p. 99.

9. E. F. Gaddihy and J. Moacanin, Space Programs Summary, 37-31, Vol. IV, p[illegible]et Propulsion Laboratory, California Institute of Technology, Pasadena, California, (1965).

10. J. L. Zakin, R. Simha and H. Hershey, NASA Technical Report under NsG-343, August 1965; J. Appl. Polymer Sci., 10, 1455 (1966).

11. M. Sasuly, "Trend Analysis of Statistics - Theory and Technique", The Brookings Institution, Washington, D. C., (1934).

12. G. M. Martin, S. S. Rogers and L. Mandelkern, J. Polymer Sci., 20, 579 (1956).

13. S. Loshaek, ibid., 15, 391 (1955).

14. R. B. Beevers and E. F. T. White, Trans. Faraday Soc., 56, 744 (1960).

15. A. H. Willbourn, ibid., 54, 717 (1958).

16. M. C. Shen, J. D. Strong and F. J. Matusik, J. Macromolecular Physics, in press.

17. W. G. Gall and N. G. McCrum, J. Polymer Sci., 50, 489 (1961).

18. R. F. Boyer, Rubber Chem. Tech., 36, 1303 (1963).

19. T. Holt and D. Edwards, J. Appl. Chem., 15, 223 (1965).

20. P. Heydemann and H. D. Guicking, Kolloid-Z., 193, 16 (1963).

21. J. Heijboer, Kolloid-Z., 148, 36 (1956).

22. K. Deutsch, E. A. W. Hoff and W. Reddish, J. Polymer Sci., 13, 565 (1954).

23. T. F. Schatzki, J. Polymer Sci., 57, 496 (1962).

24. K. Schmieder and K. Wolf, Kolloid-Z., 134, 149 (1953).

25. S. G. Turley and H. Keskkula, Polymer Preprints, 6, 524 (1965).

26. F. P. Reding, J. A. Faucher and R. D. Whitman, J. Polymer Sci., 57, 483 (1962).

27. A. E. Woodward, J. A. Sauer and R. A. Wall, J. Polymer Sci., 50, 117 (1961).

28. S. Krause, J. J. Gormely, N. Roman, J. A. Shetter and W. H. Watanabe, J. Polymer Sci., A3, 3573 (1965).

29. N. S. Steck, S. P. E. Trans., 4, 34 (1964).

TABLE I

Description of Samples Studied.

Polymer	Alkyl Side-group	Source
Polymethyl acrylate (PMA)	$-CH_3$	(a)
Polymethyl methacrylate (PMMA)	$-CH_3$	(c)
Polyethyl methacrylate (PEMA)	$-CH_2-CH_3$	(a)
Poly n-propyl methacrylate (PnPMA)	$-CH_2-CH_2-CH_3$	(b)
Poly n-butyl methacrylate (PnBMA)	$-CH_2-CH_2-CH_2-CH_3$	(a)
Poly n-hexyl methacrylate (PnHMA)	$-CH_2-CH_2-CH_2-CH_2-CH_2-CH_3$	(a)
Poly n-octyl methacrylate (PnOMA)	$-CH_2-CH_2-CH_2-CH_2-CH_2-CH_2-CH_2-CH_3$	(a)
Poly n-decyl methacrylate (PnDMA)	$-CH_2-CH_2-CH_2-CH_2-CH_2-CH_2-CH_2-CH_2-CH_2-CH_3$	(a)
Poly sec-butyl methacrylate (PsBMA)	$-\underset{\displaystyle CH_3}{\underset{\vert}{CH}}-CH_2-CH_3$	(b)
Poly iso-butyl methacrylate (PiBMA)	$-CH_2-\underset{\displaystyle CH_3}{\underset{\vert}{CH}}-CH_3$	(b)
Poly tert-butyl methacrylate (PtBMA)	$-C\,(-CH_3)_3$	(b)
Poly 2-hydroxy ethyl methacrylate (PHEMA)	$-CH_2-CH_2-OH$	(b)
Poly 2-hydroxy propyl methacrylate (PHPMA)	$-CH_2-\underset{\displaystyle OH}{\underset{\vert}{CH}}-CH_3$	(b)
Poly 2-methoxy ethyl methacrylate (PMEMA)	$-CH_2-CH_2-O-CH_3$	(b)

(a) Obtained from Dr. D. L. Glusker, Rohm and Haas Company. These samples were atactic and were those used in reference 29.

(b) Obtained from Dr. M. C. Shen, North American Aviation Science Center. These samples were all lightly cross-linked and are described in reference 16.

(c) Obtained from plexiglass by dissolution in chloroform and precipitation by methanol. This procedure was repeated and the sample dried in vacuum at 55°C.

TABLE II

Summary of LVDT and Torsion Pendulum Transition Results.

Polymer	L - T (°K)						Torsion Pendulum (°K)		
	T_g	$T_{gg}(1)$	$T_{gg}(2)$	$T_{gg}(3)$	$T_{gg}(1)/T_g$	$T_{gg}(2)/T_g$	T_g	T_{gg}	T_{gg}/T_g
PMMA	376	---	288	143	----	0.77	389	298	0.78
PEMA	337	298	258	158	0.88	0.77	346	288	0.83
PnPMA	308	284	243	188	0.92	0.79	314	283	0.92
PnBMA	291	248	222	178	0.85	0.76	297	S	----
PnHMA	268*	233	193	158	0.87	0.72	---	---	----
PnOMA	248*	213	183	146	0.86	0.74	---	---	----
PnDMA	228*	---	187	---	0.82	----	---	---	----
PsBMA	330	288	258	---	0.87	0.78	---	---	----
PiBMA	327	298	248	185	0.91	0.76	338	S	----
PtBMA	355	---	303	148	----	0.85	---	---	----
PHEMA	359	330	278	---	0.92	0.77	---	---	----
PHPMA	349	286	245	---	0.82	0.70	---	---	----
PMEMA	293	253	208	163	0.86	0.71	---	---	----

* literature values.
S shoulder

TABLE III

Summary of Expansivity and Free Volume Results.

Polymer	α'_ℓ	α'_g	$\alpha'_{g'}$	$\alpha'_{g''}$	$\alpha'_{(-140°C)}$	$3(\alpha'_\ell-\alpha'_g)\cdot T_g$	$3(\alpha_\ell-\alpha'_{g''})\cdot T_g$
			$10^4 \times 1/°C$				
PMMA	1.6	0.75	----	0.55	0.30	0.096	0.12
PEMA	1.8	1.14	0.95	0.79	0.60	0.067	0.10
PnPMA	1.9	1.37	1.12	0.81	0.64	0.049	0.10
PnBMA	2.0	1.48	1.15	0.86	0.70	0.045	0.10
PnHMA	---	1.86	1.37	1.02	0.82	-----	----
PnOMA	---	1.74	1.30	0.91	0.80	-----	----
PnDMA	---	0.93	0.67	----	0.66	-----	----
PsBMA	1.85	1.36	1.07	0.75	0.67	0.049	0.11
PiBMA	1.95	1.34	0.98	0.78	0.69	0.060	0.11
PtBMA	2.10	----	1.00	0.70	0.52	0.117	0.15
PHEMA	1.26	0.92	0.62	0.40	0.31	0.037	0.09
PHPMA	1.20	0.70	0.53	0.40	0.30	0.052	0.08
PMEMA	1.65	1.10	0.74	0.62	0.52	0.048	0.09

TABLE IV

Effects of Thermal History on Poly n-butyl methacrylate.

Run	Treatment	$\times 10^4$ (1/°C)	
		$\alpha'_{(-140°C)}$	$\alpha'_{(-70°C)}$
2.1	Cooled from T_g to -190 in 1 hour.	0.71	0.88
2.2	Annealed at 0°C for 3 days; cooled to -190 in 1 hour.	0.67	0.85
2.4	Quenched from 55°C to -190°C.	0.79	0.89
2.5	Quenched from 100°C to -190°C.	0.83	0.91
2.8	Quenched from 55 to -78°C; run immediately.	----	1.03
2.9	Quenched from 55 to -78°C; held for 18 hours.	----	0.92

LEGENDS FOR FIGURES

Fig. 1. Repeat runs of linear expansion coefficient as a function of temperature for polymethyl acrylate. (O Run 1, ● Run 2)

Fig. 2. Linear expansion coefficient as a function of temperature for polymethyl methacrylate, polyethyl methacrylate, poly n-propyl methacrylate and poly n-butyl methacrylate.

Fig. 3. Linear expansion coefficient as a function of temperature for poly n-hexyl methacrylate, poly n-octyl methacrylate and poly n-decyl methacrylate. (The T_g's shown are values taken from the literature)

Fig. 4. Linear expansion coefficient as a function of temperature for poly n-butyl methacrylate, poly sec-butyl methacrylate, poly iso-butyl methacrylate and poly t-butyl methacrylate.

Fig. 5. Linear expansion coefficient as a function of temperature for poly 2-hydroxy ethyl methacrylate and poly 2-hydroxy propyl methacrylate.

Fig. 6. Linear expansion coefficient as a function of temperature for poly 2-methoxy ethyl methacrylate.

Fig. 7. Mechanical damping as a function of temperature for polymethyl methacrylate, polyethyl methacrylate, poly n-propyl methacrylate, poly n-butyl methacrylate and poly iso-butyl methacrylate.

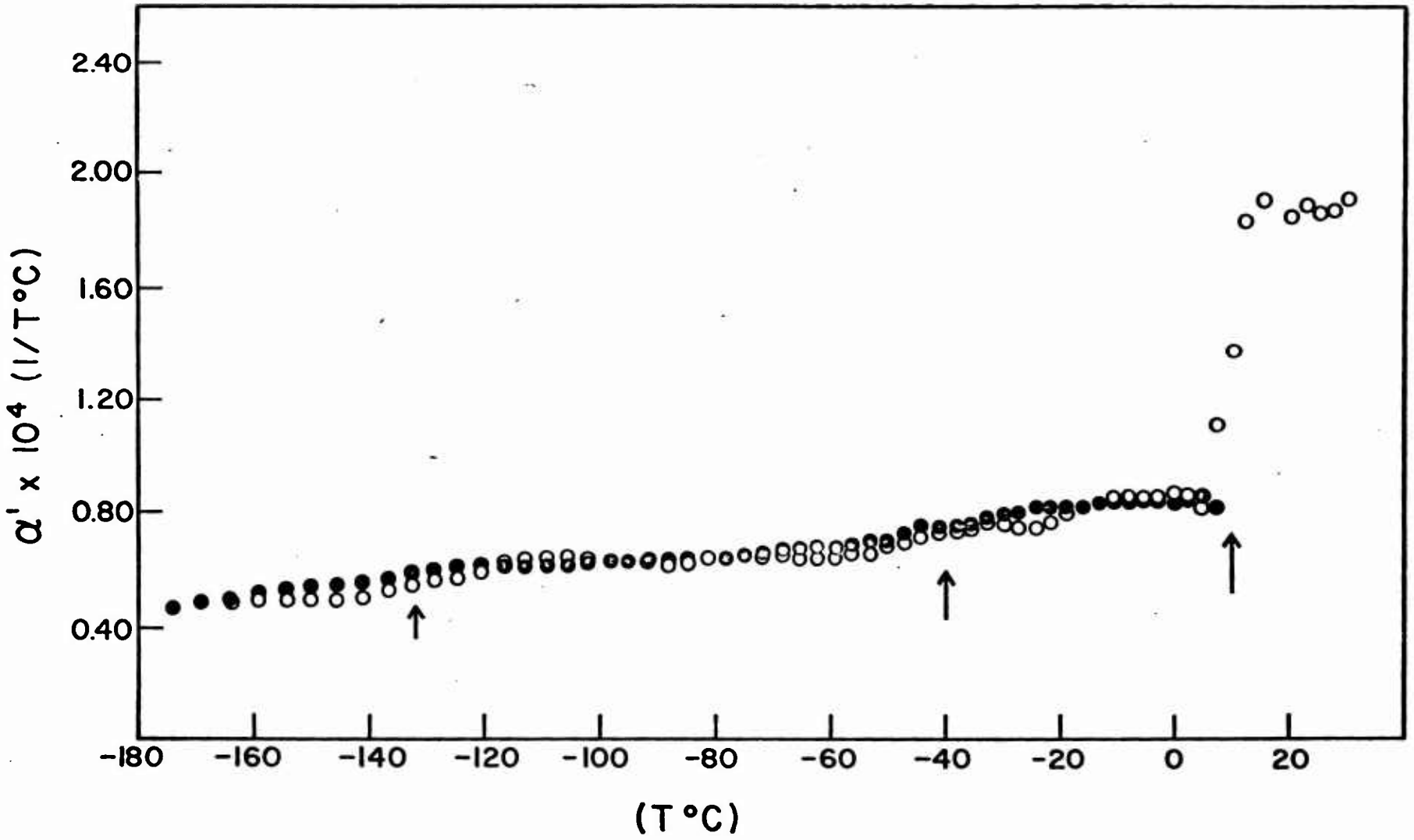
2.40
2.00
1.60
1.20
0.80
0.40
α' x 10⁴ (1/T°C)
-180
-160
-140
-120
-100
-80
-60
-40
-20
0
20
(T °C)

Fig. 1

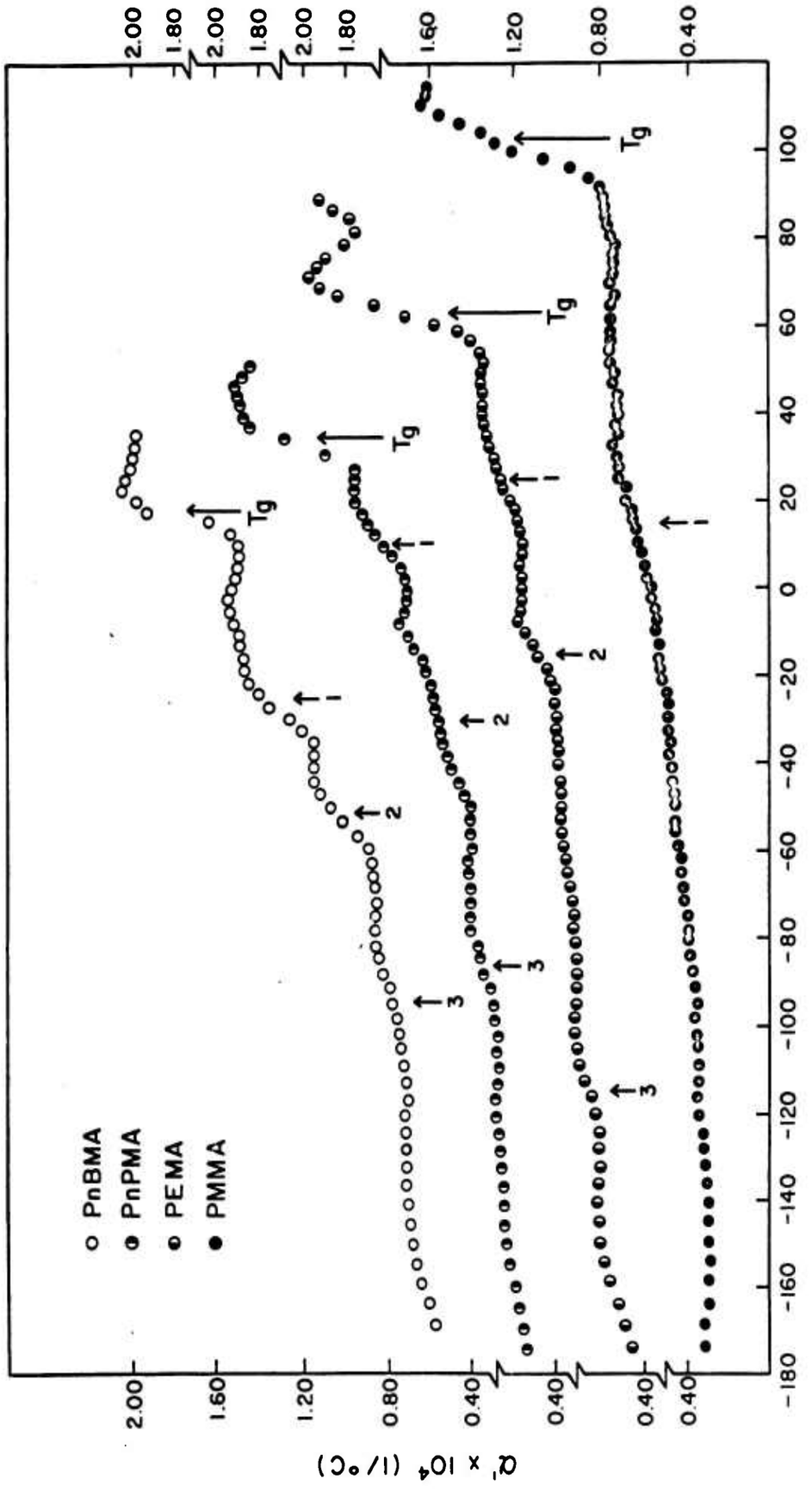

Fig. 2

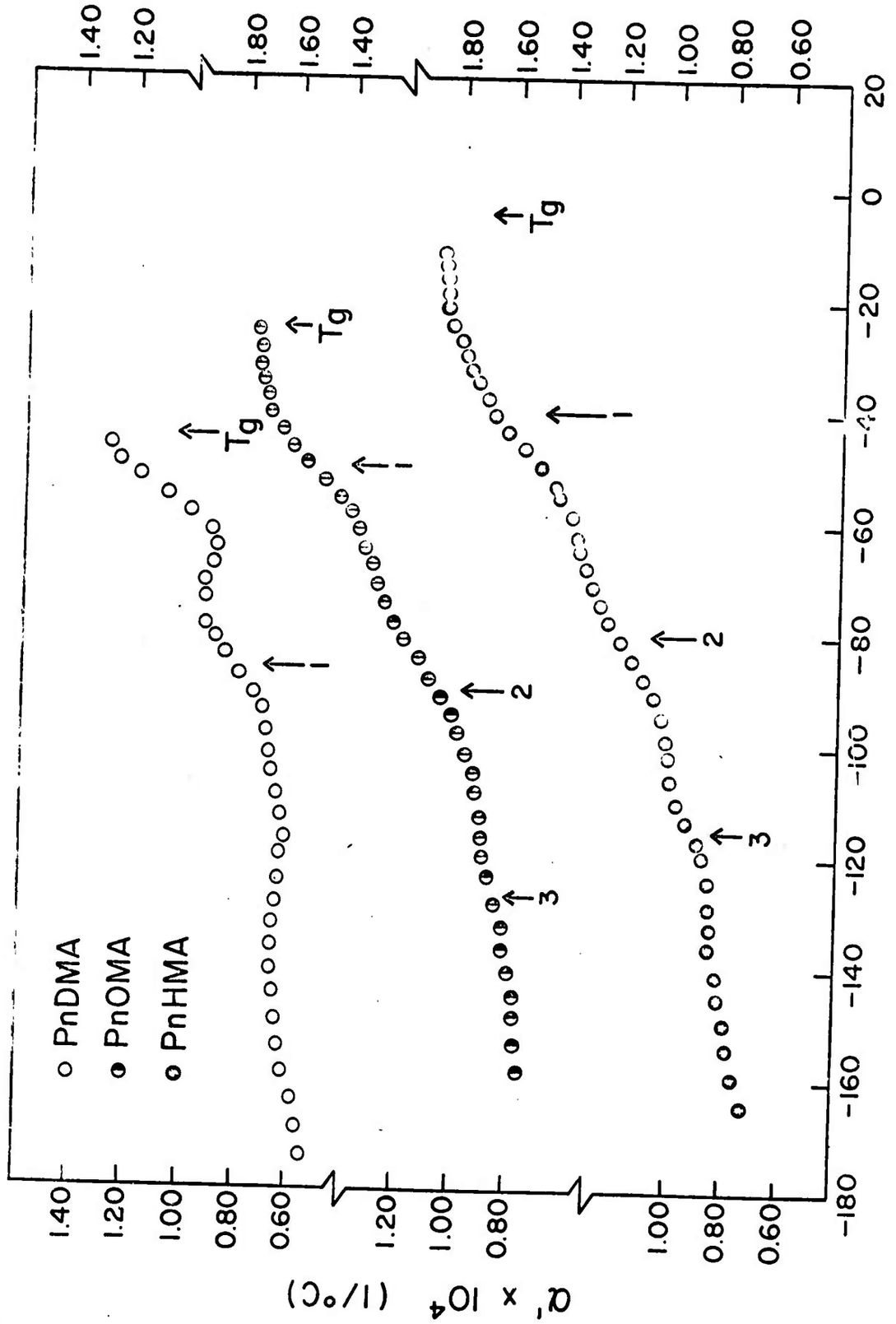

Fig. 3

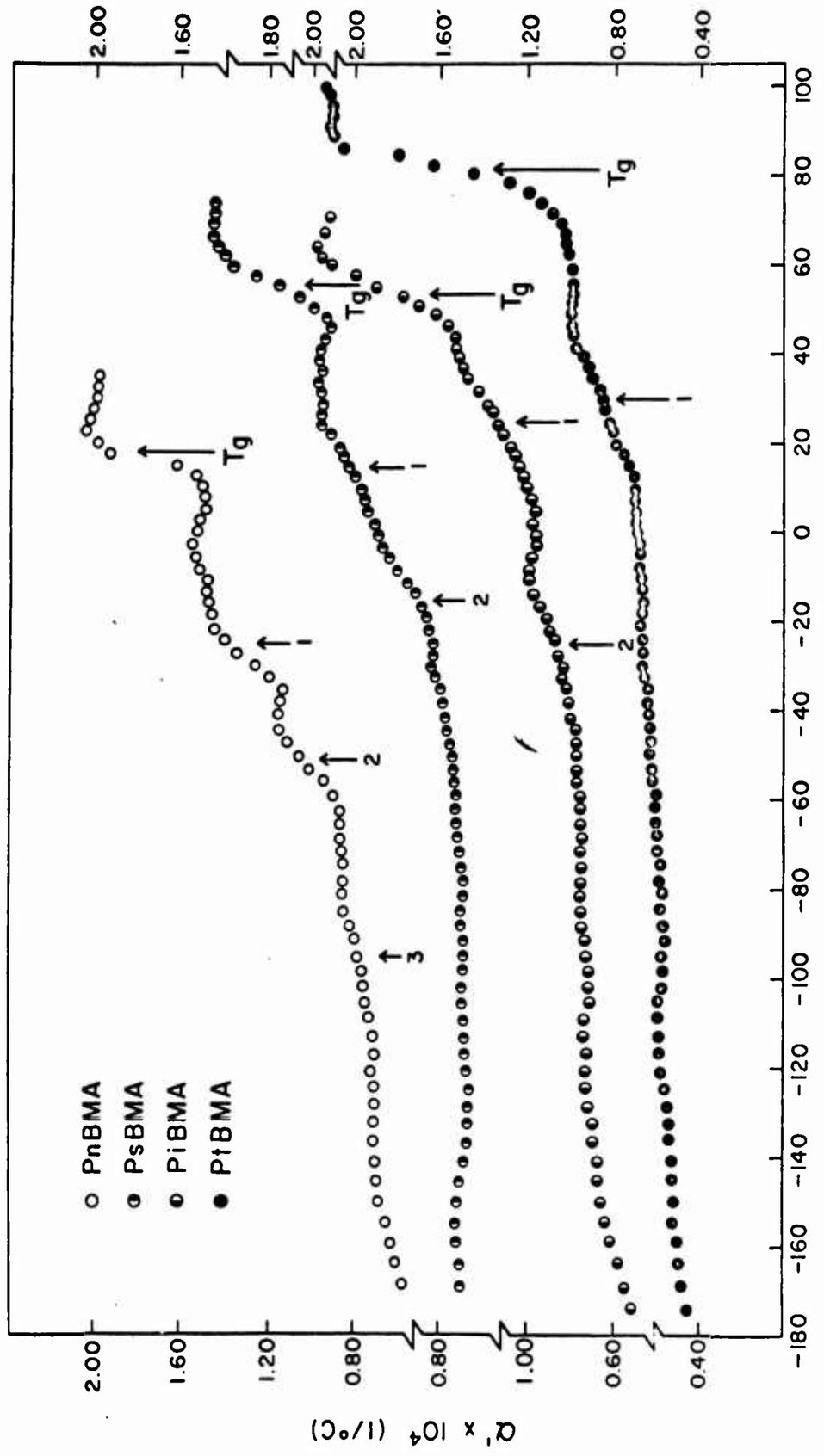

Fig. 4

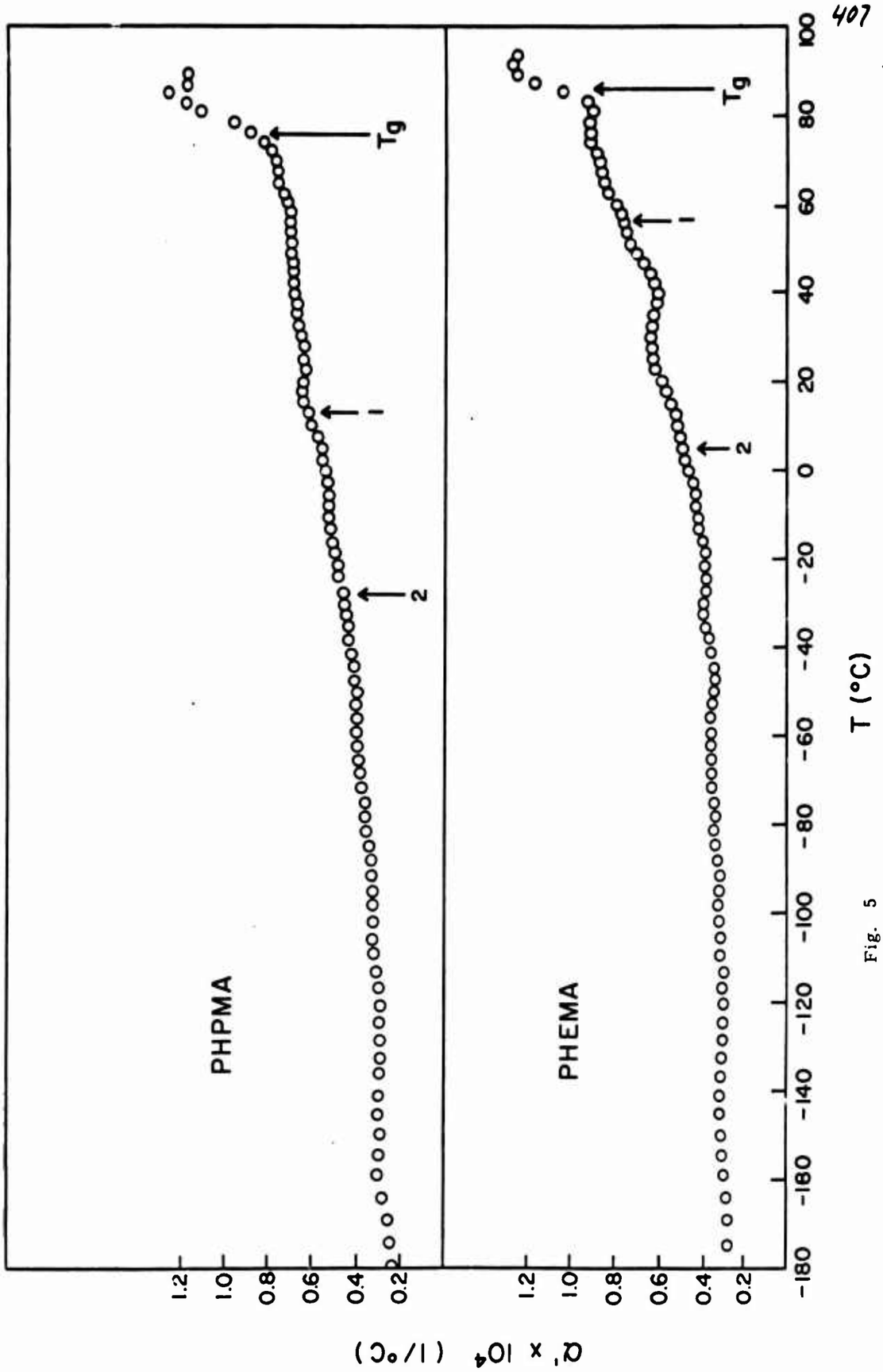
PHPMA
PHEMA
Tg
1
2
α' x 10⁴ (1/°C)
T (°C)
1.2
1.0
0.8
0.6
0.4
0.2
100
80
60
40
20
0
-20
-40
-60
-80
-100
-120
-140
-160
-180

Fig. 5

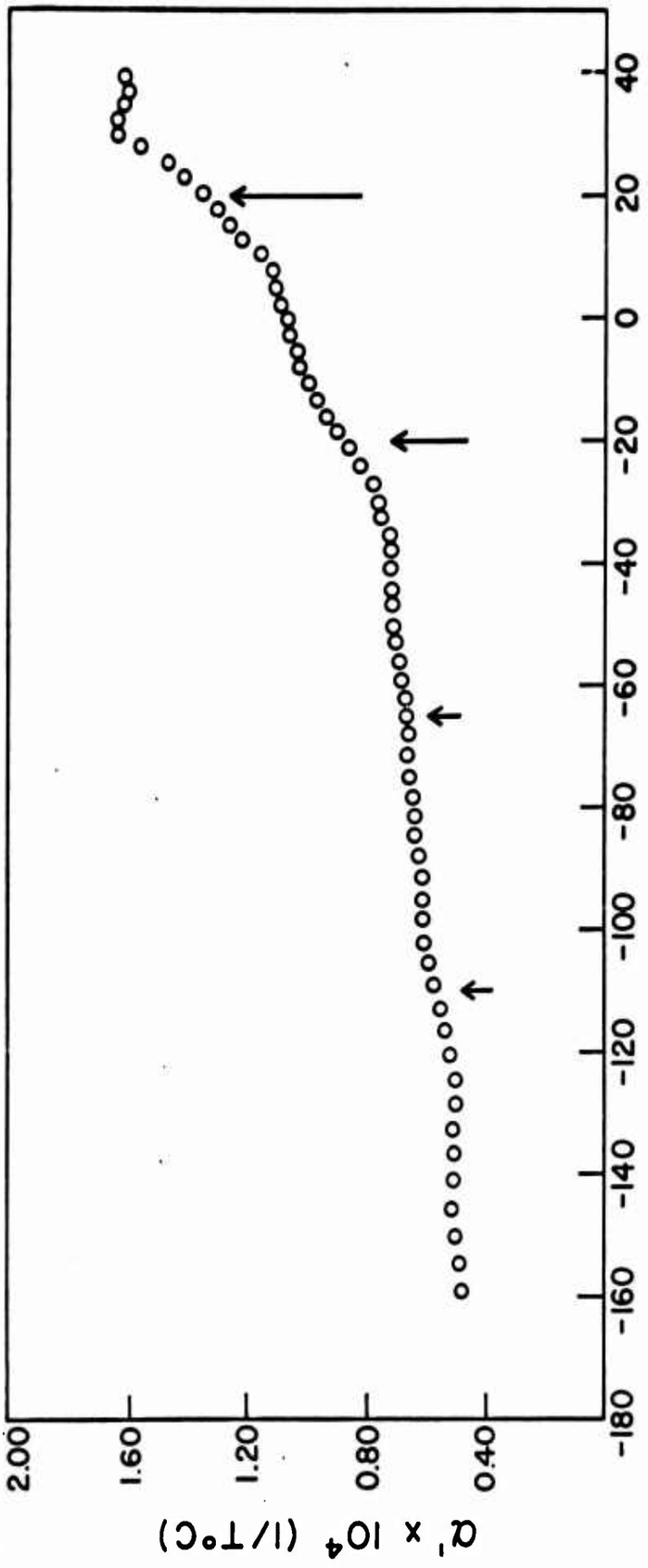
2.00
1.60
1.20
0.80
0.40
α' x 10⁴ (1/T°C)
-180
-160
-140
-120
-100
-80
-60
-40
-20
0
20
40
(T °C)

Fig. 6

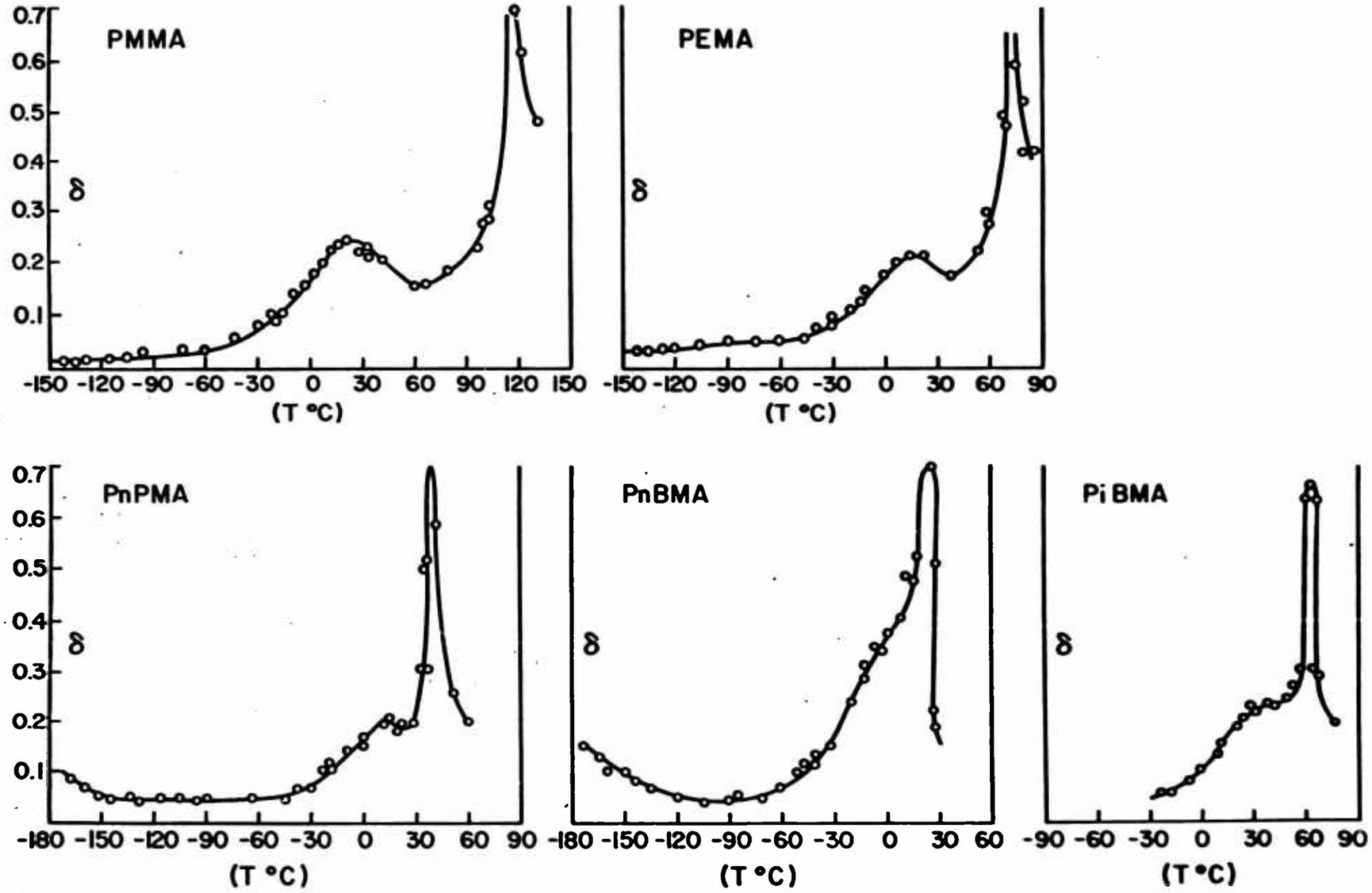
PMMA
PEMA
PnPMA
PnBMA
PiBMA
δ
0.7
0.6
0.5
0.4
0.3
0.2
0.1
-150 -120 -90 -60 -30 0 30 60 90 120 150
-150 -120 -90 -60 -30 0 30 60 90
-180 -150 -120 -90 -60 -30 0 30 60 90
-180 -150 -120 -90 -60 -30 0 30 60
-90 -60 -30 0 30 60 90
(T °C)

F. . 7

PROPERTIES OF ETHYLENE-METHACRYLIC ACID COPOLYMERS AND THEIR SODIUM SALTS: MECHANICAL RELAXATIONS

W. J. MacKnight† L. W. McKenna* and B. E. Read**
Chemistry Department and Polymer Science and Engineering Program
University of Massachusetts, Amherst, Massachusetts

ABSTRACT

A study has been made of the mechanical relaxation behavior of an ethylene-methacrylic acid copolymer containing 4.1 mole percent acid units and its partially ionized sodium salts. Degrees of ionization, estimated from infrared analysis, ranged from 0% to 78%. The weight percent crystallinity of the samples, determined by differental scanning calorimetry, varied from about 15 for the acid copolymer to about 7 for the 78% ionized copolymer. Four relaxation regions have been observed. They are labelled α, β', β and γ and each have been assigned to motions within the amorphous phase of the polymer. In plots of the logarithmic decrement against temperature (at 1 c/s), the α peak for the annealed acid copolymer occurs at 50°C and shifts to higher temperatures with increasing degree of ionization. This trend is consistent with the increase in melt flow viscosity with increasing ionization and, on this basis, the α process is attributed to the long-range diffusional motions of chain segments. The β' peak occurs at 23°C for the annealed acid copolymer and decreases in magnitude with increasing ionization. Hence the β' mechanism is attributed to the microbrownian motions of chain segments involving the breaking and reforming of intermolecular hydrogen bonds between dimerized carboxylic

acid groups. The latter assignment is supported by infrared studies of hydrogen bonding as a function of temperature. The β peak is absent for the acid copolymer but appears at -10°C for the ionised polymers and increases in height with increasing ionisation. Thus the β process is attributed to motions of branched chain segments including the ionic (carboxylate) side groups. The onset of the γ peak is observed at -120°C and is associated with the local motions of linear methylene sequences. The observation that the β peak is located at a temperature very close to the β peak (-20°C) for ordinary branched polyethylene, must cast considerable doubt on the widely held view that the ionic side groups are associated to form strong interchain links. Alternative hypotheses are suggested to explain the increase in ultimate tensile strength and melt flow viscosity with increasing ionisation.

+ To whom all correspondence should be addressed.
* On leave from the Monsanto Company, Springfield, Massachusetts.
**Visiting scientist on leave from the Molecular Science Division, National Physical Laboratory, Teddington, Middlesex, England.

INTRODUCTION

It is well known that the ionization of the carboxylic acid groups of copolymers of ethylene and methacrylic acid has profound effects on the properties of these systems[1]. In particular, the melt flow viscosity and ultimate tensile strength undergo marked increases upon ionization. These increases seem to depend on both the nature of the cation and the degree of ionization. Such effects have been attributed to the formation of strong interchain links by the association of the ionic side groups. It should be pointed out that, in view of the non-polar nature of the medium, it is probable that the ionized side groups consist of sodium carboxylate ion pairs rather than dissociated salts. In this paper are reported the results of a dynamic mechanical study of an ethylene-methacrylic acid copolymer as a function of degree of ionization with sodium hydroxide. Further studies are in progress involving both other cations and varying acid contents of the copolymer.

The structure of the acid copolymer studied may be represented schematically as

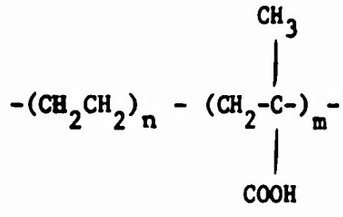

The methacrylic acid content of the copolymer is 4.1 mole percent. For a random distribution of methacrylic acid groups, this would yield an average

value of n of about 25 (for m = 1). It should be pointed out, however, that the methacrylic acid units may have a tendency to exist in blocks (m > 1). In this case the sequence length of many of the ethylene units would be much greater than 25.

EXPERIMENTAL

The starting material was a partially ionized copolymer of ethylene and methacrylic acid kindly supplied by the duPont Company. This copolymer was prepared by a free radical, high pressure process. It is known that this type of copolymerization usually leads to a random copolymer. However, there may be some tendency for the methacrylic acid units to exist in blocks and there seems to be evidence supporting this possibility[2].

The finely divided starting material was refluxed in tetrahydrofuran with dilute hydrochloric acid in order to produce the unionized copolymer. Oxygen analysis established that it contained 4.1 mole percent of methacrylic acid units. The acid copolymer was then refluxed with sodium hydroxide in tetrahydrofuran for varying periods of time and at different base concentrations to obtain the desired degrees of ionization. After this treatment, the ionized copolymers were precipitated twice in a methanol-water mixture, washed thoroughly several times, and dried in vacuo at 100°C. Samples were prepared for mechanical testing by compression molding at 180°C and 20,000 pounds pressure. Quenching was carried out by removing the mold from the press and immediately plunging it into dry ice. Samples were annealed at 95°C for 3 1/2 hours followed by slow cooling to room temperature over a 7 - 8 hour period.

Characterization of the samples thus prepared was accomplished by infrared spectroscopy and differential scanning calorimetry (DSC). The details of the methods are described elsewhere[2].

Dynamic mechanical measurements were made with a torsion pendulum of a design due to Nielsen[3]. All measurements were carried out in a dry nitrogen atmosphere. The nominal frequency was 1 cycle per second.

RESULTS

Table I summarizes the characterization results. The percent ionization was determined using the integrated absorbance per cm. sample thickness of the -COOH carbonyl stretching frequency at 1700 cm^{-1}. Temperature T_m, T_1 and T_2 are illustrated on the schematic DSC plots shown in Fig. (1). T_m, designated the melting temperature, remains practically constant over the entire range of ionization as does T_1, the minimum peak height temperature of the melting endotherm. On the other hand, T_2, the temperature of the maximum of the crystallization exotherm, shows a marked decrease with increasing ionization. It is possible that this is a consequence of the increase in the melt viscosity accompanying ionization. If the crystallization process were diffusion controlled it would be expected that greater supercooling would occur at higher degrees of ionization. The weight percent crystallinity is seen to decrease from a value of about 15 weight percent for the unionized copolymer to about 7 weight percent for the 78 percent ionized copolymer. This shows that all the samples have relatively low degrees of crystallinity as measured by the DSC technique.

The storage modulus, G', is plotted as a function of temperature in Figs. (2) and (3) for the quenched and annealed samples respectively. Fig. (2) shows that the low temperature moduli decrease with increasing ionisation while Fig. (3) shows that the difference in the low temperature moduli are decreased somewhat by annealing.

Fig. (4) shows plots of the logarithmic decrement, Λ, versus temperature for the quenched samples. In all cases, the onset of a low temperature loss peak at about -120°C may be seen. This is clearly due to the so-called γ relaxation observed also in polyethylene. In addition to the γ relaxation, the unionized acid copolymer exhibits a single loss peak at 25°C. As ionization increases, an additional loss peak, designated β, starts to develop at -10°C. This β peak increases in magnitude with increasing ionization.

For the annealed samples, Fig. (5) shows that the high temperature peak for the unionized acid copolymer splits into two peaks with maxima at 23°C and 50°C, designated β' and α respectively. The β' relaxation decreases in magnitude with increasing ionization and has virtually disappeared at 60% ionization. The α relaxation moves to higher temperature with increasing ionization. The splitting of the α peak in the 78% ionized sample may be due to overlap caused by the onset of melting.

The loss moduli, G", are plotted as a function of temperature in Figs. (6) and (7). Owing to the decrease of G' with increasing temperature these plots have the usual effect of de-emphasizing the magnitude of the α peak and enhancing that of the γ peak relative to the Λ plots. (G" G'Λ/π). Otherwise, the same trends are noted with the β and β' peaks

as in the case of the Λ plots except that a small β peak appears as a low temperature shoulder on the main β' peak of the unionized acid copolymer.

DISCUSSION

Inasmuch as the acid content of the copolymer is quite low and that infrared analysis[2] has indicated that there are approximately 5 - 10 short chain branches per 1000 main chain carbon atoms, it might be expected that the mechanical relaxations of the material would be similar to those observed in low density (branched) polyethylene at one cycle per second. The latter polymer exhibits three loss peaks[4], the α relaxation at about 50°C, the β relaxation at about -20°C, and the γ relaxation at about -120°C. These relaxations have been investigated by numerous authors[5]. The α peak seems to be due in part to motion in both the crystalline lamellae and the amorphous interlamellar regions[6-8,12] while the β peak seems to arise from the motion of branched chain segments in the amorphous phase[9]. The β relaxation in low density polyethylene may thus be related to the glass transition of the polymer[10]. The γ relaxation has been attributed to motions of short methylene sequences and both amorphous[11] and crystalline[6,7] mechanisms have been proposed.

Since the copolymers studied here have very low degrees of crystallinity, it is probable that all the relaxations observed in these polymers originate mainly in the amorphous phase.

THE α RELAXATION

The increase in magnitude of the α peak with increasing ionization

supports an amorphous origin for this peak since the amorphous content also increases with ionization. The fact that the α peak moves to higher temperatures with increasing ionization further suggests that it is due mainly to long range diffusional motions similar to those responsible for melt viscosity. This proposal is consistent with the observation that the partially ionized copolymers have larger melt viscosities than the unionized copolymer. The present results would thus seem to support an interlamellar slip mechanism for the α' type discussed by McCrum and Morris[12] which involves a viscous flow process of amorphous interlamellar material. In our view this relaxation would seem to be similar to the viscous flow regions in linear amorphous polymers, but rendered reversible by the tie points introduced by the lamellae.

THE γ RELAXATION

The γ relaxation is most evident from the G" plots (Figs. (6) and (7)) at low temperatures. Since the copolymers studied have very low crystalline contents it would seem that the γ mechanism must occur largely in the amorphous phase. Hence these data are consistent with the proposed "crankshaft" type motions of linear methylene sequences[11].

THE β' RELAXATION

The β' peak is uncovered in the Λ plots by annealing, which has the effect of increasing the temperature of the α relaxation. It is known from the infrared results[2] that the unionized carboxylic acid groups exist almost entirely in the form on interchain, hydrogen bonded dimers and the first appearance of free hydroxyl groups occurs at about 35°C. In

In view of these results and the fact that the magnitude of the β' relaxation decreases with increasing ionization, it is proposed that the β' relaxation is due to the motions of branched chain segments and involves the breaking and reforming of interchain hydrogen bonds. The mechanism is thus similar to the β mechanism in branched polyethylene except that the microbrownian motions associated with the glass transition are retarded by the hydrogen bonding. It should be pointed out that this interpretation is in accord with the views of Andrews[13] who explains amorphous relaxations in terms of the thermal breakdown of intermolecular secondary bonding of various types.

THE β RELAXATION

Since the β relaxation shows a marked increase in magnitude with increasing ionization it must be associated with the ionized carboxylate groups. Several authors[1,14,15] have expressed the opinion that ionization with both monovalent and divalent cations in ethylene-methacrylic acid copolymers and other systems leads to increased interchain bonding due to the introduction of ionic links. However, the present results cast doubt on this interpretation, at least in the case of the ethylene-methacrylic acid copolymers since the relaxation occurs at a lower temperature than the β' relaxation associated with the breaking of interchain hydrogen bonds. Thus if ionization with sodium in the ethylene-methacrylic acid copolymers studied leads to the introduction of interchain ionic bonds, such bonds must be weaker than the hydrogen bonds of the unionized acid groups. Moreover, the β relaxation in the ionized copolymers occurs at a

temperature (-10°C) quite close to that of the β relaxation in conventional low density polyethylene (-20°C). Therefore, the β process in the copolymers is attributed to motions of branched chain segments including the carboxylate side groups. Hence, ionic interchain bonds, if they exist at all, must be extremely weak, placing little restriction on the microbrownian segmental motion responsible for the β relaxation.

It would thus appear unlikely that the enhanced melt viscosity and ultimate tensile strength accompanying the ionization of the copolymers is due to the introduction of strong interchain ionic forces. The melt viscosity results might be explained on the basis of ionic repulsions which would tend to interfere with the translational motions of chains. In this connection it is interesting to note that in a study of ionized styrene-methacrylic acid copolymers, Erdi and Morawetz[14] found that while the tensile viscosity increased with ionization the activation energy for viscous flow showed the reverse trend. The latter result is consistent with the present observations and suggests that the basic event in the viscous flow process, namely short range segmental motion, occurs more easily for the ionized copolymers.

The ultimate tensile strength results are in accord with the findings of Mullins[16] for the case of natural rubber. He attributes this to the fact that weak crosslinks such as polysulfide links can break under stress thus relieving local regions of high stress concentration and enhancing the ultimate tensile properties of the material. If ionization in fact decreases the strength of intermolecular bonding then the same explanation might apply to the enhancement in tensile strength observed in the ionized

acid copolymers.

The quantitative elucidation of the effects of ionization on the mechanical properties of ethylene-methacrylic acid copolymers as well as that of cations of different size and charge is currently under investigation and will be reported in the future.

ACKNOWLEDGEMENTS

One of us (William J. MacKnight) is grateful to the National Science Foundation for partial support of this research under Grant GP 5840.

We are indebted to Dr. J. W. Brondyke of the Plastics Department of the duPont Company for supplying the starting material and to Professor Richard S. Stein for many helpful discussions.

REFERENCES

1. R. W. Rees and D. J. Vaughn, Polymer Preprints 6, 296 (1965).
2. W. J. MacKnight, L. W. McKenna, B. E. Read and R. S. Stein, to be published.
3. L. E. Nielsen, Rev. Sci. Instr. 22, 690 (1951).
4. S. G. Turley and H. Keskkula, J. Polymer Sci. C14, 69 (1966).
5. N. G. McCrum, B. E. Read and G. Williams, "Anelastic and Dielectric Effects in Polymeric Solids," Wiley, New York, Chapter 10, 1967.
6. M. Takayanagi, Proceedings of the Fourth International Congress on Rheology, Part I, pp. 161-187, Interscience, New York, 1965.
7. K. M. Sinnott, J. Polymer Sci, C14, 141 (1966).
8. J. D. Hoffmann, G. Williams and E. Passaglia, ibid, p. 173.
9. D. K. Kline, J. A. Sauer and A. E. Woodward, J. Polymer Sci. 22, 455 (1956).
10. L. E. Nielsen, J. Polymer Sci. 52, 357 (1960).
11. T. F. Schatzki, J. Polymer Sci. C14, 139 (1966).
12. N. G. McCrum and E. L. Morris, Proc. Royal Soc. A292, 506 (1966).
13. R. D. Andrews, J. Polymer Sci, C14, 261 (1966).
14. N. Z. Erdi and H. Morawetz, J. Colloid Sci., 19, 708 (1964).
15. E. P. Otocka and F. R. Eirich, Polymer Preprints 8, 66 (1967).
16. L. Mullins, paper presented at the Conference "Structure and Mechanical Properties of Polymers," Natick, Massachusetts, April 19, 1967.

TABLE I

SUMMARY OF I.R. AND D.S.C. DATA[1]

% Ionization	T_m (°C)	T_1 (°C)	ΔH_f[2] (cals. $g.^{-1}$)	Weight % Crystallinity[3]
0	100	91	9.9	14.9
20	101	91	10.7	16.2
60	100	91	8.2	12.5
78	99	86	4.6	6.9

[1] Cooling and heating rates in the Differential Scanning Calorimeter were each 10°C/min.

[2] ΔH_f = Heat of fusion.

[3] Based on a heat of fusion of 66 cals. $g.^{-1}$ for the 100% crystalline polymer.

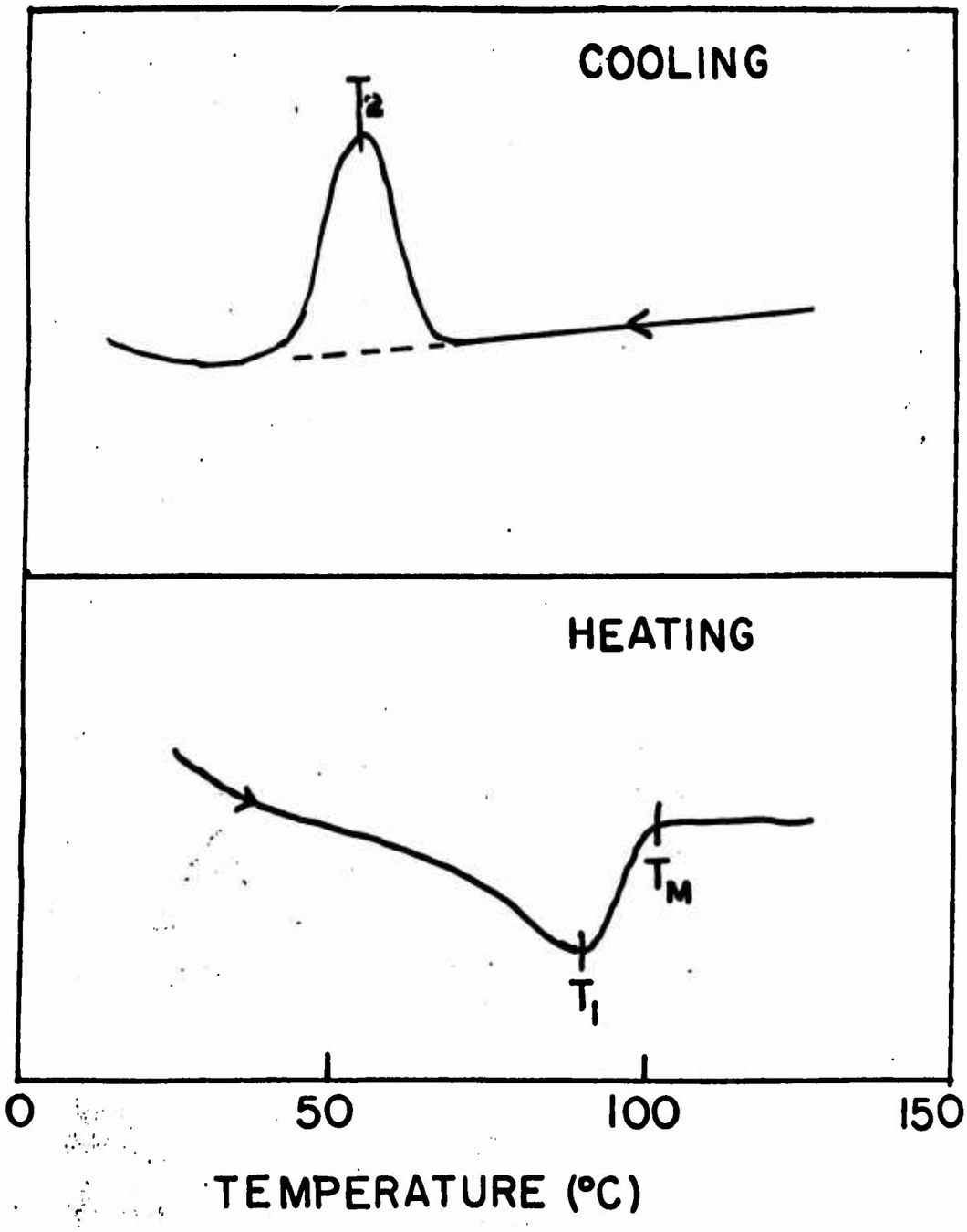

Fig. 1 - Schematic representation of differential scanning calorimetry (DSC) data showing the melting endotherm and the crystallization exotherm.

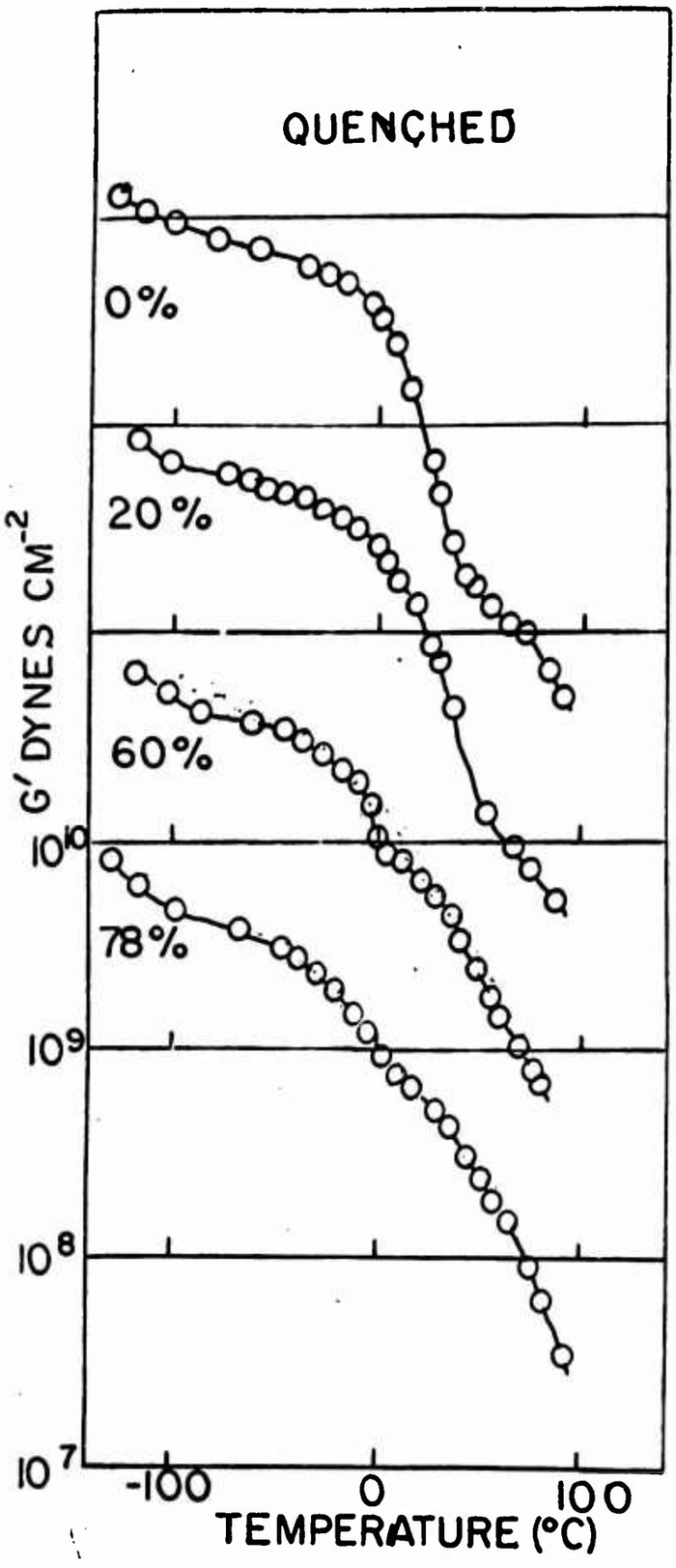

Fig. 2 - Temperature dependence of G' for quenched ethylene-methacrylic acid copolymers at various degrees of ionization. Each curve is displaced by one decade above the preceding curve.

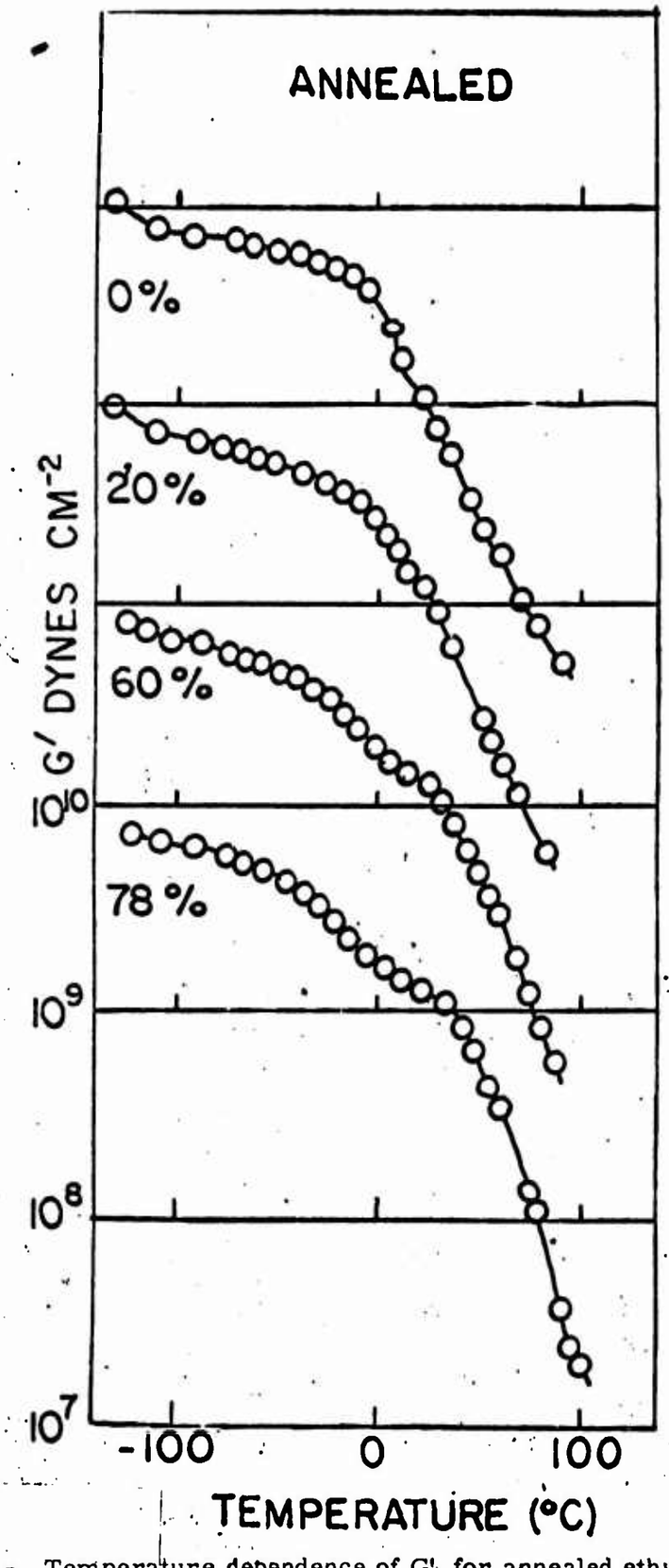

Fig. 3 - Temperature dependence of G' for annealed ethylene-methacrylic acid copolymers at various degrees of ionization. Each curve is displaced by one decade above the preceding curve.

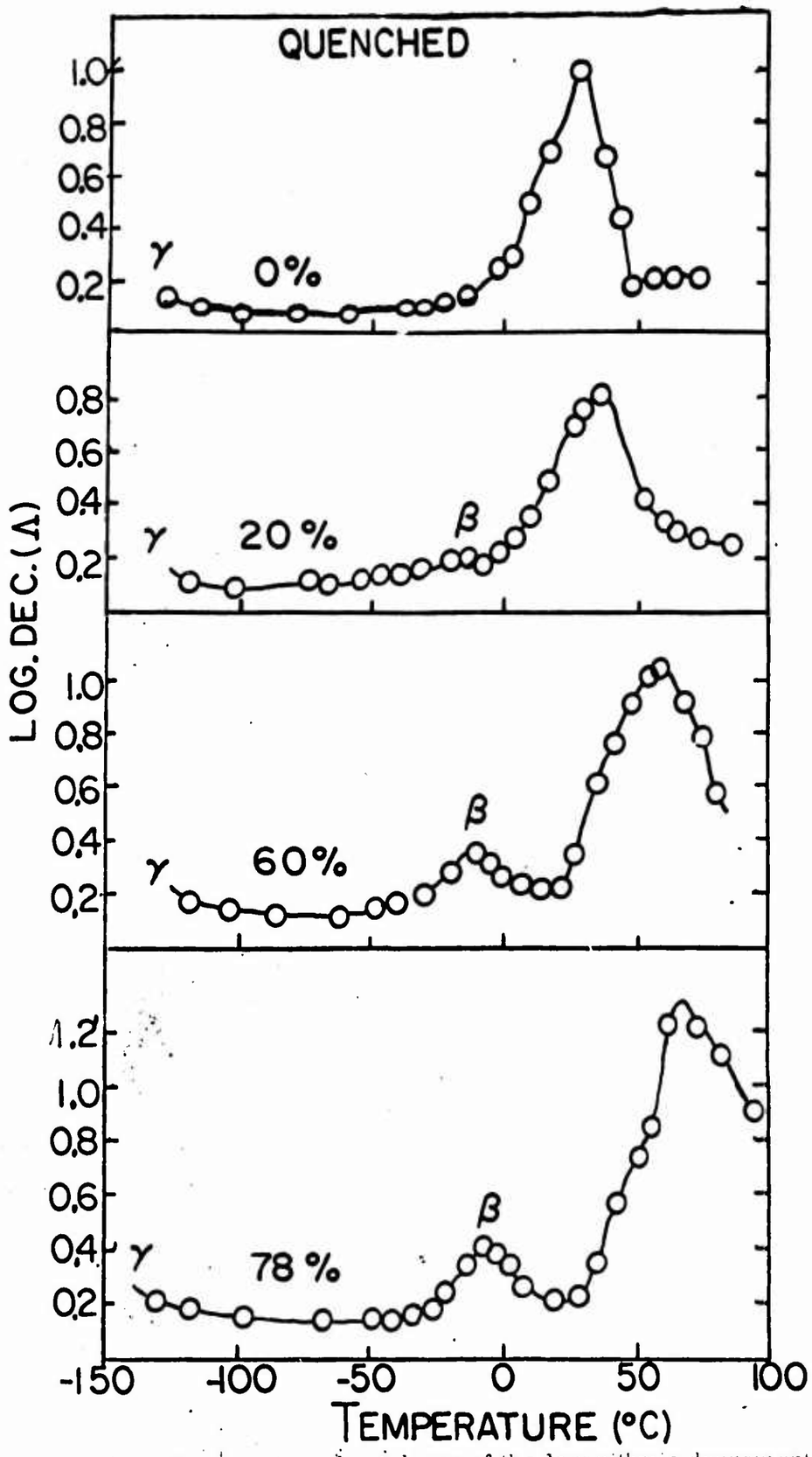

Fig. 4 - Temperature dependence of the logarithmic decrement for quenched ethylene-methacrylic acid copolymers at various degrees of ionization.

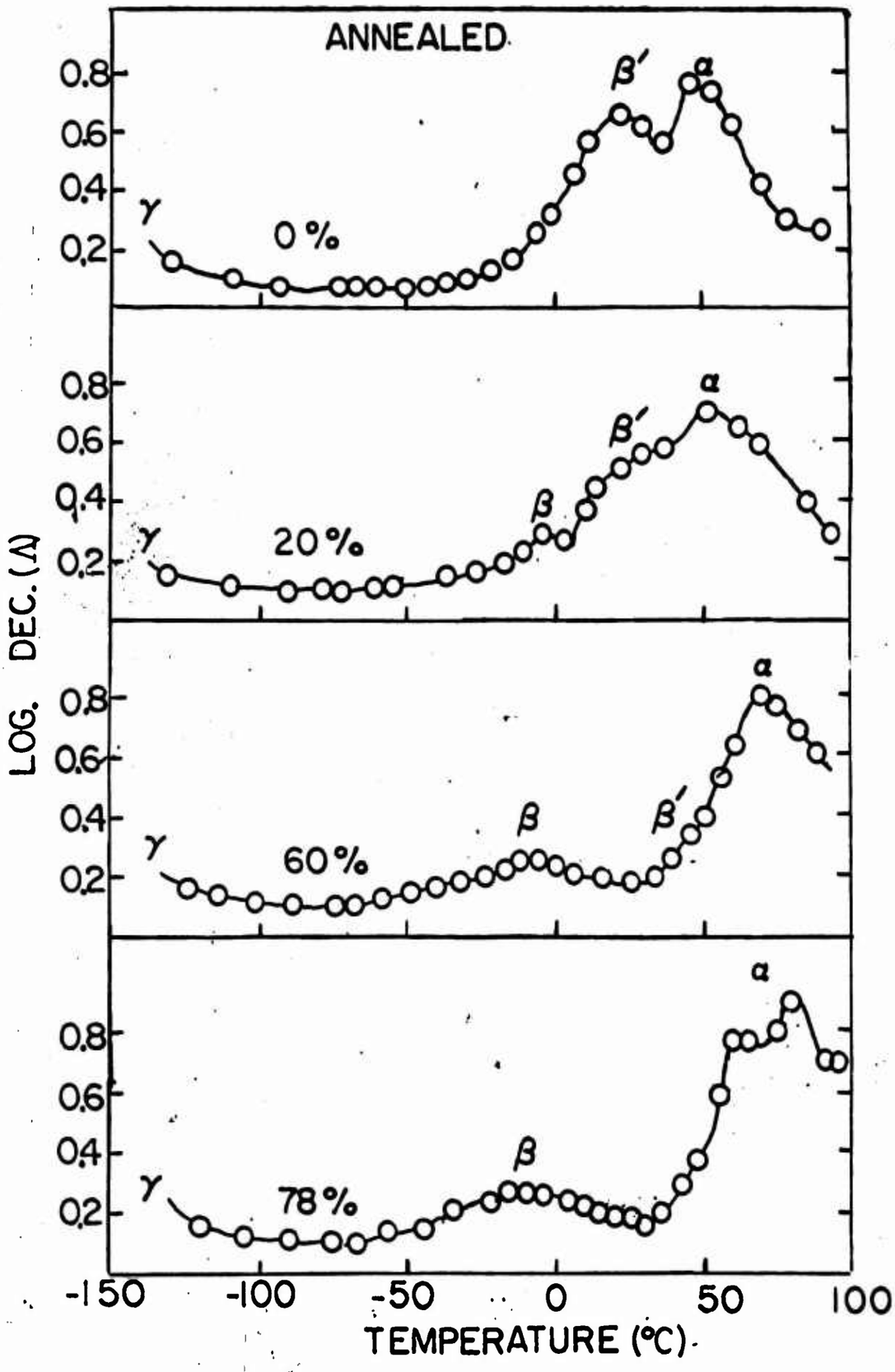

Fig. 5 - Temperature dependence of the logarithmic decrement for annealed ethylene-methacrylic acid copolymers at various degrees of ionization.

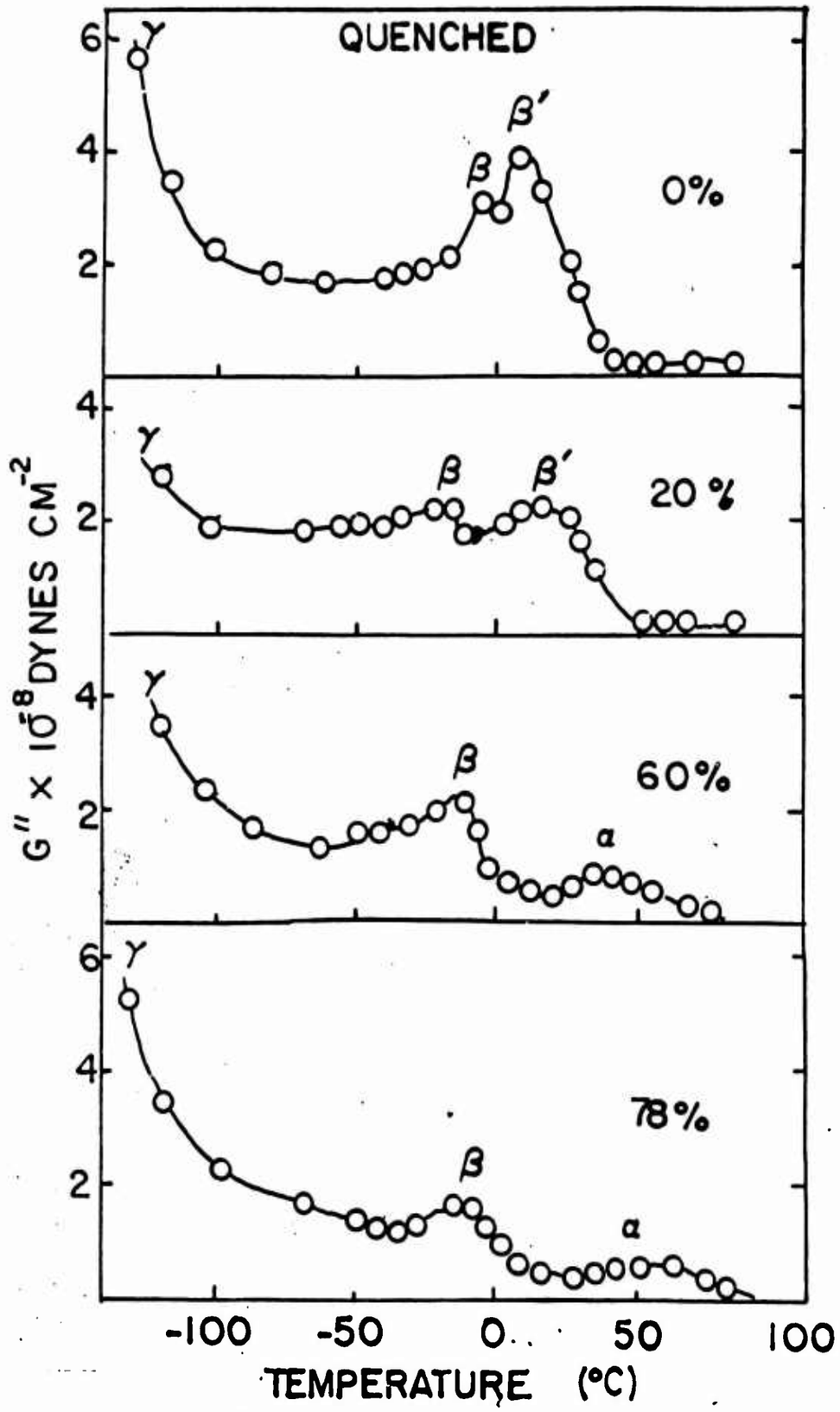

Fig. 6 - Temperature dependence of G'' for quenched ethylene-methacrylic acid copolymers at various degrees of ionization.

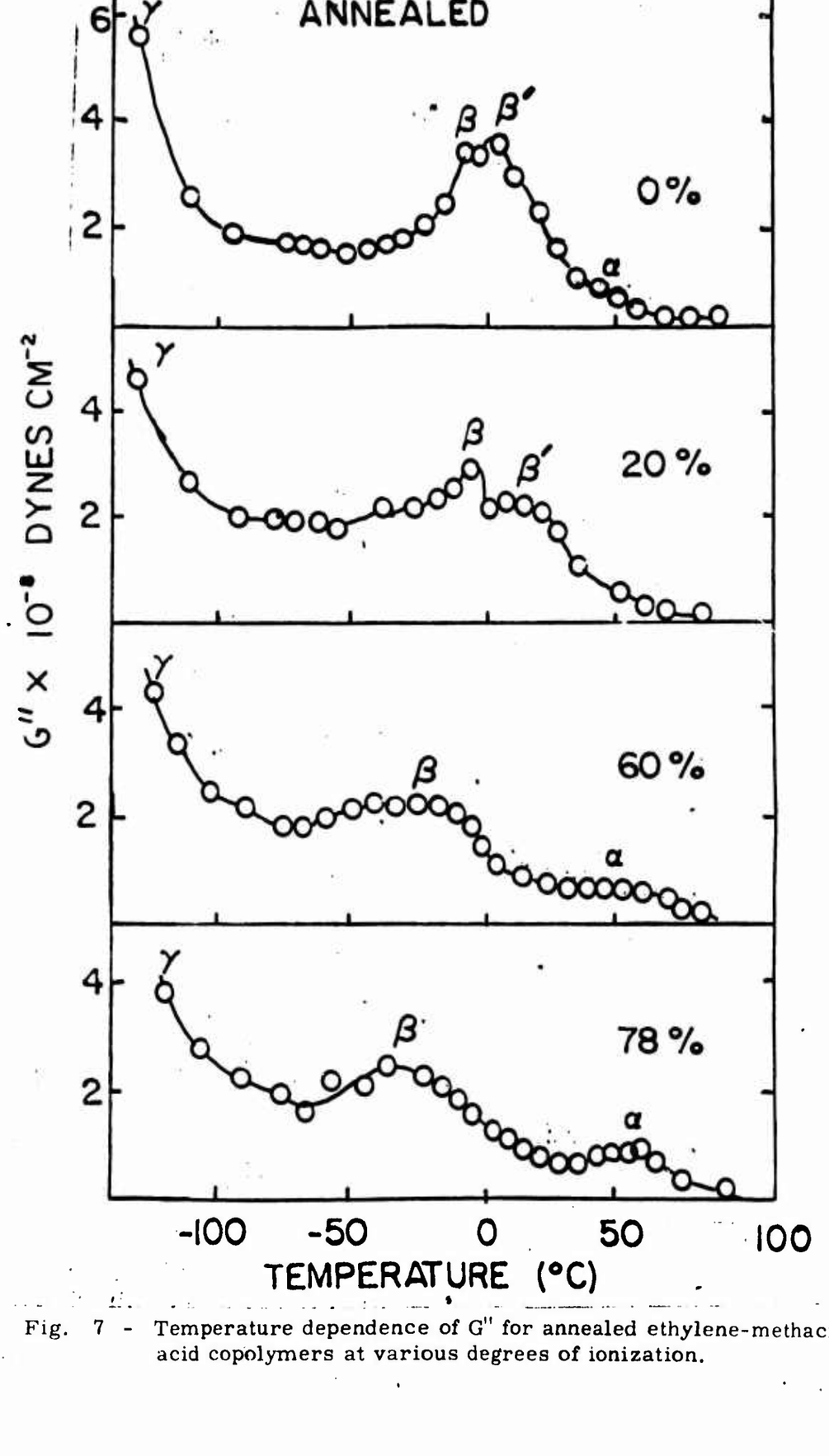

Fig. 7 - Temperature dependence of G'' for annealed ethylene-methacrylic acid copolymers at various degrees of ionization.

STUDIES IN THE FIELD OF POLYMER STRUCTURE AND MECHANICAL PROPERTIES IN THE MATERIALS SCIENCE DEPARTMENT, QUEEN MARY COLLEGE, LONDON, E.1, ENGLAND

by E. H. ANDREWS

1. Morphology and micro-kinetics of strain induced crystallization in natural rubber (Mr. P. J. Owen)

Ultrathin cast films of natural rubber (cispolyisoprene) can be crystallized at predetermined strains and at temperatures between -40°C and 10°C for study in the electron microscope[1]. Staining with osmium tetroxide vapour preserves the morphological structure, enhances contrast between crystalline and amorphous material and permits resolution better than 15 Å. At zero strain the texture is spherulitic, the spherulites (Fig. 1) consisting of lamellar and filamentous regions both limited to a dimension of some 64 Å. in the molecular chain direction (c axis). As strain is applied the filamentous structure becomes predominant and lines up perpendicular to the axis of strain. These filaments have their molecular chain direction in the direction of strain but grow along a crystallographic axis at right angles to this direction. For this reason they have been named α-filaments. The α-filaments are row nucleated (Fig. 2) from a central stem running in the strain direction and in the early stages of crystallization thus constitute a "shish-kebab" structure. With the passage of time, however, the central stem or "shish" disappears leaving only the α-filaments as in Fig. 2. The disappearance of the central stem under isothermal conditions appears to result from stress relaxation in the melt and strongly suggests that this central crystal stem is morphologically different from the α-filaments. It may consist of extended chain crystals[2] induced by the strain.

At higher strains ($>$ 300%) crystallization occurs spontaneously

at room temperature where the growth rate of α-filaments is very small, Only rows of nuclei are now apparent but their quantity is now so great as to fill the field of view. These rows of nuclei (γ-filaments) do not appear identical to the "extended chain" crystals found at lower strains, being definitely granular. They are clearly related, however, and may occur by degeneration of extended chain crystals. This effect might be similar to that obtained by annealing extended chain crystals in polyethylene. A great deal of kinetic data has been accumulated but will be published elsewhere.

2. Strength and stress-strain data on crystallized natural rubber
(Mr. P. E. Reed)

Since the microtexture of natural rubber can be varied in a controlled manner by crystallizing under different strains, and since the stress relaxes completely as a result of such crystallization, this seems an ideal system in which to study the relation between microtexture and mechanical properties. Further advantages are the use of the same starting material for all textures, the possibility of eliminating the effect of the molecular orientation by the parallel testing of orientated but uncrystallized material, and the fact that the amorphous phase can be placed at will into a glassy or rubbery condition simply by varying the temperature of test.

A great deal of work has been done along these lines using rubber crystallized at -26°C and testing in a special cryostat[3] between -26°C and -120°C. Only a sample of the results can be given here. Fig. 3 shows the ultimate breaking stress (based on cross-section area at fracture)

of a lightly vulcanized natural rubber as a function of test temperature and crystallization strain (a texture variable). The strength is little affected by texture at temperatures above about -60°C (amorphous phase rubbery), but below 80°C (amorphous phase glassy) the strength is much greater in the oriented materials then in the spherulitic ones. No similar difference is found with oriented but non-crystalline material. It appears that the oriented array of crystals allows co-operative deformation in the crystalline phase and the resulting plasticity inhibits brittle fracture and consequent low strength. This is just one example of the investigations being carried out.

3. <u>Microtexture and deformation in solid polymers studied using ultrathin sections</u> (Mr. M. W. Bennett)

A freezing ultra-microtome has been developed which allows ultrathin sections to be cut from soft polymers (e.g. low density polyethylene) and rubbers for examination in the electron microscope[4]. Such features as ringed spherulites in annealed low density polyethylene (Fig. 4) are revealed in considerable detail and may be studied before and after plastic deformation. At low rates of deformation the spherulite as a whole deforms in pseudo-affine manner but buckling is observed in the individual lamellae which compose it. At high rates, involving passage of the material through a running neck, the drawn polymer is heterogeneous consisting of (i) Spherulite kernels with recognisable rings but whose outer regions have clearly melted (ii) a "featureless" background typical of quench-cooled molten material, and (iii) lamellar regions characteristic of material crystallised from a strained melt.

4. Fatigue fracture of polyethylene (Mr. B. J. Walker)

This study is at present concerned with the macroscopic fracture-mechanics of the process, but eventually we hope to use the sectioning technique referred to earlier to study the actual generation of structural flaws. So far it has been shown conclusively that the crack growth law

$$(dc/dN) = K\mathcal{J}^n$$

applies to polyethylene (both high and low density). In this equation c is the length of a fatigue crack, N is the number of cycles, K and n are constants and $\mathcal{J}$ is a fracture parameter given by

$$\mathcal{J} = -\partial\mathcal{E}/\partial A$$

where $\mathcal{E}$ is the total elastic stored energy in the body and A is the interfacial area of the crack. Similar laws have previously been found to operate for elastomers[5], polymethylmethacrylate[6] and metals[7].

Great interest centres on the value assumed by the parameter n. In elastomers it varies from 2 to 4 and in PMMA from 2.5 to 15! In our work on polythene values of unity for a branched polymer and 3.6 for a reasonably linear one have been obtained. It is clear that the value of n is a function of the stress field geometry at the tip. In general, the sharper the tip, and the lower the plastic or hysteresial dissipation at the tip, the larger is the value of n. It is to be expected that, for polyethylene, n may be a function of temperature and this is now being investigated.

5. Stress-corrosion cracking of plastics (Mr. L. Bevan)

The propagation of a single "corrosion" crack in stressed plastics is being studied with a view to establishing the basic mechanism of environmental stress cracking. The system so far studied is PMMA in

contact with various alcohols[8]. It has been established that cracks only propagate if the parameter $\mathcal{J}$ defined earlier exceeds some critical value

$$\mathcal{J} > \mathcal{J}_c$$

Under the conditions defined by this inequality, the crack velocity is a function both of the temperature and the actual value of $\mathcal{J}$. A plot of $\mathcal{J}_c$ against temperature is constant above some value of the latter - between 15°C and 35°C according to the solvent used. Below this "critical" temperature $\mathcal{J}_c$ increases rapidly from its low value of around 1000 ergs/cm^2 (depending on the solvent) to values typical of straight mechanical fracture i.e. 10^5 ergs/cm^2. The mechanism of propagation is probably one of plasticization of a stress-dilated tip region by the solvent allowing molecular disentanglement above this "critical" temperature, but not below it.

REFERENCES

1. Andrews, E.H., Proc. Roy. Soc. A227, 562 (1964).
2. Wunderlich, B., and Arakawa, T., J. Polymer Sci. 2A, 3697 (1964).
3. Reed, P.E., J. Materials Sci. 1, 91 (1966).
4. Andrews, E.H., Bennett, M.W., and Markham, A. J. Polymer Sci. A2 in press.
5. Greensmith, H.W., Mullins, L., and Thomas, A.G., in "The Chemistry and Physics of Rubberlike Substances", p. 249, John Wiley & Sons, New York, 1963.
6. Waters, N.E., J. Materials Sci. 1, 354 (1966).
7. Paris, P.C., Proc. 10th Sagamore Army Materials Research Conf. Syracuse University Press, 1964, p. 107.
8. Andrews, E.H., and Bevan, L., in "Physical Basis of Yield and Fracture", Institute of Physics and Physical Society, (London) 1966, p. 209.

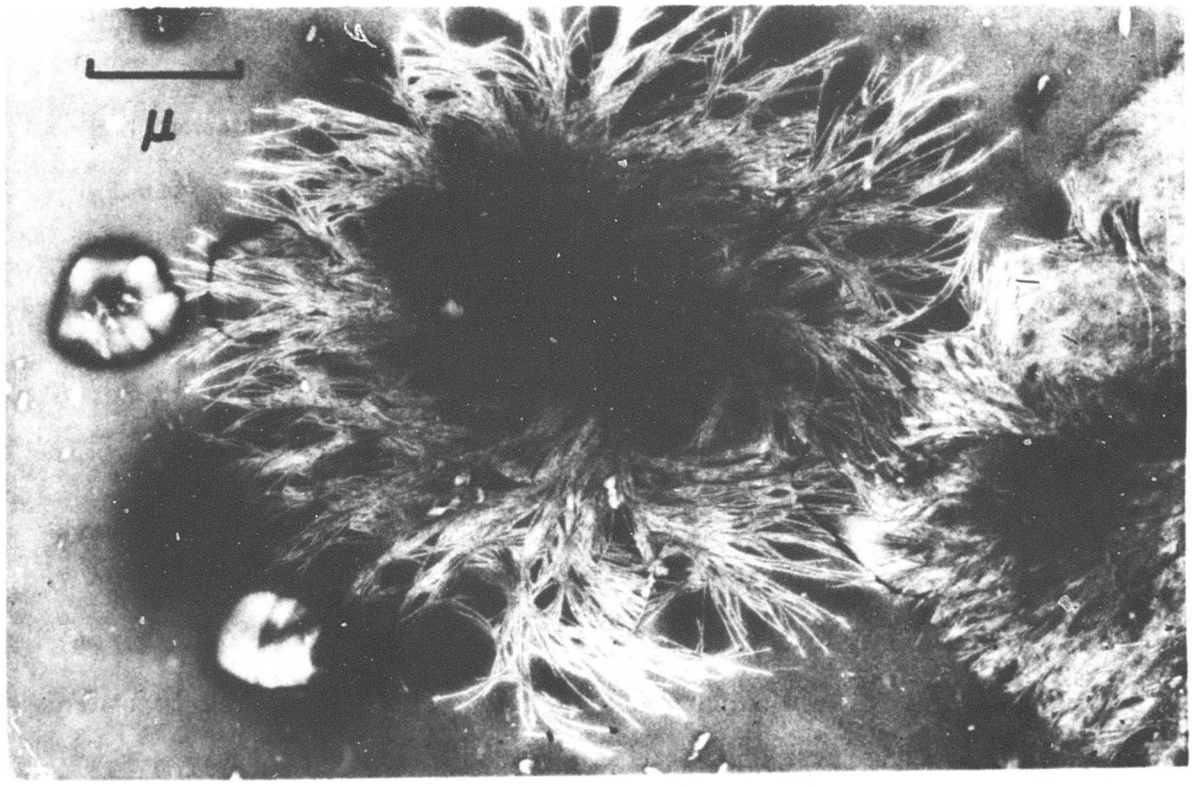

FIGURE 1. Spherulite growing in a thin film of natural rubber. The filamentous crystals, which appear white, are some 64Å wide.

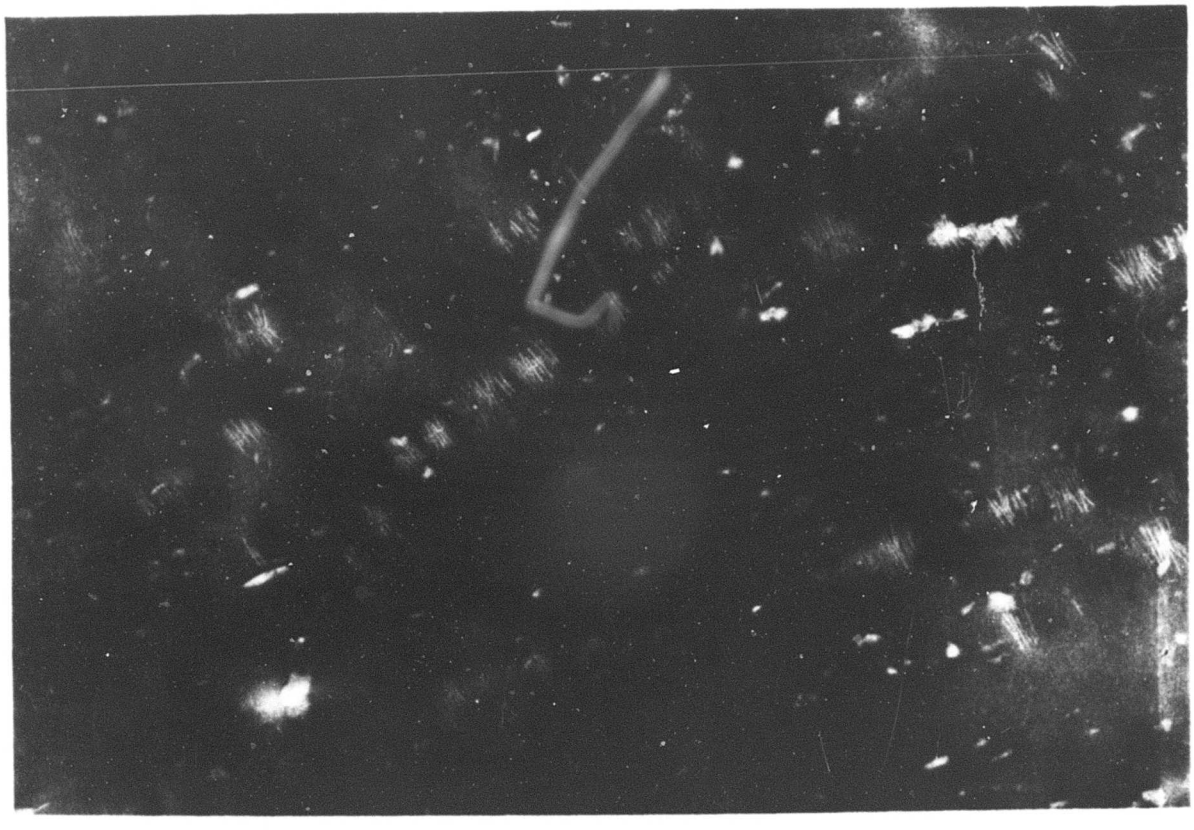

FIGURE 2. Row nucleation of α-filaments in a thin film of natural rubber held at 150% strain. The filaments are some 64 Å wide.

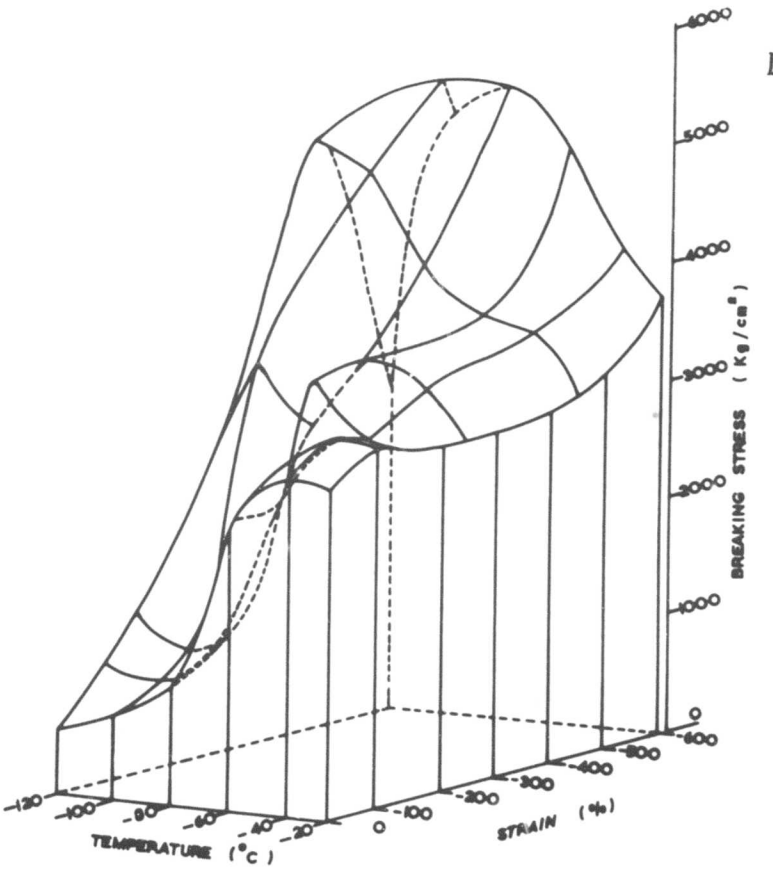

FIGURE 3. Dependence of breaking stress upon crystallization strain (i.e. changing morphology) and test temperature for crystallized natural rubber (Date of P.E. Reed).

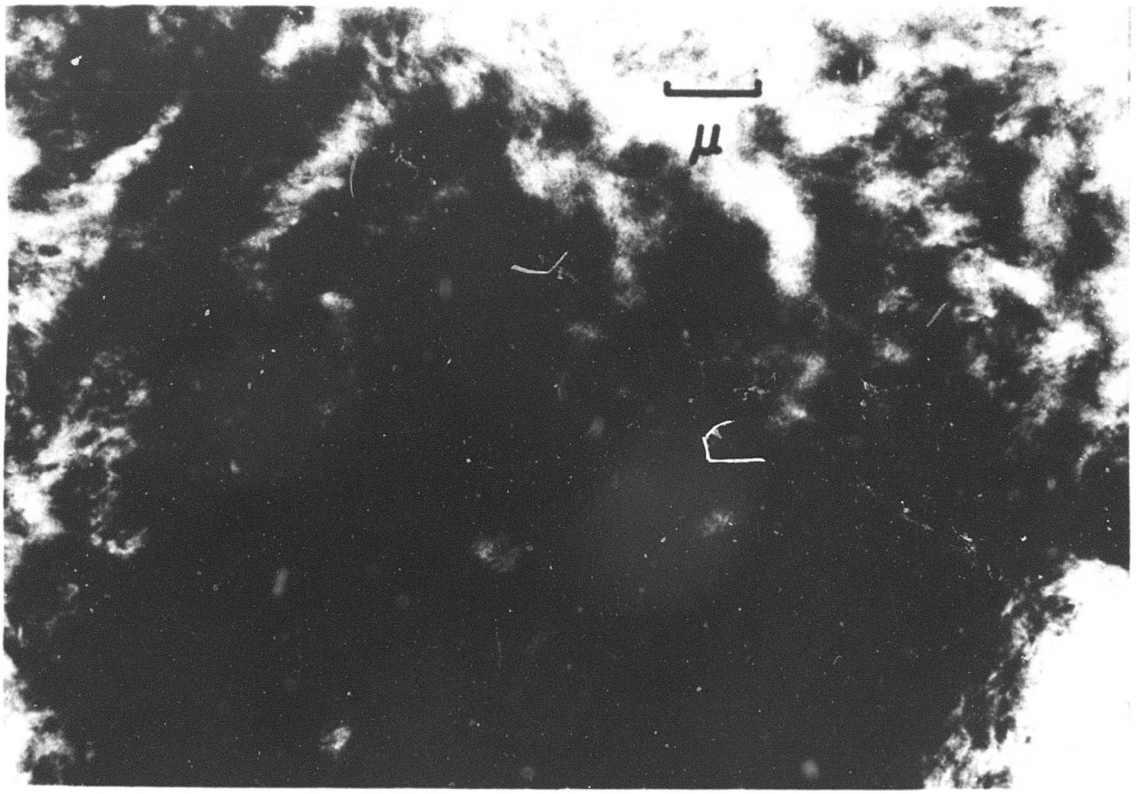

FIGURE 4. Transverse section of a ringed spherulite in annealed, branched polyethylene. The spherulite has been deformed normal to the plane of the section. The repeat distance of the dark rings is one micron and the lamellae of which they consist are approximately 200 Å thick.

437

COMMENTS ON VISCOELASTIC TRANSITIONS AND THE PROPOSED LIQUID-LIQUID TRANSITION IN POLYSTYRENE

Donald J. Plazek*

Mellon Institute
Pittsburgh, Pennsylvania 15213

*Present Address: Metallurgical and Materials Engineering
University of Pittsburgh
Pittsburgh, Pennsylvania 15213

Polymer scientists often use the word transition to refer to a change which is exhibited in a property and not in a material. This kind of transition is a rather sudden change in the value or the derivative of a property as a function of temperature or time (equivalently frequency). Such changes alone do not imply that a change occurs in the state of the material: i.e. phase changes, order-disorder transitions, degradation. Other substantiating evidence is necessary before it can be concluded that a change in property reflects a change in state.

Therefore an abrupt change in the slope of a volume-temperature curve of a polymer need not necessarily indicate a change in state. A viscoelastic transition refers to time* or frequency dependent changes in level of modulus or compliance which characterize the material in a particular state. In making linear viscoelastic dynamic (sinusoidal) measurements as a function of frequency the results should be and often are tested to be independent of the sequential order of measurement. At a given temperature and frequency, measurements made on different days must yield the same results.

*Time, here, is an experimental variable. During the passage of experiment time the character of the material is assumed invariable.

It has been suggested that the word transition be abandoned when referring to viscoelastic transitions because at times some have been mistakenly identified with thermodynamic changes in state. Dispersion and relaxation phenomenon are alternate terms that could be used without ensuing confusion. Dispersion has been criticized[1] on the bases that this word was first used to refer to the variation of refractive index with wavelength. However, it has subsequently been used to refer to the variation with wavelength of optical activity and to the frequency dependence of the complex dielectric constant. It does not appear to be unreasonable to extend the meaning of dispersion to include the frequency or wavelength dependence of any property. Because of the equivalence of creep or stress relaxation times, t, to the reciprocal of the dynamic angular frequency, ω, the change of level of strain or stress with t should be included. $\omega = 2\pi\nu$ where ν, $sec.^{-1}$, is the frequency. The words dispersion and relaxation are at present used by some in the polymer science community. Most certainly, the confusion in terminology started with the dispute over the nature of the glass "transition", T_g, which is now widely acknowledged to be kinetic; a relaxation phenomenon. Perhaps other loose talk like the freezing out of motions at T_g has also contributed to the confusion. Ample evidence exists to show that the viscoelastic mechanisms that are so prominent at temperatures above T_g are present at temperatures below at greatly enhanced times;[2,3] even though all of the mechanisms may not have the same temperature dependence and the distribution function of retardation or relaxation times may be distorted. Another practice which can be misleading is the association of a temperature

with a viscoelastic relaxation phenomenon or loss peak unless an associated frequency is specified. Within the realm of the experimentally accessible frequency range many mechanical loss peaks can be found at temperatures differing by more than 100°C.[4]

The purpose of these comments made here is to explore the principal arguments made by Dr. Boyer[5] for the existence of a liquid-liquid transition, $T_{l,l}$ in polystyrene. $T_{l,l}$ is one of many transitions which have been identified with some kind of thermodynamic change in the material on the evidence of both volume - temperature and viscoelastic measurements. Additional evidence has been proposed for $T_{l,l}$ which is claimed to be a second-order transition associated with the "freezing" of motion of molecular centers of gravity. At the same time the transition is identified as a relaxation and is said to be "strongly rate dependent."

In his summary paper Dr. Boyer said,[5] "Any proposed transition which is based on a change from segmental to cooperative action of entire polymer chains must shown up in melt viscosity data." Since all of the polymers examined recently in a review article on the viscous flow of polymers[6] could be fitted to the WLF free volume equation[7] or any equivalent form, no evidence for the $T_{l,l}$ transition can be claimed as showing up in the melt viscosity, η. To illustrate this specifically for polystyrene we have presented data in Figure 1 obtained on five samples[8] with molecular weights that range from 3.4×10^3 to 6.0×10^5. The data are plotted according to a linearized form of a free volume expression.[7]

$$\text{Log } \eta = \text{Log } A + \frac{C/2.303}{T - T_\infty}$$

η is given in poise; A, C, and T_∞ are characterizing constants. The lack of deviation from this form over the large temperature ranges shown argues against

any change in mechanism of flow in any of the samples represented. Dr. Boyer's analysis of older and less extensive data on polystyrene yields results which differ somewhat from the WLF form.

A second piece of evidence presented for $T_{l,l}$ in polystyrene is an endothermic differential thermal analysis, DTA, peak observed at 154°C for a sample with a molecular weight of 82,000. To observe the "transition" fast cooling, by plunging hot polystyrene into water, is required. This requirement quickly brought to mind our experience in purging samples of polystyrene of residual plasticizers preceding creep measurements.[8] Previously freeze-dried samples always burst into foam in vacuo at temperatures between 150°C to 170°C releasing what only could have been absorbed water vapor. In collaboration with Dr. Joseph H. Magill the hypothesis that the above endothermic peak was the evolution of steam was checked out with a Perkin Elmer Differential Scanning Calorimeter, DSC. The peak was found to be present between 170°C to 180°C (20°/min heating rate) regardless of the previous cooling rate so long as the sample was exposed for sufficiently long times to a high humidity. After the water vapor was driven off, recycling the temperature revealed no transition between 110°C to 200°C.

Isothermal measurements should not reveal thermodynamic transitions except when a system is not at equilibrium but tends in the direction of equilibrium with the passage of time. The determination of crystallization rate at a temperature below the melting point, T_m, is an example of such a measurement; but note that the material being measured is in a different thermodynamic state after being measured.

We repeat here that before and after a proper measurement of viscoelastic behavior as a function of time or frequency the material being studied is the same thermodynamically in every way. During isochronal measurements of dynamic mechanical parameters (such as the storage modulus and the loss tangent) made as a function of temperature such parameters can exhibit changes as thermodynamic transitions are approached. For example, as the melting temperature is approached from below, imperfect crystallites melt and the loss tangent increases substantially because of the higher losses occurring in the amorphous material. Here again the material is changing its thermodynamic character and such changes will always be tied to a particular temperature regardless of the frequency of measurement It is to be expected that the magnitude at a particular temperature will vary with frequency but the position of the loss peak associated with melting will not move appreciably from the measured melting point. A melting point loss peak, of course, will only be observed for a crosslinked or an extremely high molecular weight sample. The viscosity must be high at the melting point or the viscous loss, $1/\omega\eta$, will dominate and the loss tangent will increase monotonically with increasing temperature.

I have presented the reasons why viscoelastic dispersions, which are functions of time or frequency, usually should not be directly associated with thermodynamic transitions. If a loss peak seen as a function of ω is clearly absent below a given temperature and is present above (or vice versa) then and only then can it be inferred from isothermal viscoelastic measurements that the material changed its character at the given temperature. I do not believe that Dr. Boyer's appeal to the isothermal viscoelastic data of several authors[9,10,11] fulfills the requirements indicated above. In addition it can be seen in

Figure 2 that the recoverable creep compliance, $J_p(t) - t/\eta_p$, shown logarithmically as a function of Log t at 10 temperatures for a polystyrene of molecular weight 1.22×10^5, gives no indication of a second long-time dispersion at any of the temperatures[12] which is supposed to indicate the existence of $T_{l,l}$. $J_p(t)$ is the creep compliance; subscript p indicates a small rubberlike temperature dependence correction. These measurements extend to slightly higher temperatures than those stress relaxation measurements[11] referred to by Dr. Boyer. Finally, notice in Figure 2 that the transition observed, commonly called the rubberlike to glasslike transition zone[13], does not belong to any specific temperature. In fact we[8] have been able to measure part of this dispersion near 80°C as have Tobolsky, Aklonis, and Akovali[11] on similar samples. This is substantially below the conventional T_g ($\simeq$ 97°C) of this sample.

I conclude, based on the preceding remarks, that none of the evidence for the $T_{l,l}$ transition is compelling and suggest caution be exercised by those who would infer thermodynamic changes in a material from the presence of wrinkles or bends in viscoelastic or volume functions of temperature.

ACKNOWLEDGEMENT

I wish to acknowledge and thank Dr. Raymond Boyer for communicating in advance of this publication his thoughts on our differing opinions. Since each and every concept present here could not be individually referenced, I also wish to acknowledge that for the most part they have been extracted from the works of the pioneers in experimental viscoelasticity such as Drs. Herbert Leaderman, Arthur V. Tobolsky and John D. Ferry.

REFERENCES

1. R. F. Boyer, J. Polymer Sci. Part C, 14, iv, 1966.

2. A. J. Kovacs, R. A. Stratton, and J. D. Ferry, J. Phys. Chem., 67, 152 (1963).

3. D. J. Plazek and J. H. Magill, J. Chem. Phys. 45, 3038 (1966).

4. H. Nakayasu, H. Markovitz, and D. J. Plazek, Trans. Soc. Rheology, 5, 261 (1961).

5. R. F. Boyer, J. Polymer Sci. Part C, 14, 267 (1966).

6. G. C. Berry, and T. G. Fox, Adv. Polymer Sci., 5, 261 (1967).

7. M. L. Williams, R. F. Landel, and J. D. Ferry, J. Am. Chem. Soc. 77, 3701 (1955).

8. D. J. Plazek and V. M. O'Rourke, unpublished experiments.

9. J. D. Ferry, R. G. Mancke, E. Maekawa, Y. Ōyanagi, and R. A. Dicke, J. Phys. Chem., 68, 34.14 (1964).

10. E. Maekawa, R. G. Mancke and J. D. Ferry, J. Phys. Chem., 69, 2811 (1965).

11. A. V. Tobolsky, J. J. Aklonis, and G. Akovali, Jr., Chem. Phys., 42, 723 (1965).

12. D. J. Plazek, J. Polymer Sci., A-2, 6, 000 (1968).

13. J. D. Ferry, Viscoelastic Properties of Polymers (John Wiley and Sons, Inc., New York, 1961). Chapter 12.

Legends

Figure 1) Logarithm$_{10}$ of viscosity, η, dyne sec/cm^2, as a function of $1/(T - T_\infty)$ for 5 anionically polymerized polystyrene samples with molecular weights of 3.4×10^3, PC 11 [2]; 4.7×10^4, A25; 9.4×10^4, M 102; 1.89×10^5, L2; and 6.0×10^5, A19. T_∞ °C values indicated following sample designation.

Figure 2) Logarithm of reduced recoverable compliance, $[J_p(t) - t/\eta_p]$ for polystyrene, $M = 1.22 \times 10^5$, plotted against logarithm of time, t. $J_p(t) = T\rho J(t) / T_o \rho_o$ and $\eta_p = T_o \rho_o \eta / T\rho$ where ρ_o is the density at the reference temperature, T_o = 100°C. ρ is the density at the temperature, T, of measurement.

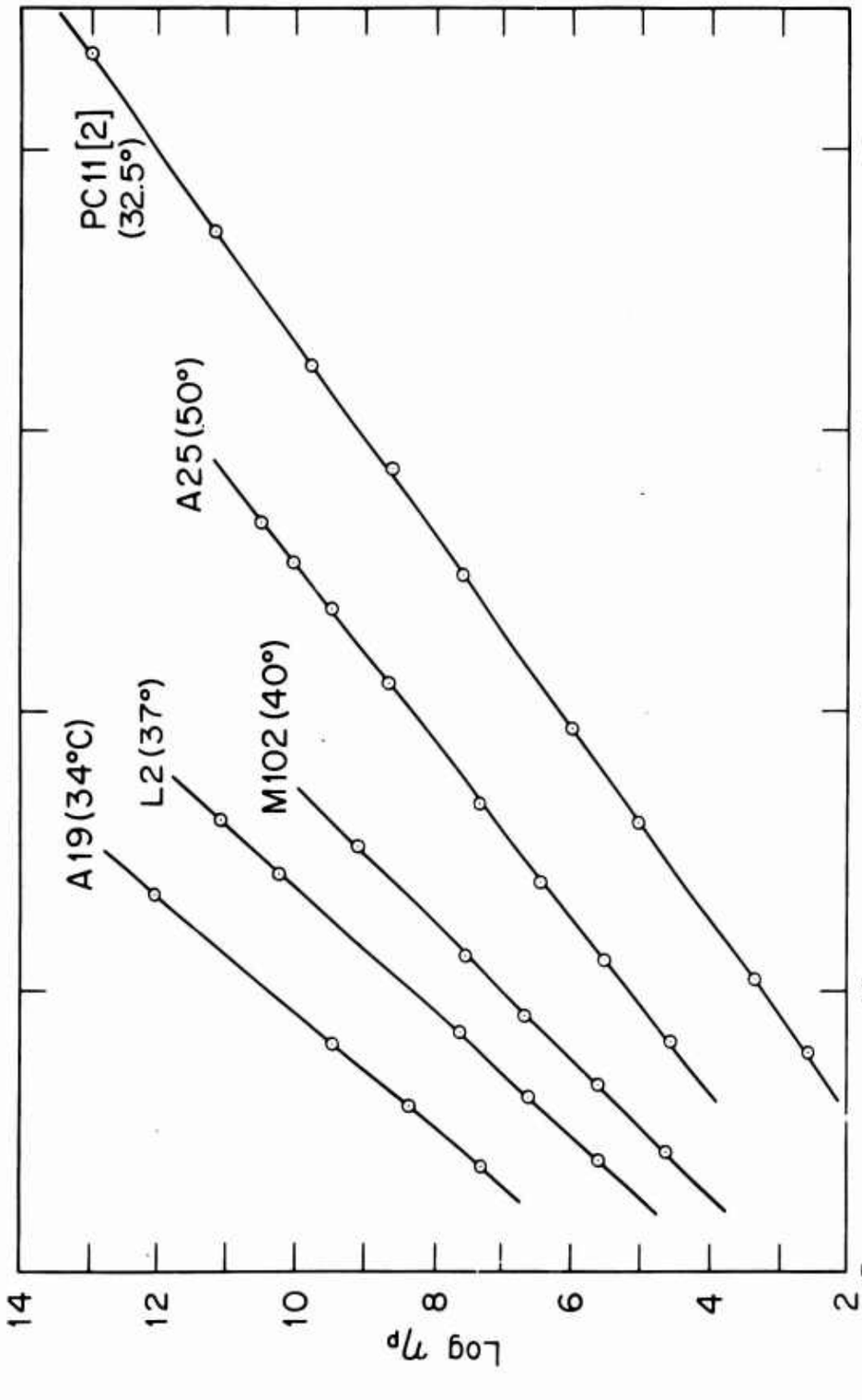
PC11 [2] (32.5°)
A25 (50°)
M102 (40°)
L2 (37°)
A19 (34°C)
Log η_p
$10^3/(T-T_\infty)$
14
12
10
8
6
4
2
5
10
15
20
25

FIGURE 1

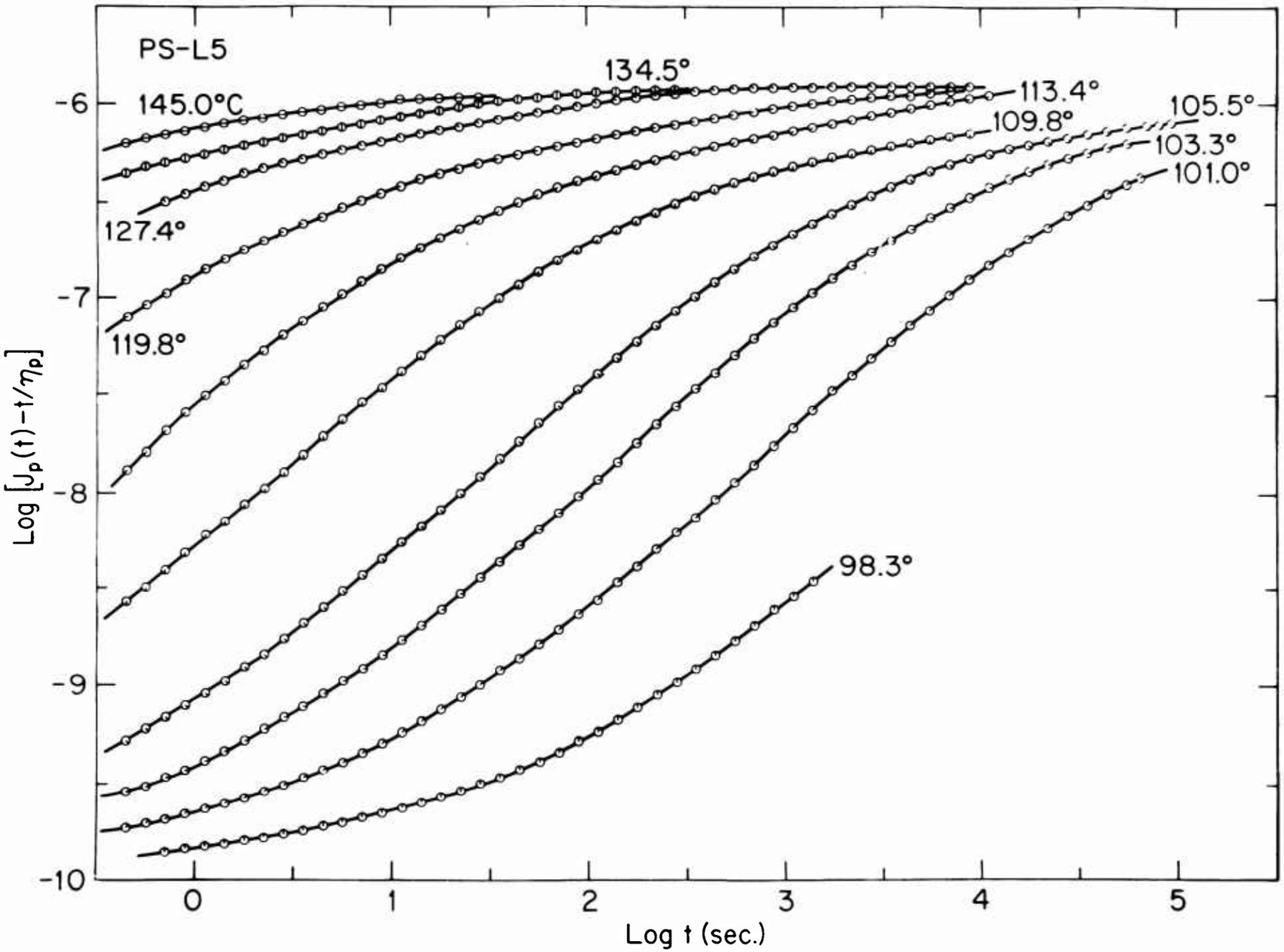
PS-L5
145.0°C
134.5°
127.4°
119.8°
113.4°
109.8°
105.5°
103.3°
101.0°
98.3°
Log [Jp(t)−t/ηp]
Log t (sec.)
-6
-7
-8
-9
-10
0
1
2
3
4
5

FIGURE 2

ATTENDANCE LIST (April 7, 1967)

Conference on Polymer Structure and Mechanical Properties

U.S. Army Natick Laboratories
Natick, Massachusetts
April 19-21, 1967

ACHHAMMER, Bernard G.
Manager, Polymer Program
Office of Advanced Research
and Technology
(Code RRM)
NASA
Washington, D.C. 20546

ADICOFF, Arnold
Research Chemist
U.S. Naval Ordnance Test Station
China Lake, California 93555

AGGARWAL, S. L.
Manager, Basic and
Materials Research
General Tire & Rubber Company
1708 Englewood Avenue
Akron, Ohio 44309

ALEXANDER, Claude H.
Manager, Product Improvement
B. F. Goodrich Chemical Company
3135 Euclid Avenue
Cleveland, Ohio 44115

ANDREWS, E. H.
Reader in Materials Science
Queen Mary College
Mile End Road
London E.1, England

ANDREWS, Rodney D., Jr.
Professor, Department of Chemistry
Stevens Institute of Technology
Castle Point Station
Hoboken, New Jersey 07030

BAER, Eric
Professor in Charge, Polymer
Science and Engineering
Materials Science Building
Case Institute of Technology
University Circle
Cleveland, Ohio 44106

BARNET, F. Robert
Supervisory Chemist
U.S. Naval Ordnance Laboratory
White Oak
Silver Spring, Maryland 20910

BARRETT, Arthur E.
Supervisor, Rubber Laboratory
(Code 130L4)
San Francisco Bay Naval Shipyard
Vallejo, California 94592

BASSETT, David Clifford
Physics Department
University of Reading
J. J. Thomson Physical Laboratory
Whiteknights Park
Reading, Berks, England

BERMAN, Saul
Chemistry Branch Staff
Office of Naval Research
Main Navy Building, Room 0408
Washington, D.C. 20360

BOSMAJIAN, George
Research Coordinator for Chemistry
U.S. Navy Marine Engineering
Laboratory
Annapolis, Maryland 21402

BOYER, Raymond F.
Director of Plastics Research
Dow Chemical Company
P. O. Box 625
Midland, Michigan 48640

BROUTMAN, Lawrence J.
Associate Professor of
Mechanics and Materials
Illinois Institute of Technology
3300 South Federal
Chicago, Illinois 60616

BRYANT, William M. D.
Research Fellow
Plastics Department
E. I. duPont deNemours & Co., Inc.
DuPont Experimental Station
Wilmington, Delaware 19898

CLOUGH, Stuart B.
Research Chemist
Clothing and Organic
Materials Division
U.S. Army Natick Laboratories
Natick, Massachusetts 01760

CUEVAS, Joseph E.
Physicist
U.S. Naval Ordnance Laboratory
White Oak
Silver Spring, Maryland 20910

CUNNINGHAM, Bernard E.
Assistant Chief, Materials
Research Branch
NASA-Ames Research Center
Moffett Field, California 94035

DESPER, C. Richard
Research Chemist
Clothing and Organic
Materials Division
U.S. Army Natick Laboratories
Natick, Massachusetts 01760

DOLE, Malcolm
Professor
Materials Research Center
Northwestern University
Evanston, Illinois 60201

DRECHSEL, Paul D.
Superintendent, Basic
Research Department
Allegany Ballistics Laboratory
Hercules, Inc.
P. O. Box 210
Cumberland, Maryland 21502

DUNBROOK, Raymond F.
2326 Alpine Avenue
Sarasota, Florida 33580

DUNLAP, Lawrence H.
Senior Research Associate
Research and Development Center
Armstrong Cork Company
2500 Columbia Avenue
Lancaster, Pennsylvania 17604

DUNN, Peter
Senior Research Scientist
Defence Standards Laboratories
P. O. Box 50, Ascot Vale
Melbourne, Victoria, Australia

EIRICH, Frederick R.
Professor, Department of Chemistry
Polytechnic Institute of Brooklyn
333 Jay Street
Brooklyn, New York 11201

FAULL, J. H., Jr.
Scientific Staff Assistant
Office of Naval Research
495 Summer Street
Boston, Massachusetts 02210

FERRY, John D.
Professor, Department of Chemistry
University of Wisconsin
Madison, Wisconsin 53706

FISCHER, Erhard W.
Professor
Institut fur Physikalische Chemie
der Universitat Mainz
Jakob Welderweg 15
Mainz, Deutschland, W. Germany

FISHER, Frank R.
Executive Secretary
Advisory Board on Military
Personnel Supplies
National Research Council
2101 Constitution Avenue
Washington, D.C. 20418

FLANAGAN, James H.
Deputy Scientific Director,
Engineering
U.S. Army Natick Laboratories
Natick, Massachusetts 01760

FOX, T. G.
Staff Fellow
Mellon Institute
4400 Fifth Avenue
Pittsburgh, Pennsylvania 15213

GEIL, Phillip H., Jr.
Associate Professor
Case Institute of Technology
University Circle
Cleveland, Ohio 44106

GENT, A. N.
Professor of Polymer Physics
and Assistant Director
Institute of Polymer Science
University of Akron
Akron, Ohio 44304

GLOOR, Walter H.
Research Engineer
Air Force Materials Laboratory
Wright-Patterson AFB, Ohio 45433

GREER, Paul S.
Associate Director
Chemistry Division
U.S. Army Research Office
Box CM, Duke Station
Durham, North Carolina 27706

HALDON, Robert A.
Department of Chemistry
University of Southern California
University Park
Los Angeles, California 90007

HANSEN, David
Associate Professor
Department of Chemical Engineering
Rensselaer Polytechnic Institute
Troy, New York 12181

HENRY, Malcolm C.
Acting Associate Director
Clothing and Organic
Materials Division
U.S. Army Natick Laboratories
Natick, Massachusetts 01760

HEYING, Theodore L.
Technical Director
Olin Mathieson Chemical Corp.
275 Winchester Avenue
New Haven, Connecticut 06511

HOBBS, Lindsey M.
Chief, Polymer Research Section
Propulsion and Vehicle
Engineering Laboratory
Materials Division
NASA-George C. Marshall Space
Flight Center
Huntsville, Alabama 35812

HOFFMAN, Allan S.
Associate Professor of
Chemical Engineering
Massachusetts Inst. of Technology
Cambridge, Massachusetts 02139

HOFFMAN, John D.
Chief, Polymers Division
A307 Polymer
National Bureau of Standards
Washington, D.C. 20234

HOWERTON, William W.
Staff Consultant
Aeronautical Materials Laboratory
Naval Air Engineering Center
Building 76-5
Philadelphia, Pennsylvania 19112

HUGGINS, Maurice L.
Senior Research Scientist
Stanford Research Institute
Menlo Park, California 94025

HUSEBY, T. W.
Member, Technical Staff
Bell Telephone Laboratories, Inc.
Murray Hill, New Jersey 07971

IKEDA, Richard M.
Research Chemist
E. I. duPont deNemours & Co., Inc.
DuPont Experimental Station
Building 334, Room 223
Wilmington, Delaware 19898

KAMBOUR, Roger P.
Research Chemist
Research and Development Center
General Electric Company
P. O. Box 8
Schenectady, New York 12305

KEITH, H. D.
Member, Technical Staff
Bell Telephone Laboratories, Inc.
Murray Hill, New Jersey 07971

KELLER, Andrew
Reader in Physics
Physics Department
H. H. Wills Physics Laboratory
University of Bristol
Royal Fort
Tyndall Avenue
Bristol 2. England

KESKKULA, Henno
Group Leader
Dow Chemical Company
335 Building
Midland, Michigan 48640

KHOURY, F. A.
Physicist
National Bureau of Standards
Washington, D.C. 20234

KINNA, Marlin A.
Project Engineer
Naval Ordnance Systems Command
Room 3612 MB
Washington, D.C. 20360

KONTOS, Emmanuel G.
Manager, Polymer Physics
Research Section
Research Center
UNIROYAL, Inc.
1361 Alps Road
Wayne, New Jersey 07470

LANDEL, Robert F.
Manager, Polymer Research Section
NASA-Jet Propulsion Laboratory
4800 Oak Grove Drive
Pasadena, California 91103

LEBOVITS, Alexander
Research Chemist
(Code 936)
U.S. Naval Applied Science Lab.
Flushing & Washington Avenues
Brooklyn, New York 11251

LEPIE, Albert H.
Research Chemist
Solid Propellants Branch
(Code 4521)
U.S. Naval Ordnance Test Station
China Lake, California 93555

LEVI, David W.
Chief, Polymer Research Branch
Picatinny Arsenal
Dover, New Jersey 07801

LICHTMAN, Joseph Z.
Materials Engineer
U.S. Naval Applied Science Lab.
Flushing & Washington Avenues
Brooklyn, New York 11251

LINDENMEYER, Paul H.
Manager, Fiber Science
Chemstrand Research Center, Inc.
P. O. Box 731
Durham, North Carolina 27702

MacKNIGHT, William J.
Assistant Professor
Polymer Science and
Engineering Program
University of Massachusetts
Amherst, Massachusetts 01002

MAGEE, Robert T.
Engineering Technician
NASA-Langley Research Center
Langley Station
Hampton, Virginia 23365

MAJOWICZ, Joseph M.
Chief, Research and Development
ATTN: CRDPES
Materials Sciences and
Technology Branch
Physical and Engineering
Sciences Division
U.S. Army Research Office
Washington, D.C. 20310

MANTZ, Brig. Gen. William M.
Commanding General
U.S. Army Natick Laboratories
Natick, Massachusetts 01760

MARTIN, Donald L., Jr.
Research Aerospace Engineering
(Materials)
Propulsion Laboratory
Research and Development Directorate
U.S. Army Materiel Command
Redstone Arsenal, Alabama 35809

MATESKY, Sol J.
Head, Electrical Systems and
Materials Branch
Naval Ordnance Systems Command
Munitions Building, Room 3612
Washington, D.C. 20360

MATSUOKA, Shiro
Supervisor, Plastics Rheology
and Processing Department
Room 1B-208
Bell Telephone Laboratories, Inc.
Murray Hill, New Jersey 07971

McABEE, Elise
Materials Engineer
Picatinny Arsenal
Dover, New Jersey 07801

McGARRY, Frederick J.
Professor of Civil Engineering
Room 1-173
Massachusetts Inst. of Technology
Cambridge, Massachusetts 02139

MEDALIA, Avrom I.
Associate Director,
Fundamental Research
Cabot Corporation
38 Memorial Drive
Cambridge, Massachusetts 02142

METZGER, Arthur C.
NASA Manager of the Resident
Apollo Spacecraft Program Office
Massachusetts Inst. of Technology
Cambridge, Massachusetts 02139

MILLER, Robert L.
Scientist
Chemstrand Research Center, Inc.
P. O. Box 731
Durham, North Carolina 27702

MOACANIN, Jovan
Group Supervisor
NASA-Jet Propulsion Laboratory
4800 Oak Grove Drive
Pasadena, California 91103

MONTERMOSO, Juan C.
Vice President,
Research and Development
Quantum, Inc.
Lufbery Avenue
Wallingford, Connecticut 06492

MORRIS, Ross E.
Head, Rubber Laboratory
(Code 130L4)
San Francisco Bay Naval Shipyard
Vallejo, California 94592

MULLINS, Leonard
Director of Research
Natural Rubber Producers'
Research Association
Tewin Road
Welwyn Garden
Hertfordshire, England

NOETHER, Herman D.
Research Associate
Celanese Research Corporation
Morris Court
Summit, New Jersey 07901

O'SHAUGHNESSY, M. T.
Manager, Fiber Physics Branch
Textile Research Laboratory
Phillips Petroleum Company
Bartlesville, Oklahoma 74003

OSSEFORT, Zachary T.
Supervisory Research Chemist
Rock Island Arsenal
Rock Island, Illinois 61201

PADDEN, Frank J., Jr.
Member, Technical Staff
Bell Telephone Laboratories, Inc.
Murray Hill, New Jersey 07971

PARKS, W. George
Executive Director
Advisory Board on Military
Personnel Supplies
National Research Council
Department of Chemistry
University of Rhode Island
Kingston, Rhode Island 02881

PETERLIN, Anton
Director, Camille Dreyfus Laboratory
Research Triangle Institute
P. O. Box 12194
Research Triangle Park
North Carolina 27709

PILSWORTH, Malcolm N., Jr.
Physicist
Pioneering Research Division
U.S. Army Natick Laboratories
Natick, Massachusetts 01760

PORTER, Roger S.
Associate Professor and Chairman
Polymer Science and
Engineering Program
University of Massachusetts
Amherst, Massachusetts 01002

POWELL, Arnet L.
Chief Scientist
Office of Naval Research
495 Summer Street
Boston, Massachusetts 02210

PREDECKI, Paul K.
Research Metallurgist
Assistant Professor
College of Engineering
Denver Research Institute
University of Denver
Denver, Colorado 80210

PRICE, Fraser P.
Physical Chemist
Research and Development Center
General Electric Company
P. O. Box 8
Schenectady, New York 12301

PRICE, Howard L.
Aerospace Technologist
NASA-Langley Research Center
Langley Station
Hampton, Virginia 23365

PROSSER, Robert A.
Research Chemist
Clothing and Organic
Materials Division
U.S. Army Natick Laboratories
Natick, Massachusetts 01760

RAUN, Milton A.
Chief, Packaging and
Materials Branch
Defense Development and
Engineering Laboratory
ATTN: SMUEA-DME-3
Edgewood Arsenal, Maryland 21010

READ, Bryan E.
Visiting Scientist
Polymer Research Institute
University of Massachusetts
Amherst, Massachusetts 01002

RIBNICK, Arthur
Staff Scientist
Textile Research Institute
P. O. Box 625
Princeton, New Jersey 08540

ROSENBLATT, David B.
Director
Pitman-Dunn Research Laboratories
Frankford Arsenal
Bridge & Tacony Streets
Philadelphia, Pennsylvania 19137

SCHNEIDER, Nathaniel S.
Group Leader, Polymer
Physical Chemistry
Clothing and Organic
Materials Division
U.S. Army Natick Laboratories
Natick, Massachusetts 01760

SCHROEDER, Hansjuergen A.
Section Manager
Olin Mathieson Chemical Corporation
275 Winchester Avenue
New Haven, Connecticut 06504

SHARMA, M. G.
Associate Professor
Department of Engineering Mechanics
105 Hammond Building
Pennsylvania State University
University Park, Pennsylvania 16802

SIELING, Dale H.
Scientific Director
U.S. Army Natick Laboratories
Natick, Massachusetts 01760

SILBERBERG, Melvin
President
Plas-Tech Equipment Corporation
4 Mercer Road
Natick, Massachusetts 01760

SIMHA, Robert
Professor, Department of Chemistry
University of Southern California
University Park
Los Angeles, California 90007
Presently:
Kennedy Memorial Foundation
Sr. Fellow
The Weizmann Institute of Science
Rehovoth, Israel

SIMMS, Bernard B.
Head, Organic Chemistry Branch
U.S. Naval Applied Science Lab.
Flushing & Washington Avenues
Brooklyn, New York 11251

SINNOTT, Kenneth M.
Research Associate
Research Division
Washington Research Center
W. R. Grace & Company
Clarksville, Maryland 21029

SMITH, Fred W.
Materials Engineer
U.S. Army Tank-Automotive Command
Warren, Michigan 48090

SMITH, Thor L.
Scientific Fellow
Stanford Research Institute
Menlo Park, California 94025

SOLLOTT, G. P.
Chief, Organic Chemistry Branch
Pitman-Dunn Research Laboratories
Frankford Arsenal
Bridge & Tacony Streets
Philadelphia, Pennsylvania 19137

STEIN, Richard S.
Professor, Department of Chemistry
University of Massachusetts
Amherst, Massachusetts 01002

STERNSTEIN, Sanford S.
Associate Professor
Department of Chemical Engineering
Rensselaer Polytechnic Institute
Troy, New York 12181

SUPNIK, Ross H.
Vice President
Plas-Tech Equipment Corporation
4 Mercer Road
Natick, Massachusetts 01760

TAKAYANAGI, Motowo
Professor of Applied Chemistry
Faculty of Engineering
Kyushu University
Hakozaki
Fukuoka, Japan

TAYLOR, Raymond L.
Staff Scientist
Quantum, Inc.
Lufbery Avenue
Wallingford, Connecticut 06492

TOBOLSKY, Arthur V.
Professor of Chemistry
Frick Chemical Laboratory
Princeton University
Princeton, New Jersey 08540

TOUCHET, Paul
Chemical Engineer
Military Technology
U.S. Army Engineer Research and
Development Laboratories
Fort Belvoir, Virginia 22060

TSCHOEGL, N. W.
Associate Professor,
Materials Science
California Institute of Technology
1201 East California Street
Pasadena, California 91109

VIETH, Wolf R.
Assistant Professor of
Chemical Engineering
Massachusetts Inst. of Technology
Cambridge, Massachusetts 02139

VINCENT, P. I.
Research Department
Plastics Division
Imperial Chemical Industries, Ltd.
Bessemer Road
Welwyn Garden City
Herts, England

WARD, I. M.
H. H. Wills Physics Laboratory
University of Bristol
Royal Fort
Tyndall Avenue
Bristol 2. England

WARFIELD, Robert W.
Chemist
U.S. Naval Ordnance Laboratory
White Oak
Silver Spring, Maryland 20910

WILDE, Anthony F.
Research Chemist
Clothing and Organic
Materials Division
U.S. Army Natick Laboratories
Natick, Massachusetts 01760

WILLIAMSON, R. Brady
Assistant Professor of
Civil Engineering
Room 1-172
Massachusetts Inst. of Technology
Cambridge, Massachusetts 02139

WINSLOW, Field H.
Head, Polymer Research and
Development Department
Bell Telephone Laboratories, Inc.
Murray Hill, New Jersey 07971

WOOD, Lawrence A.
Consultant on Rubber
A307 Polymer
National Bureau of Standards
Washington, D.C. 20234

WOODWARD, Arthur E.
Professor, Department of Chemistry
The City College of
The City University of New York
138th and Convent Avenues
New York, New York 10031

WORK, Richard N.
Professor of Physics
Arizona State University
Tempe, Arizona 85281

WUNDERLICH, Bernhard
Professor, Department of Chemistry
Rensselaer Polytechnic Institute
Troy, New York 12181

YANNAS, Ioannis V.
Assistant Professor
Fibers and Polymers Division
Massachusetts Inst. of Technology
Cambridge, Massachusetts 02139

SUPPLEMENTARY ATTENDANCE LIST (April 19, 1967)

Conference on Polymer Structure and Mechanical Properties

U.S. Army Natick Laboratories
Natick, Massachusetts 01760

19-21 April 1967

ALESI, Anthony L.
Supervisory Physical
Research Scientist
Clothing & Organic
Materials Division
U.S. Army Natick Labs
Natick, Mass. 01760

ALFREY, Turner, Jr.
Research Scientist
Dow Chemical Co.
Midland, Mich. 48640

BOONSTRA, B. B.
Associate Director
Cabot Corporation
38 Memorial Drive
Cambridge, Mass. 02142

BRINDELL, Gordon D.
Group Leader
Uniroyal Chemical
Elm Street
Nangatuck, Conn. 06770

CALDERON, Julio H.
Chemist
ERDL Fort Belvoir
7628 Angio Lane
Lorton, Va. 22079

COVINGTON, Edward R.
Senior Chemist
Southern Research Institute
2000 9th Avenue South
Birmingham, Alabama 35205

GARDNER, Frank S.
Metallurgist
Office of Naval Research
Boston Branch
495 Summer Street
Boston, Mass 02210

GOOD, C. W.
Project Leader
Research Scientist
UNIROYAL, Inc. Research Center
Wayne, N. J 07470

HEALY, Edward M.
Chemist
U. S. Army Natick Laboratories
Kansas Street
Natick, Mass 01760

HEIMBUCH, Alvin H.
Research Scientist
NASA-Ames Research Center
Gasdynamics Branch N-234
Moffett Field, Calif 94035

KILLORAN, John J
Research Chemist
U.S Army Natick Laboratories
Kansas Street
Natick, Mass 01760

KING, Abram O.
Research Chemist
U.S. Army Natick Laboratories
C&OM Division
Natick, Mass. 01760

LEVINE, Harold H.
Staff Scientist
Whittaker Corporation
Narmco R&D Division
3540 Aero Court
San Diego, Calif 92037

MARKOVITZ, Hershel
Senior Fellow
Mellon Institute
4400 Fifth Avenue
Pittsburgh, Pa. 15213

O'REILLY, James M.
Physical Chemist
General Electric R&D Center
Bldg. K1
P. O. Box 8
Schenectady, N. Y. 12301

OSWALD, Hendrikus J.
Section Supervisor
Central Research Lab.
Allied Chemical Corporation
Columbia Road
Morristown, N.J. 07960

PLAZEK, Donald J.
School of Engineering
University of Pittsburg
Pittsburgh, Pa. 15213

RELYEA, Douglas I
Senior Research Scientist
Uniroyal, Inc.
Alps Road
Wayne, N.J. 07470

REMY, David E
Chemist
U.S. Army Natick Laboratories
Natick, Mass. 01760

ROLDAN, Luis Gonzalez
Senior Scientist
C.R.L. Allied Chemical Corp.
Columbia Road
Morristown, N.J. 07960

RUSCH, Kenneth C.
Research Scientist
Ford Motor Company
Research Staff
P. O. Box 2053
Dearborn, Mich 48121

SAUER, John A.
Professor and Chairman
Department of Mechanics
Rutgers - The State University
College of Engineering
University Heights Campus
New Brunswich, N.J. 08903

SCHATZKI, Thomas F
Chemist
Shell Development Company
1400 - 53rd Street
Emeryville, Cali 94608

SCHIRALDI, Michael T
Research Chemist
Clothing & Organic
Materials Division
U.S. Army Natick Laboratories
Natick, Mass 01760

WELLS, Richard D
Textile Technologist
Fibrous Materials Research Group
U.S. Army Natick Laboratories
Natick, Mass 01760

WICKLATZ, John
Manager of Polymer Research
Central Research Laboratories
General Mills, Inc
2010 E Hennepin Avenue
Minneapolis, Minn 55413

Urs, S. V.
Section Manager, Polymer Research
Olin Mathieson Chemical Company
275 Winchester Avenue
New Haven, Conn. 06504